1. INTRODUCTION

This report contains a description of the design of the technical components of the Neutrino at Main Inject (NuMI) project at Fermilab as well as a summary of radiation safety considerations. The technical baselines for the NuMI Project have already been established and can be found in the NuMI Facility Technical Design Report, issued in October 1998. The NuMI Project was baselined in November 1998. In October 2001, revised cost and schedule of the NuMI Project were submitted as NuMI Baseline Change Proposal. This baseline Change Proposal was approved in January 2002. This report updates and expands upon the scope and the design of technical components in the NuMI Facility after the Baseline Change Proposal.

The NuMI Facility Project produces an intense beam of neutrinos to enable a new generation of experiments whose primary scientific goal is to definitively detect and study neutrino oscillations. The beam is of sufficient intensity and energy so that experiments capable of identifying muon neutrino (ν_μ) to tau neutrino (ν_τ) oscillations, as well as other possibilities, are feasible. Although not a primary goal, the intense NuMI beam could also support a strong program of neutrino scattering physics of interest to both the Elementary Particle Physics and Nuclear Physics communities.

The first step in the production of the NuMI neutrino beam is to direct a beam of protons from Fermilab's Main Injector onto a production target. Interactions of the proton beam in the target produce mesons, which are focused toward the beam axis by two magnetic horns. The mesons then decay into muons and neutrinos during their flight through a long decay tunnel. A hadron absorber downstream of the decay tunnel removes the remaining protons and mesons from the beam. The muons are absorbed by the subsequent earth shield, while the neutrinos continue through it to a "near" detector (in a new experimental hall at Fermilab) and beyond, to the "far" detector in Soudan, Minnesota. The Fermilab and Soudan experimental halls house massive detectors specially designed to detect the small fraction of the NuMI beam neutrinos that interact in them. This experiment is called MINOS (Main Injector Neutrino Oscillation Search).

The NuMI Facility includes the underground enclosures (tunnels and halls) as well as two service buildings located on the surface. The NuMI beamline and experimental facility at Fermilab are fully described in the NuMI Facility Technical Design Report. The layout of the NuMI Facility underground enclosures is illustrated in **Figure 1-1.** An aerial photograph of the

Fermilab site with the beamline superimposed is shown in **Figure 1-2** and the trajectory of the neutrino beam between Fermilab and Soudan is shown in **Figure 1-3**.

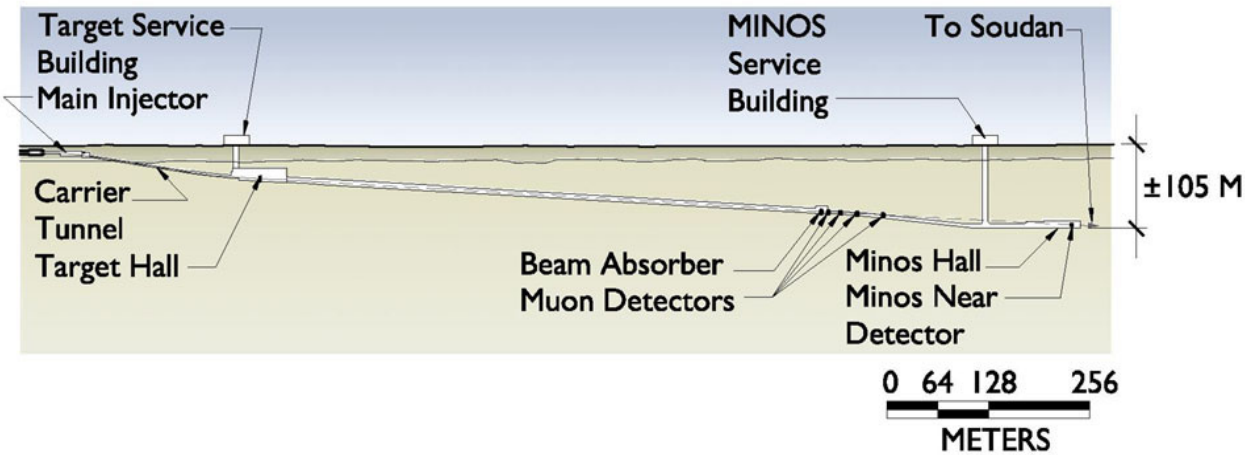

Figure 1-1 Layout of the NuMI Facility.

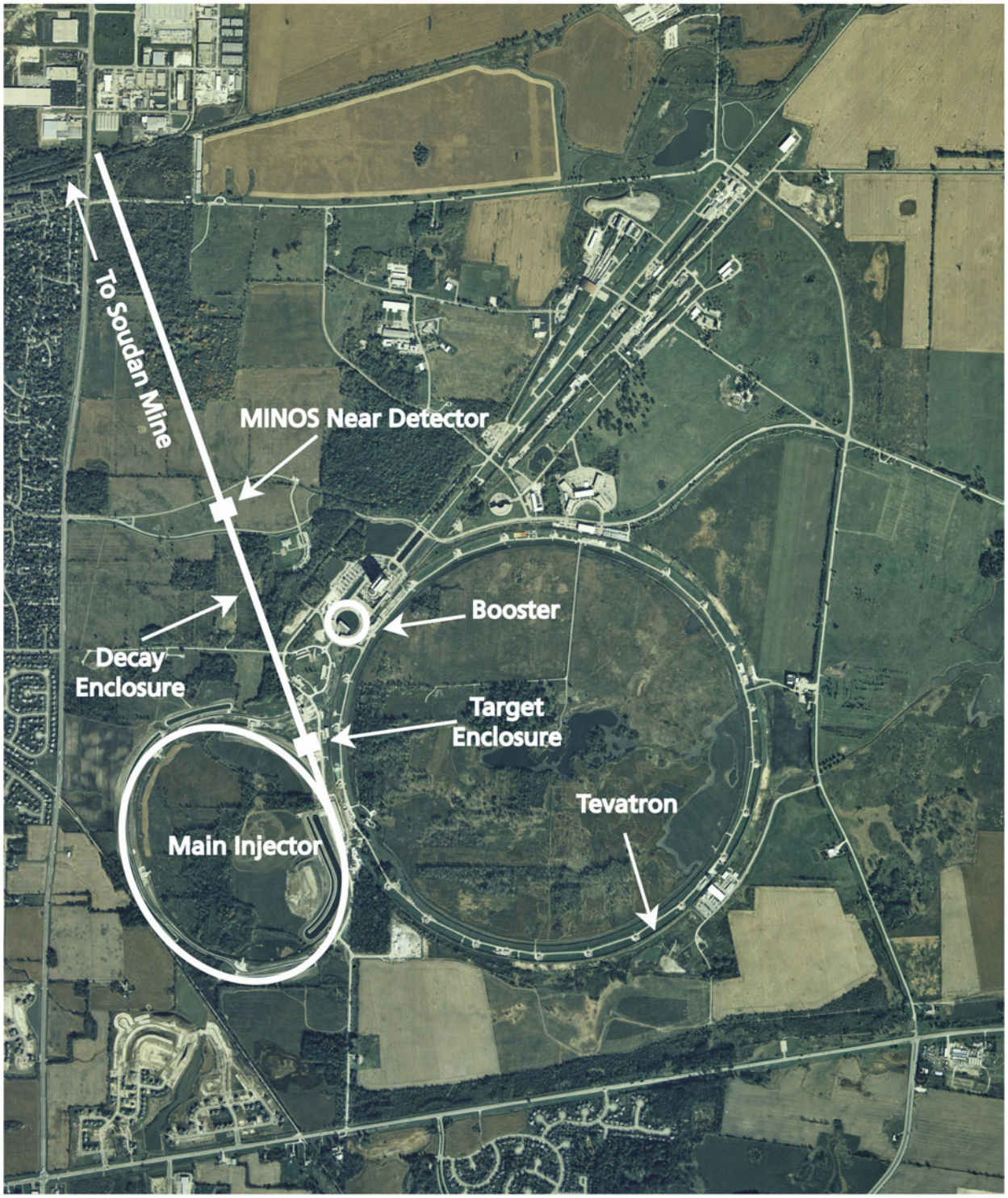

Figure 1-2 Aerial view of the Fermilab site and the NuMI beamline.

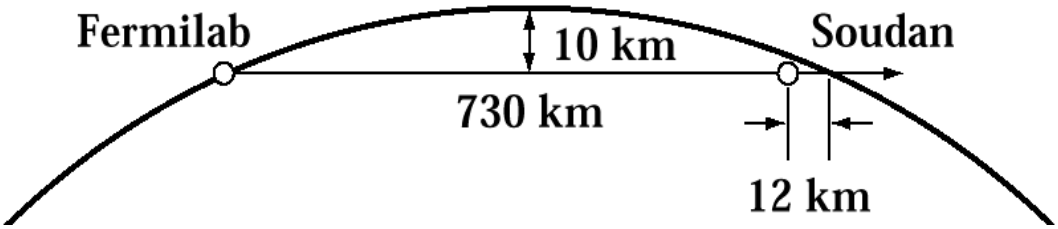

Figure 1-3 Trajectory of the neutrino beam between Fermilab and Soudan, Minnesota.

1.1 Scope and parameters

The scope of the NuMI Technical Components is laid out in **Table 1-1** and described in more detail in Chapter 2. Key parameters of the beamline are listed in **Table 1-2.**

Subsystem	Description
Primary Beam	Extraction and transport of 120 GeV proton beam from the Main Injector to the NuMI Target
Neutrino Beam Devices	Production and focusing the secondary beam from the NuMI target through the focusing horns
Power Supply Systems	Power supplies, cables and connections for NuMI beamline elements
Decay Region & Hadron Absorber	Decay pipe for neutrino-producing decays of mesons, absorber for non-decaying particles, and associated radiation shielding
Neutrino Beam Monitoring	Measurement of flux and profiles of secondary beam and muons
Survey, Alignment & Geodesy	Accurate determination of the neutrino beam centerline at Fermilab and Soudan. Accurate positioning of the neutrino beamline elements
Beamline Utilities	Water, vacuum and gas
Controls, Cables & Interlocks	Controls systems, cable specifications and installation, interlocks methodology and locations

Table 1-1 Technical components of the NuMI beamline

Downward slope of ν beam		58 mr (3.3°)
Proton intensity		2.5×10^{13} p/1.9 sec
Spill length		8 μsec
Protons on target per year		2.5×10^{20}
Target material		Graphite
Pion focusing		Wide band, 2 horn
Neutrino Energy Options		
Baseline	Low Energy	1 - 3 GeV
Option 1	Medium energy	3 - 8 GeV
Option 2	High energy	8 -16 GeV
Decay pipe		1 m radius × 675 m long
Downstream hadron monitoring		Ion chambers upstream of absorber
Muon absorber		240 m of dolomite
Muon monitoring		Ion chambers in absorber enclosure and alcoves in the dolomite shield

Table 1-2 Parameters for the NuMI beamline

1.2 Performance and Operational Goals

The Main Injector is a very high intensity proton accelerator that can provide an adequate neutrino event rate even in a detector 735 km away. Furthermore, the anticipated mode of operation of the Main Injector during the next decade is well suited to the NuMI Project. The accelerator must operate a significant fraction of the time to produce antiprotons for $\overline{p} - p$ collisions in the Tevatron. However, only one of six bunches are to be used for antiproton production, the other five being available for stationary target experiments such as MINOS. Furthermore, the Main Injector has adequate design margin and scope for upgrades in key subsystems so there is a good possibility that its intensity will increase with time and thus experiments with higher statistics and better sensitivity will be possible in the future.

The production of the neutrino beam occurs in two stages. First the 120 GeV proton beam from the Main Injector is directed by single-turn extraction into the NuMI beamline. In the NuMI beamline, the protons are focused onto a segmented target, producing secondary mesons, both pions and kaons. Because the neutrino beam must be aimed at the Soudan Underground Laboratory, the proton beam is directed downward at 58 mrad before it strikes the target. Subsequently, forward-going particles (mesons) in the energy range of interest are focused and allowed to decay, producing neutrinos. The focusing is performed by a set of two magnetic horns. These devices are shaped in such a way that, when a pulse of current passes through them, a magnetic field is generated which focuses particles in the desired momentum range over a wide range of production angles. The average meson energy is selected by adjusting the locations of the second horn and target with respect to the first horn. Thus, this “zoom” beam optics design allows the energy of the meson beam (and therefore of the neutrino beam) to be varied during the course of the experiment.

The particles selected by the focusing horns (mainly pions with a small component of kaons and uninteracting protons) are then allowed to propagate down an evacuated beam pipe (decay tunnel) 1 m in radius and 675 m long, placed in a tunnel, pointing downward towards Soudan. While traversing the beam pipe, a fraction of mesons decay, yielding forward-going neutrinos. By adjusting the energy of the parent meson beam, a neutrino beam in the desired energy range can be obtained. As mentioned above, this feature is crucial to our ability to experimentally

explore a wide range of possible oscillation parameters and to minimize the errors associated with these measurements. A hadron absorber is placed at the end of the decay pipe to remove the residual flux of protons and mesons, followed by a set of beam monitoring detectors.

The neutrino beam line has the following design objectives:

- Potentially cover the energy range 1 to 20 GeV. This is accomplished by a hadron focusing system that can be optimized to 1-3 GeV, 3-8 GeV or 8-20 GeV in neutrino energy.
- Predict the neutrino energy spectrum in the MINOS far detector to 2 or 3%, if neutrino oscillations are absent, given a measurement of the spectrum at the MINOS near detector.
- Center the neutrino beam at the detectors and to keep the effect of mis-steering to less than 2% anywhere in the neutrino spectrum.
- Long term reliability, stability and reparability such that the facility is usable for a minimum of 10 years while assuring personnel safety and allowing for future modifications and upgrades.

The integrated technical goals of the NuMI facility and MINOS experiment are listed in Table 1-3 and 1-4. The commissioning goals are the parameter values that must be achieved for approval to start operations (Critical Decision 4) and are given in Table 1-3. The operational goals, which are needed for the NuMI project to accomplish its scientific objectives, are expected to be reached after several years of operation and are given in Table 1-4. Although the NuMI Project will have sensitivity to a wide range of parameter space to search for neutrino oscillations, recent scientific results from Japan strongly indicate the most promising area to search within this parameter space. Thus the project begins in its “Low Energy” beam configuration. The commissioning goals are to be met with cosmic rays and atmospheric neutrinos to demonstrate the effectiveness of the far neutrino detector. Measurements made with the beamline monitoring instrumentation assure that the neutrino beam is aimed correctly at the MINOS far detector.

Parameter	Measurement	Commissioning Goal
Cosmic ray muons detected in the MINOS Near Detector	Near Detector data read out through DAQ system	Majority of the 153 Near Detector planes sensitive to muons
Cosmic ray muons detected in each of the two MINOS Far Detector Super Modules	Far Detector data read out through DAQ system	Majority of the 484 planes of the Far Detector sensitive to muons. Atmospheric neutrinos detected in the Far Detector.
Proton intensity in target hall	Toroid (or equivalent) beam intensity monitor at entrance to the Target Hall	Greater than $1x10^{12}$ 120 GeV protons/spill
Beam alignment	Transverse distributions of the proton beam and secondary beam.	Proton direction established to within 1 mr of the known direction to Soudan.
Near detector neutrino flux	Charged current event rate in 15 ton fiducial region	Observe neutrinos in the Near Detector produced by the NuMI beam

Table 1-3 NuMI Technical Commissioning Goals

Parameter	Measurement	Operational Goal
Proton intensity in target hall	Toroid (or equivalent) beam intensity monitor at entrance to the Target Hall	2.5×10^{13}/spill 2.5×10^{20}/year
Beam alignment	Transverse distributions of the proton beam and secondary beam	Neutrino Beam centered at Soudan to +/-0.2mr
Near detector neutrino flux	Charged current event rate in 15 ton fiducial region	1.2×10^{-14} events/proton
Far detector neutrino flux*	Charged current event rate	4×10^{-18} events/proton
Muon momentum resolution +	Curvature vs. range in magnetic overlap region	14%
Hadron energy resolution +	Test beam	$\Delta E/E = 70\%/E^{1/2} + 8\%$
Detection efficiency for charged current events +	Event length distribution	90% with <4% neutral current contamination

*Assuming 50% reduction from neutrino oscillations
+Applies to both near and far detectors

Table 1-4 NuMI Operational Technical Goals

1.3 Organization of This Report

This report is organized into five chapters with several appendices. Chapter 1 is the Introduction. Chapter 2 is the overview description of the NuMI beamline including neutrino beam fundamentals, neutrino oscillation experiments, and conceptual design of neutrino beam. Chapter 3 summarizes the design parameters of the NuMI beam as well as the design drivers and basis. Chapter 4 contains a description of the technical component subsystems as well as design specifications. Discussion and descriptions of the technical component subsystems are organized to follow the Work Breakdown Structure (WBS) of the project. Chapter 5 summarizes the radiation safety.

<u>WBS Organization</u>

Chapter 4 is organized according to the Work Breakdown Structure (WBS) that has been adopted for the NuMI Project. All technical components are contained in WBS category 1.1. The third digit of the WBS describes the component type. and serve to number the sections of chapter 4.

2. OVERVIEW OF THE NuMI BEAMLINE

The purpose of this section is to give an integrated conceptual overview and scope of the major elements of the baseline NuMI beamline. This section describes how the physics goals of the MINOS experiment impose certain requirements upon the design of the NuMI neutrino beam. Also described are general properties of neutrino beam systems and how these can be tailored to the physics needs. In particular, a quite flexible design has been adopted for NuMI, which allows a versatile future program.

2.1 Neutrino Beam Fundamentals

Most neutrino beams used in high energy physics are designed to be nearly pure beams of muon type neutrinos; ν_μ. The components to produce such a beam are illustrated in **Figure 2-1.** High energy protons interact in a target to produce a high flux of pions (π) and kaons (K), which then decay after some distance into muons and muon neutrinos (i.e. $\pi^+ \rightarrow \mu^+\nu_\mu$). Quadrupole magnets or, in the case of NuMI, focusing horns or are used to guide a large fraction of the desired π/K flux along the neutrino beam direction. The neutrinos are created by π/K decays along the length of a large diameter decay pipe. The pipe is followed by steel and earth to absorb the undecayed hadrons and the muons. A typical neutrino beamline is hundreds of meters in length from the primary target to the experimental detector, where neutrino interactions can be observed.

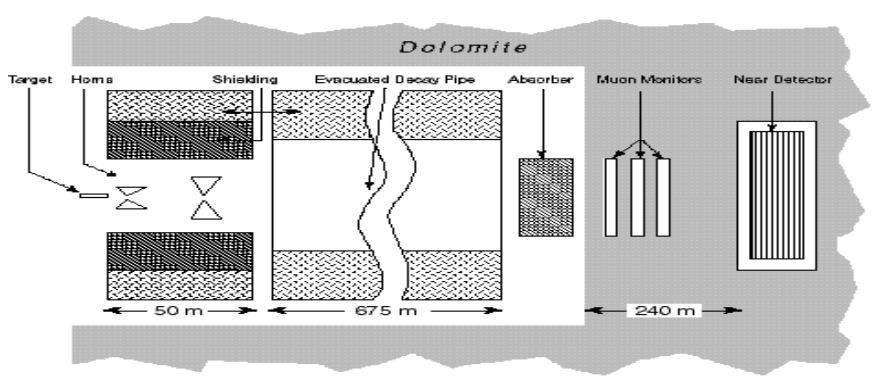

Figure 2-1 Schematic drawing of the NuMI neutrino beam-line

The energy spectrum of a neutrino beam created in this manner is calculated from measured π/K production data and simulation of focusing elements and decay kinematics. In general, secondary particles, such as π's from proton-nucleus interactions, are produced with transverse momenta of order 0.3 GeV/c. The longitudinal momenta cover a wide range, with 1 to 50 GeV/c being relevant for NuMI.

Pion decay kinematics leads to the following approximate relationships for the neutrino energy and a quantity proportional to flux

$$E_\nu = \frac{0.427 E_\pi}{(1+\gamma^2\theta^2)}$$

$$Flux = \left(\frac{2\gamma}{1+\gamma^2\theta^2}\right)^2 \frac{A}{4\pi r^2}$$

where γ is the Lorentz boost of the pion, θ is the angle between the pion and neutrino flight directions, A is the cross-sectional area of the detector, and r is the distance to it. The energy and flux of the neutrinos peak along the pion flight direction, $\theta = 0$.

The typical production angle of a pion is $p_t/p_l \sim 0.3/(m_\pi\gamma) \sim 2/\gamma$; for zero degree targeting this is the same as the angle θ above. Thus there is a factor of order 25 to be gained in the flux by focusing the pions towards the detector, the $\theta = 0$ case. This factor, and the desire to keep the radius of the decay pipe reasonably small, are the motivations for a horn focusing system. Note that for well focused pions and a detector near the axis of the pion beam, the $\theta = 0$ situation, the neutrino's energy is 43% of that of the pion. The Lorentz boost favors neutrinos from high energy pions, thus high energy neutrinos, in the flux by a factor γ^2. A further implication, since one cannot simultaneously focus pions of all energies, is that one must choose a certain neutrino energy range to emphasize.

The optimization of the focusing system is guided by the desired shape of the energy spectrum of the neutrinos which will result from the π and K decays. For the NuMI beam the shape of this spectrum is chosen to maximize the ability to search for neutrino oscillations in a particular region of parameter space, as is described in the following sections.

2.2 Neutrino Oscillation Experiments

Neutrino oscillation searches can be characterized as either "appearance" or "disappearance" experiments. In an appearance experiment, the flavor composition of the initial neutrino source should be well known, and ideally limited to a single flavor. Then if the experiment detects the interactions of neutrinos of a different flavor, it can be concluded that the original neutrinos have indeed oscillated. Alternatively, an experiment which is capable of identifying a single flavor of neutrinos, in particular that of the initial source, can measure the flux of those neutrinos at a distance from the source and determine whether or not the number of neutrinos expected (in the absence of oscillations) has arrived. If the expected number is not observed the conclusion can be drawn that the neutrinos have "disappeared" or oscillated into a different flavor. There are also a number of "pseudo-appearance" measurements that experiments can make which can provide convincing signatures of neutrino oscillations.

Beam design goals include achieving the highest possible ν_μ intensity, low backgrounds of other neutrino flavors, well understood spectra so that systematic errors are small, and the selection of a neutrino energy spectrum matched to the oscillation physics. The rest of this section describes how the energy spectrum goals drive the NuMI design.

Given the fixed distance between Fermilab and Soudan, the energy spectrum of oscillations depends only on the parameter Δm^2, with the strength characterized by the parameter θ (neutrino oscillation θ) . Several examples of oscillation probability as a function of energy, chosen to cover the Δm^2 region indicated by the atmospheric neutrino anomaly, are shown in **Figure 2-2**. At very low energy, oscillations are so rapid that the detector resolution washes out individual wiggles, although one can still look for average signals. With a beam which covers a fairly broad energy spectrum (called a wide band beam), including the highest oscillation energy, one can detect the oscillation shape, as is illustrated in **Figure 2-2** for ν_μ charged current interactions. Further, measuring the energy at which neutrinos disappear and what fraction are lost, as in **Figure 2-3**, yields precision measurements of Δm^2 and $\sin^2(2\theta)$. Producing neutrinos at even higher energies is not very useful, since the oscillation probability falls off as E^{-2}. To address the atmospheric neutrino anomaly and to provide opportunity for future neutrino studies, NuMI requires neutrinos in the energy range of order 1 to 16 GeV.

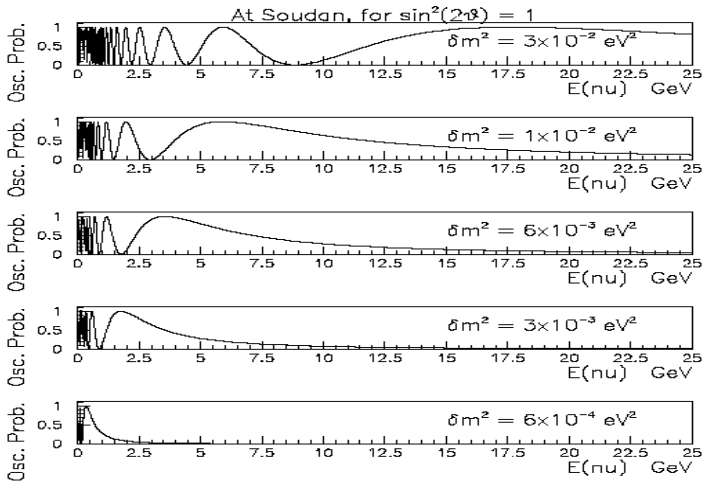

Figure 2-2 Neutrino oscillation probability as a function of energy for values of Δm^2 covering the region appropriate to the atmospheric anomaly.

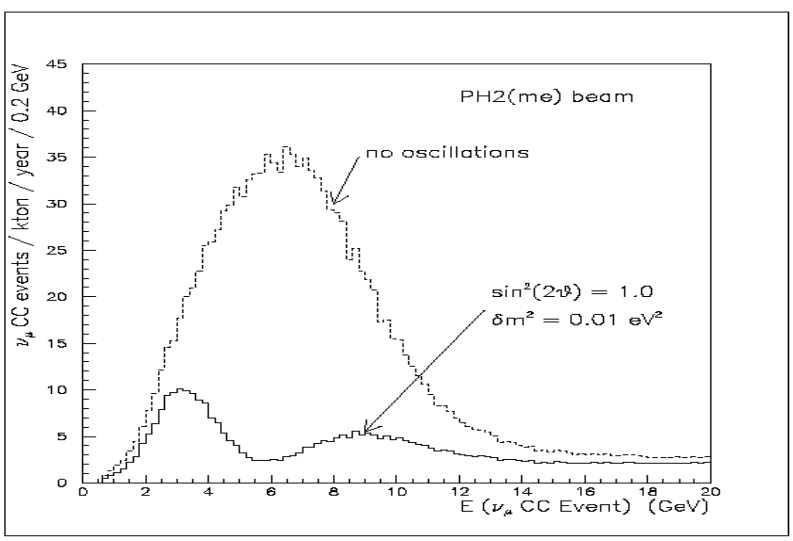

Figure 2-3 CC event total energy in the MINOS far detector distorted by oscillations.

In the case of ν_τ appearance experiments that detect events from the oscillation of $\nu_\mu \rightarrow \nu_\tau$, the energy threshold for production of a τ lepton also comes into play. Because of the energy turn-on of the ν_τ charged current cross section, as shown in **Figure 2-4**, the region from 5 GeV to 15 GeV remains the interesting one, even at low Δm^2.

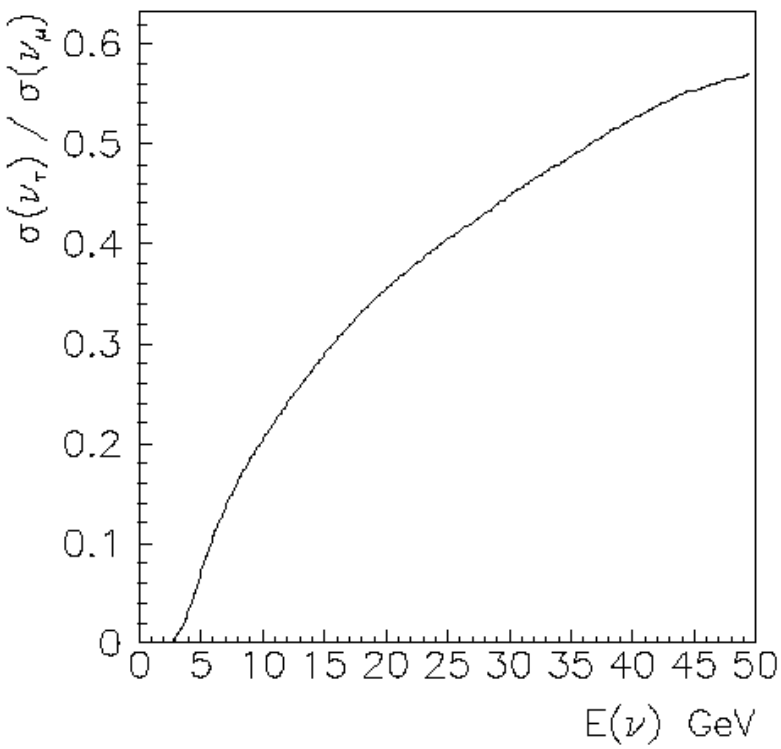

Figure 2-4 The ratio of the of ν_τ charged current interaction cross section to the ν_μ charged current interaction cross section, plotted as a function of neutrino energy.

2.3 Neutrino Beam Conceptual Design

As explained in the previous section, a neutrino beam energy spectrum that covers from 1 to 16 GeV is desired for NuMI. However, magnetic-horn beam devices typically deliver maximum focusing over a momentum bite of only about a factor of three. To address this, we have designed a horn system that can cover the energy region in three steps, using the same horns set in different positions and with different targets. The coverage for three different horn-target configurations is shown in **Figure 2-5**. The resulting event rates for the three configurations are compared in this plot with the idealized case of all pions perfectly focused down the beamline without loss. In each configuration the focusing achieves, at its optimal energy, about half the event rate of the perfect focusing case, which is typical of horn systems.

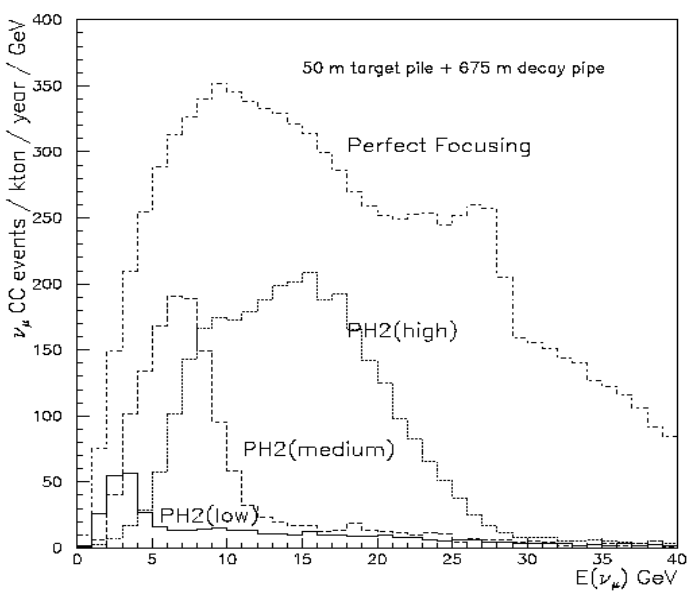

Figure 2-5 Comparison of event rates at Soudan in the case of ideal perfect focusing, and rates achieved with three configurations of the PH2 beam design.

Parabolic shaped horns were found to be better than conical ones in allowing for such reconfiguration. The NuMI beamline uses a two such horns. Thus the beams are labeled PH2(he), PH2(me) and PH2(le) for the two parabolic horn high energy, medium energy, and low energy configurations. The same set of horns could also produce an anti-neutrino beam to study possible CP violation.

2.3.1 Primary Beam System

The primary beam system for the NuMI facility encompasses the extraction and transport of 120 GeV primary protons from the Main Injector to the NuMI target. As the targeting is at zero degrees, the proton beam at the target must be aimed precisely at the MINOS far detector. The NuMI Beam design has been guided by the goals of minimizing beam losses and ensuring long term reliability and stability.

2.3.1.1 Extraction

The 120 GeV primary beam is extracted from the Main Injector ring and transferred through the Main Injector MI-60 extraction enclosure, a region known as the NuMI stub, and a steeply inclined carrier pipe to the pretarget and target regions located deep underground in newly excavated caverns. See **Figure 2-6.**

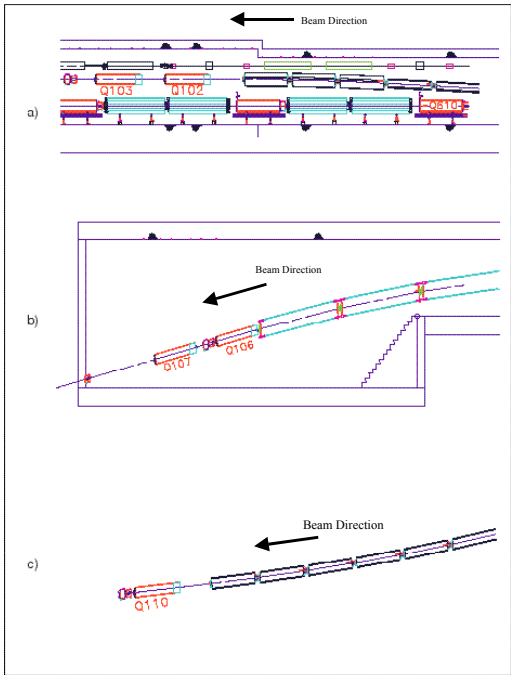

Figure 2-6 Schematic elevation view of the NuMI primary beam in a) Main Injector enclosure, b) NuMI stub, and c) pretarget hall.

The original NuMI proposal assumed a resonant extraction with a 1 msec spill. However, due to radioactivity from beam losses on the septa, this option was discarded in favor of a kicker-induced single turn mode. The 120 GeV protons are taken out of the Main Injector accelerator using a standard single turn extraction technique. The extraction mechanism is a horizontal kick, leading to Lambertson magnets that deflect primarily in the vertical. At the Lambertson magnets, the extracted beam lies outside of the circulating beam. Three Lambertsons and one C-magnet complete the extraction. The machine repetition cycle for this mode of extraction can be as low as 1.9 seconds. To produce the intensities required to achieve the MINOS experimental goals, the NuMI beam requires extraction of at least 2.5×10^{13} protons per pulse.

2.3.1.2 Transport of Primary Protons

The extracted protons are focused and bent strongly downward by a string of quadrupoles and bending magnets so that they enter the pre-target hall located 400 feet downstream of the NuMI Stub, a specially constructed appendage to the MI enclosure. For conventional construction reasons the pre-target and target halls are located in the dolomite rock formation, requiring that the initial trajectory be bent down more than is actually required to aim the neutrino beam to Soudan. Another set of bend magnets brings the protons to the correct pitch of 58 mradians for a zero targeting angle beam directed toward the experiment. The size and angular dispersion of the proton beam are controlled by a final set of quadrupoles and are matched to the diameter of the production target.

2.3.2 Neutrino Beam Devices

The neutrino beam devices transform the primary proton beam from the Main Injector into a beam of neutrinos. This is done in a three-step process. Protons strike a target to produce short lived hadrons, the hadrons are focused towards the neutrino experimental areas, and as the hadrons travel through a long pipe a fraction of them decay to neutrinos and muons. Devices called horns, which produce intense magnetic fields, focus the hadrons. At the end of the pipe the remaining hadrons are absorbed in a beam stop. Neutrinos, which are weakly interacting particles, continue through the hadron absorber and the earth to the experimental areas. To minimize the number of hadrons that are absorbed by air, the long decay pipe is evacuated.

2.3.2.1 Target

The extracted protons interact with nuclei in the target, producing pions and kaons with a broad spectrum in both longitudinal and transverse momentum. The NuMI target and focusing system have been designed as a unit in order to maximize the ν_μ charged current event rate at the MINOS far detector.

The target should be sufficiently long to enable most of the primary protons from the Main Injector to interact, but shaped so that *secondary* interactions of the π's and K's are minimized and energy absorption is low. This is achieved with a target that is long and thin, allowing secondary particles to escape through the sides, as illustrated in **Figure 2-7.** The depth of field of the horn focusing system sets a limit on the length of the target.

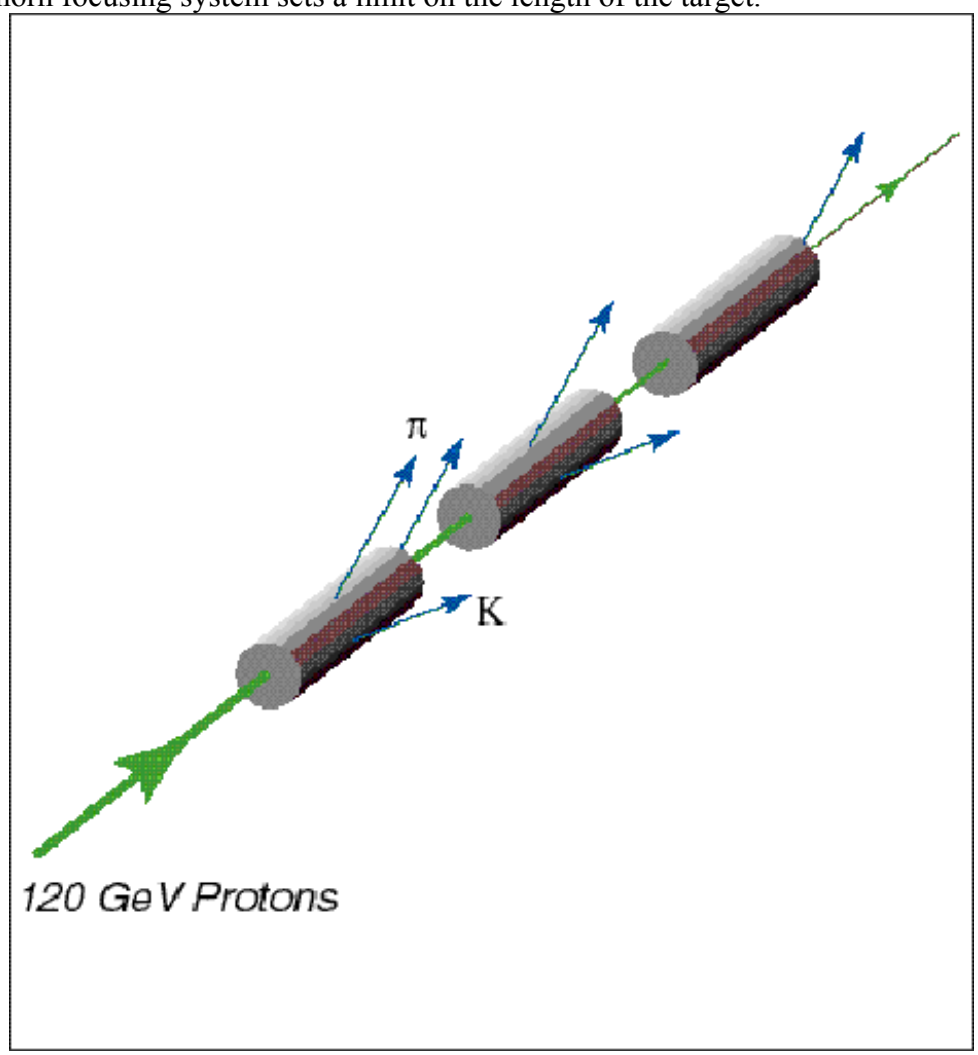

Figure 2-7 Schematic drawing of a long, slim segmented target for optimum production and decay of pions

The optimal choice of target radius is driven by two opposing trends: the *desired* flux of pions and kaons out of the target decreases with increasing radius due to particle re-absorption, but *undesirable* target stress from the heat load of the high intensity proton beam also decreases with increasing target and beam spot radius. Because the target becomes highly radioactive soon after beam start-up, replacement of a failed target is an arduous and time-consuming process. The design of the target is therefore a compromise between obtaining maximum yield and ensuring integrity against mechanical failure due to shock and heat build-up.

2.3.2.2 Horn Focusing System

The target is followed by two focusing horns, which produce toroidal magnetic fields and act as lenses to bend the secondary particles (of one sign) back to the primary proton direction. Of course the neutrinos from the decays of the π's and K's do not all follow the same path, but they are preferentially directed along the decay pipe axis. Thus the optimum design has all secondary particles directed toward the detector so that the resulting neutrino flux is maximized. However, in reality one can focus only some of the pions at all momenta or all of the pions at particular momenta, but not all pions at all momenta for all angles from the target.

NuMI has chosen horns with parabolic shaped inner conductors. These produce magnetic fields that act to first order as lenses, where the focal length is proportional to the pion momentum. Thus a selection of a particular target position causes a certain momentum to be focused by the first horn. Pions that were well focused by the first horn pass unaffected through a central aperture in the second horn. Pions that were somewhat over- or under-focused by the first horn move to larger radius and are focused by the second horn, extending the momentum bite of the system.

The pions actually pass through the current carrying inner wall of a horn to reach the focusing magnetic field. Absorption of pions in the horn walls ranges from 20% to 40% depending on the incidence angle. The design of a horn is a balance between trying to make the inner wall thin (to reduce absorption) and sturdy (since it is subjected to large pulses of electric current – 200 kA in the NuMI design). A water spray is used to keep the aluminum inner conductor below 100 C.

The deployment of the horns and target to achieve the various PH2 beam neutrino event spectra described above are shown in **Figure 2-8**.

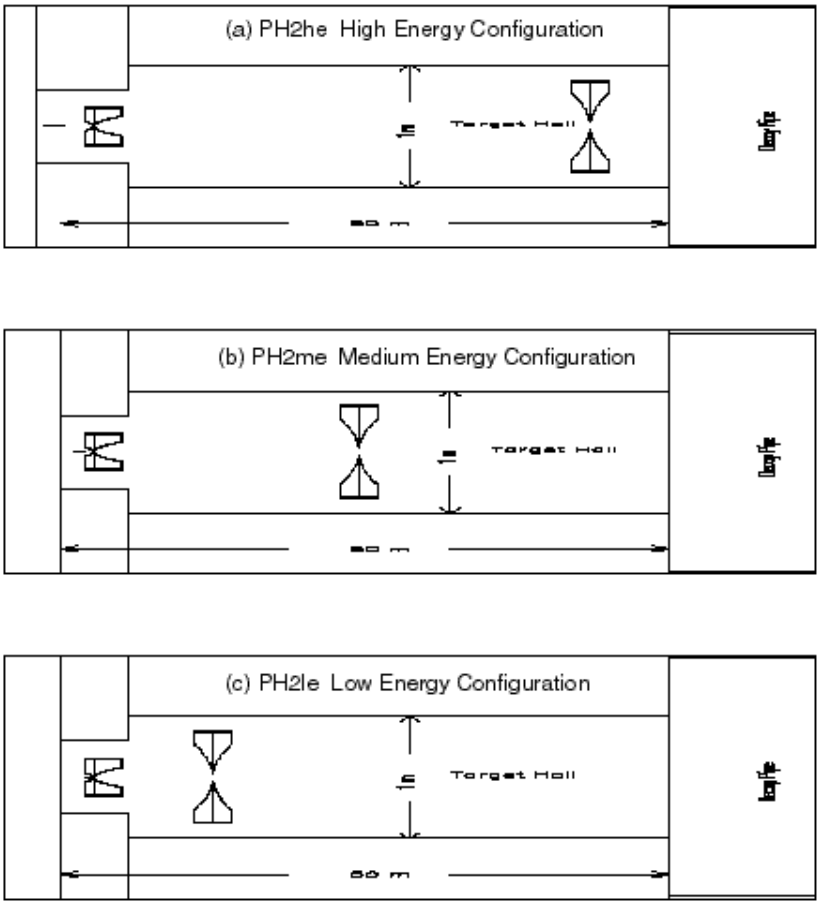

Figure 2-8 Schematic drawing of PH2 beam focusing configurations in the NuMI target hall. To change the tune to lower energy, the target is moved closer (and finally into) the first horn, and the horns are moved closer together

2.3.3 Decay Region and Hadron Absorber

The decay pipe length of 675 meters provides a sufficient flux of muon neutrinos in the wide energy band of the neutrino beam for the MINOS experiment. The decay pipe must aim at the MINOS cavern at Soudan. Misalignment of the decay pipe along its length can not occlude the 1-meter radius aperture by more than 2%. The vacuum level in the decay pipe should be 1 Torr or lower. The Hadron Absorber has to protect groundwater from irradiation under normal running conditions over long periods of time. It has to limit the levels of radiation to acceptable levels in tunnel regions accessible to personnel, for both normal running conditions and abnormal running conditions--such as the proton beam missing the target (in which case the beam is significantly narrowed in size at the hadron absorber). The absorber core and surrounding iron shielding has to maintain its integrity during both normal and abnormal running conditions.

2.3.3.1 Decay Pipe

The decay pipe provides an evacuated space for the secondary π's and K's to decay as they travel towards the MINOS detectors. The choice of length is a compromise between the neutrino flux in the detectors and cost considerations. The neutrino flux is predominantly from the pions with momentum between 2 GeV/c and 60 GeV/c. At the upper end of this range, the mean decay length of a π is several km. The number of high energy neutrinos for the long baseline experiment thus continues to increase significantly with any reasonable decay pipe length. The current baseline design is driven by cost, calling for a decay pipe length of 675 m. Combining the 675 m decay pipe with the 50 m distance from target to start of the decay pipe results in a 725 m long decay region for the NuMI beamline.

The choice of radius for the decay pipe is made by balancing the loss of secondaries that interact with the walls of the pipe against the cost increases associated with larger radius pipes. In general, for the nominal beam pipe length, the gains in neutrino flux are rather dramatic as the radius of the pipe increases to about 1 m, with comparatively modest gains over the next meter of increase.

As shown in **Figure 2-9**, a larger-radius decay pipe would be more optimal for the low energy (PH2le) configuration, while a longer one would be better for the high energy (PH2he) beam. The baseline combination of 1 m radius and 725 m decay length is a reasonable compromise.

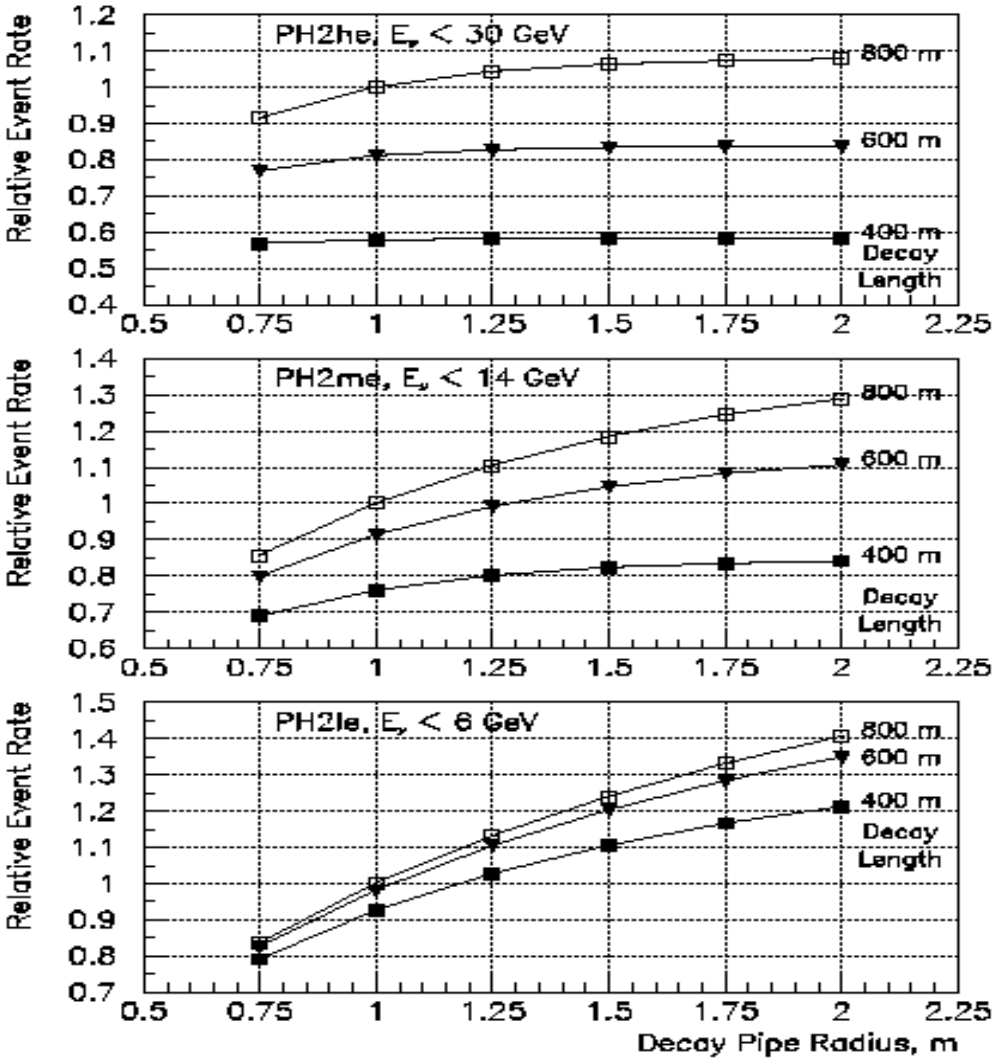

Figure 2-9 Comparison of neutrino event rates as a function of decay pipe length and radius.

2.3.3.2 Hadron Absorber

The experimental detectors are designed to observe the interactions of neutrinos. Other types of particles must be eliminated since their much higher event rates would overload the data acquisition system. All hadrons, including those primary protons that did not interact in the target, are stopped by a hadron absorber at the end of the decay pipe. Because the absorber is far downstream of the target, the natural divergence of the proton beam implies a larger spot size at the absorber, and the absorber does not have to handle nearly so high a deposition energy density as the target does. The absorber consists of a water cooled aluminum central core surrounded by steel.

2.3.3.3 Muon Shield

The hadron absorber alone is too short to eliminate the muon component of the beam, which is produced from pion decays along with neutrinos. These muons must be absorbed before reaching the MINOS near detector. Muons can be eliminated by active shielding using large and expensive magnetic devices or by providing sufficient material to absorb their energy via multiple scattering. The NuMI beamline is located in dolomite, which is a dense rock. The 240 meters of dolomite between the end of the hadron absorber and the near detector is sufficient to stop all muons coming from the decay pipe.

2.3.4 Neutrino Beam Monitoring

The neutrino beam monitoring systems enable the beam users to measure the quality of the neutrino beam being delivered to the experiments. This is accomplished by measuring the flux and spatial distribution of hadrons directly upstream of the absorber and muons at several locations within the dolomite muon shield. Hardware problems with beamline and target components will be deduced from changes in these beams. An alarm signal will be provided when performance is not nominal.

In order to detect variations, the muon intensity measurement will be normalized both to the number of incoming protons and to each other, while the measured profiles are compared to nominal profiles. Since the intensity of the NuMI beam is quite high, the actual neutrino event rate and radial distribution in the on-site neutrino beam monitor (MINOS near detector) can be

combined with the normalized measurements of the muons to insure that the systems producing the neutrino beam are functioning correctly.

3. DESIGN PARAMETERS

This section summarizes the design parameters of the NuMI.

3.1 Extraction and Primary beam

3.1.1 Proton Beam from Main Injector

Proton beam energy	120 GeV
Spill cycle time	1.87 sec
Bunch length	3-8 nsec
Batch length	84 bunches
Bunch spacing	18.8 nsec (53 MHz)
Emittance	40π mm-mr expected 500π mm-mr max
Momentum spread	2 x 10^{-4} δp/p 2σ expected 23 x 10^{-3} δp/p 2σ max
NuMI spill (pbar operation)	5 batches x 84 + 4x3 = 432 bunches = 8.14 μsec
NuMI spill (no pbar operation)	6 batches x 84 + 5x3 = 519 bunches = 9.78 μsec
Maximum intensity	4 x 10^{13} ppp (protons/spill)
Total beam power	404 kW at maximum intensity

3.1.2 Extraction Method and Parameters

Extraction	Single turn
Method	3 traveling wave kicker magnets
Position stability (transport)	± 1 mm max
Beam size @ target	1 mm H x 1 mm V (σ)
Position stability @ target	± 250 μ
Angular stability @ target	± 60 μ-radian max
Max DC beam loss (MI region)	10^{-4} at maximum intensity
Max DC beam loss (Carrier pipe)	10^{-6} at maximum intensity
Max DC beam loss (Pre-target)	10^{-4} at maximum intensity
Max beam loss - accident	5 spills at maximum intensity

3.1.3 Instrumentation

Dynamic range	100 (= $4x10^{13}/4x10^{11}$ protons/spill)
Profile monitors	Multi-wire SEM
Number of wires/plane	48 of 0.003" gold plated tungsten wires
Transport region	3 H + 3 V 1 mm wire spacing, motor-driven
Pre-Target	2 H + 2 V 0.5 mm wire spacing,motor-driven
Position reproducibility	< 50 μ
Intensity range	$2.5x10^{11}$ ppp to $4x10^{13}$ ppp
Channel signal/noise	100x over intensity range
Material in beam	$<10^{-4}$ loss
Beam position monitors	Cylindrical plate BPM
Transport region	6 H + 6 V
Position resolution	0.2 mm rms within ± 20 mm for $3x10^{10}$ to $9.5x10^{10}$ protons/bunch
Intensity resolution	± 3%
Sampling	One sample per batch
Calibration	Electronics charge injection inter-spill
Pre-target	2 H + 2 V
Position resolution	0.05 mm rms within ± 6 mm for $3x10^{10}$ to $9.5x10^{10}$ protons/bunch
Intensity resolution	± 3%
Sampling	One sample per batch
Calibration	Electronics charge injection inter-spill
Toroid intensity monitor	
Intensity resolution	3% absolute for > $1x10^{13}$ppp 30% for > $3x10^{11}$ppp
Stability	< 3% at > $1x10^{13}$ppp
Beam loss monitors	35 Sealed gas ionization chambers
Accuracy	± 30% at $2x10^{8}$ppp
Dynamic range	$2x10^{8}$ to $4x10^{13}$ppp
Monitoring	High voltage status
Function	Sensitive to small localized losses
Total Loss Monitors	4 coax hose ionization, Ar-CO2 purged
Carrier pipe region	1 of 430' long, 2 of 215' long
Pre-target region	1 spanning the entire region
Accuracy	± 30% at $2x10^{8}$ppp
Dynamic range	$2x10^{8}$ to $4x10^{13}$ppp
Monitoring	Radioactive source current inter-spill
Function	Sensitive to large losses

3.2Neutrino Beam Devices

Low Energy Beam Peak at 3 GeV

Baffle/Target Module

Module motion control	
Baffle	
composition	Graphite
aperture	5.4 mm H x 12 mm V
length	2 m
motion control	~10 cm H (manual drive)
cooling	Air or RAW under consideration
Target	
composition	Graphite segments (Poco ZXF-5Q)
length	47 of 20 mm long segments, 0.3mm spacing
density	1.686 ± 0.025 gm/cm^3
width	6.4 mm
height	18 mm
cooling	RAW cooling tubes top/bottom of fin
distance from horn 1	35 cm to Monte Carlo upstream end
motion control	~1 m Z insertion into Horn 1 (manual drive)

Neutrino Horn 1 Module

Horn shape	Double Parabolic
Construction	Nickel plated aluminum inner conductor Anodized aluminum outer conductor
Minimum aperture field-free neck	9 mm radius
Inner conductor thickness	2 mm (min) – 4.5 mm (max at neck)
Outer conductor	11.75 inch I.D. 13.75 inch O.D.
Horn Length	300 cm focus region, 132 inches overall
Current	200 kA
Motion control	±1 cm H x ±1 cm V each end (motor drive)
Horn cooling	RAW spray, 30 gal/min

Neutrino Horn 2 Module

Horn shape	Double Parabolic

Construction	Nickel plated aluminum inner conductor Anodized aluminum outer conductor
Minimum aperture field-free neck	3.9 cm radius
Inner conductor thickness	3 mm (min) - 5 mm (max)
Outer conductor	29.134 inch I.D. 31.134 inch O.D.
Horn Length	300 cm focus region, 143 inches overall
Current	200 kA
Motion control	None
Distance from Horn 1	10 m (upstream end H1 to upstream end H2)
Horn cooling	RAW spray, 30 gal/min

3.3 Power Supply Systems

Kicker Power Supply : Single pulse forming network, drives 2 magnets in parallel

Conventional Power Supplies Regulation requirements

Lam60	200 ppm
V100	400 ppm
HV101	65 ppm
V104	200 ppm
V105	60 ppm
V109	200 ppm
V110	55 ppm
Trims	0.1%
Quadrupoles	400 ppm

Horn Power Supply, current, voltage, Flat top regulation, Pulse width

The design criteria for the horn power supply and stripline are the current, current regulation, and pulse width. Horn 1 and horn 2 are connected in series with the power supply. The voltage is given at the output of the power supply. It is determined by the resistance and inductance of the strip line and horns. When we switched to single turn extraction, the power supply design was modified to give a pulse width of 2.6 msec. The section of stripline to the high energy horn 2 position was later eliminated, shortening the pulse length to 1.7 msec. The "flat-top" regulation is the allowed pulse to pulse variation.

Horn Power Supply : Series connection to Horn 1 and Horn 2

Peak current	240k A
Operating current	200k A average ± 2.5%

Current monitoring	0.4%
Operating voltage	800 V
Repeatability	± 1% pulse to pulse
Pulse width	~half-sine 1.7 ms @ base
Pulse period	1.9 sec

Horn Stripline

Construction	30 cm x 10 cm Aluminum strips, 1 cm spacing
Resistance	10 μΩ/m
Inductance	16 nH/m

3.4 Hadron Decay Pipe

Size	1.98 m inner dia x 677.1 m long
Vacuum	<1 Torr
Upstream vacuum window	4.76 mm thick steel
Downstream vacuum window	6.35 mm thick steel

3.5Hadron Absorber

Primary beam size at Absorber (target out)	5.4 cm H x 7.9 cm V (1 σ)
Primary beam size at Absorber (target in)	29 cm (rms)
Beam power - normal	64 kW (82% primary protons, 18% secondaries)
Beam power - accident	404 kW
Accident condition	1 hour (1900 pulses) mis-targeted primary proton
Absorber core	8 aluminum modules + 10 steel CCSS layers
Aluminum modules	1.29 m H x 1.29 m V x 30 cm Z RAW cooled
Steel CCSS layers	1.29 m H x 1.29 m V x 23 cm Z
Max temperature - normal	60 ^{o}C in aluminum modules 3 and 4 270 ^{o}C in steel module 1
Max temperature - accident	160 ^{o}C in aluminum modules 3 and 4 800 ^{o}C in steel module 1

3.6Neutrino Beam Monitoring

The NuMI beam monitoring system consists of 1 plane of Hadron Monitors (DHM) downstream of the decay pipe and upstream of the Hadron Absorber, 3 planes of Muon monitors located in the Hadron Absorber enclosure (Muon Alcove 0) , Muon Alcove 1 and Muon Alcove 2. The peak charged particle fluxes per spill in the various monitoring locations, assuming $4x10^{13}$ protons per spill**.**

Station	Maximum Flux/spill
DHM	$2.5x10^{9}/cm^{2}$
Alcove 0	$3.2\ x10^{7}/cm^{2}$
Alcove 1	$1.7x10^{7}/cm^{2}$
Alcove 2	$0.22x10^{7}/cm^{2}$

The following table gives the fluxes per spill, and the associated radiation doses per year, expected in the monitoring locations, as a function of particle type. Doses calculated by translating fluxes to Sieverts and then to rads, taking into account spectral information

Station	Particle	Flux (/cm^2/spill)	Dose/year(Rads)
DHM	protons	1.3×10^9	13Grad
DHM	other charged hadrons	2.0×10^9	0.3Grad
DHM	neutrons	3.5×10^9	0.2Grad
Alcove 0	neutrons	10.0×10^7	10Mrad
Alcove 0	muons	1.30×10^7	5Mrad
Alcove 1	muons	0.40×10^7	1.8Mrad
Alcove 1	neutrons	0.04×10^7	0.1Mrad
Alcove 2	muons	0.14×10^7	0.6Mrad
Alcove 2	neutrons	0.04×10^7	0.04Mrad

3.7Alignment Systems

Alignment tolerances for Low Energy beam

Beam position at target	± 0.45 mm
Beam angle at target	± 0.7 mrad
Target position - each end	± 0.5 mm
Horn 1 position - each end	± 0.5 mm
Horn 2 position - each end	± 0.5 mm
Decay pipe position	± 20 mm
Downstream Hadron monitor	± 25 mm
Muon Monitors	± 25 mm
Near Detector	± 25 mm
Far Detector	± 12 mm

3.8Water, Vacuum & Gas Systems

CUB = Central Utility Building
CW = Chilled Water
LCW = Low Conductivity Water
PW = Pond Water
RAW = Radioactive Water
SB = Service Building

Power dissipation

Beam transport magnets	628 kW
MI-62 LCW system	700/1200 (kW nominal/max) to MI Pond G
MINOS LCW system	108/200 (kW nominal/max) to MINOS SB CW
Absorber RAW	60/200 (kW nominal/max) to MINOS SB PW
Decay pipe RAW	150/200 (kW nominal/max) to CUB CW (1/2) and MINOS SB CW (1/2)
Target RAW	10/25 (kW nominal/max) to MI62 LCW
Horn 1 RAW	40/200 (kW nominal/max) to CUB CW
Horn 2 RAW	10/50 (kW nominal/max) to CUB CW

Vacuum

Main Injector extraction region	10^{-8} Torr
Primary beam transport vacuum	10^{-6} Torr
Carrier pipe	
Diameter	12”
Vacuum maximum	10^{-5} Torr
Vacuum expected	7×10^{-7} Torr maximum
Hadron Decay Pipe vacuum	0.1 to 1 Torr

Carrier Pipe size, vacuum

The 430' long carrier pipe diameter was determined by an informal cost/benefit analysis. The pipe size is much larger than all magnet apertures, however the consequence of a significant beam loss in the carrier pipe region is severe. The maximum vacuum level is determined by the ground water requirement during normal operation due to interactions with the residual gas. The

expected vacuum level is achieved in the middle of the carrier pipe by 3 large ion pumps located at each end of the carrier pipe.

3.9 Installation & Integration

Controls	Power supplies, instrumentation, vacuum, water, beam position & intensity, beam permit, beam loss budget monitor
Beam permit System	Power suppy current & voltage nominal Multi-wire fully inserted/extracted Loss monitors nominal Vacuum valves open Previous Main Injector spill transport nominal BPM positions nominal Target Budal monitor nominal

3.10 Commissioning

Beam intensity	5×10^{12} ppp
Near detector fiducial mass	0.015 kt (40 planes tgt region, 75 cm radius)
Near Detector exposure	2×10^{-6} kt-yr/day

4.1.A Appendix: Beamline Sensitivity Effects

The sensitivity of the beamline to various off-nominal conditions has been investigated. Specifically addressed are the sensitivities of focus and of trajectory.

<u>Focusing sensitivity</u> The sensitivity of the optics to different error sources has been studied in simulations. Assigning random gradient errors of $\sigma(\Delta B'/B') = 25\text{x}10^{-4}$ to the 21 quadrupoles in the line, **Figure 4.1.A-1** shows the beam sizes resulting from 20 random generator seeds. The changes in beam σ's are demonstrated to be less than ≈0.1 mm. At the target the maximum changes in beam size are on the order of 0.05 mm, within the specification.

Optical errors also arise from discrepancies between the assumed and actual MI lattice functions. **Figure 4.1.A-2**shows the β-envelopes (proportional to squares of beam sizes) that result from ±10% variations in the nominal β_X and β_Y values. The maximum β's are sufficiently well-behaved that no aperture problems arise, and the small residual mismatch at the target can be corrected with 4 or 6 final-focus quadrupoles.

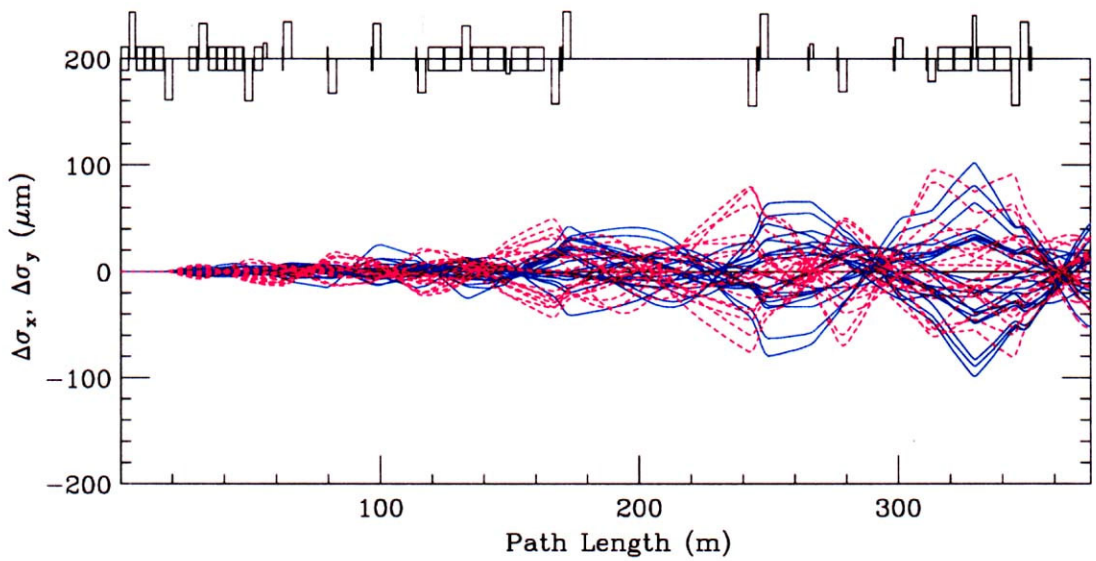

Figure 4.1.A-1. Beam size variation resulting from random gradient errors

Trajectory sensitivity and correction Most focusing elements in the line have associated position monitors. Orbit correction is an issue which, of course, must be addressed by any beamline, but for the ultra-clean transport requirements of NuMI it is critical that precise position control be available throughout.

Correction of central trajectory errors has been simulated with dipole field errors and random misalignments assigned to the beamline elements (including position monitors). Suitable error values are 0.25 mm for positions and 10^{-3} for magnetic field fractions. Figure A3 shows the deviations from the central trajectory arising from 20 random error seeds. The uncorrected

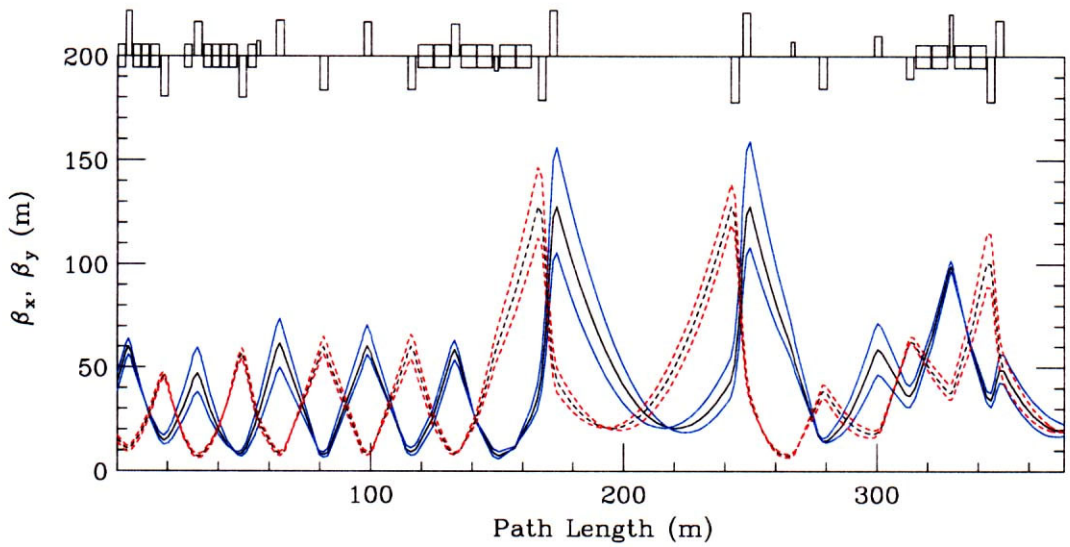

Figure 4.1.A-2. β-waves due to ±10% injection optic errors

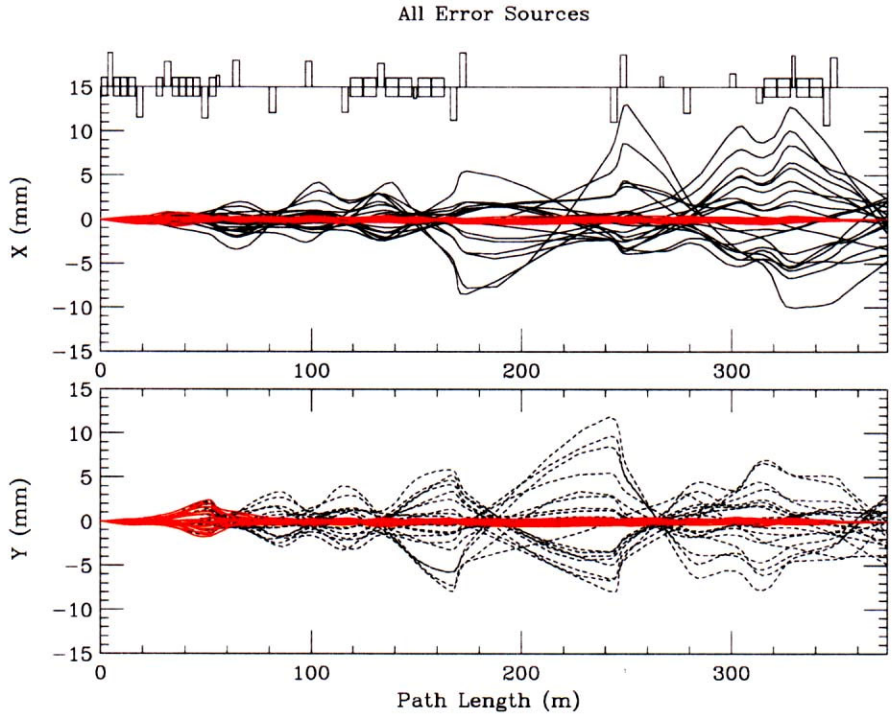

Figure 4.1.A-3. Uncorrected and corrected trajectories with random misalignments and dipole field errors

offsets in the line are Δx(rms) = 2.63 mm, Δx(max) = 13.03 mm, and Δy(rms) = 2.33 mm, Δy(max) = 11.90 mm. There is some concern, however, that the NuMI positioning errors will be greater than .25 mm, at least originally, in which case the trajectory errors will scale accordingly.

The orbits from the above analysis as corrected by the trim magnets are shown in red in the figure. They are, again, within specification, though for the vertical they require more trim strength than is available in MI vertical correctors. It is for this reason that rolled horizontal correctors are specified for the vertical plane.

The sensitivity of the line to possible dipole mispowering is a subject of considerable interest and is now presented in greater detail. **Figure 4.1.A-4a** shows the situation for the horizontal plane and **Figure 4.1.A-4b** for the vertical. What is plotted is, for each bend supply, the effect on downstream beam positions of a .1% power supply drift of the peak current. Comparing with the specification of <0.5 mm for target position (the target is located at station 356 meters), it is seen

that at least the major up and down bends will need regulation considerably greater than that used in making the figure. Taking into account the specification for stability along the beamline, the EPB string also requires more regulation. The power supply stability specifications resulting from this analysis are presented in the Section 4.3 of this Handbook. They are accomplished via techniques in use elsewhere in the laboratory.

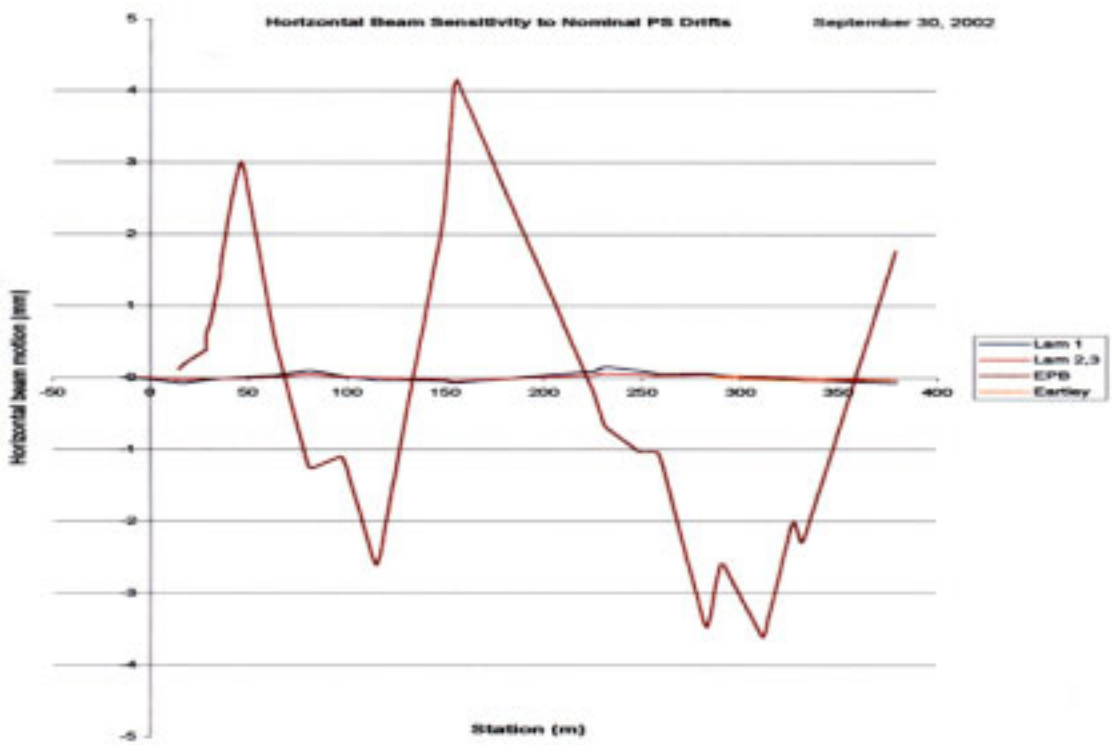

Figure 4.1.A-4a. Sensitivity in the horizontal plane to dipole power supply variations

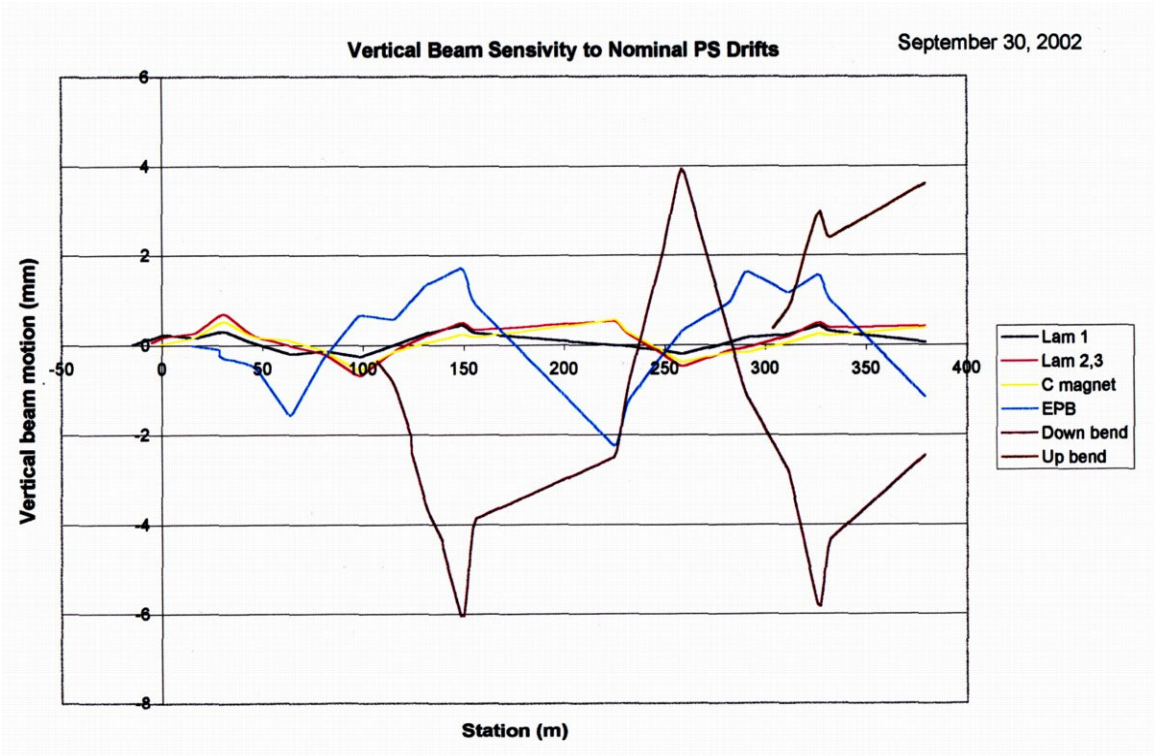

Figure 4.1.A-4b. Sensitivity in the vertical plane to dipole power supply variations

4.1.B Appendix : Aperture Considerations

Figure 4.1.B-1 shows the amplitude (root β) and dispersion (η) functions over the entire line. The beam size peaks at stations 150 m and 225 m are at the upstream and downstream ends of the unoccupied carrier region. Putting relatively large sizes at these quadrupoles allows the sizes upstream and downstream of them to be appropriately small. To prevent the running of any quadrupole at a current value that would endanger it, a limit of 16.0 T/m has been placed on the gradients.

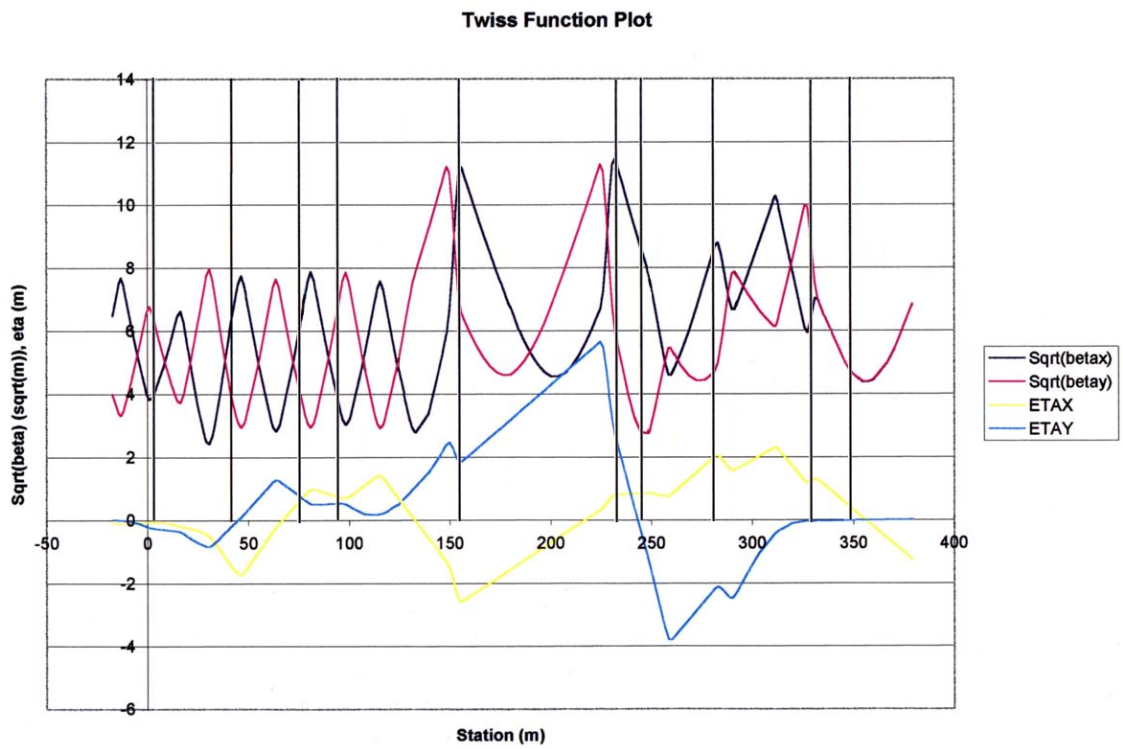

Figure 4.1.B-1. Amplitude and dispersion plots over the entire beamline. The target station value is 356 meters. The vertical lines indicate the locations of the 10 multiwire profile monitors.

Figure 4.1.B-2a shows the clearances vs. beam size over the entire line and **Figure 4.1.B-2b** shows an expanded view of the same in the Lambertson region. Considerable effort has gone into having a design for which this plot demonstrates adequate clearance over the length of the entire beamline, and several of the plot's features are worthy of detailed discussion. The aperture, or preferably clearance, shown for each element is the actual half-aperture of the device minus any sagitta in that device.

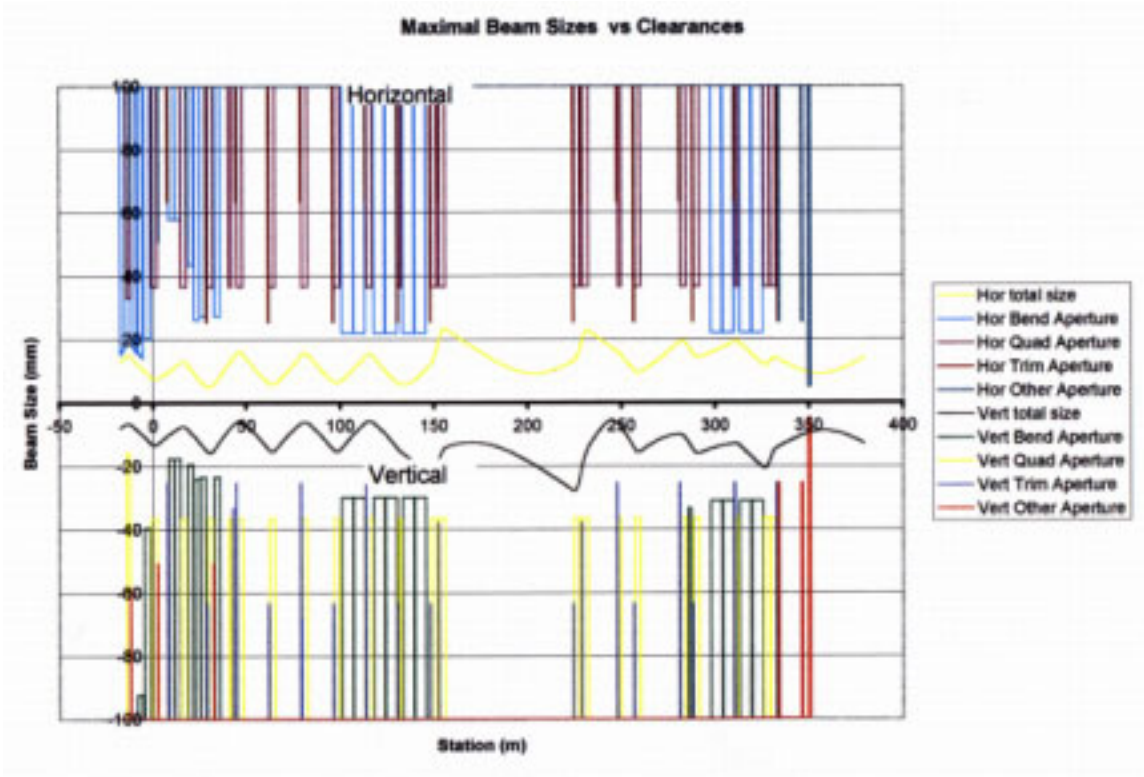

Figure 4.1.B-2a. Beam and aperture clearance plot over the entire beamline

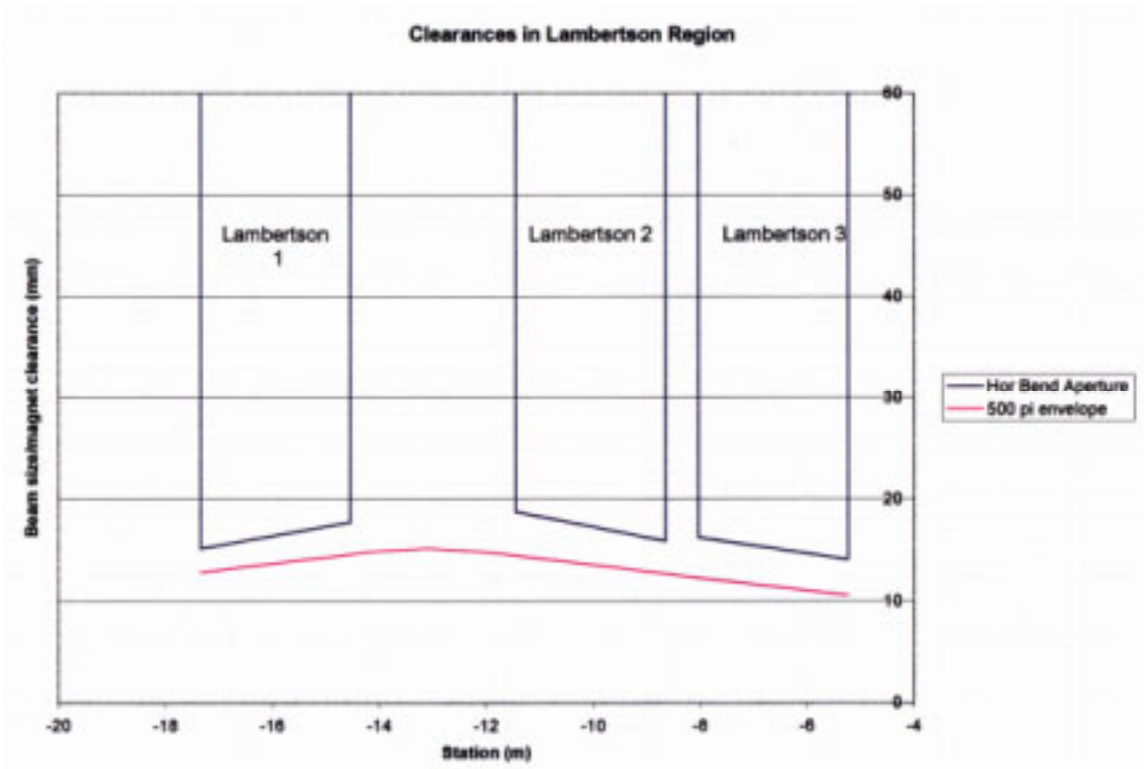

Figure 4.1.B-2b. Beam and aperture clearance plot in extraction region

However what is shown as clearance for the Lambertsons, and for MI quadrupole 608 which lies between Lambertsons 1 and 2, is worthy of special comment. The alignment of each of these magnets is determined by the path of the circulating MI beam, not the extracted beam. Thus the effective clearance is the distance from the beam center to the nearest aperture restriction, which for all Lambertsons is the septum. Note that the tighter clearance is in the horizontal plane and that the first two Lambertsons are rolled so that the horizontal distance to the septum is dependent on the height of the beam. Secondly, since the magnets are aligned along the circulating beam direction, the extracted beam is not traveling parallel to the septum face. Additionally, the beam size can change over the length of one element, again affecting the effective clearance. All of these effects have been accounted for in making the plots, which have what appears as angled magnet apertures but which really are angled beam trajectories. Similarly for the case of Q608, what are plotted as clearances are horizontal and vertical distances to the edge of a star shaped vacuum chamber.

As to the beam size plotted, what is shown corresponds to the MI *admittance*, i.e. the largest beam size that the accelerator could possibly spew forth. The figure indicates that the beamline can indeed transmit this worst possible beam. Note also that the desired criteria at the target are met – the beam size has a minimum in both planes at that location.

At station 350 m is an aperture through which the beam apparently does not fit. This aperture is that of the horn protection baffle. The worst case beam, as is plotted here, will indeed not fit through this baffle. However the more nominal beam size, as is expected in general, does fit.

Program ces (A Construction Engineering Survey format) (11/26/91) Tue Aug 24 10:37:16 2004
Site coordinates for beamline: input_ces_v2
NOTES: Coordinates are given for the entrance of the device in DUSAF coordinate system.
Site axis (EAST); site axis (NORTH); Site z-axis (ELEVATION)
Positive bearing is ccw wrt site EAST.
Pitch is the vertical angle about the x-y plane.

line	location	typ_code	distance [ft]	x [ft]	y [ft]	z [ft]	brng [deg]	pitch [deg]	yaw [deg]
0000	S1_BML	marker	-56.88634	101383.29284	97215.37729	715.72409	148.73096	0.10571	-81.69232
0001	LAM60	MI_LAM	-56.88634	101383.29284	97215.37729	715.72409	148.73096	0.10571	-81.69232
0002	LAMEND	DRIFT	-47.70000	101375.48039	97220.21061	715.74102	148.69343	0.21142	0.00000
0003	QSPOOL	drift	-46.94423	101374.83462	97220.60333	715.74381	148.69343	0.21142	0.00000
0004	QENDU	drift	-46.52756	101374.47865	97220.81983	715.74535	148.69343	0.21142	0.00000
0005	HQ608	3Q84/2	-46.40256	101374.37186	97220.88479	715.74581	148.72552	0.22202	0.00000
0006	HQ608	3Q84/2	-42.90257	101371.38043	97222.70175	715.75930	148.78998	0.24866	0.00000
0007	QENDD	drift	-39.40258	101368.38699	97224.51539	715.77442	148.82235	0.26471	0.00000
0008	BPM	MI_BPM	-39.21006	101368.22230	97224.61506	715.77531	148.82235	0.26471	0.00000
0009	D3IN	drift	-38.54339	101367.65192	97224.96018	715.77839	148.82235	0.26471	0.00000
0010	LAMEND	DRIFT	-38.29339	101367.43801	97225.08960	715.77954	148.82235	0.26471	0.00000
0011	LAM61A	MI_LAM	-37.53762	101366.79139	97225.48088	715.78302	148.81805	0.47957	-88.85429
0012	LAMEND	DRIFT	-28.35129	101358.93226	97230.23717	715.85992	148.81376	0.69442	0.00000
0013	LSPOOL	drift	-27.59552	101358.28567	97230.62854	715.86907	148.81376	0.69442	0.00000
0014	LAMEND	DRIFT	-27.09552	101357.85795	97230.88743	715.87514	148.81376	0.69442	0.00000
0015	LAM61B	MI_LAM	-26.33974	101357.21139	97231.27883	715.88430	148.81376	0.90957	-90.00021
0016	LAMEND	DRIFT	-17.15341	101349.35258	97236.03571	716.03016	148.81376	1.12472	0.00000
0017	VALVE	VALVE	-16.39760	101348.70603	97236.42705	716.04502	148.81376	1.12472	0.00000
0018	LCSPOO	drift	-15.89761	101348.27837	97236.68591	716.05483	148.81376	1.12472	0.00000
0019	CMGEND	DRIFT	-15.42198	101347.87152	97236.93217	716.06418	148.81376	1.12472	0.00000
0020	V100	MI_CMG	-14.75532	101347.30131	97237.27731	716.07724	148.81376	1.36536	-90.00021
0021	CMGEND	DRIFT	-3.75531	101337.89365	97242.97175	716.33935	148.81376	1.60600	0.00000
0022	NOVALV	drift	-3.08864	101337.32354	97243.31683	716.35805	148.81376	1.60600	0.00000
0023	Q12_UP	DRIFT	-2.58864	101336.89598	97243.57562	716.37206	148.81376	1.60600	0.00000
0024	HQD101	3Q120/2	-2.01571	101336.40602	97243.87218	716.38810	148.81376	1.60600	0.00000
0025	HQD101	3Q120/2	2.98428	101332.13027	97246.46030	716.52826	148.81376	1.60600	0.00000
0026	Q101DN	drift	7.98427	101327.85453	97249.04838	716.66838	148.81376	1.60600	0.00000
0027	IP101A	ionpump	8.89050	101327.07956	97249.51748	716.69378	148.81376	1.60600	0.00000
0028	P101SE	drift	9.39050	101326.65197	97249.77627	716.70779	148.81376	1.60600	0.00000
0029	IP101B	ionpump	15.64810	101321.30080	97253.01534	716.88318	148.81376	1.60600	0.00000
0030	V101UP	drift	16.14810	101320.87321	97253.27413	716.89719	148.81376	1.60600	0.00000
0031	VP101	BPM	16.78766	101320.32630	97253.60520	716.91510	148.81376	1.60600	0.00000
0032	BPM_DN	DRIFT	17.32100	101319.87019	97253.88125	716.93006	148.81376	1.60600	0.00000
0033	BPM_UP	DRIFT	17.42933	101319.77758	97253.93735	716.93308	148.81376	1.60600	0.00000
0034	HP101	BPM	17.70433	101319.54241	97254.07967	716.94079	148.81376	1.60600	0.00000
0035	H101DN	drift	18.23766	101319.08630	97254.35575	716.95575	148.81376	1.60600	0.00000
0036	PM101	MUWIRE	19.22982	101318.23788	97254.86930	716.98357	148.81376	1.60600	0.00000
0037	DUP4	drift	20.04648	101317.53949	97255.29204	717.00644	148.81376	1.60600	0.00000
0038	IP101C	ionpump	22.53299	101315.41318	97256.57908	717.07612	148.81376	1.60600	0.00000
0039	RWMUPS	drift	23.03299	101314.98559	97256.83790	717.09013	148.81376	1.60600	0.00000
0040	RWCM01	REWAMON	23.50172	101314.58474	97257.08052	717.10329	148.81376	1.60600	0.00000
0041	RWMDNS	drift	24.09549	101314.07700	97257.38787	717.11992	148.81376	1.60600	0.00000

0042	TOR1UP	DRIFT	24.35933	101313.85137	97257.52445	717.12731	148.81376	1.60600	0.00000
0043	TOR101	TOROID	24.57042	101313.67083	97257.63370	717.13324	148.81376	1.60600	0.00000
0044	TOR1DN	DRIFT	25.28919	101313.05620	97258.00575	717.15339	148.81376	1.60600	0.00000
0045	MIC2UP	DRIFT	25.35169	101313.00275	97258.03810	717.15513	148.81376	1.60600	0.00000
0046	HT102	MIHC	25.69234	101312.71145	97258.21444	717.16467	148.81376	1.60600	0.00000
0047	MICR_D	DRIFT	26.69234	101311.85630	97258.73206	717.19269	148.81376	1.60600	0.00000
0048	EPB_UP	DRIFT	26.99443	101311.59797	97258.88842	717.20116	148.81376	1.60600	0.00000
0049	HV01_1	EPB	27.54650	101311.12586	97259.17418	717.21664	149.14206	1.60600	0.00000
0050	EPB_DN	DRIFT	37.54655	101302.54484	97264.30127	717.49689	149.47036	1.60600	0.00000
0051	EPB_UP	DRIFT	37.99445	101302.15914	97264.52870	717.50946	149.47036	1.60600	0.00000
0052	HV01_2	EPB	38.54654	101301.68378	97264.80905	717.52494	149.79896	1.58222	-4.10925
0053	EPB_DN	DRIFT	48.54656	101293.04446	97269.83748	717.80103	150.12755	1.55845	0.00000
0054	Q12_UP	DRIFT	48.99449	101292.65621	97270.06048	717.81323	150.12755	1.55845	0.00000
0055	HQF102	3Q120/2	49.56742	101292.15959	97270.34575	717.82881	150.12755	1.55845	0.00000
0056	HQF102	3Q120/2	54.56741	101287.82551	97272.83518	717.96477	150.12755	1.55845	0.00000
0057	Q12_DN	DRIFT	59.56740	101283.49146	97275.32461	718.10076	150.12755	1.55845	0.00000
0058	BPM_UP	DRIFT	59.99447	101283.12125	97275.53727	718.11238	150.12755	1.55845	0.00000
0059	HP102	BPM	60.26947	101282.88287	97275.67418	718.11986	150.12755	1.55845	0.00000
0060	BPM_DN	DRIFT	60.80280	101282.42056	97275.93973	718.13436	150.12755	1.55845	0.00000
0061	PUMP	PUMP	60.91113	101282.32667	97275.99367	718.13731	150.12755	1.55845	0.00000
0062	EPB_UP	DRIFT	61.24446	101282.03772	97276.15961	718.14637	150.12755	1.55845	0.00000
0063	HV01_3	EPB	61.79656	101281.55918	97276.43448	718.16139	150.42978	1.42781	-23.33714
0064	EPB_DN	DRIFT	71.79658	101272.86438	97281.36787	718.41054	150.73202	1.29718	0.00000
0065	EPB_UP	DRIFT	72.24451	101272.47377	97281.58680	718.42068	150.73202	1.29718	0.00000
0066	HV01_4	EPB	72.79657	101271.99227	97281.85662	718.43318	150.97180	1.07143	-43.22909
0067	EPB_DN	DRIFT	82.79662	101263.25003	97286.70818	718.62018	151.21158	0.84569	0.00000
0068	EPB_UP	DRIFT	83.24452	101262.85751	97286.92386	718.62678	151.21158	0.84569	0.00000
0069	HV01_5	EPB	83.79662	101262.37372	97287.18971	718.63491	151.46053	0.63054	-40.76022
0070	EPB_DN	DRIFT	93.79666	101253.58939	97291.96706	718.74495	151.70948	0.41539	0.00000
0071	MICR_U	DRIFT	94.24456	101253.19497	97292.17933	718.74820	151.70948	0.41539	0.00000
0072	VT103	MIHC-R	94.73416	101252.76390	97292.41135	718.75174	151.70948	0.41539	0.00000
0073	MICR_D	DRIFT	95.73416	101251.88336	97292.88530	718.75900	151.70948	0.41539	0.00000
0074	Q12_UP	DRIFT	96.03623	101251.61735	97293.02845	718.76119	151.70948	0.41539	0.00000
0075	HQD103	3Q120/2	96.60916	101251.11288	97293.29997	718.76533	151.70948	0.41539	0.00000
0076	HQD103	3Q120/2	101.60915	101246.71024	97295.66961	718.80158	151.70948	0.41539	0.00000
0077	Q12_DN	DRIFT	106.60914	101242.30755	97298.03923	718.83780	151.70948	0.41539	0.00000
0078	BPM_UP	DRIFT	107.03620	101241.93151	97298.24162	718.84089	151.70948	0.41539	0.00000
0079	VP103	BPM	107.31120	101241.68935	97298.37197	718.84289	151.70948	0.41539	0.00000
0080	BPM_DN	DRIFT	107.84453	101241.21973	97298.62473	718.84676	151.70948	0.41539	0.00000
0081	PUMP	PUMP	107.95287	101241.12435	97298.67607	718.84755	151.70948	0.41539	0.00000
0082	EPB_UP	DRIFT	108.28620	101240.83082	97298.83404	718.84994	151.70948	0.41539	0.00000
0083	HV01_6	EPB	108.83830	101240.34470	97299.09569	718.85394	151.95815	0.19939	-40.90059
0084	EPB_DN	DRIFT	118.83831	101231.51873	97303.79680	718.88875	152.20681	-0.01662	0.00000
0085	DRC0	drift	119.28624	101231.12247	97304.00565	718.88862	152.20681	-0.01662	0.00000
0086	DRMTDX	drift	121.70743	101228.98061	97305.13462	718.88793	152.20681	-0.01662	0.00000
0087	BPM_UP	DRIFT	132.30456	101219.60599	97310.07585	718.88488	152.20681	-0.01662	0.00000
0088	HP104	BPM	132.57956	101219.36272	97310.20407	718.88478	152.20681	-0.01662	0.00000
0089	BPM_DN	DRIFT	133.11289	101218.89090	97310.45275	718.88462	152.20681	-0.01662	0.00000
0090	Q12_UP	DRIFT	133.22122	101218.79507	97310.50328	718.88462	152.20681	-0.01662	0.00000
0091	HQF104	3Q60/2	133.79415	101218.28825	97310.77040	718.88445	152.20681	-0.01662	0.00000
0092	HQF104	3Q60/2	136.29415	101216.07667	97311.93612	718.88373	152.20681	-0.01662	0.00000
0093	Q12_DN	DRIFT	138.79414	101213.86509	97313.10180	718.88301	152.20681	-0.01662	0.00000

0094	DR104D	drift	139.22121	101213.48727	97313.30094	718.88288	152.20681	-0.01662	0.00000
0095	SYTR_U	DRIFT	140.91911	101211.98524	97314.09264	718.88239	152.20681	-0.01662	0.00000
0096	H104	SYTRIM	141.56494	101211.41392	97314.39379	718.88219	152.20681	-0.01662	0.00000
0097	SYTR_D	DRIFT	144.48163	101208.83370	97315.75376	718.88137	152.20681	-0.01662	0.00000
0098	BPM_UP	DRIFT	144.93997	101208.42826	97315.96747	718.88124	152.20681	-0.01662	0.00000
0099	HP105	BPM	145.21497	101208.18498	97316.09572	718.88114	152.20681	-0.01662	0.00000
0100	BPM_DN	DRIFT	145.74830	101207.71317	97316.34441	718.88101	152.20681	-0.01662	0.00000
0101	SFOUR_	adapter	145.85663	101207.61734	97316.39490	718.88098	152.20681	-0.01662	0.00000
0102	PM105	MUWIRE	146.00246	101207.48833	97316.46291	718.88091	152.20681	-0.01662	0.00000
0103	SFOUR_	adapter	147.33579	101206.30881	97317.08460	718.88055	152.20681	-0.01662	0.00000
0104	Q12_UP	DRIFT	147.48163	101206.17981	97317.15261	718.88048	152.20681	-0.01662	0.00000
0105	HQF105	3Q120/2	148.05453	101205.67298	97317.41977	718.88032	152.20681	-0.01662	0.00000
0106	HQF105	3Q120/2	153.05452	101201.24980	97319.75116	718.87888	152.20681	-0.01662	0.00000
0107	Q12_DN	DRIFT	158.05451	101196.82664	97322.08255	718.87743	152.20681	-0.01662	0.00000
0108	MICR_U	DRIFT	158.48161	101196.44882	97322.28170	718.87734	152.20681	-0.01662	0.00000
0109	HT105	MIHC	158.97117	101196.01572	97322.50998	718.87717	152.20681	-0.01662	0.00000
0110	MICR_D	DRIFT	159.97117	101195.13107	97322.97625	718.87691	152.20681	-0.01662	0.00000
0111	DRMTU1	drift	160.27327	101194.86385	97323.11710	718.87681	152.20681	-0.01662	0.00000
0112	DRMTD	drift	182.05597	101175.59407	97333.27397	718.87054	152.20681	-0.01662	0.00000
0113	BPM_UP	DRIFT	203.11140	101156.96767	97343.09170	718.86447	152.20681	-0.01662	0.00000
0114	VP106	BPM	203.38640	101156.72439	97343.21995	718.86438	152.20681	-0.01662	0.00000
0115	BPM_DN	DRIFT	203.91974	101156.25258	97343.46860	718.86424	152.20681	-0.01662	0.00000
0116	Q12_UP	DRIFT	204.02807	101156.15674	97343.51912	718.86421	152.20681	-0.01662	0.00000
0117	HQD106	3Q120/2	204.60097	101155.64992	97343.78628	718.86405	152.20681	-0.01662	0.00000
0118	HQD106	3Q120/2	209.60096	101151.22673	97346.11768	718.86260	152.20681	-0.01662	0.00000
0119	Q12_DN	DRIFT	214.60098	101146.80358	97348.44907	718.86116	152.20681	-0.01662	0.00000
0120	MICR_U	DRIFT	215.02805	101146.42576	97348.64822	718.86103	152.20681	-0.01662	0.00000
0121	VT106	MIHC-R	215.51761	101145.99266	97348.87650	718.86090	152.20681	-0.01662	0.00000
0122	MICR_D	DRIFT	216.51761	101145.10801	97349.34277	718.86060	152.20681	-0.01662	0.00000
0123	DRMTU	drift	216.81971	101144.84079	97349.48361	718.86050	152.20681	-0.01662	0.00000
0124	DRMTD1	drift	237.27098	101126.74883	97359.01965	718.85463	152.20681	-0.01662	0.00000
0125	BPM_UP	DRIFT	258.03479	101108.38043	97368.70142	718.84866	152.20681	-0.01662	0.00000
0126	HP107	BPM	258.30979	101108.13715	97368.82964	718.84856	152.20681	-0.01662	0.00000
0127	BPM_DN	DRIFT	258.84312	101107.66534	97369.07833	718.84840	152.20681	-0.01662	0.00000
0128	SFOUR_	adapter	258.95145	101107.56950	97369.12882	718.84840	152.20681	-0.01662	0.00000
0129	PM107	MUWIRE	259.09728	101107.44050	97369.19683	718.84833	152.20681	-0.01662	0.00000
0130	SFOUR_	adapter	260.43061	101106.26098	97369.81855	718.84797	152.20681	-0.01662	0.00000
0131	Q12_UP	DRIFT	260.57645	101106.13197	97369.88653	718.84791	152.20681	-0.01662	0.00000
0132	HQF107	3Q120/2	261.14935	101105.62515	97370.15368	718.84774	152.20681	-0.01662	0.00000
0133	HQF107	3Q120/2	266.14934	101101.20196	97372.48508	718.84630	152.20681	-0.01662	0.00000
0134	Q12_DN	DRIFT	271.14933	101096.77881	97374.81647	718.84485	152.20681	-0.01662	0.00000
0135	MICR_U	DRIFT	271.57643	101096.40099	97375.01562	718.84476	152.20681	-0.01662	0.00000
0136	HT107	MIHC	272.06599	101095.96789	97375.24390	718.84459	152.20681	-0.01662	0.00000
0137	MICR_D	DRIFT	273.06599	101095.08324	97375.71017	718.84433	152.20681	-0.01662	0.00000
0138	DRMTU2	drift	273.36809	101094.81602	97375.85105	718.84423	152.20681	-0.01662	0.00000
0139	DRMTDM	drift	294.35066	101076.25405	97385.63479	718.83819	152.20681	-0.01662	0.00000
0140	MICR_U	DRIFT	312.87441	101059.86724	97394.27207	718.83285	152.20681	-0.01662	0.00000
0141	VT108	MIHC-R	313.36401	101059.43413	97394.50035	718.83272	152.20681	-0.01662	0.00000
0142	MICR_D	DRIFT	314.36400	101058.54952	97394.96663	718.83242	152.20681	-0.01662	0.00000
0143	BPM_UP	DRIFT	314.66607	101058.28227	97395.10751	718.83232	152.20681	-0.01662	0.00000
0144	VP108	BPM	314.94107	101058.03899	97395.23572	718.83226	152.20681	-0.01662	0.00000
0145	BPM_DN	DRIFT	315.47440	101057.56721	97395.48441	718.83209	152.20681	-0.01662	0.00000

0146	SFOUR_	adapter	315.58273	101057.47138	97395.53490	718.83206	152.20681	-0.01662	0.00000
0147	PM108	MUWIRE	315.72857	101057.34234	97395.60291	718.83203	152.20681	-0.01662	0.00000
0148	SFOUR_	adapter	317.06190	101056.16285	97396.22463	718.83163	152.20681	-0.01662	0.00000
0149	Q12_UP	DRIFT	317.20773	101056.03385	97396.29261	718.83160	152.20681	-0.01662	0.00000
0150	HQD108	3Q120/2	317.78066	101055.52702	97396.55977	718.83144	152.20681	-0.01662	0.00000
0151	HQD108	3Q120/2	322.78065	101051.10384	97398.89116	718.82999	152.20681	-0.01662	0.00000
0152	Q12_DN	DRIFT	327.78064	101046.68065	97401.22255	718.82855	152.20681	-0.01662	0.00000
0153	SMIDGE	drift	328.20771	101046.30283	97401.42170	718.82842	152.20681	-0.01662	0.00000
0154	FOUR_6	adapter	329.34951	101045.29279	97401.95408	718.82809	152.20681	-0.01662	0.00000
0155	B2_UPS	DRIFT	329.51617	101045.14535	97402.03180	718.82806	152.20681	-0.01662	0.00000
0156	V108_1	B2	330.13074	101044.60168	97402.31835	718.82786	152.20681	-0.76089	-90.00021
0157	B2_DNS	DRIFT	350.04792	101026.98423	97411.60429	718.56336	152.20681	-1.50516	0.00000
0158	B2_UPS	DRIFT	350.60002	101026.49601	97411.86161	718.54886	152.20681	-1.50516	0.00000
0159	V108_2	B2	351.21459	101025.95251	97412.14809	718.53272	152.20681	-2.24972	-90.00021
0160	B2_DNS	DRIFT	371.13177	101008.34713	97421.42766	717.75083	152.20681	-2.99428	0.00000
0161	FOUR_6	adapter	371.68387	101007.85940	97421.68475	717.72199	152.20681	-2.99428	0.00000
0162	MICR_U	DRIFT	371.85054	101007.71216	97421.76234	717.71326	152.20681	-2.99428	0.00000
0163	HT109	MIHC	372.34010	101007.27965	97421.99033	717.68771	152.20681	-2.99428	0.00000
0164	MICR_D	DRIFT	373.34010	101006.39622	97422.45597	717.63547	152.20681	-2.99428	0.00000
0165	Q12_UP	DRIFT	373.64220	101006.12935	97422.59662	717.61969	152.20681	-2.99428	0.00000
0166	HQF109	3Q120/2	374.21510	101005.62322	97422.86339	717.58974	152.20681	-2.99428	0.00000
0167	HQF109	3Q120/2	379.21509	101001.20607	97425.19163	717.32855	152.20681	-2.99428	0.00000
0168	Q12_DN	DRIFT	384.21508	100996.78895	97427.51984	717.06737	152.20681	-2.99428	0.00000
0169	H109UP	drift	384.64218	100996.41166	97427.71869	717.04506	152.20681	-2.99428	0.00000
0170	HP109	BPM	385.04375	100996.05690	97427.90570	717.02409	152.20681	-2.99428	0.00000
0171	FOUR_6	adapter	385.57708	100995.58574	97428.15403	716.99624	152.20681	-2.99428	0.00000
0172	V183UP	drift	385.74375	100995.43849	97428.23165	716.98751	152.20681	-2.99428	0.00000
0173	V108_3	B2	386.34007	100994.91166	97428.50931	716.95637	152.20681	-3.73884	-90.00021
0174	B2_DNS	DRIFT	406.25729	100977.33020	97437.77629	715.65762	152.20681	-4.48339	0.00000
0175	B2_UPS	DRIFT	406.80936	100976.84329	97438.03295	715.61448	152.20681	-4.48339	0.00000
0176	V108_4	B2	407.42392	100976.30126	97438.31864	715.56642	152.20681	-5.22795	-90.00021
0177	B2_DNS	DRIFT	427.34114	100958.75556	97447.56672	713.75172	152.20681	-5.97251	0.00000
0178	FOUR_6	adapter	427.89321	100958.26984	97447.82275	713.69427	152.20681	-5.97251	0.00000
0179	MICR_U	DRIFT	428.05987	100958.12318	97447.90005	713.67692	152.20681	-5.97251	0.00000
0180	VT110	MIHC-R	428.54947	100957.69244	97448.12708	713.62600	152.20681	-5.97251	0.00000
0181	MICR_D	DRIFT	429.54947	100956.81262	97448.59083	713.52193	152.20681	-5.97251	0.00000
0182	Q60_UP	DRIFT	429.85154	100956.54684	97448.73092	713.49050	152.20681	-5.97251	0.00000
0183	HQD110	3Q60/2	430.30987	100956.14356	97448.94349	713.44283	152.20681	-5.97251	0.00000
0184	HQD110	3Q60/2	432.80986	100953.94399	97450.10287	713.18269	152.20681	-5.97251	0.00000
0185	Q60_DN	DRIFT	435.30986	100951.74439	97451.26225	712.92259	152.20681	-5.97251	0.00000
0186	V110UP	drift	435.85152	100951.26781	97451.51343	712.86623	152.20681	-5.97251	0.00000
0187	VP110	BPM	436.17961	100950.97917	97451.66559	712.83210	152.20681	-5.97251	0.00000
0188	V110DN	drift	436.71294	100950.50991	97451.91290	712.77659	152.20681	-5.97251	0.00000
0189	FOUR_6	adapter	436.76819	100950.46132	97451.93853	712.77085	152.20681	-5.97251	0.00000
0190	B2_UPS	DRIFT	436.93485	100950.31467	97452.01582	712.75350	152.20681	-5.97251	0.00000
0191	V108_5	B2	437.54945	100949.77395	97452.30083	712.68955	152.20681	-6.71678	-90.00021
0192	B2_DNS	DRIFT	457.46664	100932.27589	97461.52384	710.36010	152.20681	-7.46106	0.00000
0193	B2_UPS	DRIFT	458.01870	100931.79164	97461.77909	710.28841	152.20681	-7.46106	0.00000
0194	V108_6	B2	458.63330	100931.25253	97462.06321	710.20862	152.20681	-8.20562	-90.00021
0195	B2_DNS	DRIFT	478.55049	100913.81395	97471.25489	707.36597	152.20681	-8.95017	0.00000
0196	FOUR_6	adapter	479.10255	100913.33151	97471.50919	707.28008	152.20681	-8.95017	0.00000
0197	DV1T0	drift	479.26922	100913.18587	97471.58593	707.25413	152.20681	-8.95017	0.00000

0198	P111UP	drift	479.43756	100913.03876	97471.66349	707.22795	152.20681	-8.95017	0.00000
0199	CT111T	CALTGT	479.72460	100912.78794	97471.79567	707.18330	152.20681	-8.95017	0.00000
0200	P111DN	drift	481.05793	100911.62278	97472.40981	706.97588	152.20681	-8.95017	0.00000
0201	DV2T0A	drift	481.06255	100911.61875	97472.41194	706.97516	152.20681	-8.95017	0.00000
0202	STUB_E	POINT	482.25412	100910.57748	97472.96080	706.78976	152.20681	-8.95017	0.00000
0203	DV2T0B	drift	482.25412	100910.57748	97472.96080	706.78976	152.20681	-8.95017	0.00000
0204	MICR_U	DRIFT	484.94988	100908.22174	97474.20246	706.37037	152.20681	-8.95017	0.00000
0205	VT111	MIH-OR	485.43945	100907.79392	97474.42798	706.29422	152.20681	-8.95017	0.00000
0206	MICR_D	DRIFT	486.43945	100906.92004	97474.88858	706.13865	152.20681	-8.95017	0.00000
0207	Q12_UP	DRIFT	486.74155	100906.65606	97475.02772	706.09163	152.20681	-8.95017	0.00000
0208	HQD111	3Q120/2	487.31445	100906.15541	97475.29160	706.00252	152.20681	-8.95017	0.00000
0209	HQD111	3Q120/2	492.31444	100901.78609	97477.59461	705.22464	152.20681	-8.95017	0.00000
0210	Q12_DN	DRIFT	497.31443	100897.41677	97479.89763	704.44675	152.20681	-8.95017	0.00000
0211	V111UP	drift	497.74152	100897.04355	97480.09434	704.38032	152.20681	-8.95017	0.00000
0212	VP111	BPM	498.15822	100896.67941	97480.28627	704.31549	152.20681	-8.95017	0.00000
0213	DV2TA	drift	498.69156	100896.21336	97480.53194	704.23252	152.20681	-8.95017	0.00000
0214	MICR_U	DRIFT	499.64241	100895.38243	97480.96990	704.08458	152.20681	-8.95017	0.00000
0215	HT112	MIHC-O	500.13200	100894.95461	97481.19539	704.00843	152.20681	-8.95017	0.00000
0216	MICR_D	DRIFT	501.13200	100894.08072	97481.65602	703.85286	152.20681	-8.95017	0.00000
0217	Q12_UP	DRIFT	501.43407	100893.81675	97481.79516	703.80584	152.20681	-8.95017	0.00000
0218	HQF112	3Q120/2	502.00700	100893.31609	97482.05904	703.71674	152.20681	-8.95017	0.00000
0219	HQF112	3Q120/2	507.00699	100888.94678	97484.36205	702.93885	152.20681	-8.95017	0.00000
0220	Q12_DN	DRIFT	512.00698	100884.57746	97486.66507	702.16096	152.20681	-8.95017	0.00000
0221	H112UP	drift	512.43405	100884.20424	97486.86178	702.09453	152.20681	-8.95017	0.00000
0222	HP112	BPM	512.87732	100883.81690	97487.06595	702.02556	152.20681	-8.95017	0.00000
0223	PM112U	drift	513.41069	100883.35082	97487.31159	701.94259	152.20681	-8.95017	0.00000
0224	PM112	MUWIRE	513.53362	100883.24338	97487.36825	701.92346	152.20681	-8.95017	0.00000
0225	C_P_MK	POINT	514.51351	100882.38711	97487.81956	701.77104	152.20681	-8.95017	0.00000
0226	PM112B	MUWIRE	514.51351	100882.38711	97487.81956	701.77104	152.20681	-8.95017	0.00000
0227	PM112D	drift	514.86695	100882.07822	97487.98239	701.71602	152.20681	-8.95017	0.00000
0228	DHALFX	drift	514.97574	100881.98318	97488.03248	701.69912	152.20681	-8.95017	0.00000
0229	DHALFX	drift	524.51739	100873.64507	97492.42739	700.21468	152.20681	-8.95017	0.00000
0230	DHALFX	drift	535.64237	100863.92334	97497.55159	698.48390	152.20681	-8.95017	0.00000
0231	DHALFX	drift	546.76734	100854.20157	97502.67579	696.75313	152.20681	-8.95017	0.00000
0232	DHALFX	drift	557.89232	100844.47984	97507.80000	695.02236	152.20681	-8.95017	0.00000
0233	DHALFX	drift	569.01730	100834.75811	97512.92420	693.29159	152.20681	-8.95017	0.00000
0234	DHALFX	drift	580.14228	100825.03637	97518.04840	691.56082	152.20681	-8.95017	0.00000
0235	DHALFX	drift	591.26726	100815.31464	97523.17260	689.83008	152.20681	-8.95017	0.00000
0236	DHALFX	drift	602.39223	100805.59291	97528.29681	688.09931	152.20681	-8.95017	0.00000
0237	DHALFX	drift	613.51721	100795.87118	97533.42101	686.36854	152.20681	-8.95017	0.00000
0238	DHALFX	drift	624.64219	100786.14944	97538.54521	684.63777	152.20681	-8.95017	0.00000
0239	DHALFX	drift	635.76717	100776.42771	97543.66941	682.90700	152.20681	-8.95017	0.00000
0240	DHALFX	drift	646.89214	100766.70598	97548.79362	681.17623	152.20681	-8.95017	0.00000
0241	DHALFX	drift	658.01712	100756.98425	97553.91782	679.44546	152.20681	-8.95017	0.00000
0242	DHALFX	drift	669.14210	100747.26251	97559.04199	677.71469	152.20681	-8.95017	0.00000
0243	DHALFX	drift	680.26708	100737.54075	97564.16619	675.98392	152.20681	-8.95017	0.00000
0244	DHALFX	drift	691.39206	100727.81902	97569.29039	674.25318	152.20681	-8.95017	0.00000
0245	DHALFX	drift	702.51703	100718.09728	97574.41459	672.52241	152.20681	-8.95017	0.00000
0246	DHALFX	drift	713.64201	100708.37555	97579.53880	670.79164	152.20681	-8.95017	0.00000
0247	DHALFX	drift	724.76699	100698.65382	97584.66300	669.06087	152.20681	-8.95017	0.00000
0248	BPM_UP	DRIFT	736.01693	100688.82287	97589.84478	667.31064	152.20681	-8.95017	0.00000
0249	VP113	BPM	736.29193	100688.58255	97589.97145	667.26786	152.20681	-8.95017	0.00000

0250	BPM_DN	DRIFT	736.82527	100688.11650	97590.21709	667.18489	152.20681	-8.95017	0.00000
0251	Q12_UP	DRIFT	736.93360	100688.02182	97590.26699	667.16806	152.20681	-8.95017	0.00000
0252	HQD113	3Q120/2	737.50653	100687.52116	97590.53090	667.07892	152.20681	-8.95017	0.00000
0253	HQD113	3Q120/2	742.50652	100683.15185	97592.83388	666.30103	152.20681	-8.95017	0.00000
0254	Q12_DN	DRIFT	747.50651	100678.78253	97595.13690	665.52318	152.20681	-8.95017	0.00000
0255	MICR_U	DRIFT	747.93358	100678.40931	97595.33361	665.45671	152.20681	-8.95017	0.00000
0256	VT114	MIH-OR	748.42318	100677.98148	97595.55914	665.38056	152.20681	-8.95017	0.00000
0257	MICR_D	DRIFT	749.42317	100677.10763	97596.01974	665.22498	152.20681	-8.95017	0.00000
0258	DV2T13	drift	749.72524	100676.84366	97596.15888	665.17797	152.20681	-8.95017	0.00000
0259	MICR_U	DRIFT	749.83495	100676.74779	97596.20940	665.16091	152.20681	-8.95017	0.00000
0260	HT114	MIHC-O	750.32452	100676.31997	97596.43489	665.08476	152.20681	-8.95017	0.00000
0261	MICR_D	DRIFT	751.32451	100675.44609	97596.89549	664.92918	152.20681	-8.95017	0.00000
0262	Q12_UP	DRIFT	751.62661	100675.18211	97597.03463	664.88217	152.20681	-8.95017	0.00000
0263	HQF114	3Q120/2	752.19951	100674.68146	97597.29854	664.79306	152.20681	-8.95017	0.00000
0264	HQF114	3Q120/2	757.19950	100670.31214	97599.60155	664.01517	152.20681	-8.95017	0.00000
0265	Q12_DN	DRIFT	762.19949	100665.94283	97601.90457	663.23729	152.20681	-8.95017	0.00000
0266	BPM_UP	DRIFT	762.62659	100665.56960	97602.10128	663.17085	152.20681	-8.95017	0.00000
0267	HP114	BPM	762.90159	100665.32931	97602.22793	663.12807	152.20681	-8.95017	0.00000
0268	BPM_DN	DRIFT	763.43492	100664.86324	97602.47359	663.04510	152.20681	-8.95017	0.00000
0269	SFOUR_	adapter	763.54326	100664.76858	97602.52350	663.02823	152.20681	-8.95017	0.00000
0270	PM114	MUWIRE	763.68909	100664.64112	97602.59065	663.00556	152.20681	-8.95017	0.00000
0271	V14_UP	drift	765.02242	100663.47597	97603.20479	662.79812	152.20681	-8.95017	0.00000
0272	IP114A	ionpump	765.54571	100663.01869	97603.44584	662.71672	152.20681	-8.95017	0.00000
0273	P114SE	drift	766.04571	100662.58178	97603.67612	662.63893	152.20681	-8.95017	0.00000
0274	IP114B	ionpump	780.52485	100649.92892	97610.34526	660.38634	152.20681	-8.95017	0.00000
0275	P114SE	drift	781.02485	100649.49197	97610.57558	660.30855	152.20681	-8.95017	0.00000
0276	IP114C	ionpump	795.50402	100636.83915	97617.24473	658.05597	152.20681	-8.95017	0.00000
0277	P114SE	drift	796.00402	100636.40220	97617.47504	657.97818	152.20681	-8.95017	0.00000
0278	IP114D	ionpump	810.48319	100623.74938	97624.14419	655.72556	152.20681	-8.95017	0.00000
0279	.....	drift	810.98319	100623.31243	97624.37447	655.64777	152.20681	-8.95017	0.00000
0280	BPM_UP	DRIFT	811.50648	100622.85515	97624.61551	655.56637	152.20681	-8.95017	0.00000
0281	HP115	BPM	811.78148	100622.61483	97624.74218	655.52359	152.20681	-8.95017	0.00000
0282	BPM_DN	DRIFT	812.31481	100622.14879	97624.98782	655.44062	152.20681	-8.95017	0.00000
0283	SFOUR_	adapter	812.42315	100622.05410	97625.03772	655.42375	152.20681	-8.95017	0.00000
0284	PM115	MUWIRE	812.56898	100621.92668	97625.10491	655.40108	152.20681	-8.95017	0.00000
0285	SFOUR_	adapter	813.90231	100620.76152	97625.71905	655.19364	152.20681	-8.95017	0.00000
0286	Q60_UP	DRIFT	814.04814	100620.63409	97625.78621	655.17097	152.20681	-8.95017	0.00000
0287	HQF115	3Q60/2	814.50647	100620.23357	97625.99733	655.09964	152.20681	-8.95017	0.00000
0288	HQF115	3Q60/2	817.00647	100618.04889	97627.14881	654.71070	152.20681	-8.95017	0.00000
0289	Q60_DN	DRIFT	819.50646	100615.86425	97628.30031	654.32179	152.20681	-8.95017	0.00000
0290	MICR_U	DRIFT	820.04813	100615.39089	97628.54982	654.23750	152.20681	-8.95017	0.00000
0291	HT115	MIHC	820.53770	100614.96307	97628.77531	654.16136	152.20681	-8.95017	0.00000
0292	MICR_D	DRIFT	821.53769	100614.08919	97629.23594	654.00578	152.20681	-8.95017	0.00000
0293	V15_UP	drift	821.83979	100613.82522	97629.37508	653.95876	152.20681	-8.95017	0.00000
0294	IP115A	ionpump	822.10666	100613.59201	97629.49798	653.91726	152.20681	-8.95017	0.00000
0295	P115SE	drift	822.60666	100613.15511	97629.72830	653.83947	152.20681	-8.95017	0.00000
0296	MVA15A	valve	839.78917	100598.13988	97637.64262	651.16628	152.20681	-8.95017	0.00000
0297	MVA15B	valve	840.28917	100597.70297	97637.87290	651.08853	152.20681	-8.95017	0.00000
0298	PG115	gauge	840.78916	100597.26603	97638.10321	651.01074	152.20681	-8.95017	0.00000
0299	IP115B	ionpump	841.28916	100596.82909	97638.33350	650.93295	152.20681	-8.95017	0.00000
0300	V15_DN	drift	841.78916	100596.39218	97638.56381	650.85516	152.20681	-8.95017	0.00000
0301	BPM_UP	DRIFT	842.05603	100596.15898	97638.68674	650.81363	152.20681	-8.95017	0.00000

0302	VP116	BPM	842.33103	100595.91866	97638.81338	650.77084	152.20681	-8.95017	0.00000
0303	BPM_DN	DRIFT	842.86436	100595.45258	97639.05905	650.68787	152.20681	-8.95017	0.00000
0304	Q12_UP	DRIFT	842.97269	100595.35793	97639.10895	650.67101	152.20681	-8.95017	0.00000
0305	HQD116	3Q120/2	843.54559	100594.85727	97639.37283	650.58190	152.20681	-8.95017	0.00000
0306	HQD116	3Q120/2	848.54558	100590.48796	97641.67584	649.80402	152.20681	-8.95017	0.00000
0307	Q12_DN	DRIFT	853.54557	100586.11864	97643.97886	649.02613	152.20681	-8.95017	0.00000
0308	MICR_U	DRIFT	853.97267	100585.74542	97644.17558	648.95969	152.20681	-8.95017	0.00000
0309	VT116	MIHC-R	854.46223	100585.31760	97644.40107	648.88354	152.20681	-8.95017	0.00000
0310	MICR_D	DRIFT	855.46223	100584.44371	97644.86167	648.72797	152.20681	-8.95017	0.00000
0311	V16_UP	drift	855.76433	100584.17974	97645.00081	648.68095	152.20681	-8.95017	0.00000
0312	IP116A	ionpump	856.04655	100583.93312	97645.13082	648.63706	152.20681	-8.95017	0.00000
0313	P116SE	drift	856.54655	100583.49618	97645.36111	648.55927	152.20681	-8.95017	0.00000
0314	IP116B	ionpump	872.04655	100569.95125	97652.50046	646.14785	152.20681	-8.95017	0.00000
0315	P116SE	drift	872.54655	100569.51435	97652.73078	646.07007	152.20681	-8.95017	0.00000
0316	IP116C	ionpump	888.04655	100555.96943	97659.87013	643.65865	152.20681	-8.95017	0.00000
0317	P116SE	drift	888.54655	100555.53248	97660.10041	643.58087	152.20681	-8.95017	0.00000
0318	IP116D	ionpump	904.04655	100541.98756	97667.23977	641.16945	152.20681	-8.95017	0.00000
0319	P116SE	drift	904.54655	100541.55062	97667.47008	641.09166	152.20681	-8.95017	0.00000
0320	IP116E	ionpump	920.04655	100528.00573	97674.60941	638.68025	152.20681	-8.95017	0.00000
0321	V16_DN	drift	920.54655	100527.56879	97674.83972	638.60246	152.20681	-8.95017	0.00000
0322	BPM_UP	DRIFT	920.82877	100527.32217	97674.96971	638.55857	152.20681	-8.95017	0.00000
0323	HP117	BPM	921.10377	100527.08185	97675.09638	638.51578	152.20681	-8.95017	0.00000
0324	BPM_DN	DRIFT	921.63710	100526.61578	97675.34205	638.43281	152.20681	-8.95017	0.00000
0325	SFOUR_	adapter	921.74543	100526.52113	97675.39195	638.41595	152.20681	-8.95017	0.00000
0326	PM117	MUWIRE	921.89127	100526.39366	97675.45911	638.39328	152.20681	-8.95017	0.00000
0327	SFOUR_	adapter	923.22460	100525.22854	97676.07325	638.18583	152.20681	-8.95017	0.00000
0328	Q12_UP	DRIFT	923.37043	100525.10108	97676.14041	638.16316	152.20681	-8.95017	0.00000
0329	HQF117	3Q120/2	923.94336	100524.60043	97676.40432	638.07402	152.20681	-8.95017	0.00000
0330	HQF117	3Q120/2	928.94335	100520.23111	97678.70730	637.29613	152.20681	-8.95017	0.00000
0331	Q12_DN	DRIFT	933.94334	100515.86180	97681.01031	636.51828	152.20681	-8.95017	0.00000
0332	MICR_U	DRIFT	934.37041	100515.48857	97681.20703	636.45184	152.20681	-8.95017	0.00000
0333	HT117	MIHC	934.86001	100515.06075	97681.43256	636.37566	152.20681	-8.95017	0.00000
0334	MICR_D	DRIFT	935.86000	100514.18690	97681.89315	636.22009	152.20681	-8.95017	0.00000
0335	D2MMI	drift	936.16207	100513.92292	97682.03229	636.17310	152.20681	-8.95017	0.00000
0336	SYTR_U	DRIFT	937.95846	100512.35311	97682.85972	635.89361	152.20681	-8.95017	0.00000
0337	H117	SYTRIM	938.60429	100511.78874	97683.15719	635.79315	152.19507	-8.95017	0.00000
0338	SYTR_D	DRIFT	941.52095	100509.24025	97684.50112	635.33938	152.18332	-8.95017	0.00000
0339	V17_UP	drift	941.97928	100508.83983	97684.71241	635.26809	152.18332	-8.95017	0.00000
0340	IP117	ionpump	942.23233	100508.61873	97684.82904	635.22872	152.18332	-8.95017	0.00000
0341	P117SE	drift	942.73233	100508.18189	97685.05952	635.15093	152.18332	-8.95017	0.00000
0342	V17_DN	drift	943.30566	100507.68101	97685.32382	635.06172	152.18332	-8.95017	0.00000
0343	BPM_UP	DRIFT	943.55868	100507.45994	97685.44046	635.02235	152.18332	-8.95017	0.00000
0344	VP118	BPM	943.83368	100507.21965	97685.56723	634.97957	152.18332	-8.95017	0.00000
0345	BPM_DN	DRIFT	944.36701	100506.75371	97685.81306	634.89660	152.18332	-8.95017	0.00000
0346	Q12_UP	DRIFT	944.47537	100506.65906	97685.86299	634.87977	152.18332	-8.95017	0.00000
0347	HQD118	3Q120/2	945.04827	100506.15853	97686.12710	634.79063	152.18332	-8.95017	0.00000
0348	HQD118	3Q120/2	950.04826	100501.79014	97688.43189	634.01274	152.18332	-8.95017	0.00000
0349	Q12_DN	DRIFT	955.04825	100497.42177	97690.73670	633.23489	152.18332	-8.95017	0.00000
0350	MICR_U	DRIFT	955.47535	100497.04864	97690.93359	633.16842	152.18332	-8.95017	0.00000
0351	VT118	MIHC-R	955.96492	100496.62092	97691.15928	633.09227	152.18332	-8.95017	0.00000
0352	MICR_D	DRIFT	956.96492	100495.74724	97691.62023	632.93669	152.18332	-8.95017	0.00000
0353	V18_UP	drift	957.26702	100495.48333	97691.75947	632.88971	152.18332	-8.95017	0.00000

0354	IP118A	ionpump	959.03909	100493.93507	97692.57633	632.61399	152.18332	-8.95017	0.00000
0355	P118SE	drift	959.53909	100493.49826	97692.80681	632.53620	152.18332	-8.95017	0.00000
0356	IP118B	ionpump	975.04241	100479.95337	97699.95329	630.12430	152.18332	-8.95017	0.00000
0357	V18_DN	drift	975.54241	100479.51653	97700.18377	630.04651	152.18332	-8.95017	0.00000
0358	FOUR_6	adapter	975.83532	100479.26059	97700.31877	630.00094	152.18332	-8.95017	0.00000
0359	B2_UPS	DRIFT	976.00198	100479.11499	97700.39561	629.97499	152.18332	-8.95017	0.00000
0360	V118_1	B2	976.61658	100478.57805	97700.67891	629.87938	152.18332	-8.24945	90.00021
0361	B2_DNS	DRIFT	996.53370	100461.14514	97709.87673	627.02174	152.18332	-7.54872	0.00000
0362	B2_UPS	DRIFT	997.08580	100460.66109	97710.13214	626.94921	152.18332	-7.54872	0.00000
0363	V118_2	B2	997.70037	100460.12224	97710.41642	626.86846	152.18332	-6.84771	90.00021
0364	B2_DNS	DRIFT	1017.61749	100442.63274	97719.64413	624.49383	152.18332	-6.14669	0.00000
0365	FOUR_6	adapter	1018.16958	100442.14725	97719.90026	624.43471	152.18332	-6.14669	0.00000
0366	MICR_U	DRIFT	1018.33625	100442.00069	97719.97759	624.41686	152.18332	-6.14669	0.00000
0367	HT119	MIHC	1018.82582	100441.57018	97720.20476	624.36443	152.18332	-6.14669	0.00000
0368	MICR_D	DRIFT	1019.82581	100440.69082	97720.66870	624.25738	152.18332	-6.14669	0.00000
0369	Q60_UP	DRIFT	1020.12791	100440.42517	97720.80886	624.22503	152.18332	-6.14669	0.00000
0370	HQF119	3Q60/2	1020.58625	100440.02215	97721.02152	624.17595	152.18332	-6.14669	0.00000
0371	HQF119	3Q60/2	1023.08624	100437.82376	97722.18143	623.90827	152.18332	-6.14669	0.00000
0372	Q60_DN	DRIFT	1025.58624	100435.62534	97723.34130	623.64058	152.18332	-6.14669	0.00000
0373	BPM_UP	DRIFT	1026.12790	100435.14903	97723.59264	623.58258	152.18332	-6.14669	0.00000
0374	HP119	BPM	1026.40290	100434.90720	97723.72020	623.55312	152.18332	-6.14669	0.00000
0375	BPM_DN	DRIFT	1026.93623	100434.43821	97723.96768	623.49603	152.18332	-6.14669	0.00000
0376	FOUR_6	adapter	1027.04457	100434.34296	97724.01794	623.48442	152.18332	-6.14669	0.00000
0377	B2_UPS	DRIFT	1027.21123	100434.19641	97724.09527	623.46657	152.18332	-6.14669	0.00000
0378	V118_3	B2	1027.82580	100433.65596	97724.38040	623.40075	152.18332	-5.44596	90.00021
0379	B2_DNS	DRIFT	1047.74292	100416.12030	97733.63242	621.51054	152.18332	-4.74524	0.00000
0380	B2_UPS	DRIFT	1048.29502	100415.63368	97733.88918	621.46487	152.18332	-4.74524	0.00000
0381	V118_4	B2	1048.90958	100415.09198	97734.17497	621.41401	152.18332	-4.04422	90.00021
0382	B2_DNS	DRIFT	1068.82673	100397.52069	97743.44582	620.00936	152.18332	-3.34321	0.00000
0383	FOUR_6	adapter	1069.37880	100397.03326	97743.70300	619.97714	152.18332	-3.34321	0.00000
0384	Q12_UP	DRIFT	1069.54547	100396.88608	97743.78066	619.96743	152.18332	-3.34321	0.00000
0385	HQD120	3Q120/2	1070.11840	100396.38024	97744.04756	619.93403	152.18332	-3.34321	0.00000
0386	HQD120	3Q120/2	1075.11839	100391.96555	97746.37678	619.64240	152.18332	-3.34321	0.00000
0387	Q12_DN	DRIFT	1080.11838	100387.55086	97748.70604	619.35080	152.18332	-3.34321	0.00000
0388	DRV3TB	drift	1080.54544	100387.17377	97748.90499	619.32589	152.18332	-3.34321	0.00000
0389	Q12_UP	DRIFT	1080.95532	100386.81189	97749.09594	619.30198	152.18332	-3.34321	0.00000
0390	HQF121	3Q120/2	1081.52822	100386.30605	97749.36283	619.26858	152.18332	-3.34321	0.00000
0391	HQF121	3Q120/2	1086.52821	100381.89136	97751.69206	618.97698	152.18332	-3.34321	0.00000
0392	Q12_DN	DRIFT	1091.52820	100377.47667	97754.02132	618.68538	152.18332	-3.34321	0.00000
0393	MICR_U	DRIFT	1091.95530	100377.09957	97754.22027	618.66044	152.18332	-3.34321	0.00000
0394	HT121	MIHC	1092.44486	100376.66732	97754.44836	618.63190	152.18332	-3.34321	0.00000
0395	MICR_D	DRIFT	1093.44486	100375.78439	97754.91420	618.57360	152.18332	-3.34321	0.00000
0396	MICR_U	DRIFT	1093.74696	100375.51765	97755.05492	618.55598	152.18332	-3.34321	0.00000
0397	VT121	MIHC-R	1094.23653	100375.08537	97755.28300	618.52740	152.18332	-3.34321	0.00000
0398	MICR_D	DRIFT	1095.23652	100374.20243	97755.74885	618.46910	152.18332	-3.34321	0.00000
0399	BPM_UP	DRIFT	1095.53862	100373.93573	97755.88956	618.45149	152.18332	-3.34321	0.00000
0400	HP121	SMABPM	1095.81362	100373.69292	97756.01768	618.43544	152.18332	-3.34321	0.00000
0401	BPM_DN	DRIFT	1096.34695	100373.22202	97756.26613	618.40434	152.18332	-3.34321	0.00000
0402	BPM_UP	DRIFT	1096.45529	100373.12635	97756.31659	618.39801	152.18332	-3.34321	0.00000
0403	VP121	SMABPM	1096.73029	100372.88354	97756.44471	618.38197	152.18332	-3.34321	0.00000
0404	BPM_DN	DRIFT	1097.26362	100372.41264	97756.69317	618.35086	152.18332	-3.34321	0.00000
0405	SFOUR_	adapter	1097.37195	100372.31700	97756.74363	618.34456	152.18332	-3.34321	0.00000

0406	PM121	TARGMW	1097.51779	100372.18823	97756.81157	618.33603	152.18332	-3.34321	0.00000
0407	V21_UP	drift	1098.85112	100371.01100	97757.43270	618.25828	152.18332	-3.34321	0.00000
0408	IP121A	ionpump	1099.14639	100370.75028	97757.57027	618.24105	152.18332	-3.34321	0.00000
0409	PG121	gauge	1099.64639	100370.30881	97757.80317	618.21189	152.18332	-3.34321	0.00000
0410	MAVL21	valve	1100.14639	100369.86734	97758.03611	618.18275	152.18332	-3.34321	0.00000
0411	P121SE	drift	1100.64639	100369.42587	97758.26902	618.15359	152.18332	-3.34321	0.00000
0412	IP121B	ionpump	1116.48212	100355.44388	97765.64613	617.23003	152.18332	-3.34321	0.00000
0413	P121SE	drift	1116.98212	100355.00241	97765.87904	617.20087	152.18332	-3.34321	0.00000
0414	IP121C	ionpump	1132.81788	100341.02038	97773.25613	616.27728	152.18332	-3.34321	0.00000
0415	V21_DN	drift	1133.31788	100340.57891	97773.48907	616.24814	152.18332	-3.34321	0.00000
0416	TOR_UP	DRIFT	1133.61315	100340.31822	97773.62663	616.23092	152.18332	-3.34321	0.00000
0417	TORTGT	TOROID	1133.94649	100340.02389	97773.78191	616.21146	152.18332	-3.34321	0.00000
0418	TOR_DN	DRIFT	1134.23815	100339.76638	97773.91777	616.19447	152.18332	-3.34321	0.00000
0419	BPM_UP	DRIFT	1134.61315	100339.43528	97774.09248	616.17259	152.18332	-3.34321	0.00000
0420	HPTGT	SMABPM	1134.88815	100339.19246	97774.22056	616.15654	152.18332	-3.34321	0.00000
0421	BPM_DN	DRIFT	1135.42148	100338.72157	97774.46902	616.12544	152.18332	-3.34321	0.00000
0422	BPM_UP	DRIFT	1135.52982	100338.62590	97774.51948	616.11914	152.18332	-3.34321	0.00000
0423	VPTGT	SMABPM	1135.80481	100338.38312	97774.64759	616.10310	152.18332	-3.34321	0.00000
0424	BPM_DN	DRIFT	1136.33815	100337.91218	97774.89605	616.07200	152.18332	-3.34321	0.00000
0425	PMTGT	TARGMW	1136.44648	100337.81655	97774.94651	616.06566	152.18332	-3.34321	0.00000
0426	OT_UPS	drift	1137.77981	100336.63929	97775.56767	615.98791	152.18332	-3.34321	0.00000
0427	OTRTGT	otrmon	1138.23814	100336.23463	97775.78115	615.96117	152.18332	-3.34321	0.00000
0428	OT_DNS	drift	1139.86314	100334.79985	97776.53817	615.86642	152.18332	-3.34321	0.00000
0429	OUCADR	drift	1140.20828	100334.49510	97776.69897	615.84627	152.18332	-3.34321	0.00000
0430	SH_WAL	drift	1141.20828	100333.61216	97777.16481	615.78794	152.18332	-3.34321	0.00000
0431	M_TACA	POINT	1147.20827	100328.31453	97779.95992	615.43804	152.18332	-3.34321	0.00000
0432	INCADR	drift	1147.20827	100328.31453	97779.95992	615.43804	152.18332	-3.34321	0.00000
0433	BAFL2P	BAFFLE	1160.89253	100316.23218	97786.33471	614.63995	152.18332	-3.34321	0.00000
0434	TA_OFF	drift	1165.81378	100311.88701	97788.62729	614.35294	152.18332	-3.34321	0.00000
0435	TA_UPS	drift	1167.25383	100310.61552	97789.29815	614.26895	152.18332	-3.34321	0.00000
0436	HALTA1	TAR/2	1168.04451	100309.91739	97789.66649	614.22282	152.18332	-3.34321	0.00000
0437	MCZERO	point	1169.19281	100308.90352	97790.20140	614.15586	152.18332	-3.34321	0.00000
0438	ACTRN1	horn1	1169.29123	100308.81664	97790.24727	614.15012	152.18332	-3.34321	0.00000
0439	HALTA2	TAR/2	1169.60914	100308.53593	97790.39536	614.13158	152.18332	-3.34321	0.00000
0440	ENDFIN	fin	1171.17377	100307.15444	97791.12423	614.04034	152.18332	-3.34321	0.00000
0441	DWNRN1	horn_dn	1179.03531	100300.21321	97794.78653	613.58184	152.18332	-3.34321	0.00000
0442	D2LOWE	drift	1181.72283	100297.84028	97796.03853	613.42509	152.18332	-3.34321	0.00000
0443	UPHRN2	horn_up	1201.82168	100280.09422	97805.40160	612.25291	152.18332	-3.34321	0.00000
0444	ACTRN2	horn2	1202.00114	100279.93576	97805.48520	612.24244	152.18332	-3.34321	0.00000
0445	DWNRN2	horn_dn	1211.84364	100271.24542	97810.07032	611.66840	152.18332	-3.34321	0.00000
0446	D2MEDE	drift	1217.18812	100266.52657	97812.56005	611.35672	152.18332	-3.34321	0.00000
0447	UPHRN2	horn_up	1244.47251	100242.43610	97825.27049	609.76545	152.18332	-3.34321	0.00000
0448	ACTRN2	horn2	1244.65197	100242.27766	97825.35409	609.75498	152.18332	-3.34321	0.00000
0449	DWNRN2	horn_dn	1254.49447	100233.58733	97829.93922	609.18093	152.18332	-3.34321	0.00000
0450	D2HIGE	drift	1259.83895	100228.86847	97832.42894	608.86925	152.18332	-3.34321	0.00000
0451	UPHRN2	horn_up	1290.50260	100201.79431	97846.71362	607.08091	152.18332	-3.34321	0.00000
0452	ACTRN2	horn2	1290.68206	100201.63588	97846.79722	607.07044	152.18332	-3.34321	0.00000
0453	DWNRN2	horn_dn	1300.52456	100192.94555	97851.38235	606.49639	152.18332	-3.34321	0.00000
0454	IHD3	drift	1305.86904	100188.22669	97853.87211	606.18471	152.18332	-3.34321	0.00000
0455	M_CAVE	POINT	1309.14988	100185.32991	97855.40048	605.99337	152.18332	-3.34321	0.00000
0456	OVERHA	drift	1309.14988	100185.32991	97855.40048	605.99337	152.18332	-3.34321	0.00000
0457	DKINHL	drift	1319.12085	100176.52616	97860.04545	605.41185	152.18332	-3.34321	0.00000

0458	M_THAL	POINT	1337.64936	100160.16661	97868.67697	604.33124	152.18332	-3.34321	0.00000
0459	DK_PCA	DECA44	1337.64936	100160.16661	97868.67697	604.33124	152.18332	-3.34321	0.00000
0460	DK_PCB	DEC150	1483.26094	100031.60040	97936.51020	595.83897	152.18332	-3.34321	0.00000
0461	DK_PCC	DEC150	1975.38594	99597.08384	98165.76682	567.13755	152.18332	-3.34321	0.00000
0462	DK_PCD	DEC100	2467.51094	99162.56726	98395.02345	538.43613	152.18332	-3.34321	0.00000
0463	DK_PCE	DEC100	2795.59428	98872.88956	98547.86120	519.30185	152.18332	-3.34321	0.00000
0464	DK_PCF	DEC125	3123.67761	98583.21186	98700.69896	500.16757	152.18332	-3.34321	0.00000
0465	DENCU	drift	3533.78178	98221.11471	98891.74615	476.24970	152.18332	-3.34321	0.00000
0466	DUMP	DUMP	3540.34344	98215.32115	98894.80290	475.86703	152.18332	-3.34321	0.00000
0467	DENCD	drift	3564.35914	98194.11677	98905.99064	474.46641	152.18332	-3.34321	0.00000
0468	MU_UP	drift	3583.78168	98176.96785	98915.03862	473.33367	152.18332	-3.34321	0.00000
0469	MUOND	MUON	3588.71129	98172.61530	98917.33507	473.04613	152.18332	-3.34321	0.00000
0470	MU_DN	drift	3590.35450	98171.16445	98918.10056	472.95030	152.18332	-3.34321	0.00000
0471	MUUP2	drift	3593.79862	98168.12348	98919.70501	472.74945	152.18332	-3.34321	0.00000
0472	MU_UP	drift	3633.23545	98133.30314	98938.07670	470.44945	152.18332	-3.34321	0.00000
0473	MUOND	MUON	3638.16507	98128.95062	98940.37315	470.16192	152.18332	-3.34321	0.00000
0474	MU_DN	drift	3639.80827	98127.49977	98941.13863	470.06609	152.18332	-3.34321	0.00000
0475	MUUP3	drift	3643.25239	98124.45880	98942.74309	469.86523	152.18332	-3.34321	0.00000
0476	MU_UP	drift	3702.40765	98072.22830	98970.30058	466.41521	152.18332	-3.34321	0.00000
0477	MUOND	MUON	3707.33724	98067.87575	98972.59703	466.12771	152.18332	-3.34321	0.00000
0478	MU_DN	drift	3708.98044	98066.42493	98973.36252	466.03188	152.18332	-3.34321	0.00000
0479	MUUP4	drift	3712.42460	98063.38393	98974.96698	465.83102	152.18332	-3.34321	0.00000
0480	MU_UP	drift	3811.01666	97976.33312	99020.89612	460.08100	152.18332	-3.34321	0.00000
0481	MUOND	MUON	3815.94624	97971.98060	99023.19257	459.79350	152.18332	-3.34321	0.00000
0482	MU_DN	drift	3817.58944	97970.52975	99023.95805	459.69767	152.18332	-3.34321	0.00000
0483	SHIELD	drift	3821.03360	97967.48878	99025.56251	459.49678	152.18332	-3.34321	0.00000
0484	TUNNEL	TUNNEL	4409.14181	97448.22485	99299.53296	425.19751	152.18332	-3.34321	0.00000
0485	M_ENCU	EX_ENU	4484.72906	97381.48591	99334.74533	420.78915	152.18332	-3.34321	0.00000
0486	MIN_ND	EXP	4570.37268	97305.86776	99374.64242	415.79428	152.18332	-3.34321	0.00000
0487	M_ENCD	EX_END	4624.95981	97257.67064	99400.07187	412.61069	152.18332	-3.34321	0.00000
0488	ILWIMN	drift	4634.97675	97248.82627	99404.73826	412.02647	152.18332	-3.34321	0.00000
0489	MINOFU	EXP_F2	2413631.71977	-2029749.35001	1221636.85406	-140084.03837	152.18332	-3.34321	0.00000
0490	MINOFD	EXP_F2	2413690.87500	-2029801.58051	1221664.41155	-140087.48839	152.18332	-3.34321	0.00000

THIS LOG DOCUMENTS CURRENT FILES FOR NuMI EXTRACTION / PRIMARY BEAM DESIGN, ALONG WITH DESCRIPTION OF CHANGES SINCE PREVIOUS RELEASE.

OFFICIAL BEAM DESIGN RELEASE IS DESIGNATED BY

- **NuMI0x_Vx.x beam design** with release date.

Working updates are listed with

- *file name and date, plus changes since previous release [affected systems]*

* * * * * * * * * * * *

Working update - 082504;

- *NuMI_121102_g.ces0.doc (TRANSPORT)*
  [Impacts string HV101 rolls and alignment – 1.1.6]

Changes are:

1. Rolls of magnets HV101-2,-3,-4 and -6 changed to account for altered fields due to magnetic shielding.
2. Vacuum devices downstream of HV112 are included. BEWARE, this beamsheet is inconsistent in the inclusion of vacuum devices..
3. Precise locations of some trims and instrumentation, as required to fit all components together in the tunnel, included. BEWARE, locations of trims and instrumentation are more precise in some parts of the beamline than others.

Working update - 050704;

- *NuMI_121102_f.ces0.doc (TRANSPORT)*
  [Impacts instrumentation stand placement, alignment – 1.1.6, ACNET name inputs, locations - 1.1.8, vacuum layout design – 1.1.7]

Changes are:

1. PM111 moved upstream ~ 1.2 meters to elevate better above floor for stand clearance.
2. VT113 renamed VT114 to be in sync with naming convention.
3. Move upstream BPM's (HP101, VP101) downstream by ~ 1.5 meters to just upstream of PM101. Move TOR101 to downstream of PM101 for better stand clearance.
4. Add resistive wall monitor. Position downstream of PM101.
5. Add OTR monitor. Position with downstream instrumentation station. (HPTGT, VPTGT, PMTGT).

Working update – 012204:

- *NuMI_121102_e.ces0.doc(TRANSPORT)*

Changes are:

1. Extraction region updated to most recent MI parameters – proper length MI BPM, MI quad offsets and trim dipole values.
2. Horizontal tune changed as a result of the above. Necessitated new rolls in HV101 of up to 2 milliradians.
3 Accurate instrumentation positions and device separations in stub region implemented.
4. .253" added to line just before shield wall, to return target region station values to previous norms.
5. Ds and Fs added to quadrupole names.

Warning: This beamsheet is only for the purpose of reading the annotations. The data are OUT OF DATE. 01/23/04

This file is an annotated beamsheet. Each new term or symbol is defined or explained the first time it is encountered.

Program ces (A Construction Engineering Survey format) (11/26/91) Fri May 2 13:08:54 2003
Site coordinates for beamline: input_ces_v2
NOTES: Coordinates are given for the entrance of the device in DUSAF coordinate system.
Site +x-axis (EAST); site +y-axis (NORTH); Site z-axis (ELEVATION)
Positive bearing is ccw wrt site EAST.
Pitch is the vertical polar angle out of the x-z plane.
Roll is wrt horizontal. Pos is clockwise looking downstream
Surveyor's roll is wrt nearest rectilinear direction

line	location	typ_code	distance [ft]	x [ft]	y [ft]	z [ft]	brng [deg]	pitch [deg]	roll [deg]	surveyor's roll [deg]
The first part of the beamline refers to MI60 straight section nominal										
0000	S1_BML	marker	-56.88634	101383.29651	97215.38336	715.72409	148.76849	0.00000	0.00000	
First element is a marker denoting the place at which the beamsheet starts. Distances are measured from an upstream point, the historical location of the end of the beamline's C-magnet. Distances are thus negative values up to that point.										
0001	LAM60	LAM_1	-56.88634	101383.29651	97215.38336	715.72409	148.76849	0.00000	-81.69232	8.308 wrt v
First physical element is the upstream NuMI Lambertson, LAM60. To be precise, the location is that of the beam at the plane of the upstream Lambertson steel. LAM_1 is a shorthand for this type of MI Lambertson. This device is powered by its own supply.										
0002	LAMEND	DRIFT	-47.70000	101375.44147	97220.14644	715.72409	148.76849	0.00000	0.00000	
End, nonsteel, region of Lambertson magnet. Space for coils and flanges.										
0003	.....	drift	-46.94423	101374.79522	97220.53830	715.72409	148.76849	0.00000	0.00000	
0004	.....	drift	-46.52756	101374.43892	97220.75434	715.72409	148.76849	0.00000	0.00000	
0005	HQ608	3Q84-2	-46.40256	101374.33206	97220.81917	715.72409	148.76849	0.00000	0.00000	
Main Injector quadrupole 608. 3Q84-2 is this type of MI device. All quadrupoles are designated HQ, standing for Half Quad. Since this beam sheet gives the upstream ends of devices, the first HQ location is that of the magnet upstream end, the second HQ location is that of the 'upstream end of the quad's downstream half,' namely the quad's midpoint. The subsequent location can be interpreted as the Quad downstream end.										
0006	HQ608	3Q84-2	-42.90257	101371.33928	97222.63390	715.72409	148.76849	0.00000	0.00000	
0007	.....	drift	-39.40258	101368.34651	97224.44863	715.72409	148.76849	0.00000	0.00000	
0008	.....	drift	-39.21006	101368.18191	97224.54846	715.72409	148.76849	0.00000	0.00000	
0009	.....	drift	-38.54339	101367.61186	97224.89413	715.72409	148.76849	0.00000	0.00000	
0010	LAMEND	DRIFT	-38.29339	101367.39809	97225.02376	715.72409	148.76849	0.00000	0.00000	
0011	LAM61A	LAM_1	-37.53762	101366.75183	97225.41562	715.72409	148.76849	0.00000	-88.85429	1.146 wrt v
LAM61A and LAM61B are the downstream two Lambertsons. They are powered by a single supply.										
0012	LAMEND	DRIFT	-28.35129	101358.89679	97230.17870	715.72409	148.76849	0.00000	0.00000	
0013	.....	drift	-27.59552	101358.25053	97230.57056	715.72409	148.76849	0.00000	0.00000	
0014	LAMEND	DRIFT	-27.09552	101357.82301	97230.82982	715.72409	148.76849	0.00000	0.00000	
0015	LAM61B	LAM_1	-26.33974	101357.17675	97231.22168	715.72409	148.76849	0.00000	-90.00000	0.
0016	LAMEND	DRIFT	-17.15341	101349.32171	97235.98479	715.72409	148.76849	0.00000	0.00000	
The remainder of the beamline refers to the NuMI extracted beam										
0017	VALVE	VALVE	-16.39760	101348.67545	97236.37666	715.72409	148.78282	0.56236	0.00000	
Space reserved for a vacuum valve.										
0018	.....	drift	-15.89761	101348.27988	97236.68843	716.05483	148.79714	1.12472	0.00000	
0019	CMGEND	DRIFT	-15.42198	101347.87142	97236.93200	716.06418	148.81261	1.12472	0.00000	
0020	V100	CMG_1	-14.75532	101347.30121	97237.27718	716.07724	148.81261	1.36536	-90.00000	0.

Unofficial annotated beamsheet (Warning: Not for use as a survey document)

Main Injector style C-magnet. V indicates vertical bend. 1xx is the arbitrary designation for this beamline. 101 through 121 are quadrupole locations. This magnet is before the first quad, thus denoted 100

0021	CMGEND	DRIFT	-3.75531	101337.89362	97242.97172	716.33935	148.81261	1.60600	0.00000
0022	.....	drift	-3.08864	101337.32351	97243.31680	716.35805	148.81261	1.60600	0.00000
0023	Q12_UP	DRIFT	-2.58864	101336.89595	97243.57562	716.37206	148.81261	1.60600	0.00000

Each magnet has an upstream and downstream extension. This is the upstream one for a 3Q120 magnet. All other magnets have something similar.

0024	HQ101	3Q120-2	-2.01571	101336.40602	97243.87218	716.38810	148.81261	1.60600	0.00000

Half quads, as explained above.

0025	HQ101	3Q120-2	2.98428	101332.13031	97246.46033	716.52826	148.81261	1.60600	0.00000
0026	Q12_DN	DRIFT	7.98427	101327.85459	97249.04848	716.66838	148.81261	1.60600	0.00000
0027	.....	drift	8.41133	101327.48937	97249.26954	716.68036	148.81261	1.60600	0.00000
0028	BPM_UP	DRIFT	10.17800	101325.97861	97250.18404	716.72987	148.81261	1.60600	0.00000

BPM Beam Position Monitor _UP, upstream extension for vacuum connection. Similarly for _DN

0029	VP101	BPM	10.45900	101325.74344	97250.32637	716.73758	148.81261	1.60600	0.00000

VP Vertical Position, similarly for HP. 101 for nearby quad. For historical reasons all instrumentation is given the location type of DRIFT. A more modern nomenclature is MONITOR. In either case the beam passes through undeflected.

0030	BPM_DN	DRIFT	10.98633	101325.28738	97250.60245	716.75250	148.81261	1.60600	0.00000
0031	BPM_UP	DRIFT	11.09466	101325.19472	97250.65852	716.75555	148.81261	1.60600	0.00000
0032	HP101	BPM	11.36966	101324.95955	97250.80087	716.76326	148.81261	1.60600	0.00000
0033	BPM_DN	DRIFT	11.90299	101324.50349	97251.07695	716.77823	148.81261	1.60600	0.00000
0034	.....	drift	12.01133	101324.41084	97251.13302	716.78124	148.81261	1.60600	0.00000
0035	TOR_UP	DRIFT	17.64649	101319.59198	97254.04995	716.93918	148.81261	1.60600	0.00000
0036	TOR101	TOROID	17.97982	101319.30694	97254.22249	716.94853	148.81261	1.60600	0.00000

Toroid intensity monitor

0037	TOR_DN	DRIFT	18.27149	101319.05753	97254.37347	716.95670	148.81261	1.60600	0.00000
0038	PM101	SMALMW	18.64649	101318.73683	97254.56756	716.96720	148.81261	1.60600	0.00000

PM Profile Monitor, SMALW indicates a type with a smaller than normal footprint for use in this crowded area.

0039	.....	drift	19.46315	101318.03847	97254.99030	716.99010	148.81261	1.60600	0.00000
0040	MICR_U	DRIFT	25.20274	101313.13028	97257.96129	717.15096	148.81261	1.60600	0.00000

MI Corrector (alternatively Trim) upstream extension. Similarly MICR_D

0041	HT102	MIHC	25.69230	101312.71161	97258.21474	717.16467	148.81261	1.60600	0.00000	0.

Horizontal Trim of type MIHC, which is MI Horizontal Corrector

0042	MICR_D	DRIFT	26.69230	101311.85650	97258.73235	717.19269	148.81261	1.60600	0.00000	
0043	EPB_UP	DRIFT	26.99440	101311.59816	97258.88872	717.20116	148.81261	1.60600	0.00000	
0044	HV01_1	EPB	27.54647	101311.12605	97259.17448	717.21664	149.14206	1.60600	0.00000	0.

EPB External Proton Beam, a common type of bending magnet. HV indicates rolled such as to bend both horizontally and vertically. This is a string of six magnets _1 through _6

0045	EPB_DN	DRIFT	37.54651	101302.54503	97264.30157	717.49689	149.47151	1.60600	0.00000	
0046	EPB_UP	DRIFT	37.99445	101302.15934	97264.52903	717.50946	149.47151	1.60600	0.00000	
0047	HV01_2	EPB	38.54651	101301.68398	97264.80934	717.52494	149.70982	1.58366	-3.84340	-3.84 wrt h
0048	EPB_DN	DRIFT	48.54656	101293.04459	97269.83764	717.80132	150.12812	1.56131	0.00000	
0049	Q12_UP	DRIFT	48.99446	101292.65631	97270.06068	717.81352	150.12812	1.56131	0.00000	
0050	HQ102	3Q120-2	49.56739	101292.15972	97270.34591	717.82911	150.12812	1.56131	0.00000	
0051	HQ102	3Q120-2	54.56738	101287.82561	97272.83528	717.96536	150.12812	1.56131	0.00000	
0052	Q12_DN	DRIFT	59.56737	101283.49153	97275.32467	718.10161	150.12812	1.56131	0.00000	
0053	BPM_UP	DRIFT	59.99443	101283.12132	97275.53731	718.11326	150.12812	1.56131	0.00000	
0054	HP102	BPM	60.26943	101282.88293	97275.67421	718.12074	150.12812	1.56131	0.00000	
0055	BPM_DN	DRIFT	60.80277	101282.42063	97275.93973	718.13528	150.12812	1.56131	0.00000	
0056	.....	drift	60.91110	101282.32673	97275.99367	718.13823	150.12812	1.56131	0.00000	
0057	EPB_UP	DRIFT	61.24443	101282.03779	97276.15965	718.14732	150.12812	1.56131	0.00000	
0058	HV01_3	EPB	61.79653	101281.55925	97276.43451	718.16238	150.42835	1.42638	-24.16621	-24.17 wrt h
0059	EPB_DN	DRIFT	71.79658	101272.86455	97281.36807	718.41133	150.72858	1.29145	0.00000	

Unofficial, unauthorized drain sheet
(reader's guide to the beamline)

0060	EPB_UP	DRIFT	72.24447	101272.47393	97281.58703	718.42140	150.72858	1.29145	0.00000	
0061	HV01_4	EPB	72.79654	101271.99247	97281.85691	718.43386	150.96980	1.06771	-42.83203	-42.83 wrt h
0062	EPB_DN	DRIFT	82.79659	101263.25036	97286.70877	718.62018	151.21101	0.84397	0.00000	
0063	EPB_UP	DRIFT	83.24452	101262.85787	97286.92445	718.62678	151.21101	0.84397	0.00000	
0064	HV01_5	EPB	83.79658	101262.37408	97287.19030	718.63491	151.45996	0.62882	-40.76022	-40.76 wrt h
0065	EPB_DN	DRIFT	93.79663	101253.58978	97291.96775	718.74463	151.70891	0.41368	0.00000	
0066	MICR_U	DRIFT	94.24453	101253.19539	97292.18002	718.74784	151.70891	0.41368	0.00000	
0067	VT103	MIHC-R	94.73413	101252.76429	97292.41204	718.75138	151.70891	0.41368	90.00000	0.

Magnets used for vertical correctors are MI horizontal corrector devices rolled 90 degrees. MI vertical correctors are not strong enough to be effective.

0068	MICR_D	DRIFT	95.73413	101251.88378	97292.88599	718.75860	151.70891	0.41368	0.00000	
0069	Q12_UP	DRIFT	96.03619	101251.61777	97293.02917	718.76077	151.70891	0.41368	0.00000	
0070	HQ103	3Q120-2	96.60912	101251.11331	97293.30069	718.76490	151.70891	0.41368	0.00000	
0071	HQ103	3Q120-2	101.60911	101246.71066	97295.67037	718.80099	151.70891	0.41368	0.00000	
0072	Q12_DN	DRIFT	106.60910	101242.30805	97298.04008	718.83708	151.70891	0.41368	0.00000	
0073	BPM_UP	DRIFT	107.03617	101241.93196	97298.24248	718.84013	151.70891	0.41368	0.00000	
0074	VP103	BPM	107.31117	101241.68984	97298.37282	718.84213	151.70891	0.41368	0.00000	
0075	BPM_DN	DRIFT	107.84450	101241.22022	97298.62558	718.84597	151.70891	0.41368	0.00000	
0076	.....	drift	107.95284	101241.12485	97298.67692	718.84676	151.70891	0.41368	0.00000	
0077	EPB_UP	DRIFT	108.28617	101240.83131	97298.83490	718.84915	151.70891	0.41368	0.00000	
0078	HV01_6	EPB	108.83827	101240.34519	97299.09654	718.85316	151.95786	0.19853	-40.76022	-40.76 wrt h
0079	EPB_DN	DRIFT	118.83831	101231.51926	97303.79771	718.88777	152.20681	-0.01662	0.00000	
0080	.....	drift	119.28621	101231.12300	97304.00657	718.88764	152.20681	-0.01662	0.00000	
0081	.....	drift	121.70740	101228.98110	97305.13551	718.88692	152.20681	-0.01662	0.00000	
0082	BPM_UP	DRIFT	132.30453	101219.60652	97310.07674	718.88380	152.20681	-0.01662	0.00000	
0083	HP104	BPM	132.57952	101219.36324	97310.20499	718.88373	152.20681	-0.01662	0.00000	
0084	BPM_DN	DRIFT	133.11286	101218.89143	97310.45367	718.88357	152.20681	-0.01662	0.00000	
0085	Q12_UP	DRIFT	133.22119	101218.79559	97310.50416	718.88354	152.20681	-0.01662	0.00000	
0086	HQ104	3Q60-2	133.79412	101218.28877	97310.77132	718.88337	152.20681	-0.01662	0.00000	

This quad, along with a few others, is 60 inches long, instead of the more common 120 inches

0087	HQ104	3Q60-2	136.29412	101216.07719	97311.93700	718.88262	152.20681	-0.01662	0.00000	
0088	Q12_DN	DRIFT	138.79411	101213.86558	97313.10272	718.88190	152.20681	-0.01662	0.00000	
0089	.....	drift	139.22118	101213.48780	97313.30183	718.88176	152.20681	-0.01662	0.00000	
0090	SYTR_U	DRIFT	140.91911	101211.98573	97314.09356	718.88127	152.20681	-0.01662	0.00000	
0091	H104	SYTRIM	141.56494	101211.41441	97314.39468	718.88108	152.20681	-0.01662	0.00000	0.

First of two magnets of type SwitchYard Trim, more strength than a MI trim. This one produces a modest horizontal bend.

0092	SYTR_D	DRIFT	144.48160	101208.83423	97315.75468	718.88022	152.20681	-0.01662	0.00000	
0093	BPM_UP	DRIFT	144.93993	101208.42878	97315.96839	718.88009	152.20681	-0.01662	0.00000	
0094	HP105	BPM	145.21493	101208.18551	97316.09661	718.88003	152.20681	-0.01662	0.00000	
0095	BPM_DN	DRIFT	145.74826	101207.71369	97316.34529	718.87986	152.20681	-0.01662	0.00000	
0096	.....	drift	145.85660	101207.61786	97316.39579	718.87983	152.20681	-0.01662	0.00000	
0097	PM105	MUWIRE	146.00243	101207.48886	97316.46380	718.87980	152.20681	-0.01662	0.00000	
0098	.....	drift	147.33576	101206.30933	97317.08552	718.87940	152.20681	-0.01662	0.00000	
0099	Q12_UP	DRIFT	147.48159	101206.18033	97317.15350	718.87934	152.20681	-0.01662	0.00000	
0100	HQ105	3Q120-2	148.05449	101205.67351	97317.42065	718.87917	152.20681	-0.01662	0.00000	
0101	HQ105	3Q120-2	153.05448	101201.25032	97319.75205	718.87770	152.20681	-0.01662	0.00000	
0102	Q12_DN	DRIFT	158.05447	101196.82713	97322.08344	718.87625	152.20681	-0.01662	0.00000	
0103	MICR_U	DRIFT	158.48157	101196.44935	97322.28259	718.87612	152.20681	-0.01662	0.00000	
0104	HT105	MIHC	158.97114	101196.01624	97322.51087	718.87596	152.20681	-0.01662	0.00000	0.
0105	MICR_D	DRIFT	159.97114	101195.13160	97322.97714	718.87569	152.20681	-0.01662	0.00000	
0106	.....	drift	160.27324	101194.86434	97323.11798	718.87560	152.20681	-0.01662	0.00000	
0107	.....	drift	182.05594	101175.59456	97333.27482	718.86920	152.20681	-0.01662	0.00000	

Unofficial Document
(reader's copy) Not to be used for any purpose

0108	BPM_UP	DRIFT	203.11137	101156.96813	97343.09255	718.86300	152.20681	-0.01662	0.00000	
0109	VP106	BPM	203.38637	101156.72485	97343.22077	718.86293	152.20681	-0.01662	0.00000	
0110	BPM_DN	DRIFT	203.91970	101156.25307	97343.46945	718.86277	152.20681	-0.01662	0.00000	
0111	Q12_UP	DRIFT	204.02804	101156.15723	97343.51998	718.86274	152.20681	-0.01662	0.00000	
0112	HQ106	3Q120-2	204.60097	101155.65041	97343.78710	718.86257	152.20681	-0.01662	0.00000	
0113	HQ106	3Q120-2	209.60096	101151.22722	97346.11850	718.86110	152.20681	-0.01662	0.00000	
0114	Q12_DN	DRIFT	214.60095	101146.80404	97348.44989	718.85962	152.20681	-0.01662	0.00000	
0115	MICR_U	DRIFT	215.02801	101146.42625	97348.64904	718.85952	152.20681	-0.01662	0.00000	
0116	VT106	MIHC-R	215.51761	101145.99315	97348.87732	718.85936	152.20681	-0.01662	90.00000	0.
0117	MICR_D	DRIFT	216.51761	101145.10850	97349.34362	718.85906	152.20681	-0.01662	0.00000	
0118	.....	drift	216.81968	101144.84125	97349.48447	718.85900	152.20681	-0.01662	0.00000	
0119	.....	drift	237.27095	101126.74929	97359.02047	718.85296	152.20681	-0.01662	0.00000	
0120	BPM_UP	DRIFT	258.03475	101108.38089	97368.70221	718.84689	152.20681	-0.01662	0.00000	
0121	HP107	BPM	258.30975	101108.13761	97368.83043	718.84679	152.20681	-0.01662	0.00000	
0122	BPM_DN	DRIFT	258.84308	101107.66580	97369.07911	718.84663	152.20681	-0.01662	0.00000	
0123	.....	drift	258.95142	101107.56996	97369.12964	718.84659	152.20681	-0.01662	0.00000	
0124	PM107	MUWIRE	259.08725	101107.44096	97369.19765	718.84656	152.20681	-0.01662	0.00000	
0125	.....	drift	260.43058	101106.26144	97369.81933	718.84617	152.20681	-0.01662	0.00000	
0126	Q12_UP	DRIFT	260.57641	101106.13243	97369.88735	718.84613	152.20681	-0.01662	0.00000	
0127	HQ107	3Q120-2	261.14931	101105.62561	97370.15447	718.84597	152.20681	-0.01662	0.00000	
0128	HQ107	3Q120-2	266.14930	101101.20242	97372.48586	718.84449	152.20681	-0.01662	0.00000	
0129	Q12_DN	DRIFT	271.14929	101096.77927	97374.81726	718.84302	152.20681	-0.01662	0.00000	
0130	MICR_U	DRIFT	271.57639	101096.40145	97375.01640	718.84289	152.20681	-0.01662	0.00000	
0131	HT107	MIHC	272.06596	101095.96835	97375.24468	718.84276	152.20681	-0.01662	0.00000	0.
0132	MICR_D	DRIFT	273.06596	101095.08370	97375.71096	718.84246	152.20681	-0.01662	0.00000	
0133	.....	drift	273.36806	101094.81648	97375.85184	718.84236	152.20681	-0.01662	0.00000	
0134	.....	drift	294.35063	101076.25451	97385.63558	718.83619	152.20681	-0.01662	0.00000	
0135	MICR_U	DRIFT	312.87441	101059.86770	97394.27283	718.83078	152.20681	-0.01662	0.00000	
0136	VT108	MIHC-R	313.36397	101059.43459	97394.50111	718.83062	152.20681	-0.01662	90.00000	0.
0137	MICR_D	DRIFT	314.36397	101058.54995	97394.96738	718.83032	152.20681	-0.01662	0.00000	
0138	BPM_UP	DRIFT	314.66607	101058.28273	97395.10826	718.83026	152.20681	-0.01662	0.00000	
0139	VP108	BPM	314.94107	101058.03945	97395.23648	718.83016	152.20681	-0.01662	0.00000	
0140	BPM_DN	DRIFT	315.47440	101057.56764	97395.48516	718.82999	152.20681	-0.01662	0.00000	
0141	.....	drift	315.58273	101057.47180	97395.53569	718.82996	152.20681	-0.01662	0.00000	
0142	PM108	MUWIRE	315.72857	101057.34280	97395.60367	718.82993	152.20681	-0.01662	0.00000	
0143	.....	drift	317.06190	101056.16327	97396.22538	718.82953	152.20681	-0.01662	0.00000	
0144	Q12_UP	DRIFT	317.20773	101056.03427	97396.29336	718.82950	152.20681	-0.01662	0.00000	
0145	HQ108	3Q120-2	317.78063	101055.52745	97396.56052	718.82934	152.20681	-0.01662	0.00000	
0146	HQ108	3Q120-2	322.78062	101051.10426	97398.89191	718.82786	152.20681	-0.01662	0.00000	
0147	Q12_DN	DRIFT	327.78061	101046.68111	97401.22331	718.82638	152.20681	-0.01662	0.00000	
0148	.....	drift	328.20771	101046.30329	97401.42245	718.82625	152.20681	-0.01662	0.00000	
0149	.....	drift	329.34947	101045.29322	97401.95483	718.82592	152.20681	-0.01662	0.00000	
0150	B2_UPS	DRIFT	329.51614	101045.14578	97402.03256	718.82589	152.20681	-0.01662	0.00000	
0151	V108_1	B2	330.13070	101044.60211	97402.31911	718.82569	152.20681	-0.76117	-90.00000	0.

The major downbend at 108, and the subsequent upbend at 118, are accomplished with B2 magnets. These were the major bend components of the Main Ring. Each is 239” long.

0152	B2_DNS	DRIFT	350.04792	101026.98466	97411.60501	718.56110	152.20681	-1.50573	0.00000	
0153	B2_UPS	DRIFT	350.59999	101026.49644	97411.86236	718.54659	152.20681	-1.50573	0.00000	
0154	V108_2	B2	351.21459	101025.95293	97412.14881	718.53042	152.20681	-2.25001	-90.00000	0.
0155	B2_DNS	DRIFT	371.13177	101008.34756	97421.42839	717.74847	152.20681	-2.99428	0.00000	
0156	.....	drift	371.68384	101007.85983	97421.68544	717.71963	152.20681	-2.99428	0.00000	
0157	MICR_U	DRIFT	371.85050	101007.71258	97421.76306	717.71093	152.20681	-2.99428	0.00000	

Unofficial Document
(reader's guide only)
Source data bearing sheet

0158	HT109	MIHC	372.34010	101007.28007	97421.99102	717.68534	152.20681	-2.99428	0.00000	0.
0159	MICR_D	DRIFT	373.34010	101006.39664	97422.45666	717.63311	152.20681	-2.99428	0.00000	
0160	Q12_UP	DRIFT	373.64217	101006.12978	97422.59735	717.61733	152.20681	-2.99428	0.00000	
0161	HQ109	3Q120-2	374.21510	101005.62364	97422.86411	717.58741	152.20681	-2.99428	0.00000	
0162	HQ109	3Q120-2	379.21509	101001.20649	97425.19232	717.32619	152.20681	-2.99428	0.00000	
0163	Q12_DN	DRIFT	384.21508	100996.78938	97427.52053	717.06500	152.20681	-2.99428	0.00000	
0164	BPM_UP	DRIFT	384.64214	100996.41208	97427.71942	717.04269	152.20681	-2.99428	0.00000	
0165	HP109	BPM	384.91714	100996.16914	97427.84747	717.02832	152.20681	-2.99428	0.00000	
0166	BPM_DN	DRIFT	385.45048	100995.69798	97428.09579	717.00047	152.20681	-2.99428	0.00000	
0167	.....	drift	385.55881	100995.60227	97428.14625	716.99479	152.20681	-2.99428	0.00000	
0168	B2_UPS	DRIFT	385.72548	100995.45503	97428.22384	716.98610	152.20681	-2.99428	0.00000	
0169	V108_3	B2	386.34007	100994.91208	97428.51003	716.95398	152.20681	-3.73884	-90.00000	0.
0170	B2_DNS	DRIFT	406.25726	100977.33059	97437.77697	715.65520	152.20681	-4.48339	0.00000	
0171	B2_UPS	DRIFT	406.80932	100976.84368	97438.03360	715.61205	152.20681	-4.48339	0.00000	
0172	V108_4	B2	407.42392	100976.30169	97438.31930	715.56402	152.20681	-5.22767	-90.00000	0.
0173	B2_DNS	DRIFT	427.34111	100958.75599	97447.56741	713.74929	152.20681	-5.97194	0.00000	
0174	.....	drift	427.89317	100958.27023	97447.82341	713.69185	152.20681	-5.97194	0.00000	
0175	MICR_U	DRIFT	428.05984	100958.12361	97447.90071	713.67449	152.20681	-5.97194	0.00000	
0176	VT110	MIHC-R	428.54944	100957.69283	97448.12777	713.62357	152.20681	-5.97194	90.00000	0.
0177	MICR_D	DRIFT	429.54944	100956.81301	97448.59152	713.51950	152.20681	-5.97194	0.00000	
0178	Q60_UP	DRIFT	429.85150	100956.54723	97448.73161	713.48807	152.20681	-5.97194	0.00000	
0179	HQ110	3Q60-2	430.30983	100956.14395	97448.94414	713.44040	152.20681	-5.97194	0.00000	
0180	HQ110	3Q60-2	432.80983	100953.94436	97450.10352	713.18030	152.20681	-5.97194	0.00000	
0181	Q60_DN	DRIFT	435.30982	100951.74478	97451.26291	712.92016	152.20681	-5.97194	0.00000	
0182	BPM_UP	DRIFT	435.85149	100951.26821	97451.51409	712.86380	152.20681	-5.97194	0.00000	
0183	VP110	BPM	436.12649	100951.02628	97451.64161	712.83519	152.20681	-5.97194	0.00000	
0184	BPM_DN	DRIFT	436.65982	100950.55702	97451.88895	712.77971	152.20681	-5.97194	0.00000	
0185	.....	drift	436.76816	100950.46171	97451.93918	712.76842	152.20681	-5.97194	0.00000	
0186	B2_UPS	DRIFT	436.93482	100950.31506	97452.01648	712.75110	152.20681	-5.97194	0.00000	
0187	V108_5	B2	437.54942	100949.77435	97452.30149	712.68716	152.20681	-6.71650	-90.00000	0.
0188	B2_DNS	DRIFT	457.46660	100932.27628	97461.52447	710.35770	152.20681	-7.46106	0.00000	
0189	B2_UPS	DRIFT	458.01867	100931.79200	97461.77972	710.28601	152.20681	-7.46106	0.00000	
0190	V108_6	B2	458.63327	100931.25293	97462.06387	710.20622	152.20681	-8.20562	-90.00021	0.
0191	B2_DNS	DRIFT	478.55045	100913.81431	97471.25552	707.36364	152.20681	-8.95017	0.00000	
0192	.....	drift	479.10252	100913.33187	97471.50981	707.27775	152.20681	-8.95017	0.00000	
0193	.....	drift	479.26922	100913.18623	97471.58659	707.25103	152.20681	-8.95017	0.00000	
0194	STUB_E	POINT	482.25412	100910.57780	97472.96145	706.78746	152.20681	-8.95017	0.00000	

Marker for the end of the original NuMI stub.

0195	.....	drift	482.25412	100910.57780	97472.96145	706.78746	152.20681	-8.95017	0.00000	
0196	.....	drift	483.32485	100909.64211	97473.45463	706.62086	152.20681	-8.95017	0.00000	
0197	PM111T	TARGMW	483.47069	100909.51468	97473.52178	706.59819	152.20681	-8.95017	0.00000	

This is a thin target device, probably implemented as a thick wire profile monitor, which can be inserted into the beam to create known losses. The purpose is for calibration of downstream loss monitors.

0198	.....	drift	484.80402	100908.34953	97474.13592	706.39078	152.20681	-8.95017	0.00000	
0199	MICR_U	DRIFT	484.94985	100908.22210	97474.20308	706.36808	152.20681	-8.95017	0.00000	
0200	VT111	MIH-OR	485.43945	100907.79428	97474.42861	706.29193	152.20681	-8.95017	90.00000	0.

This vertical trim is, as for the others, a rolled MI horizontal device. Additionally this one has the gap opened 50%, for aperture reasons, with a corresponding decrease in maximal field.

0201	MICR_D	DRIFT	486.43945	100906.92040	97474.88920	706.13635	152.20681	-8.95017	0.00000	
0202	Q12_UP	DRIFT	486.74151	100906.65642	97475.02834	706.08934	152.20681	-8.95017	0.00000	
0203	HQ111	3Q120-2	487.31445	100906.15577	97475.29222	706.00023	152.20681	-8.95017	0.00000	
0204	HQ111	3Q120-2	492.31444	100901.78645	97477.59523	705.22238	152.20681	-8.95017	0.00000	

Unofficial Bonus Material (readers should be aware that the beam sheet)

0205	Q12_DN	DRIFT	497.31443	100897.41714	97479.89825	704.44452	152.20681	-8.95017	0.00000	
0206	BPM_UP	DRIFT	497.74149	100897.04391	97480.09497	704.37805	152.20681	-8.95017	0.00000	
0207	VP111	BPM	498.01649	100896.80359	97480.22164	704.33527	152.20681	-8.95017	0.00000	
0208	BPM_DN	DRIFT	498.54982	100896.33754	97480.46728	704.25230	152.20681	-8.95017	0.00000	
0209	.....	drift	498.65816	100896.24286	97480.51718	704.23547	152.20681	-8.95017	0.00000	
0210	MICR_U	DRIFT	499.64241	100895.38279	97480.97052	704.08235	152.20681	-8.95017	0.00000	
0211	HT112	MIHC-O	500.13197	100894.95494	97481.19601	704.00617	152.20681	-8.95017	0.00000	0.

Horizontal corrector with gap opened 50%.

0212	MICR_D	DRIFT	501.13197	100894.08109	97481.65661	703.85059	152.20681	-8.95017	0.00000	
0213	Q12_UP	DRIFT	501.43407	100893.81711	97481.79575	703.80361	152.20681	-8.95017	0.00000	
0214	HQ112	3Q120-2	502.00697	100893.31645	97482.05966	703.71447	152.20681	-8.95017	0.00000	
0215	HQ112	3Q120-2	507.00696	100888.94714	97484.36268	702.93662	152.20681	-8.95017	0.00000	
0216	Q12_DN	DRIFT	512.00695	100884.57779	97486.66566	702.15877	152.20681	-8.95017	0.00000	
0217	BPM_UP	DRIFT	512.43405	100884.20460	97486.86237	702.09233	152.20681	-8.95017	0.00000	
0218	HP112	BPM	512.70905	100883.96427	97486.98905	702.04955	152.20681	-8.95017	0.00000	
0219	BPM_DN	DRIFT	513.24238	100883.49820	97487.23472	701.96658	152.20681	-8.95017	0.00000	
0220	.....	drift	513.35071	100883.40355	97487.28462	701.94971	152.20681	-8.95017	0.00000	
0221	PM112	MUWIRE	513.49655	100883.27612	97487.35178	701.92704	152.20681	-8.95017	0.00000	
0222	C_P_MK	POINT	514.51347	100882.38744	97487.82018	701.76884	152.20681	-8.95017	0.00000	

Marker indicating the beginning of the carrier pipe, or Hobbit. The subsequent string of drifts represents the unoccupied carrier region.

0223	.....	drift	514.51347	100882.38744	97487.82018	701.76884	152.20681	-8.95017	0.00000	
0224	.....	drift	514.82988	100882.11097	97487.96592	701.71959	152.20681	-8.95017	0.00000	
0225	.....	drift	514.97571	100881.98350	97488.03307	701.69692	152.20681	-8.95017	0.00000	
0226	.....	drift	524.51736	100873.64540	97492.42798	700.21251	152.20681	-8.95017	0.00000	
0227	.....	drift	535.64233	100863.92363	97497.55218	698.48177	152.20681	-8.95017	0.00000	
0228	.....	drift	546.76731	100854.20190	97502.67639	696.75107	152.20681	-8.95017	0.00000	
0229	.....	drift	557.89229	100844.48013	97507.80059	695.02033	152.20681	-8.95017	0.00000	
0230	.....	drift	569.01727	100834.75840	97512.92479	693.28962	152.20681	-8.95017	0.00000	
0231	.....	drift	580.14225	100825.03667	97518.04896	691.55889	152.20681	-8.95017	0.00000	
0232	.....	drift	591.26722	100815.31490	97523.17316	689.82815	152.20681	-8.95017	0.00000	
0233	.....	drift	602.39220	100805.59317	97528.29736	688.09744	152.20681	-8.95017	0.00000	
0234	.....	drift	613.51718	100795.87141	97533.42157	686.36670	152.20681	-8.95017	0.00000	
0235	.....	drift	624.64216	100786.14967	97538.54577	684.63597	152.20681	-8.95017	0.00000	
0236	.....	drift	635.76713	100776.42794	97543.66994	682.90526	152.20681	-8.95017	0.00000	
0237	.....	drift	646.89211	100766.70618	97548.79414	681.17452	152.20681	-8.95017	0.00000	
0238	.....	drift	658.01709	100756.98444	97553.91834	679.44379	152.20681	-8.95017	0.00000	
0239	.....	drift	669.14207	100747.26268	97559.04255	677.71308	152.20681	-8.95017	0.00000	
0240	.....	drift	680.26704	100737.54095	97564.16672	675.98234	152.20681	-8.95017	0.00000	
0241	.....	drift	691.39202	100727.81921	97569.29092	674.25164	152.20681	-8.95017	0.00000	
0242	.....	drift	702.51700	100718.09745	97574.41512	672.52090	152.20681	-8.95017	0.00000	
0243	.....	drift	713.64198	100708.37572	97579.53932	670.79016	152.20681	-8.95017	0.00000	
0244	.....	drift	724.76696	100698.65395	97584.66352	669.05946	152.20681	-8.95017	0.00000	
0245	BPM_UP	DRIFT	736.01690	100688.82300	97589.84527	667.30926	152.20681	-8.95017	0.00000	
0246	VP113	BPM	736.29190	100688.58268	97589.97195	667.26648	152.20681	-8.95017	0.00000	
0247	BPM_DN	DRIFT	736.82523	100688.11664	97590.21758	667.18351	152.20681	-8.95017	0.00000	
0248	Q12_UP	DRIFT	736.93357	100688.02195	97590.26748	667.16668	152.20681	-8.95017	0.00000	
0249	HQ113	3Q120-2	737.50650	100687.52130	97590.53139	667.07754	152.20681	-8.95017	0.00000	
0250	HQ113	3Q120-2	742.50649	100683.15198	97592.83441	666.29968	152.20681	-8.95017	0.00000	
0251	Q12_DN	DRIFT	747.50648	100678.78266	97595.13739	665.52183	152.20681	-8.95017	0.00000	
0252	MICR_U	DRIFT	747.93354	100678.40944	97595.33411	665.45539	152.20681	-8.95017	0.00000	
0253	VT113	MIH-OR	748.42314	100677.98162	97595.55963	665.37921	152.20681	-8.95017	90.00000	0.
0254	MICR_D	DRIFT	749.42314	100677.10773	97596.02023	665.22364	152.20681	-8.95017	0.00000	

Unofficial Bmad Lattice (reassembled by hand from the baseline lattice)

0255	.....	drift	749.72521	100676.84376	97596.15937	665.17666	152.20681	-8.95017	0.00000	
0256	MICR_U	DRIFT	749.83492	100676.74792	97596.20989	665.15959	152.20681	-8.95017	0.00000	
0257	HT114	MIHC-O	750.32448	100676.32007	97596.43538	665.08341	152.20681	-8.95017	0.00000	0.
0258	MICR_D	DRIFT	751.32448	100675.44622	97596.89598	664.92787	152.20681	-8.95017	0.00000	
0259	Q12_UP	DRIFT	751.62658	100675.18225	97597.03512	664.88086	152.20681	-8.95017	0.00000	
0260	HQ114	3Q120-2	752.19948	100674.68159	97597.29903	664.79172	152.20681	-8.95017	0.00000	
0261	HQ114	3Q120-2	757.19947	100670.31227	97599.60201	664.01386	152.20681	-8.95017	0.00000	
0262	Q12_DN	DRIFT	762.19946	100665.94293	97601.90503	663.23601	152.20681	-8.95017	0.00000	
0263	BPM_UP	DRIFT	762.62656	100665.56973	97602.10174	663.16957	152.20681	-8.95017	0.00000	
0264	HP114	BPM	762.90156	100665.32941	97602.22842	663.12679	152.20681	-8.95017	0.00000	
0265	BPM_DN	DRIFT	763.43489	100664.86334	97602.47409	663.04382	152.20681	-8.95017	0.00000	
0266	.....	drift	763.54322	100664.76868	97602.52395	663.02699	152.20681	-8.95017	0.00000	
0267	PM114	MUWIRE	763.68906	100664.64126	97602.59115	663.00428	152.20681	-8.95017	0.00000	
0268	.....	drift	765.02239	100663.47610	97603.20529	662.79687	152.20681	-8.95017	0.00000	
0269	.....	drift	765.16822	100663.34864	97603.27244	662.77417	152.20681	-8.95017	0.00000	
0270	.....	drift	772.80905	100656.67155	97606.79186	661.58549	152.20681	-8.95017	0.00000	
0271	.....	drift	782.48341	100648.21747	97611.24789	660.08044	152.20681	-8.95017	0.00000	
0272	.....	drift	792.15777	100639.76339	97615.70392	658.57539	152.20681	-8.95017	0.00000	
0273	.....	drift	801.83209	100631.30930	97620.15994	657.07034	152.20681	-8.95017	0.00000	
0274	BPM_UP	DRIFT	811.50645	100622.85522	97624.61597	655.56529	152.20681	-8.95017	0.00000	
0275	HP115	BPM	811.78145	100622.61490	97624.74264	655.52251	152.20681	-8.95017	0.00000	
0276	BPM_DN	DRIFT	812.31478	100622.14885	97624.98828	655.43954	152.20681	-8.95017	0.00000	
0277	.....	drift	812.42311	100622.05417	97625.03818	655.42267	152.20681	-8.95017	0.00000	
0278	PM115	MUWIRE	812.56895	100621.92674	97625.10534	655.39997	152.20681	-8.95017	0.00000	
0279	.....	drift	813.90228	100620.76159	97625.71948	655.19255	152.20681	-8.95017	0.00000	
0280	Q60_UP	DRIFT	814.04811	100620.63413	97625.78667	655.16985	152.20681	-8.95017	0.00000	
0281	HQ115	3Q60-2	814.50644	100620.23363	97625.99776	655.09856	152.20681	-8.95017	0.00000	
0282	HQ115	3Q60-2	817.00644	100618.04896	97627.14927	654.70965	152.20681	-8.95017	0.00000	
0283	Q60_DN	DRIFT	819.50643	100615.86429	97628.30077	654.32071	152.20681	-8.95017	0.00000	
0284	MICR_U	DRIFT	820.04810	100615.39096	97628.55028	654.23645	152.20681	-8.95017	0.00000	
0285	HT115	MIHC	820.53770	100614.96314	97628.77577	654.16027	152.20681	-8.95017	0.00000	0.
0286	MICR_D	DRIFT	821.53769	100614.08926	97629.23637	654.00470	152.20681	-8.95017	0.00000	
0287	.....	drift	821.83976	100613.82528	97629.37551	653.95771	152.20681	-8.95017	0.00000	
0288	BPM_UP	DRIFT	842.05599	100596.15898	97638.68717	650.81264	152.20681	-8.95017	0.00000	
0289	VP116	BPM	842.33099	100595.91869	97638.81384	650.76986	152.20681	-8.95017	0.00000	
0290	BPM_DN	DRIFT	842.86432	100595.45261	97639.05948	650.68089	152.20681	-8.95017	0.00000	
0291	Q12_UP	DRIFT	842.97266	100595.35796	97639.10938	650.67002	152.20681	-8.95017	0.00000	
0292	HQ116	3Q120-2	843.54559	100594.85731	97639.37329	650.58092	152.20681	-8.95017	0.00000	
0293	HQ116	3Q120-2	848.54558	100590.48796	97641.67627	649.80306	152.20681	-8.95017	0.00000	
0294	Q12_DN	DRIFT	853.54557	100586.11864	97643.97929	649.02521	152.20681	-8.95017	0.00000	
0295	MICR_U	DRIFT	853.97264	100585.74545	97644.17600	648.95877	152.20681	-8.95017	0.00000	
0296	VT116	MIHC-R	854.46223	100585.31760	97644.40153	648.88259	152.20681	-8.95017	90.00000	0.
0297	MICR_D	DRIFT	855.46223	100584.44375	97644.86212	648.72702	152.20681	-8.95017	0.00000	
0298	.....	drift	855.76430	100584.17977	97645.00126	648.68003	152.20681	-8.95017	0.00000	
0299	.....	drift	868.77720	100572.80824	97650.99502	646.65560	152.20681	-8.95017	0.00000	
0300	.....	drift	881.79010	100561.43670	97656.98881	644.63116	152.20681	-8.95017	0.00000	
0301	.....	drift	894.80297	100550.06517	97662.98259	642.60672	152.20681	-8.95017	0.00000	
0302	.....	drift	907.81587	100538.69364	97668.97635	640.58231	152.20681	-8.95017	0.00000	
0303	BPM_UP	DRIFT	920.82877	100527.32211	97674.97014	638.55788	152.20681	-8.95017	0.00000	
0304	HP117	BPM	921.10377	100527.08179	97675.09681	638.51509	152.20681	-8.95017	0.00000	
0305	BPM_DN	DRIFT	921.63710	100526.61574	97675.34244	638.43212	152.20681	-8.95017	0.00000	
0306	.....	drift	921.74543	100526.52106	97675.39235	638.41526	152.20681	-8.95017	0.00000	

Unofficial Download
(remove this boilerplate by buying an official copy)

0307	PM117	MUWIRE	921.89127	100526.39363	97675.45950	638.39259	152.20681	-8.95017	0.00000	
0308	.....	drift	923.22460	100525.22848	97676.07364	638.18514	152.20681	-8.95017	0.00000	
0309	Q12_UP	DRIFT	923.37043	100525.10102	97676.14083	638.16247	152.20681	-8.95017	0.00000	
0310	HQ117	3Q120-2	923.94333	100524.60036	97676.40471	638.07333	152.20681	-8.95017	0.00000	
0311	HQ117	3Q120-2	928.94332	100520.23105	97678.70773	637.29548	152.20681	-8.95017	0.00000	
0312	Q12_DN	DRIFT	933.94331	100515.86173	97681.01074	636.51762	152.20681	-8.95017	0.00000	
0313	MICR_U	DRIFT	934.37041	100515.48850	97681.20746	636.45119	152.20681	-8.95017	0.00000	
0314	HT117	MIHC	934.86001	100515.06068	97681.43295	636.37501	152.20681	-8.95017	0.00000	0.
0315	MICR_D	DRIFT	935.86000	100514.18683	97681.89355	636.21946	152.20681	-8.95017	0.00000	
0316	.....	drift	936.16207	100513.92286	97682.03269	636.17245	152.20681	-8.95017	0.00000	
0317	SYTR_U	DRIFT	937.95846	100512.35304	97682.86011	635.89299	152.20681	-8.95017	0.00000	
0318	H117	SYTRIM	938.60429	100511.78867	97683.15759	635.79253	152.19507	-8.95017	0.00000	

This is the second Switchyard trim magnet. It serves as a strong horizontal trim, and runs at zero field as its design value.

0319	SYTR_D	DRIFT	941.52095	100509.24016	97684.50155	635.33876	152.18332	-8.95017	0.00000	
0320	.....	drift	941.97928	100508.83973	97684.71280	635.26746	152.18332	-8.95017	0.00000	
0321	BPM_UP	DRIFT	943.55871	100507.45984	97685.44085	635.02176	152.18332	-8.95017	0.00000	
0322	VP118	BPM	943.83371	100507.21959	97685.56762	634.97898	152.18332	-8.95017	0.00000	
0323	BPM_DN	DRIFT	944.36704	100506.75361	97685.81345	634.89601	152.18332	-8.95017	0.00000	
0324	Q12_UP	DRIFT	944.47537	100506.65899	97685.86339	634.87914	152.18332	-8.95017	0.00000	
0325	HQ118	3Q120-2	945.04827	100506.15844	97686.12749	634.79000	152.18332	-8.95017	0.00000	
0326	HQ118	3Q120-2	950.04826	100501.79007	97688.43231	634.01215	152.18332	-8.95017	0.00000	
0327	Q12_DN	DRIFT	955.04825	100497.42168	97690.73713	633.23430	152.18332	-8.95017	0.00000	
0328	MICR_U	DRIFT	955.47535	100497.04855	97690.93398	633.16786	152.18332	-8.95017	0.00000	
0329	VT118	MIHC-R	955.96492	100496.62082	97691.15967	633.09171	152.18332	-8.95017	90.00000	0.
0330	MICR_D	DRIFT	956.96492	100495.74714	97691.62063	632.93614	152.18332	-8.95017	0.00000	
0331	.....	drift	957.26702	100495.48323	97691.75990	632.88912	152.18332	-8.95017	0.00000	
0332	PM118T	TARGMW	957.41285	100495.35580	97691.82712	632.86645	152.18332	-8.95017	0.00000	

A second thin target device for loss monitor calibration.

0333	.....	drift	958.74618	100494.19091	97692.44172	632.65900	152.18332	-8.95017	0.00000	
0334	.....	drift	958.89201	100494.06351	97692.50895	632.63633	152.18332	-8.95017	0.00000	
0335	.....	drift	975.83535	100479.26049	97700.31920	630.00045	152.18332	-8.95017	0.00000	
0336	B2_UPS	DRIFT	976.00202	100479.11489	97700.39604	629.97449	152.18332	-8.95017	0.00000	
0337	V118_1	B2	976.61658	100478.57795	97700.67934	629.87889	152.18332	-8.24916	90.00000	0.
0338	B2_DNS	DRIFT	996.53370	100461.14504	97709.87718	627.02132	152.18332	-7.54815	0.00000	
0339	B2_UPS	DRIFT	997.08580	100460.66099	97710.13256	626.94878	152.18332	-7.54815	0.00000	
0340	V118_2	B2	997.70040	100460.12214	97710.41688	626.86804	152.18332	-6.84742	90.00000	0.
0341	B2_DNS	DRIFT	1017.61752	100442.63261	97719.64459	624.49344	152.18332	-6.14669	0.00000	
0342	.....	drift	1018.16958	100442.14715	97719.90072	624.43435	152.18332	-6.14669	0.00000	
0343	MICR_U	DRIFT	1018.33625	100442.00059	97719.97805	624.41650	152.18332	-6.14669	0.00000	
0344	HT119	MIHC	1018.82585	100441.57008	97720.20518	624.36407	152.18332	-6.14669	0.00000	0.
0345	MICR_D	DRIFT	1019.82585	100440.69072	97720.66916	624.25699	152.18332	-6.14669	0.00000	
0346	Q60_UP	DRIFT	1020.12791	100440.42507	97720.80932	624.22464	152.18332	-6.14669	0.00000	
0347	HQ119	3Q60-2	1020.58625	100440.02202	97721.02195	624.17556	152.18332	-6.14669	0.00000	
0348	HQ119	3Q60-2	1023.08624	100437.82363	97722.18185	623.90787	152.18332	-6.14669	0.00000	
0349	Q60_DN	DRIFT	1025.58624	100435.62524	97723.34176	623.64019	152.18332	-6.14669	0.00000	
0350	BPM_UP	DRIFT	1026.12790	100435.14893	97723.59307	623.58218	152.18332	-6.14669	0.00000	
0351	HP119	BPM	1026.40290	100434.90710	97723.72066	623.55276	152.18332	-6.14669	0.00000	
0352	BPM_DN	DRIFT	1026.93623	100434.43811	97723.96810	623.49564	152.18332	-6.14669	0.00000	
0353	.....	drift	1027.04457	100434.34283	97724.01836	623.48405	152.18332	-6.14669	0.00000	
0354	B2_UPS	DRIFT	1027.21123	100434.19628	97724.09569	623.46621	152.18332	-6.14669	0.00000	
0355	V118_3	B2	1027.82583	100433.65586	97724.38083	623.40039	152.18332	-5.44596	90.00000	0.
0356	B2_DNS	DRIFT	1047.74295	100416.12020	97733.63288	621.51017	152.18332	-4.74524	0.00000	

Unofficial Document
(Teachers and students may find it useful to be aware of)

0357	B2_UPS	DRIFT	1048.29502	100415.63358	97733.88964	621.46451	152.18332	-4.74524	0.00000	
0358	V118_4	B2	1048.90961	100415.09189	97734.17543	621.41368	152.18332	-4.04422	90.00000	0.
0359	B2_DNS	DRIFT	1068.82673	100397.52060	97743.44628	620.00900	152.18332	-3.34321	0.00000	
0360	.....	drift	1069.37880	100397.03313	97743.70346	619.97681	152.18332	-3.34321	0.00000	
0361	Q12_UP	DRIFT	1069.54547	100396.88598	97743.78112	619.96710	152.18332	-3.34321	0.00000	
0362	HQ120	3Q120-2	1070.11840	100396.38015	97744.04802	619.93367	152.18332	-3.34321	0.00000	
0363	HQ120	3Q120-2	1075.11839	100391.96546	97746.37728	619.64207	152.18332	-3.34321	0.00000	
0364	Q12_DN	DRIFT	1080.11838	100387.55077	97748.70650	619.35047	152.18332	-3.34321	0.00000	
0365	.....	drift	1080.54544	100387.17367	97748.90545	619.32557	152.18332	-3.34321	0.00000	
0366	Q12_UP	DRIFT	1080.95532	100386.81179	97749.09640	619.30165	152.18332	-3.34321	0.00000	
0367	HQ121	3Q120-2	1081.52822	100386.30595	97749.36329	619.26825	152.18332	-3.34321	0.00000	
0368	HQ121	3Q120-2	1086.52821	100381.89126	97751.69255	618.97662	152.18332	-3.34321	0.00000	
0369	Q12_DN	DRIFT	1091.52820	100377.47657	97754.02178	618.68502	152.18332	-3.34321	0.00000	
0370	MICR_U	DRIFT	1091.95530	100377.09948	97754.22076	618.66011	152.18332	-3.34321	0.00000	
0371	HT121	MIHC	1092.44490	100376.66719	97754.44881	618.63157	152.18332	-3.34321	0.00000	0.
0372	MICR_D	DRIFT	1093.44489	100375.78425	97754.91466	618.57324	152.18332	-3.34321	0.00000	
0373	MICR_U	DRIFT	1093.74096	100375.51756	97755.05541	618.55562	152.18332	-3.34321	0.00000	
0374	VT121	MIHC-R	1094.23653	100375.08527	97755.28346	618.52708	152.18332	-3.34321	90.00000	0.
0375	MICR_D	DRIFT	1095.23652	100374.20234	97755.74930	618.46874	152.18332	-3.34321	0.00000	
0376	BPM_UP	DRIFT	1095.53862	100373.93560	97755.89005	618.45113	152.18332	-3.34321	0.00000	
0377	HP121	SMABPM	1095.81362	100373.69282	97756.01817	618.43508	152.18332	-3.34321	0.00000	

The final two BPMs in each plane, this one and others to follow, are two times as accurate as the others. This is accomplished by having the plates closer together, thus the nomenclature SMAllBPM.

0378	BPM_DN	DRIFT	1096.34695	100373.22192	97756.26659	618.40398	152.18332	-3.34321	0.00000	
0379	BPM_UP	DRIFT	1096.45529	100373.12625	97756.31709	618.39765	152.18332	-3.34321	0.00000	
0380	VP121	SMABPM	1096.73029	100372.88344	97756.44517	618.38164	152.18332	-3.34321	0.00000	
0381	BPM_DN	DRIFT	1097.26362	100372.41254	97756.69363	618.35050	152.18332	-3.34321	0.00000	
0382	.....	drift	1097.37195	100372.31691	97756.74409	618.34420	152.18332	-3.34321	0.00000	
0383	PM121	TAMUWI	1097.51779	100372.18813	97756.81203	618.33571	152.18332	-3.34321	0.00000	

The final two multiwires, this one and another to follow, are for targeting, thus TargetMUltiWIre. The wire pitch is half as great as in the others, and the area seen is correspondingly reduced.

0384	.....	drift	1098.85112	100371.01087	97757.43316	618.25792	152.18332	-3.34321	0.00000	
0385	.....	drift	1098.99695	100370.88213	97757.50111	618.24942	152.18332	-3.34321	0.00000	
0386	TOR_UP	DRIFT	1135.37883	100338.75913	97774.44963	616.12757	152.18332	-3.34321	0.00000	
0387	TORTGT	TOROID	1135.71216	100338.46481	97774.60491	616.10812	152.18332	-3.34321	0.00000	

Target toroid

0388	TOR_DN	DRIFT	1136.00383	100338.20730	97774.74080	616.09112	152.18332	-3.34321	0.00000	
0389	BPM_UP	DRIFT	1136.37883	100337.87619	97774.91547	616.06924	152.18332	-3.34321	0.00000	
0390	HPTGT	SMABPM	1136.65383	100337.63338	97775.04359	616.05320	152.18332	-3.34321	0.00000	

Target horizontal BPM, vertical follows

0391	BPM_DN	DRIFT	1137.18716	100337.16248	97775.29205	616.02209	152.18332	-3.34321	0.00000	
0392	BPM_UP	DRIFT	1137.29549	100337.06681	97775.34251	616.01580	152.18332	-3.34321	0.00000	
0393	VPTGT	SMABPM	1137.57049	100336.82403	97775.47062	615.99975	152.18332	-3.34321	0.00000	
0394	BPM_DN	DRIFT	1138.10383	100336.35310	97775.71908	615.96865	152.18332	-3.34321	0.00000	
0395	.....	drift	1138.21216	100336.25746	97775.76954	615.96232	152.18332	-3.34321	0.00000	
0396	PMTGT	TAMUWI	1138.35799	100336.12869	97775.83749	615.95382	152.18332	-3.34321	0.00000	

Target multiwire

0397	.....	drift	1139.69132	100334.95146	97776.45861	615.87606	152.18332	-3.34321	0.00000	
0398	.....	drift	1139.83716	100334.82269	97776.52656	615.86757	152.18332	-3.34321	0.00000	
0399	.....	drift	1141.18591	100333.63181	97777.15487	615.78889	152.18332	-3.34321	0.00000	
0400	M_TACA	POINT	1147.18589	100328.33419	97779.94998	615.43896	152.18332	-3.34321	0.00000	

Beginning of shielding cave

Unofficial Beamline Data Sheet
(remove this boilerplate)

0401	.....	drift	1147.18589	100328.33419	97779.94998	615.43896	152.18332	-3.34321	0.00000
0402	BAFL2P	BAFFLE	1160.87015	100316.25183	97786.32480	614.64086	152.18332	-3.34321	0.00000

Horn protection baffle

0403	.....	drift	1165.79140	100311.90666	97788.61735	614.35386	152.18332	-3.34321	0.00000
0404	.....	drift	1167.23146	100310.63517	97789.28821	614.26987	152.18332	-3.34321	0.00000
0405	HALTA1	TAR-2	1168.02214	100309.93708	97789.65655	614.22374	152.18332	-3.34321	0.00000

Upstream part of target. Note that this region contains both horn and target.

0406	MCZERO	TAR-2	1169.17043	100308.92320	97790.19149	614.15678	152.18332	-3.34321	0.00000

Coordinate system origin for Monte Carlo neutrino studies.

0407	ACTRN1	ACTRN1	1169.26886	100308.83629	97790.23733	614.15104	152.18332	-3.34321	0.00000

Marks the beginning of the active part of horn one, which is overlapped with the target.

0408	HALTA2	TAR-2	1169.58677	100308.55558	97790.38542	614.13250	152.18332	-3.34321	0.00000

Downstream part of target, still overlapped with horn one.

0409	ENDFIN	ENDFIN	1171.15140	100307.17412	97791.11433	614.04126	152.18332	-3.34321	0.00000

Target downstream cooling fin

0410	DWNRN1	DWNRN1	1179.01293	100300.23286	97794.77662	613.58276	152.18332	-3.34321	0.00000

Horn one downstream extension

0411	.....	drift	1181.70046	100297.85994	97796.02859	613.42600	152.18332	-3.34321	0.00000
0412	UPHRN2	UPHRN2	1201.79930	100280.11388	97805.39166	612.25380	152.18332	-3.34321	0.00000

Upstream extension, active part, and downstream extension of horn two.

0413	ACTRN2	ACTRN2	1201.97876	100279.95541	97805.47525	612.24333	152.18332	-3.34321	0.00000
0414	DWNRN2	DWNRN2	1211.82126	100271.26511	97810.06038	611.66931	152.18332	-3.34321	0.00000
0415	.....	drift	1217.16574	100266.54625	97812.55014	611.35760	152.18332	-3.34321	0.00000
0416	UPHRN2	UPHRN2	1244.45014	100242.45578	97825.26058	609.76633	152.18332	-3.34321	0.00000

Space for horn two in medium energy neutrino configuration. Similarly location for high energy follows

0417	ACTRN2	ACTRN2	1244.62960	100242.29732	97825.34418	609.75587	152.18332	-3.34321	0.00000
0418	DWNRN2	DWNRN2	1254.47210	100233.60701	97829.92931	609.18185	152.18332	-3.34321	0.00000
0419	.....	drift	1259.81657	100228.88816	97832.41903	608.87014	152.18332	-3.34321	0.00000
0420	UPHRN2	UPHRN2	1290.48023	100201.81400	97846.70372	607.08179	152.18332	-3.34321	0.00000
0421	ACTRN2	ACTRN2	1290.65969	100201.65557	97846.78734	607.07133	152.18332	-3.34321	0.00000
0422	DWNRN2	DWNRN2	1300.50219	100192.96523	97851.37247	606.49720	152.18332	-3.34321	0.00000
0423	.....	drift	1305.84667	100188.24638	97853.86220	606.18557	152.18332	-3.34321	0.00000
0424	M_CAVE	POINT	1309.12750	100185.34960	97855.39057	605.99423	152.18332	-3.34321	0.00000

marks end of target cave

0425	OVERHA	OVERHA	1309.12750	100185.34960	97855.39057	605.99423	152.18332	-3.34321	0.00000

Horn room overhangs decay region approx 10'

0426	DKINHL	DKINHL	1319.09848	100176.54584	97860.03555	605.41270	152.18332	-3.34321	0.00000

Part of decay region inside target hall.

0427	M_THAL	POINT	1337.62698	100160.18629	97868.66709	604.33209	152.18332	-3.34321	0.00000

Marks end of target hall

0428	DK_PCA	DECA44	1337.62698	100160.18629	97868.66709	604.33209	152.18332	-3.34321	0.00000

Six regions of decay region beyond target hall

0429	DK_PCB	DEC150	1483.23857	100031.62011	97936.50032	595.83975	152.18332	-3.34321	0.00000
0430	DK_PCC	DEC150	1975.36357	99597.10363	98165.75711	567.13817	152.18332	-3.34321	0.00000
0431	DK_PCD	DEC100	2467.48857	99162.58714	98395.01387	538.43655	152.18332	-3.34321	0.00000
0432	DK_PCE	DEC100	2795.57190	98872.90950	98547.85172	519.30214	152.18332	-3.34321	0.00000
0433	DK_PCF	DEC125	3123.65524	98583.23187	98700.68957	500.16773	152.18332	-3.34321	0.00000
0434	DENCU	DU_ENU	3533.75940	98221.13479	98891.73686	476.24974	152.18332	-3.34321	0.00000

Absorber (dump) enclosure upstream of absorber, followed by device itself and downstream part of enclosure

0435	DUMP	DUMP	3540.32107	98215.34123	98894.79361	475.86703	152.18332	-3.34321	0.00000
0436	DENCD	DU_END	3564.33677	98194.13685	98905.98135	474.46641	152.18332	-3.34321	0.00000
0437	.....	drift	3583.75930	98176.98793	98915.02937	473.33363	152.18332	-3.34321	0.00000

Unofficial unedited beamsheet
(Leader's saved beamsheet)

0438	MUOND	MUON	3588.68892	98172.63538	98917.32582	473.04613	152.18332	-3.34321	0.00000

First muon alcove, others follow

0439	.....	drift	3590.33212	98171.18453	98918.09130	472.95030	152.18332	-3.34321	0.00000
0440	.....	drift	3593.77628	98168.14356	98919.69576	472.74945	152.18332	-3.34321	0.00000
0441	.....	drift	3633.21311	98133.32325	98938.06744	470.44942	152.18332	-3.34321	0.00000
0442	MUOND	MUON	3638.14269	98128.97070	98940.36390	470.16192	152.18332	-3.34321	0.00000
0443	.....	drift	3639.78590	98127.51985	98941.12938	470.06609	152.18332	-3.34321	0.00000
0444	.....	drift	3643.23005	98124.47888	98942.73384	469.86520	152.18332	-3.34321	0.00000
0445	.....	drift	3702.38528	98072.24841	98970.29133	466.41518	152.18332	-3.34321	0.00000
0446	MUOND	MUON	3707.31490	98067.89586	98972.58782	466.12768	152.18332	-3.34321	0.00000
0447	.....	drift	3708.95807	98066.44501	98973.35330	466.03184	152.18332	-3.34321	0.00000
0448	.....	drift	3712.40222	98063.40404	98974.95776	465.83096	152.18332	-3.34321	0.00000
0449	.....	drift	3810.99428	97976.35326	99020.88693	460.08090	152.18332	-3.34321	0.00000
0450	MUOND	MUON	3815.92390	97972.00071	99023.18338	459.79340	152.18332	-3.34321	0.00000
0451	.....	drift	3817.56710	97970.54986	99023.94887	459.69757	152.18332	-3.34321	0.00000
0452	.....	drift	3821.01126	97967.50889	99025.55333	459.49669	152.18332	-3.34321	0.00000
0453	TUNNEL	TUNNEL	4409.11943	97448.24510	99299.52394	425.19718	152.18332	-3.34321	0.00000

Beam is in rock here, but constructed tunnel is parallel to it

0454	M_ENCU	EX_ENU	4484.70668	97381.50616	99334.73630	420.78879	152.18332	-3.34321	0.00000

MINOS near detector hall upstream region, followed by detector itself and downstream part of hall.

0455	MIN_ND	EXP	4570.35031	97305.88800	99374.63344	415.79389	152.18332	-3.34321	0.00000
0456	M_ENCD	EX_END	4624.93744	97257.69088	99400.06291	412.61026	152.18332	-3.34321	0.00000
0457	.....	drift	4634.95438	97248.84655	99404.72931	412.02608	152.18332	-3.34321	0.00000

Drift space, Fermilab to Soudan

0458	MINOFU	EXP_F2	2413631.69740	-2029748.91592	1221637.51292	-140084.96990	152.18332	-3.34321	0.00000

Far detector upstream end, similarly downstream end follows. Note that the coordinate system is flat, not curved with earth. Thus detector is at 140,000’ below sea level.

0459	MINOFD	EXP_F2	2413690.85266	-2029801.14639	1221665.07041	-140088.41992	152.18332	-3.34321	0.00000

Unofficial annotated beam sheet
(read it's guide to the beamsheet)

4.1 PRIMARY BEAM SYSTEMS

4.1.1 Introduction

The first element in the production chain of NuMI neutrinos is the 120 GeV primary proton beam. This beam is extracted from the Main Injector and transmitted roughly 1200 feet to an underground target hall. The chief criteria, which have guided the design of this beamline, have been transmission of high intensity with minimum losses and precision of targeting.

The beamline specification calls for the transmission of a $4x10^{13}$ proton pulse every 1.9 seconds. While generation of this intensity is not yet possible in the accelerator complex, 50% of it is achievable at present and upgrades are being planned to reach, or exceed, the specified value. At the design intensity, NuMI would use each year a number of protons comparable to that accelerated in Fermilab's entire history to this point.

There are problems associated with transmission of such an intense beam, chiefly associated with the necessity of maintaining minimal losses. The chief concerns are those of activating components and, due to the location of the beamline, contaminating groundwater. If a significant amount of beam, of order one percent, were chronically lost in any region of the line, the components in that region would be activated to a level of greater than 10 rads per hour, making maintenance problematical.

Typically groundwater contamination has not been a problem at Fermilab. This is because the water has been situated many feet below the level of beamlines and accelerators. Basically, in the time taken for any radionuclides to migrate down to the level of an aquifer, several half-lives will have passed and the activity will have been greatly reduced. However for NuMI the primary beam is transmitted to and into the aquifer region. Thus the decay time argument does not apply and the loss criteria are made much more stringent.

The criteria for targeting of the proton beam, specified in detail below, are not unprecedented. However they are nonetheless severe. The one feature that is new is the requirement to point the beam accurately at a distant location, namely the Soudan mine. The secondary hadron and neutrino beams are produced at zero degrees relative to the proton beam and thus it is imperative that the proton beam be accurately directed at Soudan at the point of targeting. Since a primary signature of neutrino oscillations is a shortage of muon neutrinos at the far detector, it is imperative to assure that no deficit arises due simply to poorly aimed beam.

4.1.1.1 Specifications

The specifications established for the proton beam are as follows.

- Positional precision and stability The position specification on the target is established by the physics of the experiment as 0.5 mm. The instrumentation specified will be adequate to fix the beam center within ±100μ and the program Autotune will be used to maintain the position to high precision. The position stability upstream of the target is not fixed by physics. However variation which can be corrected to the 1 mm level is required by aperture considerations.

The level of concern over positional instability depends on how such instability occurs over time. If a variation happens over minutes or hours it can be correctable to a certain level by tuning. If any instability were to be seen as a pulse to pulse jitter, correction would not be possible. A more detailed discussion of stability, in particular in how it pertains to power supply regulation, is found in Appendix A.

.

- Beam angle Assigning an appropriate fraction of the angle error budget, as determined from physics, to the primary beam, yields a required precision of 60 μrad at the target. The final two instrumentation stations are located 12.5 m apart, so that a 1 mm relative position error between them will lead approximately to 80 μrad. The instrumentation itself will operate with a precision of an order of magnitude better than this 1 mm value, so that the real limitation will be on the relative alignment of two detectors.

- Beam size The beam spot on target is to be round with a σ of 1 mm. A different size might be specified for beam intensity different from the nominal 4×10^{13} protons per pulse. The specification on this size is ±10%. It is also necessary that the beam size not change significantly over the 95.4 cm target length. Note that there is a potential contribution to the spot size due to momentum spread, but that the beam design has dispersion functions of effectively zero at the target to prevent this.

- Loss levels Losses must be minimized as they lead to air activation, component residual activity, potential equipment damage and groundwater irradiation or contamination. Loss limits in different regions along the beamline have been determined and are presented in detail in Chapter 5. The most sensitive location is that where the line traverses the interface between soil and rock. The fraction of beam loss in this, rather limited, region must be kept below a few $\times 10^{-6}$,

or a handful of full intensity pulses in the average water residency time of four months. The more downstream locations, the pretarget hall and occupied parts of the carrier tunnel, with relative loss limits of 1.4×10^{-4}, are in some ways more worrisome in that smaller beam missteerings in the stub could lead to striking components there.

4.1.2 System Description: Beamline elements

4.1.2.1 Kicker The requirements on the extraction kicker were originally presumed to be similar to those of the long-batch kicker, which used to be operational at MI52. However the MI52 first Lambertson has been found to be quite highly activated, and our simulations show that indeed the two kicker configuration which precedes it does not provide enough kick to clear the septum cleanly. Since the NuMI extraction region must transmit roughly five times as much beam as MI52 does with a likely larger transverse emittance, it has been decided to construct three, rather than two, kicker magnet modules. The three magnets will together supply 3.8 kG-m of integrated field, and achieve adequate separation at the Lambertson.

The normal operating mode will be one in which five Booster batches, each consisting of 84 18.9nsec bunches, are extracted, a single Booster batch having previously been sent to the antiproton source on the same accelerating cycle. However for periods when antiproton is not in a stacking mode it will be desired to extract six Booster batches to NuMI. This latter mode has essentially the same requirements as did six batch extraction to the Tevatron, which was effected by the MI52 long batch device. The specifications for the kicker system are given in **Table 4.1-1** and a cross-sectional view of a kicker magnet is given in **Figure 4.1-1**. The magnets are to be located in the region downstream of quadrupole Q602.

Physical & Good Field Aperture:	81 mm H x 33 mm V elliptical shape
Kick Angle @ 120 GeV:	950 μrad to inside of ring
Field Rise Time (1%-99%):	1.30 μs
Field Fall Time:	N/A
Field Flattop Time:	9.78 μs minimum (6 batches)
Flattop Integrated Field:	3.8 kG - m
During Pulse:	±0.5%
Pulse to Pulse:	±0.5%
Repetition Rate:	1.9 seconds
Required Charging Time:	1.5 seconds

Table 4.1-1 Extraction Kicker Specifications **(**Specifications from MI Note #258, 1/6/00 D.E.J.)

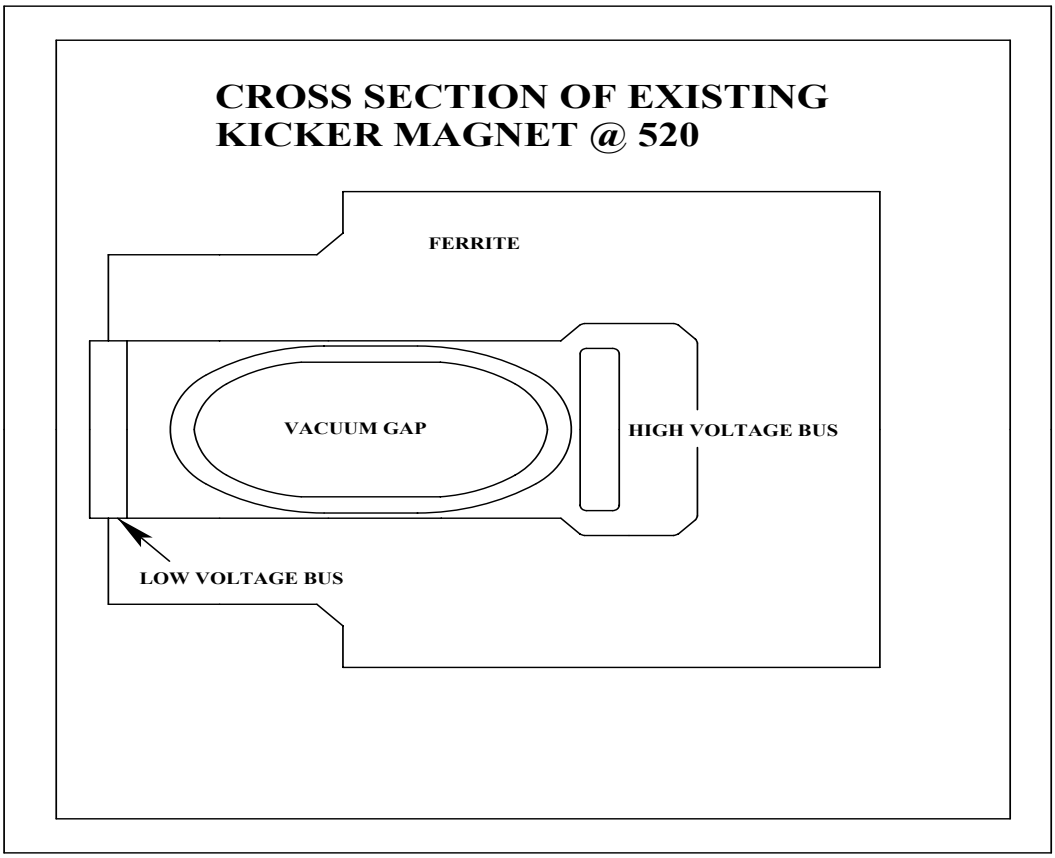

Figure 4.1-1: Kicker magnet cross section

A measured waveform from an existing kicker is shown in **Figure 4.1-2**. It is seen to satisfy the given specifications. However note that there is no criterion given in those specifications for fall time and that there is ringing after the pulse is completed. This feature implies that there can be no beam left in the Main Injector after NuMI extraction and thus that this kicker design is not satisfactory for any scenario in which NuMI beam is extracted first on any given cycle, with extraction to antiproton following.

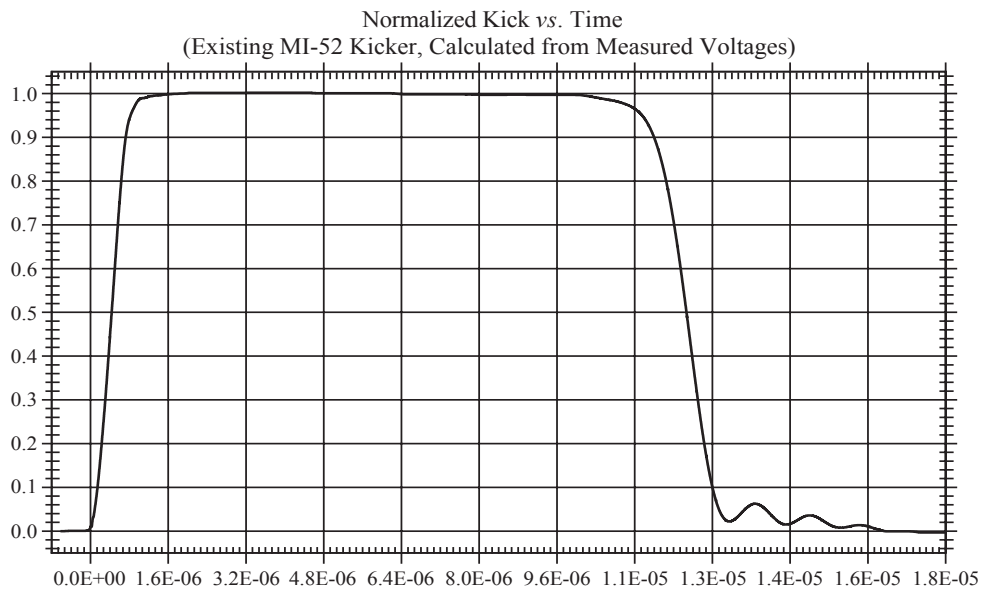

Figure 4.1-2: Measured MI52 long-batch kicker waveform

4.1.2.2 Extraction region The primary active elements for extraction are the three Lambertson magnets. The methodology followed for establishing beam orbits in the MI60 region, where these magnets are located, is as follows. A horizontal excursion of the circulating beam is established, primarily by offsetting several quadrupoles; the required displacements are given in **Table 4.1-2**. Once extraction energy has been approached and beam size has decreased, corrector magnets are used to make an additional contribution to the excursion; **Table 4.1-2** includes the fields. The bumps are all constructed to be local so that the circulating beam is unaffected outside the extraction region. With the circulating beam on its 'extractable' orbit the kicker is fired and creates an extraction bump extending from location 602 through 608 and terminating in the field region of the Lambertsons.

Quadrupole displacements: (x positive is toward the outside of the ring)

Q602: X = 3.1 mm
Q606: X = -.55 mm
Q608: X = -3.9 mm
Q610: X = -3.7 mm
Q612: X = -3.4 mm

Horizontal corrector fields at extraction:

H602: B = -.726 kG
H604: B = -.039 kG
H606: B = .208 kG
H608: B = 1.341 kG
H610: B = 1.427 kG
H612: B = 1.509 kG

Lambertson fields & septa positions:

LAM60A: B = 5.324 kG; X = 2.0 mm, Y = -1.5 mm, rotation = .145 radians
LAM60B: B = 10.734 kG; X = 2.0 mm, Y = 0, rotation = .020 radians
LAM60C: B = 10.734 kG, X = 2.0 mm, Y = 0, no rotation from vertical

Table 4.1-2 Extraction Parameters

A complication is that the strongly focusing MI lattice requires that a quadrupole, Q608, be placed between the Lambertsons. One effect is that the extracted beam passes through this magnet off-center and sees considerable quadrupole steering. This steering must be counteracted by a horizontal kick from the Lambertsons and thus the first two are rolled to provide an outward deflection in what is primarily a vertical bend. A second problem is that the, primarily vertical, kick that Lambertson 1 generates makes the aperture of the quadrupole limiting on the beam which can be transmitted into the line. Due to this effect the first Lambertson is run at a reduced current. To effect extraction Lambertsons 2 and 3 must be run somewhat above their nominal value, though still within their specified current limit. **Figure 4.1-3** shows the circulating and extracted orbits together with an expanded view of the 608 region. The clearances of the beam vs. septa and apertures in the extraction region are discussed in Appendix B.

Figure 4.1-3a. Circulating and extracted beam orbits in the MI60 region

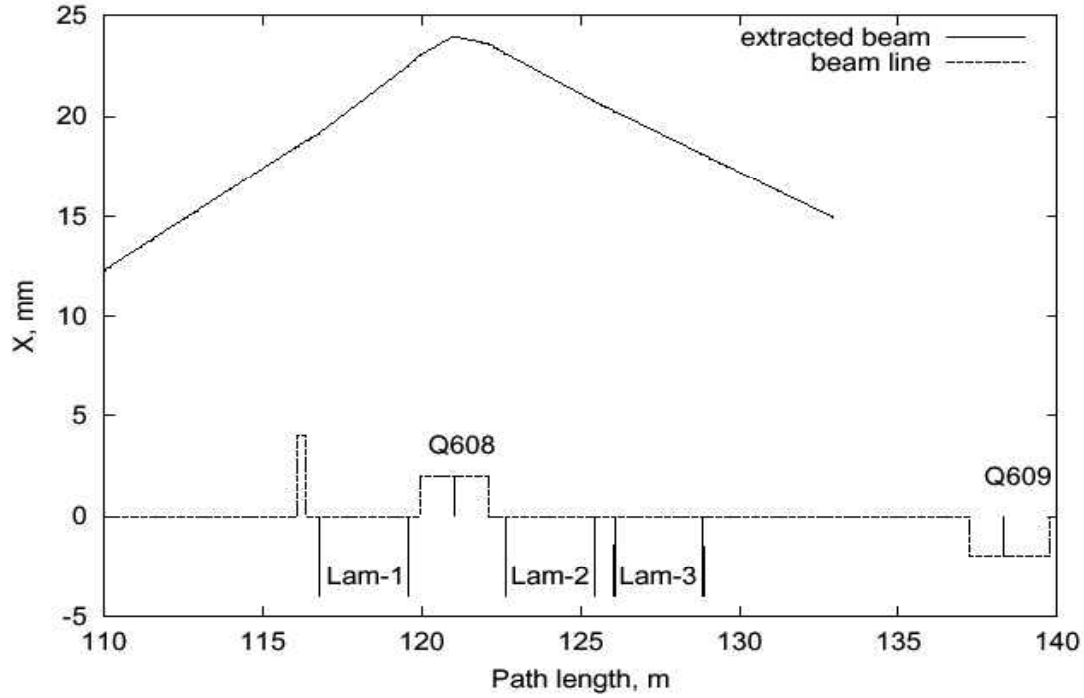

Figure 4.1-3b. Extracted beam orbit through Lambertsons

Figure 4.1-4 shows the results of a tracking study through the extraction channel. The quantity plotted is the fractional beam loss through the extraction region as a function of kicker strength. The losses on the left side of the figure, for too small kick, are found to occur primarily on the septum of Lambertson 1; while those on the right, for too strong kick, occur on the Q608 aperture. The chosen strength of 3.8 kG-m is well centered in the minimal loss region.

The final extraction element is a standard MI C-magnet, installed as a pure vertical bend and positioned as far upstream as possible given physical constraints.

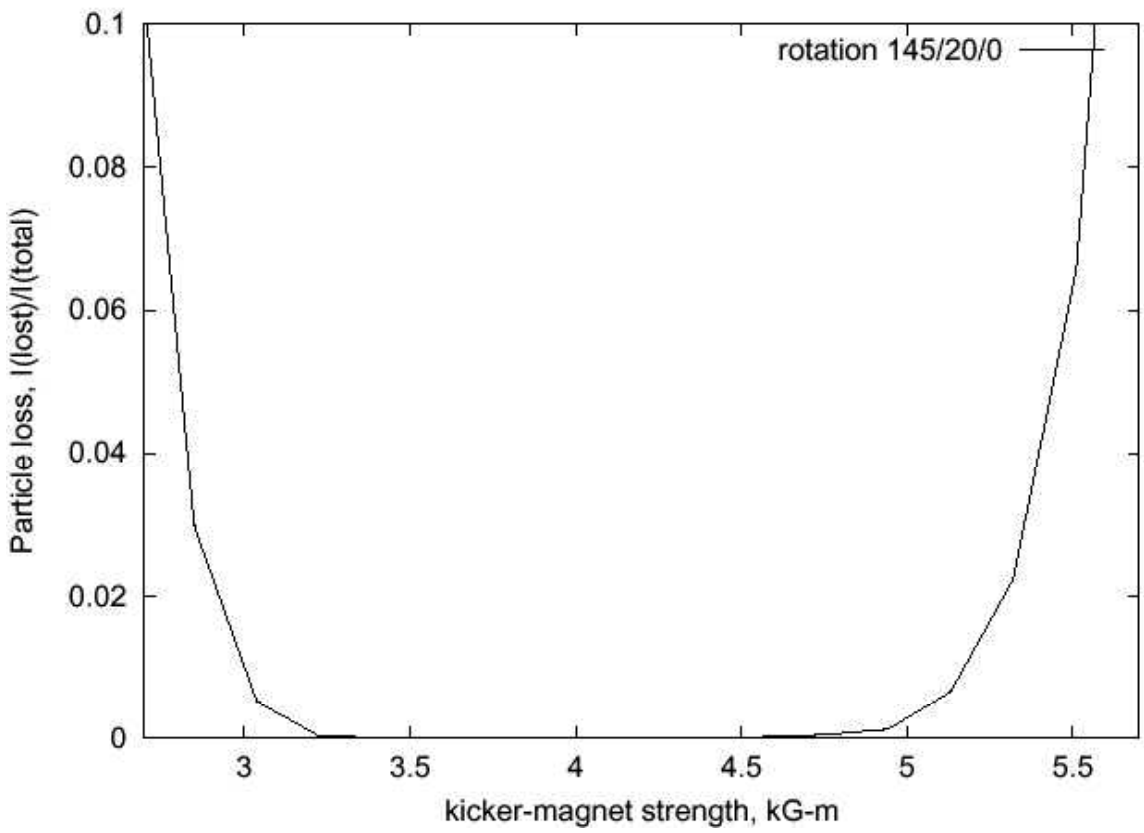

Figure 4.1-4. Extraction losses vs. kicker strength

4.1.2.3 Beam transport and targeting The beam transport consists of three bend regions together with quadrupole focusing in the straight sections connecting them. The quadrupole layout and design principles are discussed in detail in TM-2174 (May 28, 2002; John Johnstone, author). **Table 4.1-3** presents all of the elements of the line.

Element	Number	Purpose/Comment
Dipoles:		
EPB	6	Transport in MI60 region
B2	10	Downbend in NuMI stub, upbend in pretarget
Eartley	2	Trim in MI60 (provides a strong horizontal corrector in this area), 1 horizontal bend in pretarget
Quadrupoles:		
3Q120	17	Transport and targeting
3Q60	4	Transport
Trims:		
Horizontal	10	MI IDH correctors, two to have aperture increased from 1.0” to 1.5”
Vertical	9	MI IDH correctors rolled 90 degrees, two to have aperture increased from 1.0” to 1.5”
Beam instrumentation:		
Horizontal BPMs	13	Two nearest target to have double resolution
Vertical BPMs	11	Two nearest target to have double resolution
Multiwires	10	Two nearest target have .5 mm wire spacing, others have 1 mm wire spacing
Toroids	2	Measure intensity in line with some redundancy
Total loss monitors	4	Integrate losses over major beamline sections
Sealed loss monitors	35	Localize any loss points

Table 4.1-3 Components of the Primary Proton Line

There are 21 quadrupoles in total. The first 15 provide a match with the MI optics, a suitably focused transfer through the MI tunnel and a well-behaved passage through the carrier region where no components are installed. The last 6 form the final focus optics to obtain the desired beam size at the target and also to eliminate vertical and insofar as possible horizontal dispersion there. The final focus segment is optically flexible and can comfortably accommodate tuning to different beam sizes and shapes.

4.1.2.4.Layout Figure 4.1-5a shows the extraction region (partially obscured) and the first beamline bend. It is seen that the NuMI line in this region fits comfortably between the MI below

and the Recycler ring above. The bend in this region comes from a string of six EPB dipoles, powered in series to the design field of 15.0 kG but rolled at five separate angles. In the horizontal plane the deflection is such as to accomplish most of the horizontal bend required to hit Soudan, a small final bend in pretarget accomplishing the remainder. In the vertical the goal is to have the beam exit this region level, or nearly so, so as to avoid generating interferences with existing equipment. The actual pitch angle achieved is -.27 milliradians. **Figure 4.1-5b** shows the NuMI line passing above the A150 line in the MI tunnel.

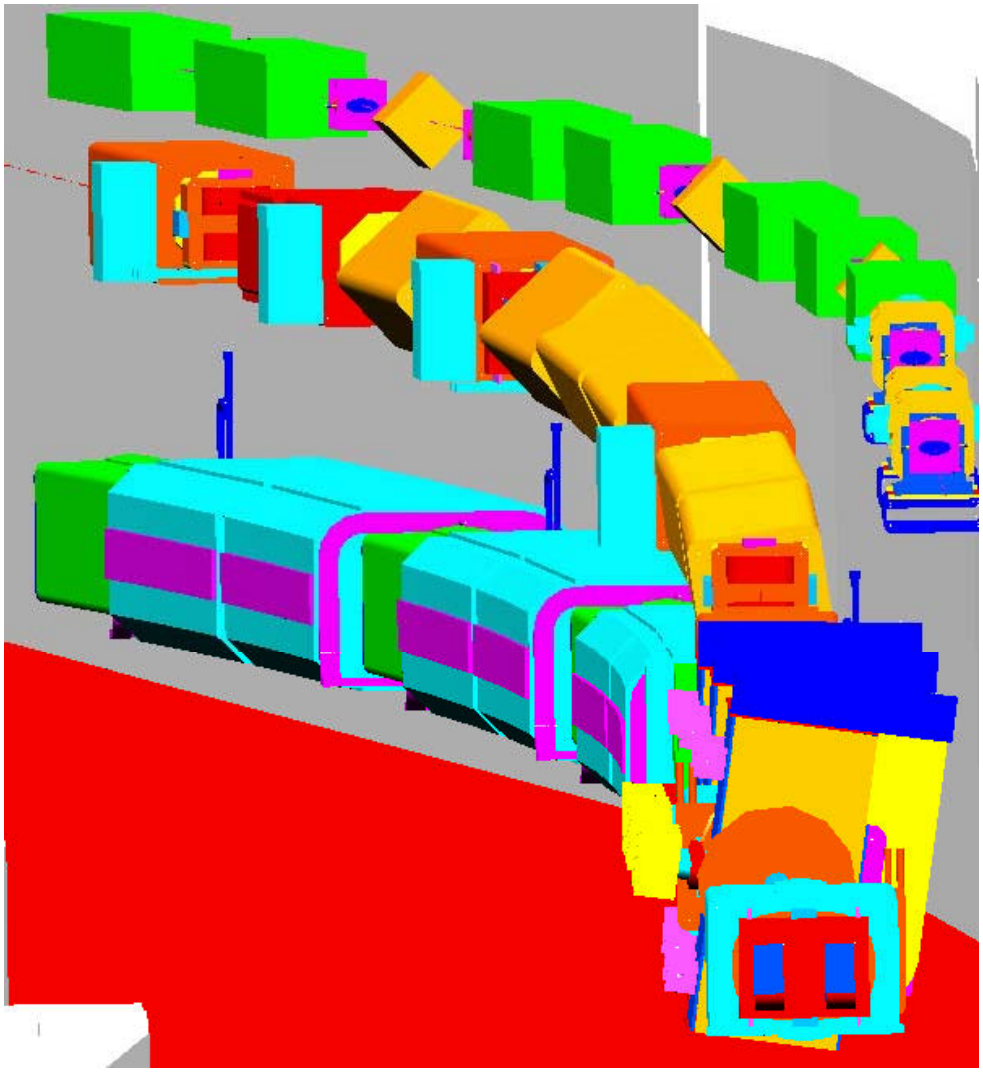

Figure 4.1-5a. The MI60 region, of the NuMI beamline. The MI ring is on the bottom, the Recycler ring is on the top and the NuMI line is between.

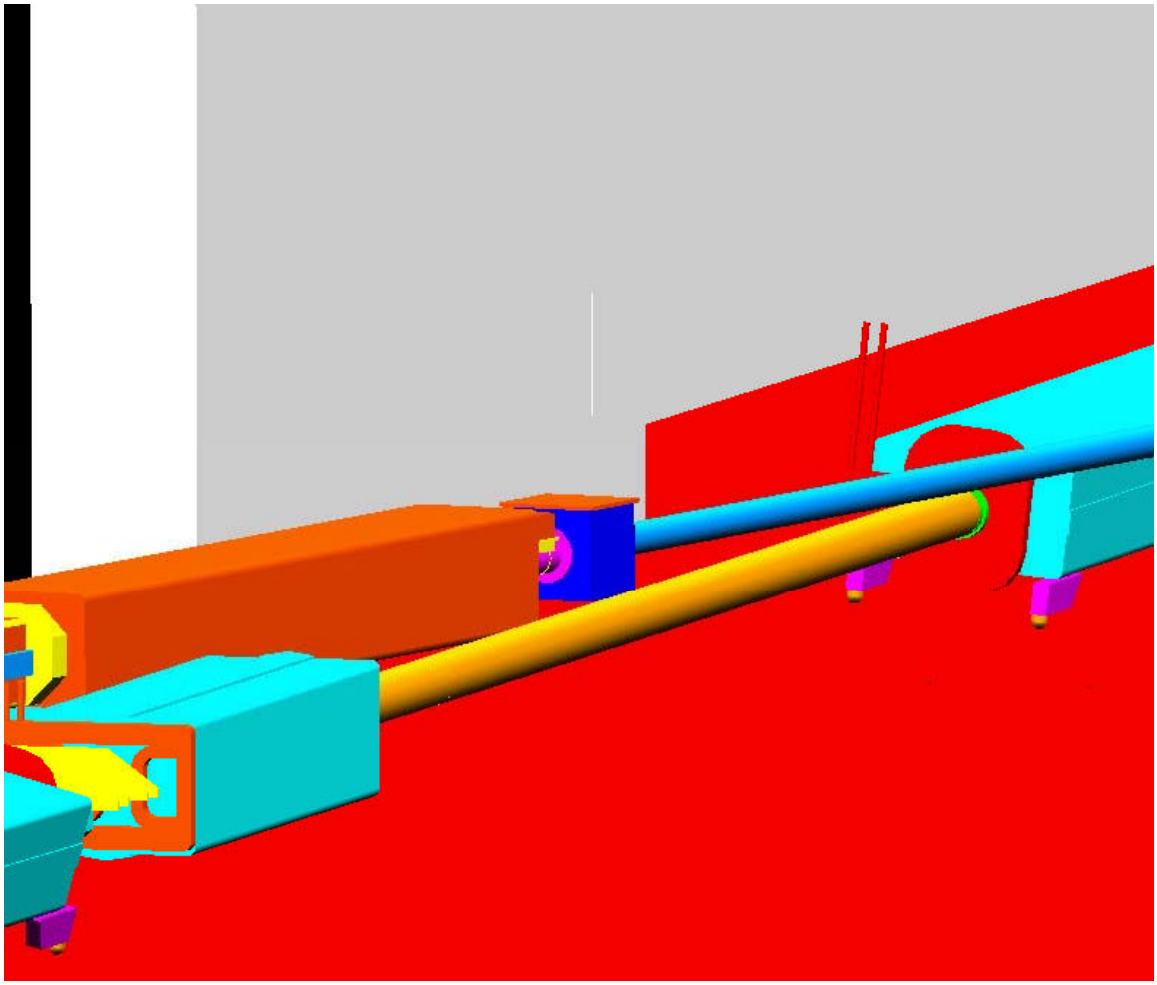

Figure 4.1-5b. View of the region where the NuMI beamline passes above the A150 line

To be directed toward Soudan vertically it is necessary to bend the protons at a pitch of -58 milliradians. What is actually done is to bend by -156 milliradians, the goal having been from a civil construction standpoint to descend below clay soil into bedrock as soon as possible, and then to bend back +98 milliradians to set the final pitch. The downbend occurs in a region known as the northeast extraction enclosure (NuMI stub), basically an alcove-like extension of the MI60 straight section. This region and the beamline in it are pictured in **Figure 4.1-5c**. The downbend is accomplished by a string of six Main Ring B2 magnets, rolled by 90 degrees. The bend field of 17.1 kG is safely below the design value of 17.8 kG. If left uncompensated this major downbend would generate a significant vertical dispersion. A major accomplishment of the optics design is that dispersions are kept reasonable throughout.

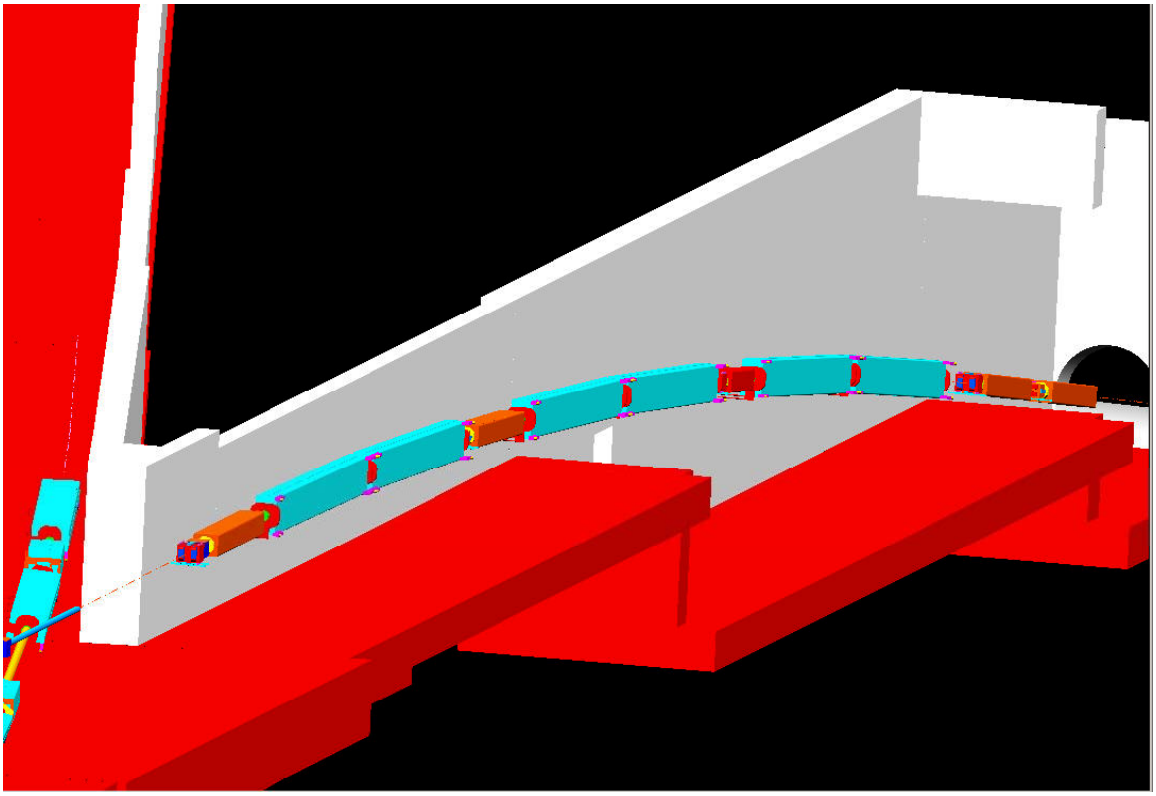

Figure 4.1-5c. View of the NuMI beamline as it traverses the MI northeast extraction enclosure (NuMI stub)

Figure 4.1-5d (in preparation) shows the downstream end of the beamline, the upbend and the focusing region that takes beam to the target. Also present here is the small horizontal bend (.40 milliradians) necessary to hit the target while simultaneously having beam directed toward Soudan. This is effected by a 5' long "Eartley" dipole. The major upbend here is again achieved by rolled B2 dipoles, in this case running at 16.1 kG.

A feature to note, which is only partially indicated by the figure, is that there is a considerable drift space, nearly 23 meters in total, from the last magnet to the target. Some of this space is inside the shielding pile and is reserved for an upstream move of the target if the need ever arises to change the secondary beam focus and raise the neutrino energy. Also inside the shielding is a graphite collimator, or baffle, whose purpose is to protect the target water system and the focusing horns from errant primary beam.

Some of the drift space (~14.25 meters in length) outside the shielding is available for instrumentation. At the upstream end of this space is a complete instrumentation station, with

horizontal and vertical BPMs and a multiwire profile monitor. Each of these monitors is specified to have double the accuracy of the ones in the transport region. Similar instrumentation is placed at the downstream end of the free space. Such good instrumentation at two separate locations allows the proton beam direction on target to be measured quite accurately, assuring that the protons, and thus the secondary mesons and neutrinos, are directed accurately toward Soudan. The target profile monitor is also crucial for ascertaining the beam spot size near the target. The beam will begin to miss the target in the horizontal direction if its width becomes significantly larger than the specified 1 mm sigma.

4.1.3 System Description: Instrumentation

4.1.3.1 Overview

The instrumentation of this beamline is designed to serve two purposes. The first is to assure that the beam is accurately on target and is directed accurately toward the far detector. The pointing requirement on the primary beam, 60μrad as noted above, is about as stringent as those requirements of other fixed target experiments. The second purpose of the instrumentation is to aid in the effort to keep any losses at an absolutely minimum level. It will do this by providing: position information to assure that the beam is in the center of its vacuum chamber, profiles to allow unexpected beam tails and halo to be observed, sensitive loss measurements to allow beam problems to be immediately addressed and intensity measurements in the ring and in the line to serve redundantly with the loss monitors in the case of large losses.

All of the instruments specified are of types that already exist in either the Main Injector complex, the Tevatron or the Switchyard. However NuMI will utilize unprecedented beam intensities at this energy, coupled with the requirement for rigorous control of beam loss. This places a stringent requirement on beam instrumentation precision, calibration and robustness.

4.1.3.2 Profile Monitors

Profile monitors will be of the type known as multi-wires. The operational principle is that of secondary electron emission from wires, which are placed in the beam. There are neither gas nor gas containment windows, which would provide additional material in the beam beyond the wires themselves. There are 10 of these devices, each having 48 horizontal and 48 vertical wires. The wire spacing is 1mm for the upstream eight units and 0.5mm for the last two, which are used in targeting the beam. Placement of the multi-wires along the beam transport is shown

in **Figure 4.1.B-1**,(in Appendix B) along with beam amplitude and dispersion functions. All units will have motion control into and out of the beam as directed through the control system.

A new design is under development to provide profile monitor grids which will scatter an order of magnitude less beam than for the standard 75 micron Tungsten-Rhenium wires, which intercept 10% of the beam and scatter 10^{-4} of it. This is important to enable utilization of the profile monitors during high intensity operation, while maintaining needed beam loss sensitivity for the beam permit system. Prototype beam tests are planned for March '03.

The amplifiers, which produce profile read-back signals, have gains variable in steps over two orders of magnitude, to facilitate operation at different beam intensities. Typical intensity profile readouts from a series of multi-wires are seen in **Figure 4.1-6**. Changing amplitude and dispersion functions affect profile widths significantly.

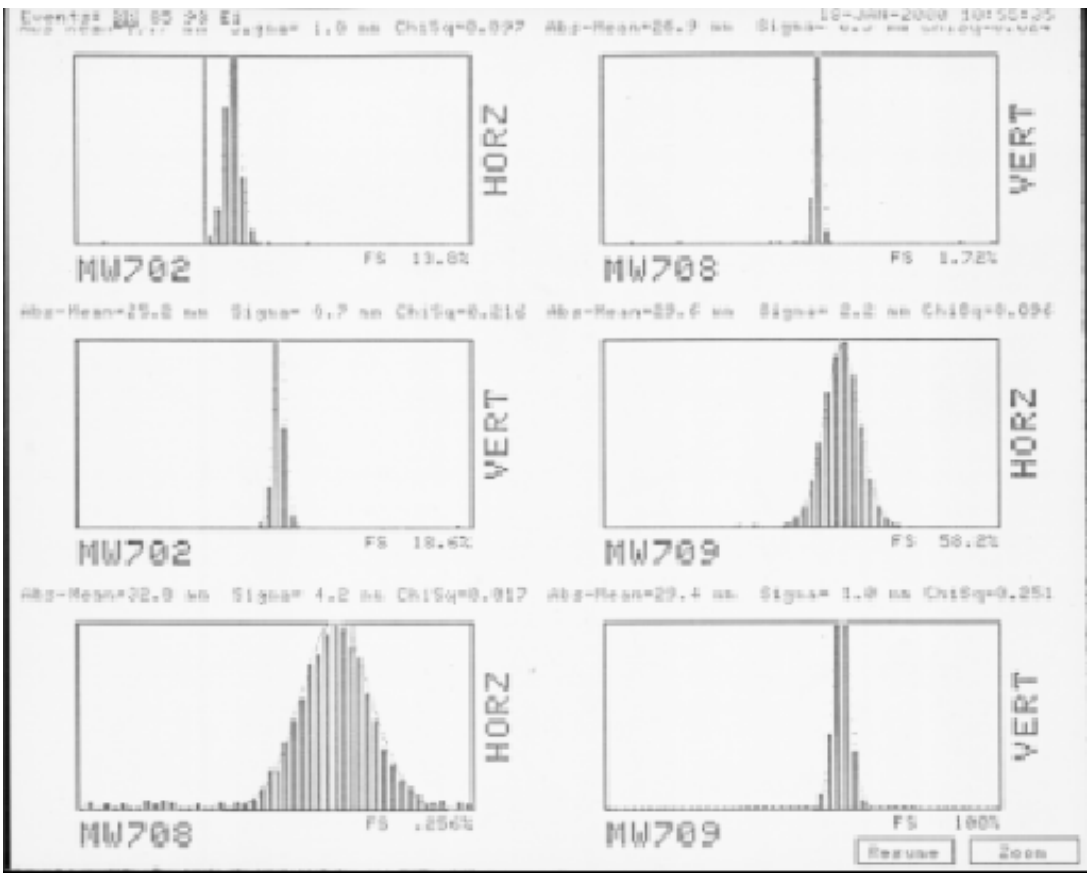

Figure 4.1-6: Horizontal and vertical profiles for a series of three multiwire monitors

4.1.3.3 Position/intensity monitors (BPM's)

There are specified 24 position/intensity monitors, 13 horizontal and 11 vertical. The detectors are standard design split plate Beam Position Monitors. These intercept no beam and will provide position information during normal operation. All units have intensity, as well as position, readouts. BPM specifications are provided in **Table 4.1-4**.

	Transport BPM	Target BPM
# Channels	21	4
System Type	Single Pass	Single Pass
Beam Bunch Freq	53 MHz	53 MHz
# Bunches	80 x (1 to 6)	80 x (1 to 6)
Dynamic Range (particles/bunch)	3e9 – 6e10	3e9 – 6e10
Processing BW	Single batch	Single batch
Position Accuracy (mm) RMS	0.2 @ 1e10 0.3 @ 4.5e9 (over +/- 20 mm)	0.1 @ 1e10 0.15 @ 4.5e9 (over +/- 6 mm)
Plate Diameter (mm)	100	50
Stability (mm)	**	**
Resolution (mm)	**	**
Processing Technology	TBD	TBD
Signal Cables	3/8 in. Heliax	3/8 in. Heliax

** As necessary to provide specified position accuracy in stable and robust form for each beam pulse.

Table 4.1-4 Beam Position Monitor specifications

A significant overlap in beam parameters is seen with those of the Main Injector. Selection of the electronics processing technology will be based on beam tests currently in progress. An important consideration is standardization with other Beams Division systems, currently in planning, to facilitate long term high quality support.

4.1.3.4 Toroid intensity monitors

Toroids are often used for intensity measurements as they provide better accuracy than BPMs, are stable, reliable and subject to absolute calibrations. There is a toroid in the MI ring - observation of the change in ring intensity obtained from it over NuMI extraction provides a measure of the beam delivered. There will be two similar devices in the NuMI line to assure within a few percent accuracy that all beam removed from the MI indeed enters the line and arrives in the vicinity of the target.

4.1.3.5 Loss monitors

Two types of loss monitors will be used, both copies of existing equipment. First there are standard sealed units, 35 in number. These are placed at every location along the beamline where the aperture becomes smaller, as well as at every second magnet in bend strings. A photograph of a sealed unit, indicating the dimensions, is shown as **Figure 4.1-7**. The second type is known as total loss monitors. The present plans are for three of these - two in the carrier tunnel covering separately soil and rock regions, and one covering the length of the pretarget hall. The total loss monitors are sensitive in a calibrated fashion to any and all losses over the region covered.

The electronics to be used for the loss monitors will be like that developed for the Main Injector beamlines, where several decades of linearity have been demonstrated, see **Figure 4.1-8**. These monitors will likely provide the first warning of many types of beam delivery problems. The intensity monitors will see losses at the level of a few percent, but the loss monitors will be several orders of magnitude more sensitive and will provide a primary means of troubleshooting.

Figure 4.1-7: A standard sealed unit loss monitor

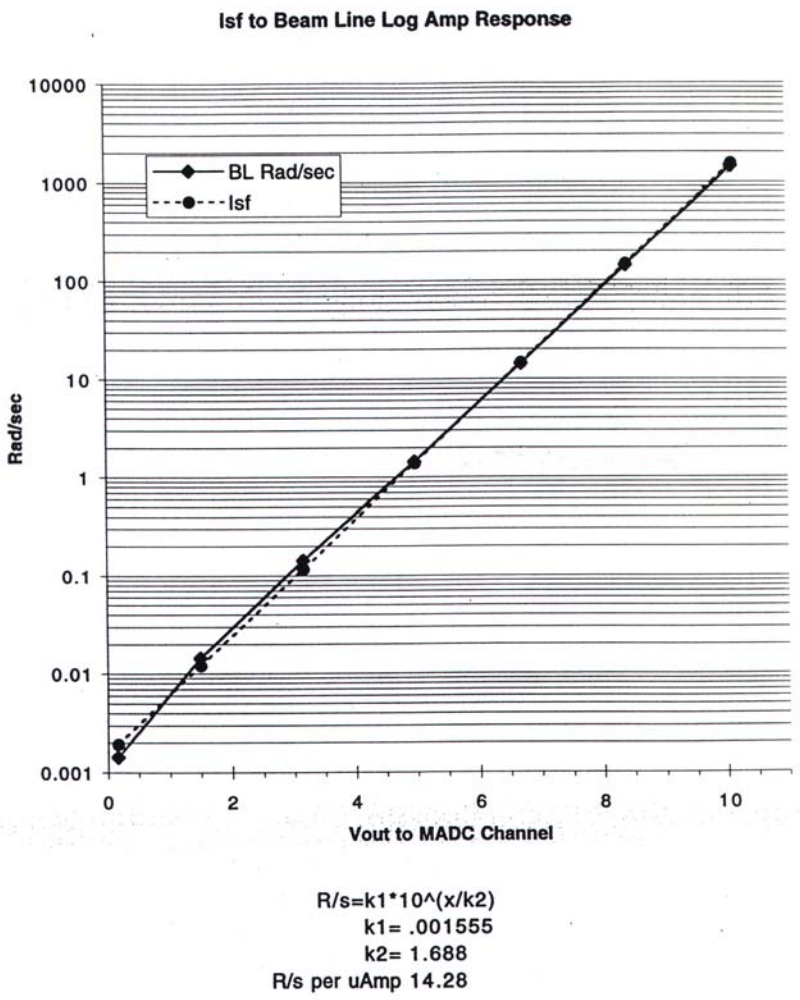

Figure 4.1-8: Measurement of the range and linearity of a standard loss monitor

4.2.11 Target Hall Crane Camera System

4.2.11.1 Target hall crane camera system overview

The purpose of the NuMI target hall crane camera system is twofold. First, to safely operate the crane from a remote location not within line-of-sight of the crane or load. Secondly, to allow precision placement and picks of crane loads. This is to be accomplished using ten miniature video cameras located on the crane with the video signals transmitted wirelessly to receivers at the upstream end of the target hall. These signals will be hard wired to the crane remote operating station in the target hall passageway where they will be displayed on four good resolution video monitors. The crane motion will be controlled using the vendor supplied IR remote controls. The goal is to position the crane and load to within 0.5 inch along the beam direction (x) and transverse to the beam direction (y).

4.2.11.2 Algorithm for precision location of the crane

The travel of the crane in the x direction is from 8 to 211 feet from the upstream face of the target hall. The travel of the crane trolley in the y direction is about 18 feet approximately centered on the proton beam line. A special high contrast scale with one inch graticule spacing is fixed to the crane rail for the full x range and viewed by a video camera (C1) fixed to the crane bridge. The x position is determined by viewing the location of a pointer (fixed to the crane bridge) in the field of the scale. Tests at MI-8 indicate that a resolution of better than 0.5 inch can be achieved. A similar technique is used for the y direction where the scale is attached to the crane bridge and the video camera (C2) and pointer are attached to the crane trolley.

4.2.11.3 Algorithm for location of the crane hook

The crane design specification allows the hook to drop essentially vertically, i.e. with fixed x,y position. However the hook can be remotely controlled to rotate in the horizontal plane. A video camera (C3) is mounted on the bridge trolley to monitor the angular orientation of the hook relative to a scale located on the hook system.

4.2.11.4 Algorithm for safe motion of the crane

Since the crane will not normally be within the line of sight of the operator it is necessary to provide a general view of the region around the crane. A view of the general areas upstream and downstream of the bridge position will be given by video cameras (C4 and C5) mounted on the crane bridge. These cameras leave a blind spot below the bridge. Two video cameras (C6 and C7) will be mounted on the bridge one at each end and will view the area below the crane. As will be seen below in section F, these cameras may require remote control of tilt, zoom and focus.

4.2.11.5 Viewing the crane hook area

The crane hook can be used to lift loads directly, or to attach to special lifting fixtures to lift T-Blocks or Horn/Target Modules. These functions require a good view of the hook area. A video camera (C8) will be mounted on the bridge trolley to monitor the hook area. This camera may require remote control of the tilt, zoom and focus.

4.2.11.6 High quality view of H-Block covers, etc.

To remove and install the H-Blocks, T-Blocks, Modules, etc. it is necessary to have a high-resolution view of the lifting regions, alignment indicators and general view of the top area of the subject unit as well as the area of the slot in which the unit is installed. Video cameras C6, C7 and C8 can provide most of these functions since they can be remotely controlled for tilt, zoom and focus. To see the alignment indicators for installing the T-Blocks, two additional video camera (C9 and C10) will be installed either on a special outrigger attached to the T-Block lifting fixture, or directly on the bridge.

4.2.11.7 Video transmission from the crane to the remote crane operations area.

To minimize cables in the target hall it is proposed to use a wireless video transmission system. For quality and noise reduction the 2.4 GHz non-license frequency band is used. The ten video cameras on the bridge will be connected to four video transmitters each operating at a different frequency within the 2.4 GHz band. Eight signals in two sets of four signals each will be combined using two quad processors. These two video transmitters will send signals that can be viewed on two monitors each displaying in real time four signals, one in each quadrant of the monitor screen. The remaining two signals will be transmitted individually.

The outputs of the four transmitters are combined using an impedance matched power combiner and transmitted using a high gain reflective grid antenna with 8-degree beam width. The antenna is mounted on the upstream side of the bridge and focused horizontally pointing to the upstream wall of the target hall. The receiving antenna is identical in design, mounted on the upstream target hall wall focused horizontally but displaced 5 feet below the axis of the transmitting antenna. This arrangement gives a received signal strength with is somewhat uniform (within a factor of 10) over the range in x of the crane bridge.

The received signal is power divided into four video receivers with frequencies matched to the four video transmitters. The output of the four receivers will be hard wired to four good resolution monitors in the remote crane operations area. For improved resolution the complete video systems should be a color system.

4.2.11.8 Noise in the video system

The main sources of noise in the video system are from (1) radiation from the buss bar sliders which provide power to the bridge and trolley and (2) video signals reflected from the walls of the target hall and arriving at the receiver antenna out of phase with the direct signals. Using very focused transmitting and receiving antennas can minimize both of these sources of noise. In addition the transmitting antenna must be on the opposite end of the bridge from the crane exposed buss system. It may also be necessary to place electrostatic shielding around the buss scraper area. The extent of these noise problems can be tested using the crane in MI-8. An undesirable backup would be to use either an optical fiber or RF cables festooned from the bridge to the remote crane operation area.

4.2.11.9 Power for cameras and transmitters

The video cameras and transmitters use 12-volt power. It is proposed to take 110-volt AC power from the bridge power system to operate a single well-regulated and filtered 12-volt power supply. A festooned system will connect power and video signal cables between the crane bridge and the trolley.

4.2.12 Target Pile Shielding & Carriages

The target pile is installed in the target hall pit. The pit cross section is illustrated in **Figure 4.2-35**. The pit elevation view is illustrated in **Figure 4.2-36**. The pit floor slopes downward from the upstream end to the downstream end of the hall at a theoretical angle of 3.34349° with respect to the LTCSZ (x, y) plane. The pit is 52.5 meters long. The decay pipe protrudes into the pit at the downstream end by about 0.35 meters. The last 4.3 meters of the beam-left pit sidewall at the downstream end is 0.16 meters wider as shown by the dashed line in Figure 4.2-35. This part of the wall is offset to form part of the downstream air labyrinth (with the steel shielding installed). This labyrinth is the passageway that the cooling airflow passes through to exit the target pile and enter the air-cooling equipment located in the target hall. The beam-left pit sidewall stops about 0.5 meters short of the decay pipe shielding concrete. The cooling airflow flows from the passageway mentioned above, through this 0.5-meter opening in the sidewall, and into a plenum located alongside the decay pipe shielding concrete. The cooling airflow turns upward in the plenum and enters the return duct at the top of the decay pipe shielding concrete. The pit walls and floor are concrete and about 1 meter thick.

The major components of the target pile are the steel and concrete shielding, the carriages, and the air-cooling system. The target, baffle, horn 1, horn 2, and beam monitoring instrumentation are installed in the target pile chase.

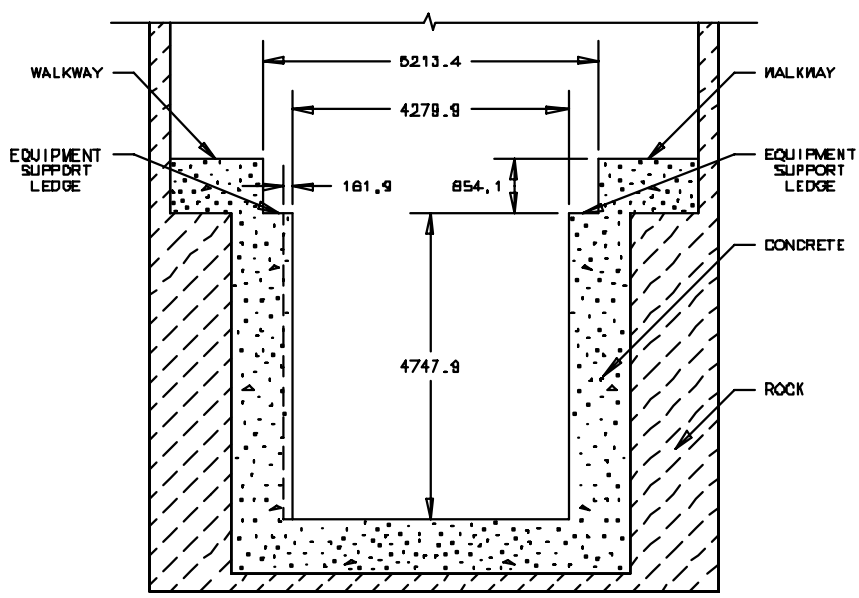

Figure 4.2-35 Target hall pit cross section

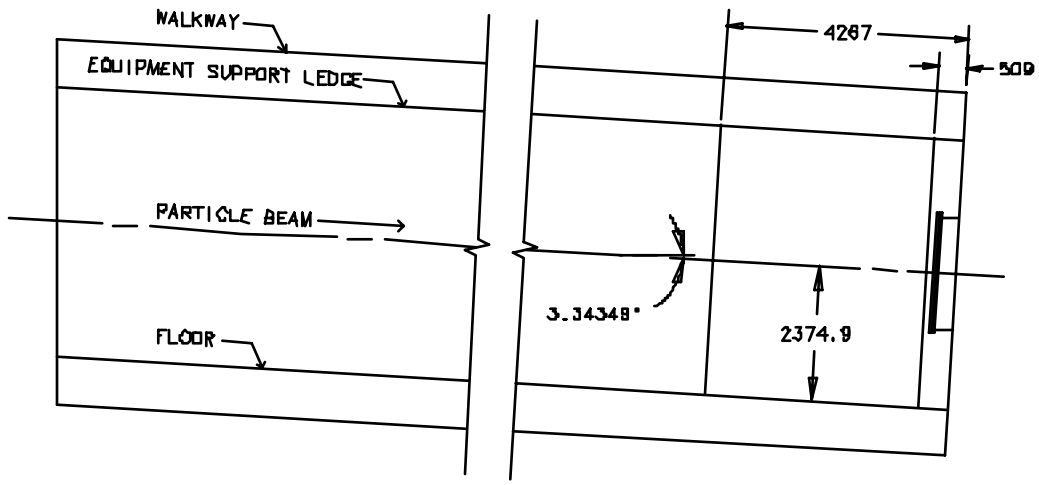

Figure 4.2-36 Target hall pit elevation view

4.2.12.1 Steel and Concrete Shielding

The steel shielding has a rectangular cross section with a central square chase. Beam line components and instrumentation are installed in the chase. The chase also serves as a channel for the cooling airflow. The cross sectional view of the floor and walls of the steel shielding, the concrete pit, and the concrete covers is illustrated in **Figure 4.2-37**. The floor and walls are primarily built using steel blocks referred to as "Duratek blocks" or "blue blocks". These steel blocks measure 1.33 meters x 1.33 meters x 0.67 meters. A company named Duratek manufactured the blocks. Most of these blocks have integral lifting handles and are painted blue. The remaining Duratek blocks are painted green and have integral pick points. The steel blocks in every wall layer are stacked in an interlocked fashion like masonry bricks in a house, that is, gaps between blocks in a row are offset from gaps in the rows immediately below and above it. All wall and floor layers are staggered with respect to each other so the gaps between blocks do not line up and form a line-of-sight crack through the target pile. There is always 0.67 meters of steel between an inner layer gap and the outside surface of the pile. Gaps between blocks can be as large as 2.54 centimeters. In addition to the Duratek blocks, steel blocks of various sizes are used at both the upstream and downstream ends of the pile to fill gaps caused by staggering the Duratek block layers. The "top-out rail" is a layer of steel installed on top of both inner wall layers. Its function is to provide a defined surface for supporting T-blocks anywhere along the length of the target pile. The top-out rails are installed at a prescribed elevation. The steel shielding is installed on four grout rails. The grout rails are installed at a prescribed elevation.

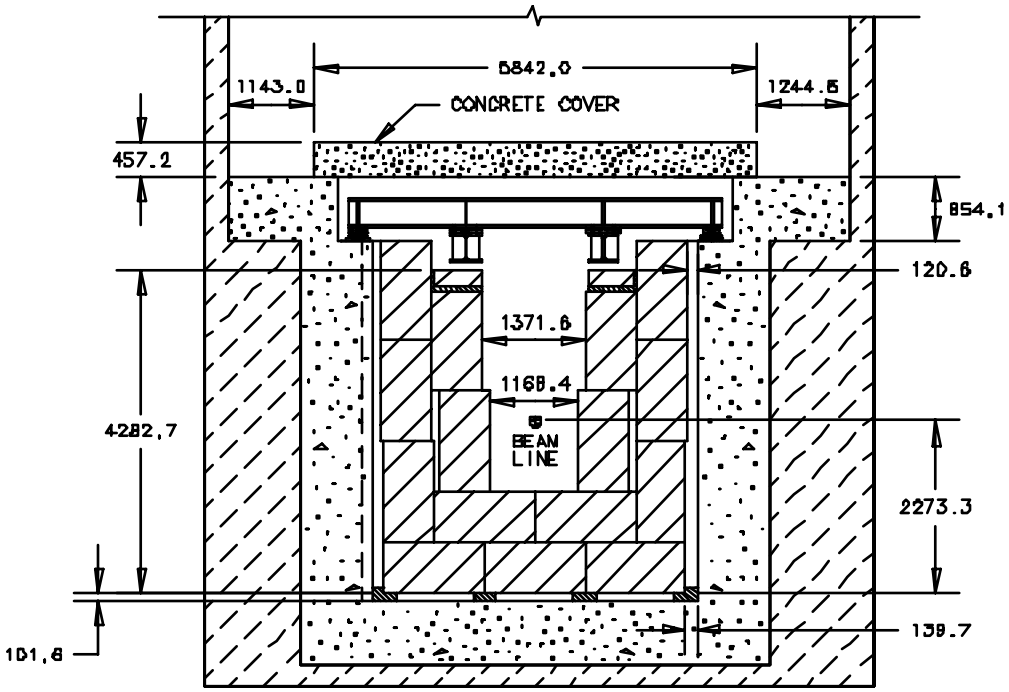

Figure 4.2-37 Steel walls and floor, concrete shielding

Two methods are used to close the top of the shielding block pile. “T-blocks” are used where beam line equipment is installed. A horn 1 module T-block is shown in **Figure 4.2-38**. Duratek blocks are used in all other areas. Two layers of Duratek blocks are used to close the top of the pile between horn 2 and the downstream air labyrinth, as illustrated in **Figure 4.2-39**. Three layers are used between horn 1 and horn 2. As shown in the figure, the Duratek blocks sit on the lower blocks in the inner wall. The inner walls are installed with a 0.1 meter offset between the lower and upper rows of blocks to make this support ledge. Additionally, the ledge forms a radiation labyrinth with two 90° bends when the beam component module is installed. These labyrinths attenuate radiation leakage through the gap between the upper row of Duratek blocks in the inner wall and the module.

Figure 4.2-38 Horn 1 module T-block

Figure 4.2-39 Steel shielding downstream of horn 2

The steel shielding is completely surrounded by concrete. The pit and decay pipe shielding concrete are discussed above. Concrete covers close off the top of the pit. The covers are steel reinforced concrete beams with dimensions of 0.46 by 0.92 by 5.8 meters. A 1.83-meter thick masonry wall is installed at the upstream end of the pit to shield the pre-target area.

The open space between steel shielding blocks, pit floor, and pit walls form cooling channels for the exterior surface of the pile. The channels are named “bottom” and “side”, respectively. The space between the top of the steel shielding pile and the concrete covers is named the “top” channel. The cooling airflow enters the target pile at the downstream end and flows upstream in the top, bottom and side channels. All of the air exits the bottom and side channels at the upstream end of the pile, turns 180°, and enters the chase. All of the air flowing in the top channel flows vertically downward through clearances between the T-blocks and into the chase. The cooling airflow exits the target pile at the downstream end of the chase.

An aluminum air seal is installed across the opening of the pit just under the concrete covers. The covers hold this air seal down when the air-cooling system pressurizes the target pile. The outer surfaces of both the floor and the walls are wrapped with a thin layer of aluminum sheeting that terminates at the top-out rail. This layer of aluminum is provided to

minimize air leakage from the bottom and side channels into the chase through gaps between the Duratek blocks. A grout air seal between the bottom and side channels prevents air leakage from the bottom channels into the side channels. A soft, elastomer seal is provided at the top of each side channel to minimize air leakage into the top channel. Aluminum sheeting is installed over top-closure Duratek blocks and sealed to the top-out rail, as shown in **Figure 4.2-39**. This is done to minimize the leakage of cooling air from the top channel, through the blocks, and into the chase. An aluminum air seal is installed across the upstream end of the pit. This wall of aluminum sheeting is provided to minimize air leakage into the pre-target area and into the equipment morgue.

An air labyrinth is installed at the downstream end of the target pile. Its purpose is to provide a way for the cooling airflow to exit the target pile and to attenuate radiation leakage out of the airflow path to an acceptable level. The air labyrinth consists of the "grill", the pit passageways discussed in the paragraph about the Target Hall pit, and the outer ceiling. The grill is a 0.61 meter thick layer of steel at the very downstream end of the hall with eight, 0.23 by 1.91 meter, equally spaced slots through it. The cooling airflow makes a hard 90 turn upward at the downstream end of the chase, flows through the slots, makes a hard 90 beam-left turn upon exiting the grill and flows into the pit passageways. The outer ceiling consists of two 0.23 meter thick layers of steel slabs installed on the pit horn support ledge directly above the air labyrinth grill. It attenuates radiation leakage through the grill into the target hall. The gaps between slabs are staggered so there is no line of sight crack through the outer ceiling. Aluminum sheeting is installed between the two layers to keep the supply airflow, which enters the target pile in the area above the outer ceiling and below the concrete covers, from leaking into the return air flowing in the air labyrinth. The shielding installation drawings are 8875.126-ME-406820 through 406830.

4.2.12.2 Carriages

A carriage is the structural support for a beam line component module. The Horn 1 carriage is shown in **Figure 4.2-40**. There are three carriages: Horn 1, Horn 2, and Target/Baffle. Horn 1 and Horn 2 carriages are identical. The Target/Baffle carriage is a slightly longer version of the Horn 1/Horn 2 carriage. A carriage consists of two support beams, two cross beams, and four adjustable feet. An adjustable foot is installed at each end of both cross beams. The support beams are parallel to the beam line. The ends of the support beams bolt to the cross beams. The ends of the cross beams sit on the horn support ledge. The carriages are initially installed at

prescribed locations and adjusted as necessary to correctly position the beam line component. The vertical shim stack in each support foot is welded in place after this is accomplished. All of the support feet are free to rotate about all three axes. The upstream, beam-right support foot is not allowed to translate. The downstream, beam-right support foot is free to translate only in the longitudinal, i.e., particle beam, direction. The other two support feet are free to translate in both the lateral and longitudinal directions. The installation assembly drawing for the Horn 1 carriage is 8875.126-ME-427286, 8875.126-ME-427287 for the Horn 2 carriage, and 8875.126-ME-427288 for the Target/Baffle carriage.

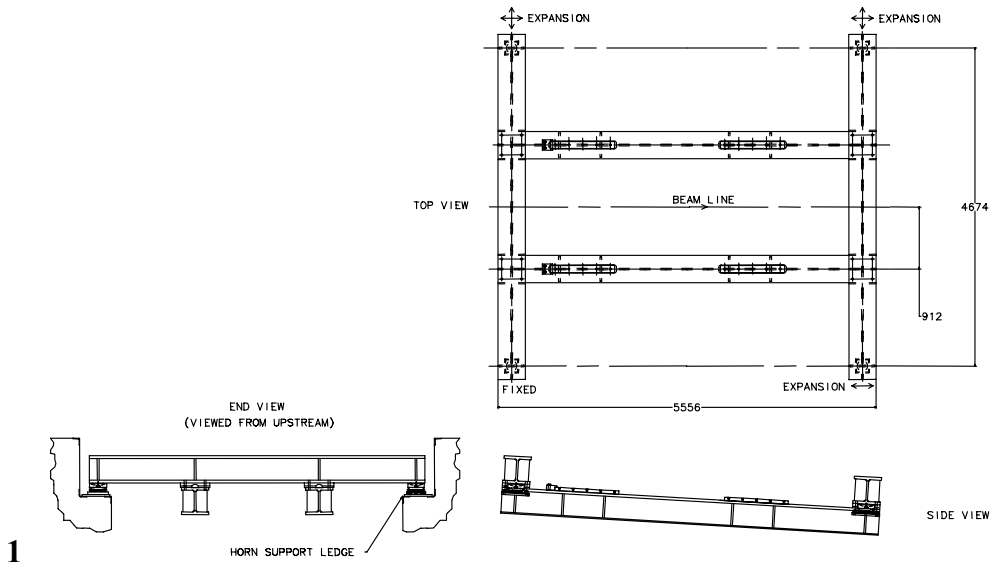

1

Figure 4.2-40 Horn 1 carriage

4.2.13 Target Pile Air Cooling System

The purpose of the air cooling system is (1) to keep the pit floor and walls at approximately 12.8 °C, (2) to remove the following heat loads: beam heating - 158 kW, stripline - 2.4 kW, ambient - 3.4 kW, fan - 50 kW, (3) to dehumidify at a rate of 20 kilograms/hour at the 158 kW beam heating load, and (4) filter particulates from the airflow. The automatically controlled system is designed to provide 240 kW of cooling, and to circulate and filter 750 Nm^3 of air per hour. The high efficiency particulate filters have a minimum removal efficiency of 99.97% with 0.3-micron size particles. The dehumidification rate is based on a leak exchange rate between the target hall and the target pile of 2.5% of the design airflow rate. The filters are installed in bag-in/bag-out housings.

The flow schematic is shown in **Figure 4.2-**41 **a & b**. It is discussed below, starting where the cooling airflow exits the target pile.

Temperature and humidity of the air exiting the target pile are monitored. Humidity of the target hall is also monitored.

Pressure drop across the particulate and high efficiency filter banks are individually monitored. High differential pressure across either bank will shutdown the fan. It is very important to change the filters at the specified pressure drops. In particular, the prefilter will come apart at high-pressure drops, and unload the particulates trapped in it. This will unnecessarily load the much more expensive high efficiency filters, most likely requiring that they be changed immediately.

The airflow is cooled after filtering. An automatically controlled air damper is installed in parallel with the evaporator coils. It will make moderate adjustments in the amount of air flowing to the evaporators to reduce the reheat duty. Air damper position can also be positioned manually. An electrically operated solenoid valve starts or stops the flow of high-pressure liquid refrigerant 22 to each evaporator coil based on the system heat load. Solenoid valve operation can be either automatic or manual. The full-open and full-closed state of each solenoid valve is monitored using limit switches. A self-operated, thermal expansion valve automatically controls flow of refrigerant 22 to each evaporator coil. Evaporator coil header pressure is used to automatically adjust condenser unit capacity to match the system heat load. Operating status of the condensing unit is monitored.

The single-speed fan boosts the airflow to operating pressure after cooling. Fan differential pressure is monitored. The particle beam will shutdown if fan differential pressure is too low. Fan inlet and outlet temperatures are monitored. The fan can be started and stopped in either the target hall or the power supply room.

The reheater heats the airflow to operating temperature when needed. Reheater operation can be either automatic or manual. The heating element is equipped with a high temperature switch to protect it from burning out. Temperature and humidity of the air entering the target pile are monitored. The particle beam will shutdown if supply air temperature to the target pile is high or low for too long.

Slow start, smart motor contactors energize the fan and refrigeration compressor motors. Each contactor will protect its motor from being damaged by current and voltage irregularities. Each motor winding has an internal high temperature switch that is included in the control logic to further protect the motor from damage.

A PLC, programmable logic controller, is used to automatically control the solenoid valves that start and stop high-pressure refrigerant flow to each evaporator coil. Control logic for the fan is hardwired. All monitoring instruments are wired to PLC input modules. The PLC transmits all monitored signals to Acnet via Ethernet. The signals will be displayed on Actnet parameter pages. Selected signals are included on alarm pages and on graphic displays.

The instrument list is given in **Table 4.2-16.5a** and **Table 4.2-16.5b .**

BPS --> Beam Permit System; PSR --> Power Supply Room; PLC --> Programmable Logic Controller; WC --> Water Column

TAG NO.	DESCRIPTION	LOCATION	UNITS	NORMAL OPERATING RANGE	NORMAL OPERATING VALUE	CALIBRATION RANGE	ACCURACY [+ / -]	ANALOG SIGNAL	DISCRETE SIGNAL	MANUFACTURER
AE -	Analysis Element - Supply air relative humidity	Local	%	55 to 65	-	0 - 100				
AE -	Analysis Element - Return air relative humidity	Local	%	30 to 65	-	0 - 100				
AE -	Analysis Element - Target hall relative humidity	Local	%	50 to 100	-	0 - 100				
AIT -	Analysis Indicating Transmitter - Supply air relative humidity	PSR	%	55 to 65	-	0 - 100				
AIT -	Analysis Indicating Transmitter - Return air relative humidity	PSR	%	30 to 65	-	0 - 100				
AIT -	Analysis Indicating Transmitter - Target hall relative humidity	PSR	%	50 to 100	-	0 - 100				
HC -	Hand control, Open Auto Close - Evaporator #1 upper coil	PSR	-	-	-	-	-	-	0 to 110 VAC	
HC -	Hand control, Open Auto Close - Evaporator #1 lower coil	PSR	-	-	-	-	-	-	0 to 110 VAC	
HC -	Hand control, Open Auto Close - Evaporator #2 upper coil	PSR	-	-	-	-	-	-	0 to 110 VAC	
HC -	Hand control, Open Auto Close - Evaporator #2 lower coil	PSR	-	-	-	-	-	-	0 to 110 VAC	
HC -	Hand control, Open Auto Close - Evaporator #3 upper coil	PSR	-	-	-	-	-	-	0 to 110 VAC	
HC -	Hand control, Open Auto Close - Evaporator #3 lower coil	PSR	-	-	-	-	-	-	0 to 110 VAC	
HC -	Hand control, Open Auto Close - Evaporator #1 upper coil	Acnet command to PLC	-	-	-	-	-	-	-	-
HC -	Hand control, Open Auto Close - Evaporator #1 lower coil	Acnet command to PLC	-	-	-	-	-	-	-	-
HC -	Hand control, Open Auto Close - Evaporator #2 upper coil	Acnet command to PLC	-	-	-	-	-	-	-	-
HC -	Hand control, Open Auto Close - Evaporator #2 lower coil	Acnet command to PLC	-	-	-	-	-	-	-	-
HC -	Hand control, Open Auto Close - Evaporator #3 upper coil	Acnet command to PLC	-	-	-	-	-	-	-	-
HC -	Hand control, Open Auto Close - Evaporator #3 lower coil	Acnet command to PLC	-	-	-	-	-	-	-	-
HC -	Hand control, Start - Fan	PSR	-	-	-	-	-	-	0 to 110 VAC	
HC -	Hand control, Start - Fan	Local	-	-	-	-	-	-	0 to 110 VAC	
HC -	Hand control, Stop - Fan	PSR	-	-	-	-	-	-	0 to 110 VAC	
HC -	Hand control, Stop - Fan	Local	-	-	-	-	-	-	0 to 110 VAC	
HC -	Hand control, On Off Auto - Reheater	PSR - Vendor panel	-	-	-	-	-	-		-
IE -	Current Element - Fan motor	Fan motor contactor	%	55 to 70	65	0 - 100		_ to _ VDC	-	
ISL -	Current Switch Low - Fan motor (Fan "on" signal to software logic)	Fan motor contactor	%	0 - 100	25			-	0 to 24 VDC	
ISL -	Current Switch Low - Fan motor (Fan "on" signal to hardwired logic)	Fan motor contactor	%	0 - 100	25			-	0 to 24 VDC	
JL -	Power Light - Reheater on	PSR - Vendor panel	-	-	-	-	-	-	-	-
PDI -	Pressure Differential Indicator / Switch - Prefilter bank	PSR	inches WC	0.7 to 1.3	< 1.5	0 to 3	± 2% FS	-	-	Dwyer
PDI -	Pressure Differential Indicator / Switch - High efficiency filter bank	PSR	inches WC	1.5 to 3	< 3	0 to 5	± 2% FS	-	-	Dwyer
PDI -	Pressure Differential Indicator / Switch - Fan	PSR	inches WC	10 to 13	12	0 to 15	± 2% FS	-	-	Dwyer
PDIT -	Pressure Differential Transmitter - Fan	PSR	inches WC	10 to 13	12	0 to 20	1% FS	0 to 10 VDC	-	Orange Research
PDSHH -	Pressure Differential Switch High - Prefilter bank	PSR	inches WC	-	1.25	-	-	-	0 to 24 VDC	Dwyer
PDSHH -	Pressure Differential Switch High - High efficiency filter bank	PSR	inches WC	-	2.75	-	-	-	0 to 24 VDC	Dwyer
PDSHH -	Pressure Differential Switch High High - Prefilter bank	PSR	inches WC	-	1.5	-	-	-	0 to 24 VDC	Dwyer
PDSHH -	Pressure Differential Switch High High - High efficiency filter bank	PSR	inches WC	-	3	-	-	-	0 to 24 VDC	Dwyer
PDSLL -	Pressure Differential Switch Low Low - Fan	PSR	inches WC	-	8	-	-	-	0 to 24 VDC	Dwyer
PDT -	Pressure Differential Transmitter - Prefilter bank	PSR	inches WC	0.7 to 1.3	< 1.5	0 to 2.5	± 0.25% FS	4 to 20 mA	-	Setra
PDT -	Pressure Differential Transmitter - High efficiency filter bank	PSR	inches WC	1.5 to 3	< 3	0 to 5	± 0.25% FS	4 to 20 mA	-	Setra
PDT -	Pressure Differential Transmitter - Fan	PSR	inches WC	10 to 13	12	0 to 25	± 0.25% FS	4 to 20 mA	-	Setra
PI -	Pressure Indicator - Evaporator coils	PSR	psig	58 to 69	61.75	0 to 100	± 2% FS	-	-	Dwyer
PIT -	Pressure Transmitter - Evaporator coils	PSR	psig	58 to 69	61.75	0 to 100	± 0.11% FS	4 to 20 mA	-	Setra
TE -	Temperature Element - Return air temperature from target pile	Local	°F	50 to 80	< 80	40 to 100	±0.5	-	-	Minco
TE -	Temperature Element - Supply air temperature to target pile	Local	°F	50 to 60	55	40 to 100	±0.5	-	-	Minco
TE -	Temperature Element - Fan inlet temperature	Local	°F	45 to 55	50	40 to 100	±0.5	-	-	Minco
TE -	Temperature Element - Fan discharge temperature	Local	°F	50 to 60	55	40 to 100	±0.5	-	-	Minco
TE -	Temperature Element - Target pile pit wall #1 @ horn 1 midpoint	Local	°F	50 to 60	55	40 to 100	±2	-	-	Omega
TE -	Temperature Element - Target pile pit wall #2 @ horn 1 midpoint	Local	°F	50 to 60	55	40 to 100	±2	-	-	Omega
TE -	Temperature Element - Target pile pit floor #1 @ horn 1 midpoint	Local	°F	50 to 60	55	40 to 100	±2	-	-	Omega
TE -	Temperature Element - Target pile pit floor #2 @ horn 1 midpoint	Local	°F	50 to 60	55	40 to 100	±2	-	-	Omega
TE -	Temperature Element - Duratek block inner wall #1 @ horn 1 midpoint	Local	°F	50 to 60	55	40 to 100	±2	-	-	Omega
TE -	Temperature Element - Duratek block inner wall #2 @ horn 1 midpoint	Local	°F	50 to 60	55	40 to 100	±2	-	-	Omega
TE -	Temperature Element - Horn 1 carriage support beam @ midpoint	Local	°F	50 to 60	55	40 to 100	±2	-	-	Omega
TE -	Temperature Element - Free air at upstream end of horn 1 carriage	Local	°F	50 to 60	55	40 to 100	±2	-	-	Omega
TIC -	Temperature Indicating Controller - Air damper	PSR	°F	50 to 60	55	40 to 100	-	4 to 20 mA	-	
TIC -	Temperature Indicating Controller - Reheater control	PSR - Vendor panel	°F	50 to 60	55	40 to 100	-	4 to 20 mA	-	
TSH -	Target pile supply air temperature high - Reheater control	PSR - Vendor panel	°F	50 to 65	65	-				
TSHH -	Heating element temperature high - Reheater control	PSR - Vendor panel	°F							
TSHH -	Target pile supply air temperature high high	Local	°F	50 to 70	70	-		-	0 to 24 VDC	
TT -	Temperature Transmitter - Fan discharge temperature	PSR	°F	50 to 60	55	40 to 100		4 to 20 mA	-	
TTI - - 1	Temperature Transmitting Indicator - to PLC	PSR	°F	50 to 60	55	40 to 100		4 to 20 mA	-	
TTI - - 2	Temperature Transmitting Indicator - to Reheater control	PSR	°F	50 to 60	55	40 to 100		4 to 20 mA	-	
ZSH -	Position Indicator - Fan contactor closed (auxiliary contact)	Motor contactor	-	-	-	-	-	-	0 to 110 VAC	
ZSH -	Position Indicator - Solenoid valve HV-nnn open	Local	-	-	-	-	-	-	0 to 24 VDC	
ZSH -	Position Indicator - Solenoid valve HV-nnn open	Local	-	-	-	-	-	-	0 to 24 VDC	
ZSH -	Position Indicator - Solenoid valve HV-nnn open	Local	-	-	-	-	-	-	0 to 24 VDC	
ZSH -	Position Indicator - Solenoid valve HV-nnn open	Local	-	-	-	-	-	-	0 to 24 VDC	
ZSH -	Position Indicator - Solenoid valve HV-nnn open	Local	-	-	-	-	-	-	0 to 24 VDC	
ZSH -	Position Indicator - Solenoid valve HV-nnn open	Local	-	-	-	-	-	-	0 to 24 VDC	
ZSL -	Position Indicator - Solenoid valve HV-nnn closed	Local	-	-	-	-	-	-	0 to 24 VDC	
ZSL -	Position Indicator - Solenoid valve HV-nnn closed	Local	-	-	-	-	-	-	0 to 24 VDC	
ZSL -	Position Indicator - Solenoid valve HV-nnn closed	Local	-	-	-	-	-	-	0 to 24 VDC	
ZSL -	Position Indicator - Solenoid valve HV-nnn closed	Local	-	-	-	-	-	-	0 to 24 VDC	
ZSL -	Position Indicator - Solenoid valve HV-nnn closed	Local	-	-	-	-	-	-	0 to 24 VDC	
ZSL -	Position Indicator - Solenoid valve HV-nnn closed	Local	-	-	-	-	-	-	0 to 24 VDC	
ZT -	Position Transmitter - Air damper	Local	%			0 to 100		4 to 20 mA	-	
ZTI -	Position Transmitting Indicator - Air damper	PSR	%			0 to 100		4 to 20 mA	-	
Energize HV -	PLC logic output signal	PLC	-	-	-	-	-	-	0 to 110 VAC	-
Energize HV -	PLC logic output signal	PLC	-	-	-	-	-	-	0 to 110 VAC	-
Energize HV -	PLC logic output signal	PLC	-	-	-	-	-	-	0 to 110 VAC	-
Energize HV -	PLC logic output signal	PLC	-	-	-	-	-	-	0 to 110 VAC	-
Energize HV -	PLC logic output signal	PLC	-	-	-	-	-	-	0 to 110 VAC	-
Energize HV -	PLC logic output signal	PLC	-	-	-	-	-	-	0 to 110 VAC	-

Table 4.2-16.5a Air-cooling system instrument list – Part 1

TAG NO.	MODEL NUMBER	INSTRUMENT DESCRIPTION	CABLE	WIRED TO	PLC INPUT MODULES	PLC OUTPUT HARDWIRED TO	PLC OUTPUT MODULES	ACNET PARAMETER PAGE	ACNET GRAPHIC DISPLAY	ACNET ALARM SET POINT
AE -				AIT -	-	-	-	-	-	-
AE -				AIT -	-	-	-	-	-	-
AE -				AIT -	-	-	-	-	-	-
AIT -				PLC	AIM1 Ch 1	-	-	Yes	Yes	65
AIT -				PLC	AIM1 Ch 2	-	-	Yes	Yes	65
AIT -				PLC	AIM1 Ch 3	-	-	Yes	Yes	-
HC -				HV -	-	-	-	-	-	-
HC -				HV -	-	-	-	-	-	-
HC -				HV -	-	-	-	-	-	-
HC -				HV -	-	-	-	-	-	-
HC -				HV -	-	-	-	-	-	-
HC -				HV -	-	-	-	-	-	-
HC -	-	-	-	-	-	-	-	Yes	-	-
HC -	-	-	-	-	-	-	-	Yes	-	-
HC -	-	-	-	-	-	-	-	Yes	-	-
HC -	-	-	-	-	-	-	-	Yes	-	-
HC -	-	-	-	-	-	-	-	Yes	-	-
HC -	-	-	-	-	-	-	-	Yes	-	-
HC -				Fan motor contactor control circuit	-	-	-	-	-	-
HC -				Fan motor contactor control circuit	-	-	-	-	-	-
HC -				Fan motor contactor control circuit	-	-	-	-	-	-
HC -				Fan motor contactor control circuit	-	-	-	-	-	-
HC -	-	-	-	Vendor panel wiring	-	-	-	-	-	-
IE -				II -	-	-	-	-	-	-
ISL -	On II -			PLC	DIM1 Ch 1	-	-	Yes	-	-
ISL -	On II -			Fan motor contactor	-	-	-	-	-	-
JL -	-	-	-	Reheater vendor panel wiring	-	-	-	-	-	-
PDI -	Photohelic 3003MR	Differential pressure gauge with two switches	-	-	-	-	-	-	-	-
PDI -	Photohelic 3005MR	Differential pressure gauge with two switches	-	-	-	-	-	-	-	-
PDI -	Photohelic 3015MR	Differential pressure gauge with two switches	-	-	-	-	-	-	-	-
PDIT -	20107 w/LCD Display	Beryllium copper diaphragm with inductive pickup		BPS	-	-	-	-	-	-
PDSHH -	On PDI -	Phototransistor actuated SPDT relay, 1.0 amp @30 vdc		PLC	DIM1 Ch 2	-	-	Yes	-	-
PDSHH -	On PDI -	Phototransistor actuated SPDT relay, 1.0 amp @30 vdc		PLC	DIM1 Ch 3	-	-	Yes	-	-
PDSHH -	On PDI -	Phototransistor actuated SPDT relay, 1.0 amp @30 vdc		PLC	DIM1 Ch 4	-	-	No	-	-
PDSHH -	On PDI -	Phototransistor actuated SPDT relay, 1.0 amp @30 vdc		PLC	DIM1 Ch 5	-	-	No	-	-
PDSLL -	On PDI -	Phototransistor actuated SPDT relay, 1.0 amp @30 vdc		PLC	DIM1 Ch 6	-	-	No	-	-
PDT -	C-264 Option 717	Variable capacitance		PLC	AIM1 Ch 4	-	-	Yes	Yes	1.25
PDT -	C-264 Option 717	Variable capacitance		PLC	AIM1 Ch 5	-	-	Yes	Yes	2.75
PDT -	C-264 Option 717	Variable capacitance		PLC	AIM1 Ch 6	-	-	Yes	Yes	8
PI -	Photohelic A36010S	Pressure gauge with two switches	-	-	-	-	-	-	-	-
PIT -	C-204	Variable capacitance		Refrigerator compressor control	-	-	-	-	-	-
TE -	S457PEZ24	Bendable averaging RTD, 100 Ω at 0 ºC		PLC	RTD IM1 Ch 1	-	-	Yes	No	-
TE -	S457PEZ12	Bendable averaging RTD, 100 Ω at 0 ºC		TTI -	-	-	-	-	-	-
TE -	S457PEZ12	Bendable averaging RTD, 100 Ω at 0 ºC		PLC	RTD IM1 Ch 2	-	-	Yes	No	-
TE -	S457PEZ12	Bendable averaging RTD, 100 Ω at 0 ºC		TIC -	-	-	-	-	-	-
TE -		Omegaclad Type J - MgO insulation and metal sheath		PLC	T/C IM1 Ch 1	-	-	Yes	No	-
TE -		Omegaclad Type J - MgO insulation and metal sheath		PLC	T/C IM1 Ch 2	-	-	Yes	No	-
TE -		Omegaclad Type J - MgO insulation and metal sheath		PLC	T/C IM1 Ch 3	-	-	Yes	No	-
TE -		Omegaclad Type J - MgO insulation and metal sheath		PLC	T/C IM1 Ch 4	-	-	Yes	No	-
TE -		Omegaclad Type J - MgO insulation and metal sheath		PLC	T/C IM1 Ch 5	-	-	Yes	No	-
TE -		Omegaclad Type J - MgO insulation and metal sheath		PLC	T/C IM1 Ch 6	-	-	Yes	No	-
TE -		Omegaclad Type J - MgO insulation and metal sheath		PLC	T/C IM1 Ch 7	-	-	Yes	No	-
TE -		Omegaclad Type J - MgO insulation and metal sheath		PLC	T/C IM1 Ch 8	-	-	Yes	No	-
TIC -				Air damper positioner	-	-	-	-	-	-
TIC -				Reheater SCRs	-	-	-	-	-	-
TSH -			-	Reheater vendor panel wiring	-	-	-	-	-	-
TSHH -			-	Reheater vendor panel wiring	-	-	-	-	-	-
TSHH -				PLC	DIM1 Ch 7	-	-	Yes	-	-
TT -	On TIC -			PLC	AIM1 Ch 7	-	-	Yes	-	-
TTI - - 1				PLC	AIM1 Ch 8	-	-	Yes	Yes	60
TTI - - 2				Reheater vendor panel	-	-	-	-	-	-
ZSH -				Fan motor contactor control circuit	-	-	-	-	-	-
ZSH -				PLC	DIM1 Ch 8	-	-	Yes	-	-
ZSH -				PLC	DIM2 Ch 1	-	-	Yes	-	-
ZSH -				PLC	DIM2 Ch 2	-	-	Yes	-	-
ZSH -				PLC	DIM2 Ch 3	-	-	Yes	-	-
ZSH -				PLC	DIM2 Ch 4	-	-	Yes	-	-
ZSH -				PLC	DIM2 Ch 5	-	-	Yes	-	-
ZSL -				PLC	DIM2 Ch 6	-	-	Yes	-	-
ZSL -				PLC	DIM2 Ch 7	-	-	Yes	-	-
ZSL -				PLC	DIM2 Ch 8	-	-	Yes	-	-
ZSL -				PLC	DIM3 Ch 1	-	-	Yes	-	-
ZSL -				PLC	DIM3 Ch 2	-	-	Yes	-	-
ZSL -				PLC	DIM3 Ch 3	-	-	Yes	-	-
ZT -				ZTI -	-	-	-	-	-	-
ZTI -				PLC	DIM3 Ch 4	-	-	Yes	-	-
Energize HV -	-	-		-	-	Solenoid valve to evap #1 upper coil	DOM1 Ch 1	-	-	-
Energize HV -	-	-		-	-	Solenoid valve to evap #1 lower coil	DOM1 Ch 2	-	-	-
Energize HV -	-	-		-	-	Solenoid valve to evap #2 upper coil	DOM1 Ch 3	-	-	-
Energize HV -	-	-		-	-	Solenoid valve to evap #2 lower coil	DOM1 Ch 4	-	-	-
Energize HV -	-	-		-	-	Solenoid valve to evap #3 upper coil	DOM1 Ch 5	-	-	-
Energize HV -	-	-		-	-	Solenoid valve to evap #3 lower coil	DOM1 Ch 6	-	-	-

Table 4.2-16.5b Air-cooling system instrument list – Part 2

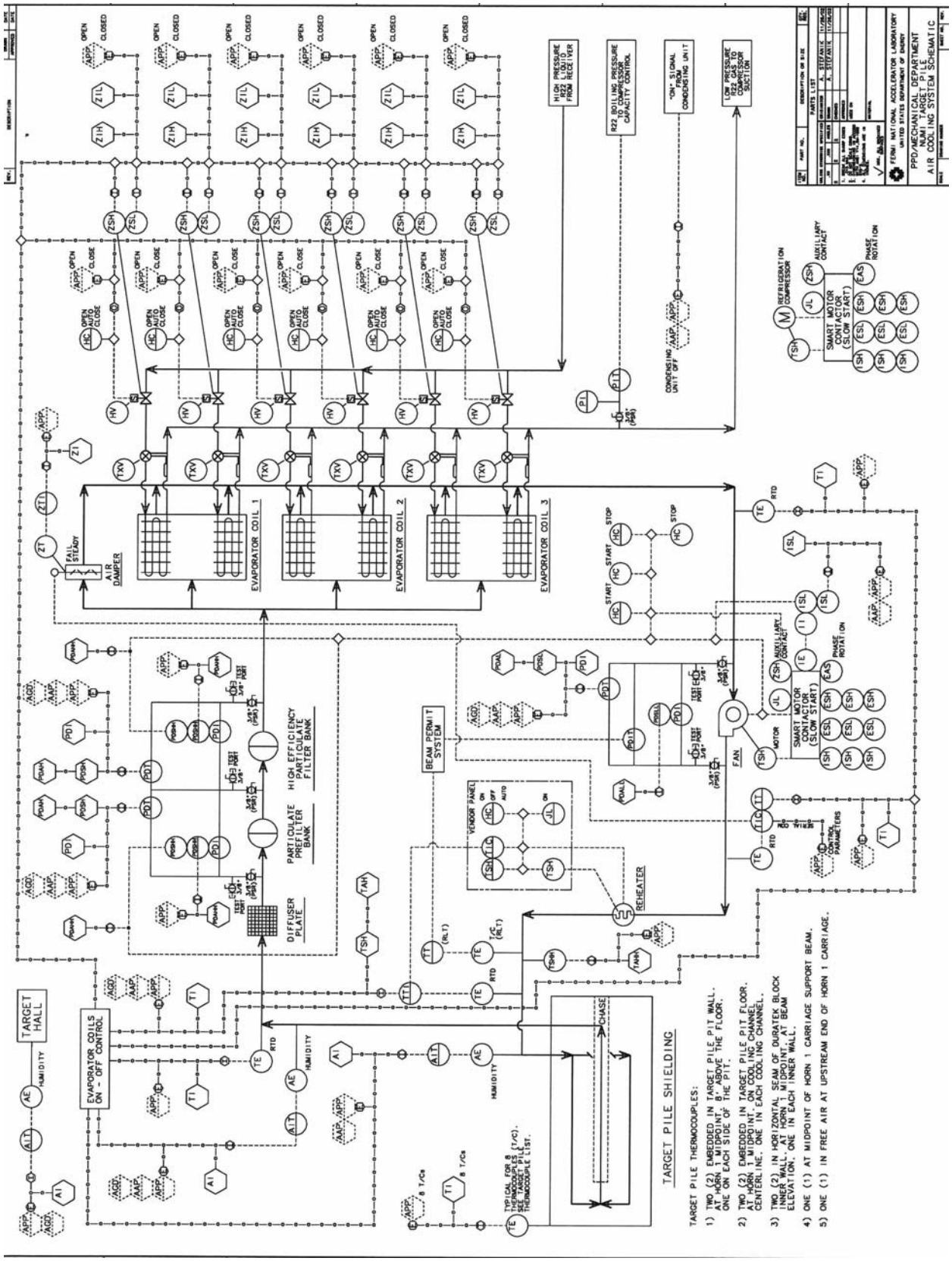

Figure 4.2-41a: Air-cooling system flow schematic

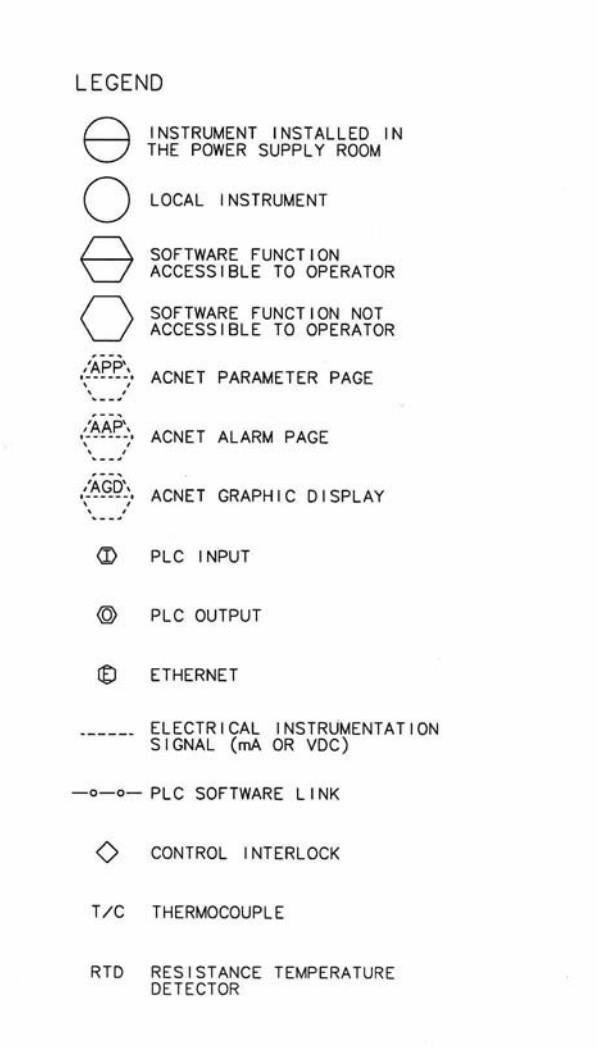

Figure 4.2-41b: Legend for Air-cooling system flow schematic

4.2.14 Target Pile Installation Equipment

Standard rigging equipment is used to install many of the target pile components. The blue blocks have integral lifting handles that are designed to work with standard equipment. All of the steel slabs are drilled and tapped so they can be lifted with swivel hoist rings. The concrete covers are equipped with Swift Lift anchors and can be lifted using the matching lifting eye.

Special lifting fixtures are needed to lift green Duratek blocks (**Figure 4.2-43**), T-blocks (**Figure 4.2-44**), the modules (**Figure 4.2-45**), and top-closure Duratek blocks (**Figure 4.2-46**). Duratek blocks are lowered down the access shaft in a custom designed basket. A transporter from the neutrino fixed target beam line will be used to transport materials from the access shaft to the target hall. The transporter is pulled and pushed using a standard, hand-operated, electric driver. The transporter rides on rails that are welded to the steel floor plates. The rails are removed after installation. It might be necessary to design a coupling to connect the driver to the transporter. A special fixture is needed to hold the work cell door on the transporter and to install it. Special wheeled frames are used to move the modules.

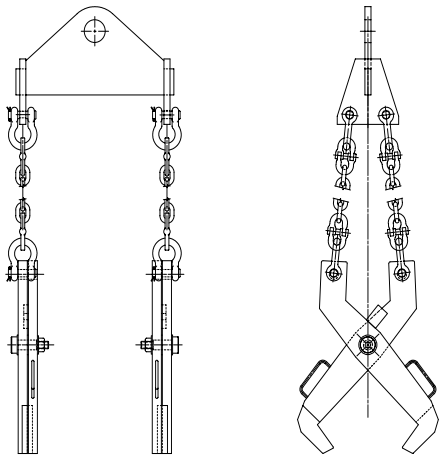

Figure 4.2-43 Green Duratek block lifting fixture

Figure 4.2-44 T-block lifting fixture

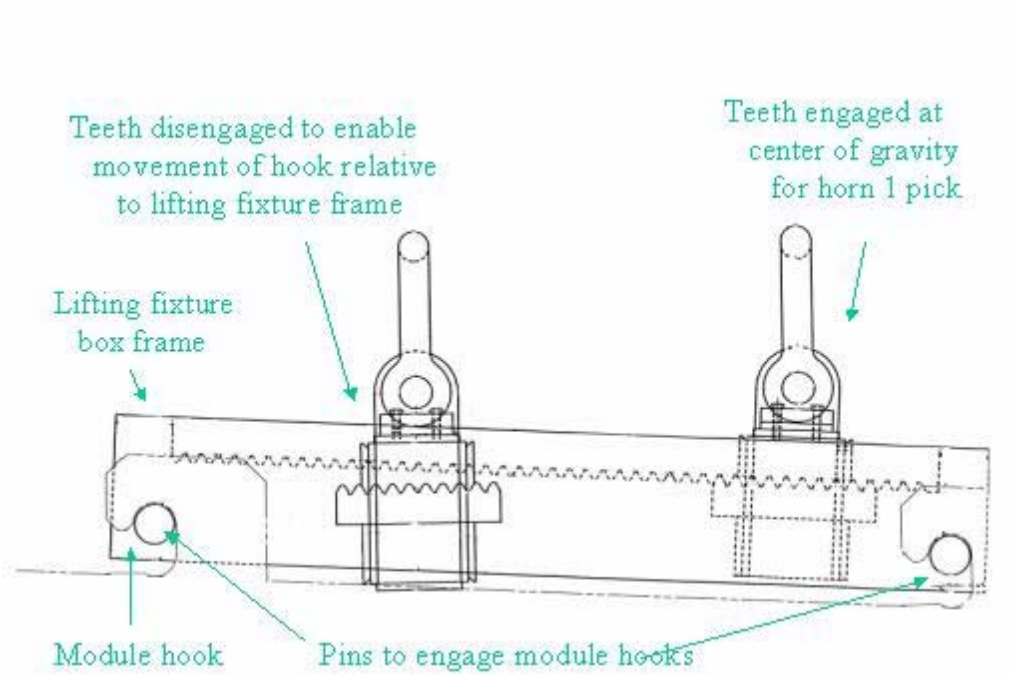

Figure 4.2-45 Module lifting fixture

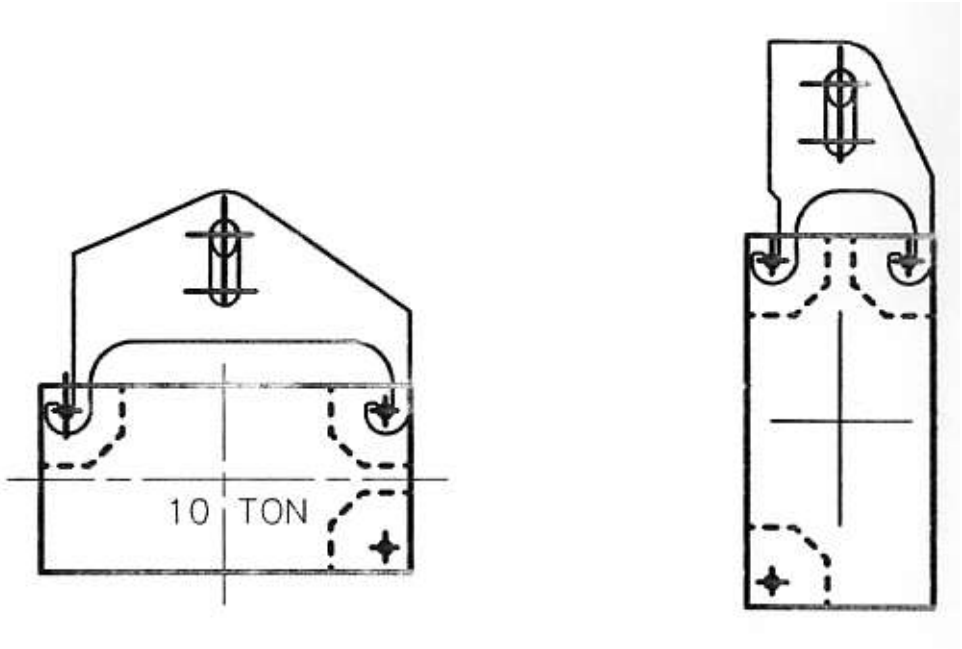

Figure 4.2-46 Blue Duratek block lifting fixture

4.2.15 Target Hall Instrumentation

Instrumentation of the target hall is described in this section. The instrumentation consists of environmental sensors, beam synchronous sensors and motion control devices. They are summarized according to the three categories in **Table 4.2-17**, below. A detailed instrumentation list is shown in **Table 4.2-18**.

Environmental sensors are used to measure temperature, humidity and pressure in various locations of the hall and on some of the beam line elements. These sensors are connected to either a PLC or an Analog Entry Box (AEB). The PLC digitizes input signals and transmits this data to ACNET via an Ethernet connection. The AEB transmits signals to an MADC, where signals are digitized and transmitted to ACNET via CAMAC. In parallel, the AEB transmits data to a Process Channel Interface (PCI) with output signals to the Beam Permit. If any specified AEB input signal falls outside the allowed range the PCI signal will drop Beam Permit. At this time there are five Beam Permit inputs: three baffle temperature sensors, one air supply temperature sensor and one air supply fan differential pressure sensor. A block diagram of the signal paths is shown in **Figure 4.2-47**.

Beam-synchronous sensors are used to measure the horn current pulse, the horn magnet fields (with "Bdot" pickup coils), beam on target (Budal monitor) and residual radiation into the Beam Loss Monitors (BLMs). The BLMs will be used with low-intensity beams to locate the optimal beam path through the horns. They may also be used for beam timing measurements. All signals from beam-synchronous sensors are connected to AEB inputs.

Note: The timing of the beam as derived from Budal or BLM signals will be compared to the timing of the pulsed horn, as derived from the B-dot detectors or the transducer output from the horn power supply system. In the event the relative timing changes significantly (>1% field decrease from maximum) an ACNET alarm will be set. This translates to a 133-microsecond window of coincidence (beam starts 76.5 μsec before maximal horn current or beam starts 66.5 msec after maximal horn current: 143-μsec window).

Horn 1 and the baffle/target positions are adjustable via motor controls. All motors are located on top of the modules, shielded from the primary radiation. Vertical and horizontal angle and position will be adjustable for horn 1 and target/baffle. In addition, target/baffle has 100 inches of longitudinal motion (along the beamline) to facilitate changes to the neutrino beam energy. Limit switches, including those for longitudinal motion, are placed on top of the modules.

Position readback will be obtained with precision LVDTs, also located on top of the modules. Motion parameters are summarized in **Table 4.2-19**. ACNET is used for motion control via ethernet-VME-ACS communication, as shown in **Figure 4.2-48**.

Note: Motion of the target/baffle must be interlocked so that it is not possible for the target to collide with the horn.

Table 4.2-17. Instrumentation Summary

ENVIRONMENT			**Synchronous with Beam**	**Input**	**MOTION Controls**	
Readout frequency~ 0.1Hz	**Input Channels**		Measured during beam spill	**Channels**	**and Readback**	**ACS**
	AEB	**PLC**		**AEB**		
						Quantity
Temperature			**Budal Monitor**		**Motor Control**	
Baffle: also to Beam Permit	3		Target (x, y)	2	Tgt mod; trans & angle	4
Baffle/Target Carrier		2	**Total**	**2**	Tgt/baffle motion in Z	1
Horn #1 Module support		4			Hrn #1 mod trans&angle	4
Horn #1 Carriage		2	**Bdot**		**Total**	**9**
Horn #1 Body		6	Hrn #1 Field	3		
Horn #2 Module support		4	Hrn #2 Field	3		
Horn #2 Body		6				
Target pile shielding		6	**Total**	**6**		
Air Temp(pile supply/return)	1	2				
Fan Temp (inlet/outlet)		2			**LVDT**	
Total	**4**	**34**			Tgt mod; trans & angle	4
			Horn Currents		Hrn #1 mod trans&angle	4
Pressure			Striplines	4	Tgt/baffle motion in Z	1

Filter bank in/out differential		2	Sum of striplines	1		**Total**	**9**
Fan i/o diff ; Beam Permit	1	1	**Total**	**5**			
Evaporator coil		1					
Total	**1**	**4**					

Target Pressure			**Beam Loss Monitor**		**Limit Switch Circuits**	
Pirani Vacuum Gauge	1		Horn 1	1	Tgt module	10
He Pressure Gauge	1		Horn 2	1	Hrn #1 module	8
Total	**2**		**Total**	**2**	**Total**	**18**
					(Note: Limit switches may be doubled up for redundancy)	
Humidity						
Air (supply/return) & Tgt hall		3	**Timing**			
			Bdot & Budal, possibly more	1		
Total		**3**	Budal, Stripline Current	0	**Interlock switch**	**1**
Other			**Total**	**1**	or more	
Fan Current		1				
Target - Ground Impedance	1					
Total	**1**	**1**				
Subtotal: Channel Count	**7**	**42**	**Subtotal: Channel Count**	**16**		

Table 4.2-18 Detailed List of Instrumentation

11/13/2002 Draft:

R.L.T.

Component	Quantity	Device	#	Detail	ACNET Alarm	Range	Error	ACNET Readout/ Control
Target Pile	Pre-filter, High-eff. filter	Pressure differential	2		**A**	3"	0.25%	PLC/ethern
	Fan in/out	Pressure differential	1	**Permit**	**A**	13"	0.25%	AEB
	Fan in/out	Pressure differential	1		**A**	13"	0.25%	PLC/ethern
	Humidity, Supply/Return	Rel Humidity Transmitter	2			100%		PLC/ethern
	Humidity, Target Hall	Rel Humidity Transmitter	1			100%		PLC/ethern
	Evaporator coil	Pressure	1					PLC/ethern
	Fan Curent	Transducer	1			100%		PLC/ethern
	Pit Temperatures	Thermocouple	6		**A**	50˚C	1˚C	PLC/ethern
	Air Temp (supply to pile)	Thermocouple	1	**Permit**	**A**	50˚C	1˚C	AEB
	Air Temp (supply to pile)	RTD	1		**A**	30˚C	0.25˚C	PLC/ethern
	Air Temp (return from pile)	RTD	1		**A**	30˚C	0.25˚C	
	Fan Inlet Temperature	RTD	1		**A**	30˚C	0.25˚C	PLC/ethern
	Fan Discharge Temp	RTD	1		**A**	30˚C	0.25˚C	PLC/ethern
Baffle	Temperature	Thermocouple (2 + 1 spare)	3	**Permit**	**A**	50˚C	1˚C	AEB
Target	Beam on target	Budal Monitor; current	2	1X, 1Y				AEB
	Target-ground impedance	To be decided	1		**A**			AEB
	Vacuum	Pirani Gauge	1		**A**			AEB
	He Pressure	Pressure Gauge	1		**A**			AEB
Tgt/Bffl Carrier	Temperature	Thermocouple	2		**A**	50˚C	1˚C	PLC/ethern
Target	Space Frame angle	Motor Control	4	2X, 2Y		*	*	ACS

Module		and transverse motion	LVDT (pos'n readback)	4	2X, 2Y		*	*	ACS
			Limit Switch Circuits	8			*	*	ACS
		Target Motion - Z axis	Motor Control	1	Z only		*	*	ACS
			Scaled-motion LVDT	1			*	*	ACS
			Z-Limit Switch Circuits	2			*	*	ACS
		Motion Interlock	Limit Switch	1					
							*	*	
Horn	**1**								
Module		Horn angle and	Motor Control	4	2X,2Y		*	*	ACS
		Transverse Motion	LVDT (pos'n readback)	4	2X,2Y		*	*	ACS
			Limit Switch Circuits	8			*	*	ACS
		Support temperature	Thermocouple	4		**A**	50˚C	1˚C	PLC/ethern
		Carriage temperature	Thermocouple	2		**A**	50˚C	1˚C	PLC/ethern
Shielding Block		Horn alignment	Beam loss monitor	1					AEB
Horn	**2**								
Module		Suport temperature	Thermocouple	4		**A**	50˚C	1˚C	PLC/ethern
Shielding Block		Horn Aligment	Beam loss monitor	1					AEB
Horn 1		Magnetic Field	Bdot coil	3		**A'**		0.40%	AEB
		Temperature	Thermocouple	6		**A**	50˚C	1˚C	PLC/ethern
Horn 2		Magnetic Field	Bdot coil	3		**A'**		0.40%	AEB
		Temperature	Thermocouple	6		**A**	50˚C	1˚C	PLC/ethern
Power Supply		Stripline Currents	Summing Module	4					AEB
		Total Current	Summing Module	1					AEB
Timing		Horn Current/ Beam Spill	Bdot coil & Budal Monitor	1		**A'**	200 us	10 us	AEB
		or	BLM &Stripline current, etc				200 us	10 us	AEB

Table 4.2-19 Motion Control

Device	Motion Vertical Upstream	Motion Vertical Downstream	Motion Transverse Upstream	Motion Transverse Downstream	Motion Longitudinal
Horn 1					
Motor	Superior KMT063S09	Superior KMT063S09	Superior KMT063S09	Superior KMT063S09	
Gearbox ratio	40:1	40:1	100:1	100:1	
LVDT range	1" (.004")	1" (.004")	1" (.004")	1" (.004")	
Limit Switches	2 (+/- 3mm) *strip line*	2 (+/- 3mm) *strip line*	2 (+/- 3mm) *strip line*	2 (+/- 3mm) *strip line*	
Target/Baffle					
Motor	To be specified	To be specified	To be specified	To be specified	To be specified
Gearbox ratio	To be specified	To be specified	100:1	100:1	1:1
LVDT range	**8"** (.004") *	**8"** (.004") *	1" (.004")	1" (.004")	~10" (.040")**
Limit Switches	2 (+0.3/-7.5")	2 (+0.3"/-7.5")	2 (+/-0.3")	2 (+/-0.3")	4 redundant
1" LVDT at top 0r 8"LVDT if possible					
geared down from 100"	100" (linear gear)				

a) to ACNET via AEB & MADC
b) to Beam Permit via PCI
c) to ACNET via the PLC

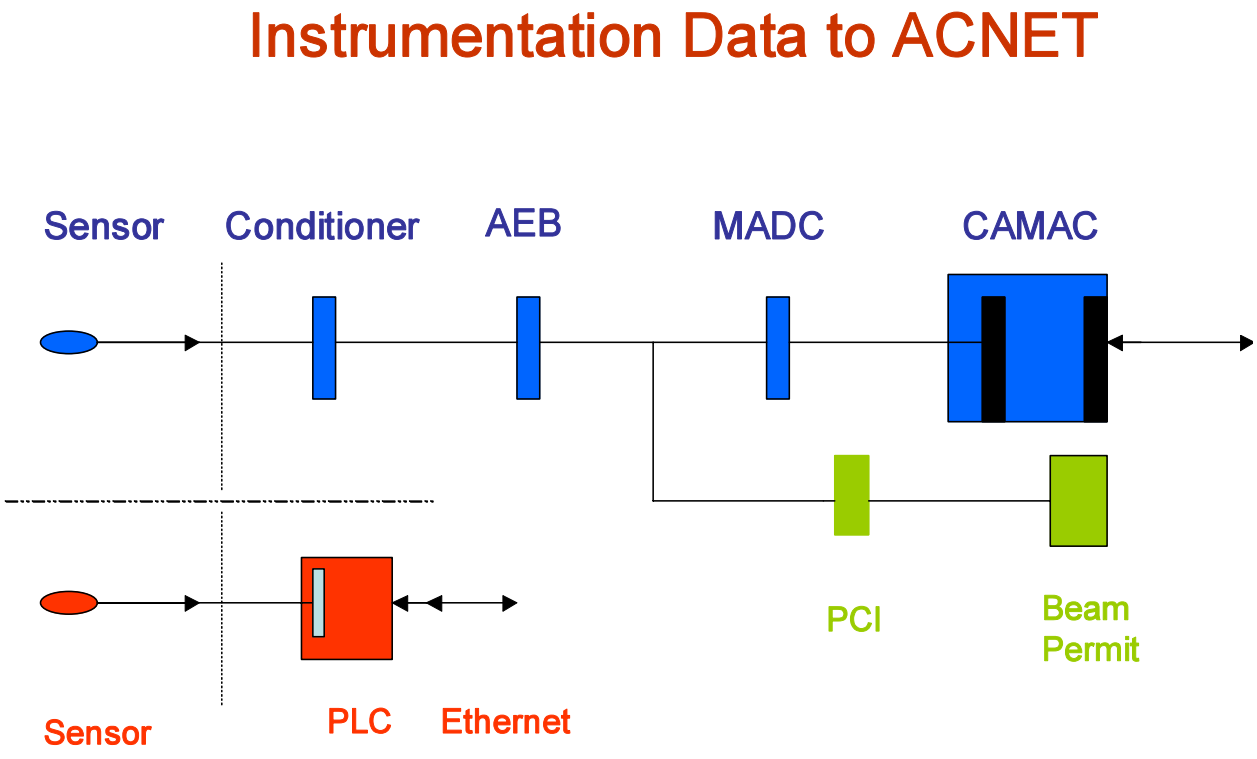

Figure 4.2-47 Instrumentation Readout Paths

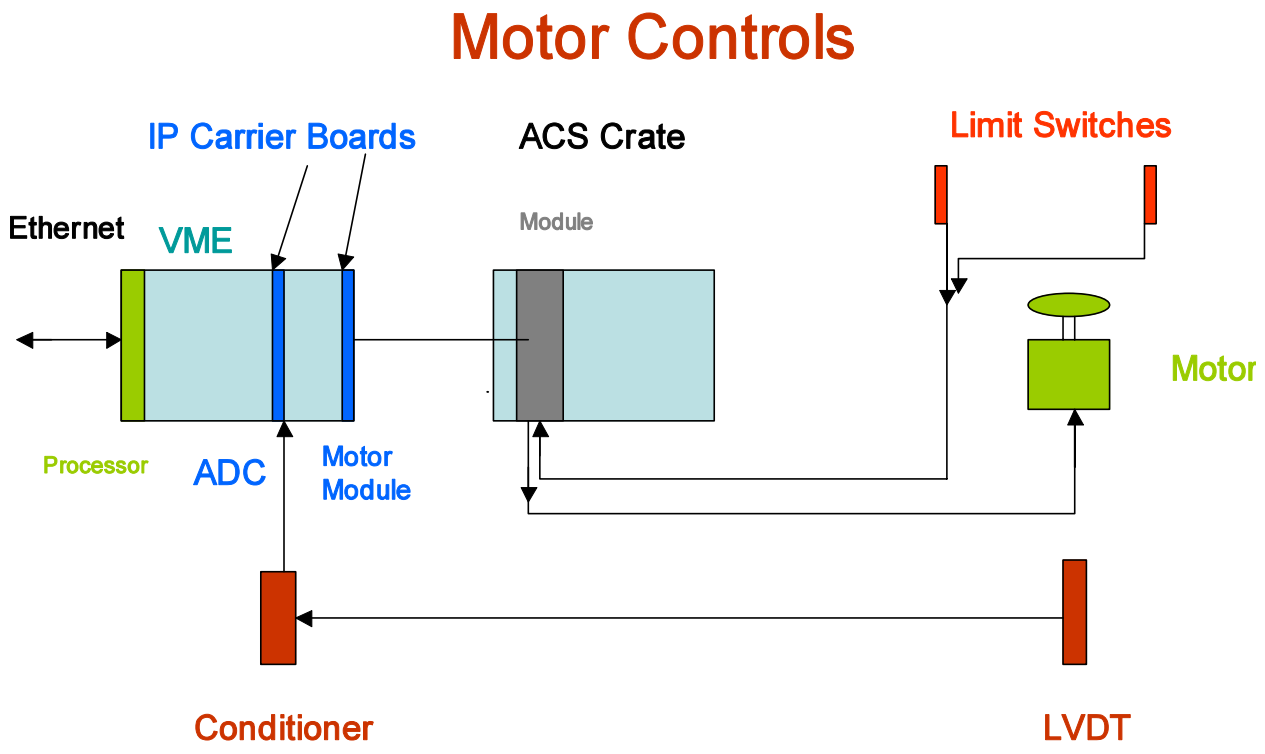

Figure 4.2-48 Instrumentation Readout Paths Motor Controls

4.2 NEUTRINO BEAM DEVICES (WBS 1.1.2)

4.2.1 Target Hall Devices Overview

The components included in the target hall devices (Figure 1 and Figure 2) are:

- Radiation shielding
- Baffle
- Target

Beam focusing horns, including field monitoring probes and a cross hair system to check the horn position with beam

Target/baffle carrier, which moves target to change neutrino beam energy

- Modules that carrier and horns are attached to, providing positioning and shielding
- Work cell, where broken components that are hanging from modules that are also radioactivated can be replaced
- Recirculating air cooling system for target pile
- Remote stripline connection for horns
- Instrumentation

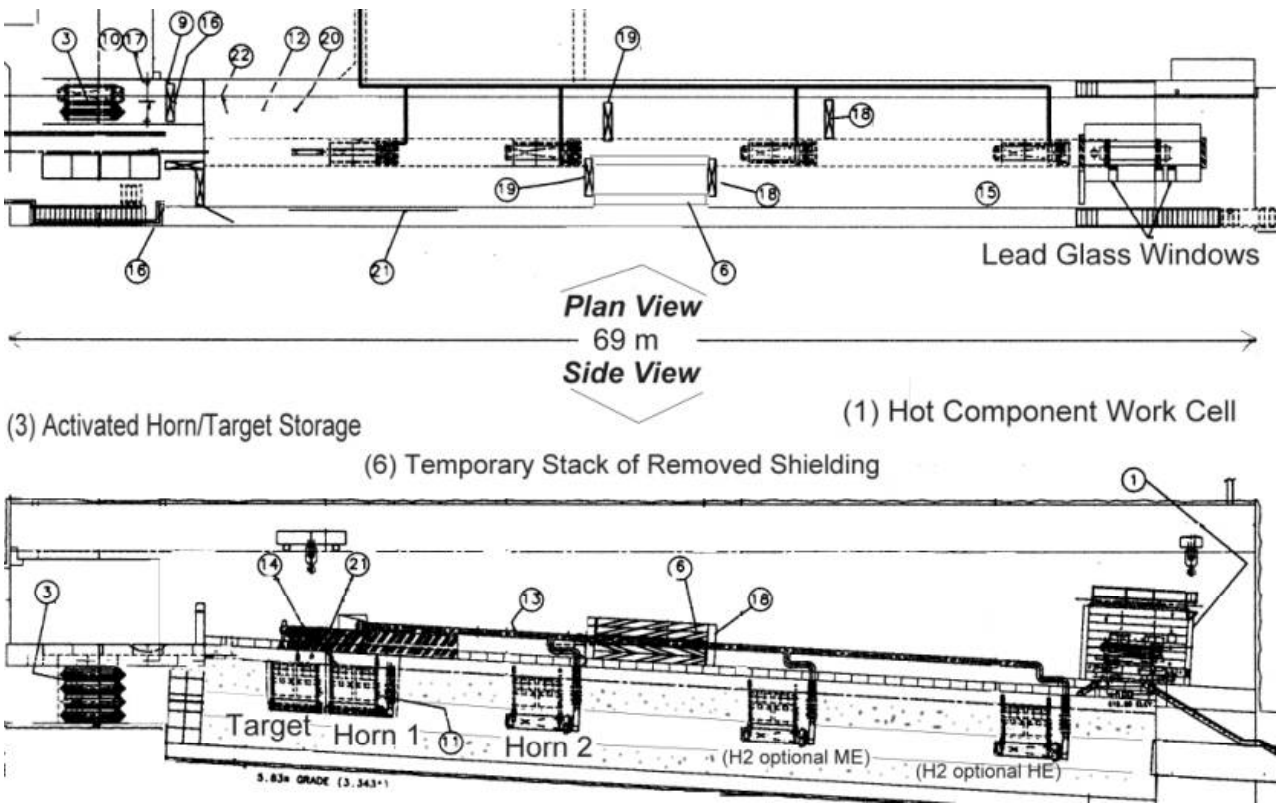

Figure 4.2-1 Plan and elevation views of the NuMI target hall.

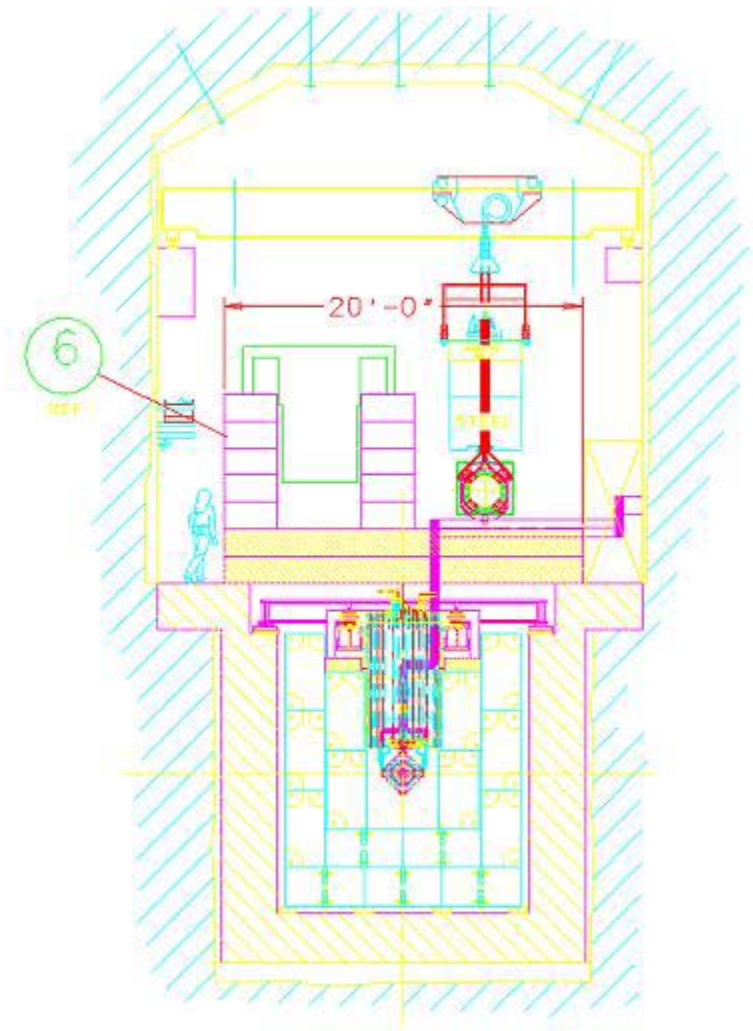

Figure 4.2-2 Cross sectional view of the NuMI target hall, showing a temporary stackup of removed shielding, and a module plus horn being transported.

Four coordinate systems are involved in the target hall design. LTCSZ and LTCSH are used by the surveyors for the overall NuMI layout. For the target hall layout drawings, it is convenient to use a third system, a Cartesian system where local gravity is vertical. The factor that drives the use of three coordinate systems instead of just one is that the curvature of the earth is significant over the length of the NuMI complex. The beam Monte Carlo is the fourth system.

The "Target Hall Drawing Coordinate System" is LTCSZ with a rotation (-62.18329 deg) about the z-axis such that the horizontal component of the neutrino beam is pointed along the drawing

y-axis. The vertical angle of the beam is –3.34349 deg. The beamsheet point DKINHL is taken as the (0,0,0) to anchor target hall drawings.

In the Monte Carlo coordinate system, the idealized start of horn 1 is (0,0,0), and the coordinate system is aligned with the beam. **Table 4.2-1** explains the relationship between beamsheet acronyms, physical devices, and the coordinate along the beam.

Beamsheet Nomenclature			MC coordinate L.E. beam
BAFL2P	**start of baffle**	**baffle is 150 cm long**	**-221.593cm**
HALTA1	**start of 1st half of target**	**leading edge of vertical fin; total target vertical fin is 95.38 cm long**	**-35 cm**
UPHRN1	*upstream-most edge of horn*	*start of curved end-bell of horn*	*-3.208 cm*
MCZERO	**Zero of GNUMI MC in target hall**	**where idealized horn 1 begins; middle of curved end bell of real horn**	**0 cm**
ACTRN1	**Horn 1 insertion point**	**start of real horn parabolic section; 3cm after start of 3 meter long idealized horn**	**3 cm**
HALTA2	**start of 2nd half of target fin**	**Focus point of the primary beam optics**	**12.69 cm**
DWNRN1	*extent of idealized horn 1*	*end of 3 meter long idealized horn 1*	*3 m*
UPHRN2	*upstream-most edge of horn*	*start of curved end-bell of horn*	*9.95202 m (9.955 m old)*
ACTRN2	**Horn 2 insertion point**	**also start of idealized horn 2**	**10 m**
DWNRN2	*extent of idealized horn 2*	*end of 3 meter long idealized horn 2*	*13 m*
DKINHL	**theoretical start of decay pipe, not including flange, window; also known as target hall endpoint**	**Used as zero for local cartesian coordinate system for target hall drawings**	**45.6982 m**

Table 4.2-1 Definitions of beamsheet terms, with relation to the Monte Carlo coordinate system along the beam direction.

Radiation dose to equipment is an integral design consideration, see **Figure 4.2-3** for a summary of radiation levels.

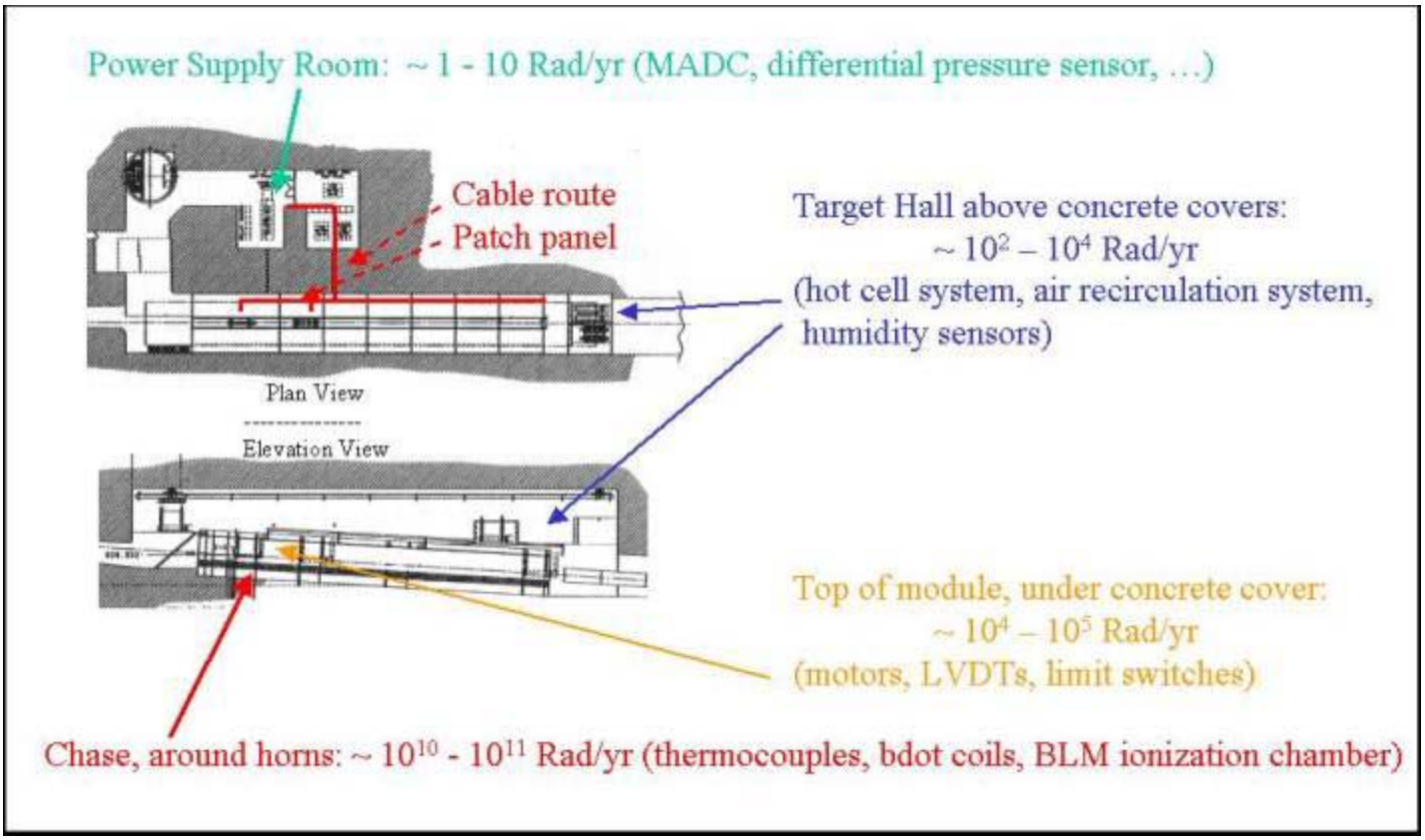

Figure 4.2-3 Overview of radiation levels in target hall.

4.2.2 Target Hall Baffle

4.2.2.1 Baffle Functions and Requirements

The baffle must:

- Prevent mis-steered primary proton beam from causing damage to the horn neck and target cooling/support components.

- Be capable of operating continuously with 3% beam scraping at design luminosity.

- Withstand full intensity of beam for a number of pulses it will take to detect mis-steering of beam and shut beam off.

- Incorporate monitoring that will shut beam off in case of continued large loss of beam on baffle. It may be useful for efficient running that loss of one pulse on baffle not turn off the beam.

- Construction and alignment tolerance of hole through baffle must be 0.5 mm or better.

In addition:

- Incorporate monitoring that allows detection and monitoring of beam-baffle scraping at order of 1% accuracy. (E.g. if 2% of the beam is being scraped, measure (2+/-1)%). Since actual full power beam running is expected be around $2x10^{13}$ during the first couple years running, this means an accuracy of $+/-2x10^{11}$ or better.

- Incorporate monitoring that allows a crosscheck of alignment via e.g. low intensity beam-scan to 0.5 mm.

- Have the baffle move along the beamline with the target, as this increases the available target travel (the overall length for extraction of a broken target/baffle module is limited, and by having the target stick out one end of the carrier at one extreme of motion and the baffle stick out of the carrier at the other extreme one makes maximum usage of this length).

4.2.2.2 Baffle hardware design

The baffle, **Figure 4.2-4**, is mounted with the target to eliminate the expense of another module to support and align it. The baffle and target can be pre-aligned to each other before attachment to the module, and move as a unit. The baffle construction tolerance is 0.2 mm RMS; the goal for overall baffle position accuracy is 0.5 mm, including thermal effects, survey tolerance, and carrier wobble.

.

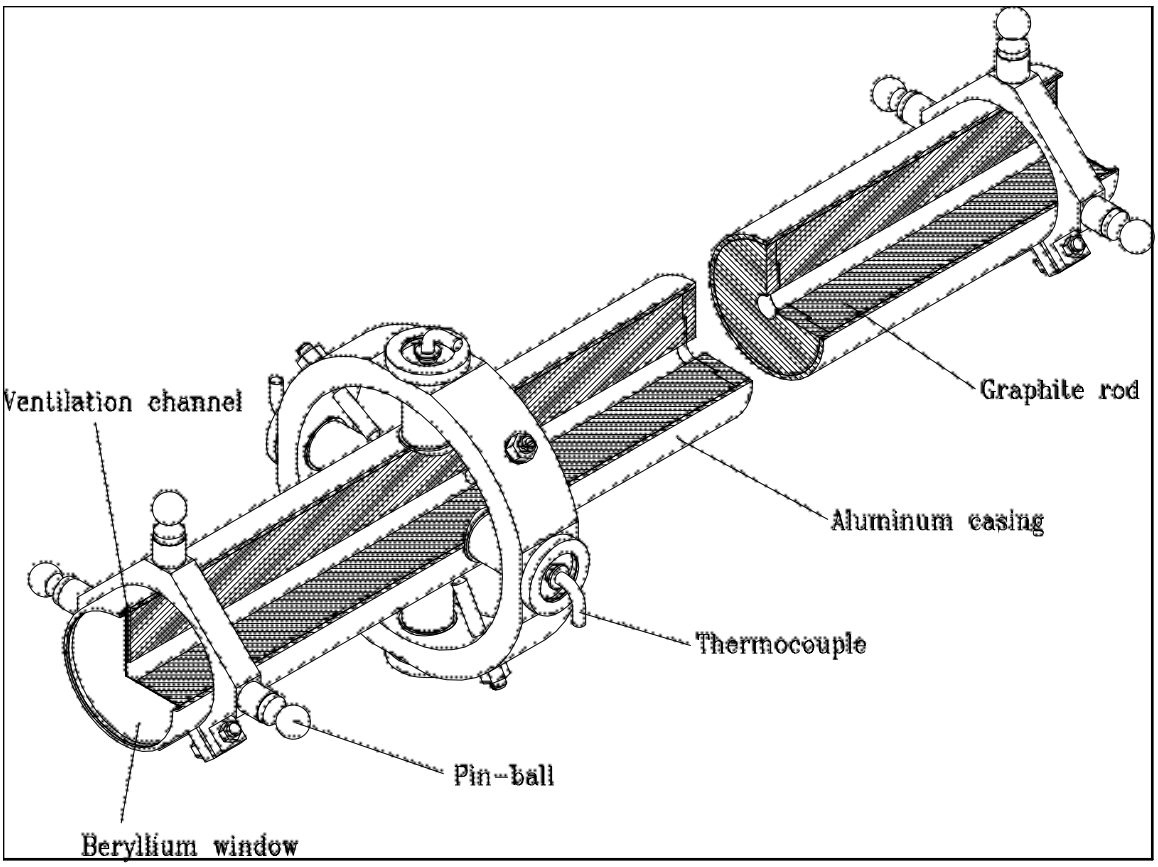

Figure 4.2-4 Baffle. 150 cm long, 11 mm diameter hole, 57 mm diameter graphite core, 61 mm diameter aluminum casing. Cooling fins not shown. Thermocouples will be located near the downstream end of the baffle

Baffle hole size, baffle location – beam accident geometry

The baffle hole is made as large as possible, while still providing protection to the horn and target. **Figure 4.2-5** and **Figure 4.2-6** show the layout of the baffle relative to the target and horn.

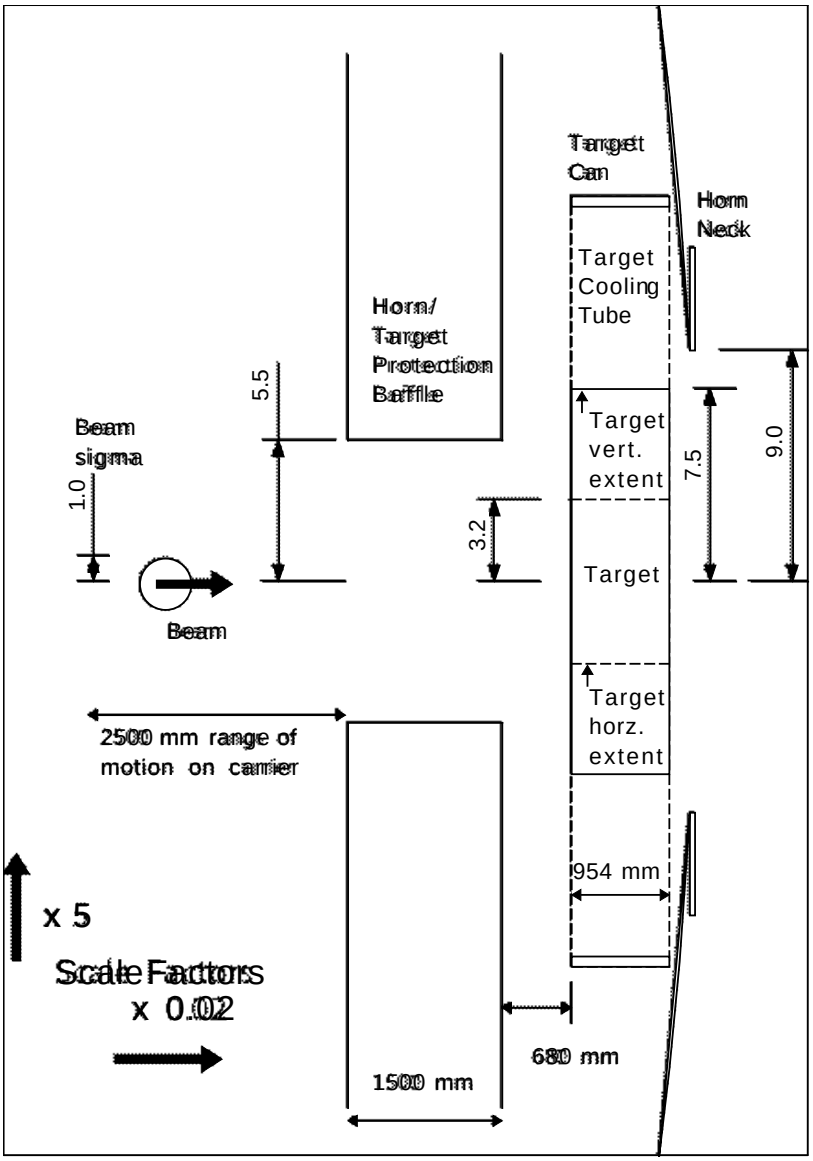

Figure 4.2-5 Plan view of baffle, target, and horn geometry. Since target is rectangular rather than cylindrical, limits of its horizontal and vertical extent are shown. Note large factor between horizontal and vertical scales

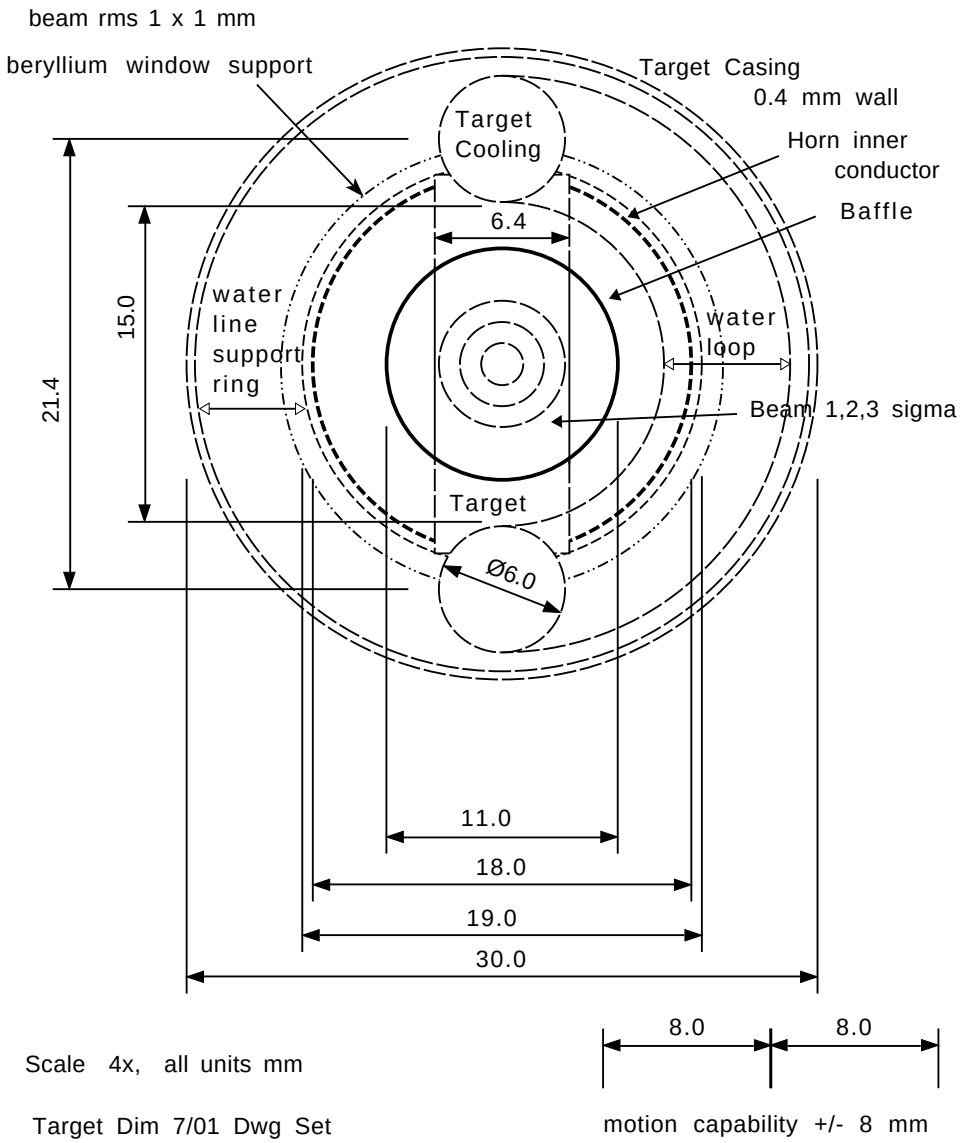

Figure 4.2-6 Beam-eye view of baffle inner radius and comparison to beam spot, target fin, horn neck, and target cooling and support structure.

The horn protection system actually consists of two baffle locations, a relatively large opening after the last bend string (but unfortunately before the last quad), and a second baffle in the target hall. Peter Lucas produced a spreadsheet that takes into account the magnetic field, and gives the maximum radius that the beam could reach while still passing through the two baffles. These limits are set entirely by the two baffles and the intervening magnet, and do not try to identify magnet failures that could actually produce these deviations. Examining some variations run by Adam Para, the pattern is roughly that the fully protected region is the baffle radius plus (0.5 mr horizontal, 0.7 mr vertical) times the distance downstream of the baffle.

Table 4.2-2 lists three items to be protected by the baffle. In it, are derived maximum baffle radii using the above rule of thumb for two cases: (1) having the baffle close to the target, and moving with the target, or (2) at a fixed upstream location which would still allow target movement to the HE location without moving the baffle. Baffle radius is reduced by 0.5 mm to allow for alignment tolerance. Numbers are in coordinate system where horn 1 starts at Z=0cm (i.e. the GNUMI Monte Carlo coordinate system). The horn neck is at (Z,R) = (0.8m,9mm); the top edge is shadowed by the target, so only the horizontal edge is included in the calculation. The target cooling line solder starts at (Z,R) = (-0.35m,7.5mm) at top and bottom of graphite fin; after some distance down target, the graphite contributes to shielding the tube. The cooling loop tube between supply and return is at the end of the target (Z,R) = (0.6m,7.7mm), and is exposed in the horizontal direction.

Baffle hole R(max)	Baffle Z=-2m	Baffle Z=-5m
Horn 1 neck, X direction	7.1 mm	5.6 mm
Target cooling tube, Y direction, LE position	5.8 mm	3.7 mm
Target cooling loop, X direction, LE position	5.9 mm	4.4 mm

Table 4.2-2 Maximum baffle hole radius allowed for different layouts of baffle, horn and target.

From the above table, it is seen that a 5.5 mm radius baffle hole protects the horn for all baffle locations, for all different energy beams. If the target and baffle move together, then a 5.5 mm radius baffle will also protect the target for all beam configurations; however a fixed location baffle would require a smaller hole to protect the target. It is also seen that the X and Y requirements are very similar, and a circular hole thus makes sense. From the above

arguments, the baffle is mounted near the target, moves with the target, and the radius of the hole is selected to be 5.5 mm.

In the current layout, the baffle ends at -103 cm in the Monte Carlo coordinate system, or 68 cm before the leading edge of the target vertical fin.

Baffle material

Calculations have been done of energy deposition, heat rise, and stress for the standard NuMI beam (4e13 protons in a 0.7 mm sigma-x 1.4 mm sigma-y beam spot) hitting Nickel, Copper, Aluminum, and Graphite. Nickel and Copper are clearly unsuitable. Aluminum is marginal; it would exceed its yield point and creep modestly with accident pulses [ref. i]. Graphite is satisfactory [ref. ii]. Beryllium would also work, but is rejected because it would generate mixed waste unnecessarily. We have selected Graphite; it is reasonable to use the same grade selected for the target, ZXF-5Q, since we already have experience with it in the target beam test.

Baffle outer radius

IHEP has proposed shrink-wrapping the graphite in a long aluminum tube [ref. ii]. This provides good thermal contact with the graphite that will be maintained under beam heating in spite of the larger thermal expansion coefficient of aluminum. Also it can be done with high accuracy. The technology they describe would limit baffle diameter to 60 mm; 60 mm would appear to be a reasonable match to NuMI requirements. The graphite diameter is 57.1 mm, which is a standard stock graphite rod size.

Baffle length

Calculations have been done to find out how long the graphite baffle must be to protect the horn inner conductor, the target cooling tube and solder joint to the graphite, and the target ceramic. The position of the baffle was also varied. The position/length selected is that which has the upstream end of the baffle as close to the target as will still provide a good safety margin. This allows the greatest possible target motion. The result chosen is150 cm long baffle with 68 cm spacing between baffle and target fin. Curiously, extending the baffle length in the space between target and baffle further actually makes the energy deposition in the target fixturing worse, although it reduces the energy deposition in the horn neck. Please

see [ref. ii] for derivations of acceptable temperature rises. **Figure 4.2-7** and **Figure 4.2-8** include temperature rises for baffle lengths and positions calculated after [ref. ii] was written. The chosen operating point as shown in **Figure 4.2-8** corresponds to (a) cooling pipe steel stress of 50 MPa compared to 340 MPa yield, (b) Aluminum horn neck stress of 70 MPa compared to 210 MPa yield, (c) ceramic insulator stress of 30 MPa compared to 170 MPa yield, and (d) target solder joint temperature rise of 70 K over approximately 30 deg C operating temperature compared to 340 deg C melting point.

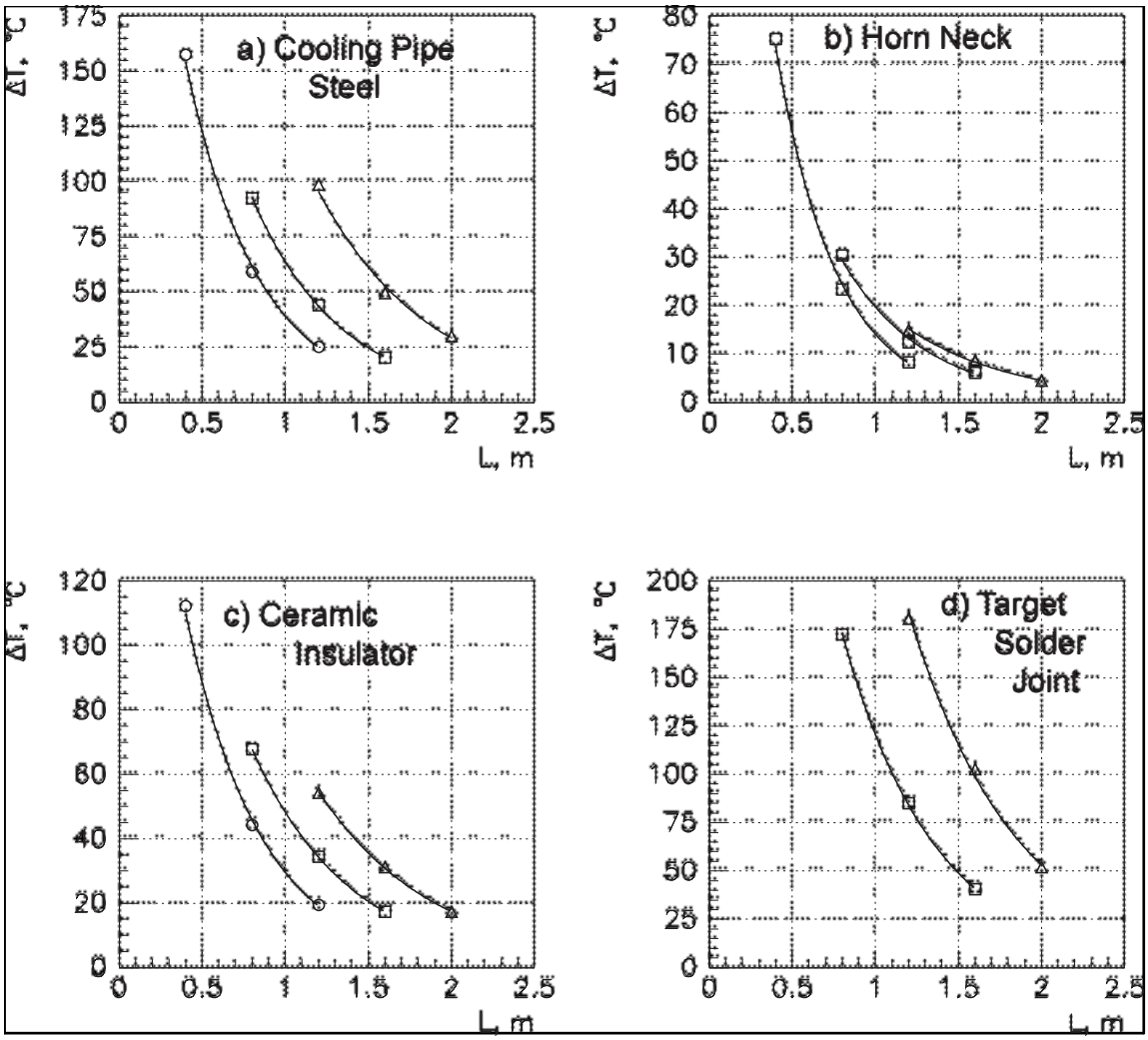

Figure 4.2-7 Temperature rise of protected components for an accident spill as a function of the length of the baffle. The distance Lbt between the downstream end of the baffle and the target vertical fin is 176 cm (circles), 86 cm (boxes), and 41 cm (triangles).

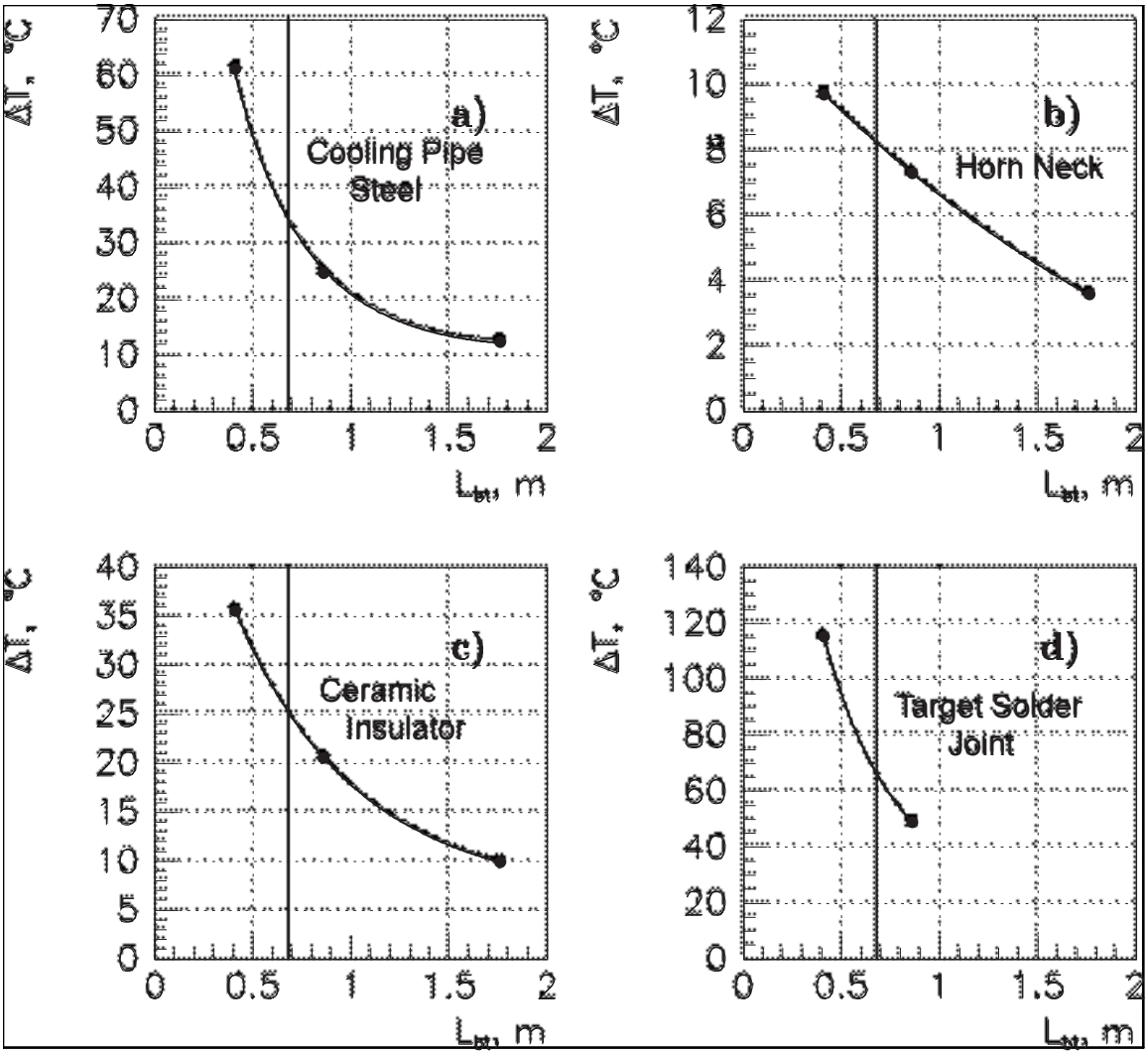

Figure 4.2-8 Temperature rise of protected components for an accident spill as a function of the position of a 1.5 m long baffle. Lbt is the distance from the end of the baffle to the start of the target vertical fin. The chosen design value of 68 cm is marked.

<u>Baffle atmosphere and windows</u>

[ref. ii] documents that the maximum temperature in the core of an accident shower along the inner edge of the baffle is 344 deg C, at which temperature no detectable oxidation is expected. The oxidation threshold (temperature resulting in 1% weight loss in 24 hours) for ZXF-5Q is 450 deg C. Hence an inert atmosphere in the baffle is not required.

Beryllium windows are provided to prevent erosion of the graphite by the strong wind in the target pile. A ventilation hole is provided to prevent air pressure buildup. To help keep ventilation hole clear of debris, the hole should not be oriented upward; to help prevent

contamination falling out of the hole, it should not be oriented down; hence we plan to orient the hole horizontally.

Baffle thermal warp

A thermal gradient laterally across the baffle can be caused by azimuthally asymmetric beam loss, air flow, or cooling fin contact. This would cause the baffle to warp. The following arguments indicate such effects are not a problem for us.

A zeroth order model with a linear temperature gradient across the cylinder gives a warp of the center relative to the ends of ($\alpha TL^2/8w$) where α is the coefficient of thermal expansion, T is the maximum temperature difference, L is the length of the baffle, and w is the width of the baffle. For a warp of 0.5 mm, this implies a temperature difference of 13.3 K for graphite across the baffle. Numerically modeling non-realistic extreme cases where the entire fin cooling was on one half of the baffle or the entire heat deposition was on one half of the baffle for 3% continuous scraping gave only a few degree temperature differences even at the higher temperature downstream end of the baffle. Hence this effect can be safely ignored.

4.2.2.3 Baffle cooling and monitoring

Calorimetric methods are a simple and direct way of monitoring the beam loss on the baffle. For this to work, the cooling of the baffle should be adjusted so that temperature rises are easily measured with standard thermocouples but the baffle will not overheat. The simplest is to rely on heat transfer to the existing air flow, with the addition of fins to increase the heat transfer. However, heat transfer efficiency is hard to precisely calculate a priori, so a large safety factor should be built in for the operating parameters.

Figure 4.2-9 shows the energy distribution when beam hits the front of the baffle [ref. iii]. This corresponds to an average temperature rise of 11 K per pulse at the downstream end of the baffle for full power beam. Since the largest temperature rise is downstream, the monitoring thermocouples should be mounted near the downstream end.

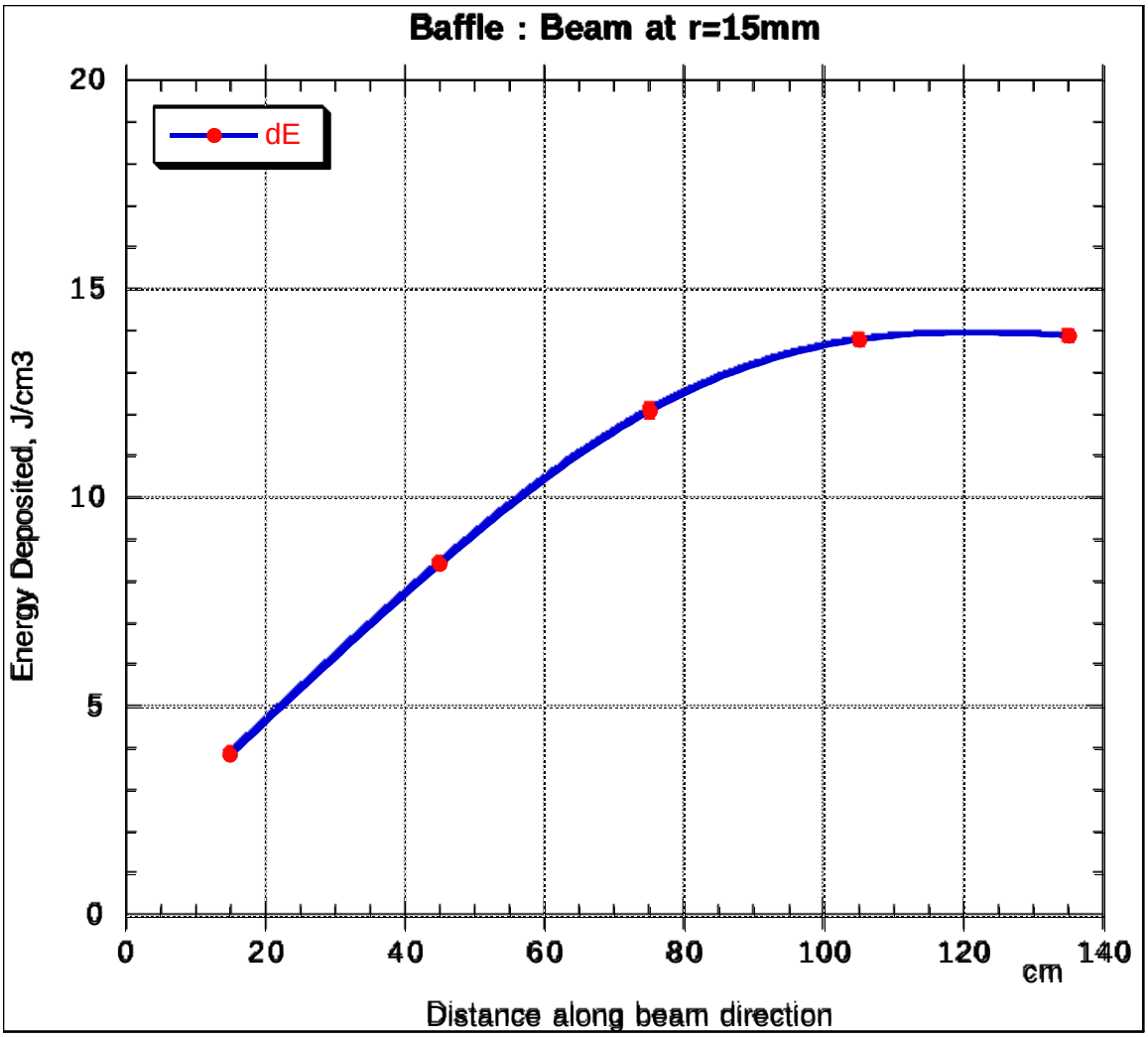

Figure 4.2-9 Energy deposited in baffle (J/cm3/pulse) as a function of position along baffle for 4e13 protons hitting baffle, averaged over 3 cm baffle radius and 30 cm long baffle segments. Integral is 42 kJ/pulse, corresponding to 22 kW at 1.87 second repetition rate, or 5.5% of the 400 kW total beam power.

To first order, the time constant for heat transfer to the cooling air is (Vdc/Ah), and the asymptotic temperature rise is (PV/Ah), where V is the volume of graphite, d is the density of graphite 1.8 g/cm3, c is the specific heat capacity of graphite 0.7 J/gK, A is the surface area of the graphite segment, h is the heat transfer coefficient from baffle to air, and P is the power deposited per unit volume. For a 3 cm radius cylinder, V/A = 1.5 cm. The cooling air flow along the surface of the baffle is about 4 m/s, which would give h~12W/m2K for flow parallel to a fin-less cylindrical baffle [ref. ii]. The actual flow pattern is hard to predict, and with transverse flow the heat transfer coefficient could be double this. For use in selecting a strategy, a hypothetical fin with five times the heat transfer of the cylinder is chosen as a reasonable operating point, and shown in comparison in the table. The cooling air

temperature will be about 16 deg C. Note that [ref. ii] includes full three-dimensional modeling of the heat transfers, with results that agree well at the downstream end of the baffle with the simple approximation given here.

The baffle fin design has not been finalized, but Figure 4.2-10 shows a concept. It consists of two half rings 1.5 mm thick with pins 2 mm in diameter. Pins of 15 mm height are located with period 7 mm along the circumference and 9 mm along the baffle. The internal radius of a half ring is the same as the external radius of the baffle casing. These half rings are pressed to the baffle casing via a stainless steel clamp, providing pressure about 10-20 MPa. Such a pressure should provide a good thermal contact between radiator and casing. Another

The

air

e to

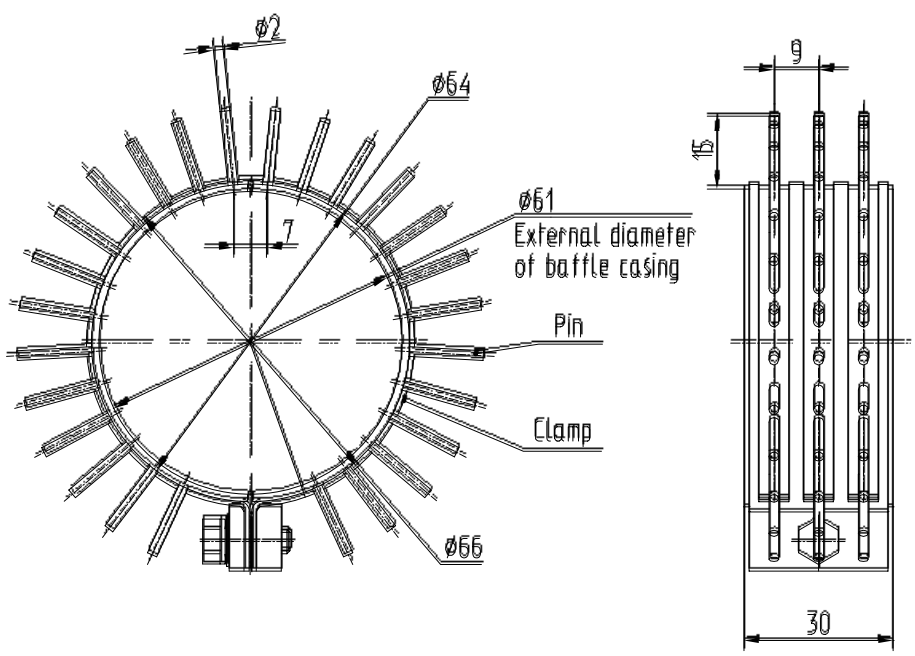

ents.

120

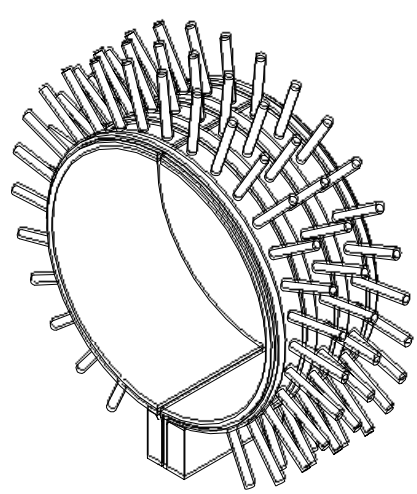

ered

Accident scenario

To prevent damage to the aluminum baffle tube, an interlock will be set to prevent further beam pulses at a thermocouple readback of about 120 deg C. The interlock could be set lower if found to be operationally desirable. This would prevent more than at most a dozen continuous accident pulses; however the interlock will probably not be set tight enough to trip the beam from a single accident pulse. With the fin, the baffle will cool off in a few minutes, allowing one to turn the beam back on quickly.

Continuous scraping

We are optimistic that beam scraping will be low. The fin design nevertheless would allow 3% continuous beam scraping with a safety factor of 2 in the heat transfer coefficient h before reaching the 120 deg C trip point.

The 19 K temperature rise per 1% beam loss is an order of magnitude larger than needed for monitoring the beam loss at the required level, providing a large safety factor on the value of h being larger than the design specification.

Backgrounds to the calorimetric monitoring of the baffle scraping have also been calculated. The energy deposit in the baffle is 0.10 J/cm3/pulse for 1% scraping, compared to 0.04 J/cm3/pulse from interactions in the target pile air and 0.0002 J/cm3/pulse backscatter from the target [ref. iii].

Note that the thermal monitoring does not give pulse-by-pulse monitoring of the scraping, but an average with a few minute time constant. We have not yet found an argument showing a necessity for pulse-by-pulse monitoring of scraping.

Calibration

The actual temperature response of the baffle will be calibrated during commissioning by steering 100% of the beam at low intensity on to the baffle. Note that a constant beam intensity should be maintained for a period of several time constants for this measurement.

Commissioning alignment scan

The fin parameter set also allows an alignment check of the baffle via beam scan during commissioning, or whenever one wants to recheck alignment. It is conservative to turn down beam power during scans; beam intensity as low as $8x10^{11}$ protons per pulse is easy to achieve. Such a single pulse (2% of maximum beam) into the baffle would produce only a 0.2 K temperature rise in the baffle, so one would need to use a large number of pulses per point (say 30 over a one minute period), or else a higher intensity beam (in which case one could limit the repetition rate) to produce a robust thermocouple response. With the standard 1 mm RMS beam spot, an alignment check accuracy of a fraction of 1 mm would be expected, based on experience with similar temperature scans done during the NuMI target test.

Usable signals from the alignment check baffle scan will most likely also be detected in the horn 1 alignment ionization chamber and the hadron monitor in front of the absorber, providing redundancy.

Since the baffle and target are pre-aligned on a common carrier, the combination of baffle scan and Budal-monitor target scan can demonstrate that the combined baffle/target system is at the correct angle as well as in the correct position.

4.2.2.4 Effect of scraping on the neutrino spectrum

The effect on the neutrino spectrum of beam tails hitting the baffle has been modeled in GNUMI, and is illustrated in **Figure 4.2-11**. The effect of scraping is mostly significant between 5 GeV and 8 GeV. In a 10-ktyear exposure, there will be of order 500 events in this range collected in the MINOS far detector, giving a statistical error of 4%. Thus knowing a scraping correction to 1% accuracy would keep the systematic error negligible compared to the statistical error. As shown in the figure, 1% beam scraping produces about a 1% change in the double ratio (beam scraping correction), hence measuring the scraping to +/- 1% of the total beam power is a reasonable specification.

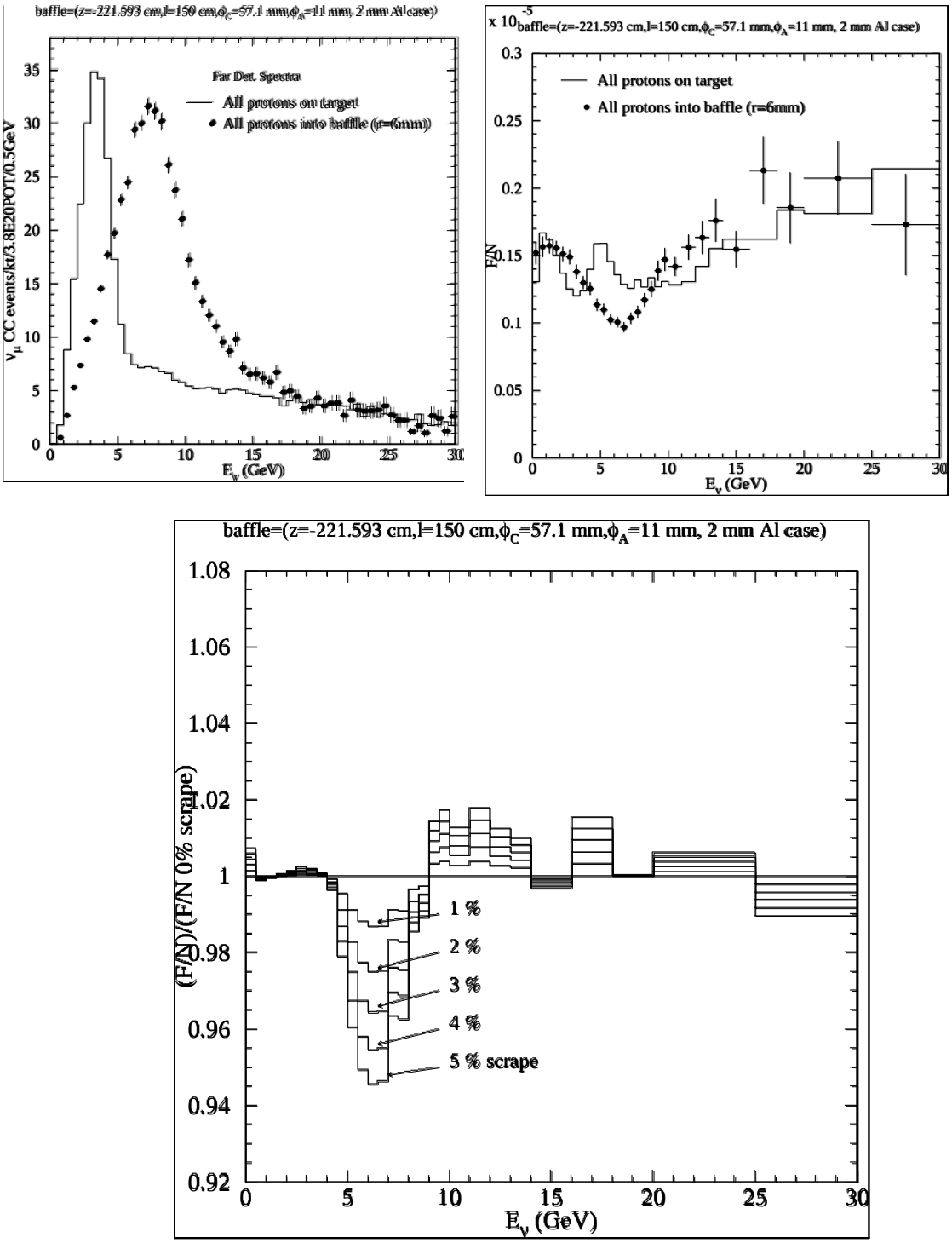

Figure 4.2-11 Effect of various amounts of beam-baffle scraping on neutrino spectrum. Top plots show spectra separately for 100% of beam on target or baffle. (Mark Messier, 6/12/02)

It would be nice to keep the scraping to less than 1%, so that no correction at all would need to be applied. For a gaussian beam with 1 mm RMS, 99% of the beam is within 3 mm radius. In our case, the baffle hole is 5.5 mm radius, and even after allowing for 0.5 mm alignment tolerances the loss from a gaussian beam would be negligible. However, only experience with the real beam will tell us if there are significant non-gaussian tails, or jitter in the beam position that cause losses on the baffle.

Note this simulation had baffle to target distance of 37 cm instead of our current choice of 68 cm, but that should have only a minor effect. In a similar study with the baffle a couple meters further back, Brajesh Choudhary found the scraping sensitivity to be twice as large, which may be another motivation for keeping the baffle close to the target.

References

---

[i] Thermal Stress Analysis of Numi Baffle – II, MSG-EAR-0282, Bob Wands, 4/2/01 and Thermal Stress Analysis of NuMI Baffle, MSG-EAR-00279, Bob Wands, 11/8/00.

[ii] Technical Design of the Target Pile Protection Baffle-draft, S.Filippov, V. Garkusha, R. Gibadullin, F. Novoskoltsev, I. Ponimash, T. Ryabova, V. Zarucheisky, (IHEP) 4/30/02.

[iii] MARS Simulation: Baffle Heating, B. Lundberg, 6/9/02.

4.2.3 Target

The neutrino beam is produced by pion decay. Those pions are produced by interactions of the primary proton beam with the target. The proton beam spot size should be no smaller than 1.0 mm RMS horizontally and vertically at full baseline beam intensity to limit beam induced stress on the target.

The target material is graphite, type ZXF-5Q (POCO Graphite), density 1.78 g/cm^3. The graphite segments are machined as narrow fins and mounted to stainless steel water-cooling pipes, as shown in **Figure 4.2-12** and **Figure 4.2-13**. The airtight casing has beryllium windows for the primary beam entrance and exit.

The main target is 47 vertical target segments, each 20.0 mm long, with 0.3 mm spacing between segments, for a total length of 95.38 cm. The segments are 6.4 mm wide. The height is sculpted (see Figure 2). A 48th segment (not shown) is mounted horizontally, in the target canister, with the fin center 157.3 mm upstream of the upstream edge of the main target.

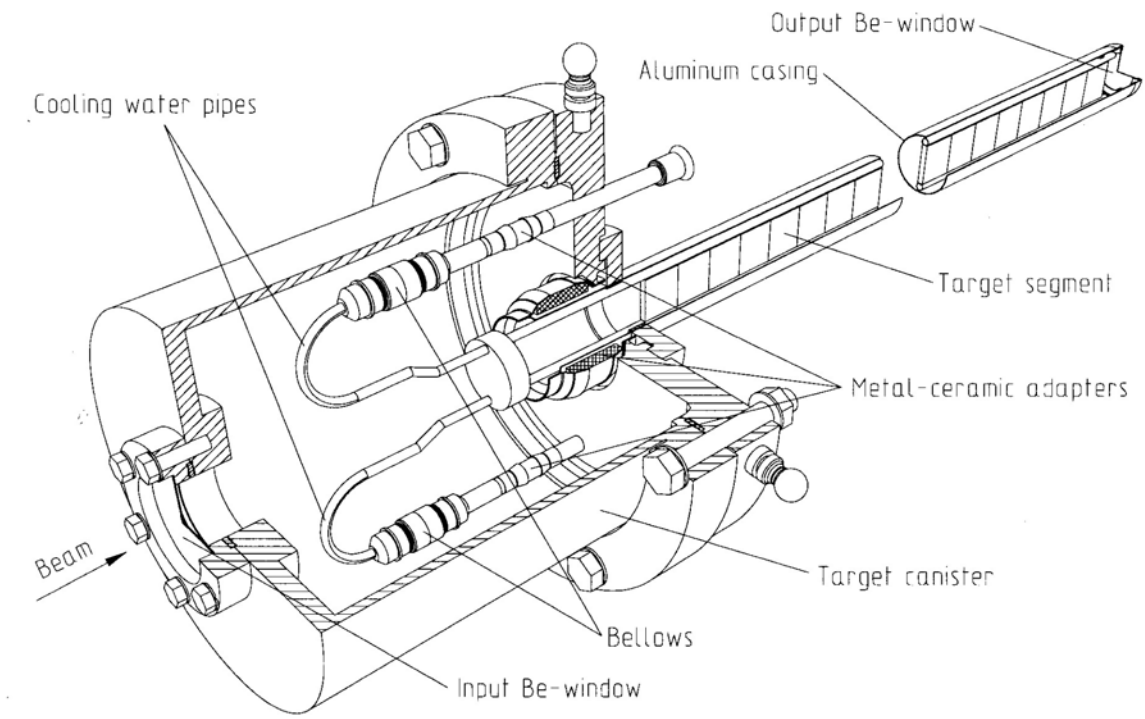

Figure 4.2-12 The target and target vacuum canister.

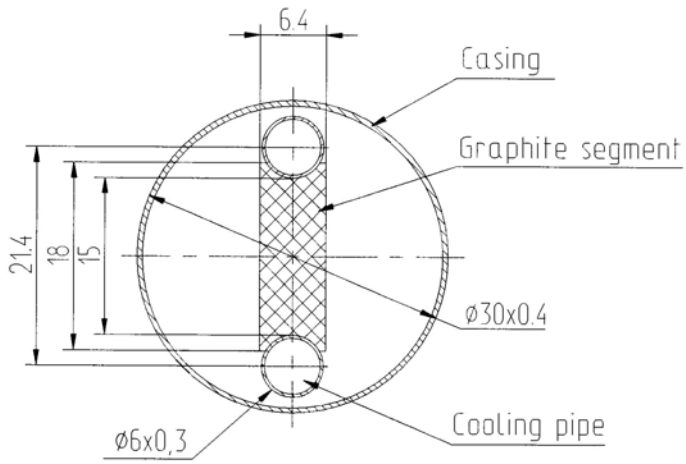

Figure 4.2-13 Beam's eye view of target. Dimensions shown in mm.

The target fin plus cooling tube is electrically isolated from the casing by ceramic spacers and water line breaks. A wire connected to the cooling tube allows measurement of the delta-ray charge knocked out of the target when it is hit by beam. This horizontal "Budal monitor" provides a cross check of the position of the target by measuring the response as the beam is scanned horizontally across the target.

The Budal signal on the 48th target segment is separately read out, and provides a position check as the beam is scanned vertically across the target. The cooling for this segment is provided by conduction through its clamping plates to the canister. The clamping plates are anodized to provide the required electrical isolation.

The aluminum casing around the target is electrically insulated from the base canister. This provides an electrical break from possible voltage from the horn inner conductor. A wire connected to this casing can be used to check if the casing is touching the horn (there is only 2.7 mm clearance between the target casing and horn).

The target casing may be evacuated during low intensity beam scans, which should improve the signal-to-noise of the Budal monitor. During high intensity running, the target canister will be He filled, to provide heat transfer from the aluminum casing to the cooling pipes.

During continuous operation, the center of the highest temperature segment will cycle between 58 deg C and 330 deg C, with resultant stresses, energy deposit and water cooling parameters shown in **Table 4.2-4** through **Table 4.2-6**.

	Center of segment	Corner of segment
Max. equivalent stress	27.4 MPa	23.5 MPa
Type of stress	All-axis-compression	All-axis-stretch
Strength limits	210 MPa compressive	95 MPa tensile
Derating factor high cycle fatigue endurance	0.5 to 0.6	0.5 to 0.6
Resulting safety factor after many cycles	2.2	1.8

Table 4.2-4 Thermal stresses in target segment with highest energy deposition density.

Graphite Segments	2.96 kw
Cooling pipes and water	0.42 kw
Aluminum casing	0.15 kw
Total	3.52 kw

Table 4.2-5 Energy deposition in target for baseline beam intensity (4e13 protons per 1.87 seconds).

Velocity of cooling water	**2 m/s**	**3 m/s**	**4 m/s**
Heat transfer coefficient, $kW/m^2/K$	10	14	18
Pressure drop, atm	0.32	0.68	1.2
Water flow rate, l/min	2.7	4.1	5.5
Water temperature rise, K	18	12	8.8

Table 4.2-6 Water cooling parameters as a function of water velocity.

The construction drawing set for the target is IHEP 7589-00-00-00. See also "Advanced Conceptual Design of the Low Energy Target and Beam Plug" (NuMI-B-543), "Dynamic Stress Calculations for ME and LE Targets and Results of Prototyping for the LE target" (NuMI-B-675), "Further Studies of Target for the Low Energy NuMI Beam" (March 30, 2001), "Temperature and Stresses in the LE Target with 6.4 mm Wide Segments" (June 20, 2001), and "NuMI LOW ENERGY TARGET SPECIFICATION" (June 25, 2001), for more details.

4.2.4 Focusing horns

Figure 4.2-14 and **Figure 4.2-15** show the horns, which are pulsed to produce toroidal magnetic fields. Slightly idealized parameterizations of the conductor shapes are listed in **Table 4.2-7**. The field strength falls off linearly with radius. The highest field is at the neck of horn 1 (3 Tesla at 200 kA).

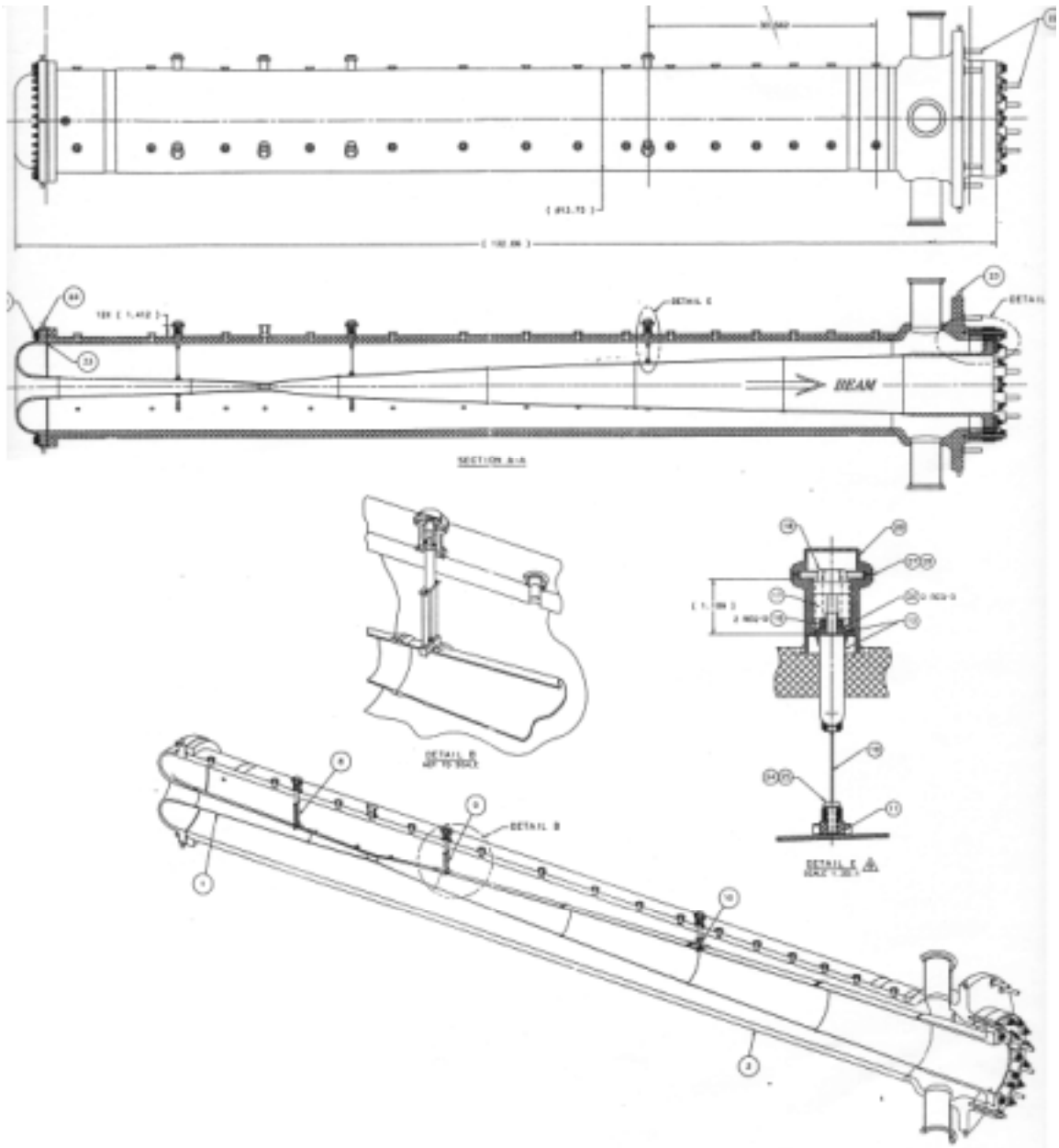

Figure 4.2-14 Horn 1 assembly drawing, with detail of inner conductor support spider. (From drawing 8875.112-ME-363092)

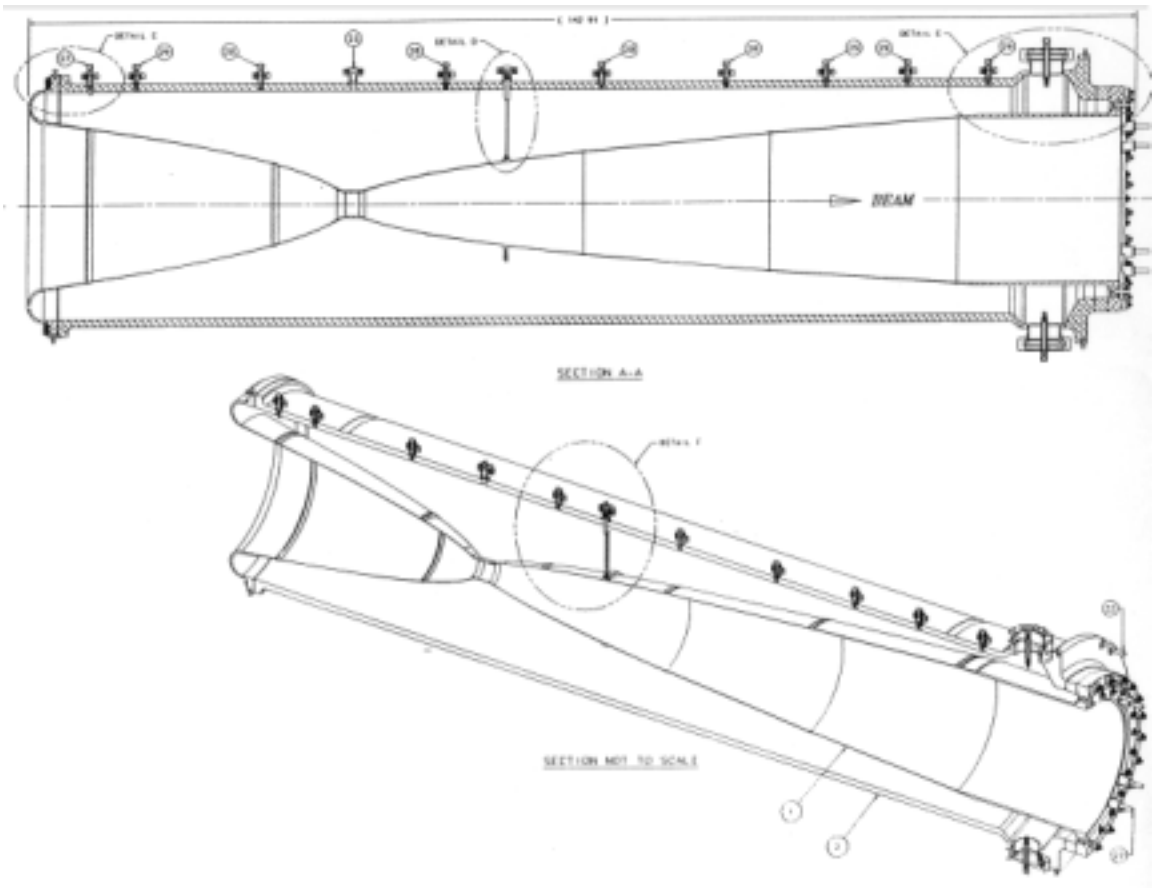

Figure 4.2-15 Horn 2 assembly drawing. (From drawing 8875.112-ME-363382).

PH2M Horn Parameters

Horn#1	Upstream		Neck	Downstream	
Z, cm	0.–44.047	44.047–80.	80.–83.982	83.982–95.128	95.128–300.
R_{in}^{IC}, cm	$\sqrt{\frac{92.8454-Z}{7.0483}}-0.2$	$\sqrt{\frac{85.7091-Z}{7.0483}}$	0.90	$\sqrt{\frac{Z-82.2125}{2.1850}}$	$\sqrt{\frac{Z-80.}{2.1850}}-0.2$
R_{out}^{IC}, cm	$\sqrt{\frac{92.8454-Z}{7.0483}}$		1.35	$\sqrt{\frac{Z-80.}{2.1850}}$	
R_{in}^{OC}, cm			~~15.83~~ 14.92		
R_{out}^{OC}, cm			~~16.20~~ 17.46		

Horn#2	Upstream	Neck	Downstream
Z, cm	0.–97.617	97.617–104.803	104.803–300.
R_{in}^{IC}, cm	$\sqrt{\frac{100.-Z}{0.1351}}$ ~~0.2~~ 0.3	~~4.00~~ 3.90	$\sqrt{\frac{Z-100.}{0.2723}}$ ~~0.2~~ 0.3
R_{out}^{IC}, cm	$\sqrt{\frac{100.-Z}{0.1351}}$	~~4.20~~ 4.40	$\sqrt{\frac{Z-100.}{0.2723}}$
R_{in}^{OC}, cm		37.00 ✓	
R_{out}^{OC}, cm		~~37.87~~ 39.54	

.

Table 4.2-7 Idealized equations describing shape of horn conductors. Z is distance along beamline, and R gives inner and outer edges of inner and outer conductors. See construction drawings for details of rounded corners, endcaps, cooling ports, etc.

The horns are designed for 205 kA maximum current pulse of 5.2 ms half-sine wave width, with a repetition rate of 1.87 sec. The pulse width planned for use with the low energy beam is between 1.7 ms and 2.3 ms, which will reduce the joule heating. However, the horn is still baselined to be able to run at 5.2 ms pulse width, and the following section is entirely based on that more stringent case as indicated in **Table 4.2-8**.

Parameter		Horn 1		Horn 2	
Inductance (nH)		690		~457	
Resistance (μΩ)		208 (meas.)		<112	
Average Power from Current Pulse (kW)		17.0		<7.5	
Power Flux at Neck (W/cm2)		14.5		<4.7	
Temperature Rise at Neck (^{o}C)		22.8		<7.1	
Outer conductor beam energy deposition (kW)		14.5		5.4	

Table 4.2-8 Electrical parameters for 5.2 ms pulse width.

Summary of stresses:

• US end cap: minimum stress before pulse is -1030 psi; maximum stress at mid-pulse is -9020 psi; mean stress is -5025 psi with an alternating stress of 3995 psi; Stress ratio R=0.11

• Under the above calculated stress levels, allowable maximum stress for 10^7 cycles at the endcap is 26.5 ksi resulting in fatigue safety factor of 2.9

• Neck of horn: stress at mid-pulse is +4351 psi; stress at end of pulse is -3742 psi; mean stress is 304 psi with alternating stress 4047 psi; Stress ratio R = -0.86 (*Note: Negative value of R results in lower value of fatigue stress limit)*

• Under the above calculated stress levels, allowable maximum stress for 10^7 cycles at neck is 15.3 ksi resulting in fatigue safety factor of 3.5

• Stress in conductor weldment regions is very low (<<4 kpsi)

∗ *Fatigue data from Aerospace Structural Metals Handbook*

Fabrication

•Inner conductor fabricated from 6061-T6 billet per QQA 200/8

•Relatively good strength (UTS ~ 45 ksi, YS ~ 40 ksi, R=-1 FS ~ 16 ksi)

Welding:

•Single pass, full penetration CNC TIG weld is required to minimizing conductor distortion, assure repeatability, and control internal weld porosity

• Proper cleaning, handling, fixtures, and weld parameters are crucial to minimize conductor distortion and internal weld porosity.

Coating:

•Inner Conductor and conductor supports are coated high phosphorus electroless nickel (0.0005” - 0.0007” thick).

•Outer conductor is anodized: Type III (hard coat sulfuric acid, 0.0023”), R_c 60-65, dielectric strength of ~800 V/mil

•Stripline contact surfaces use 0.0005” silver brush plating

Mechanical:

•Water Seals- Total of 64 water seals in horn

- Utilize EVAC aluminum delta seals on KF style flange

•Bolted Connections

- Utilize TimeSert threaded inserts, pullout exceeds 9600 lb. on 3/8” insert
- As a reference, maximum end wall reaction is approximately 4270 lb.

•Current Contact Surfaces

- Current surfaces have 32 μin finish, 0.0003”-0.0005” silver plate finish
- Interface clamping pressure exceeds 1400 psi
- Prototype horn 1 contact area is 9.2 in^2 for 7250 Arms.

4.2.5 Horn Magnetic Field Monitor

The magnetic field of Horns 1 and 2 will be monitored by a set of three pickup coils (Bdot coils) in each horn. These will be inserted and mounted through ports located at the "neck" of each horn. The coils will be spaced with a 120 degree azimuth separation around the horn: one coil located at top of horn and the other two located toward the bottom 120 degrees from the top one.

The coil assembly**, Figure 4.2-16**, will consist of 8 turns of 0.010" stainless steel wire wound on a zirconia ceramic structure. The ceramic mount will have grooves ground onto the end to locate the wire. Staggered 1/16" holes will be drilled into the upper body of the mount to secure the wire coils. The holes will be drilled after a "green" firing of the zirconia which will then undergo the final firing.

The voltage induced in the coil by the pulsing of the horn will be readout by an instrumentation amplifier into either a sample and hold synchronized to the current pulse timing or a peak sensing circuit. The required accuracy of 0.3% has been demonstrated on a prototype coil during testing of the horn 1 prototype. Modulation of the prototype coil signal with the horn cooling water temperature was observed due to thermoelectric voltage generation at the silver solder joints between the stainless steel coil and its stainless feedthrough/mount. The production coil will be welded to the feedthrough using stainless steel. It is believed that this will eliminate the thermoelectric caused modulation. It has been demonstrated that a baseline subtraction using a pedestal read ~1ms after the end of the current pulse corrects for the modulation. Such a subtraction will be employed as a fallback if modulation is observed in the production coil. The coil may also be used for timing synchronization by measuring the time of the peak of the coil pickup.

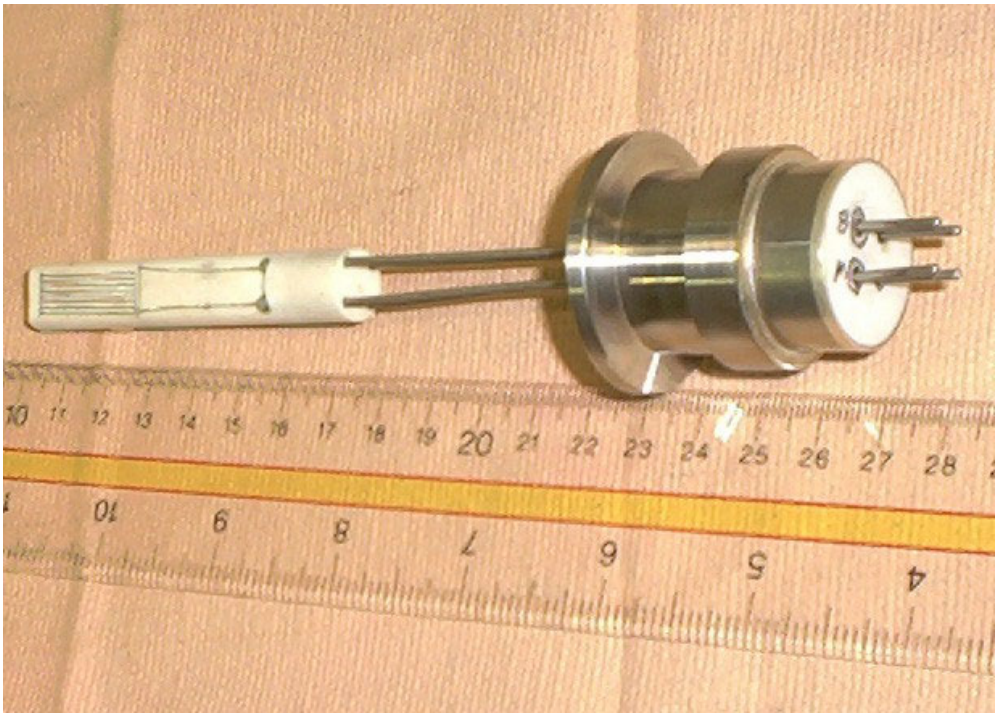

Figure 4.2-16 The prototype horn magnetic field monitoring probe.

4.2.7 Remote Clamp and Stripline Block

A stripline stub is permanently connected to a horn. This mates to the stripline at the bottom of the module. The remote clamp is used to apply pressure between the two sections of stripline to make a good electrical connection. The remote clamp is mounted on the stripline block, which provides radiation shielding, see **Figure 4.2-**18. The entire stripline block and remote clamp can be lifted out of the module for replacement if the remote clamp fails.

Once the bottom of a module is radioactivated, the replacement of a horn must be done remotely, in the work cell. The remote clamp toggles, and is tightened or released via a long shaft through the shielding. A set of daggers aid in bringing the striplines into proper alignment when a new horn is inserted.

The requirement for clamping pressure is set at 1400 psi. The stripline contact area is 9 sq. in. per layer. Allowing for a reasonable safety factor, the clamp was designed to provide 32000 lbs of force. In a test of the prototype, the actual force exerted was 38000 lbs. Belville washers serve two functions. They spring the contacts apart when the force is released, and provide a tolerance for minor thickness variations when toggle is in the clamped position. The nominal clearance between stripline contact surfaces during insertion is 0.03 inch, for each of eight surfaces, thus the clamp must close at least 0.24 inch.

Ceramic insulators are used in the remote clamp because of the high radiation environment.

The stripline penetration through the stripline block jogs to prevent line-of-sight from the top of the module to the high radiation area below.

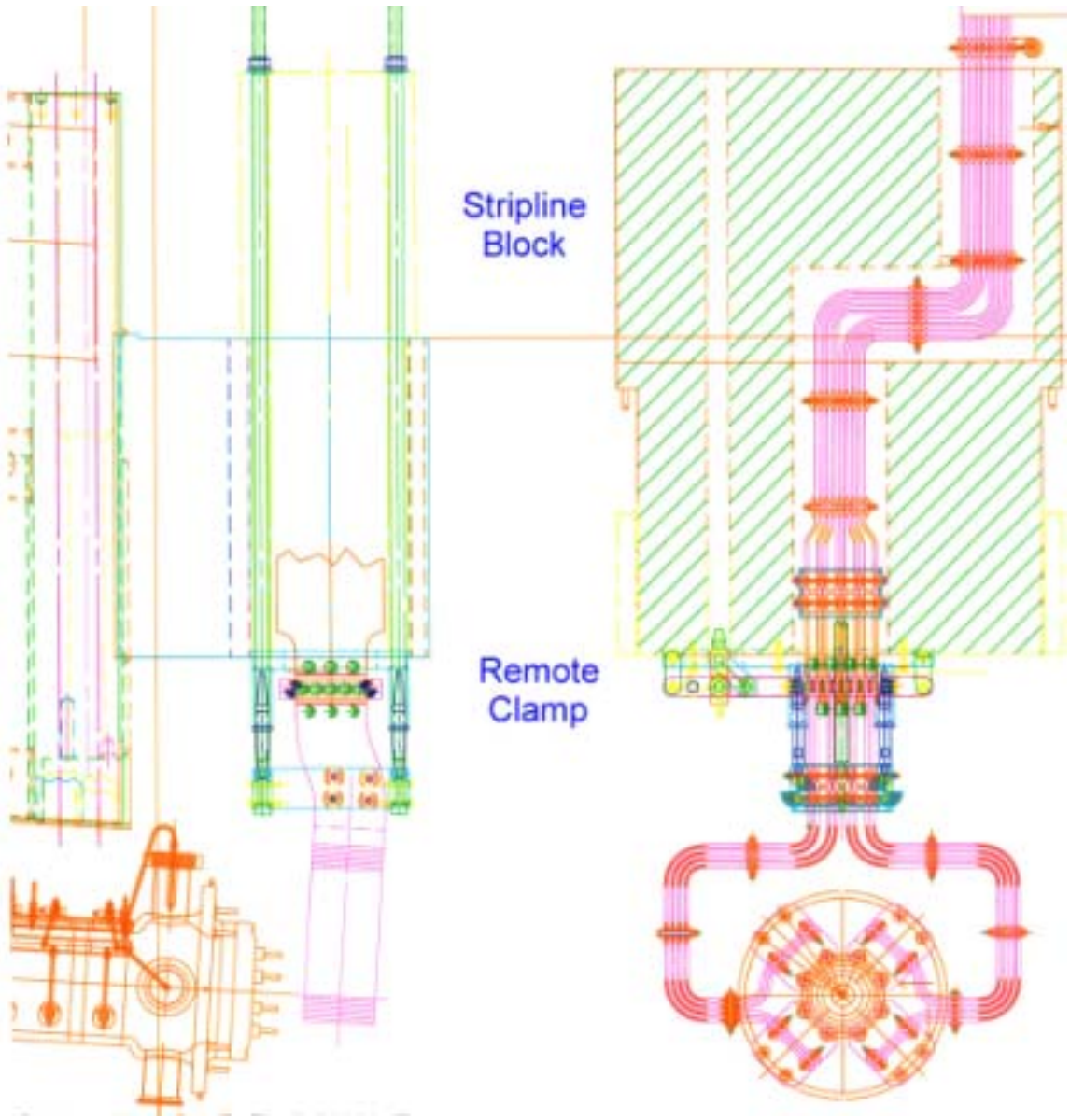

Figure 4.2-18 Side and end views of the stripline block and remote clamp in place with the horn and module.

4.2.8 Target/baffle Carrier Design

4.2.8.1 Carrier Definition

"Module" refers to the heavy shielding module that supports beam components below it, and has positioning motors mounted on top of it. The target/baffle carrier is a frame mounted on shafts through the target/baffle module. The module provides motion control of the target transverse to the beam by moving the shafts vertically and horizontally. The carrier supplies precision motion control of the target along the beam. When maintenance is required that cannot be done in situ, the entire module with carrier and components still mounted on it is moved to the work cell. The module, carrier, target and baffle are shown **in Figure 4.2-19** and **Figure 4.2-20**.

Please refer to the engineering drawing set for up-to-date definitive dimensions and layout. The integration drawing for the modules, carrier, and horn 1 is **8874.000-ME-363028**. The final carrier drawings have not been made yet.

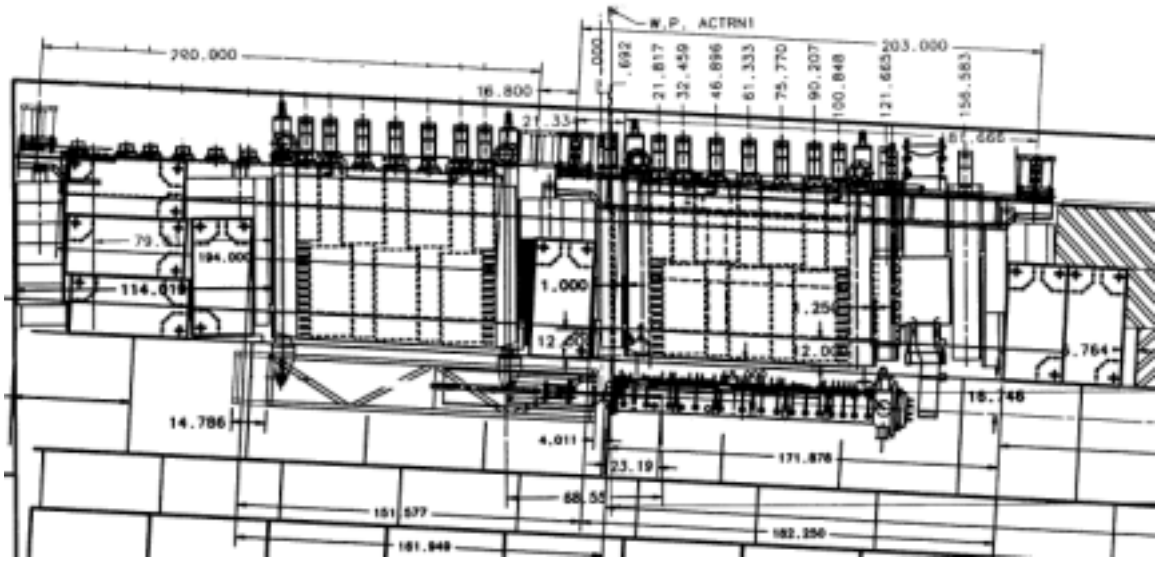

Figure 4.2-19 Modules in target hall shielding. Target/baffle carrier mounted below target/baffle module, with target and baffle extended into the low energy position. Also visible are carriage cross beams, steel shielding, horn 1 mounted below horn 1 module.

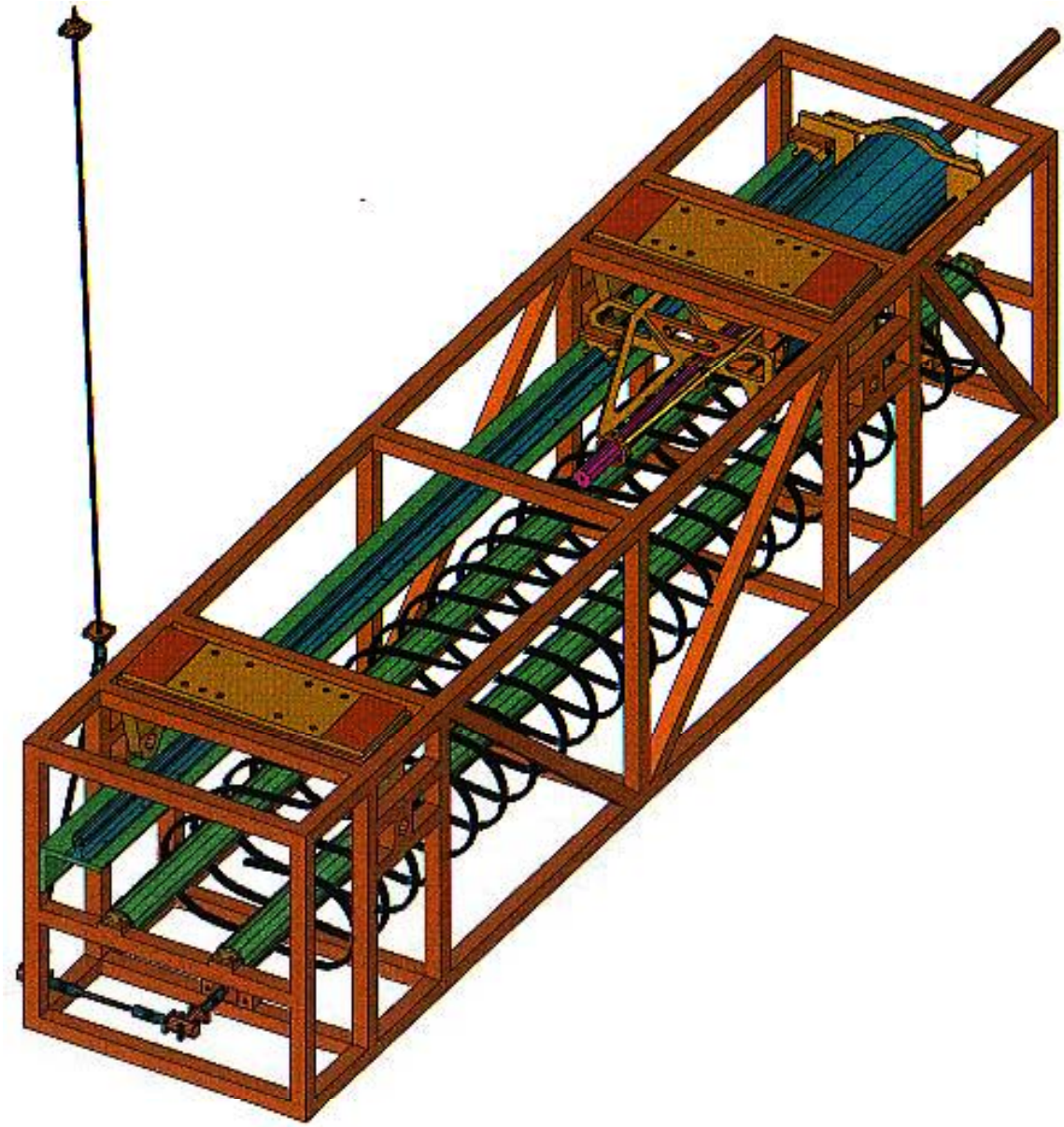

Figure 4.2-20 Target/baffle carrier with target and baffle mounted. Target shown extended into the low energy neutrino beam position

4.2.8.2 Target/Baffle Carrier Functions and Requirements

Target/Baffle Carrier must:

- Remotely drive target into horn along beam axis after module is set in place: target casing extends 66.2 cm into horn, target carrier frame has 7.1 cm clearance to horn, thus minimum of 73.3 cm forward travel.

- Provide target motion capability to 250 cm retracted from the standard low energy running position, to enable changing the energy tune of the neutrino beam.

- Set position of target and baffle to 0.5 mm transversely, and 1 mm longitudinally along beam line.

- Maintain position of target and baffle to 0.5 mm transversely and 1 mm longitudinally under beam heating from $4x10^{13}$ protons / 1.87 sec striking target; this includes other beam energy tunes in addition to the standard low energy beam position.

- Provide the motion capability of the target and baffle utilities: target water supply line, target water return line, target vacuum line, two Budal target monitor electrical lines, 8 thermocouple electrical lines.

- Maintain 1 inch clearance to target hall chase walls, in addition to the allowance for +/- 8 mm horizontal and +8 mm / -7.5 inch vertical motion of support shafts.

- Provide a 2 cm radius "stay-clear" through the support structure that allows beam scans of downstream components when the target/baffle carrier is remotely lowered off beam axis (by ~ 7.5 inch).

- Survive radiation dose of up to 10^{11} rad/year for up to 10 years (except for the drive shaft end which is above the module).

- Be short enough that it can be extracted through the target module carriage (199 inches) and inserted in the work cell (216 inches) with the target frozen in the extended position, or frozen with the baffle sticking out the back end in the target fully retracted position.

In addition, carrier will provide:

- Four tooling balls for survey, located at beamline elevation, one on each side of the beamline at each module endwall, visible through holes in the endwall.

- A pair of limit switches at each end of the travel of the target/baffle.

- Rotary encoder on drive shaft at the top of the module to give remote readback of location of target along beamline.

- Include baffling to direct part of the chase air stream to the target that is otherwise blocked by the target base and support tube. Airflow must also be maintained over the length of the baffle and the target.

- Rust prevention coating of drive shaft and any other (non-stainless) steel parts.

Note secondary containment of radioactive water leaks is built into the target pile design, and is not a carrier design consideration.

4.2.8.3 Target Motion Capability

<u>Low Energy Target Insertion</u>

For the Low Energy Beam, the target will extend 66 cm into the horn with only 3 mm transverse clearance at the tip. The choice was made not to mount the target on the horn itself for fear of vibration damage to the target from horn pulsing. The target module will be set in place with the target in a retracted position. After the target module is surveyed into position, and the axis of the carrier aligned with the beamline (and horn) axis using the module motor drives, the target will be extended along the beam line into the horn using the carrier motor drive.

Other Neutrino Energy Tunes

In NuMI-NOTE-BEAM-0783 [ref. i], the case was made that by extending the range of motion of the low energy target upstream one obtains the capability to quickly and easily change the energy of the neutrino beam. Such alternate energy tunes are labeled "semi-medium" and "semi-high" energy beams, and produce decent rates and spectra, although not quite the performance that can be obtained with optimized targets and horn 2 positions for the alternate tunes.

When moving the target, one is taking the chance that it could become stuck in some location. The target is in a high-radiation environment (e.g. humidity can turn to nitric acid), and repairs to the carrier mechanisms after being irradiated is mostly limited to replacement. Proper choice of materials can help mitigate this. However, this is a risk explicitly taken, and reinforces the need to have a complete spare target/baffle/carrier unit at beam-turn-on.

Extended target motion by relocating target module

The target carrier allows for 2.5 m of target motion without moving the target module. The target can be moved even further upstream by moving the target module, although this is not a trivial exercise. The current baseline design allows space for one to move the target module 2 m upstream by unstacking some shielding, using the crane to move the 20 ton module, restacking shielding, and then doing a survey to check the final position. This would result in a total target range of 4.5 meters, but the last 0.5 m or so may be precluded by interference between the baffle and target hall upstream wall and beam pipe. (The standard high energy target position was 3.65 m upstream of the low energy position, and is reachable in this scheme.) The target/baffle carriage cross beams which limit the upstream movement of the module can be seen in **Figure 4.2-19**. Three pieces of steel shielding required for this new position are not in the baseline project, and would have to be acquired before the move.

Restriction of motion by carriage, workcell

Carrier frame	**Fixed frame**	**160 in.**
Moving components	**Total moving components**	**315.97 cm = 124.40 in.**
	Baffle length	150 cm
	Baffle to vertical Target fin	68 cm
	Target fin length	95.38 cm
	Target casing beyond fin	2.59 cm
Length normal extraction	**Components inside frame**	**160 in.**
Total length L.E. position	**Frame with target extended**	**188.86 in.**
	Target extension	28.86 in.
	Frame length	160 in
Total length fully retracted	**2.5 m upstream of L.E.**	**193.97 in**
	Baffle extension	33.97 in.
	Frame length	160 in

Table 4.2-10 Length of target/baffle/carrier unit in various configurations.

The opening in the target carriage shielding is 199.389 inches. The work cell is 216 inches long. These two openings set the maximum length of the target/baffle carrier and range of motion. The module with target/baffle possibly frozen in the fully extended or fully retracted position must be able to navigate through these openings, with operators controlling the crane by camera and remote control due to the high residual radiation.

In the target extended downstream position, the length of carrier plus target is 189 inches. With 250 cm of motion capability, with the baffle extended out the upstream end, the baffle plus carrier is 194 inches long. See also Figure 4.2-21.

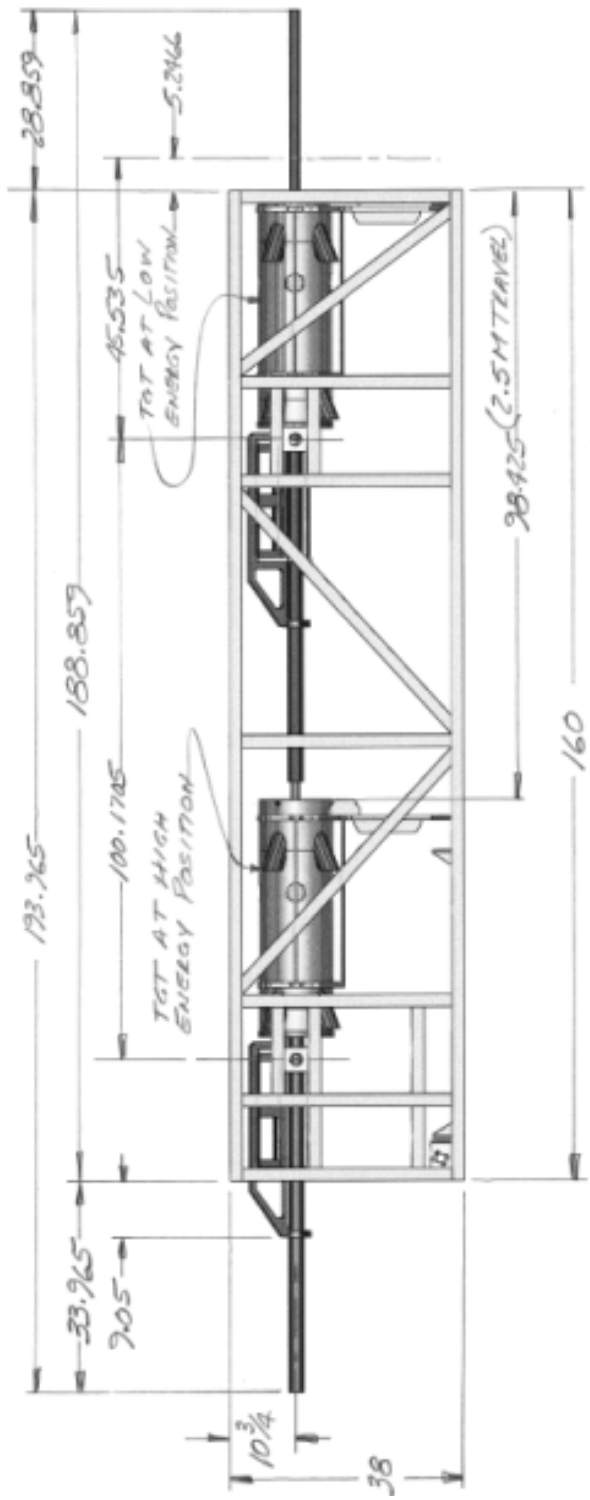

Figure 4.2-21 (Rotated) target carrier side view. Target and baffle are shown in both Low Energy Beam extended position, and in fully retracted highest energy beam position.

4.2.8.4 Target/baffle carrier hardware design

Carrier mechanical design

The target and baffle frames have rollers that ride on aluminum rails, as shown **in Figure 4.2-22**. The rails are at beam height, and are supported by an aluminum tube space frame. Two hangers (sometimes miscalled clamps) connect the space frame to the shafts (not shown in the figure), which come through the module. The mass of the various components is summarized in **Table 4.2-11**.

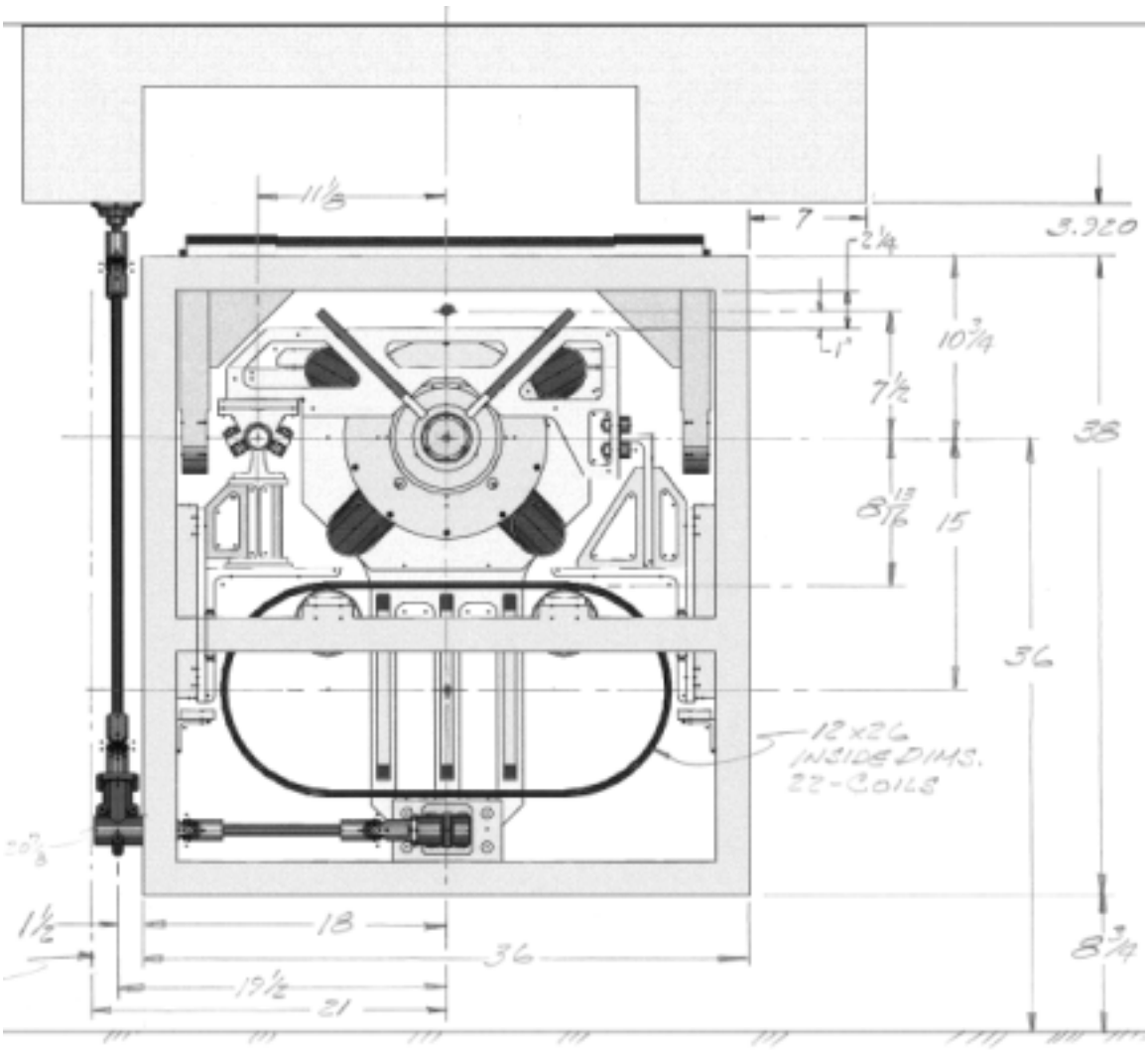

Figure 1.2-22 Target carrier end view.

Components			215 lb
	Target Assy.	150 lb	
	Baffle Assy.	65 lb	
Coils			47 lb
	One steel loop	0.581 lb	
	Water in loop	0.194 lb	
	3x22 steel loops	38.3 lb	
	2x22 water loops	8.5 lb	
Carriage Assy.			598 lb
	Frame Assy.	231 lb	
	Target baffle left support	120 lb	
	Target baffle right support	110 lb	
	Shaft support	44 lb	
	Coil support	23 lb	
	Drive system	70 lb	
Drive shaft loads			82 lb
	Components on 0.058 slope	12 lb	
	Rolling friction (0.05 coef.)	11 lb	
	Coil contraction, max.	30 lb	
	Friction coil on supports (0.61 coef.)	29 lb	

Table 4.2-11 Approximate mass of carrier components, and loads.

The aluminum rails are coated with tungsten-disulfide to provide a tough surface for the rollers to ride on.

The rollers are commercially available cam-followers, black oxide coated steel in an aluminum housing. (These may be replaced with stainless steel if we can locate a vendor). They will be run dry, i.e. without grease. It is expected that the target location will only be changed a few hundred times, so the number of cycles is relatively small.

The drive shaft is 1-inch diameter 17-4 PH heat-treated stainless steel.

Carrier thermal considerations

When running in the ME or HE locations, some of the target support shafts and rails will be downstream of the target, and thus receive substantial energy deposition from the secondary beam. MARS was used to calculate the energy depositions [ref. ii, see Figure 5 for summary of study]. In order to maintain thermal position stability, several measures are taken.

Water cooling is supplied to the downstream module-to-carrier hanger (sometimes known as the clamp, in analogy to its use for horn 1), and the lower part of the support shaft is made of low-expansion steel. The water-cooled clamp design is copied from the horn 1 module design [ref. iii]. The bearing between this clamp and the carrier is on beam-centerline vertically. The clamp water cooling is not required for low energy beam running. Thus its water loop is separate on the module from the target water loop, so that failure in this system would not require replacing the target for low energy running.

The carrier frame and rails are made of minimal volume to surface ratio aluminum and are kept at larger radius to the beam centerline. For initial design studies, a frame constructed of ¼ inch thick wall ¾ inch square aluminum tubing was assumed. The beam-heating of the tubing plateaus about 1 m downstream of the start of the target (**Figure 4.2-23**). At a radius of 25 cm from the beam, the energy deposition in the aluminum is around 0.032 watts/gram. Assuming a heat transfer coefficient of 10 w/m^2K to the 18 deg C air flowing in the chase, the asymptotic temperature calculated was 55 deg C, which is acceptable for the frame. The final design uses thinner 1/8 inch wall 2 inch square tubing, and thus should experience less than half the temperature rise. The beam heating upstream of the target is negligible.

The drive shaft is placed at a radius of 40 cm from the beam-centerline. At that radius and downstream of the target, it is estimated that its temperature will be between 100degC and 150degC. The part that sets the target location is upstream of the target, and will remain cool. The downstream end of the shaft can be constrained transversely, but allowance must be made for a 2 mm longitudinal expansion of the downstream part when running higher energy tunes.

R. Rameika
B. Lundberg
March 2002

Energy deposition in target support structure

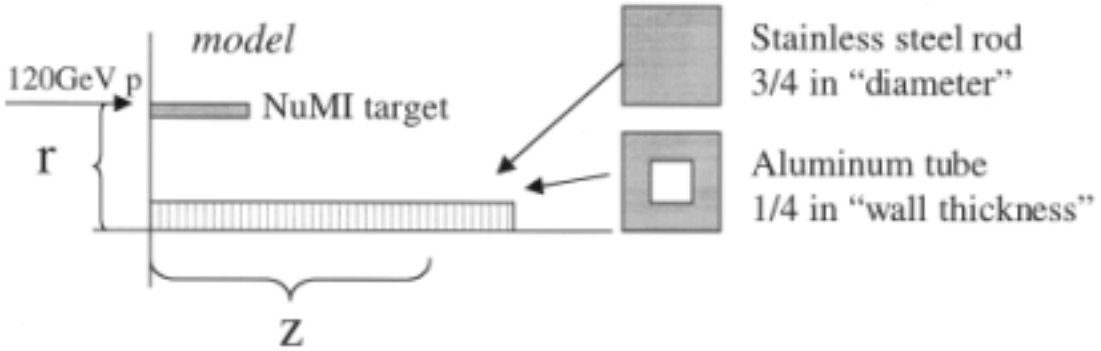

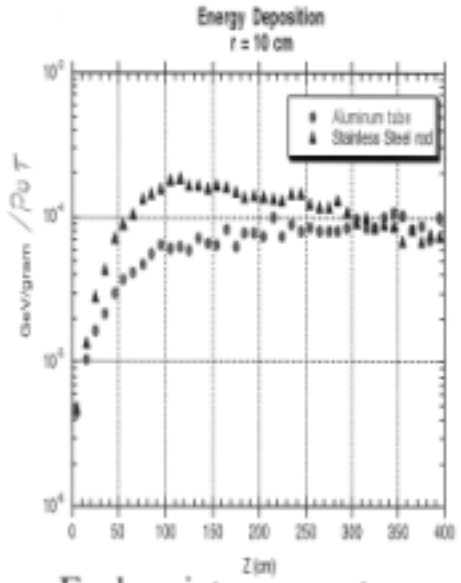

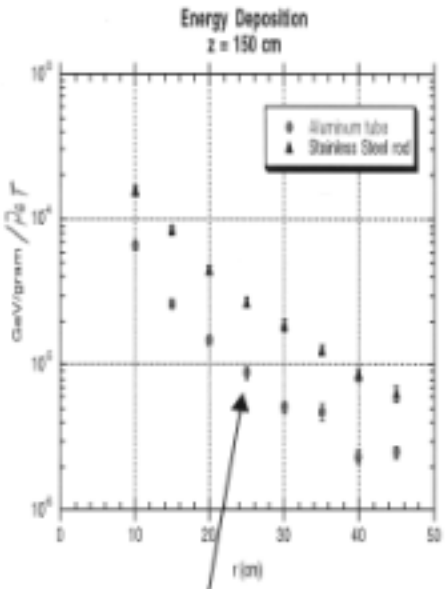

Each point represents a "zone" of 10 cm in length.

Material	ρ (g/cm^3)	Vol (cm^3)	Watts/cm at z=150 cm; r=25 cm	Watts/cm^3	Watts/gram
Aluminum	2.7	3.23	0.28	0.087	0.032
Stainless Steel	8.02	3.63	2.8	0.77	0.096

(for 4e13 ppp)
1.87sec ref. rate

Figure 4.2-23 Summary from study of beam energy deposition in carrier using MARS.

Carrier Frame Stiffness

Analysis of carrier support frame distortion has been carried out for three positions of the target; fully extended, fully retracted, and halfway in between. The vertical mis-alignment of points on the target and baffle due to changes in the loading of the carrier frame was at most about 0.2 mm.

During the assembly of the target on the carrier frame, the target will be aligned such that the upstream and downstream ends of the target fin are vertically on axis; because of the sag of the target tube due to gravity, the middle of the target will be a fraction of a mm above the beam axis.

The sag of the drive shaft is 5/16 inch when the target is in the fully extended position.

Flexible utility lines

The 2.5 m travel of the target is accommodated by compressing a coil of 22 loops of pipe, 3/8" O.D. 0.028" wall stainless, total length 38 m per line. Three lines are used: water supply, water return, vacuum. In the LE position, the coil is unloaded. Fully retracted by the 2.5 m, the coil force is of order 30 lbs. The drive shaft is kept under tension, eliminating worry about buckling. (Putting the drive shaft in compression might have forced use of a larger diameter shaft, exacerbating cooling problems due to the larger volume to surface ratio). The maximum stress on the water line is calculated to be 18 ksi, which is below the yield stress with shear factor of 35 ksi x 0.577 = 20 ksi.

Radiation hard thermocouple cable is produced commercially, consisting of a stainless steel sheath encapsulating a pair of wires in magnesium oxide insulation. We will use this cable for all electrical routing on the carrier. The flex necessary for the target motion will be obtained in similar fashion to that for the utility lines, i.e. a coil that expands or contracts, resting on an immobile support shaft. The voltage standoff required is reasonably modest. The target tube may see a voltage of order 50 Volts from the horn, since it follows the horn voltage closely due to beam ionization of the air between the horn and target tube. The Budal monitor may be run with a bias voltage of up to 75 volts, although a smaller bias (down to zero) can be used if necessary.

Target Module Endwall Penetrations

The Horn 1 module upstream endwall has six penetrations for utilities, as shown in **Figure 4.2-24**. Target module upstream and downstream endwalls will copy this, with the assignments for usage shown in **Table 4.2-12**.

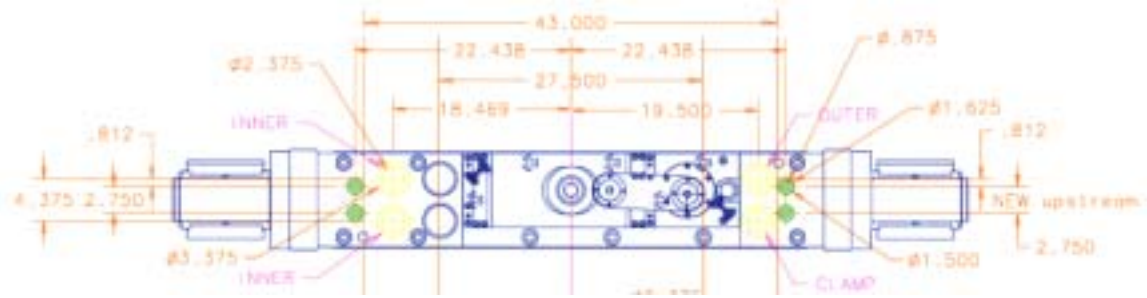

Figure 4.2-24 Top view of Horn 1 module upstream endwall, which will be copied for the target module. Utility penetrations include those labeled clamp, outer, inner, and the two large holes to the right of those labeled inner.

Upstream endwall	
1	Upstream Left Survey Port
2	Upstream Right Survey Port
3	Drive Shaft for 2.5 m motion
4	Target water supply
5	Target water return
6	Target vacuum/helium line
Downstream endwall	
1	Downstream Left Survey Port
2	Downstream Right Survey Port
3	Clamp water supply
4	Clamp water return
5	Electrical feed through #1
6	Electrical feed through #2

Table 4.2-12 Allocation of target-module endwall utility penetrations.

Each electrical feed through contains five two-pin plugs. Connections are as show **in Table 4.2-13**, where the third baffle thermocouple could be re-allocated if some other electrical connection is required.

Plug	Pin 1	Pin 2
1	Target Budal horizontal fin	Shield for horizontal fin signal
2	Target Budal vertical fin	Shield for vertical fin signal
3	Carrier thermocouple 1	Carrier thermocouple 1
4	Carrier thermocouple 2	Carrier thermocouple 2
5	Baffle thermocouple 1	Baffle thermocouple 1
6	Baffle thermocouple 2	Baffle thermocouple 2
7	Baffle thermocouple 3 (or spare)	Baffle thermocouple 3 (or spare)
8	Wire from target vacuum jacket	Ground for limit switches
9	U.S. limit switch 1	U.S. limit switch 2
10	D.S. limit switch 1	D.S. limit switch 2

Table 1.2-13 Target carrier electrical pin allocation.

References

[i] Proposal for Continuously-Variable Beam Energy, M. Kostin, S. Kopp, M. Messier, D. Harris, J. Hylen, A. Para, NuMI-NOTE-BEAM-0783, 10/17/01.

[ii] Energy deposition in target support structure, R. Rameika, B. Lundberg, 3/02.

[iii] Thermal Analysis of Clamp Using MARS Analysis Heat Generations, Bob Wands, 9/12/01.

4.5 NEUTRINO BEAM MONITORING (WBS 1.1.5)

4.5.1 Introduction

The neutrino beam monitoring system enables the users to verify the quality of the beam being delivered to the experiment(s). The monitors measure the flux and spatial distribution of:

- secondary hadrons (and non-interacting primary protons) measured by the "Hadron Monitor", located just upstream of the hadron absorber,
- muons, which are directly associated with the production of neutrinos, measured by the "Muon Monitors," located downstream of the hadron absorber and at various locations within the dolomite muon shield.

The locations of the monitors are shown in **Figure 4.5-1**. The monitors' intensity measurements are normalized to the incoming proton intensity while the measured spatial distributions of particles are compared to nominal spatial distributions recorded as the beam is being commissioned.

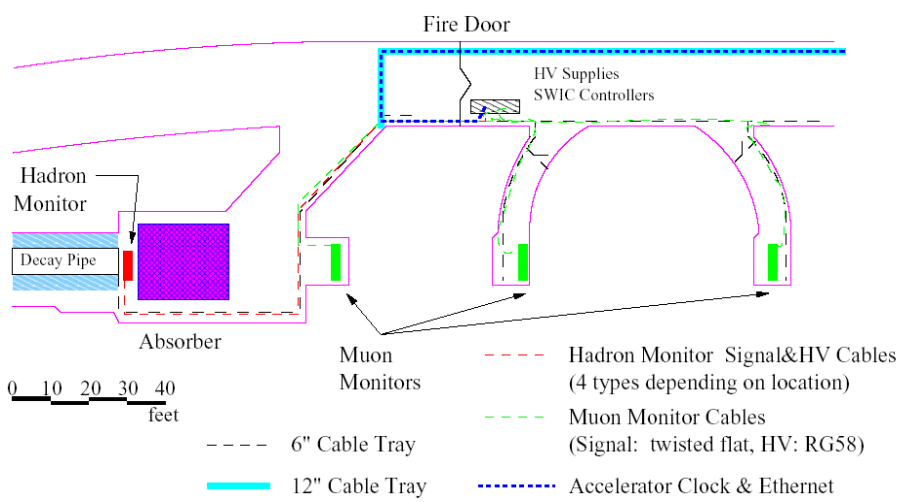

Figure 4.5-1 Plan view of the monitoring system: the hadron monitor is upstream of the absorber stack and the muon monitors are in the absorber enclosure and within the dolomite shielding

Both the Muon and Hadron Monitors are used to commission the NuMI beamline. In addition, during normal neutrino beam running for the MINOS experiment, the monitors serve as accurate neutrino rate monitors. Finally, during periodic specialized runs the monitors serve to re-check the neutrino beam direction toward Soudan.

4.5.2 The Hadron Monitor

4.5.2.1 System Function

The hadron monitor is designed primarily for commissioning the NuMI beamline. Specifically, it will align the proton beam prior to the installation of the horns and target in the target hall. The proton beam alignment is set within the quantitative limits described in Section 4.6 (about 50μrad).[1] **Figure 4.5-2** shows the signal expected in the Hadron Monitor during commissioning.

During normal neutrino beam operations with the horns and target in place, the hadron monitor tracks the proton spot, and can also monitor the integrity of the NuMI target. However, these latter functions are redundant with other instrumentation, such as the multiwires and BPM's or the muon monitors, so are not essential. If the Hadron Monitor should fail after extended running, it will have been highly radioactivated by the beam. As a result, the hadron monitor will only be replaced if a long shutdown permits. The likelihood or urgency of the replacement requirement will depend on operational experience with the NuMI beam. **Figure 4.5-2** shows the expected signal during normal beam operations: the magnitude of particle scattering in the target serves as a check of the full target integrity.

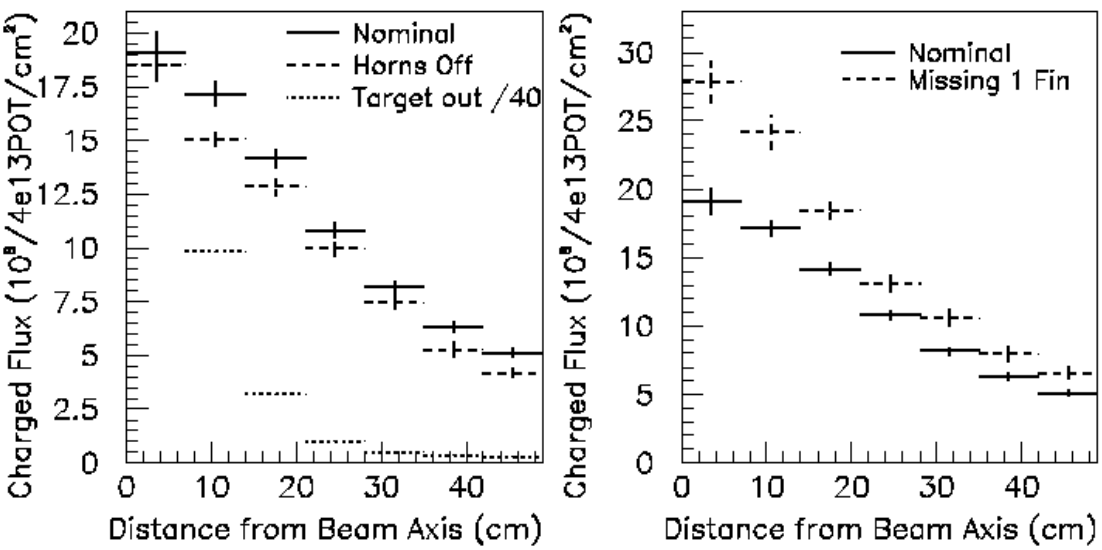

Figure 4.5-2 (left) Charged particle fluxes at the hadron monitor as a function of the distance from the center of the beamline. Fluxes for running with the target in (nominal) and out are shown. (right) Effect on Hadron Monitor signals if 15 cm of the 1 m target breaks off.

[1] Smart, W. NuMI-L-221, 31 Oct. 1996

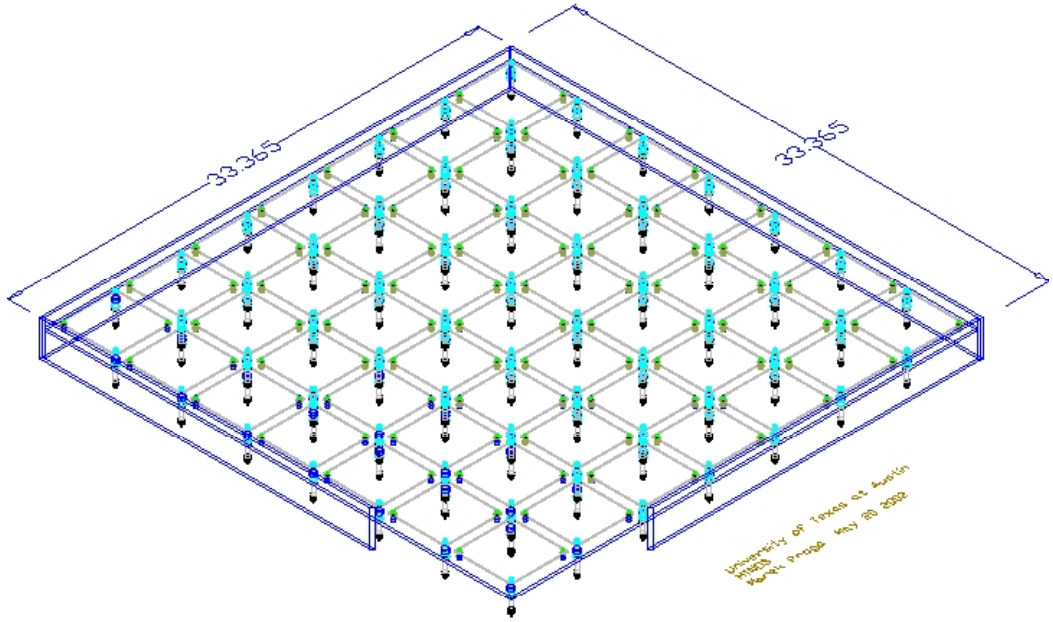

Figure 4.5-3 Schematic layout of the Hadron Monitor gas vessel and 7x7 array of ion chambers.

4.5.2.2 System Description

The hadron monitor is a 1x1 m^2 Aluminum gas vessel encasing an array of parallel plate ionization chambers (see **Figure4.5-3**). The chambers are mounted to the rear wall of the gas vessel on electrical feedthroughs. A thin front window of 0.010" Aluminum is mounted to the box. It is welded to a flange that compresses an Aluminum wire gasket to the box. It is not anticipated to open this lid for chamber repair after the hadron monitor has been in the beam. The vessel is 34” x 34”. Each 4”x4” ion chamber plate is separated from its neighbor by 0.5”.

Figure4.5-4 shows the drawings for the ceramic plates of the parallel plate ion chambers. The wafers are 1mm 96% pure Aluminum oxide, with Pt-Ag alloy electrodes.[2] Electrical connections to the grounded guard ring, the sense pad, and the HV plane are made through the corner holes to the rear of the board, where solder connections are made. Deviations from flatness, based on a preliminary order of 20 boards, are less than 0.003" across the 4" plate. The plates are separated by 1mm, the gap defined by precision ceramic washers.

[2] Cer-Tek, Incorporated, El Paso, Texas.

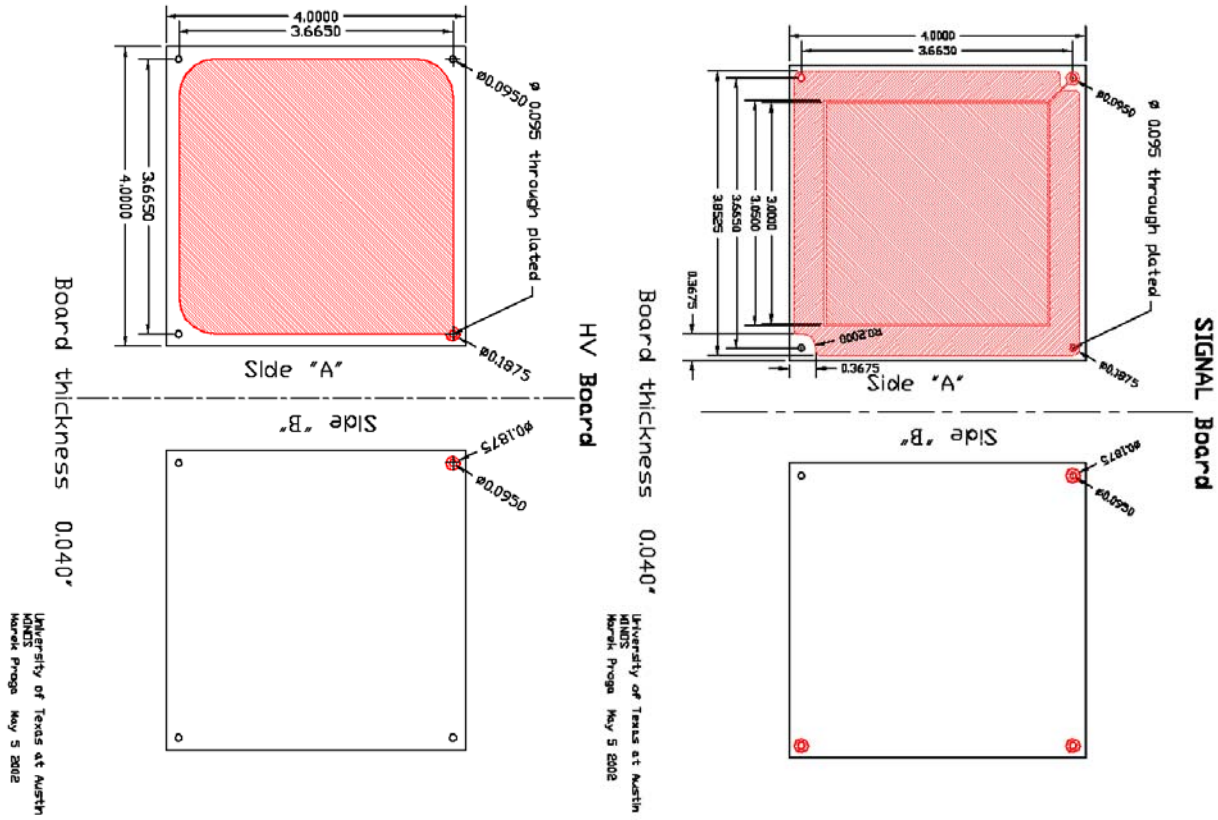

Figure 4.5-4 Design of the metalized ceramic pads that make up one parallel plate ion chamber inside the hadron monitor: (above) HV plan (below) signal plane with guard ring.

Figure 4.5-5 shows how the parallel plate chambers are mounted on the rear wall. Two commercially available HV feedthroughs (rated to 10 kV in vacuum) penetrate the rear Aluminum wall of the hadron monitor box.[3] The feedthroughs consist of a central stainless pin Kovar-sealed to a ceramic insulator. The ion chamber plates are soldered directly to the feedthrough pins at the corners, thus providing both the mechanical support of the chamber and the electrical contacts. An explosion-bonded Al-Stainless piece is used to make the weldments between the feedthroughs and aluminum box.

The cables delivering HV and bringing signals out of the hadron monitor consist of two pieces. Immediately behind the monitor, where the rad levels are highest, the coax cables are made of aluminum central and outer conductors with ceramic tubing as the dielectric. All the parts are made of commercially available wire or tubing. At the edge of the monitor, these

[3] Made by Insulator Seal, Incorporated, Hayward, CA.

cables are attached to kapton-insulated coax cable.[4] The kapton cable brings the lines out to the edge of the absorber shielding when the hadron monitor is in place, where a transition box will convert this to standard twist-n-flat.

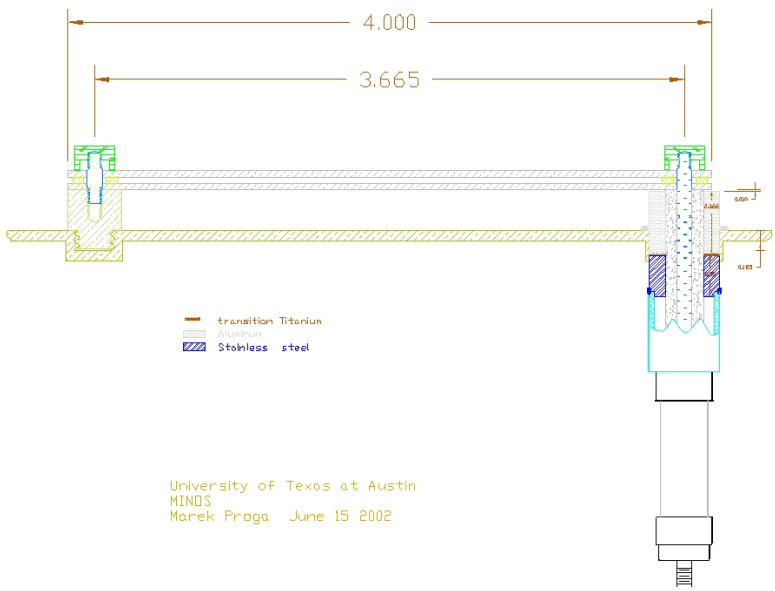

Figure 4.5-5: The mounting and signal feedthrough for a single ion chamber. Ceramic-insulated feedthroughs both support the chamber and deliver HV/signal through the gas vessel wall. The HV and signal feedthroughs are at opposite diagonal corners of the plates, and the other two corners are simple Aluminum standoffs.

4.5.2.3 Fluences, Doses

The hadron monitor is exposed to up to 10^9 charged particles/cm^2/spill during beam operation, consisting predominantly of 120 GeV protons which fail to react in the target. In addition, the monitor sees 2 x 10^9 neutrons/cm^2/spill, largely as a result of splashback from the hadron absorber located 80 cm downstream of the monitor. The particle fluences result in 1.3GRads/year at the monitor center and 1.0Grad/yr at its edge

It is estimated that the total mass of the Hadron Monitor, including all cables that must be disposed of with the detector in the event of failure, is of order 55 pounds. Of this mass, 47lbs. is Aluminum or Aluminum oxide so will have short half life after irradiation by the beam. The remaining 5 pounds is predominantly stainless steel used to make the vacuum connections, and will account for 90% of the residual activation. The residual activation is approximately 50Rem/hr on contact after 1 year of irradiation and 1 week cooldown.

---

[4] Insulator Seal, Inc.

4.5.2.4 System Repair

Should the hadron monitor fail and require replacement, the failed monitor will be disposed of. Given the intense activation of both the monitor and the surrounding shielding and absorber core, special care must be taken for personnel safety.

A conceptual idea for the sequence is indicated in **Figure 4.5-6**. The cables and gas lines for the hadron monitor protrude through the polyethylene blocks. Disconnections of these cables will be the first task. Provision for disconnections will be made just outside the absorber shielding. As the exterior of the absorber is expected to be 20 mRem/hr on contact after operations, this disconnection must be readily done.

Second, the two polyethylene blocks (not shown in the figure) must be extracted from the slot in the concrete shielding. They can be pulled out using pulley (A) and lowered down to ground level using pulley (B). Because these blocks will be activated they will be lowered into a shielded cart. The cart is rolled out of the passageway.

Removal of the hadron monitor is also accomplished using the two pulleys (A) and (B). Two steel cables will have been attached to the hadron monitor when it was inserted into the absorber and left attached to the hadron monitor (*i.e.*: they also protruded through the polyethylene blocks). These cables will be used to extract the hadron monitor (over pulley (A)) and lower it into a shielded coffin/cart (over pulley (B)). Because the cords were left attached to the HadMon during installation, the personnel can stand far away from the slot during this procedure. In **Figure 4.5-6**, the hadron monitor is shown at three successive locations during the procedure to extract it from the absorber (indicated as (1) through (3)).

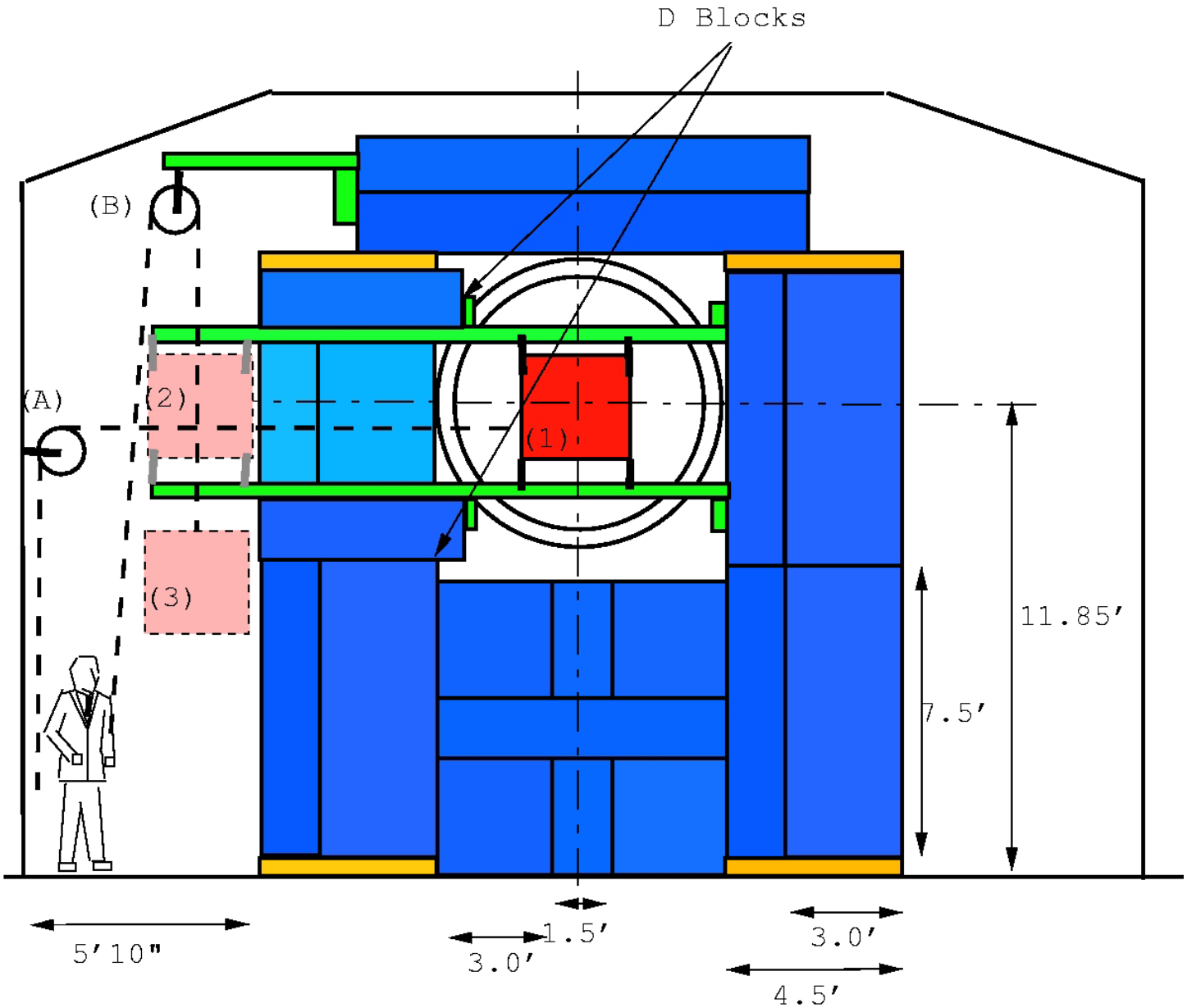

Figure 4.5-6 Rail and Pulley system for hadron monitoring replacement scheme as viewed from the downstream end of the absorber alcove.

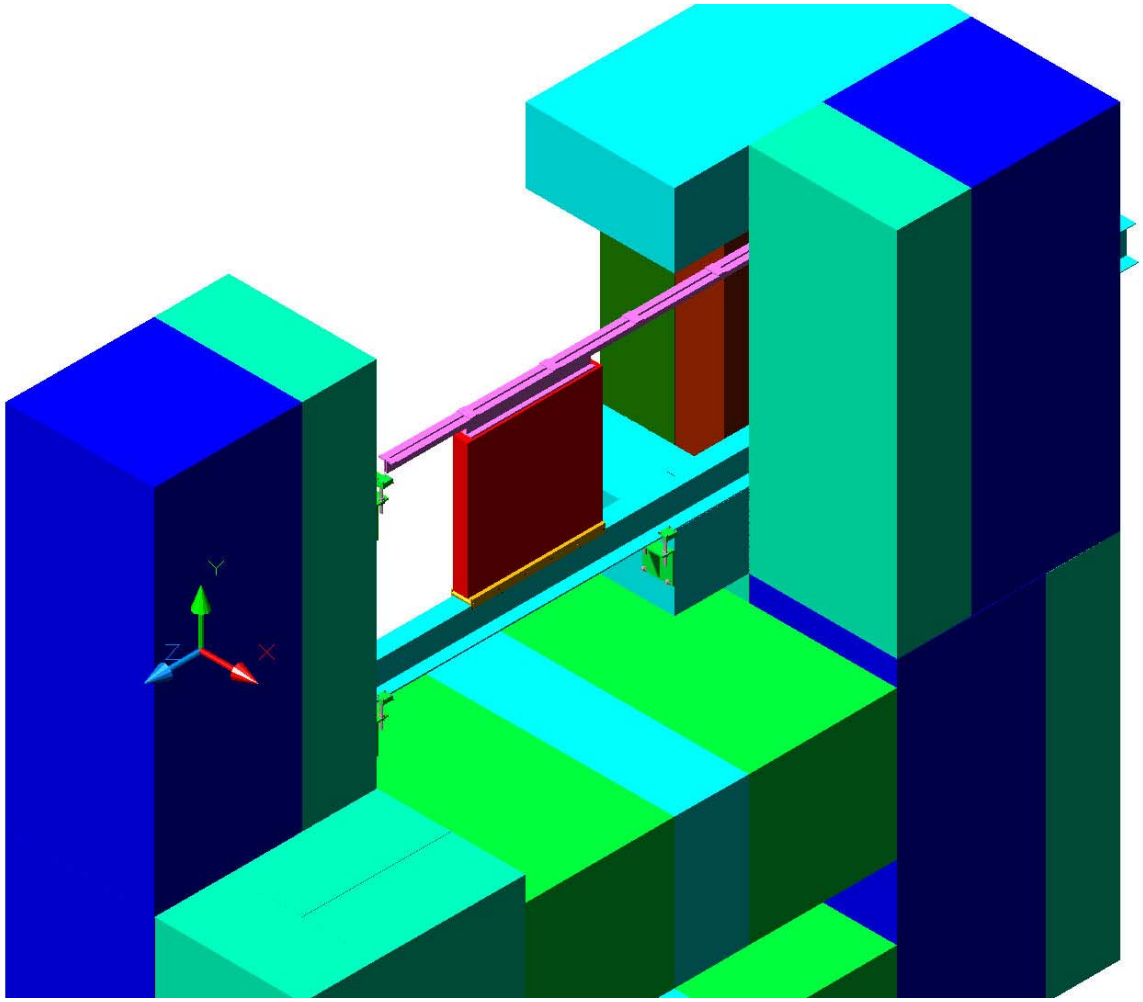

Figure 4.5-7 Rail system for hadron monitor replacement scheme.

The rail system to install and align the Hadron Monitor is shown in **Figure 4.5-7**. The lower rail is a 6" I-beam and supports the monitor weight. The monitor is in sliding contact with the rail. The upper rail consists of 6" "L" bracket that is straddled by fins on the top of the monitor so as to maintain verticality. A hard stop on the lower rail defines the fully-inserted monitor position, as well as the reproducible position to which replacement monitors may be inserted. Alignment and placement of the monitor is done during initial installation, but not after replacement.

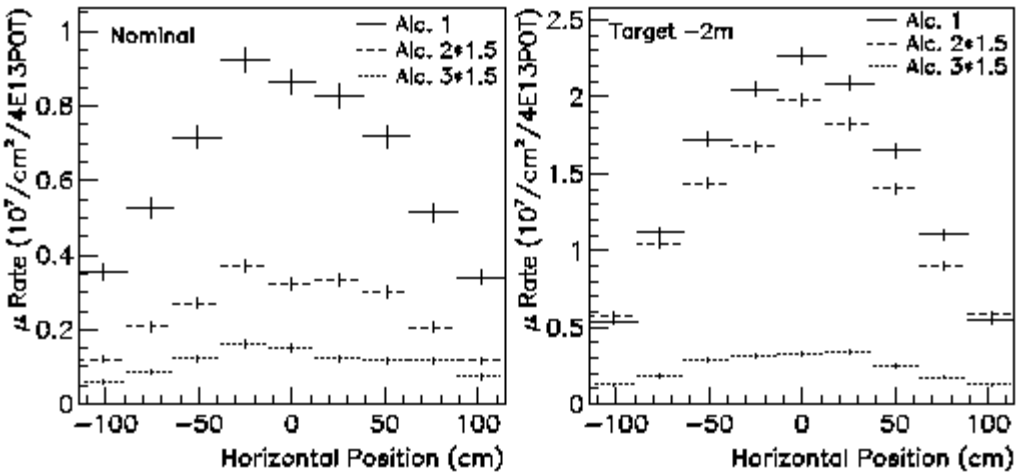

Figure 4.5-8 Muon fluxes in the 3 muon monitoring locations: Alcoves 1, 2 and 3 . Fuxes assume 4x 10^{13} protons on target per spill, and only include the muons, as predicted by GEANT. Shown are the fluxes in the three alcoves for nominal low-energy beam running (left plot), for special monitoring runs in the semi-medium energy beam (right). The fluxes in alcoves 2 and 3 have been multiplied by 1.5 (for both plots) so the shapes can been seen on the figure.

4.5.3 The Muon Monitors

4.5.3.1 System Function

The muon monitors are three arrays of ionization chambers located in the four 'alcoves' downstream of the hadron absorber in the NuMI beamline. Each alcove will see different fluxes of charged particles due to the attenuation expected in the absorber and dolomite rock between alcoves, with the downstream alcove seeing the most energetic muons only (see **Figure 4.5-8**).

The muon monitors are approximately 2 m by 2 m arrays of ion chambers that measure an ionized charge proportional to the number of muons passing through the array. Because each muon plane is segmented into an array of 9 by 9 chambers, the individual signals from each chamber in the array help locate the center of the muon (hence neutrino) beam. The chambers will not be absolutely calibrated to provide a charge-per-muon conversion factor, but will be relatively calibrated and this calibration will be tracked over time during operation of the NuMI beam. In this way, the relative signal seen from chamber to chamber indicates the relative magnitude of (muon) beam intensity at a particular location within each muon array, and also the comparison of rates between alcoves can be used to infer information on the energy spectrum of muons.

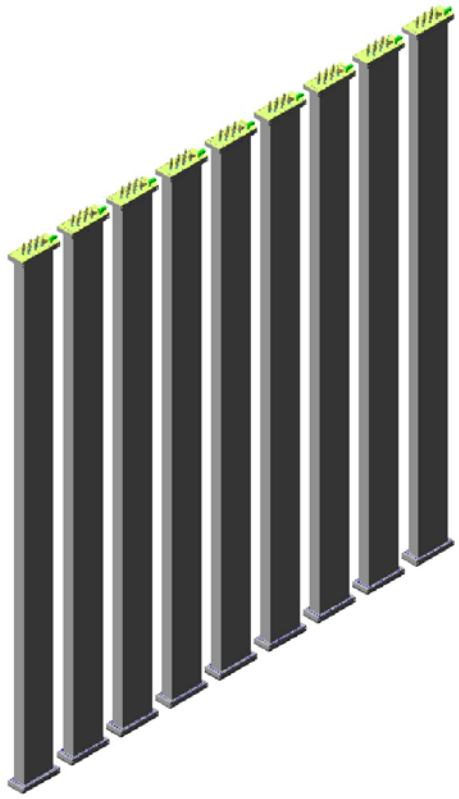

Figure 4.5-9 One array of 9 muon chamber tubes. Each tube is 2m in length, and separated from neighboring tubes by 25 cm (center-to-center).

An ion chamber tube is approximately 8 feet in length, made of 6" by 2" extruded aluminum tubing, 1/8" wall. Nine tubes will be used to form the 9 by 9 array (see **Figure 4.5-9**). The tube has 3/4" thick endflanges welded to each end to which are bolted endplates which handle all electrical and gas connections. The endplates are gas-sealed to the endflanges by an Aluminum wire gasket that is compressed by the endplate and endflanges.

The ion chambers themselves are mounted onto trays that slide into the tubes. A drawing of one of the ion chambers mounted on the channel is shown in **Figure 4.5-10**. The tray is rigidly bolted to one of the endplates via a tab (shown in red in the figure). The channel is shown in light blue, the endplate is shown in dark gray. The 6" by 2" tube and its endflange is also shown (in mustard brown). Not shown in the figure are the two kapton-insulated coax cables per ion chamber, which bring signal and HV to the chamber from the feedthroughs at the endplate.

The muon monitors use the same ceramic plate ion chamber electrodes as the hadron monitor. The gas gap, however, will be 3mm (not 1mm as in the hadron monitor). With this gas gap and Helium gas, it is anticipated to collect 1400, 170 and 80 pC per in the central ion chamber in Alcoves 1, 2, and 3, respectively.

The endplate with all electrical (signal and HV) connections is shown in **Figure 4.5-11**. The high voltage and signal feedthroughs are commercially-available ceramic-insulated vacuum feedthroughs. The signals for the 9 chambers are fed into a 9-pin D-type connector[5] with ceramic insulator, gold-plated stainless pins, and a stainless jacket. It is welded directly to the endplate. The high voltage (typically less than 600 Volts) is brought in through a straight-pin feedthrough.[6] One HV feedthrough delivers the HV for one chamber.

To maintain chamber-to-chamber calibrations over the course of NuMI operations, as well as help calibrate temperature or pressure variations, each chamber will have a 1 μCi Am^{241} alpha source (E = 5.4 MeV) mounted to it. During dedicated calibration runs, the electronics will trigger between NuMI spills so as to integrate the charge from the ionization created by the alpha's, not the NuMI beam. Such sources in bench measurements have been shown to ionize approximately 2.5pA of current in He gas, which is sufficient for calibration but a small background to actual beam spill measurements.

[5] Ceramaseal, Incorporated.

[6] Insulator Seal, Incorporated.

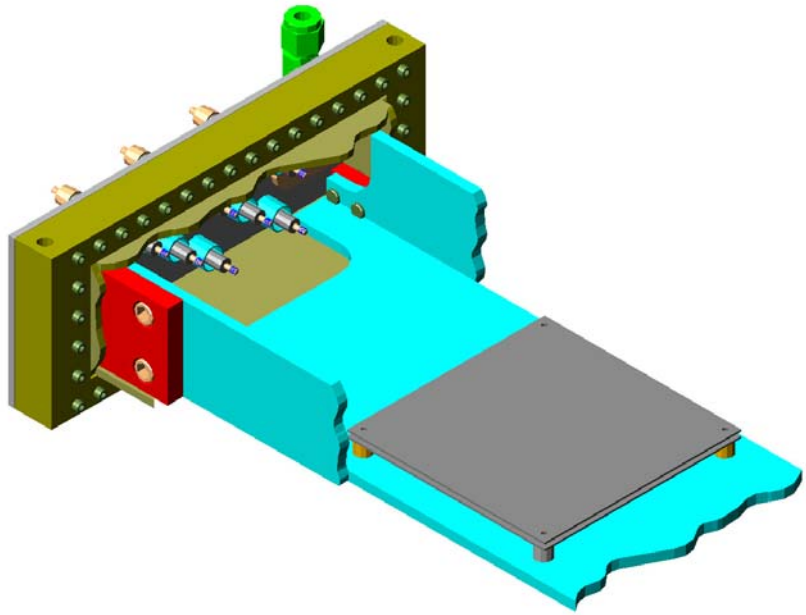

Figure 4.5-10. Tray inside a muon tube onto which the parallel plate chambers are mounted. Each ion chamber is connected to the electrical feedthroughs at the endplate by coax kapton cable (not indicated in drawing).

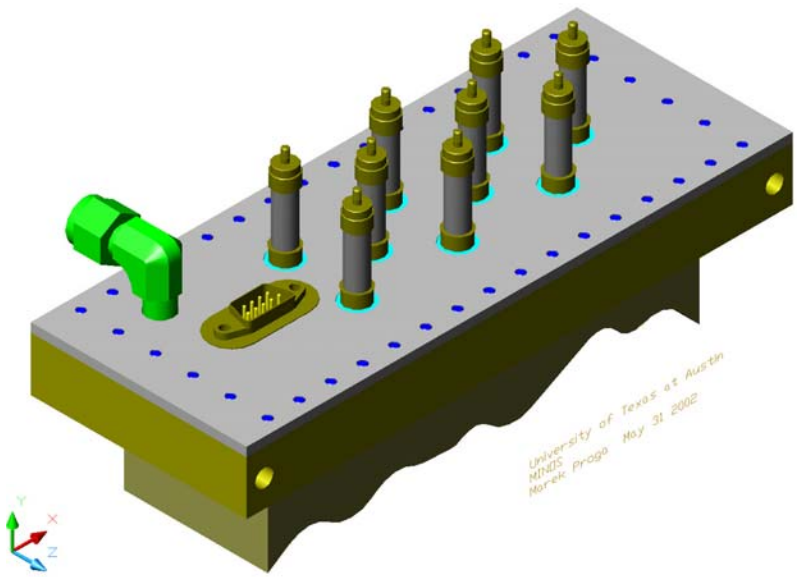

Figure 4.5-11. Endplate of the muon monitor tube will electrical feedthroughs. A single 9-pin D-type connector brings out the signal lines and a ceramic HV feedthrough is used for each individual chamber HV. A Swagelok feedthrough brings in the gas line.

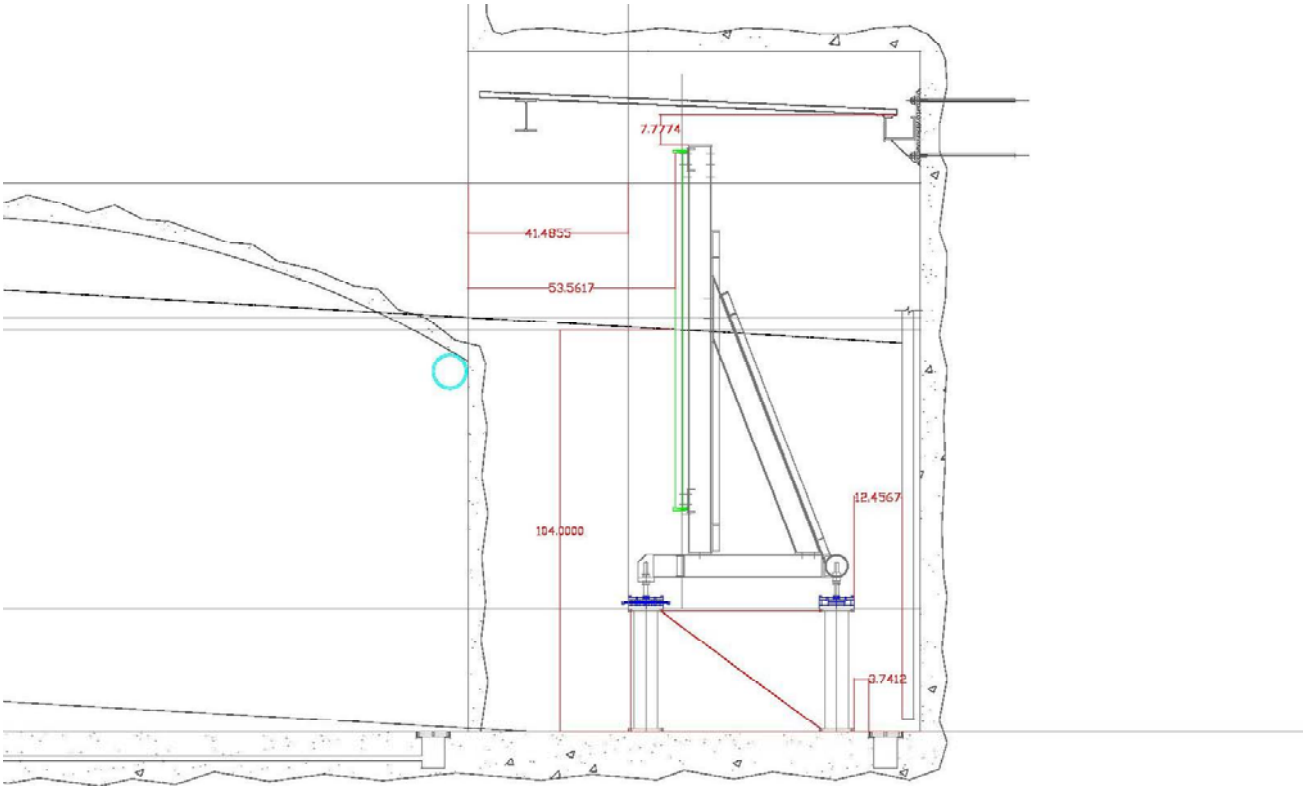

Figure 4.5-12. Elevation view of the support structure and the muon monitor in Alcove 1. The muon detectors are supported at beam center. The top of the detector is 7" from the drip ceiling.

A frame has been designed to support the muon beam monitoring chambers at beam height in any of four alcoves downstream of the hadron beam absorber. **Figure 4.5-12** shows a side view of this frame as seen in Alcove 1. Unobstructed access to the detectors is permitted from the upstream side for quick mounting or service of individual muon tubes. The chamber tubes hang by studs that fasten to the upper cross beam of the picture frame. The upper studs serve to locate the tube centers. Lower studs are less constrained in order to allow for welding inaccuracies and warp in the extruded tubes. We strive for 1 mm relative placement of the tubes on the frame. Cabling and gas supply will be routed along the bottom of the picture frame. Gas exhaust will be routed along the top of the picture frame. Deflection of the upper beam when loaded with the muon chambers should be about 0.050 inches.

Components of the frame are entirely aluminum except for steel jackscrews in the floor mounts. Because of the difficulty of transporting a frame to its final location underground, these frames have been made of smaller sections, which will be bolted together in the final alcove location. The three principal pieces are a rectangular picture frame on which the chamber tubes are mounted vertically, a diagonal bracing section which supports the picture frame, and a rectangular base section which has a 3-point mount on the floor.

Beam height in each alcove determines the vertical location of the frame. A single frame design should work well for all four muon alcoves. Jack screws in the feet allow a vertical adjustment of ±3 inches. Larger adjustments may be accomplished via extra bolt holes which allow the horizontal supports of the picture frame to be adjusted an additional amount vertically. Once the frame is bolted to the floor, no horizontal position adjustment is possible. The mounting frame is about 6 inches below the drip ceiling and 15 inches from the downstream wall. There exist about 52 inches of working space upstream of the muon chambers in alcoves 2 and 3. Part of this space may later be filled with light material (such as polyethylene) to reduce electrons in the beam flux.

4.5.4 System Description: Electronics

The essential features of the electronics used to acquire data are shown in the simplified schematic of **Figure 4.5-13**. An operational amplifier takes the signal and stores it on a precision 100pF integration capacitor. The voltage on the capacitor is subsequently digitized by an ADC for computer read-out. Voltage on the input to the integrator is maintained at a virtual ground subject to the limitations of the amplifier. This differs from pulse height read out systems that employ a load resistor to develop a voltage at this point in the circuit. The integration capacitors will be modified where necessary to accommodate the range in expected signal size. An additional resistor has been added across the common integrator output buses to eliminate cross talk for large signals.

The complete system used for data acquisition is the same as those used for SWIC Readout (**Figure 4.5-14)**. Each SWIC electronics box has 96 channels, each of the monitors use that same electronics (although the hadron monitor, of course, does not fill all the channels). There is a slight modification to the integration capacitor and an additional resistance is needed to reduce channel cross talk for large output signals. The integration time is to be 5msec.

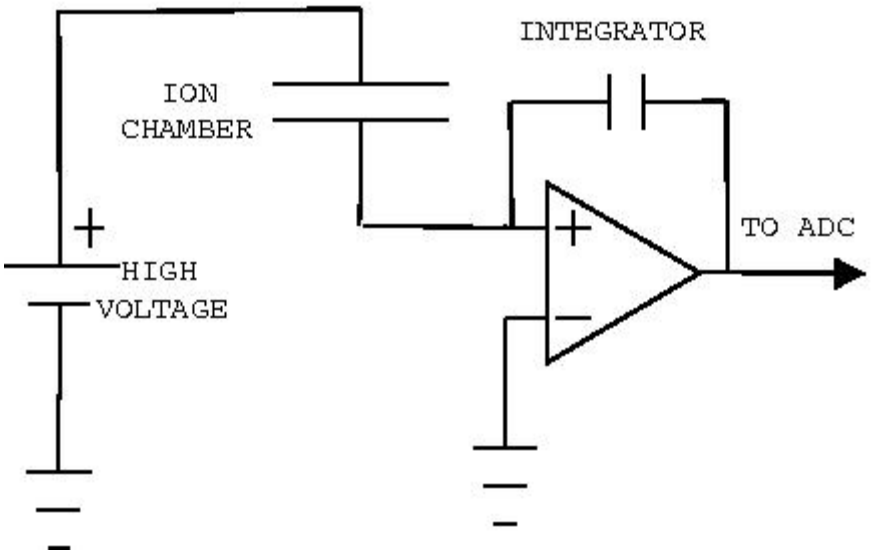

Figure 4.5-13: Schematic of ionization chamber and input stage of electronics

The map of where the electronics is placed can be seen in plan view in **Figure 4.5-1**. The electronics racks and high voltage are located in the bypass tunnel, which leads off to the west from the absorber cavern. Although the downstream hadron monitor is not shown in the diagram, both the hadron and the muon monitor in Alcove 1 will be serviced by SWIC controllers near the electronics rack. Electronics for all monitoring locations are accessible during normal running.

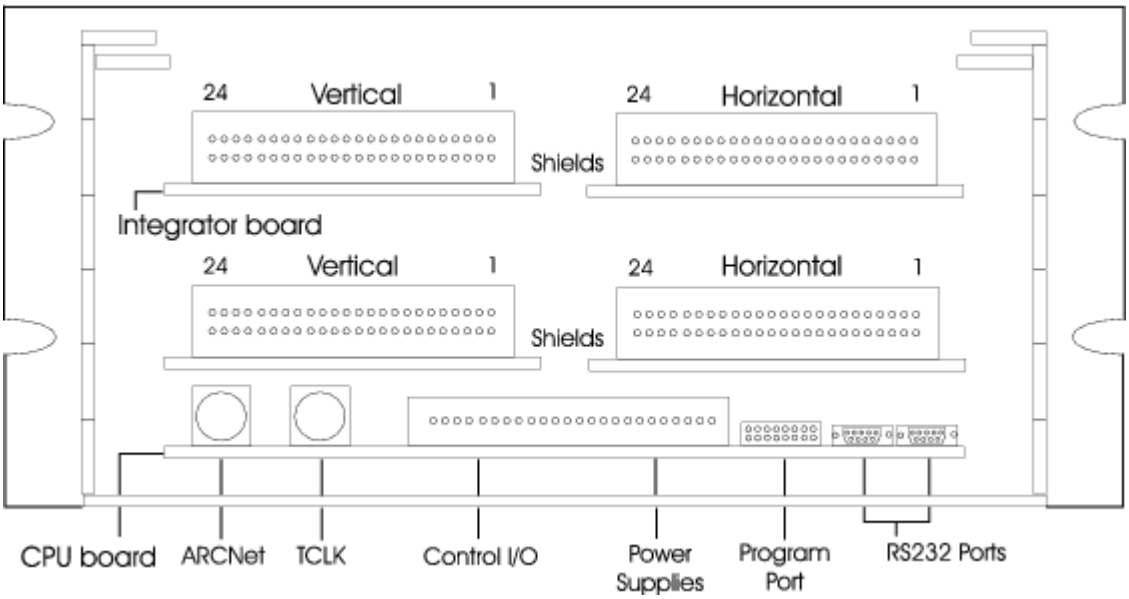

Figure 4.5-14 Layout of the 96-channel SWIC box.

4.5.5 System Description: Gas System

The monitors are to be supplied with helium, which must be maintained at a high purity (less than 10ppm impurities). Gas will be stored near the MINOS shaft, sent through a two stage regulator followed by a line filter to a gas distribution panel in the hallway near the electronics, which splits the one line to four, which then go to each of the four monitoring planes.
Exhaust gas is returned to the distribution panel where there will be bubblers, and then sent to an external vent, part of the HVAC system. **Figure 4.5-15** shows a schematic of the gas system.

There are two sets of "8-pack" high-pressure manifolds, one of which will be set up to a two-stage regulator. This allows operation in the semi-automatic mode, with one side in reserve at all times. The gas pressure after the two-stage regulator will be approximately 30psi. The gas will then be put through a line filter, and sent to the distribution panel near the electronics for the monitoring system. Each line going to a plane of monitors will be connected to two flowmeters in parallel, as well as a pressure gauge, and finally a valve to allow one to turn off the flow to only one alcove in case a muon tube needs to be replaced.

Gas is supplied to the main distribution rack located outside the last radiation barrier, via a continuous length of, 3/8" OD stainless tubing. The main distribution rack allows for adjustment

of flow to a given alcove. Four sets of flow-meters control gas flow to each of the four monitoring planes. One flow meter will allow for fast purging of the monitor, while the other will be used for normal low flow running.

The chambers are to be operated at slight overpressure (<0.5 inches of water). Each tube has a gas volume of approximately 15 liters (three stations having total volume of 405 liters). The hadron monitor is 19 liters. Each bottle contains about 8000 l of gas, (300 ft^3). At the rate of one volume change per ~2hrs for all three alcoves plus the hadron monitor, we consume an 8-cylinder pack every week.

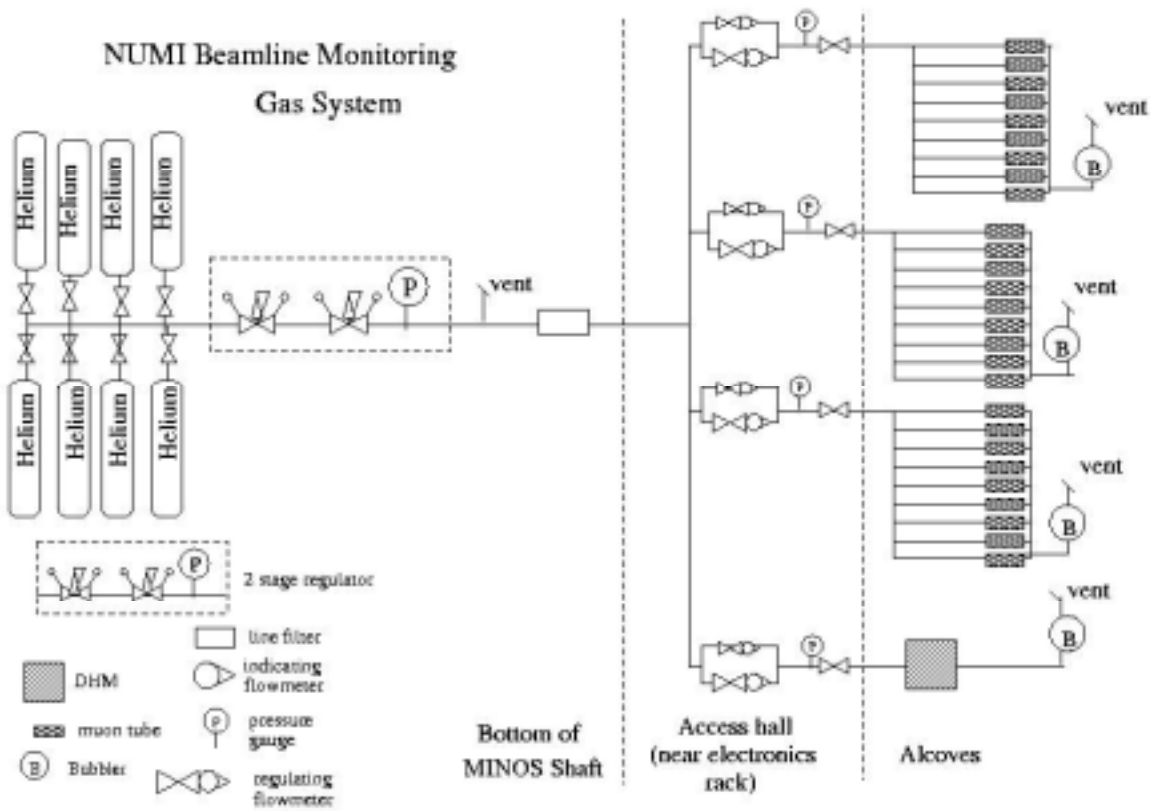

Figure 4.5-15 This shows a schematic drawing of the gas system.

4.5.6 System Description: Online Information

There is much information to be recorded during data taking to be able to ensure both that the monitors themselves are performing well, and ultimately that the beamline itself is performing as expected. Of course the information about the beamline is contained in the signals of these

arrays, and the concurrent calibration constants that are to be calculated online. This information is to be summarized as an overall flux of particles (and a peak flux for the Downstream hadron monitor), and some shape information, including the first and second moments of the horizontal and vertical projections of the signals. The information that arrives at the monitors spill by spill will be transferred by the XML-RPC system which is currently also being used by MiniBooNE.

Because ionization chambers are used, we record signals from the detectors along with calibrations that are going on during off-spill gates. An ethernet controlled DAC sets voltages on 16 channels of modified Droege HV supplies. Seven of these supplies serve the Downstream Hadron Monitor. Each of the three muon alcoves is served by three HV channels. The current and voltage of each channel is read back over ethernet. Low voltages in the SWIC electronics and the HV NIM bins are also remotely monitored. Pressure, humidity, and temperature are monitored at the location of each detector. An overview of the ethernet system can be found in **Figure 4.5-16**.

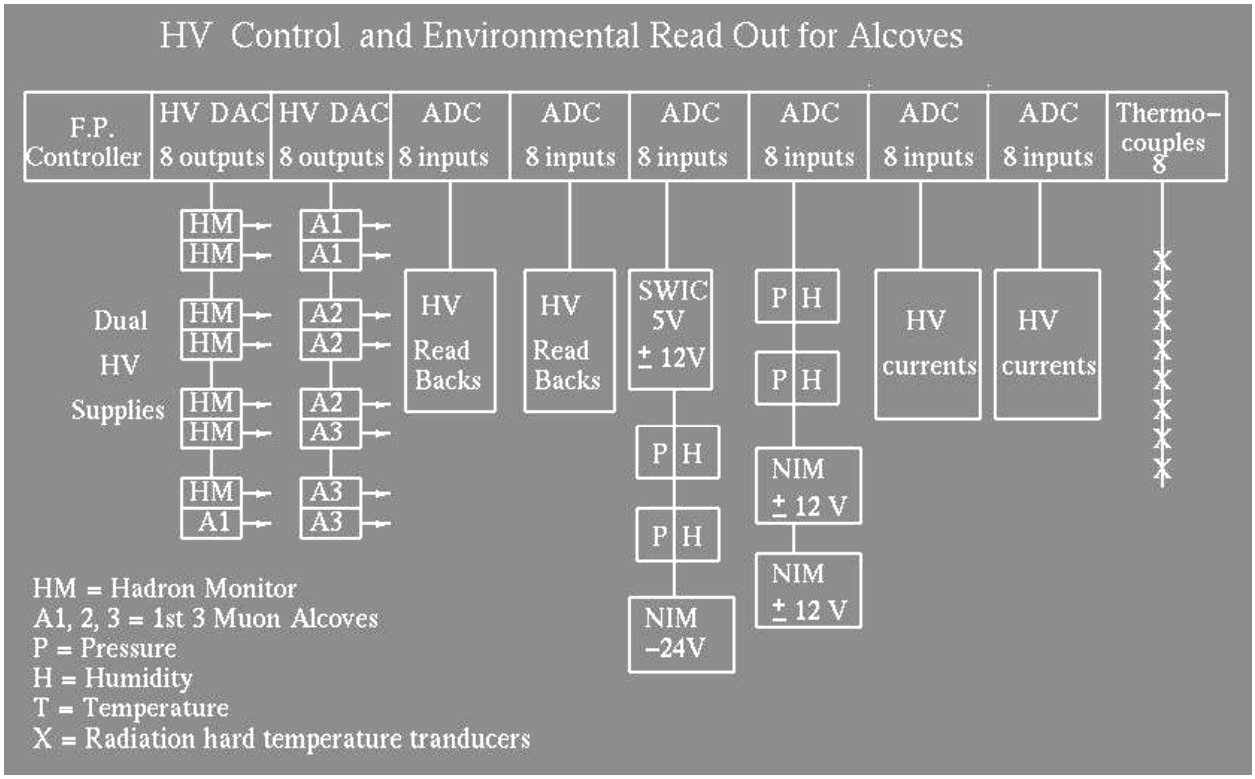

Figure 4.5-16 This shows the list of devices that DCS expects to get from the beamline monitoring devices.

The DCS will export its data to the rotorooter process and then on to the DISPATCHER where it along with the RPC XML data will be put in offline data streams, and will be available to the experimenters. Summary information will be put into the main ORACLE database by an offline job. In addition it is planned to store all the data acquired by the DCS on a disk of the DCS computer where time histories and correlations can be extracted if needed.

4.6 SURVEY, ALIGNMENT, AND GEODESY (WBS 1.1.6)

4.6.1 Introduction

For a long baseline neutrino experiment, properly aligning the neutrino beam to hit the far detector 735 km away is clearly important. Actually, as shown in **Figure 4.6-1**, the NuMI beam, for low neutrino energies, is several kilometers wide and modern geodetic survey techniques, especially the Global Positioning System (GPS) satellites, make hitting the far detector relatively straightforward. For the NuMI beamline, the physics-driven alignment goals from the MINOS experiment require that the neutrino beam center must be within 100 meters of the far detector.

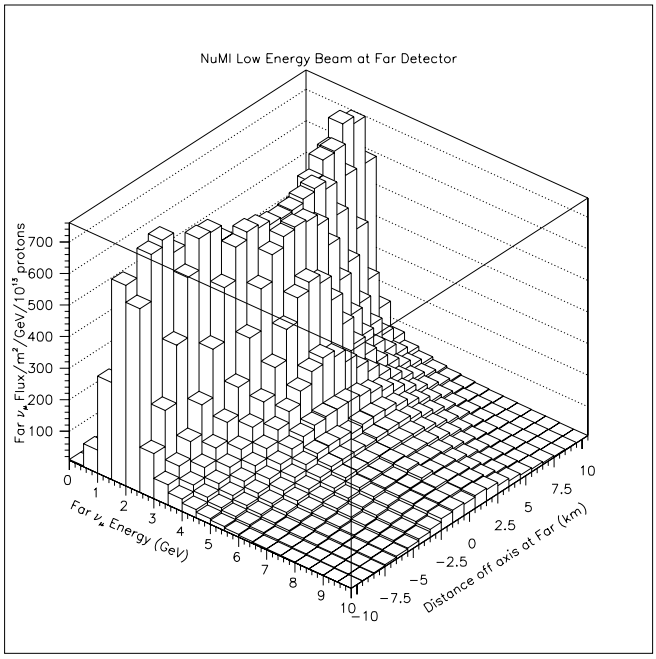

Figure 4.6-1 Transverse distribution of the NuMI low energy tune neutrino beam at the far detector as a function of energy. Note that at low neutrino energy the beam is several kilometers wide

4.6.2 System Description: Determining the Line from Fermilab to Soudan

The relative positions of Fermilab and Soudan on the surface are determined by making simultaneous measurements using the Global Positioning System (GPS) satellites. Simultaneous GPS data at both Fermilab and Soudan were recorded in April 1999 as shown in **Table 4.6-1**. The data was analyzed at Fermilab and, independently, by the National Geodetic Survey (NGS). The agreement between the NGS result and two methods of analysis at Fermilab was excellent. The Fermilab to Soudan vector, averaged over the period of the observations used, is known to better than 1 cm horizontally and 6 cm vertically, well within requirements. The differential earth tide effect between Fermilab and Soudan is approximately the same as this uncertainty.

Included in **Table 4.6-1** are the results from two less precise measurements also using professional GPS receivers, which agree to better than 1 meter, and a later result using an amateur hand held receiver. All four results are within the 12-meter tolerance goal for this measurement. Accuracy of a differential GPS measurement is increased by including CORS (Continuously Observed Reference Station) data in the analysis (**Figure 4.6-2**), simultaneous observations from both positions, and using the precise satellite positions calculated by NGS from the CORS data.

Year	Receiver	Measure time (hour)	Include CORS	Simulta-neous	Precision Satellite Positions	Deviation from 1999 (meter)
1999	Professional	26	Yes	Yes	Yes	
1998	Professional	6	No	Yes	No	0.231
1994	Professional	1	No	No	No	0.785
2000	Hand held	<1	No	No	No	10.140

Year			Azimuth			Vertical	Distance (meter)	north (meter)	east (meter)	up (meter)	$\lvert(\delta n,\delta e,\delta u)\rvert$ (meter)
1999	336	5	52.383	-3	17	17.882	735273.058	671108.532	-297424.016	-42175.390	
1998			-0.033			-0.008	-0.196	-0.229	-0.029	-0.018	0.231
1994			-0.007			0.001	-0.785	-0.725	0.296	0.049	0.785
2000			0.654			2.278	5.608	6.487	-0.330	7.787	10.140

Table 4.6-1. Relative position of the SHAFT monument on the surface at Soudan as measured from Fermilab surface monument 66589 by GPS. Results are given in the Local Geodetic Coordinate System (reference SHAFT). The values for the most accurate measurement are given on the first line, followed by the differences (other – best) of the three additional measurements relative to the best one. The professional receivers used were Trimble 4000 SSi's; the hand held receiver was a Garmin GPS III+ (Best Buy ~$350).

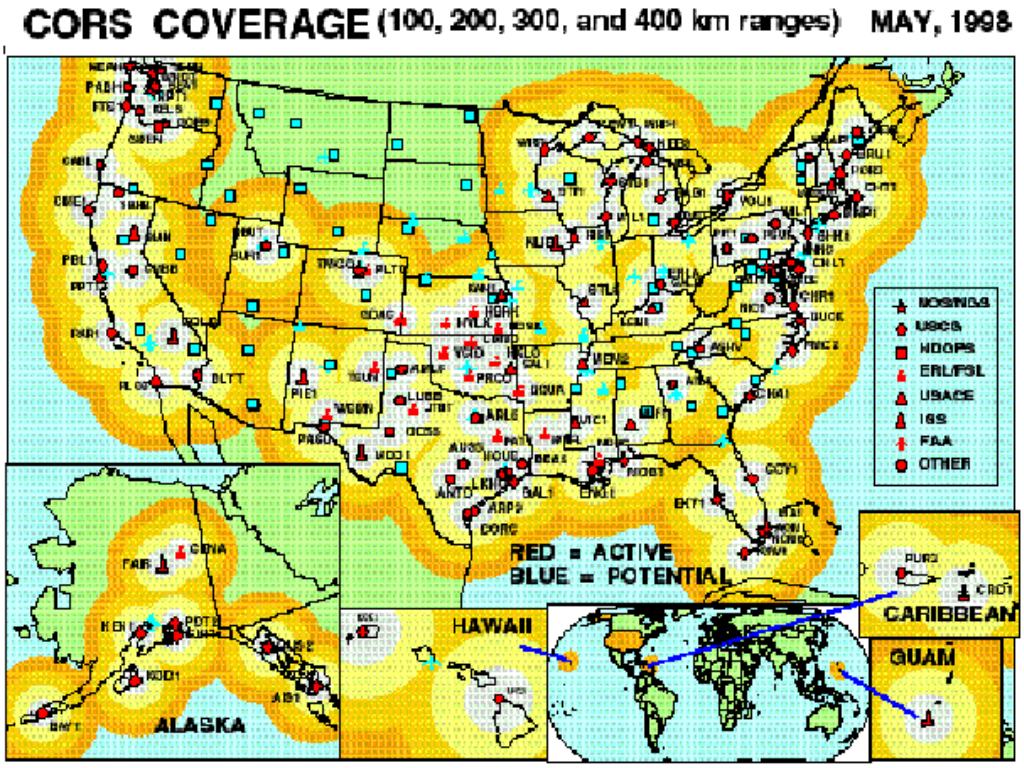

Figure 4.6-2 CORS (Continuously Observed Reference Station) network. GPS data are recorded for over 100 accurately known locations in the United States, including 4 in Wisconsin. (Source: National Geodetic Survey www page: http://www.ngs.noaa.gov/CORS/Maps.html

The position of the 27th level at the bottom of the Soudan Mine, relative to the surface, is determined using inertial survey. An inertial survey unit and operator were rented from the University of Calgary during the April 1999 GPS trip to Soudan. The inertial survey unit used (Honeywell Laseref III IMU) contains a triad of accelerometers and optical gyroscopes to measure force and angular velocity. The accelerometers are double integrated to yield position change along each of the 3 axes. Internal consistency of the several inertial survey runs indicated a 0.7 m per coordinate precision for the surface to bottom of the mine measurement, many times better than the 12 m goal. As shown in **Table 4.6-2,** these measurements agreed to better than 4 m per coordinate with the old mine values for the 27th level relative to the surface.

	east	north	up
	meter	meter	meter
1999 INS values	-15.2	148.2	-710.1
INS-old mine #'s	-0.2	3.7	-3.4

Table 4.6-2. Inertial Survey (INS) measurement from the surface to level 27 at Soudan. The average of the 4 INS runs made on April 20, 1999 is given, together with the change of these measurements from the old mine values.

Conventional survey techniques are used to determine the position of the MINOS far detector relative to the bottom of the shaft at Soudan. **Table 4.6-3** gives the position of monuments in the MINOS cavern and the nominal detector axis and edges in the Cartesian Local Geodetic Coordinate System (LGCS) relative to the surface monument called “SHAFT” (which was used in the surface GPS measurement above). **Table 4.6-4** gives the same points in the Cartesian beam coordinate system, with origin at the nominal detector center, Y axis along the neutrino beam direction, and X axis horizontal.

POINT NAME	X(+EAST) (Meter)	Y(+NORTH) (Meter)	Z(+UP) (Meter)
BRASS_1	37.3668	10.8767	-709.1782
BRASS_2	32.5269	20.5614	-709.1638
BRASS_3	24.9370	35.7484	-709.1476
BRASS_4	17.9893	49.6496	-709.1606
BRASS_5	3.3012	79.0429	-709.1639
CP_E11	27.1329	39.8453	-705.0098
CP_E14	24.6850	44.7639	-705.0327
CP_E17	22.2376	49.6672	-705.0330
CP_E2	34.2510	25.6183	-705.0434
CP_E5	31.7950	30.5282	-705.0347
CP_E8	29.3449	35.4377	-705.0233
CP_W11	19.5038	36.0554	-705.0210
CP_W14	17.0549	40.9669	-705.0257
CP_W17	14.6069	45.8628	-705.0210
CP_W2	26.6014	21.8538	-705.0311
CP_W5	24.1563	26.7486	-705.0431
CP_W8	21.7098	31.6510	-705.0386
EI_01	34.1657	23.6082	-709.2540
EI_035	31.8929	28.1608	-709.2580
EI_065	29.5962	32.7045	-709.2534
EI_10	27.2189	37.4801	-709.2451
EI_125	24.9455	42.0243	-709.2487
EI_155	22.6748	46.5704	-709.2416
EI_18	20.5332	50.8897	-709.2587
EO_01	37.0840	23.7565	-709.2491
EO_09	29.9725	38.0342	-709.2452
EO_19	21.3997	54.7230	-709.2630
PP1	8.2536	51.7757	-707.5768
PP2	4.2885	59.6857	-707.5483
PP3	1.1212	66.0377	-707.5610
VULCAN_E	31.7687	30.2899	-707.0321
VULCAN_W	24.2997	26.7597	-706.8035
WBE_1	17.6527	55.4088	-709.2568
WBE_1_5	16.7981	60.6413	-709.2508
WBE_2	13.3126	64.1350	-709.2516
WBE_2_5	11.7837	70.7375	-709.2529
WBE_3	8.2340	74.4346	-709.2519
WBW_1	10.6467	51.9149	-709.2533
WBW_1_5	7.8540	55.7006	-709.2597
WBW_1_7	7.2439	59.4027	-709.2612
WBW_2	6.2549	60.6034	-709.2562
WBW_2_2	5.2874	63.5825	-709.2643
WBW_2_5	2.4974	66.3988	-709.2517
WBW_3	1.1941	70.8040	-709.2534
WI_01	28.3010	20.6410	-709.2532
WI_035	26.0234	25.2087	-709.2504
WI_065	23.7625	29.7489	-709.2521
WI_10	21.3667	34.5228	-709.2503
WI_125	19.1039	39.0775	-709.2530
WI_155	16.8175	43.6237	-709.2527
WI_18	14.6497	47.9674	-709.2615
WO_01	26.9941	18.7946	-709.2483
WO_09	19.8536	32.9234	-709.2434
WO_185	12.3356	47.9075	-709.2598
DetCtr_dsgn	24.4433	35.7132	-704.5203
DetCtr_meas	24.3847	35.8303	-704.5203
dcs_origin	31.3726	21.8483	-704.5203
FD_ds_axis	17.3968	49.8124	-704.5203
FD_us_right	34.9506	23.6365	-704.5203
FD_us_left	27.7946	20.0601	-704.5203
FD_us_top	31.3726	21.8483	-700.5203
FD_us_bot	31.3726	21.8483	-708.5203
FD_us_t,r	34.9506	23.6365	-700.5203

Table 4.6-3. Far Cavern Monuments and Detector Points in the Local Geodetic coordinate system, reference point Shaft Monument, with the X axis East, Y axis North, Z axis up, to make a right handed orthogonal system.

POINT NAME	X(+"West") (Meter)	Y(+"Up") (Meter)	Z(+"North") (Meter)
BRASS_1	-0.3794	-3.0428	-28.3462
BRASS_2	-0.4095	-3.6472	-17.5364
BRASS_3	-0.4565	-4.6014	-0.5853
BRASS_4	-0.4992	-5.5025	14.9291
BRASS_5	-0.5917	-7.3838	47.7340
CP_E11	-4.2597	-0.6231	2.3193
CP_E14	-4.2841	-0.9599	7.8030
CP_E17	-4.3020	-1.2735	13.2742
CP_E2	-4.2228	0.2526	-13.5649
CP_E5	-4.2360	-0.0525	-8.0835
CP_E8	-4.2543	-0.3547	-2.6049
CP_W11	4.2588	-0.6368	2.3626
CP_W14	4.2385	-0.9551	7.8415
CP_W17	4.2244	-1.2633	13.3066
CP_W2	4.3026	0.2605	-13.4884
CP_W5	4.2864	-0.0642	-8.0265
CP_W8	4.2681	-0.3728	-2.5563
EI_01	-3.2430	-3.8507	-15.5599
EI_035	-3.2593	-4.1455	-10.4801
EI_065	-3.2502	-4.4319	-5.3970
EI_10	-3.2733	-4.7285	-0.0707
EI_125	-3.2853	-5.0225	5.0019
EI_155	-3.3005	-5.3058	10.0756
EI_18	-3.3291	-5.5984	14.8878
EO_01	-5.9165	-3.7784	-16.7371
EO_09	-5.9821	-4.6861	-0.8124
EO_19	-5.8262	-5.7762	17.9173
PP1	7.2417	-4.2800	21.2850
PP2	7.2279	-4.7573	30.1203
PP3	7.2018	-5.1756	37.2058
VULCAN_E	-4.1054	-2.0351	-8.3983
VULCAN_W	4.1533	-1.8186	-8.1816
WBE_1	-2.7874	-5.9013	20.2109
WBE_1_5	-4.3762	-6.1844	25.2611
WBE_2	-2.8332	-6.4531	29.9410
WBE_2_5	-4.4354	-6.8308	36.5153
WBE_3	-2.9265	-7.1097	41.4054
WBW_1	5.0414	-5.8994	20.2393
WBW_1_5	5.8343	-6.1708	24.8684
WBW_1_7	4.7151	-6.3770	28.4437
WBW_2	5.0588	-6.4587	29.9586
WBW_2_2	4.5839	-6.6437	33.0491
WBW_2_5	5.8101	-6.8466	36.8136
WBW_3	4.9941	-7.1067	41.3270
WI_01	3.3296	-3.8491	-15.5740
WI_035	3.3108	-4.1380	-10.4782
WI_065	3.2895	-4.4296	-5.4146
WI_10	3.2836	-4.7331	-0.0819
WI_125	3.2575	-5.0264	4.9954
WI_155	3.2563	-5.3170	10.0758
WI_18	3.2401	-5.6032	14.9219
WO_01	5.3270	-3.7835	-16.6339
WO_09	5.3542	-4.6834	-0.8288
WO_185	5.3342	-5.6579	15.9071
DetCtr_dsgn	0.0003	0.0075	-0.1307
DetCtr_meas	0.0000	0.0000	0.0000
dcs_origin	0.0431	0.8934	-15.6053
FD_ds_axis	-0.0432	-0.8934	15.6054
FD_us_right	-3.9568	0.8940	-15.6163
FD_us_left	4.0431	0.8927	-15.5944
FD_us_top	0.0431	4.8868	-15.3767
FD_us_bot	0.0431	-3.1001	-15.8340
FD_us_t,r	-3.9568	4.8875	-15.3877

Table 4.6-4. Far Cavern Monuments and Detector Points. In the "Beam" coordinate system with the Z-axis along the beam direction, X-axis horizontal, beam left, and Y-axis to make a right handed orthogonal system.

The line from Fermilab to Soudan is transferred from the surface at Fermilab to underground using conventional survey techniques. The most difficult parameter is the azimuth (horizontal angle). **Table 4.6-5** shows the two methods we are using to determine underground azimuth and the offset (horizontal deviation from the ideal beam line) resulting from the expected angular error at several distances. A gyro-theodolite is a precision theodolite combined with an accurate gyrocompass. One accurate to 15 microradians has been loaned to Fermilab by SLAC and has been in use on NuMI since mid 2001. Both mechanical and optical plumbing is being used down the sight risers and shafts constructed at Fermilab.

Transferring Azimuth	Fermilab Surface to Tunnels				
Method:		Accuracy at:			
	distance >	84 m	460 m	1040 m	735 km
	Accuracy	Downstream	Mid Decay	MINOS	Soudan
	(milliradian)	Target Hall	Tunnel Vent	near det	far det
Best Gyro	0.015	1.3 mm	7 mm	16 mm	11 m
Widely Separated Plumb Bobs	0.012	1.0 mm	6 mm	12 mm	9 m

Table 4.6-5 The two methods being used to determine underground azimuth and the offset (horizontal deviation from the ideal beam line) resulting from the expected angular error at several distances

4.6.3 System Description*:* Beamline Element Accuracy Requirements

The PBEAM_WMC Monte Carlo was used to calculate the effect of misalignments of each beamline element on the determination of the far detector spectrum (without oscillations) from the measured near detector spectrum. PBEAM is first run with all beam elements at their nominal values and positions ("on axis"). A parameter is selected to investigate and its position is varied from its nominal value. For example, in the Monte Carlo the first focussing horn is moved 4 mm transverse to the beam axis ("Horn 1 X shift of 4 mm"), and the resulting spectra at both near and far detectors are calculated.

The ratio R_{far} , obtained by dividing the far detector flux with the beamline element displaced by the far detector flux with the beamline element on axis, is shown in **Figure 4.6-3a**. A dashed

line has been drawn for a flux ratio of 1.0, which would be the result if there were no change in the flux. **Figure 4.6-3b** is a similar graph for the near detector. The ratio of these ratios (far ratio to near ratio, RR) is shown in **Figure 4.6-3c**. It is easy to pick out the largest fractional difference (in the interval 1 to 10 GeV), which occurs near 5 GeV. Beam element misalignments breaking the azimuthal symmetry of the neutrino beam, such as this horn 1 X shift, are measurable in the near detector.

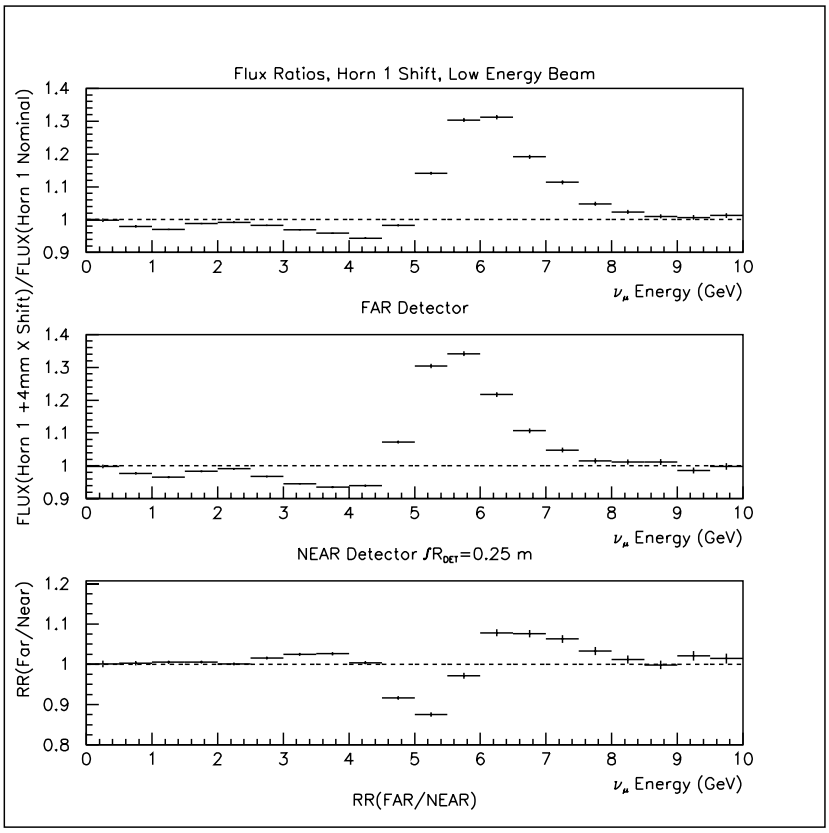

Fig 4.6-3 Effect of a 4 mm offset of horn 1 on (top) the far detector flux, (middle) near detector at 316.6 m beyond the end of the decay pipe, (bottom) far over near ratio(RR). These results are for the low energy beam configuration.

Figure 4.6-4 displays RR-1 for several horn 1 X shifts. These all start at RR-1=0 at low energy, but have been offset by multiples of 10% to clearly display the several curves on a single graph. To obtain sufficient statistical precision from the Monte Carlo in a reasonable time, X shifts much larger than the expected alignment tolerance of 0.35 mm have been calculated. At each peak and valley shown in **Figure 4.6-4**, the data are fit to the formula $RR\text{-}1=Ax^p$. This formula forces the required result of RR=1 at x=0, i.e. no effect on the spectrum if there is no misalignment. The value of RR at the expected alignment tolerance is calculated using the parameters A and p determined by the fit.

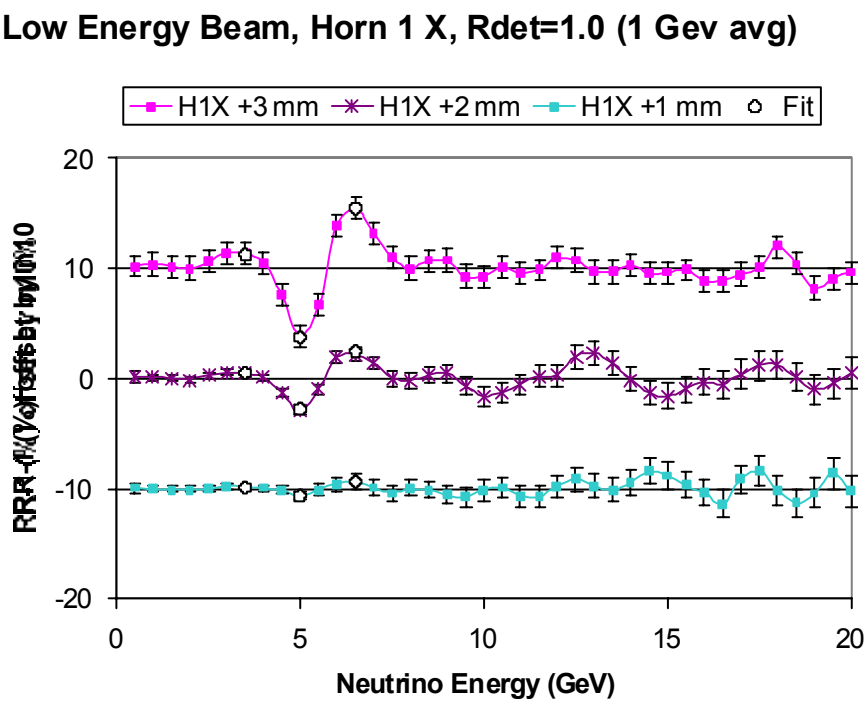

Fig 4.6-4 Curves of RR-1 for several horn 1 X shifts. These all start at RR-1=0 at low energy, but have been offset by multiples of 10% to clearly display the several curves on a single graph. These results are for the low energy beam configuration.

This analysis is repeated for all beam element misalignments shown in **Table 4.6-6**. A similar table is prepared for each 1 GeV neutrino energy interval and, to be conservative, lists the largest deviation of RR found for any neutrino energy up to the table value. The overall effect on RR is found by adding the individual element terms in quadrature. The table takes into account that most misalignments can occur in two transverse planes.

In the table, angle parameters are expressed by a single linear distance; the downstream end of the device is displaced by this amount and the upstream end is displaced by an equal amount in the opposite direction. These two displacements are what are actually measured by the surveyors. The length of the device, in meters, is given in square brackets after the description.

Up to 8 GeV Neutrino Energy							
R=0.25 E	p	A	Misaligned	Expected	Units	(RR-1)exp	Squared
(GeV)		(%)				(%)	(%)2
5.0	2.000	-0.7443	1XP	0.35	mm	-0.091	0.0083
6.0	1.000	0.5864	1AP [3]	0.35	mm	0.205	0.0421
8.0	1.500	-0.4806	2XP	0.35	mm	-0.100	0.0099
6.0	1.000	0.0608	2AP [3]	0.35	mm	0.021	0.0005
5.0	1.500	-0.0272	BAP [10]	0.35	mm	-0.006	0.0000
5.0	1.500	-1.8539	BXP	0.45	mm	-0.554	0.3070<
8.0	1.000	0.9807	TAP [.95]	0.35	mm	0.343	0.1178
8.0	1.000	1.7554	TXP	0.35	mm	0.614	0.3775<<
8.0	1.500	-0.7742	FXP	0.12	100m	-0.032	0.0010
8.0	1.156	1.6285	NXP	0.25	10cm	0.328	0.1076
6.5	1.000	-6.1960	DDM	0.025	m	-0.155	0.0240
7.5	1.000	3.4942	DUM	0.025	m	0.087	0.0076
					Sum		1.0033
					X2		2.0066
					RMS	1.417	
7.0	1.500	0.2646	DRM	2.00	cm	0.748	0.5601<
4.5	1.000	1.2792	HCM	0.50	%	0.640	0.4091
					Sum		2.9758
			All Misalignments:		RMS	1.725	
key:	1st char			2nd char			
	1	horn 1		A	Angle		
	2	horn 2		C	Current		
	B	Beam		D	Downstream		
	D	Decay Pipe X		R	Radius		
	F	Far Det		U	Upstream		
	H	Horns		X	Traverse Offset		
	N	Near Det					
	T	Target		3rd char			
				P	Plus		
				M	Minus		

Table 4.6-6 The expected percentage error in RR from each misalignment at 8 GeV neutrino energy. These results are for the low energy beam configuration

This result is plotted in **Figure 4.6-5** as a function of neutrino energy. Also shown is the statistical error from a two-year run. The MINOS physics requirement is that the error due to neutrino beam misalignments be comfortably below the 2 year run statistical error, and **Figure 4.6-5** shows this to be the case for the low energy beam.

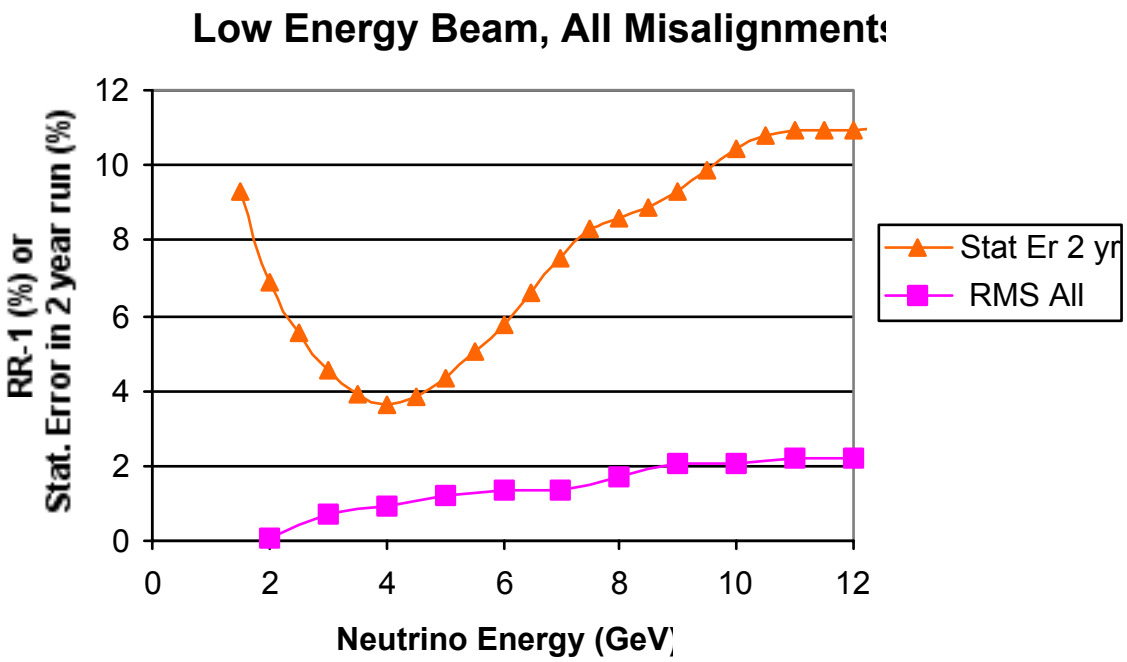

Figure 4.6-5 The expected percentage error in RR from all misalignments listed in **Table 4.6-6**. Also shown is the statistical error for a two-year run. These results are for the low energy beam configuration

4.6.4 System Description: Construction QA

Fermilab surveyors are providing NuMI tunnels and halls quality assurance. Most of the decay tunnel was excavated using a 21.5-foot diameter Tunnel Boring Machine (TBM). **Figure 4.6-6** shows the vertical and horizontal deviations of the center of the TBM decay tunnel from the specified line from Fermilab to Soudan. Measurement of the completed tunnel by both the SA Healy (civil subcontractor) and Fermilab surveyors are shown. Agreement with the design is excellent; most vertical and horizontal centers are within 2 inches. No attempt was made by the two groups of surveyors to measure at the same station (horizontal distance along the tunnel), so

local tunnel variations could explain part of the differences between the measurements. The agreement for horizontal is worse than vertical; this is likely conformation that azimuth is the most difficult parameter to transfer underground. The Fermilab surveyors used the 15 microradian gyro-theodolite (0.36 inch in 2000 feet), while the SA Healy surveyors used a less precise 100 microradian instrument (2.4 inch in 2000 feet).

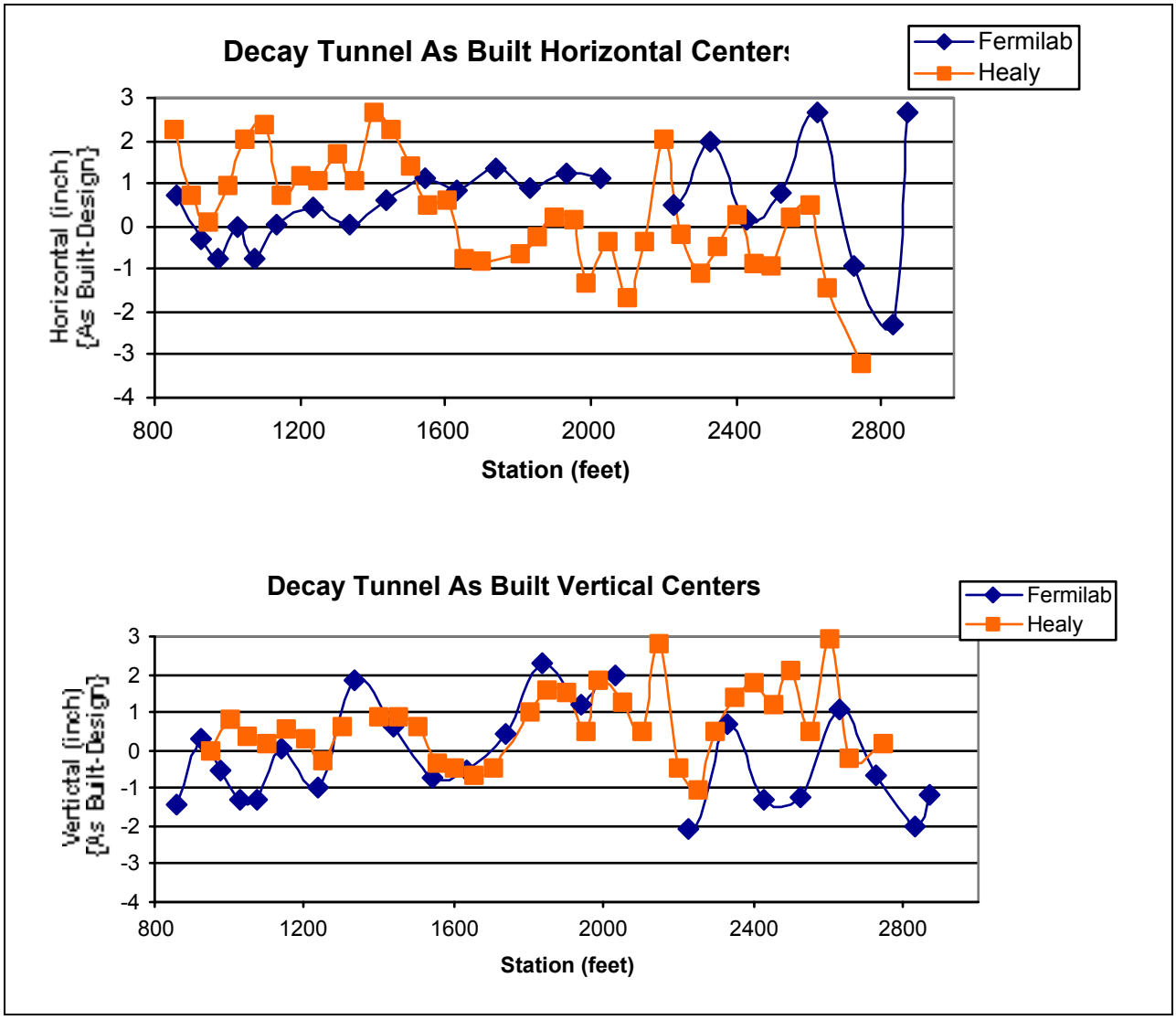

FIgure 4.6-6 The vertical and horizontal deviations of the "as built" center of the TBM decay tunnel from the specification. Measurements of the completed tunnel by both the SA Healy (civil subcontractor) and Fermilab surveyors are shown.

4.7 WATER, VACUUM AND GAS SYSTEMS (WBS 1.1.7)

4.7.1 Introduction

In this section are grouped together details of the various utilities required for the NuMI beams. Water and gas would normally be expected to fall under the heading of utilities, and for NuMI it has been decided to include vacuum as well.

4.7.2 System Description: Water systems

Cooling water at Fermilab falls into three categories - **Industrial Cooling Water (ICW)**, **Low Conductivity Water (LCW)** and **RadioActive Water (RAW)**. These systems are needed to remove, directly or indirectly, the heat generated by the operation of electrical devices and to dispose of the energy deposited in various components by high energy beams. Without functional cooling systems, many beamline components would be damaged and fail due to excessive thermal buildup. There are seven NuMI water systems.

4.7.2.1 The MI-62 (Upstream) LCW system. This system provides cooling water to all of the extraction and pre-target magnets. The MI-62 LCW system rejects its heat to the pond G pond water system. There are two installed pumps, one pump runs, one in hot stand-by. Controls for the MI-62 water system will also include controls and instrumentation for the pond water (PW) system. The MI-62 (Upstream) LCW system is not anticipated to become activated. See Drawing 8875.117-ME-406228, NuMI Extraction & Pre-Target (Upstream) LCW System P&ID

Approximate System Volume:	4200 gallons
Approximate Pump Specifications:	600 gallons per minute 440 feet total developed head 125 horsepower
Heat Load	760 kW
Nominal Heat Exchanger Capacity	1200 kW

4.7.2.2 The MINOS LCW system. This system provides cooling water to the MINOS Near Detector Coil, its power supply and the electronics racks located in the MINOS Near Detector Hall. The MINOS LCW system rejects its heat to a FESS provided chilled water system in the MINOS Service Building and MINOS Cavern. There are two installed pumps, one pump runs, one in hot stand-by. Control of the FESS provided chilled water system is outside of the scope of the NuMI Water Systems Controls. The MINOS (Downstream) LCW system is not anticipated to become activated. See Drawing 8875.117-ME-406230, NuMI Downstream P&ID.

Approximate System Volume:	310 gallons
Approximate Pump Specifications:	145 gallons per minute 110 feet total developed head 3 horsepower
Heat Load	109 kW
Nominal Heat Exchanger Capacity	150 kW

4.7.2.3 The Decay Pipe Cooling RAW system. This system provides cooling to the 2300 feet long vacuum decay pipe located in the tunnel between the NuMI Target Hall and the NuMI Absorber Caverns. The Decay Pipe Cooling RAW System rejects its heat to a FESS provided chilled water system at the upstream end of the decay pipe and also rejects its heat at the downstream end to the same FESS provided chilled water system that accepts heat from the MINOS LCW System. There are two installed pumps, one pump runs, one in hot stand-by. Control of these systems is outside of the scope of the NuMI Water Systems Controls.

The water in this system will become activated. Kamran Vasiri has calculated the activation of the Decay Pipe Cooling System. After one year of operation and one hour of cool down, the total activity in the decay pipe cooling system should be approximately 87 mCi/year. Dose rate to a person standing next to the pump suction tank should be approximately 1 mrem per hour. See Drawing 8875.117-ME-406231,NuMI Decay Pipe Cooling P&ID

Approximate System Volume:	725 gallons
Approximate Pump Specifications:	24 gallons per minute 270 feet total developed head 7.5 horsepower
Heat Load	140 kW
Nominal Heat Exchanger Capacity	150 kW

4.7.2..4 The Absorber Cooling RAW System. This system provides cooling to the NuMI Absorber (Beam Dump), which is located in the NuMI Absorber Cavern at the downstream end of the decay pipe. The Absorber Cooling RAW system rejects its heat to an Intermediate Water System, which in turn rejects its heat to a pond water system at the MINOS service building. There are two installed pumps, one pump runs, one in hot stand-by. Control of the intermediate system is within the scope of the NuMI Water Systems Controls but the pond water system is not.

The water in this system will become activated. Kamran Vasiri has calculated the affect of a complete failure of the water containment systems for the absorber RAW system. Based on the concentration of tritium in the absorber cooling water of 16,000 pCi/ml (represents one year of running) and a water inflow rate of 150 gpm (conservative) the concentration of tritium in the sump discharge water would be less then 1500 pCi/ml. This is less than the allowable limit of 2000 pCi/ml. See Drawing 8875.117-ME-406229, NuMI Absorber RAW System P&ID

Absorber Core Cooling System

Approximate System Volume:	90 gallons
Approximate Pump Specifications:	506 gallons per minute 65 feet total developed head 3 horsepower
Heat Load	150 kW
Nominal Heat Exchanger Capacity	150 kW

Absorber Intermediate Cooling System:

Approximate System Volume:	880 gallons
Approximate Pump Specifications:	50 gallons per minute 52 feet total developed head 3 horsepower
Heat Load	150 kW
Nominal Heat Exchanger Capacity	150 kW

4.7.2..5 The Target & Baffle RAW System. This system provides cooling to the NuMI Target and Beam Baffles located in the NuMI Target Hall. There are two installed pumps, one pump

runs, one in hot stand-by. This system rejects its heat to the MI-62 LCW system. See Drawing 8875.117-ME-406232, NuMI Target & Baffle P&ID. The water in this system will become activated. Kamran Vaziri has calculated the amount of radioactivity as a function of time in the target RAW system to be about 3.5 curies after one year of operation. Of this, approximately 0.8 Curies is the relatively long-lived isotope tritium. Dose rate at one foot from the piping for this system will be about 14.3 rads per hour. Only 0.2 rads per hour is from ^{7}Be, the rest is from short-lived isotopes. Approximately 1 cm^3 of hydrogen gas will be produced each day for this system.

Approximate System Volume:	85 gallons
Approximate Pump Specifications:	10gallons per minute 42 feet total developed head 1/2 horsepower
Heat Load	~5 kW
Nominal Heat Exchanger Capacity	20 kW

4.7.2..6 The Horn 1 RAW System. This system provides cooling to Horn 1 located in the NuMI Target Hall. The Horn 1 RAW System rejects its heat to a FESS provided chilled water system. There are two installed pumps, one pump runs, one in hot stand-by. Control of this FESS provided chilled water system is outside of the scope of the NuMI Water Systems Controls. See Drawing 8875.117-ME-406477,NuMI Horn #1 and Horn #2 RAW Water P&ID The water in this system will become activated. Kamran Vaziri has calculated the amount of radioactivity as a function of time in the horn1 cooling water. He has also calculated the amount of shielding needed around the DI bottles necessary to keep the dose to about 1 mrem per hour for people in close proximity to the DI bottles. Approximately 3 inches of lead are sufficient.

Approximate System Volume:	105gallons
Approximate Pump Specifications:	110 gallons per minute 106 feet total developed head 5 horsepower
Heat Load	43.5 kW
Nominal Heat Exchanger Capacity	90 kW

4.7.2..7 The Horn 2 RAW System. This system provides cooling to Horn 2 located in the NuMI Target Hall. There are two installed pumps, one pump runs, one in hot stand-by. The Horn 2 RAW System rejects its heat to a FESS provided chilled water system. Control of this FESS provided chilled water system is outside of the scope of the NuMI Water Systems Controls. The water in this system will become activated.

Approximate System Volume:	95 gallons
Approximate Pump Specifications:	110 gallons per minute 103 feet total developed head 5 horsepower
Heat Load	40 kW
Nominal Heat Exchanger Capacity	50 kW

4.7.3 System Description: Vacuum Systems

Transport of the NuMI proton and hadron beams requires that various levels of vacuum be established in the MI tunnel, extraction stub, carrier pipe, pretarget area and decay pipe. Since the NuMI beamlines are single pass, requirements are not so stringent as they are in a circular machine. The novel feature is the 675 m long decay pipe, which has a very large evacuated volume. There are two vacuum systems:

4.7.3.1 The primary beam transport system. This vacuum system starts in the extraction area at the Lambertson magnets and continues through magnet bends 1 and 2, through the carrier pipe, to the pre-target area, through the final bend, bend 3, and just into the target pile. This vacuum system ends just before the second horn protection baffle. The vacuum in the primary beam transport system needs to operate at 1×10^{-6} torr in the vicinity of the beam instrumentation but can rise to a higher level of 1×10^{-5} torr in the middle of the carrier pipe. See Drawing 8875.117-MC-406XXX, NuMI Proton Beam-line Vacuum P&ID.

4.7.3..2 The decay pipe vacuum system. This system starts just downstream of the target pile and extends 2214 feet (675 meters) to just upstream of the beam absorber. This system needs to operate at a pressure of approximately 1 torr. See Drawing 8875.117-ME-406092,NuMI-Vacuum Decay Pipe Vacuum P&ID.

4.7.4 System Description: Utility System Controls

For each of the seven water systems and the two vacuum systems listed above, the following summary lists the interlocks, alarms, permits, analog variables, ON-OFF signals to and from ACNET, and finally the local instrumentation.

Interlocks: Each water system has one or more pumps, which are protected by a series of interlocks. These pump interlocks may be implemented in hard wired relay logic (ladder logic) or implemented in a Programmable Logic Controller (PLC). The decision as to which method to use has not yet been.

Analog Variables: Each system will have a number of instruments, which output analog variables to be displayed on an ACNET parameter page and/or a customized application program. Typically, these variables include water system pressures, temperatures, flow rates, expansion tank liquid levels, and resistivity. These signals may be chosen to be 4-20 ma signals or 0 to 10 VDC signals. The decision as to whether these analog signals are fed directly into a MADC or are fed into a PLC has not yet been made

Alarms: From the set of analog variables, there will be alarms for conditions where the analog variable either exceeds or is less than a given value. The intent is that when the variable exceeds or falls under a given value, an alarm will be displayed on the alarms display in the main control room. These alarms will be generated in ACNET in comparing the value of the analog variables to predetermined 'limits'.

ON-OFF signals to ACNET: Each system will generate digital status for reading by ACNET. For example, the intent is to monitor current switches on the pump motors and to indicate on an ACNET console that a particular pump is drawing current (on) or not drawings current (off).

ON-OFF signals from ACNET: Each system will receive one or more digital commands from ACNET. These signals will be used to start or stop pumps based on an operator's command at the ACNET console.

Permits. These permits will be for 'beam permits' or 'power supply permits' or both. The intent of these permits is to generate a signal that indicates satisfactory operation of the system.

Should the parameters of the system indicate that the system is not operating satisfactory, the permit signal will be removed.

Local instrumentation: This is instrumentation, which is non-interfaced to the control system. This instrumentation is typically comprised of pressure gauges, thermometers, flow meters and level gauges. This local instrumentation provides a visual indication and is intended to aid in system commissioning and to de-bug system problems in the event of a failure or poor performance.

4.7.4.1 MI-62 (Up Stream) LCW System

LCW Pump Motor Interlocks

Contactor –	3phase rotation Over-current Motor Internal Over-temperature Switch (Wired Normally Closed)
Expansion Tank Liquid Level	Low Low Low
LCW Supply Temperature	Low Low (permit if value > 60 degrees F)
LCW Supply Temperature	High High (permit if value < 110 degreesF)

Pond Water Pump Motor Interlocks

Contactor –	3 phase rotation Over-current Motor Internal Over-temperature Switch (Wired Normally Closed)
Differential Pressure Across Pump	Low (w/ 15 second time delay)

Analog Variables to ACNET

- LCW Supply Pressure
- LCW Pump Suction Pressure
- LCW Supply Temperature
- LCW Return Temperature

- LCW Supply Resistivity (4-20 ma Signal)
- LCW Resistivity Out of the DI Bottles (4-20 ma Signal)
- LCW Resistivity at the NuMI TSB Power Supply Room (4-20 ma Signal)
- LCW Expansion Tank Liquid Level
- Differential Pressure Across Pond Water Strainer
- Pond Water Pump Suction Pressure
- Pond Water Pump Discharge (Supply) Pressure
- Pond Water Supply Temperature
- Pond Water Return Temperature

Alarms to ACNET

- Pond Water Supply Pressure Low for15 Seconds
- High Differential Pressure Across Pond Water Strainer
- Expansion Tank Pressure Low
- Expansion Tank Liquid Level Low
- Expansion Tank Liquid Level High
- LCW Supply Temperature High (alarm if value > 100 Degrees Fahrenheit.)
- LCW Supply Temperature Low (alarm if value < 70 Degrees Fahrenheit.)

ON-OFF Signals to ACNET

- LCW Pump Current Switches

ON-OFF Signals from ACNET

- LCW Pump Remote Start and Stop Switches

Inputs to Beam Permit

- Sum of Magnet Power Supply Permit Inputs

Inputs to Beam Line Magnet Power Supply Permit

- Either LCW Pump Drawing Current
- Expansion Tank Liquid Level Not Low Low
- LCW Supply Temperature Not High (permit if value < 110 degrees Fahrenheit.)

Local Instrumentation (Gauges w/o wires)

Pressure Gauges

- LCW Pump Suction (2) Range is 0 to 30 psig
- LCW Pump Discharge (2) Range is 0 to 300 psig

- Expansion Tank (1) Range is 0 to 60 psig
- Power Supply LCW Supply Headers (2) Range is 0 to 200 psig
- Power Supply LCW Return Headers (2) Range is 0 to 200 psig
- Power Supply LCW Supply Header in Tunnel (1) Range is 0 to 300 psig
- Power Supply LCW Return Header in Tunnel (1) Range is 0 to 300 psig
- Pond Water Basket Strainer Inlet and Outlet (2) Range is 0 to 200 psig
- DI-Bottle inlet header (1) Range is 0 to 60 psig
- DI-Bottle outlet header (1) Range is 0 to 60 psig
- LCW Supply Header in Tunnel at TSB (1) Range is 0 to 300 psig
- LCW Return Header in Tunnel at TSB (1) Range is 0 to 300 psig

Temperature Gauges

- Heat Exchanger (4) Range is approximately 0 to 200 degree Fahrenheit.

Flow Gauges

- Di-Bottle Flow (1) Range is 6 to 60 gpm
- LCW Make-Up (1) Range is 6 to 60 gpm

Level Gauges (Sight Glasses)

- Expansion Tank

4.7.4.2 MINOS (Down Stream) LCW System

Pump Motor Interlocks

Contactor –	3 phase rotation Over-current Motor Internal Over-temperature Switch (Wired Normally Closed)
Expansion Tank Liquid Level	Low Low
LCW Supply Temperature	Low Low (permit if value > 60 degrees F) w/ 5 minute time delay

Analog Variables to ACNET

- LCW Supply Pressure
- LCW Pump Suction Pressure
- LCW Booster Pump Discharge Pressure
- LCW Supply Temperature
- LCW Supply Resistivity (4-20 ma Signal)
- LCW Resistivity Out of the DI Bottles (4-20 ma Signal)
- LCW Expansion Tank Liquid Level

Alarms to ACNET

- Expansion Tank Liquid Level Low
- Expansion Tank Liquid Level High
- LCW Supply Temperature High (alarm if value > 75 Degrees Fahrenheit.)
- LCW Supply Temperature Low (alarm if value < 65 Degrees Fahrenheit.)

ON-OFF Signals to ACNET

- LCW Pump Current Switches
- Booster Pump Current Switch

ON-OFF Signals from ACNET

- LCW Pump Remote Start and Stop Switches

Inputs to Beam Permit

None

Inputs to Near Detector Magnet Power Supply Permit

- Either LCW Pump Drawing Current
- Booster LCW Pump Drawing Current
- Expansion Tank Liquid Level Not Low Low
- LCW Supply Temperature Not High (allow permit if value < 80 degrees F)

Local Instrumentation (Gauges w/o wires)

Pressure Gauges

- LCW Pump Suction (2) Range is 0 to 30 psig
- LCW Pump Discharge (1) Range is 0 to 60 psig
- LCW Booster Pump Discharge (2) Range is 0 to 100 psig
- Expansion Tank (1) Range is 0 to 60 psig
- DI-Bottle inlet header (1) Range is 0 to 60 psig
- LCW Supply Header (1) Range is 0 to 60 psig
- LCW Return Header (1) Range is 0 to 60 psig

Temperature Gauges

- Heat Exchanger (4) Range is approximately 20 to 140 degree Fahrenheit.

Flow Gauges

- Di-Bottle Flow (1) Range is 2 to 20 gpm

Level Gauges (Sight Glasses)

- Expansion Tank

4.7.4.3 Decay Pipe Cooling RAW System

Pump Motor Interlocks

Contactor	3 phase rotation Over-current Motor Internal Over-temperature Switch (Wired Normally Closed)
Expansion Tank Liquid Level	Low Low

Analog Variables to ACNET

- Pump Discharge Pressure
- Pump Suction Pressure
- Water Supply Temperature (2 points)
- Water Return Temperature (2 points)
- Water Expansion Tank Liquid Level

Alarms to ACNET

- Expansion Tank Liquid Level Low
- Expansion Tank Liquid Level High
- Cooling Water Supply Temperature High (alarm if value > 75 Degrees Fahrenheit.)
  (This temperature will be measured at two locations)
- Cooling Water Return Temperature High (alarm if value > 95 Degrees Fahrenheit.)
  (This temperature will be measured at two locations)

ON-OFF Signals to ACNET

- RAW Pump Current Switches
- Flow Switch low.

ON-OFF Signals from ACNET

- RAW Pump Remote Start and Stop Switches

Inputs to Beam Permit

- Return Water Temperature Not High (measured at 2 points)
- Pump Differential Pressure Not Low (1 minute time delay)
- Pump Differential Pressure Not High (1 minute time delay)
- Either Pump Drawing Current

- Expansion Tank Level not Low Low

Local Instrumentation (Gauges w/o wires)

Pressure Gauges

- Pump Suction (2) Range is 0 to 60 psig
- Pump Discharge (1) Range is 0 to 200 psig
- Expansion Tank (1) Range is 0 to 60 psig
- DI-Bottle inlet header (1) Range is 0 to 60 psig
- Heat Exchanger Inlet in Tunnel at TSB (1) Range is 0 to 100 psig
- Heat Exchanger Outlet in Tunnel at TSB (1) Range is 0 to 100 psig
- Heat Exchanger Inlet in Tunnel at D.S. End (1) Range is 0 to 100 psig
- Heat Exchanger Outlet in Tunnel at D.S. End (1) Range is 0 to 100 psig
- Full Flow Filter Differential Pressure (1) Range is 0 to 10 psig

Temperature Gauges

- Heat Exchangers Inlets and Outlets (8) Range is approximately 20 to 140 degree F

Flow Gauges

- Di-Bottle Flow (1) Range is 2 to 20 gpm

Level Gauges (Sight Glasses)

- Expansion Tank

4.7.4.4 Absorber Cooling RAW System

Pump Motor Interlocks

Absorber RAW Pumps:

Contactor	3 phase rotation Over-current Motor Internal Over-temperature Switch (Wired Normally Closed)
Absorber RAW Expansion Tank Liquid Level	Low Low

Absorber Intermediate Loop Pumps:

Contactor	3 phase rotation Over-current Motor Internal Over-temperature Switch (Wired Normally Closed)
Absorber Intermediate Loop Expansion Tank Liquid Level	Low Low

Analog Variables to ACNET

- Absorber RAW Pump Discharge Pressure (Supply Pressure)
- Absorber RAW Return Pressure
- Absorber RAW Pump Suction Pressure
- Absorber RAW Water Supply Temperature
- Absorber RAW Water Return Temperature
- Absorber RAW Water Expansion Tank Liquid Level
- Absorber RAW Resistivity out of the DI Bottle (4-20 ma Signal)
- Absorber Intermediate Loop Supply Temperature

Alarms to ACNET

- Absorber RAW Expansion Tank Liquid Level Low
- Absorber RAW Expansion Tank Liquid Level High
- Absorber RAW Water Supply Temperature High (alarm if value > 105 Degrees F.)
- Absorber RAW Water Return Temperature High (alarm if value > 125 Degrees F.)
- Absorber Intermediate Expansion Tank Liquid Level Low

- Absorber Intermediate Expansion Tank Liquid Level High
- Absorber Intermediate Water Supply Temperature High (alarm if value > 95 Degrees F)

ON-OFF Signals to ACNET

- Absorber RAW Pump Current Switches (2)
- Absorber Intermediate Pump Current Switches (2)

ON-OFF Signals from ACNET

- Absorber RAW Pump Remote Start and Stop Switches

Inputs to Beam Permit

- Absorber RAW Return Water Temperature Not High (permit if value < 130 Degrees F)
- Absorber RAW Pump Differential Pressure Not Low
- Absorber RAW Pump Differential Pressure Not High
- Either Absorber RAW Pump Drawing Current
- Absorber RAW Expansion Tank Level not Low Low
- Either Absorber Intermediate Pump Drawing Current
- Absorber Intermediate Expansion Tank Level not Low Low

Local Instrumentation (Gauges w/o wires)

Pressure Gauges

- RAW Pump Suction (2) Range is 0 to 60 psig
- RAW Pump Discharge (2) Range is 0 to 100 psig
- Intermediate Pump Suction (2) Range is 0 to 60 psig
- Intermediate Pump Discharge (2) Range is 0 to 100 psig
- RAW Expansion Tank (1) Range is 0 to 60 psig
- Intermediate Expansion Tank (1) Range is 0 to 60 psig
- DI-Bottle inlet header (1) Range is 0 to 60 psig
- RAW Full Flow Filter Differential Pressure (1) Range is 0 to 10 psig
- Intermediate Full Flow Filter Differential Pressure (1) Range is 0 to 10 psig
- RAW Return Header (1) Range is 0 to 100 psig
- Intermediate Return Header (1) Range is 0 to 100 psig

Temperature Gauges

- Heat Exchangers Inlets and Outlets (8) Range is ≈ 20 to 140 degree Fahrenheit.

Flow Gauges

- Di-Bottle Flow (1) Range is 2 to 20 gpm

Level Gauges (Sight Glasses)

- RAW Expansion Tank
- Intermediate Expansion Tank

4.7.4.5 Target & Baffle RAW System

Pump Motor Interlocks

Target RAW Pumps:

Contactor	3 phase rotation Over-current Motor Internal Over-temperature Switch (Wired Normally Closed)
Target RAW Expansion Tank Liquid Level	Low Low

Analog Variables to ACNET

- Target RAW Pump Discharge Pressure (Supply Pressure)
- Target RAW Return Pressure
- Target RAW Pump Suction Pressure
- Target RAW Water Supply Temperature
- Target RAW Water Return Temperature
- Target RAW Water Expansion Tank Liquid Level
- Target RAW Resistivity out of the DI Bottle (4-20 ma Signal)

Alarms to ACNET

- Target RAW Expansion Tank Liquid Level Low
- Target RAW Expansion Tank Liquid Level High
- Target RAW Water Supply Temperature High (alarm if value > 105 Degrees F)
- Target RAW Water Return Temperature High (alarm if value > 125 Degrees F)

ON-OFF Signals to ACNET

- Target RAW Pump Current Switches (2)

ON-OFF Signals from ACNET

- Target RAW Pump Remote Start and Stop Switches

Inputs to Beam Permit

- Target RAW Return Water Temperature Not High (permit if value < 130 Degrees F)
- Target RAW Pump Differential Pressure Not Low
- Target RAW Pump Differential Pressure Not High

- Either Target RAW Pump Drawing Current
- Target RAW Expansion Tank Level not Low Low

Local Instrumentation (Gauges w/o wires)

Pressure Gauges

- Target RAW Pump Suction (2) Range is 0 to 30 psig
- Target RAW Pump Discharge (2) Range is 0 to 60 psig
- Target RAW Expansion Tank (1) Range is 0 to 60 psig
- DI-Bottle inlet header (1) Range is 0 to 60 psig
- Target RAW Full Flow Filter Differential Pressure (1) Range is 0 to 10 psig
- Target RAW Return Header (1) Range is 0 to 100 psig

Temperature Gauges

- Heat Exchangers Inlets and Outlets (4) Range is 40 to 180 degree Fahrenheit.

Flow Gauges

- Di-Bottle Flow (1) Range is 2 to 20 gpm

Level Gauges (Sight Glasses)

- RAW Expansion Tank

4.7.4.6 Horn 1 RAW System

Pump Motor Interlocks

Horn 1 RAW Pumps:

Contactor	3 phase rotation Over-current Motor Internal Over-temperature Switch (Wired Normally Closed)
Horn 1 RAW Expansion Tank Liquid Level	Low Low
Horn 1 Pump Running Local Indicator Lights	On/Off

Analog Variables to ACNET

- Horn 1 RAW Pump Discharge Pressure (Supply Pressure)
- Horn 1 RAW Expansion Tank Pressure
- Horn 1 RAW Pump Suction Pressure
- Horn 1 RAW Water Supply Temperature
- Horn 1 RAW Water Return Temperature
- Horn 1 RAW Water Expansion Tank Liquid Level
- Horn 1 RAW Resistivity out of the DI Bottle (4-20 ma Signal)

Alarms to ACNET

- Horn 1 RAW Expansion Tank Liquid Level Low
- Horn 1 RAW Expansion Tank Liquid Level High
- Horn 1 RAW Water Supply Temperature High (alarm if value > 75 Degrees F)
- Horn 1 RAW Water Return Temperature High (alarm if value > 85 Degrees F)

ON-OFF Signals to ACNET

- Horn 1 RAW Pump Current Switches (2)

ON-OFF Signals from ACNET

- Horn 1 RAW Pump Remote Start and Stop Switches

Inputs to Power Supply Permit

- Horn 1 RAW Return Water Temperature Not High (permit if value > 90 Degrees F)
- Horn 1 RAW Pump Differential Pressure Not Low
- Horn 1 RAW Pump Differential Pressure Not High

- Either Horn 1 RAW Pump Drawing Current
- Horn 1 RAW Expansion Tank Level not Low Low

Local Instrumentation (Gauges w/o wires)

Pressure Gauges

- Horn 1 RAW Pump Suction (2) Range is 0 to 60 psig
- Horn 1 RAW Pump Discharge (2) Range is 0 to 100 psig
- Horn 1 RAW Expansion Tank (1) Range is 0 to 60 psig
- DI-Bottle inlet header (1) Range is 0 to 60 psig
- Horn 1 RAW Full Flow Filter Differential Pressure (1) Range is 0 to 10 psig
- Horn 1 RAW Jet Pump Motive (1) Range is 0 to 60 psig
- Horn 1 RAW Supply Header (2) Range is 0 to 60 psig
- Horn 1 RAW Jet Pump Suction (1) Range is -30 inches Hg to 15 psig
- DI Bottle Outlet Filter Inlet Range is 0 to 30 psig.

Temperature Gauges

- Heat Exchangers Inlets and Outlets (4) Range is 20 to 120 degree Fahrenheit.
- Return Water Temperature Range is 20 to 120 degree Fahrenheit

Flow Gauges

- Di-Bottle Flow (1) Range is 2 to 20 gpm
- Horn 1 Inner Conductor A Flow, Range is 2 to 20 gpm
- Horn 1 Inner Conductor B Flow, Range is 2 to 20 gpm
- Horn 1 Outer Conductor Flow, Range is 2 to 20 gpm
- Horn 1 Clamp Flow, Range is 2 to 20 gpm

Level Gauges (Sight Glasses)

- RAW Expansion Tank

OtherInstrumentation:

- Pump Hour Meter (2)

4.7.4.7 Horn 2 RAW System

Pump Motor Interlocks

Horn 2 RAW Pumps:

Contactor	3 phase rotation Over-current Motor Internal Over-temperature Switch (Wired Normally Closed)
Horn 2 RAW Expansion Tank Liquid Level	Low Low
Horn 2 Pump Running Local Indicator Lights	On/Off

Analog Variables to ACNET

- Horn 2 RAW Pump Discharge Pressure (Supply Pressure)
- Horn 2 RAW Expansion Tank Pressure
- Horn 2 RAW Pump Suction Pressure
- Horn 2 RAW Water Supply Temperature
- Horn 2 RAW Water Return Temperature
- Horn 2 RAW Water Expansion Tank Liquid Level
- Horn 2 RAW Resistivity out of the DI Bottle (4-20 ma Signal)

Alarms to ACNET

- Horn 2 RAW Expansion Tank Liquid Level Low
- Horn 2 RAW Expansion Tank Liquid Level High
- Horn 2 RAW Water Supply Temperature High (alarm if value > 75 Degrees F)
- Horn 2 RAW Water Return Temperature High (alarm if value > 85 Degrees F)

ON-OFF Signals to ACNET

- Horn 2 RAW Pump Current Switches (2)

ON-OFF Signals from ACNET

- Horn 2 RAW Pump Remote Start and Stop Switches

Inputs to Power Supply Permit

- Horn 2 RAW Return Water Temperature Not High (permit if value < 90 Degrees F)
- Horn 2 RAW Pump Differential Pressure Not Low

- Horn 2 RAW Pump Differential Pressure Not High
- Either Horn 2 RAW Pump Drawing Current
- Horn 2 RAW Expansion Tank Level not Low Low

Local Instrumentation (Gauges w/o wires)

Pressure Gauges

- Horn 2 RAW Pump Suction (2) Range is 0 to 60 psig
- Horn 2 RAW Pump Discharge (2) Range is 0 to 100 psig
- Horn 2 RAW Expansion Tank (1) Range is 0 to 60 psig
- DI-Bottle inlet header (1) Range is 0 to 60 psig
- Horn 2 RAW Full Flow Filter Differential Pressure (1) Range is 0 to 10 psig
- Horn 2 RAW Jet Pump Motive (1) Range is 0 to 60 psig
- Horn 2 RAW Supply Header (1) Range is 0 to 100 psig
- Horn 2 RAW Jet Pump Suction (1) Range is 30 inches Hg to 15 psig
- DI Bottle Outlet Filter Inlet Range is 0 to 30 psig.

Temperature Gauges

- Heat Exchangers Inlets and Outlets (4) Range is ≈ 20 to 120 degree Fahrenheit.
- Return Water Temperature Range is ≈ 20 to 120 degree Fahrenheit

Flow Gauges

- Di-Bottle Flow (1) Range is 2 to 20 gpm
- Horn 2 Inner Conductor A Flow, Range is 2 to 20 gpm
- Horn 2 Inner Conductor B Flow, Range is 2 to 20 gpm
- Horn 2 Outer Conductor Flow, Range is 2 to 20 gpm
- Horn 2 Clamp Flow, Range is 2 to 20 gpm

Level Gauges (Sight Glasses)

- RAW Expansion Tank

OtherInstrumentation:

- Pump Hour Meter (2)

4.7.4.8 Vacuum Decay Vacuum System

Vacuum Pump Motor Interlocks

Vacuum Decay Pipe Pumps:

Contactor	3 phase rotation Over-current Motor Internal Over-temperature Switch (Wired Normally Closed)

Vacuum Pump Inlet Isolation Valve Interlocks

Allow valve to open if:

Pump Inlet Pressure is less than the header pressure **and**
Hand switch is in the Auto Position **and**
Vacuum Pump is running.

Analog Variables to ACNET

- Vacuum Decay Pipe Vacuum Header Pressure (2)
- Vacuum Decay Pipe Pump Inlet Pressure (2)
- Vacuum Decay Pipe Pump Exhaust Line Pressure (1)
- Vacuum Decay Pipe Pump Oil Temperature (2)

Alarms in ACNET

- Vacuum Decay Pipe Vacuum Header Pressure High
- Vacuum Decay Pipe Vacuum Exhaust Header Pressure High

ON-OFF Signals to ACNET

- Vacuum Decay Pipe Pump Current Switches (2)
- Vacuum Decay Pipe Pump Inlet Isolation Valves Open Limit Switch (2)
- Vacuum Decay Pipe Pump Inlet Isolation Valves Close Limit Switch (2)

ON-OFF Signals from ACNET

- Vacuum Decay Pipe Pump Remote Start and Stop Switches
- Vacuum Decay Pipe Pump Inlet Isolation Valves Open and Close Hand Switch (2)

Inputs to Beam Permit

- Vacuum Decay Pipe Pressure Satisfactory

Local Instrumentation (Gauges w/o wires)

Temperature Gauges

- Vacuum Pump Oil Temperature Gauge, Range is ≈ 40 to 180 degree Fahrenheit.

Level Gauges (Sight Glasses)

- Vacuum Pump Oil Level Sight Glass

APPENDIX 1 – Piping Schematics

Drawing 8875.117-MC-406233
NuMI Water Systems Piping and Instrumentation Diagram (P&ID) Legend

Drawing 8875.117-ME-406228
NuMI Extraction & Pre-Target (Upstream) LCW System P&ID

Drawing 8875.117-ME-406230
NuMI Downstream P&ID

Drawing 8875.117-ME-406229
NuMI Absorber RAW System P&ID

Drawing 8875.117-ME-406231
NuMI Decay Pipe Cooling P&ID

Drawing 8875.117-ME-406232
NuMI Target & Baffle P&ID

Drawing 8875.117-ME-406477
NuMI Horn #1 and Horn #2 RAW Water P&ID

Drawing 8875.117-ME-406092
NuMI-Vacuum Decay Pipe Vacuum P&ID

Drawing 8875.117-MC-406XXX
NuMI Proton Beam-line Vacuum P&ID

5 RADIATION SAFETY[1]

5.5 Introduction

Chapter 4 of this Handbook presented technical designs for each of the subsystems required to produce the neutrino beam for the NuMI physics program. Inherent in the designs is the fact that radiation protection is of the greatest importance in both primary and secondary beam areas. The purpose of this chapter is to present the various radiation-related matters, to explain the methodology that has guided the designs of the radiation protection systems in the project and to show the results.

The design of the Fermilab Main Injector (MI) permits the acceleration of numbers of protons not previously encountered in the energy regime above 100 GeV. The NuMI Facility design assumes that Main Injector protons will be transported to the target at a maximum intensity of 4×10^{13} protons every 1.87 seconds. This is called the Safety Envelope. Normal running will be allowed up to 10% less than this safety envelope. Physics goals of the MINOS experiment assume a value for beam on target of 3.7×10^{20} protons per year. For the purposes of designing radiation protection for the NuMI Facility, the above intensities translate to a maximum instantaneous proton rate of 2.1×10^{13} protons per second and an annual "dc" average (assuming 55% efficiency for beam) of $\sim1\times10^{13}$ protons per second.

As discussed in Chapter 4, an important consideration in the design of the NuMI Facility has been the desire to maintain the flexibility to accommodate a variety of neutrino beam configurations. This flexibility includes designing a Target Hall in which the location of the beam line components such as the target and the focusing horns may vary depending on the desired range of neutrino energy. Maintaining this flexibility has an impact on the design of the radiation shielding because of the desire to minimize the need to reconfigure the Target Hall shielding after the facility has begun operation.

There are four types of radiation that are of concern in the design of a facility such as NuMI. These are 1) the prompt radiation field, 2) the residual radiation field, 3) airborne activation and 4) soil/rock and groundwater activation. All these will be discussed. We have also included a section on Decontamination and Decommissioning (D&D).

[1] The approved NuMI/MINOS SA can be found on the web; it contains the most up to date information on radiation safety. Contact Nancy Grossman for access to this password protected document.

The program MARS[2] has been adopted as the Fermilab standard shielding code. Thus the design of the NuMI shielding is based on the use of the MARS simulation code. The "output" of the MARS program can be converted to activation level or, dose equivalents, used to determine the probability of radionuclide production in the air, soil or rock in which the nuclear interactions occur. These doses can then be compared to the various regulatory limits for each type of radiation exposure.

Evaluation of the radiation protection requirements for the NuMI facility has shown that various radiation safety factors drive the design of the facility. The design of the shielding for the target/focusing region (except the top), decay region, and two sides of the Hadron Absorber are driven by groundwater activation. Residual activation levels drive the shielding on top of the target/focusing region, and two sides of the Hadron Absorber. The level of primary beamline losses allowed are driven by groundwater or residual dose rate concerns, depending on the region of the primary beam. The air within the target chase is highly activated and thus must be contained in the target chase to the extent possible. This drives some design issues with the target chase shielding. Similarly the air in the region of the Hadron Absorber is highly activated and must be minimized and allowed to decay in transit to the vent.

Figure 5-1 shows a conceptual drawing of the NuMI Project. Radiation safety items are shown such as interlocked gates and doors, air monitoring locations, and labyrinths and penetrations. Refer to this picture when locating items described in the text.

[2] N. V. Mokhov, “The MARS Code System User’s Guide”,Fermilab-FN-628 (1995); Update Version 13(98), February, 1998

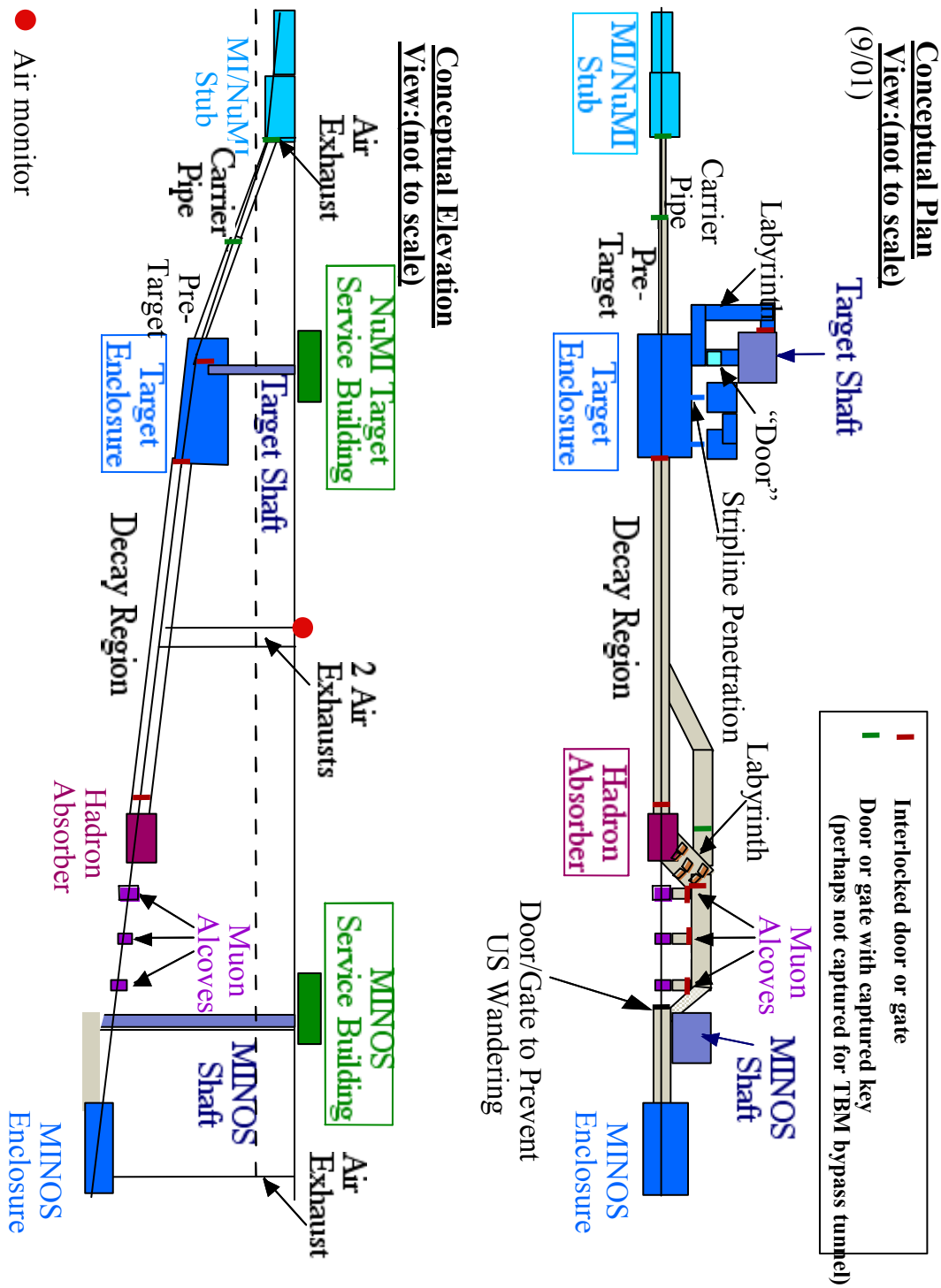

Figure 5-1 Conceptual Drawing of the NuMI Project, showing Radiation Safety Items

5.2 Access Requirements and Interlocks

The personnel safety interlock system is fail safe and redundant. The primary critical device for NuMI will be the Lambertson string (LAM601, LAM6023) located in MI-60. The secondary critical device will be the set of bend magnets HV102. (**Need MARS runs of this.)**

The personnel safety interlock system will "request" the abort signal required to stop NuMI extraction, in those situations when a radiation or critical equipment protection limit has been exceeded. The interlocks for the portions of the NuMI facility in the MI enclosure, NuMI Stub Enclosure, and lined section of the carrier tunnel will be an integral part of the MI interlocks system.

The NuMI safety interlock system will prevent personnel access, when the beam is enabled, to the Carrier Tunnel unlined section, Pretarget and Target Hall area, decay pipe tunnel, Hadron Absorber area and muon alcoves. There will also be interlocked detectors that will disable the beam if the radiation levels become too high in the power supply room, upstream shaft area and bypass tunnel.

5.3 Groundwater

Groundwater activation and contamination can occur when radionuclides produced in the soil or rock surrounding an accelerator or beam line enclosure have a finite probability of getting into water passing through the soil or rock. Groundwater activation also can occur when the beam produces radionuclides, namely tritium, directly in the water contained in the soil or rock. This activated water can then migrate to a potential source of potable water.

The NuMI primary proton beam, and the secondary hadron beam, must be directed toward the MINOS far detector in Soudan, implying a 58 mradian downward slope. As a consequence the Target Hall and much of the hadron decay region pass through the local aquifer. This has led to careful consideration and analysis of the processes that might lead to potential contamination of the groundwater resources. The key issue for NuMI is that radionuclides produced in the rock and water surrounding part of the beam line are produced in the groundwater resource. Thus we cannot take credit for decay in transit to the groundwater resource, as other facilities not

constructed so deeply have. Several analyses and designs[3,4,5] laid the groundwork for the present model, which has resulted in the understanding of the problem. A Fermilab TM describing this methodology has been completed and is being circulated for approval. It takes into consideration the flow rate of water within the aquifer. Previous methodologies assumed static water conditions, which is extremely unrealistic within the aquifer. In the unlined sections of the NuMI tunnel, all the water nearby is captured by the tunnel and thus cannot make it to a well for consumption.

5.5.1 Specifications

Table 5-1 gives the limits on the concentrations of ^{22}Na and ^{3}H allowed.

	^{22}Na (pCi/ml)	^{3}H (pCi/ml)
Groundwater	0.4	20
Surface Water	10	2000

Table 5-1 Regulatory limits on allowed radionuclide concentrations in groundwater and surface water.

The sum of the fractions of radionuclide contamination (relative to the regulatory limits) must be less than one for all radionuclides;

$$\sum_i \frac{C_i}{C_{reg\ i}} \leq 1$$

where the sum is over radionuclides, i, C_i is the concentration of radionuclide *i* in the water and $C_{reg\ i}$ is the regulatory limit concentration.

Fermilab ES&H policy requires that a facility design must demonstrate that beamline operation will *not* result in activation levels above the regulatory limits, including all uncertainties in the methodology and input parameters. Verification that such limits are not violated is accomplished during the facility operation through the Lab-wide monitoring program (FESHM).

---

[3] A.Wehman, S. Childress, "Tritium Production in the Dolomitic Rock Adjacent to NuMI Beam Tunnels", Draft (1998) NuMI-B-495A(1999)

[4] B. Freeman, "A NUMI Wide-Band Beam Shield Design That Meets the Concentration Model Groundwater Criteria, NuMI-B-155, June 13, 1995.

[5] A. Wehmann,et.al.,"Groundwater Protection for the NuMI Project, FERMILAB-TM-2009, October 10, 1997.

5.5.2 Primary Beam Region

The primary beam region is separated into seven different sections based on the geology and geometry of the sections. Both geometry and geology affect the water flow rates. **Figure 5-2** shows the seven sections. The sections of main concern are the lined sections 1 and 2.

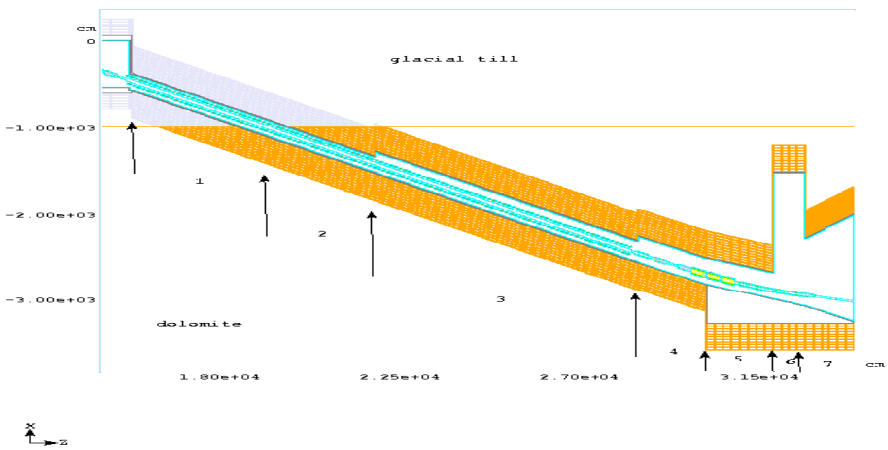

Figure 5-2: Seven Groundwater Sections of the NuMI Primary Beam

Section 1, the glacial till region, is not in the aquifer and the water travels slowly (cm/yr) through the soil to the aquifer. Thus much of the radioactivity has decayed by the time the water reaches the aquifer. Section 2, where the tunnel is lined, in the aquifer and in the mixed rock glacial till, is the area of the utmost concern. Here predicting the water velocity is difficult due to the variable nature of the geology in this region. We conservatively assume the water flows with the regional gradient towards the Fox River. This velocity (4 to 50 feet per year) is slow enough to allow activation of the water near the tunnel. The remaining sections (3 through 7) are unlined and have high water inflow velocities (several hundred feet per year), thus not allowing the water to get very activated and not allowing the water to get to a well. In all cases the inflow rates assumed in the calculations is below that measured in May 2002.

One should also note that the unlined tunnel downstream collects a large amount of water from the critical section 2. This is because two drainpipes were installed under the lined carrier tunnel. These two pipes extend ~50 feet and 6 feet respectively from the unlined section upstream into the lined section. They collect water in this region at a rate of **~5 gpm** (update value) as of March 2002. The groundwater activation calculation conservatively assumes the tunnel collects none of the water in section 2.

Table 5-2 shows the calculated residency time of the water in each of the 7 sections, based on conservative (slow) flow rates. The last two columns show the number of accident pulses allowed in each section, and the accident condition that can cause such an accident pulse. These results are all based on comparison to the groundwater limit. This table is being updated for the new beam optics. It is envisioned that the results will not change significantly. The region of most concern, as expected, is region 2. The final column in the table shows that power supply regulation is very important. (See Section 4.3.1). In order to have stable, controllable beam, the power supplies will be regulated at least an order of magnitude below that which is shown to create these accident conditions.

The radiation safety system will have interlocked detectors to watch losses in the primary beam. If excessive losses are seen, it will trip the critical devices and remove the beam permit. Also the beam permit system will check the power supply current at flattop before each pulse, losses on the last pulse and many other status items. The permit system will not allow extraction if anything is not within tolerance (See Section 4.1). All of this will make the occurrence of more than one accident pulse very unlikely.

Region	Water residency time (years)	Water residency time (days)	Lost pulses allowed in residency time	Accident Condition
1. Lined Carrier Pipe GT Accident	8.00000	2920.00	4.E+11	V105, 0.6%
2. Lined Carrier Pipe (Interface) Accident	1.50919	550.85	125	V104-2, 30%
3. Unlined Carrier Pipe Accident	0.00487	1.78	204	V104-2, 13%
4. Pre Target Accident (US)	0.01082	3.95	178	V105, 0.2%
5. Pre Target Accident (Mid)	0.01821	6.65	656	V105, 0.2%
6. Pre Target Accident (Shaft)	0.04618	16.86	5799	V105, 0.2%
7. Pre Target Accident (DS)	0.04028	14.70	16693	V105, 0.2%

Table 5-2 Primary Beam Accident Conditions and Lost Pulses Allowed

Due to all the mitigating factors for accident pulses, the DC or normal operational losses are of the biggest concern. These are the continually occurring losses that one can run with while still meeting all the regulatory requirements and not overly irradiating the components that personnel need to access. These are estimated using MARS, to be at a level of 10^{-4} of 4E13ppp (at 1.87 sec per pulse) for all regions, but region 2 where it is 10^{-6}. MARS simulations show that with the required power supply regulation no beam normal beam losses should occur, assuming 500π beam at $1x10^{-3}\Delta p/p$. As described in Section 4.1,the NuMI beam optics is designed to accept the largest beam the MI can provide.

5.5.3 Secondary Beam Region

Similar to the primary beam, the secondary beam is broken down into 5 different regions. Table 5-3 shows the estimated star densities from MARS simulations of the secondary beam components and shielding, and the resulting estimates of activation of the water flowing into the tunnel relative to the groundwater regulatory limit. **Figure 5-3** shows the activation levels of the inflow waters relative to the groundwater regulatory limits, including uncertainties. In all areas we are below the groundwater regulatory limit, including uncertainties.

Region	Star Density (stars per cm3/p)	Star Density Limit (stars/cm3/p)	Average Value Relative to Limit (% Uncertainty)
Target Hall	1.33E-11	4.10E-11	0.185 (75%)
DK Middle Silurian	4.58E-11	6.80E-11	0.402 (66%)
DK Lower Silurian	2.02E-11	4.80E-11	0.258 (64%)
DK Upper Ordovician	1.23E-11	5.40E-11	0.142 (61%)
Hadron Absorber	7.8e-12	4.7e-11	0.101 (64%)

Table 5-3: Secondary Beam Star Densities and Estimated Activation Levels

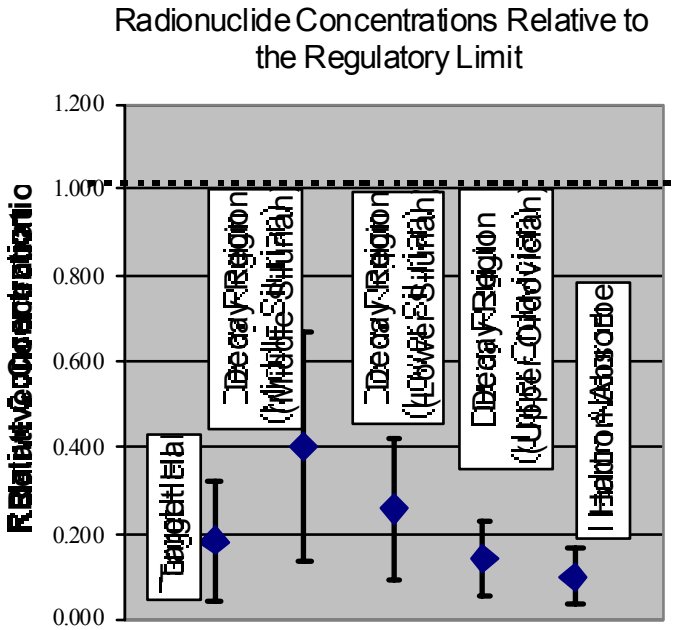

Figure 5-3: Secondary Beam Groundwater Inflow Activation Levels Relative to Regularity Limits

5.3.4 Monitoring

Operation of the NuMI Facility will be included in the comprehensive laboratory-monitoring program. Wells are an integral part of the Fermilab environmental monitoring strategy. Samples of well water would initially be examined every month, with the sampling rate eventually being reduced once NuMI has reached steady-state operation. NuMI, in collaboration with the ES&H Section, is in the process of determining the number and locations of NuMI monitoring wells.

In addition, regular sampling will be done on the water that is pumped from the NuMI downstream shaft region to the surface waters. Regular sampling will also be done for radionuclide levels in cooling water systems, including both the closed loop RAW system serving components experiencing higher activation levels, and the **LCW cooling system** serving conventional beam transport elements. RAW spills are controlled by a combination of continuous water level sensing, secondary containment vessel collection and tightly controlled sump discharge.

5.4 Airborne Activation

Airborne activation results from the interaction of primary and secondary particles directly with target nuclei of the air (or other gaseous medium) in its path. A secondary source of airborne activity is dust, formed by natural erosion or wear or by work on radioactive accelerator

components. The third source of airborne radioactivity results from the emission of gaseous radioactivity from liquids irradiated in the accelerator produced radiation environment. For NuMI, the main concern is radioactive air. Activities in radioactive air consist primarily of ^{11}C and ^{13}N with smaller concentrations of ^{15}O and ^{41}Ar; all with relatively short half-lives. ^{11}C, having a 20 minutes half-life, tends to be the dominant concern.

5.5.4 Specifications

Federal regulations, which are further implemented by the State of Illinois, govern the releases of airborne radionuclides, excluding radon and radon progeny, by U. S. Department of Energy Facilities (CFR89)[6]. These regulations place an annual limit of 10 mrem/year on the dose equivalent that can be delivered to a member of the public due to the release of airborne radionuclides from DOE facilities. The methodology for determining the dose equivalent is also specified. The regulations further require the application of continuous monitoring in accordance with U. S. Environmental Protection Agency specifications if the dose equivalent should exceed 0.1 mrem/year. Requirements for monitoring systems that meet these specifications are quite stringent and could tightly constrain Fermilab operations. These limits apply to the total release from the Laboratory.

Consistent with these requirements, in March 1999, Fermilab submitted an application renewal to the Illinois Environmental Protection Agency for its lifetime air pollution-operating permit[7]. This application addressed the radionuclide emissions from NuMI and other Fermilab facilities. It specified that the doses to the public will be kept well below 0.1 mrem/year for all Fermilab operations. The average annual activity release is to be kept less than 100 Ci. In consideration of the overall program of operations at Fermilab, the NuMI project management in consultation with the staff of the Fermilab ES&H Section established an administrative goal for the NuMI project of a maximum annual release of 45 Ci. The corresponding maximum anticipated dose equivalent due to NuMI operations that might be received by an individual hypothetically present full-time at the Fermilab site boundary is estimated to be 0.025 mrem.

---

[6] Dagenais (Da84) has provided estimates of the buildup of radon in tunnels made of the rock found at the level of the NuMI facilities on the Fermilab site. These results, including worst-case estimates, indicate occupational exposure to radon and radon progeny under the ventilation conditions present in the NuMI facility to be unimportant compared to the applicable regulatory limits of (CFR93).

[7] In response to this application, Illinois Environmental Protection Agency permit was issued on June 16, 1999.

5.4.2 Air Activation Results for NuMI

Delayed ventilation is used at NuMI to control radioactive air emissions. It is the simplest method and the one historically used at Fermilab. Since the vast majority of the radioactive atoms produced are short lived (20.5 minutes for ^{11}C), a delay time of one hour from production to exhaust will reduce the radioactivity by roughly one order of magnitude at the stack. Since the sealed chase inside the Target Hall is the main source of air activation, the largest delay is from the Target Hall to the vent part way down the Decay Tunnel. The area between the Hadron Absorber and the decay pipe also has high air activation levels. We are in the process of more accurately estimating these levels and determining the best ways to mitigate them. Most likely we will significantly reduce the airflow rate from the Hadron Absorber to the vent and build an aluminum box to contain the air just downstream of the decay pipe. Details of the air activation methodology and its application to NuMI are covered in TM-2089, and draft documents on the updated air activation methodology.

	Ventilation Rate (cfm)	Yearly Release 1% ^{41}Ar (Ci/yr)	Yearly Release 2.5% ^{41}Ar (Ci/yr)
Carrier Tunnel	1000	To be determined	1
Pre-Target Hall	900	To be determined	1
Target Hall	800 (700 leakage rate from chase)	To be determined	40
Upstream 1/2 Decay Region	800	To be determined	0.01
Downstream 1/2 Decay Region	3500	To be determined	0.01
Hadron Absorber	2250 (200 leakage rate from core/aluminum box)	To be determined	Being calculated

Table 5-4 Summary of air emission calculations at NuMI stacks. Note that the ventilation rate in the pre-target area can be reduced if necessary.

5.5 Prompt Radiation

The prompt radiation field at particle accelerators and beam lines exists only while they are in operation. Depending on the configuration of the facility and its components, the prompt radiation fields may include thermal neutrons, fast neutrons, photons and/or muons.

The prompt radiation field must be predicted and mitigated for both normal operations and accident conditions. There are two areas of concern; the radiation field outside of enclosures, which are normally embedded and/or covered by bulk shielding comprised of rock and/or soil, and the "leakage" of radiation through labyrinths and penetrations. For the former it is appropriate to use the results, which have been well established by the simulations done for a relevant set of case studies. These results are documented[8,9] and accepted for use in the design of bulk shielding at Fermilab.

Since most of the NuMI Facility lies deep underground, there are only a few areas where the issue of prompt radiation from NuMI operations must be considered. These areas are the MI/NuMI Stub, power supply room/upstream shaft area and bypass tunnel (see **Figure 5-1**). Interlocks and interlocked detectors will be used in some of these areas. There is also the issue of prompt radiation from the MI in areas where NuMI wishes to have access when NuMI is not operating, but the MI is operating. This includes the unlined section of the Carrier Tunnel and downstream.

5.5.1 Primary Beam

MI/NuMI Stub: In particular, this includes the regions of the Main Injector where the NuMI extraction devices are located, also the NuMI Extraction Stub (Figure A). The design goal is to have the surface areas above all Main Injector related beams be classified as Unlimited Occupancy. The applicable criterion applied to the MI indicates the need for 24.5 feet of soil equivalent over most of the enclosure and 25 feet over extraction regions, with stairways, cable penetrations etc. being treated separately. The as-built drawing which includes the MI-60 extraction region and the NuMI Stub[10] shows that the stated shielding criteria (24.5 and 25 feet) have been satisfied.

---

[8] A. Van Ginneken and M. Awschalom, "High Energy Particle Interactions in Large targets", Fermilab, 1975, (available from the Publication's Office).

[9] J. D. Cossairt, "A Collection of Casim Calculations", TM-1140, October 22, 1982.

[10] Radiation Safety 9667-C7

Table 5-5 shows the various penetrations and labyrinths in the primary beam region, their dose rates at the exit under normal and accident conditions and the mitigation that will be used. Accident pulses will normally be limited to one pulse due to the beam permit system or radiation safety system detecting the accident condition. Thus the column to look at for the accident condition is the dose rate/pulse. All of these areas have sufficiently low dose rates for their locations.

Access	Normal (mrem/hr)	Accident (mrem/hr)	Accident (mrem/pulse)	Mitigation
Survey Riser SR-1 (498)	1.48	14765.41	7.79	plug
Exhaust Air Vent EAV-1 (935)	0.29	2852.87	1.51	fence
Survey Riser SR-2 (954)	0.29	2852.87	1.51	plug
Target Hall Labyrinth	2.44E-03	24.37	0.013	OK
Target Hall Equipment Door	0.25	2476.83	1.31	OK

Table 5-5: Primary Beam Labyrinth and Penetration Calculations

5.5.5 Secondary Beam

In the secondary beam, two areas will have beam on access. These areas are the power supply room and upstream shaft area adjacent to the Target Hall. The design goal is to have these areas be Controlled Areas. **Table 5-6** shows anticipated levels in these areas due to the transmission line penetration, labyrinth and the equipment door. Two interlocked detectors will be located in this region, one in the Power Supply Room and one in the shaft area.

Access	Normal (mrem/hr)	Accident (mrem/hr)	Accident (mrem/pulse)	Mitigation (possible)
Target Hall Labyrinth	1.36E-03	-	-	OK
Target Hall Equipment Door	0.74	-	-	OK

Stripline Penetration (PS Room)	2.77	-	-	(shield)
Raw Penetration	60.80	-	-	plug
Survey Riser SR-3 (1321)	0.002	-	-	plug

Table 5-6: Secondary Beam Labyrinth and Penetration Dose Rates

Dose rates at the exit of the Hadron Absorber labyrinth are estimated at 7 mrem/hr beam on. Dose rates in the bypass tunnel are estimated at less than 0.05 mrem/hr. When beam is first commissioned at lower intensities, these values will be checked with radiation monitors.

5.6 Residual Dose Rates

The residual radiation field is that which remains after the beam has been shut down. In most situations at Fermilab, the residual radiation field is almost exclusively gamma rays, with the occasional presence of beta rays near a contaminated surface.

Location	Dose Rate (on contact)
Target Hall: concrete floor of work area	< 1 mrem/hr
Target Hall: Top of T-Block (horn 1)	~ 5 mrem/hr
Target Hall: Bottom of concrete "cap"	~ 2 mrem/hr
Target Hall: near work cell	~ 1 mrem/hr
Target Hall: near air handling equipment	~1 mrem/hr
Target Hall: DS horn baffle (old result)	25 rem/hr
Target Hall: bottom of T-Blocks above horn 1 (average)	100 rem/hr
Target Hall: inside cave walls around horn 1	80 rem/hr
Target Hall: horn 1 outer conductor	600 rem/hr
Target Hall: target	6000 rem/hr
Target Hall: upstream wall	~2 mrem/hr
Decay Region: outside edge of concrete	~100 mrem/hr
Decay Region: emergency egress (rock & conc)	~100 mrem/hr
Decay Region: upstream window	5 rem/hr
Decay Region: downstream window	700 mrem/hr
Decay Region: decay pipe	30-200 rem/hr
Hadron Absorber: Core Near Beam	~100's rem/hr
Hadron Absorber: Core Sides	~ 10's rem/hr
Hadron Absorber: Steel Blocks	~1's rem/hr
Hadron Absorber: Front	~ 1's rem/hr
Hadron Absorber: Labyrinth Side	~100 mrem/hr
Hadron Absorber: Non-Labyrinth Side	
Hadron Absorber: Top	
Hadron Absorber: Back	< 30 mrem/hr

Table 5-7: Estimated Residual Dose Rates for Various Beamline Elements

Table 5-7 shows the estimated residual dose rates for various beamline elements. Blank cells are in the process of being estimated. Underlined numbers are being updated.

5.7 RAW Water Systems

Here we describe the results of the calculation of the induced activity in the NuMI Radioactive Water (RAW) Systems. The interaction between the ionizing radiation and water leads to the formation of short-lived radical species (OH, H and electrons mainly) and stable molecular species (O_2, H_2O_2 and H_2). While most of the ions recombine to form water, hydrogen gas and other species are also produced. The amount of hydrogen gas produced is calculated to assess the level of safety precautions required.

The most significant radioisotopes, from a contaminant aspect are ^{3}H, and to a lesser extent ^{7}Be, because of their rather long half lives. However, from a dose rate from a RAW system point of view, tritium dose not contribute, because of its very low energy decay beta particle. Only 10% of beryllium decays are via gamma emissions, while 11C, 13N and 15O are positron emitters producing 0.511MeV gamma rays. Therefore, allowing cooling time before getting near a RAW system is very effective way of reducing the dose rates.

Fermilab Radiological Control Manual (FRCM) suggests keeping the tritium concentrations in the cooling system below 0.67 microCuries/cc. However, some of the NuMI RAW systems may exceed this limit due to high particle fluxes or it may not be feasible to replace the cooling water frequent enough to keep the concentrations below the FRCM value. For these cases, multi-tier containment methods are used, with the proper operational precautions during the handling of the RAW systems. When possible the high tritium concentration water is disposed of as solidified low-level radioactive waste.

Table 5-8 and **Table 5-9** summarize the results for five NuMI RAW systems. One can see that the horn 1 system has the highest levels. These results, are conservatively calculated (reference RAW Note), and thus an overestimate. The table also shows the estimated shielding needed for the RAW systems and DI bottles and tanks. A 1.5' thick concrete wall is planned for the RAW room which houses the horn 1, horn 2, target and decay pipe RAW systems. With this wall, dose rates are estimated at less than 5 mrem/hr outside the room's door.

The flux densities used in calculating activities and dose rates are shown in **Table 5-8** for the decay pipe and Hadron Absorber Systems. For the target system, a flux density of 0.12 hadrons/cm^2/proton was used. This corresponds to 10 times the flux density at the horn 1 neck. This is a conservatively high estimate. For horn 1, the flux density used for the water between the conductors was 0.019 hadrons/cm^2/proton and 0.0053 hadrons/cm^2/proton for the water in the tank under the horn. For horn 2 the flux density used for the water between the conductors is

0.0025 hadrons/cm^2/proton and 0.0019 hadrons/cm^2/proton for the tank under the horn. The target cooling tubes have an inner diameter of 5.4 mm, and thus the amount of water present is extremely small.

Cooling System	Size (gallons)	MARS Flux Density Used (parts/cm2/p)	Tritium (Ci/yr)	Total Activity (Ci/yr) 1 hour Cooldown	Ci/ml/yr (1 hour cooldown)
Target & Baffle	See text	10*Horn1 neck	0.080	0.63	1.65E-06
Horn 1	~105	see text	1.820	14.23	3.76E-05
Horn 2	~105	see text	0.538	4.20	1.11E-05
Decay Pipe	5500	4.66E-05	0.011	0.09	5.27E-09
Hadron Absorber	130	1.30E-05	0.006	0.04	1.00E-07

Table 5-8: RAW System Activity

Cooling System	Size (gallons)	mrem/hr @1' (0 cooldown)	Local Secondary Containment	Hydrogen Gas	DOSE on contact (0 cooldown) (Rad/hr)	DOSE @1' (0 cooldown) (Rad/hr)
Target & Baffle	See text	44 rem/hr with no shielding from horn 1 RAW, with 18" planned concrete shielding, expect < 5 mrem/hr on the outside of the RAW room door.	contained in target	1 cc/day	2.9	0.9
Horn 1	~105		contained in chase shielding and Al liner	3.5 gal/day	66.6	20.0
Horn 2	~105		contained in chase shielding and Al liner	0.6 gal/day	19.7	5.9
Decay Pipe	5500		contained in concrete	52 gal/yr	0.009	0.003
Hadron Absorber	130	87	yes	14 gal/yr	0.185	0.056

Table 5-9 RAW System Dose Rates and Hydrogen Gas Production

Since 4% hydrogen gas in air is considered explosive, a helium purging system will be added to the horn RAW systems. The Hadron Absorber RAW system needs to be vented to the exhaust stack and the Decay Pipe RAW system might need daily purging/venting with small amounts of Helium gas.

5.8 Hot Component Handling

See Section 4.2.

5.9 Decontamination & Decommissioning (D&D)

The guidelines of the FESHM 8070 will be used for the D&D of the NuMI Beamline. No hazardous materials have been used in the construction of the beamline. Items put in the NuMI tunnel during construction are being chemically analyzed for D&D. Therefore, no mixed waste or potential contaminant of the ground water will be produced. The major radioactive isotopes produced will have 2.6 and 5.3 year half-lives. There are sump pumps that remove the water that flows into the NuMI tunnel. This will continue after the conclusion of the experiment. Accidental flooding of the tunnel in the future will not have any detrimental effects on the ground water. All the materials used in the construction of the beamline are naturally occurring in the surrounding soil.

4.2.10 Work Cell Design

4.2.10.1 Work Cell function and specifications

The purpose of the NuMI Target Hall Work Cell is to provide a well-shielded facility for repairing or replacing NuMI target and horn assemblies that have developed faults during operation. In normal NuMI beamline operation these components are mounted on steel framework structures called "modules" that provide mechanical support, utility connections and precise positioning. (A single module serves both the production target and the upstream baffle assembly.) The target and horn assemblies and their modules become intensely radioactive during beamline operation. The modules are designed to be reused (there are no spares) but a failed target or horn assembly will usually be replaced with a spare because it will be too radioactive for repairs to be practical.

The Work Cell provides facilities for performing the following operations with minimal radiation exposure to the personnel involved:

1. Place a failed target or horn assembly, mounted on its module, in the work cell using the overhead bridge crane. The upstream steel door of the Work Cell must be opened and closed by remote control during this operation.

2. Install top shield cover, except at end-wall and stripline penetrations, to allow personnel access to top of module.

3. Repair the failed component or detach it from its module if repairs are not possible.

4. In the case where repairs are not possible, remove the module and the failed component separately from the Work Cell. (The module is temporarily returned to the target chase and the horn or target assembly is placed in the morgue.)

5. Move a replacement target or horn into the Work Cell and place it on the lifting table.

6. Move the module into the Work Cell and use the lifting table to align the component accurately relative to the module.

7. Make the required mechanical connections between the module and component.

8. Test utility lines and connections (water, vacuum, instrumentation) of the module-component assembly.

9. Remove the module-component assembly from the Work Cell and reinstall it in the target chase.

4.2.10.2 Work Cell design

The Work Cell consists of the following major components:

1. Three-foot thick concrete shield-block side walls (East and West).

2. One-foot thick steel end walls (North and South). The South wall is remotely movable. It opens by sliding to the East on upper and lower rails with Hillman rollers.

3. Rails for supporting target and horn modules in the same way they are supported in the target chase.

4. Electrical power for South door, lifting tables, etc.

5. A remotely controlled Lifting Table (also known as the Motion Table) that provides x-y-z positioning capability for aligning the horn or target relative to the module before the two are mechanically connected. The system provides position ranges of: x = ±6 inches, y = 0 to 25 inches, z= ±9 inches.

6. Three apertures in the East concrete side wall that are filled with (manually) removable lead bricks and lead-glass blocks. The lead-glass blocks allow workers to view the connections between the component (target or horn assembly) that must be disconnected or connected by remote control.

7. A fourth aperture, located in the downstream (North) steel end wall is also filled with removable lead bricks and lead-glass blocks. This provides a view of the connection between the horn and the stripline flexible joint as well as access to that joint if a stripline needs to be disconnected from a horn.

8. Removable steel cover plates that provide radiation shielding and personnel access to the top of the Work Cell after a module assembly has been placed inside.

9. Note: the Work Cell structure is built on the same 3.5-degree slope as the target chase so that the module can be supported in the same manner in both locations.

10. Note: the mechanical, water and electrical connections between a module and its target or horn assembly are made from the top of the Work Cell by way of the same penetrations,

through the module end walls and stripline-penetration shielding block, that are used when the module is installed in the target chase.

11. Note: transportation and lifting fixtures for moving and installing the steel doors and the concrete shield blocks of the Work Cell are included in the Work Cell construction task.

Most of the figures that follow are derived from current engineering drawings of the Work Cell and its components. They are intended only to illustrate the major design features of the device and should not be used to obtain exact specifications or dimensions.

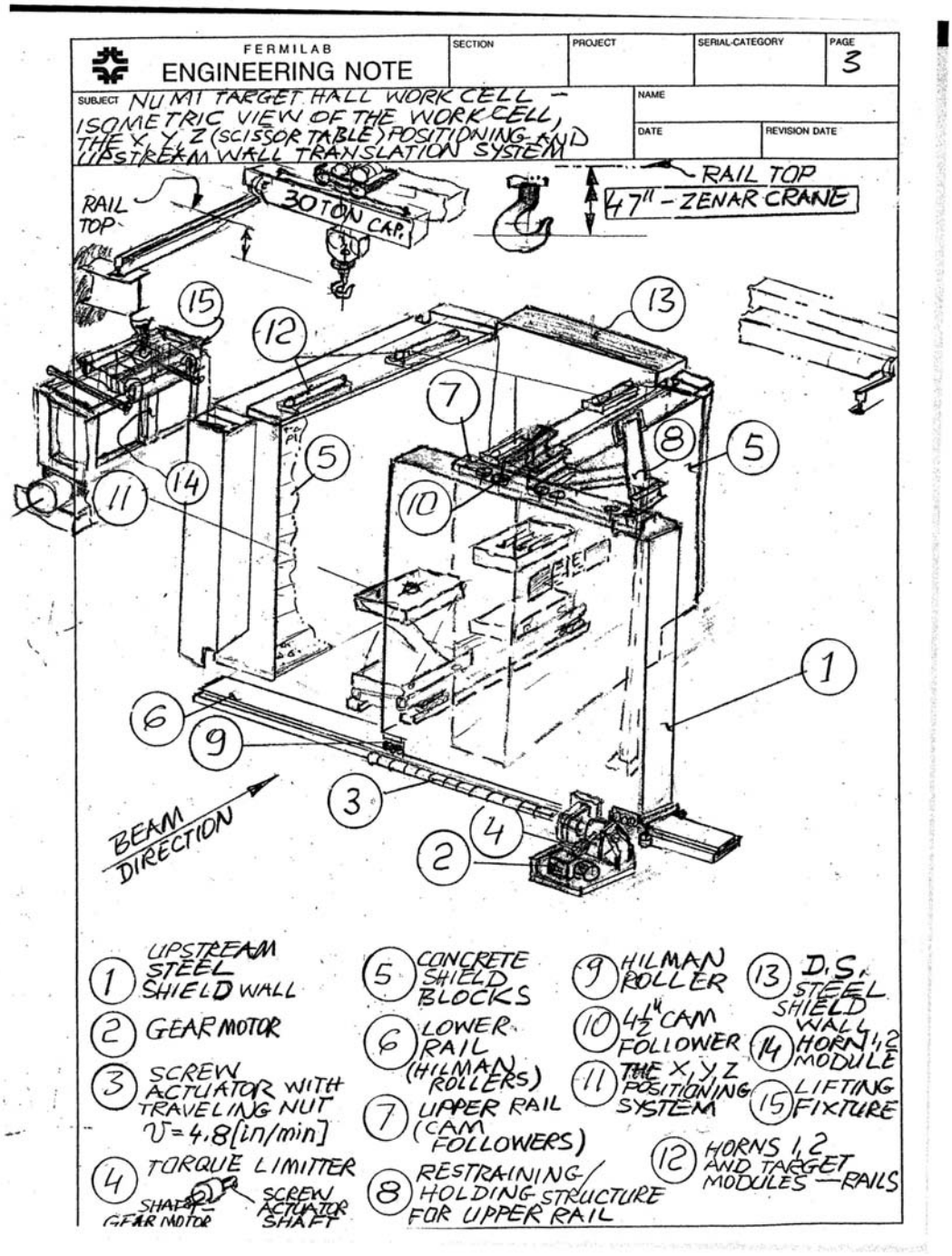

Figure 4.2-30 Sketch of the main Work Cell components.

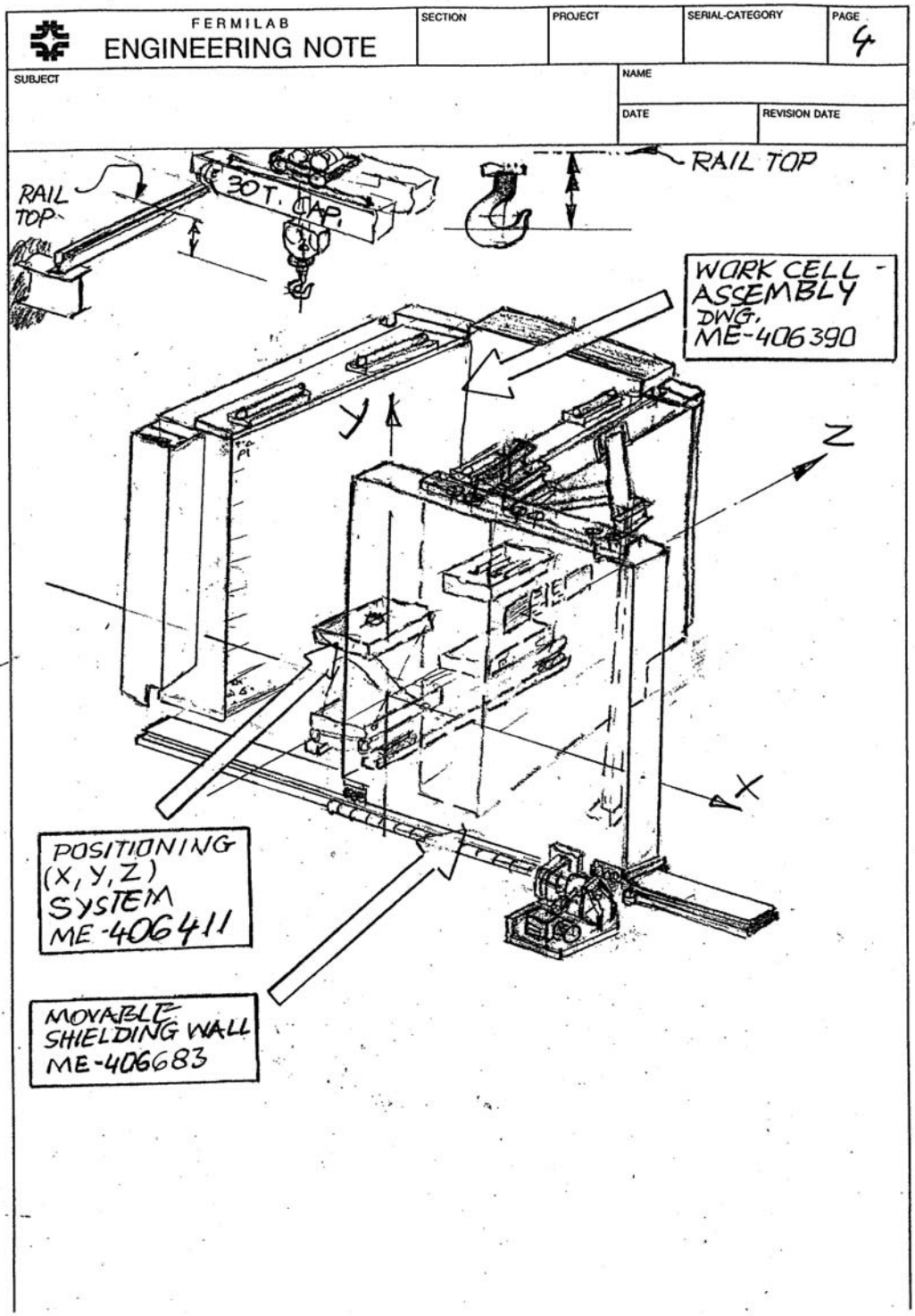

Figure 4.2-31 Work Cell sketch showing coordinate systems and drawing numbers.

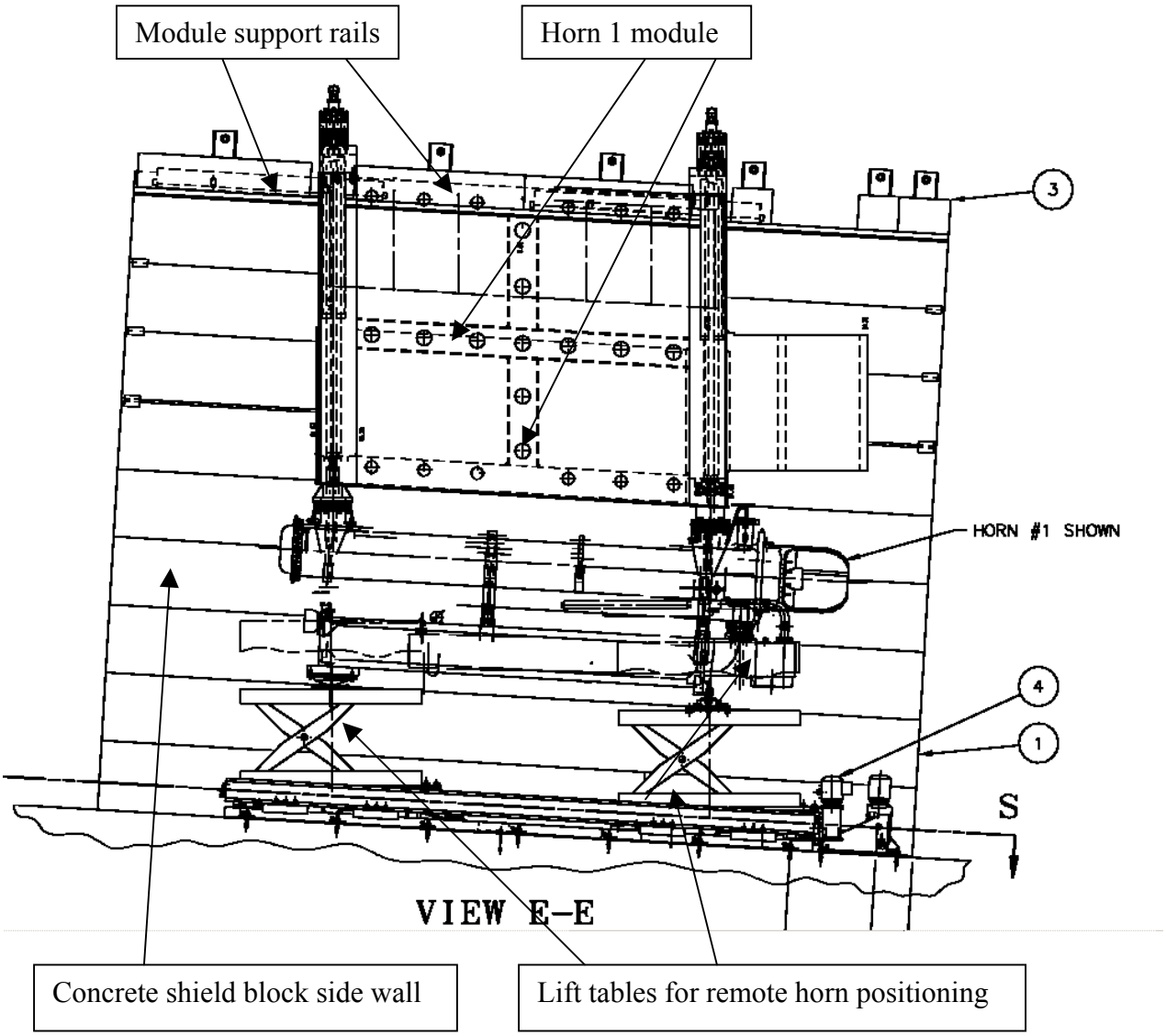

Figure 4.2-32 Side elevation view of the Work Cell assembly with Horn 1 module installed.

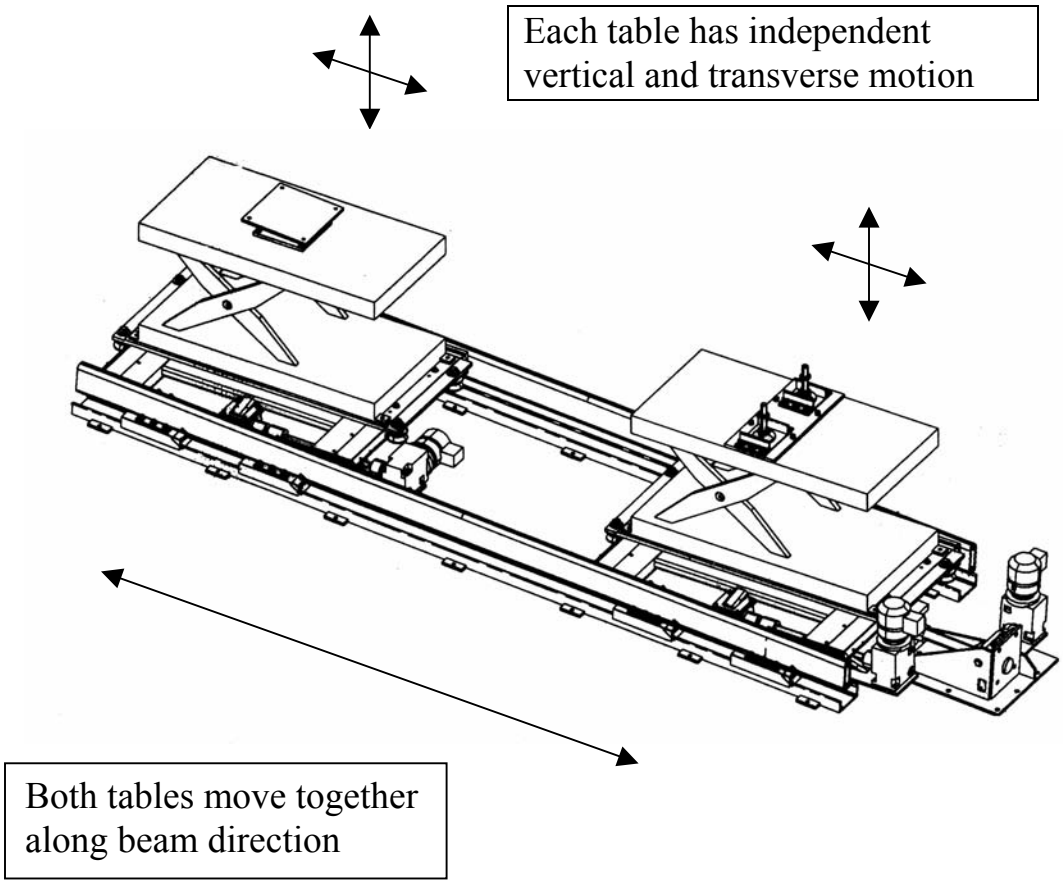

Figure 4.2-33 Sketch of Lifting Table.

	29	MD-406576	TRACK - BASE PLATE 1	2
	28	MD-406589	WALKWAY-RAILING BRACKET ASSEMBLY A	8
	27	MD-406593	WALKWAY ASSEMBLY	1
	26	MC-406585	WALKWAY - KICKER SUPPORT ASSEMBLY #2	3
	25	MC-406579	WALKWAY - KICKER SUPPORT ASSEMBLY #1	2
A	24	FURNISHED	GLASS BRICK (6 x 6 x 18)	6
	23	COML.	FERRY HD SCREW, 3/8-16UNC-2A x 1 LG. S.S. 304, CAP SCREW HEX.HD.	36
	22	COML.	HILTI HDI 3/8 DROP-IN ANCHOR ITEM NUMBER 0045731	36
	21	COML.	PIPE, 1 1/2 SCH. 40 x 37.00 LG., ALUMINUM E6061-T6	4

D

Table 4.2-16a Key to numbered components in drawings that follow.

3. ITEM 9 TO BE FIELD INSTALLED. STEPS MUST BE LEVEL. DRILL (2) 9/16 THRU HOLES INTO ITEM 37 PER DIMENSIONS IN DETAIL N. USE FOOTING OF ITEM 9 TO LOCATE ANCHOR POSITIONS. SHIM IF REQUIRED AT BOTH FOOTING AND LANDING.

2. FIELD WELD ITEMS 3, 4 AND 6 PRIOR TO ANCHORING TO CONCRETE BLOCKS (ITEMS 1 & 2) ON SOUTH AND NORTH ELEVATIONS.

1. ALL STEEL (ALLOY & CARBON) SHALL BE PAINTED WITH 2 COATS PRIMER (ITEM #47) & 1 COAT HIGH GLOSS WHITE (ITEM #48). ALL WELDS,BURNS ETC. SHALL BE TOUCHED-UP WITH SAME PAINT.

NOTES:

ITEM	PART NO.	DESCRIPTION OR SIZE	QTY.
70	COML	HILTI DROP-IN ANCHOR, HDI(SS303)1/2, HILTI P/N 45739	2
69	1210-0740	NUT, HEX, FULL, TYPE 18-8 S.S., 1/2-12UNC-2B THD	2
68	1218-0635	SCREW, CAP HEX HD, TYPE 18-8 S.S., 1/2-13UNC-2A x 1.50 LG	2
67	COML	BAR GRATING FASTENER - FLAT-HEAD J-BOLT, McMASTER-CARR P/N 6268T28	12
66	COML	C 6 x 13 x 183.00 LG STEEL CHANNEL	1
65	MC-427002	EAST CHANNEL MTG PLATE	2
64	1218-1140	WASHER, LOCK, TYPE 18-8 S.S., SCREW SIZE 1/2	32
63	1226-0630	SCREW, CAP HEX HD, TYPE 18-8 S.S., 1/2-13UNC-2A x 1.00 LG	30
62	FURNISHED	LEAD BRICK - 2 x 4 x 8	194
61	MC-406998	WINDOW CORNER SPLICE PLATE	4

PARTS LIST

ITEM	PART NO.	DESCRIPTION OR SIZE	QTY.
		ALUMINUM E6061-T6	
20	COML.	PIPE, 1 1/2 SCH. 40 x 32.50 LG., ALUMINUM E6061-T6	4
19	COML.	PIPE, 1 1/2 SCH. 40 x 22.00 LG., ALUMINUM E6061-T6	3
18	COML.	PIPE, 1 1/2 SCH. 40 x 58.00 LG., ALUMINUM E6061-T6	12
17	COML.	PIPE, 1 1/2 SCH. 40 x 48.00 LG., ALUMINUM E6061-T6	8
16	COML.	PIPE, 1 1/2 SCH. 40 x 43.00 LG., ALUMINUM E6061-T6	4
15	COML.	PIPE, 1 1/2 SCH. 40 x 68.00 LG., ALUMINUM E6061-T6	2
14	COML.	PIPE, 1 1/2 SCH. 40 x 9.50 LG., ALUMINUM E6061-T6	8
13	COML.	FLANGE, HOLLAENDER FITTING NO. 48	2
12	COML.	SIDE OUTLET ELL, HOLLAENDER FITTING NO. 9	9
11	COML.	CROSS, HOLLAENDER FITTING NO. 7	13
10	COML.	TEE, HOLLAENDER FITTING NO. 5	14
9	COML.	SPACE SAVER STAIRWAY, McMASTER-CARR #7948T999, 167.50" TOP STEP HGT. 68 DEG. CARBON STEEL, GRAY	1
8	MD-406681	DOWNSTREAM SHIELD WALL BLOCK #1	1
7	MC-406685	DOWNSTREAM SHIELD WALL BLOCK #2	3
6	MC-406686	SHIELD WALL BLOCK 4	3
5	MC-406698	WALL BRACKET 3	1
4	MD-406627	WALL BRACKET 2	2
3	MD-406624	WALL BRACKET 1	7
2	FURNISHED	"D" BLOCK (3 x 6 x 1.5) WEST WALL ONLY	9
1	FURNISHED	"J" BLOCK (3 x 12 x 1.5) WEST WALL ONLY	9

PARTS LIST

UNLESS OTHERWISE SPECIFIED	ORIGINATOR	A.SZYMULANSKI	07-JUN-2001
FRACTIONS / DECIMALS / ANGLES	DRAWN	L.SZCZEPANIK	19-DEC-2001
± .06 / ± --- / ± —	CHECKED	D.FRIEND	08-MAY-2002
1. BREAK ALL SHARP EDGES .015 MAX. 2. DO NOT SCALE DRAWING. 3. DIMENSIONS BASED UPON ANSI Y14.5M-1982 4. MAX. ALL MACH. SURFACES 250	APPROVED	A.SZYMULANSKI	08-MAY-2002
	USED ON	ME-406747	
	MATERIAL	SEE PARTS LIST	

FERMI NATIONAL ACCELERATOR LABORATORY
UNITED STATES DEPARTMENT OF ENERGY

PPD/MECHANICAL DEPARTMENT
NUMI TARGET HALL-WORK CELL
WORK CELL ASSEMBLY

SCALE	DRAWING NUMBER	SHEET	REV
FULL	8875.126-ME-406570	1 OF 2	A

CREATED WITH : Idea8m4 GROUP: PPD/MECHANICAL DEPARTMENT

Table 4.2-16b Key to numbered components in drawings that follow (continued)

60	MC-406997	WINDOW FRAME SPLICE PLATE	4
59	MC-406996	VERTICAL WINDOW FRAME SECTION	2
58	MC-406995	HORIZONTAL WINDOW FRAME SECTION	2
57	MC-406993	STOP BRKT SPLICE PLATE	2
56	COML.	HOT ROLLED FLAT, 1/2 x 4 x 3.00 LG. CARBON STEEL ASTM A-36	2
55	COML.	HOT ROLLED FLAT, 1/2 x 4 x 2.00 LG. CARBON STEEL ASTM A-36	9
54	COML.	HOT ROLLED FLAT, 1/4 x 4 x 3.00 LG. CARBON STEEL ASTM A-36	2
53	COML.	HOT ROLLED FLAT, 1/4 x 4 x 2.00 LG. CARBON STEEL ASTM A-36	9
52	COML.	SHIMS - LEAD	AS REQD
51	———	———	—
50	MC-406992	LEAD GLASS STOP BRKT WELDMENT	4
49	COML.	1 x 3 x 4.00 LG. ASTM A 36 STEEL FLAT	2
48	1825-3750	PAINT, HIGH GLOSS WHITE RUSTOLEUM #27881	AS REQ'D
47	1825-4000	PAINT, RED PRIMER RUSTOLEUM #769	AS REQ'D
46	COML.	WASHER, FLAT, ALLOY STEEL FOR 5/8" BOLT	32
45	COML.	CAP SCREW, HEX. HD, ALLOY STEEL 5/8-11UNC-2A x 2.00 LG.	32
44	COML.	HILTI KWIK BOLT, 5/8 x 4 3/4 LG. HILTI #000453712	48
43	COML.	C 6 x 13 x 225.00 LG STEEL CHANNEL	1
42	MC-406651	WALL BRACKET	4
41	COML.	1/2 x 3 x 182.00 LG STEEL ANGLE	2
40	COML.	3/8 FLAT WASHER	40
39	COML.	CONCRETE GROUT, HIGH STRENGTH MASTERFLOW 928, ASTM C-1107	AS REQ'D
38	ME-406748	EAST WALL ASSEMBLY	1
37	MD-406750	KICKER SUPPORT ASSY 3	1
36	COML.	HILTI KWIK BOLT 3/4 x 8" ITEM # 000453738	10
35	COML.	1/2-13 UNC x 5.50 LG. HILTI S.S. KWIK BOLT ITEM NO. 000453936	32
34	COML.	5/8-11 UNC x 7.00 LG. HILTI KWIK BOLT ITEM NO. 000453738	83
33	COML.	FLAT WASHER FOR 7/8 BOLT ALLOY STEEL	24
32	COML.	7/8-9 UNC-2A x 8.75 LG. HEX. BOLT ALLOY STEEL	24
31	MC-406582	TRACK - WELDMENT	4
30	MD-406578	TRACK - BASE PLATE 2	2
29	MD-406576	TRACK - BASE PLATE 1	2
28	MD-406589	WALKWAY-RAILING BRACKET ASSEMBLY A	8
27	MD-406593	WALKWAY ASSEMBLY	1
26	MC-406585	WALKWAY - KICKER SUPPORT ASSEMBLY #2	3

Table 4.2-16c Key to numbered components in drawings that follow (continued)

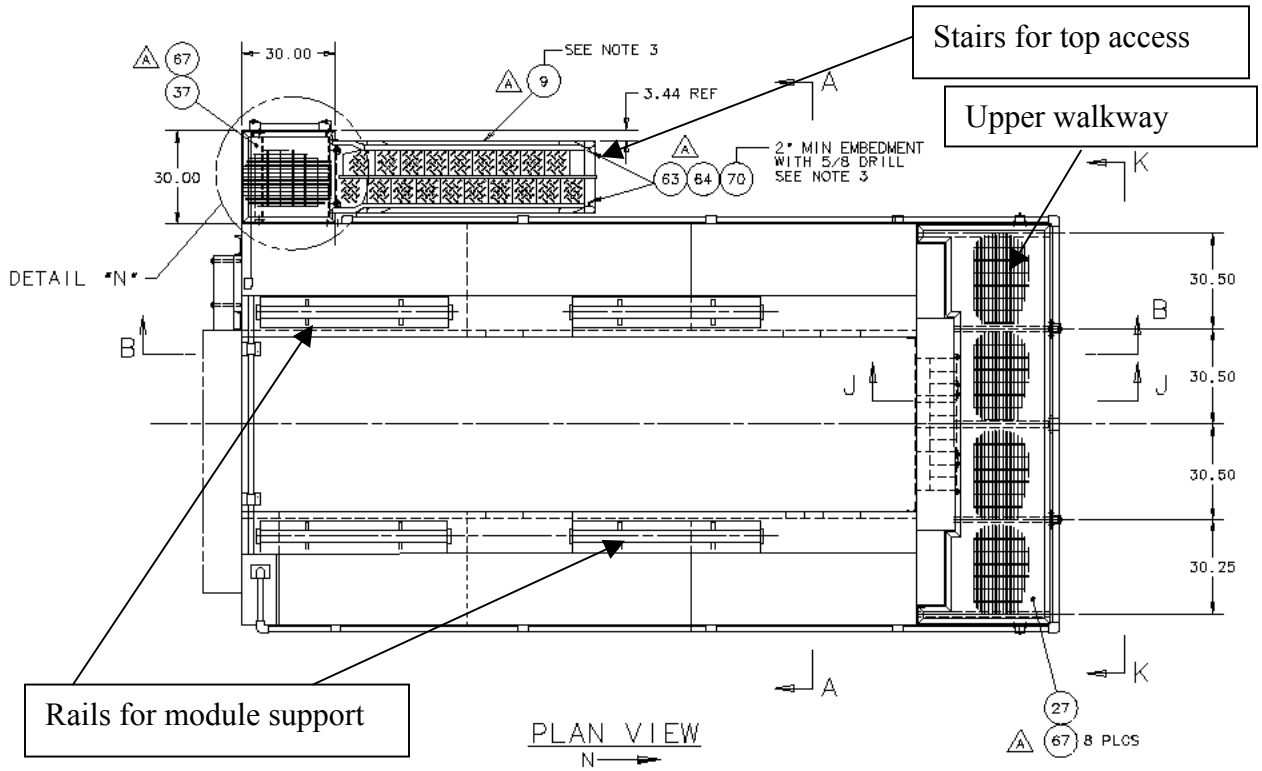

Figure 4.2-34a Plan view of the Work Cell assembly.

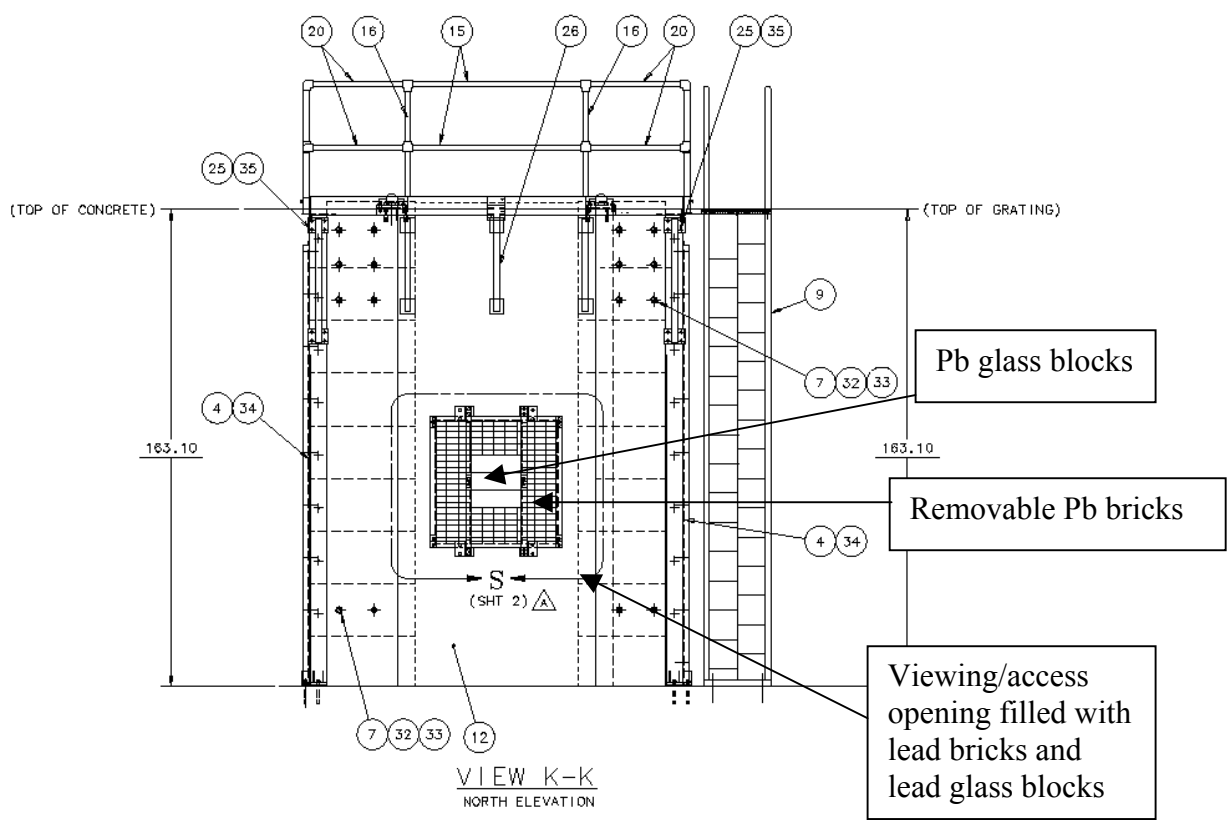

Figure 4.2-34b North end elevation of the Work Cell assembly.

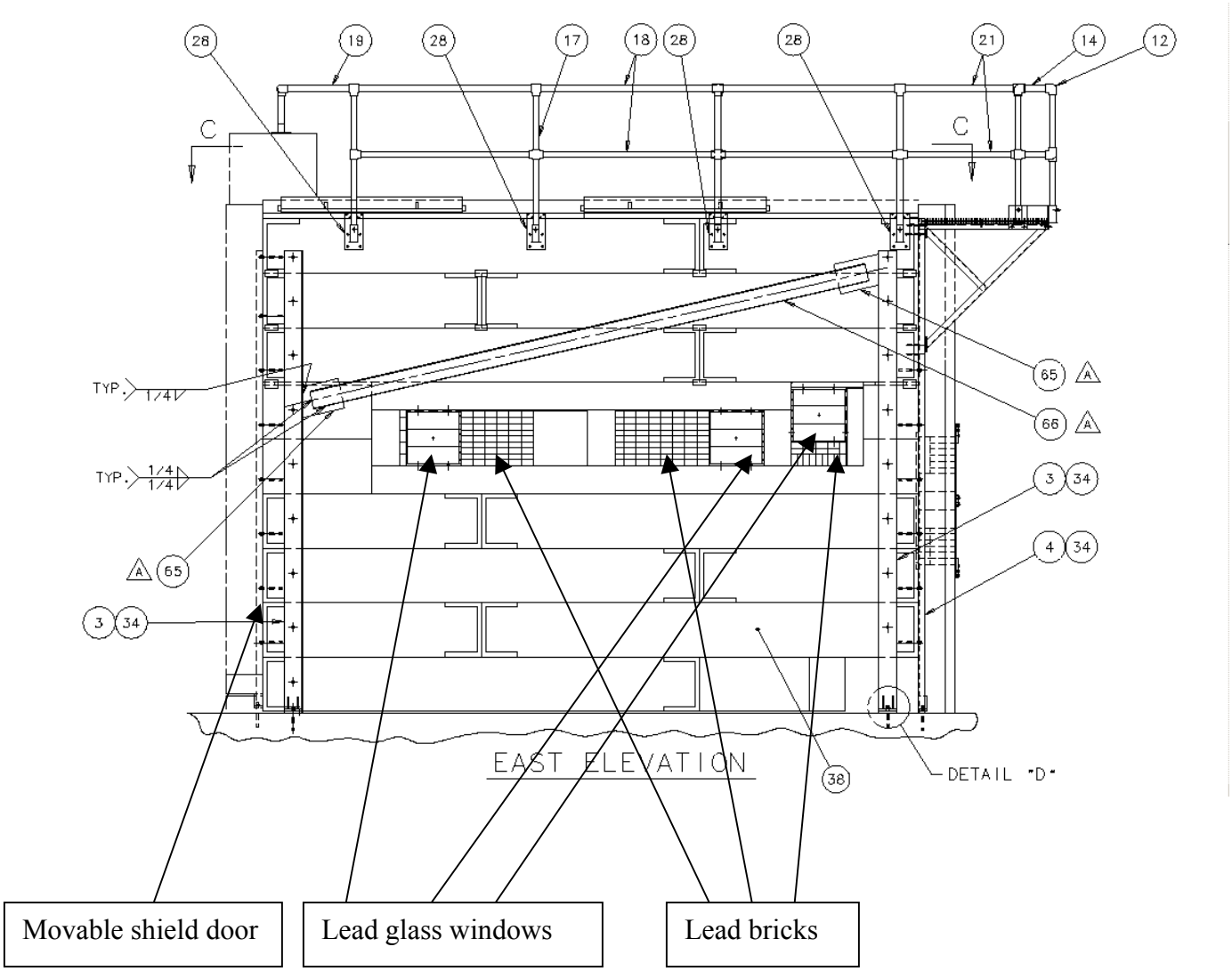

Figure 4.2-34c-Side elevation view of East wall of Work Cell.

4.2.6 Horn Alignment Cross-hair System

4.2.6.1 Alignment cross-hair function and specifications

The purpose of the NuMI horn alignment cross-hair system is to allow locations of the NuMI magnetic horns to be determined relative to the incident proton beam centerline. This is to be accomplished by scanning the incident beam, at low intensity (roughly 10^{12} protons per pulse), horizontally and vertically across the cross-hair locations. The locations of the cross hairs are determined by observing the changes in signal level in a beam loss monitor (BLM) located downstream of each horn. The BLMs are mounted well away from the beam axis and detect secondaries from beam proton interactions in the cross-hair material. The cross hairs consist of horizontal and vertical aluminum strips attached to the downstream end of Horn 1 and the upstream and downstream ends of Horn 2. While it is not possible to attach a cross-hair structure to the upstream end of Horn 1 due to the production target location, the narrow neck of the inner conductor of Horn 1 provides essentially the same alignment function as an upstream cross-hair structure when it is scanned by the incident beam.

Adam Para described the initial conceptual design of the cross-hair alignment system in NuMI-B-796. Byron Lundberg used MARS to perform a series of beam-heating calculations for different cross-hair materials (NuMI-NOTE-BEAM-882). It can be concluded from this study that aluminum will survive normal full-intensity operation of the NuMI beam if the cross hairs were centered 2.5 mm from the beam centerline and are not more than 1.0 mm wide.

The performance of the cross-hair system has been simulated and documented by Debbie Harris (NuMI-NOTE-BEAM-864). The simulation was performed only for the low-energy neutrino beam configuration. The conclusion of this study is that the transverse alignments of the upstream and downstream ends of each horn can be determined to a precision of ±0.5 mm. The study concluded that the aluminum cross-hair material of the cross hairs should be 6 mm deep along the beam line for the downstream cross hairs on both horns and 18 mm deep for the Horn 2 upstream cross hairs, in order to achieve an acceptable signal to noise ratio in the BLMs. It has been decided to double the thickness of the cross hair material (to 12 mm and 36 mm respectively) to allow for the possibility of worse signal to noise. The simulations indicate signal-to-noise ratios of 0.6 to 0.8 for the cross-hair scans (with the doubled thicknesses) and >10 for the Horn 1 neck scan. The simulations also indicate that the cross-hair material causes changes of less than 0.2% in the neutrino flux and the near/far detector event rates.

The cross hair system consists of the following components:

1. Three aluminum cross hair structures and hardware to mount them to the horns. The locations must not be permanently affected (±0.25 mm) by temperature changes, horn pulsing and other perturbations that occur during NuMI operation. **Figure 4.2-17** shows an end-on view of the Horn 1 cross-hair structure.
2. Two beam loss monitors (BLMs), one located downstream of each horn, and associated hardware and readout electronics, including gun-drilled holes for cable penetrations. BLMs will remain in position during high intensity running but they must be replaceable if they are damaged.
3. Vertical and horizontal trim magnets, located roughly 23 m upstream of the upstream face of Horn 1. These are used to perform scans of each set of cross hairs and of the neck of Horn 1.

The cross-hair system specifications include the following:

1. The system must determine the transverse location of Horn 1 to a precision of ±0.5 mm and of Horn 2 to ±1.0 mm, relative to the proton beam centerline. These requirements limit the distortion of the neutrino energy spectrum by horn misalignment to an acceptable level.
2. The proton beam location is assumed to be determined to a precision of ±0.1 mm and ±15 μrad by multiwire chambers upstream of the NuMI target.
3. The system requires the ability to perform horizontal and vertical scans of the proton beam position, at low intensity, over a range of ±3.5 mm at the locations of the cross hairs and ±12 mm at the location of the neck of Horn 1. Scans are performed with the target and baffle moved out of the beam.
4. BLM response should be stable and sensitive to rate changes of ~5% at intensities expected during scans (10^7 particles/cm^2/10^{12} protons/spill).
5. The proton beam is assumed to have an rms size of 1 mm and divergence of 0.9×10^{-4} in both horizontal and vertical at the NuMI target. Primary beam instrumentation that monitors proton beam intensity and location must perform according to the same specifications at low intensity (10^{12} protons per pulse) as at high intensity.
6. The signal-to-noise determined by the simulation will degrade if the material in the beam is increased beyond that assumed.
7. The cross hairs are mounted permanently to the horns at locations close enough to the beam centerline to provide adequate signals for the scans and far enough away to prevent damage to the cross hairs during full intensity running.
8. The cross hair material should have a negligible (<1%) effect on the neutrino flux.
9. The upstream and downstream cross hairs on Horn 2 should be located on opposite sides of the beam so that they can be scanned individually.

B. Alignment cross-hair system parameters

Table 4.2-9 summarizes the parameters used for the locations and dimensions of the aluminum cross hair material in the simulations study (NuMI-NOTE-BEAM-864). The

BLMs for Horns 1 and 2 are located at z = 4.01 m and 14.14 m respectively (in the Monte Carlo coordinate system, relative to z = 0 at MCZERO at the entrance to Horn 1). Note that the GEANT simulation used slightly different values for these locations, z = 4.099 m and z = 14.573 m respectively. The signal-to-background ratio was found to be independent of the distance between a BLM and the beam centerline for distances of 15 to 35 cm. Each BLM is located at beam elevation and displaced horizontally by 30 cm from the beam centerline. Each will collect a charge of roughly 33 nC during a beam spill of 10^{12} protons on target.

Horn Alignment Cross-hair Parameters in GEANT Simulation						
Parameter	**Horn 1**		**Horn 2 Upstream**		**Horn 2 Downstream**	
Center in x (cm)	-0.250	0.000	0.250	0.000	-0.250	0.000
Center in y (cm)	0.000	-0.250	0.000	0.250	0.000	-0.250
Upstream edge z (m)	3.434	3.440	9.922	9.940	13.624	13.630
Length (cm)	0.600	0.600	1.800	1.800	0.600	0.600
Thickness in x (cm)	0.100	34.000	0.100	34.000	0.100	34.000
Thickness in y (cm)	34.000	0.100	34.000	0.100	34.000	0.100

Table 4.2-9. Characteristics of the three sets of cross hairs according to GEANT

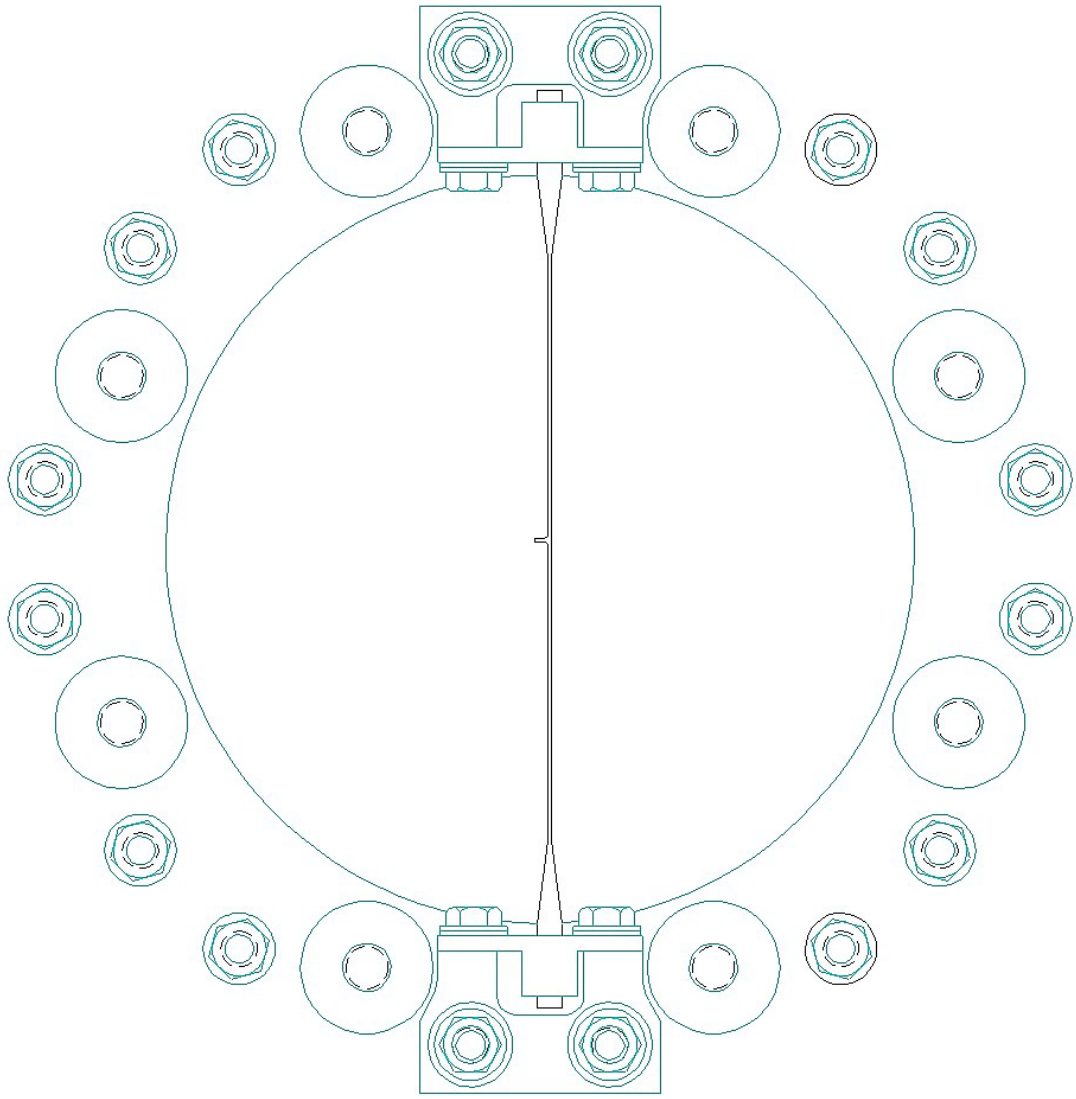

Figure 4.2-17. Drawing of the Horn 1 cross-hair structure.

This is an end-on view, looking into the proton beam, showing how the cross hair is mounted on bolts that are also used to tie the inner and outer conductors together. The aluminum cross hair material is 12-mm thick (along the beam direction) and 1-mm wide. The horizontal member is made only long enough (4-mm long, measured from the center of the vertical member) for incident beam scans, in order to reduce the amount of material in the beam and to simplify the support structure. Belleville washers provide a tension of about 80 pounds (at room temperature) on the vertical member, which is adequate to maintain positive tension at 100 C above room temperature (e.g., from beam heating). The cross-hair material is nickel plated to protect against corrosion.

4.2.9 Target and Horn Support Modules

4.2.9.1 Support module function and specifications

The NuMI target and horn support modules provide mechanical support, cooling water, instrumentation connections and precision alignment capabilities for the production target and magnetic focusing horns in the NuMI target chase. The NuMI beam requires three very similar support modules for (1) the carrier that holds the production target and its upstream baffle, (2) Horn 1 and (3) Horn 2. The intensely radioactive environment of the target chase requires the use of radiation-hard materials and the ability to control, align and service the Target/Baffle and horn assemblies by remote control. Heating caused by the beam and by horn currents places strict requirements on component materials and on cooling to maintain precise alignment. The three support modules are currently in different stages of construction. Horn 1 module: all components have been ordered and most have been delivered. Horn 2 module: all components have been ordered and some have been delivered. Target/Baffle module: all components have been ordered and some have been delivered, including the mainframe.

The most important support module features are:

1. Component materials will maintain alignment and functionality in a corrosive, intensely radioactive environment that is subject to variable heating by the proton beam and horn currents.
2. Modules provide feed-through connections for cooling water, instrumentation cabling, the horn stripline (Horn 1 and 2 modules only) and vacuum (Target/Baffle module only) as required.
3. Modules provide radiation shielding for (beam-off) work by personnel near the feed-through connections at the top of a module and for target hall equipment that cannot be easily removed when the beam is on.
4. The modular design allows failed components to be replaced in the work cell.
5. The mechanical support for a horn or the Target/Baffle carrier can be engaged or disengaged, while the module is in the work cell, using long vertical drawbars that are operated from the top of the module. Similarly, water, electrical and vacuum lines can be connected or disconnected from a horn or the Target/Baffle carrier from the top of a module in the work cell.
6. Modules provide precise, remotely controlled motion of the target and baffle assemblies and of Horn 1 transverse to the beamline, and of the target and baffle along the beamline (e.g., to insert the target into Horn 1 for low energy running).

These design features are accomplished by constructing each module from an open box-like steel structure, the module mainframe, and by independently supporting the shielding blocks (T blocks) that occupy open space within and adjacent to the mainframe. Most feed-through connections utilize “gun-drilled” holes through the 10-inch thick upstream and downstream end-walls of each module. Engineering design issues and the details of module construction are described in the Engineering Handbook document for each module. A preliminary version of the Horn 1 Module Engineering Handbook has been

prepared by Rafael Silva. Handbooks for the Horn 2 and Target/Baffle modules are being prepared by Rafael and by Ernie Villegas, respectively.

Figure 4.2-25 shows schematically how the Horn 1 module and its T-blocks are supported in the target chase. **Figure 4.2-26** shows the relative locations of the Target/Baffle module, the carrier assembly and the Horn 1 module.

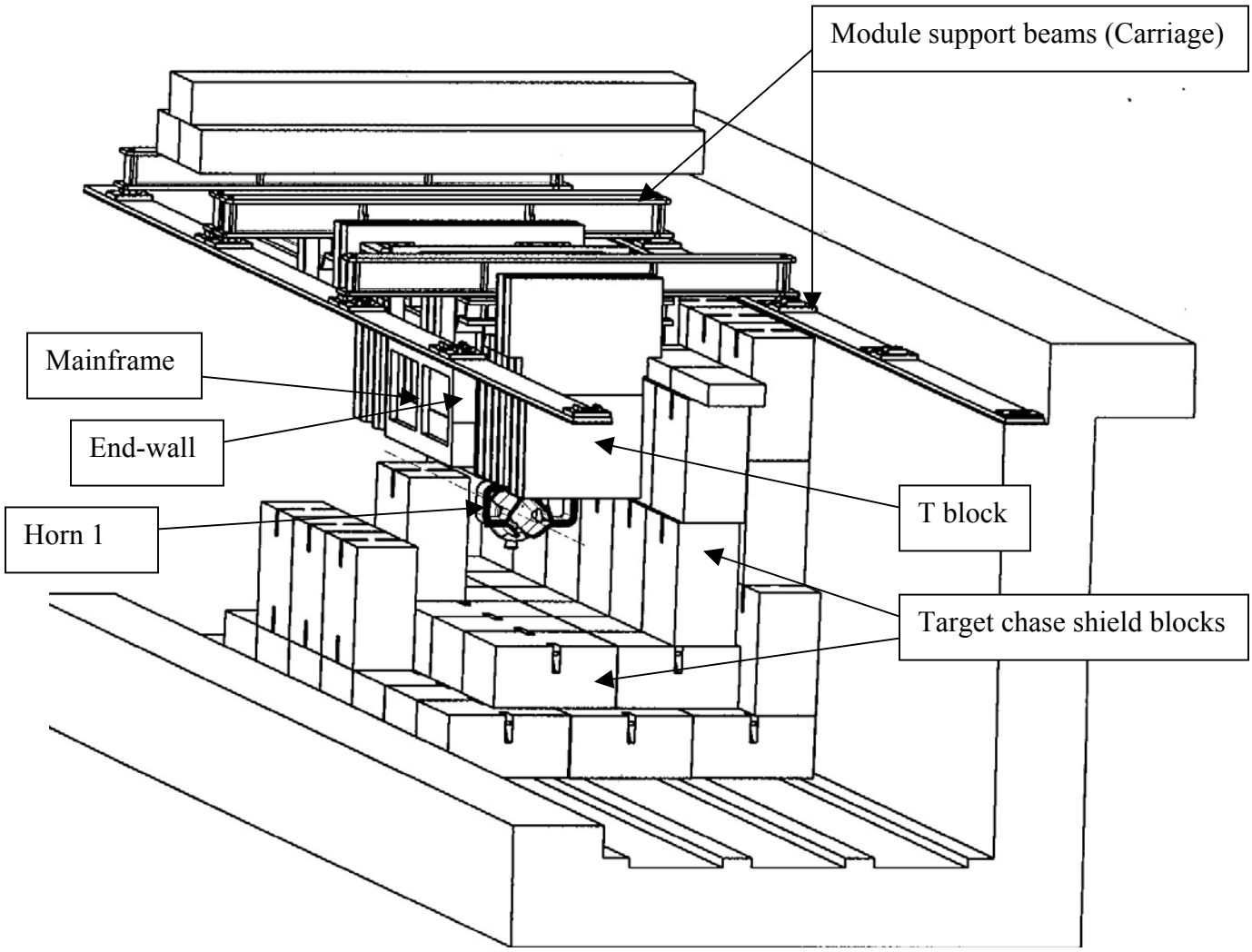

Figure 4.2-25. Schematic representation of the NuMI target chase showing the Horn 1 module and its T-blocks.

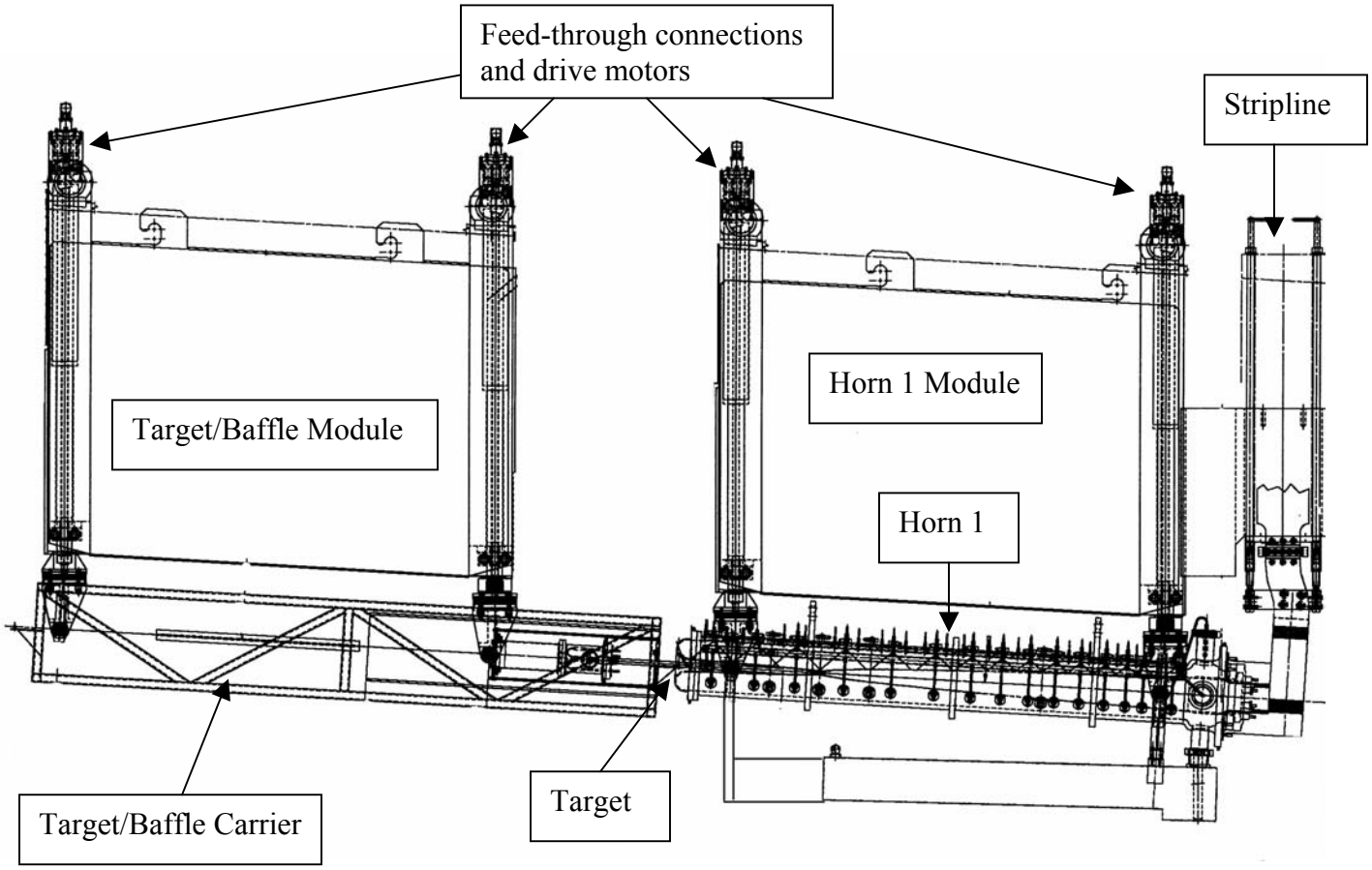

Figure 4.2-26. Schematic representation of the locations of the Target/Baffle and Horn 1 modules, the Target/Baffle carrier and Horn 1.

4.2.9.2. Support module parameters

Each support module consists of the following components:

1. Module mainframe (including stripline support block for Horn 1 and 2 modules).
2. Upstream and downstream supports for a horn or the Target/Baffle carrier.
3. Steel shielding T-blocks that are supported independently of the mainframe.
4. Remotely controlled horizontal and vertical motion (except Horn 2 module).
5. Remotely accessible precision alignment fixtures (tooling balls).
6. Cooling water supply and return connections.
7. Electrical feed-through connections for thermocouples and other instrumentation.
8. Vacuum connections (Target/Baffle module only).

Figures 4.2-27, **Figures 4.2-28** and **Figures 4.2-29** show some of the construction details of the Horn 1 and Target/Baffle modules. **Tables 4.2-14** and **4.2-15** summarize the support module design parameters and alignment tolerances.

.

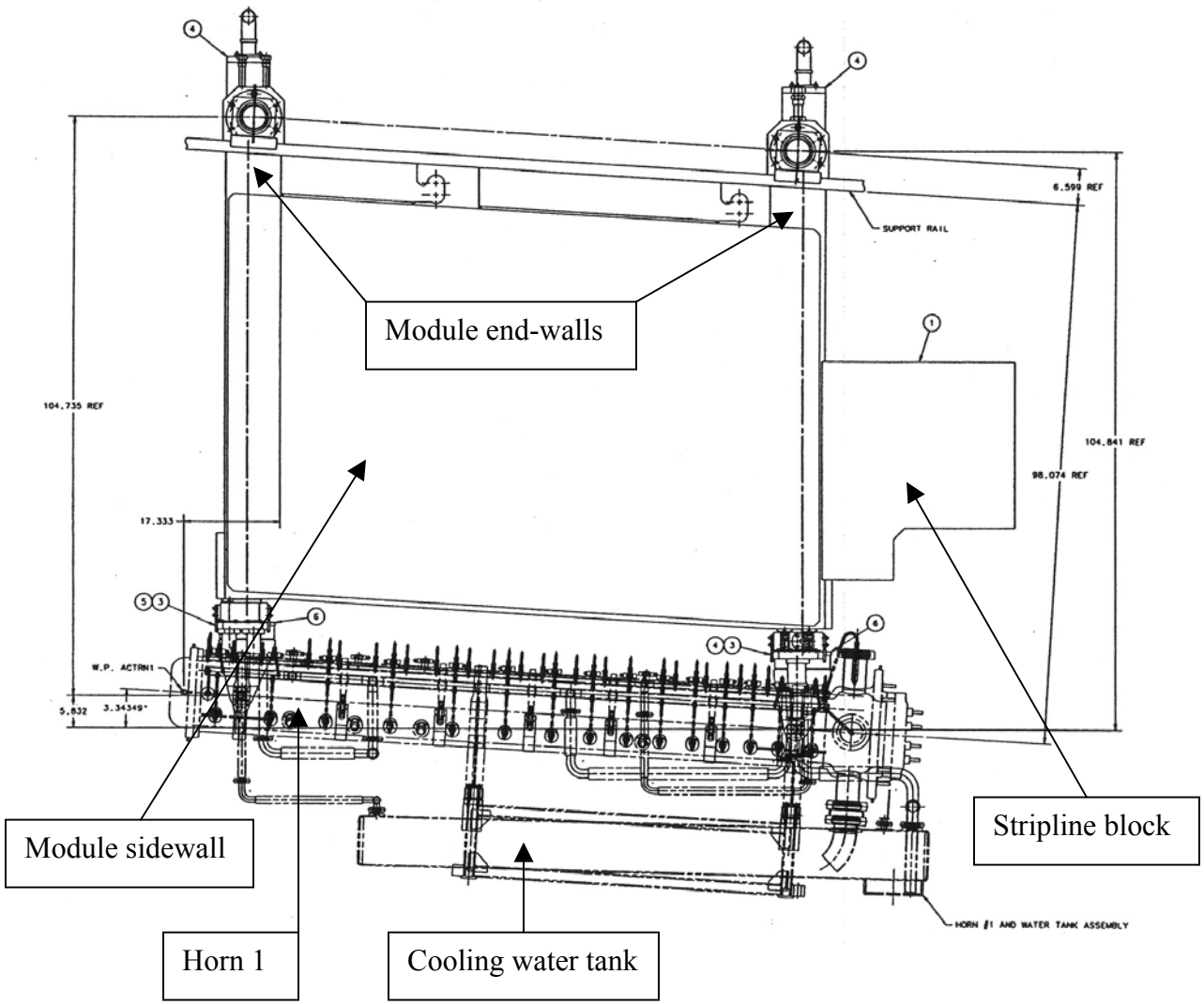

Figure 4.2-27. Side view of the Horn 1 module.

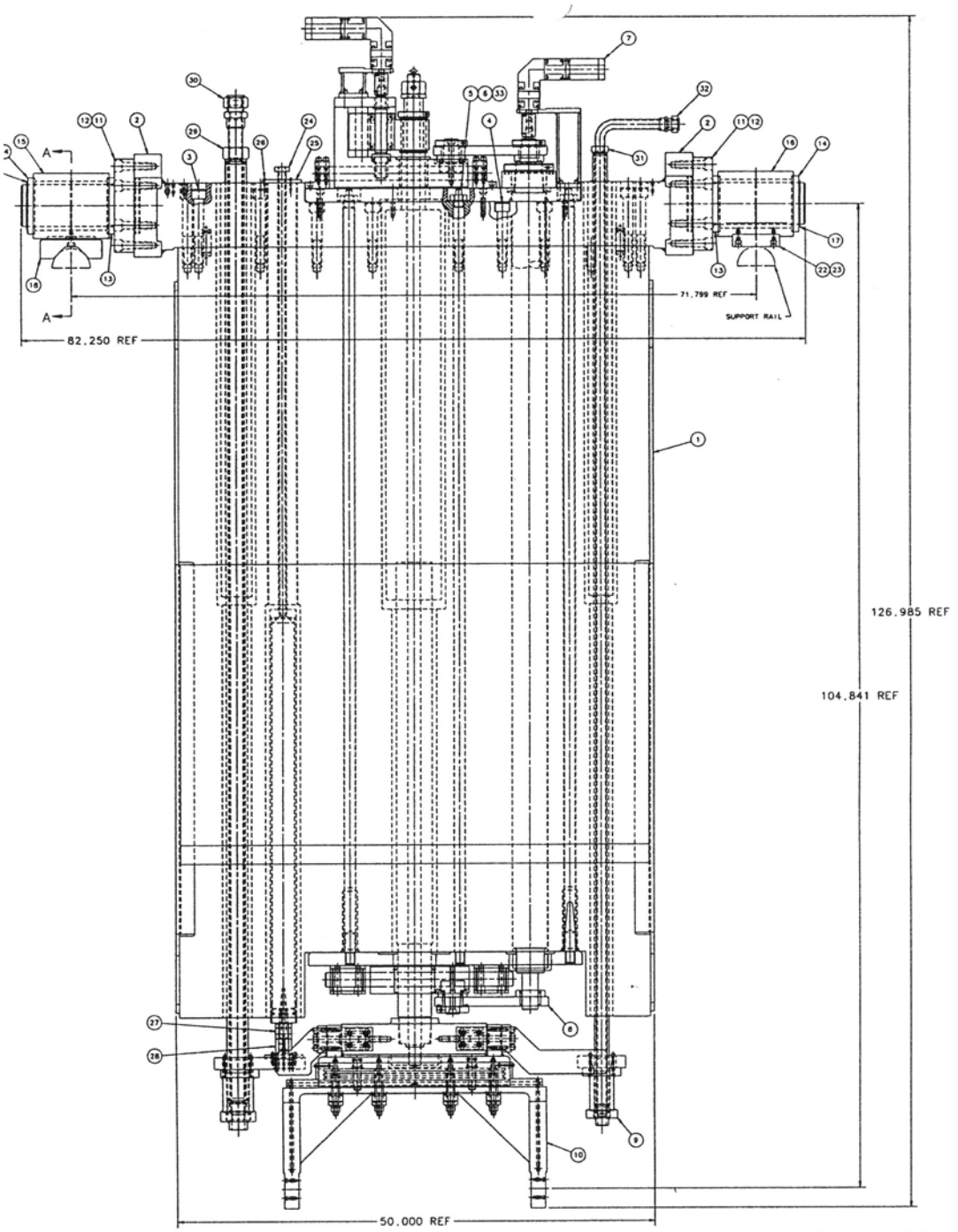

Figure 4.2-28. End view of Horn 1 module end-wall showing drive motors, water and electrical feed-through holes and the penetrations for support drawbars and for making water and electrical connections to Horn 1.

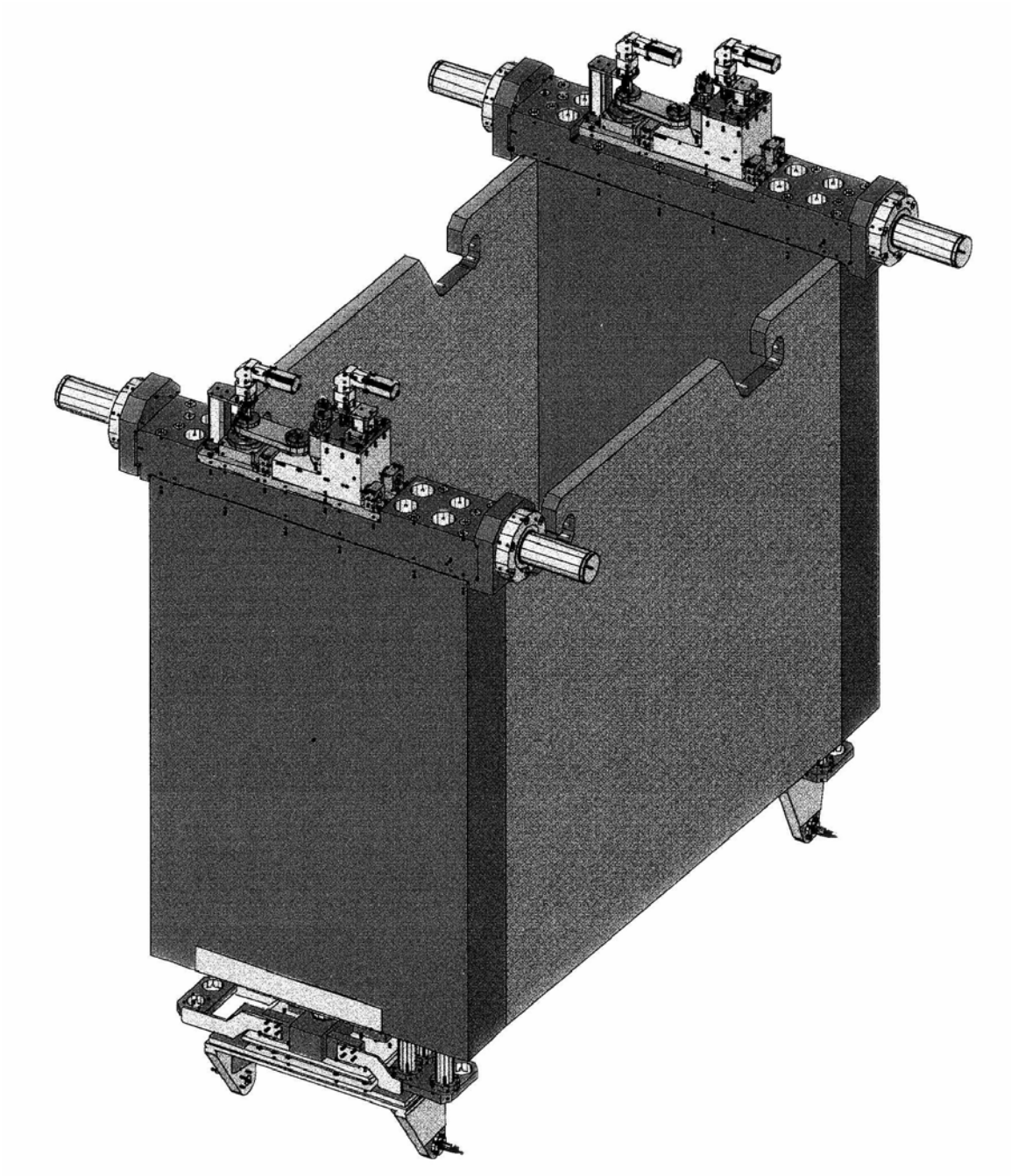

Figure 4.2-29. Isometric drawing of the Target/Baffle module mainframe.

Target/Baffle and Horn Support Module Parameters, November 2002				
Parameter	Horn 1 Module	Horn 2 Module	Target/baffle Module	Comments
Module weight	51,000 lb	~ 51,000 lb	~ 27,200 lb	Total weight (module + component + fixure) limited by 30-ton crane
Component weight (horns, carrier)	1,140 lb	2,120 lb	6,200 lb	Horn weights don't include clamps, stripline
Target chase clearance	2 cm	2 cm	2 cm	Minimum clearance to chase walls
Vertical motion range	+/- 3 mm	Fixed	+ 8 mm to - 200 mm	
Horizontal motion range	+/- 3 mm	Fixed	+/- 8 mm	
Longitudinal motion range	Fixed	Fixed	2.5 m	
Component alignment goal	+/- 0.5 mm	+/- 1.0 mm	+/- 0.5 mm	See Table 2 for details
Design radiation dose - top	10^5 Rad/year	10^5 Rad/year	10^5 Rad/year	
Design radiation dose - bottom	10^{11} Rad/year	10^{11} Rad/year	10^{11} Rad/year	

Table 4.2-14: Summary of current best estimates of support module parameters.

	Target/Baffle	Horn 1	Horn 2
Component alignment goal	+/- 0.5 mm	+/- 0.5 mm	+/- 1 mm
Component motion relative to module			
Motorized vertical range of motion	+8/-200 mm	+/- 3 mm	none
Motorized horizontal range of motion	+/- 8 mm	+/- 3 mm	none
Motorized range of motion along beamline	2500 mm	none	none
Motion due to thermal expansion	<0.5 mm	<0.5mm	~1 mm
Module to Carriage adjustment	None	None	None
Module tolerance	1.5 mm	1.5 mm	1.5 mm
Carriage internal tolerance	1.5 mm	1.5 mm	1.5 mm
Carriage adjustment vertical shim pack	+/- 8mm, 0.8 mm steps	+/- 8mm, 0.8 mm steps	+/- 8 mm, 0.8 mm steps
Carriage adjustment horizontal slip plate	> +/- 8 mm	> +/- 8 mm	> +/- 8 mm
Carriage sag when module put in place*	~ 1.8 mm	~ 1.8 mm	~ 1.8 mm

* Due to the carriage sag under weight we plan to adjust carriage shim pack after module is in place. Displacement due to thermal expansion will tend to be in the downward direction.

Table 4.2-15: Adjustments and tolerances for component positioning in the target hall.

4.3 POWER SUPPLY SYSTEMS (WBS 1.1.3)

4.3.1. Introduction

The extraction/primary beam power supply system consists of the power supplies for the beamline elements, their local controls and regulation equipment, the cables and connections from the power supplies to the 480 VAC power panels and the cables and connections from the power supplies to the devices that they drive.

Table 4.3-1 summarizes the number and types of power supplies needed for the NuMI beamline. For beam tuning and focusing, each trim and quadrupole magnet has its own power supply. On the other hand the bend circuits use several 500 kW supplies in series (or for the V108 circuit a Main Ring Power Supply) in order to obtain the desired voltage levels. All power supplies are standard refurbished FNAL power supplies, with the exception of the kicker power supply and horn power supply. Some of the MI correction element power supplies will need to be built, but from a standard, existing FNAL design. The kicker and horn power supplies are designed and built specifically for the NuMI application. The horn power supply uses a transmission line to supply current to the two horns. The kicker power supply uses standard RG220 cable. The following sections describe the power supply system, starting with the conventional, mostly refurbished power supplies, then the kicker power supply and finally the horn power supply and its transmission line. Cables are covered briefly at the end.

Type	Number
Kicker Power Supply (requires a 60 kV charging power supply)	1
Horn Power Supply (requires 2 charging power supplies and a transmission line)	1
PEI 240 kW (horn power supply charging power supplies)	2
Main Ring Style	1
PEI 500 kW	10
PEI 20 kW	23
MI Correction element power supplies	19

Table 4.3-1 Summary of Number of Power Supplies and Types

4.3.2. System Description: Conventional Power Supplies

Table 4.3-2 through **Table 4.3-4** list the power supply circuits (except for the kicker), corresponding magnet types, numbers of magnets, their resistance, inductance, cabling information, current and voltage information, power supplies required and their corresponding voltages, currents and power. The two 240 kW power supplies used for charging the horn power supply capacitor bank are discussed in the section on the horn power supply. The others are discussed here.

Table 4.3-2 : Power Supplies in MI60

(See document TDH_V2_4.3_Tables_2-4.xls for tables 4.3-2 through 4.3-4)

Table 4.3-3: Power Supplies in MI62

Table 4.3-4: Power Supplies in Target Service Building

All the magnet supplies will be ramped. There will be seven high-current bend circuits: the kicker magnet (I:KPS6N), the first Lambertson magnet (I:LAM60), the second and third Lambertson magnets (I:LAM61), the C-magnet (E:V100) and three bend circuits (E:HV101, E:V108, E:V118). The power supplies are located in three areas, MI-60, MI-62 and MI-65. The extraction system power supplies (I:KPS6N, I:LAM60, I:LAM601, E:V100, E:HV101), the first 12 corrector element power supplies, and the first 6 quad power supplies are located in MI60. The second bend power supplies (E:V108), one 20 kW power supply (E:H104), and 6 quad power supplies are located in MI62. The final bend power supply (E:V118), one 20 kW power supply (E:H117), 9 quad power supplies and 9 corrector power supplies are located in MI-65.

The kicker power supply is covered in Section 4.3.3. The first Lambertson magnet, due to aperture restrictions in quad Q608 downstream of it, is run at a lower current than the last two Lambertson magnets. Thus there are two separate 500 KW power supplies for the three Lambertson magnets (I:LAM60, I:LAM61). The C-magnet is powered by a 500 kW supply (E:V100). The first bend string (E:HV101) consists of six EPB magnets powered by three 500 kW supplies in series. The second bend (E:V108) consists of six B2 magnets powered by a Main Ring type power supply. The circuit E:V118, the four B2 magnets, is powered by a four 500 kW supplies, run as 2 sets of 2 500kW supplies in series. There will also be 21 quadrupole circuits, each with a 20kW power supply and two dipole circuits, each with a 20kW power supply. There are nineteen low-current circuits for Main Injector corrector magnets. Several quadrupole circuits may be combined in the future to run from one power supply if it is shown to be an effective way to operate. The critical devices will be the E:HV101 and I:LAM61 circuits. Standard FNAL hardware is used for the critical device circuits.

4.3.2.1 Upgrades and Improvements to Conventional Power Supplies

All of the large NuMI power supplies (240kW, 500kW, Main Ring) and most of the smaller NuMI power supplies (20 kW and MI corrector power supplies) are re-used power supplies from decommissioned beamlines. The 20 kW and MI corrector power supplies did not need to be upgraded or refurbished. The others were re-furbished and upgraded to meet the anticipated 10-year lifetime of the NuMI beamline. The refurbishing included new voltage regulators, new gate firing circuits, water lines, and ramp calculators were installed. The power supplies were also modified for two-quadrant operation (invert) by removing diodes and adding silicon controlled rectifier switches (SCRs). Each circuit is set to use the maximum power supply voltage tap possible.

4.3.2.2 Power Supply Regulation

To meet the beamline specifications given in Section 4.1 particular concern needs to be given to the six bend supplies; the criteria are somewhat less stringent for quadrupoles and dipole correctors. There are three sources of current variation for magnet strings. One is the 720 Hz line ripple. The other two sources of current variation are line voltage changes and load changes. Simulations of a particular power supply (or series of power supplies) can be used to see the

effects of these changes on the resulting flattop current. The present cost estimates for the NuMI beamline power supply regulation include costs for standard regulation plus the costs of a filter choke for three of the six magnet strings. An analysis of the power supply stability requirements for the new beam optics has been completed and is shown in **Table 4.3-5** through **Table 4.3-8**. Details are given in Section 4.1. A change request will be made to incorporate these requirements into the present cost and schedule. These beam stability criteria listed in Section 4.1, lead to the stability limits listed in **Table 4.3-5**, where instability in ppm is the plus or minus variation allowed in that loop relative to its operating current at flattop.

String	Maximum Current of PS	Peak Current (amps)	Corresponding target RMS in microns	Allowed Instability in ppm
Lam60	2500	916	160	900
Lam61	2500	1985	300	730
V100	5000	2692	200	670
HV101	2500	1670	20	100
V108	4250	4442	200	60
V118	5000	4173	200	70

Table 4.3-5: Power Supply Regulation Requirements due to Beam Stability

The power supplies also need to regulate well to minimize beam loss. The fractional losses at $4x10^{13}$ppp in the primary beam line should be kept below 10^{-4} in most locations and 10^{-6} in the central region of the carrier tunnel. MARS simulations of losses along the beamline are nearly complete. The results will be summarized in **Table 4.3-6**. One can clearly see that the requirements for power supply regulation to limit beam loss for groundwater activation are much less than those needed for beam stability and physics. (This is known from the data we have from the present study of beam loss using MARS and STRUCT.)

String	Maximum Current of PS	Peak Current (amps)	Corresponding Fractional Beam Loss	Allowed Instability in ppm	Allowed Instability Percentage Change
Lam60	2500	916			
Lam61	2500	1985			
V100	5000	2692			
HV101	2500	1670			
V108	4250	4442			
V118	5000	4173			

Table 4.3-6: Power Supply Regulation Requirements due to Beam Loss

4.3.2.3 Line Ripple

Filter chokes are used to filter out the 720Hz ripple on the line. When a PS current is changed, even if it is line-synched, it shifts slightly on the 720Hz ripple, which is quite sharply peaked. As a result, there is a fair amount of current variation despite line synching. Even extraction can vary by up to 30 microseconds. **Table 4.3-7** shows the current variation that would occur assuming no filter chokes, for each string. We will use filters on all the circuits listed **Table 4.3-7**. This requires 7 filters since the V119 string is two sets of 500 kW PEI's in series and thus requires two filters. One might argue that the Lam61 string does not need a filter, but the difference between allowable instability and the level without a filter is only a factor of 2. The requirement numbers were obtained by looking at single string variation, not multiple, thus we should err on the side of better regulation per string than the allowed instability ppm numbers show.

String	Maximum Current of PS	Peak Current (amps)	Allowed Instability in ppm	Variation due to 720 Hz in ppm with no Filters	Variation due to 720 Hz in ppm with Filters
Lam60	2500	916	900	1606	209
Lam61	2500	1985	730	349	17
V100	5000	2692	670	528	14
HV101	2500	1670	100	225	12
V108	4250	4442	60	202	4
V118	5000	4173	70	324	7

Table 4.3-7: Current Variation due to Line Ripple

4.3.2.4 Current Variation due to Line Voltage and Load Changes

Line voltage changes were simulated for the NuMI V108 string. Assuming a constant reference voltage, a 5% change in line voltage was easily corrected for at the level of 100 ma (at a flattop current of 4250 amps) by the standard voltage regulation loop of the power supply. This corresponds to ~24 ppm change. This level of line voltage change is the most one would expect and results in a current variation well below that required by NuMI. Thus standard regulation is sufficient for line voltage changes.

Load changes were similarly simulated for the NuMI V118 string. A 5% change in load resistance (corresponding to about a 10° C change in the copper of the magnet, or the LCW changing 15^{0} C) resulted in a 1 amp change out of 4250 amps. This corresponds to a 240 ppm change. Other magnet strings have not been simulated, but would probably come to a similar result. **Table 4.3-8** shows the current variations due to load changes when using special FNAL electronics. Due to beam requirements and concerns about ease of bringing up the beam,, special FNAL electronics will be installed on circuits all 6 strings.

String	Maximum Current of PS	Peak Current (amps)	Allowed Instability in ppm	Variation due to Load Changes (ppm)	Variation due to Load Changes with FNAL Electronics (ppm)	Extra Factor Needed (regulation/spec)
Lam60	2500	916	900	653	326	0.36
Lam61	2500	1985	730	277	138	0.19
V100	5000	2692	670	287	144	0.21
HV101	2500	1670	100	304	152	1.52
V108	4250	4443	60	191	96	1.59
V118	5000	4173	70	240	120	1.72

Table 4.3-8: Current Variation due to Load Changes

4.3.2.5 Regulation Requirements

The conclusion is that filter chokes and FNAL electronics will be used for all 6 strings and either a BμLB or JITtER system will be installed for the three major bend strings (HV101, V108, V118). A BμLB system is more expensive and regulates throughout the ramp where as the JITtER system, under development in Beams Division, will sample and correct at the start of flat top. The JITtER system should be easier to support and less expensive and sufficient for NuMI, if the development shows it to be a reliable system.

Autotune will greatly help, but has its drawbacks as one must have beam and working beam position monitors to use Autotune. When beam first starts up, Autotune will not be able to correct things immediately. Thus we will use both Autotune and an additional level of power supply regulation. In addition, each string will be tuned for the maximum bandwidth. This is the standard way of starting up a power supply system.

The remaining types of power supplies in the primary beam line are 20 KW PEI's for the quadrupole magnets, 200 turn switchyard dipoles, and Main Injector (MI) trim power supplies. The 20kw PEIs have standard regulation of +/-0.05% of the maximum current of the power supply (100 or 200 amps). The MI trim magnets standard power supply regulation is +/-0.1% of the maximum current of the power supply (12 amps). We believe that this level of regulation is sufficient for the NuMI beamline.

4.3.2.6 Controls

The NuMI power supplies will have the same controls as the P1, P2, P3 and A1 lines. Operations will have only to adjust one point per load. The groups of supplies will be regulated by one current regulator, and thus will act as one. Each supply will have an SCR Unit with a closed voltage loop, the same as the single supplies. The supplies will all receive the same voltage reference. Each magnet load will have one current reference. We use C468 ramp generators, which are current referenced. We are installing a local DAC, which has better temperature drift numbers, in the current regulation system to improve the noise.

4.3.3. Extraction Kicker Power Supply

The requirements on the extraction kicker are similar to those of the long-batch kicker, which is operational at MI52. The normal operating mode will be one in which six Booster batches, each consisting of 82 x 18.9 nsec bunches, fill the Main Injector. The first Booster batch is sent to the antiproton source and the remaining five are extracted to NuMI. However, for periods when antiproton is not in a stacking mode it will be desirable to be able to extract six Booster batches to NuMI. Three kicker magnets are to be used in NuMI. The magnets are to be located in the region downstream of quadrupole Q602, with the power supply upstairs in the MI60 South Power Supply Room.

The kicker power supply will power two of the three magnets in series and then those in parallel with a third kicker magnet. The pulse-forming network (PFN) consists of two 32 section 10 ohm PFN's in parallel with one thyratron switch driving the magnets. A 60 kV power supply will be used to charge the PFN.

4.3.3.1 Specifications

The specifications for the kicker system are given in **Table 4.3-9**.

4.3.3.2 Thyraton

Figure 4.3-1 shows the NuMI thyratron enclosure. The CX1592C from Marconi Applied Technologies (née EEV) was selected for the thyratron, with thought of minimizing pre-fire rates. This is the same thyratron used for proton extraction for pbar production. A new triggering method, recommended by Marconi, will be used to give a longer thyratron life because of the longer length of the current pulse.

Kick Angle @ 120 GeV protons	900 μrad (3.6 kG-m), to radial inside of MI, nominal
Current Per Magnet	2460 A Nominal/ 2730 A Maximum
Nominal integrated field	3.6 kG – m (1.2 kG-m per magnet)
Maximum integrated field (110%)	4.0 kG-m
Field Rise Time (1%-99%):	1.30 μs
Field Fall Time:	N/A
Field Flattop Time:	9.78 μs minimum (6 batches)
Flattop During Pulse:	+/- 1%, best effort to +/- 0.5%
Flattop pulse to pulse:	+/- 0.5%
Maximum PFN Charge Voltage	60 kV
Maximum PFN Output Current	6000 A
Repetition Rate:	1.9 seconds
Maximum Charging Time:	1.5 seconds
Pulse Forming Network Length	11.5 μs minimum (=9.78 μs + 2 x 0.60 μs + 0.50 μs)
MI reset to transfer/next MI reset	1.25 seconds/1.83 seconds

Table 4.3-9: Specifications for the NuMI Kicker Power Supply

Figure 4.3-1: Thyratron Enclosure

4.3.3.3 Pulse Forming Network (PFN)

The design of the PFN must have a ripple period close to magnet transit time for best performance. The design of the PFN has to meet not only electrical constraints, but also physical size and cable routing constraints. The NuMI kicker power supply has two PFN's in parallel. Each PFN has 32 sections, 20 nF/section, 2.0 μH/section and a 49 kV nominal kick. The NuMI PFN also has increase coupling (12% vs. 2%) and longer lifetime capacitors versus the MI-52 design. **Figure 4.3-2** shows a schematic of the PFN design. **Figure 4.3-3** will show a simulation of the total integrated field. The simulation used as much detail as possible concerning the magnet and PFN. The purple line is for two magnets in series, the red line is for a single magnet. Once can see the rise time requirement of 130 nsec may be hard to meet with 6 Booster batches.

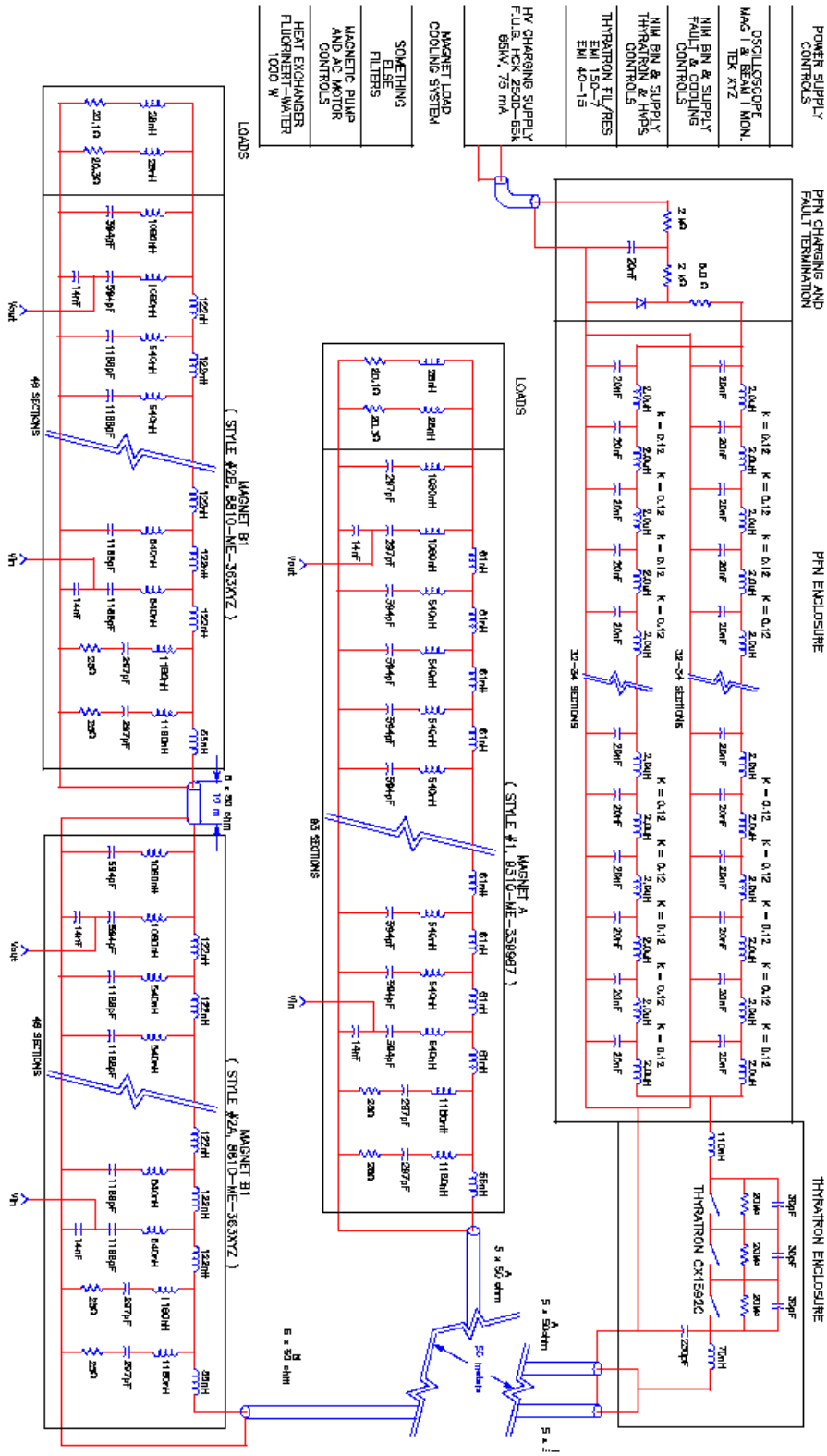

Figure 4.3-2: NuMI Kicker Design Schematic

Updated figure has not been made yet.

Figure 4.3-3: Simulated Kicker Integrated Field

4.3.3.4 Charging Power Supply

The charging power supply specification has been written. (ES-370-035), and needs to be reviewed.

4.3.3.5 Controls

The kicker will use a NIM bin based controls system. The modules are copies of the existing kicker controls for MI. Two special cables have been installed between MI-52 and MI-60 for fast inhibit & permit signals. **Table 4.3-10** shows the kicker fault signals that will be monitored.

Reset and if clears no problem	**Investigate before resetting**
Personnel Safety	HV Power Supply in Range (Absolute)
Trigger Supply Out of Limits	Magnet Current in Range (Absolute)
Filament Supply Out of Limits	Thyratron Prefire
Thyratron Oil Level Low	Thyratron No Fire
Thyratron Temperature High	Open Fault in Cable or Magnet or Loads
Magnet Fluorinert Level Low	(Magnet I)/(Charge V) Out of Limits
Magnet Load Temperature High	Shorting Fault in Cable or PFN or Loads
Magnet Load Fluorinert Flow Low	
Magnet Load Fluorinert Level Low	

Table 4.3-10: Kicker Fault Signals

4.3.4. Horn Power Supply

4.3.4.1 Horn Power Supply Specifications

The horn power supply must deliver 200 kA (average, ± 2.5%) pulses every 1.9 s. with a pulse-to-pulse repeatability of 1% and current monitoring to 0.4%. As a safety margin the power supply system will be designed to operate at up to 240kA. This results in a system load current of 7250 Arms operationally (8700 Arms design). The specifications are given in **Table 4.3-11**. The horn power supply system is located in the power supply room, underground, next to the Target Hall. The main components are the charging power supply, the capacitor bank, the silicon controlled rectifier (SCR) switches, the current transducers, and the safety system. The *NuMI Horn Power Supply Manual*, revised 4/02 is the most complete description of the horn power supply system.

Pulse width	2.6/5.2 ms
Bank Voltage	860/515 V
Pulse	1/2 sine
RMS current	5125/7250 A
Peak current	205 kA peak
Average flattop current	200 kA (average, ± 2.5%)
Pulse to pulse repeatability	1%
Current monitoring	0.4%
Repetition rate	1.87 seconds
Duty	continuous
di/dt, horn	268/146 A/us

Table 4.3-11: Power Supply System Output, operational level

In the horn power supply system, energy is stored in a capacitor bank and switched via a parallel array of SCR switches into the horn load. A parallel strip transmission line is used to connect the power supply to the horns. The circuit is a damped LC discharge circuit that will reach peak current when the SCR switch releases stored energy from the capacitor bank to the horns via the transmission line. The horn power supply can provide either a 2.6 msec or a 5.2 msec "flattop" pulse, depending on how the capacitors are connected. **Table 4.3-12** shows the design parameters for the horn power supply operating in these two modes. Also shown, for completeness, are the parameters for the prototype horn power supply used for testing horns at MI8.

	Prototype Horn Power Supply	Operational Horn Power Supply (5.2 msec)	Operational Horn Power Supply (2.6 msec)
Operational Current (kA)	200	205	205
Peak Possible Current (kA)	200	240	240
Peak Voltage (V)	800	550	1100
1/2 sine wave pulse base length	800-850 μsec	5.2 msec	2.6 msec
Repetition rate	0.5 Hz (up to 1.5 Hz)	0.5 Hz	0.5 Hz
Peak Current per capacitor	Varies	2 kA	4 kA
RMS current per capacitor	Varies	72.5 A	145 A
Total Capacitance		0.9 F	0.225 F
Comments	Current depends on the resistance of the circuit and the voltage limit of the PEI PS)	12 sets of 10 capacitors	Change 120 parallel caps divided into 12 cells to 60 series pairs; need two 240kw PEI's in series to get voltage (1100V)

Table 4.3-12 Design Parameters of Horn Power Supplies

4.3.4.2 Horn Power Supply Overall Design

The circuit used to provide current to the horns is a damped R-L-C discharge circuit as shown in **Figure 4.3-4.** It achieves peak current when the SCR (Silicon Controlled Rectifier) switch releases stored energy from the capacitor bank to the horns via the stripline. The load elements, listed in **Table 4.3-13**, are for the full-length stripline installation in the Target Hall and factor in skin effects and temperature rise. Power dissipation is given for the two possible pulse widths that can be generated.

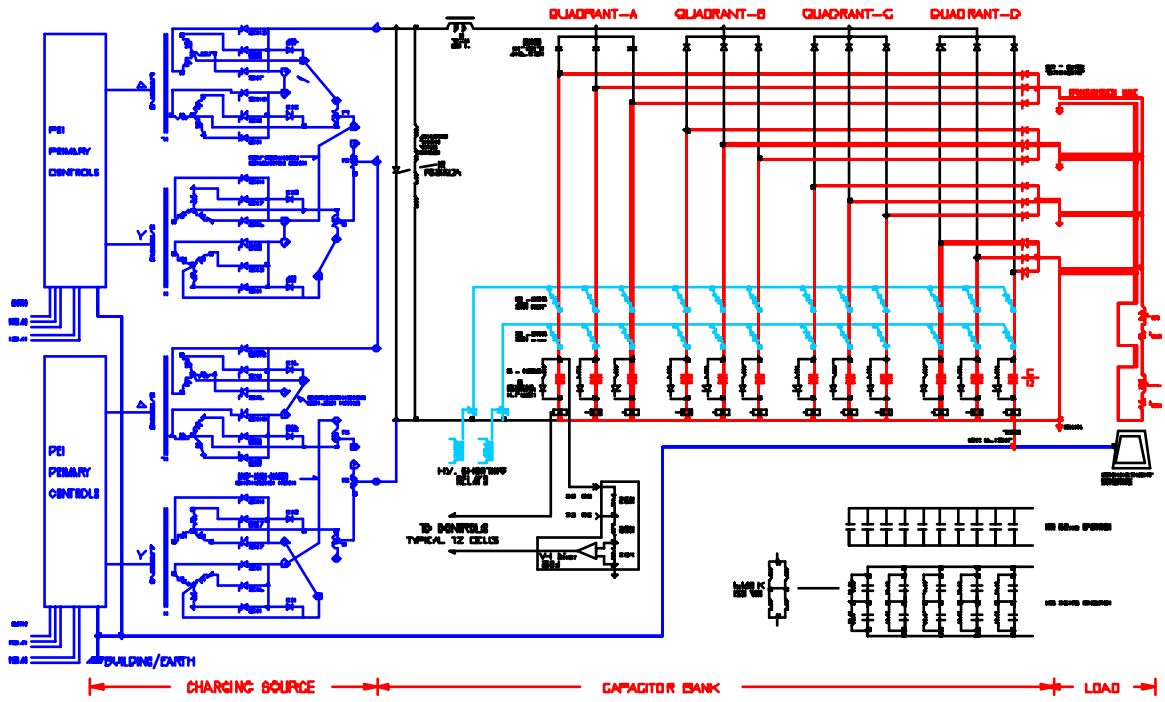

Figure 4.3-4 Horn Power Supply system schematic diagram.

Element	L, μH	R, mΩ	$P_{2.6}$ / $P_{5.2}$, kW
Horn #1	0.689	0.270	7.1/ 4.2
Horn #2	0.510	0.071	1.9/3.7
Transmission line:			
Transmission line: P. S. to beamline, 9.5 m.*	0.152	0.095	2.5/5.0
Transmission line: Between horns, 53.5 m.*	0.856	0.535	14.1/28.1
Cap. Bank, connections	0.1	0.050	1.3/2.6
Stripline connections*	0.1	0.010	0.26/0.52
Total	2.407	1.031	27.1/54.2

(*Estimate; from drawings, 7-Dec-01)

Table 4.3-13 Horn Power Supply Beamline Load Elements

Energy to provide the high current pulse for the NuMI horns is supplied by DC power sources (240 kW PEIs) that are used to charge the capacitor bank during the quiescent period between horn pulses. When the capacitor bank is configured to provide 2.6 ms pulse widths, the stored energy in the bank is 85 kJ. When configured for 5.2 ms pulse widths, the operating level of stored energy is 120 kJ.

With any array of capacitors connected in parallel, a capacitor experiencing a fault will have to absorb in addition to its own stored energy, the energy of all the capacitors connected in parallel with it and do so without case rupture. For this reason the capacitor bank is divided into twelve isolated sections, or cells, making the maximum amount of stored energy in any cell 12 kJ or less. All of the cells are isolated by diodes from each other and the charging source, and by SCRs from each other and the load. Consequently, the cells cannot communicate with each other under fault conditions. Having the capacitor cells isolated from each other forces current sharing among each of the twelve SCRs switching load (horn) current.

The style of case construction specified for these capacitors utilizes 14-gauge steel, instead of the normal 16 gauge, and have a fault energy containment rating of 25 kJ to provide a safety factor greater than two in each of the cells. The capacitor bank is assembled in four groups of three cells. Each group of three cells is referred to as a 'quadrant.' The quadrants are labeled "A" through "D."

The bank normally operates with 120 capacitors in service, 30 in each quadrant. Provision was made to accommodate a maximum of 144 capacitors. All safety margins are determined for the maximum capability (240 kA design level) of the capacitor bank when used for NuMI beamline service. A basic schematic diagram of the high power elements is shown in **Figure 4.3-4**. FNAL drawing #9820-MD-370111 includes additional detail.

To minimize the voltage from the outer conductor of horn 1 to the target, located within the throat of horn 1 for the low energy beam, horn 1 is installed in the return side of the transmission line, nearest (electrically) to the capacitor bank. To achieve current flow in the proper direction, i.e. current in the center conductor of the horn in the same direction as the beam, it is necessary to make the positive side of the capacitor bank 'ground.' The capacitors in the bank are non-polarized and the PEIs can operate equally well with either terminal declared 'ground' since the PEI output floats.

The low-side bus from each capacitor cell (row) within each quadrant is connected to all of the others, and then connection to the enclosure frame is at a single point. All connections to an earth ground and the horn modules in the beamline installation are made to this point via the LEM® current monitor. The LEM provides for detection of fault currents in the grounding cables. The LEM signal output is tied into the controls interlock chain to terminate system operation in the event significant ground currents are detected.

Any electrical fault from the stripline or horns to the mounting structures or shielding steel in the beamline installation will allow the capacitor bank output current to return to the capacitors by a an alternate path, and ultimately through the cables connecting to the single point frame ground of the enclosure. The LEM current transducer will detect current in these cables.

4.3.4.3 Capacitor Bank Electrical Components

The capacitor bank specifications are given in **Table 4.3-14**. Based upon the inductance and resistance values provided for the two horns and the transmission line, the capacitance required for the bank is 0.90 Farads. The capacitor bank will be recharged by two of the standard Fermilab 240 kW power supplies. During operation of the horns the calculated power consumption is 83 kW. The required voltage for operation is 515 volts. To avoid creating transients on the power line a 1 mH inductance will be inserted between the power supply and the capacitor bank. The design uses 120 parallel capacitor units (7.5mF, 670V) divided into 12 cells, 10 units per cell and two empty slots per cell in case more capacitance is needed to make up for less than expected inductance for the target hall circuit. This design provides the 5.2 msec pulse. To obtain the 2.6 msec (half pulse), the 120 pairs in parallel are switched to 60 series pairs (with each pair being 3.75uF, 1340 V) in parallel. This yields a total capacitance of 0.225F or 1/4 the full pulse design amount. The 2.6 msec operational setup requires two 240 kW PEIs to run in series to obtain the 1100 volts needed for operation. This has been done before at Fermilab. The pulse waveform is given in **Figure 4.3-5**.

Peak current, maximum	240 kA (Design Rating; 120%)
Peak current, operating	205 kA
RMS current	8700 A (Design Rating; 120%)
Capacitance/unit	7,500 +/- 5% uF
Number of cells	12
Installed capacitors/cell	10
Total No. Caps installed	120
Max. No. capacitors/cell	12
Maximum No. capacitors	144
Capacitance/cell	18.75 mF / 75 mF
Installed Capacitance	0.9 Farad
Max. capacitance	1.08 Farad
Capacitor voltage rating	670 $V_{Working}$ /1340 $V_{Hi\text{-}pot}$
Switching element	SCR array, 12 parallel devices
SCR Mfg, Part Number	Eupec, Inc., T2710N20TOF

Table 4.3-14: Capacitor Bank Specifications

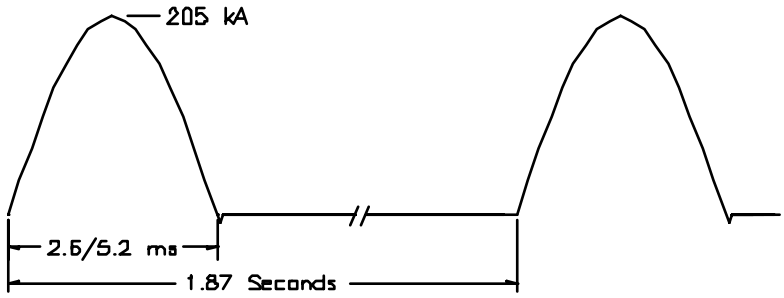

Figure 4.3-5: Capacitor Bank Pulse Train Waveform

We have chosen the metalized polypropylene construction for the capacitors specifically because they fail gracefully, or experience soft failures. They are fitted with pressure switches to detect any pressure build-up co-incident with soft failures and these switches will be tied into the interlock system of the controls. We have specified a capacitor case containment rating of 25 kilo-Joules when the maximum operating energy in any one cell is 15.7kJ. The nominal operating energy in each cell is 10.6 kJ. The absolute max energy available, assuming the PEI goes to full it's full output of 800 volts, is 22.4 kJ per cell. All of the cells are isolated from each other by semi-conductors, SCRs or diodes.

Capacitor Row Buses

The capacitor row bus extension tabs are constructed of 0.063" copper sheet stock with tab extensions to the respective positive and negative bushings of every second capacitor in the row. This every-other-one arrangement allows the free terminals of the capacitor pairs to be connected in a series, or parallel arrangement depending on the pulse width desired. For 2.6 msec operation the parallel arrangement is used.

Silicon Controlled Rectifier (SCR) Modules

The SCRs used in the capacitor bank to switch stored energy from the capacitors are assembled into modular sub-assemblies. Twelve assemblies, one for each capacitor row, are used in the capacitor bank. The assembly includes two water-cooled heat sinks, an SCR, bus bar terminals, and a compression clamp to hold the SCR under 10,000 lb. pressure. The modular approach is instituted to allow quick change-out in the event of an SCR failure. A snubber network is installed across each output SCR to protect it from voltage transients. The combination of a 1 uF capacitor in series with two parallel-connected non-inductive resistors is used. The respective snubber circuits are mounted adjacent to each SCR. **Table 4.3-15** shows the SCR ratings.

V_{DSM}, V_{RSM}	2,200, 2,300 V
I_{av}	3,700 A
I_{rms}	5,800 A
I_{tsm}	54,000 A

Table 4.3-15: SCR Ratings

Firing Circuits

Firing circuits provide the signal to the respective SCR gate terminals that initiate conduction of the devices. The firing circuits used to trigger the output SCRs are adapted from the Fermilab Low Beta Power Supply system. Circuit modifications are incorporated to increase the trigger pulse current amplitude to 6 Amps during the initial microsecond, decaying in several additional microseconds to 1 Amp for the remainder of the pulse. These modifications are documented by FNAL drawing # 9820-EC-370116. Each of the 12 output SCRs in the capacitor bank has a dedicated firing circuit. Three identical circuits are included on a single printed circuit board. Four printed circuit boards are installed, one for each quadrant of the capacitor bank. The overall pulse width of the gate signal for the SCRs is controlled by the electronics in the Trigger Fan-out Box and must be adjusted such that the pulse width does not exceed the on time of the SCRs.

The output SCRs of the capacitor bank float at the operating voltage of the system. The firing circuit board components provide 1,500 Vdc isolation between the low-level input pulse and the 120 Vac power, and the output pulse to the SCRs. Consequently, the majority of the components on the circuit board and the co-axial cables carrying the trigger pulse to each SCR float at high voltage as well. The co-axial cable outer jacket is not rated, with respect to ground, for the potentials the system may be operating at. Subsequently, the gate pulse co-axial cables are dressed away from structures at ground potential, or double insulated in areas where structures are unavoidable. Red colored RG-58 co-ax cable was installed to signify the application is operating at high voltage.

Trigger Fan-out Box

The trigger fan-out box is mounted to the ceiling of the enclosure, above the 'C' quadrant capacitor structure. It receives the 'SCR Trigger' pulse from the controls via fiber optic cable. A second fiber optic cable carries a 'status' signal back to the controls to verify that the trigger fan-out circuit has all of the appropriate voltages present. The status information is included in the interlock chain and must be present for system operation

Four parallel outputs from this circuitry are connected to the respective SCR firing-circuit pc-board of each quadrant. Two additional 'sync pulse' outputs are generated within and are available externally at the connector feed-thru panel, located above quadrant 'C.' The two sync signals are 1-μs in width, TTL level, buffered and synchronous with the trigger for the capacitor bank output SCRs.

Voltage Dividers
A voltage divider is installed in each of the capacitor cells (rows) to monitor the performance of the respective cells. The control electronics monitors these signals on a continuous basis throughout the operating cycle, looking for any imbalance. The frequency compensated voltage divider circuitry includes a voltage to current converter with a low impedance output. This approach was implemented for improved noise immunity and the ability to drive long signal lines to the control electronics.

Output Current Transformers
A passive current transformer (CT) is installed in the low-side bus of each capacitor row. Its output is 1 volt/kA and appears as a voltage source with 50 ohms in series. The twelve individual signals, one from each CT, pass through the connector panel located above quadrant C of the enclosure. The 50 ohm input impedance of each channel of the control electronics provides termination for the current transformers.

Reverse Energy Discharge Resistor and Diode
Energy reflected from the load inductance will be stored in the capacitor bank, but have the opposite polarity. Because of the relatively large amount of resistance in the stripline and horns the amount of energy reflected is approximately 1.5 kJ (15%), to low to have made the additional components necessary for energy recovery circuitry economically worthwhile. Consequently, the reverse energy is dissipated in a resistor switched into the circuit by a freewheeling diode. The resistor-diode combination is connected in anti-parallel across each capacitor cell. The diode for each cell is mounted as a water-cooled assembly to the capacitor low-side bus, adjacent to the current transformers.

Humidity Sensor
A humidity sensor is installed within the capacitor bank enclosure on the ceiling of "C" quadrant. It was included in the equipment to monitor enclosure humidity. It has a measuring range of 0-100% and an accuracy at 20˚C of; +/- 2% from 0 – 90% RH, +/-3% from 90 – 100% RH. Temperature dependence: +/- 0.02 ˚C /˚C. It operates on +5 Vdc and has an output of 0 –1 V with respect to common for 0 – 100 % RH indication. Connection to it is via a dedicated connector on the enclosure feed-thru panel.

4.3.4.4 Charging Power Supply Design Issues

Two 240 kW PEI power supplies are used for charging the capacitor bank. Their specifications are given in **Table 4.3-16**. These PEI power supplies used for the capacitor bank were originally designed for powering magnets under constant current or programmed functions. When used for charging capacitors, the charging current will go to zero once the capacitors have achieved the desired voltage, confusing the power supply regulator. As an aid to voltage regulation, a resistor is installed across the PEI output to pull a small amount of current at all times. The resistor is constructed of four series connected, water-cooled elements as used in domestic electric water heaters. Their combined series resistance of the four elements is 138 Ohms. These resistors are mounted within the capacitor bank.

PEI (Power Energy Industries)	240 kW
Maximum output voltage, Volts	200/400/800
Maximum output current, Amps	1200/600/300
Voltage regulation	0.1 %
Current regulation	0.05 %

Table 4.3-16: Charging Power Supply Specifications

A 10 mH inductor is connected between the PEI charging source (supply) and the capacitor bank. Its purpose is to limit undershoot current that occurs as a result of reverse recovered charge on the capacitor bank at the end of each discharge pulse. Design specifications of the choke are provided in FNAL Specification # 9820-ES-370036.

A by-pass diode is located within the capacitor bank enclosure, adjacent to the choke. This single diode appears electrically across the multiple series by-pass diodes of the PEIs and is meant to carry all of the remaining undershoot current, diverting it around the PEIs. Its anode is connected to the input end of the choke (PEI negative connection) and its cathode to ground (PEI positive connection).

Diodes are installed between the capacitor bank side (electrical) of the charging choke and each capacitor cell of the bank. Their purpose is two-fold. First, they provide isolation of the PEIs to prevent the delivery of stored energy from the capacitor bank into any fault that may occur in the charging supplies. Their second purpose is to provide isolation from cell to cell, preventing stored energy delivery into a faulted cell from the remainder of the capacitor bank. The diodes are of modular construction and are installed in sets of three on water-cooled heat sinks. The assemblies are located between the capacitor support structure and the G-10 SCR panel, in each quadrant, near the floor of the enclosure.

4.3.4.5 Electrical Safety

Bleeder Resistor P.C. Board

When the capacitor bank is configured with series pairs (2.6 or 5.2?msec) of capacitors, bleeder resistor boards must be installed as a safety measure. The low side terminal of all series pairs is grounded via the high current bus in each capacitor row. The high side terminal of the pair will be grounded when the LOTO procedure is carried out to completion. The mid-point between the capacitors, however, is not grounded and could retain a charge relative to ground. The installation of the bleeder resistors (100 kOhm) will provide a leakage path to effect discharge of any remaining stored energy after the system is shut down. Additionally, bleeder resistors will prevent any accumulation of stored charge from incidental energy sources. The resistance value is high to keep power loss in the aggregate of the bleeder networks to an acceptable level. Redundancy for safety is established on each PC board by the use of four resistor elements connected in a bridge configuration, two in series by two in parallel with the mid point of the series resistors connect together. Hence, two resistors must fail before the bleeder network becomes inoperative.

The time required to achieve full discharge is equal to five R-C time constants (63 minutes). The bleeder resistors are not to be relied upon to discharge the capacitor bank for maintenance purposes. LOTO procedures must be followed before any maintenance is to be performed within the capacitor bank enclosure or the PEI power supplies.

Energy Dump Resistors and Shorting Relays

A separate dump resistor is installed for each capacitor cell and is connected to a common shorting (grounding) relay, maintaining the cell-to-cell isolation necessary for safety. A second identical set of resistors and shorting relay is also installed to provide redundancy. These resistors are air-cooled and rated to absorb 27 kJ each, sufficient for the maximum stored energy of system operation with greater than a factor of two safety margin. When system shutdown occurs during a charge cycle, or an interlock interrupts normal cycling, energy stored in the capacitors will be switched by the shorting relay into the dump resistors where it will be safely dissipated.

Ground-sticks

A pair of ground-sticks is provided on each side of the capacitor bank enclosure, secured to the inside of one of the center bay doors. One of the pair includes a resistor assembly that will limit potential discharge current to a safe level. The 'hard-ground' stick does not use resistors. The two ground-sticks are inserted into the retaining mounts on the center bay door of one side of the enclosure. The storage points on the doors are equipped with interlock switches to assure the system is not energized while a ground-stick may be applied to the capacitor bank circuitry. When the ground-sticks are stowed it is essential they be fully seated in the holders in order to make-up the interlocks.

4.3.4.6 Controls

General Description

The control system was established as a joint development effort between the NuMI and MiniBoone projects since the two systems are similar in most requirements. Some functions required by the MiniBoone system are not used for NuMI. Hence, some LEDs are not illuminated during normal operation when in use for the NUMI horn system. The controls system consists of five plug-in modules in a rack-mounted frame. Two modules of the same model are used to monitor current and voltage balance in the capacitor bank, however they are not interchangeable due to different calibrations for the respective functions. A separate chassis mounted just below the controls chassis provides DC power for the control modules.

Monitored system parameters:

1. Output current of each cell to 0.4 % or better
2. Current in each transmission line pair
3. Current imbalance between stripline pairs
4. Total output current
5. Capacitor voltage in each cell
6. Capacitor bank over voltage and over current
7. PEI over current
8. Ground faults
9. Over temperature conditions of horns
10. Coolant flow loss to horns, PEIs, capacitor bank
11. Capacitor over-pressure
12. Equipment entry

The local resident power supply controller, beside permitting local operation of the equipment separate from control-room operators, is to monitor all of the operating parameters watching for of limit conditions and safely shutting the system down when such condition are detected. All safety related interlocks would be by hardware. We do not depend on software of personnel safety. There is no other solid-state device that even comes close to the switching capability and ruggedness of SCRs. It has be recognized that the very nature of SCRs is that once triggered there is no way to turn them off other than there being an occurrence of a subsequent 'current zero. We will, however, detect any and every fault in the equipment and turn it off to prevent a second pulse.

4.3.4.7 Cooling System

Figure 4.3-6 shows the capacitor bank water system schematic. With two exceptions, all the heat generating components, resistors, charging choke, diodes and SCRs associated with the capacitor bank in the enclosure, are cooled directly by water. The first exception is the capacitor energy dump resistors, which operate only momentarily when the system is turned off or the interlock system interrupts normal operation. Consequently, a negligible amount of additional heat is dissipated within the enclosure from these resistors. The second exception is the stripline. It is convection cooled and releases its heat to the air within the enclosure. A cooling water supply temperature of 95˚F, contributing some heat to the enclosure, plus the heat given off by the stripline serve to keep the enclosure internal temperature well above the ambient dew point during operation. This heat is conducted through the capacitor bank enclosure walls and radiated to the exterior environment.

Water Flow, typical:

Capacitor bank	9 gpm @ 80 psi differential
PEI, each	6 gpm @ 80 psi differential
Δp Switch setting	60 psi, PEIs and Cap.Bank, each

Water is carried either by copper pipe or Nylo-Seal® nylon tubing. Nylo-Seal has a working pressure rating of 400 psi., and a burst pressure rating of 1200 psi. Swagelok and Parker fittings

are used throughout for the plastic tubing. Flow balancing valves are installed internal to the enclosure to establish the flow rate to the various parallel water paths. A self-regulating flow control valve controls the total water flow rate for the capacitor bank. The 10-gpm device is

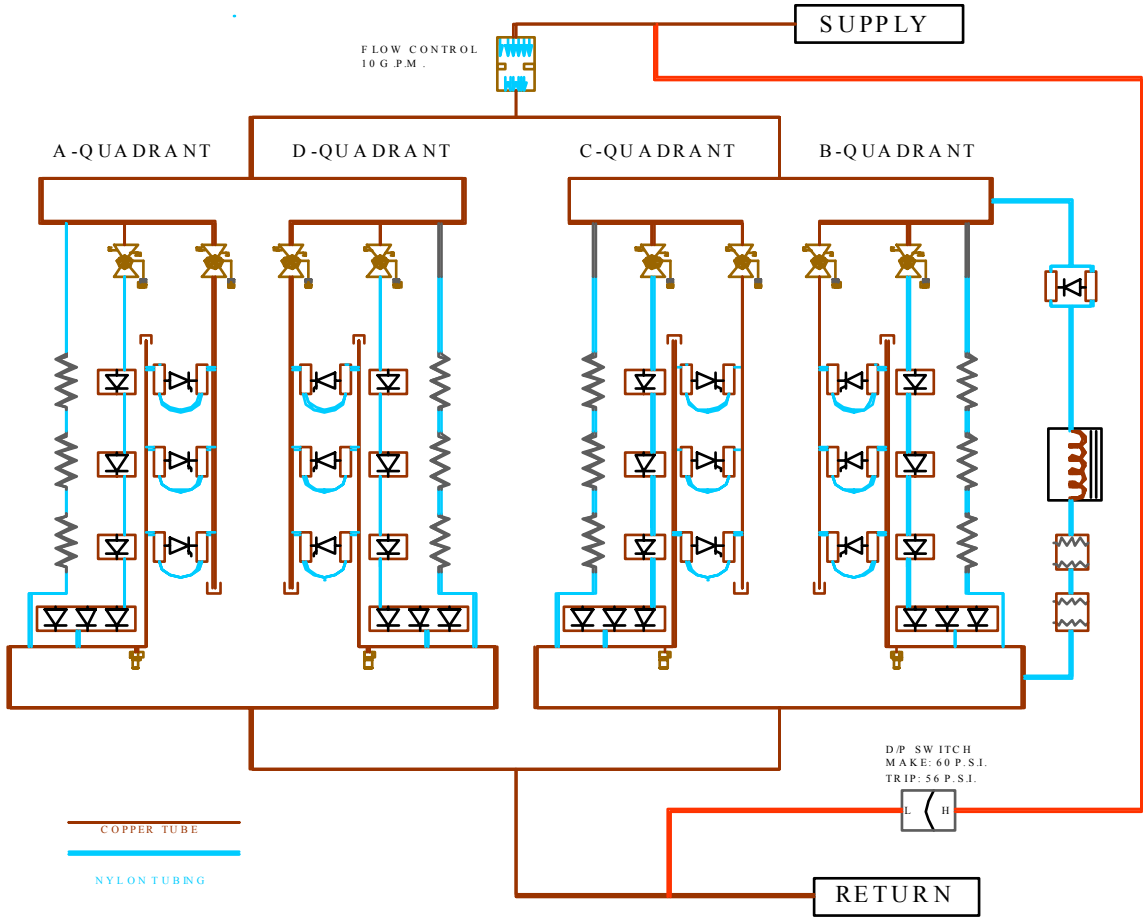

installed in the supply side water line.

Figure 4.3-6: Capacitor bank water system schematic. (See Drawing #9820-MC-370054 for complete information and symbol key.)

4.3.4.8 Mechanical Design

Enclosure

The enclosure is constructed to Fermilab specifications per FNAL drawing number 2782.000-ME-314551. It measures 75" high x 210" long x 69" wide. We have specified a cabinet constructed of 14 Ga. steel to offer an added layer of personnel protection. It is constructed of mild steel and built in three sections; a center section housing the SCR switch assembly, and the two identical capacitor bank sections, one on either side of the center unit. All are constructed as a floor pan and a roof pan, separated vertically by mullions that form the corners and supports for the enclosure doors. The sections have mating flanges secured by multiple bolts to make up the complete enclosure. In the area adjacent to each flange bolt the steel has been left un-painted and silver-plated by the enclosure vendor. The plated areas were coated with moisture excluding

grease prior to assembly to preserve optimum electrical contact between the enclosure sections. All sides of the enclosure are equipped with doors to allow full access to internal components. The door mullions in front of the capacitors in each quadrant are removable to facilitate capacitor replacement. **Table 4.3-17** lists the enclosure mechanical parameters.

Length	209 inches, (5.31 m), without doors installed
Width	70 inches, (1.78 m), without doors installed
Height	79 inches, (2 m), [81" including C-channel]
Weight	22,000 lbs., (10,000 kg)

Table 4.3-17: Enclosure Mechanical Parameters

All doors are readily removable, with the exception of the two doors on the end of the enclosure adjacent to the output stripline. By necessity those two doors have been modified to slide on tracks, rather than swing, and are not easily removed.

Oil containment

The most likely capacitor failure mode, in terms of oil leakage, is the loss of seal under one or more bushings. Placing capacitors with their bushings "up" would be the preferred orientation, negating any leakage concerns. However, to facilitate removal and replacement and to permit a compact design that could be lowered as an assembled and tested unit into the underground cavern, the capacitors are mounted horizontally with their bushings toward the outside of the enclosure. The two-inch lip-height of the floor pans in the capacitor sections of the enclosure provides 14 gallons of potential oil containment in the event of capacitor leakage. The capacitors used in the capacitor bank are impregnated with rapeseed (Canola) oil, a biodegradable vegetable oil. Each capacitor contains approximately 2.5 gallons of oil. Therefore, as many as 5 units in either enclosure end-section could spill their entire contents without exceeding the oil containment capacity for that section.

All penetrations in the enclosure floor pans have been sealed or curbed to prevent leakage to the outside. With any capacitor losing oil, it is likely that electrical failure of the capacitor will follow at some point. Any capacitor electrical failure will contribute to a current imbalance of the capacitor bank output and eventually be detected by the local controls, resulting in shutdown of the power supply system.

Capacitor Support Structure

The capacitors constitute 50% of the total weight of the enclosure assembly. During transport the structures supporting the capacitors in each quadrant are lifted directly via the four hoist rings on top of the enclosure. Each hoist ring is rated for 10,000 lbs vertical lift capacity. Internal and external structural members cross brace the capacitor supports to allow transport of the capacitor bank as a single unit. The balance of the weight of the components within the enclosure is carried through the enclosure structure to the capacitor supports. The 1" thick G-10 panels that mount the switching SCRs in each quadrant also serve as torsional webs to give the enclosure torsional stiffness.

Ground-cable Penetration

Ground cables connecting the capacitor bank low-side terminal to the horn modules, via the LEM, for ground fault detection exit the enclosure through a curbed hole in the base of the enclosure on the output stripline end. The purpose of this curb is to maintain the oil containment capability of the enclosure floor pan. The cable opening is sufficiently large to allow for the installation of two 900-mcm-ground cables with some room to spare. The excess opening should be sealed off after the installation in the underground power supply room to prevent the entrance of vermin.

4.3.5. Transmission Line

4.3.5.1 Overall Design and Specifications

A parallel strip transmission line is used to connect the power supply to the horns. The circuit is a damped LC discharge circuit that reaches peak current when the SCR switch releases stored energy from the capacitor bank to the horns via the transmission line. A transmission line consisting of a four-layer assembly of two parallel plates is necessary to connect the output of the power supply system to the horns. **Figure 4.3-7** and **Figure 4.3-8** show the layout and dimensions of the transmission line. In **Figure 4.3-8** the upper portion of figure shows the stripline cross section at a typical joint, held at 28,000 lbs by the spring style bar clamp. The lower portion of figure illustrates the mid-line style of aluminum bar clamp. An insulator separates each pair of aluminum alloy bus conductors. Aluminum spacers separate adjacent pairs. Inside the Target Hall beamline shield the insulation is a 1cm air gap with TS ceramic spacers. Outside the shield, Kapton polyimide insulation of 0.5 mm total thickness is used. The completed assembly is held in compression by ceramic sleeved through bolts at the spacer locations and compression clamps in the region where Kapton is used (if it is used). This configuration yields an equivalent transmission line width of 1.2 meters in a compact cross section. **Table 4.3-18** lists estimated transmission line dimensions and parameters.

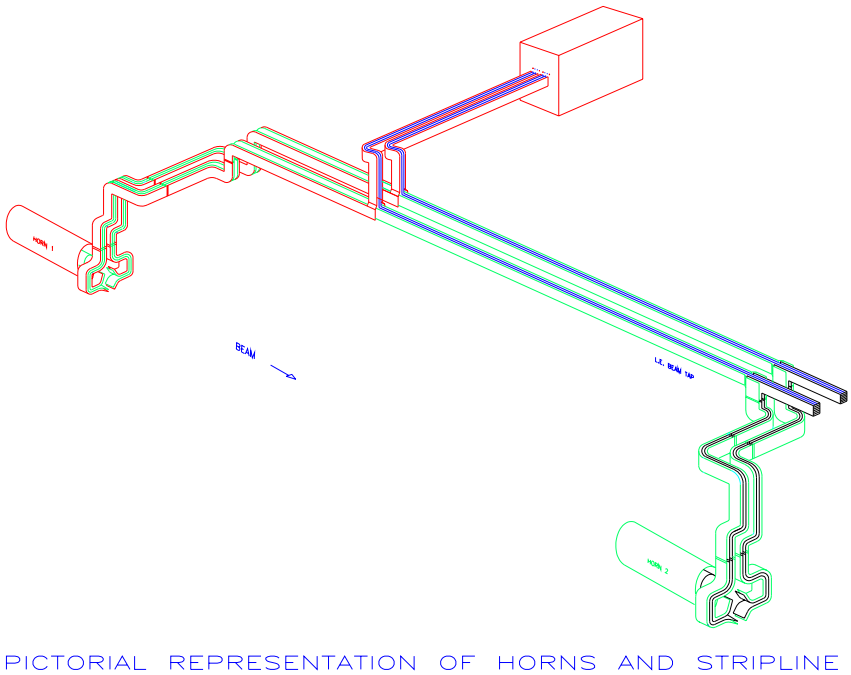

Figure 4.3-7: Stripline Pictorial Representation

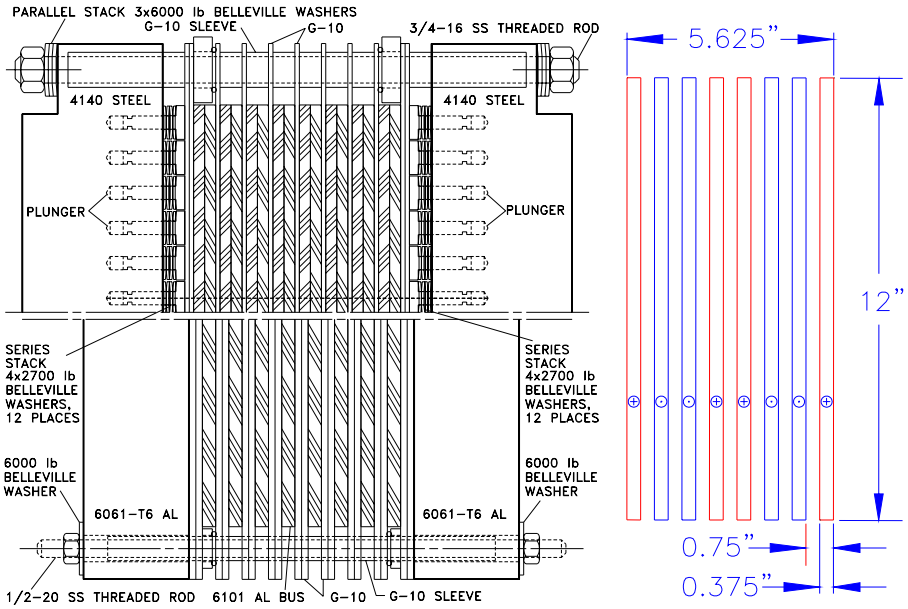

Figure 4.3-8: Stripline Drawing and Pictorial Cross Section.

The transmission line must deliver 200 kA (average, ± 2.5%) pulses every 1.9 seconds to the horn. As a safety margin the power supply system, including the transmission line, is designed to operate at up to 240kA. This results in a system load current of 7250 A_{rms} operationally (8700 A_{rms} design). The estimated circuit parameters were listed in **Table 4.3-13**. These calculated load values include effects of DC resistance, skin effect, temperature, transmission line conductor cross section and spacing.

Conductor material	6101-T61 Aluminum alloy
Conductor width	12 inches, (30.5 cm)
Conductor width at horn joints	8 inches, (20.3 cm)
Conductor thickness	0.375 inches, (0.953 cm)
Conductor spacing	0.375 inches, (0.953 cm)
No. parallel pairs	4
Inductance @ 100Hz	4.9 nH/ft., 16 nH/m of length
Resistance @ 100Hz	3.05 uΩ/ft., 10 uΩ/m of length
Power loss, 2.6 mS	80 W/ft., 260 W/m of length
Power loss, 5.2 mS	160W/ft., 530 W/m of length

Table 4.3-18: Transmission Line Parameters

The transmission line is a 12,000 lb. structure and thus its support is non-trivial. The transmission line is in approximately 20' long sections. Transmission line joints are to be welded except where connection/disconnection is needed. One piece of the transmission line runs across from the Target Hall to the horn power supply room (see **Figure 4.3-9**). The second long piece of the transmission line runs along the Target Enclosure to the horns. Disconnects/connects are will be located in the horn power supply room, in the Target Hall where the transmission line emerges from the penetration, above the shielding at each horn and inside the shielding at each horn.

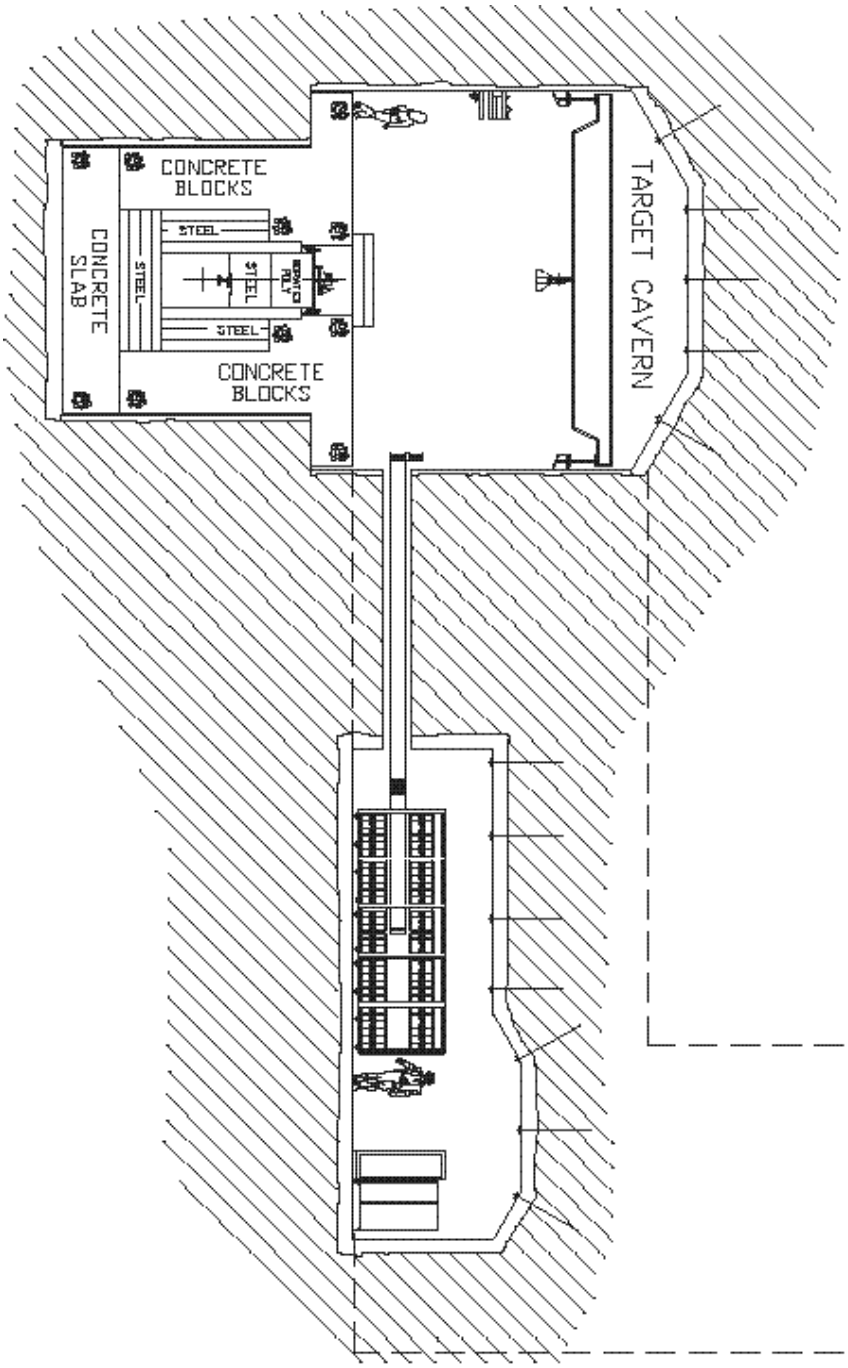

Figure 4.3-9: Target Hall and Power Supply Room Cross Section Conceptual Drawing

Transmission Line Cooling:
The target chase is cooled by 28,000 cfm flowing in the beam direction in the horn region. The beam heating in this region is less than 183 KW/m^3. The electrical heating is estimated at ~27 KW/m^3. For the stripline between the remote disconnect clamp block and the horn, the air flow through the target pile for the target pile cooling provides satisfactory cooling of the stripling to

remove the energy deposited from beam heating and from i^2r losses. The thermal analysis results are shown in **Figure 4.3-10**. The highest temperatures seen are 88°C at 4E13 ppp.

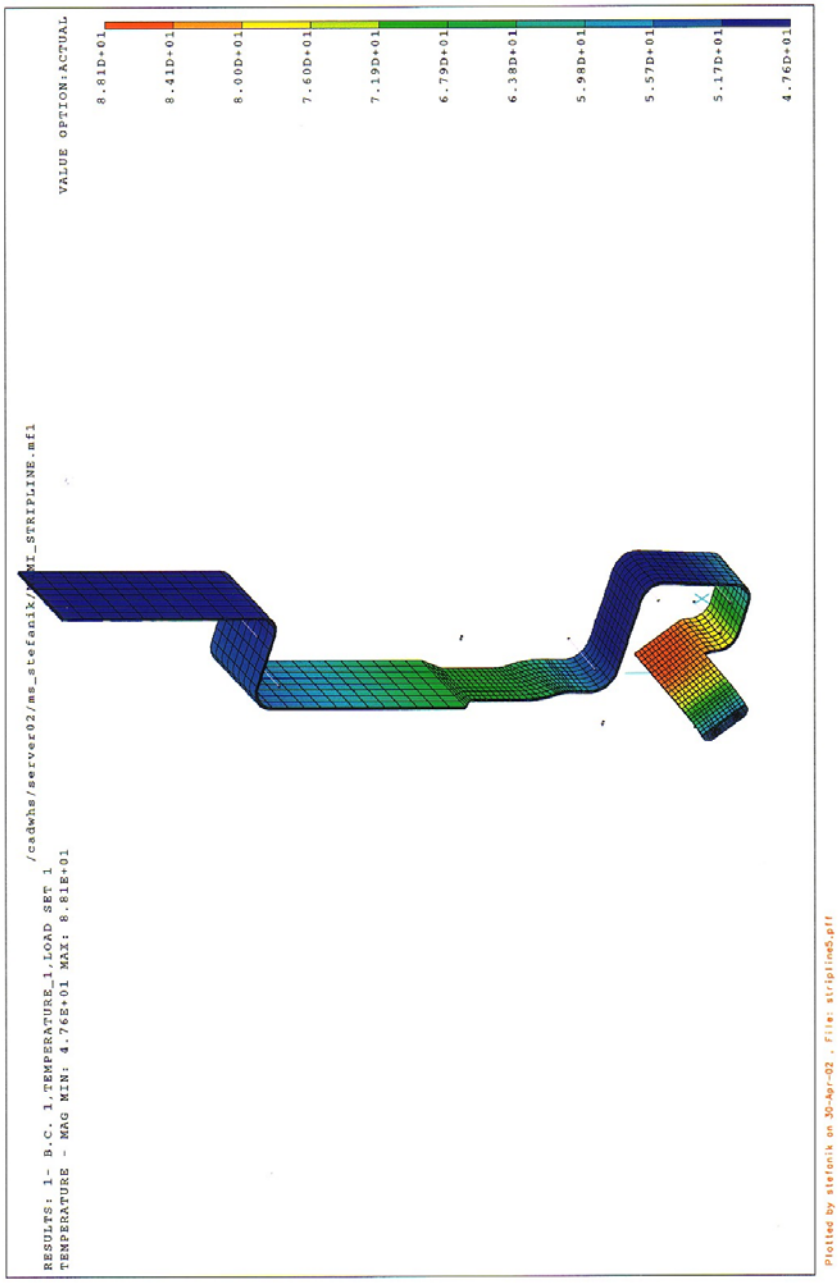

Figure 4.3-10: Transmission Line Beam Heating with AirFlow, Horn 1 Region

4.3.5.2 Transmission Line Joints

The transmission line joint, where the transmission line connects to the horns, is a complicated region. **Figure 4.3-11** and **Figure 4.3-12** show the plan and elevation view for the design in the area. The eight strips of the transmission line must connect to the bell shape of the horn. For horn 1, some amount of movement (+/- 3 mm horizontally and/or vertically) is desired also.

This area will become highly radioactive and thus the desire is to have the joints last as least as long as the horns do. Add to this that they will be pulsed every 1.9 seconds with 200 kA, which causes some amount of vibration and one can see the difficult issues with this area of the design.

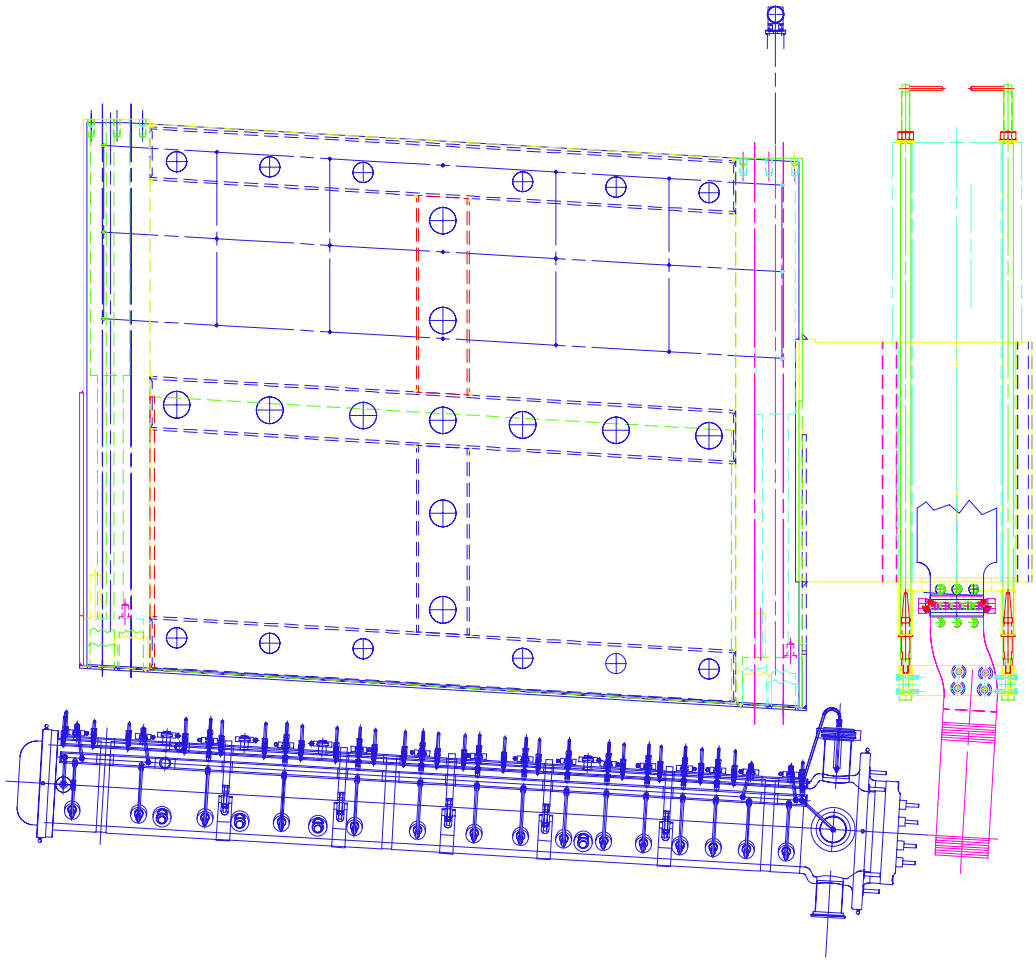

Figure 4.3-11: Horn, Remote Clamp and Transmission Line Elevation View

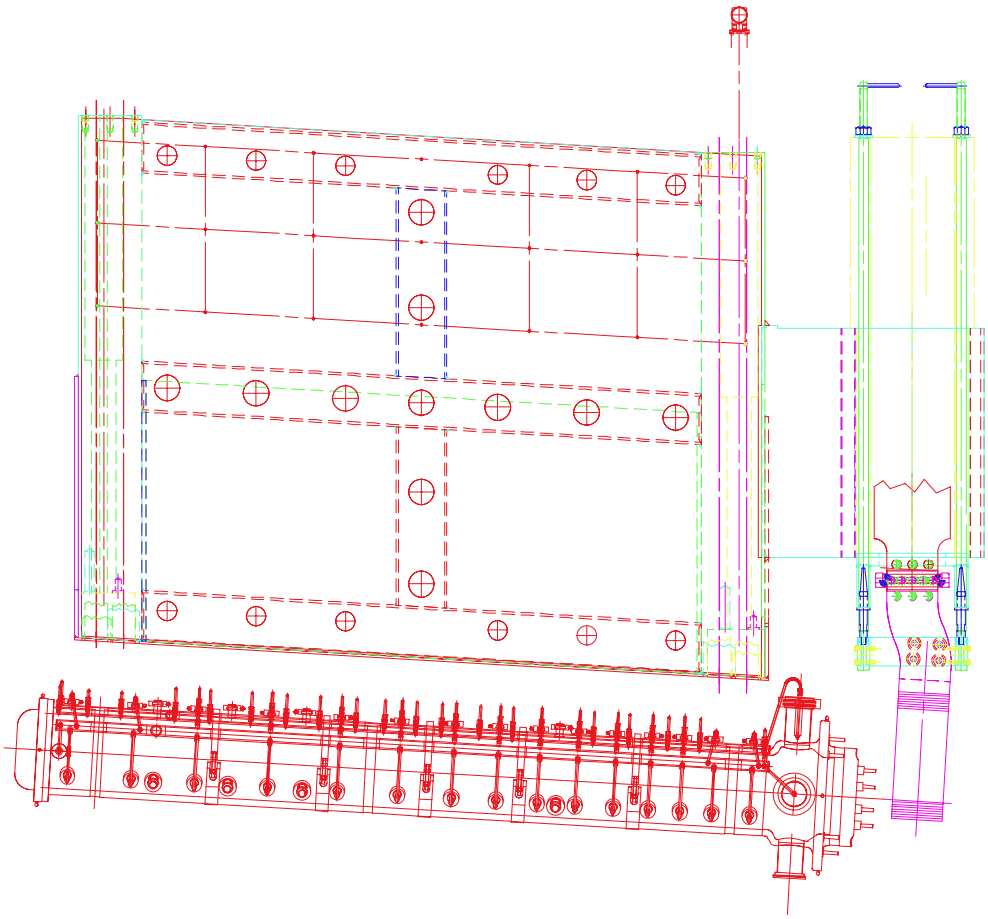

Figure 4.3-12: Horn, Remote Clamp and Transmission Line Cross Section

Fatigue Lifetime:
The part of transmission line connected to horn, the joint, will be replaced each time a horn is replaced. The horns are designed to last at least 10 million pulses. Thus the joints are designed to last 10 million pulses also. The horn fatigue lifetime safety factor for 10 million pulses is about 3.5. The maximum force desired on the horn upon displacing horn 1, is ~ 400 lbs. A fatigue lifetime safety factor similar to that of horn 1 is desired with this design. ANSYS analyses have been completed on the horn 1 joint design, using the appropriate thermal loads (88°C), magnetic loads, and the maximal (3mm) offsets. They indicate a fatigue lifetime safety factor at least as large as that for the horns.

The horn 2 joint is based on the same design as the horn 1 joint, but scaled up to horn 2 dimensions. ANSYS results show that it is flexible enough to accommodate the expansion of horn 2. Horn 2 expands 0.033 cm and the ANSYS results show a maximum force of ~ 50 lbs on the horn.

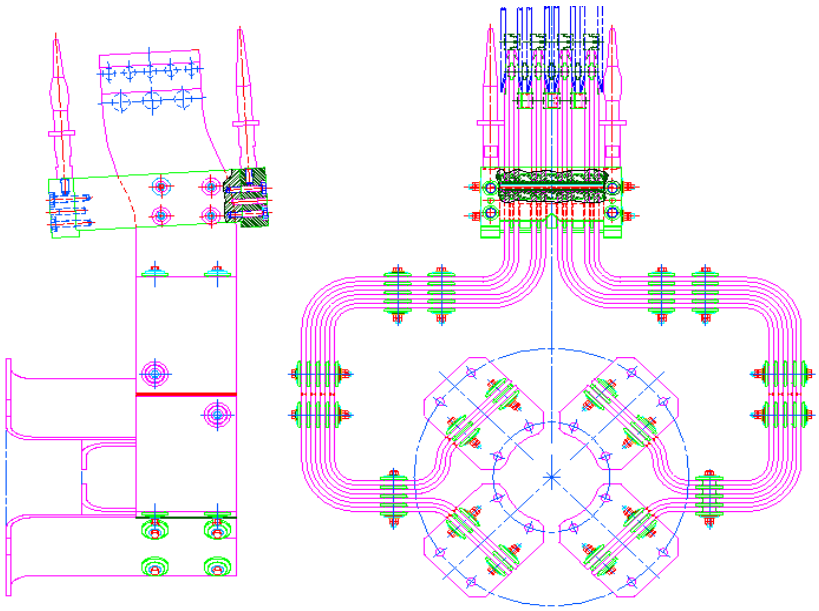

Figure 4.3-13**: Horn 1 Joint Cross Section and Elevation**

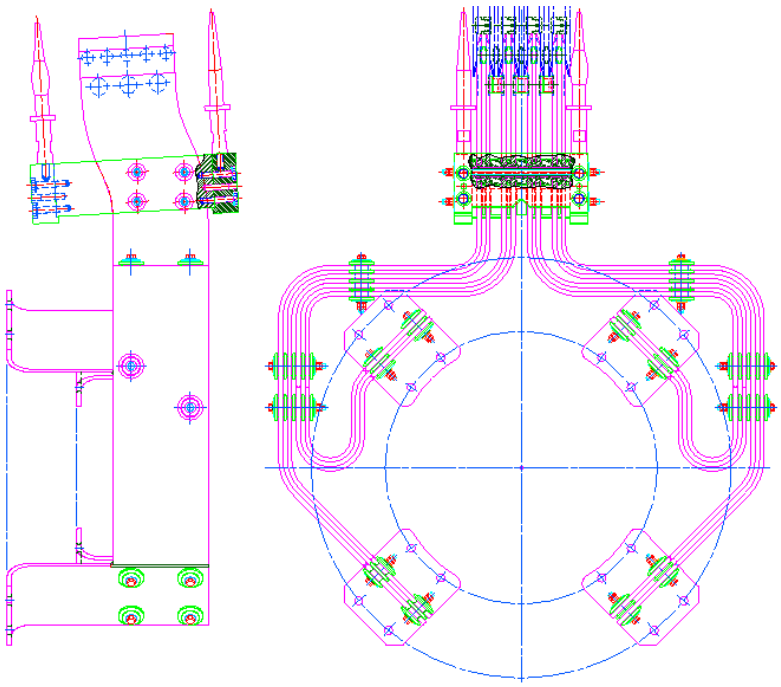

Figure 4.3-14: **Horn 2 Joint Cross Section**

4.3.5.3 Transmission Line Routing through the Shield Block and Beyond

The transmission line joint fingers connect with the transmission line section through the shield block at the remote clamp, as shown in **Figure 4.3-12**. The routing through the block is such to minimize weight and residual activation levels at the top of the block. Clamps and snubbers are used to minimize vibration. There are "quick" disconnecting joints at the remote clamp at the bottom of the module, at the top of the module, and beyond the edge of the T-blocks. In this manner, one can remove the section of stripline from top of module to beyond the module sides. Then one can remove the T-blocks, and the stripline-stuffing block. Next one removes the horn with transmission line joint and remaining stripline part in the module to work cell for replacement. At the work cell, one disconnects the section routed through the module from the joint and horn by disengaging the remote clamp.

The part of the stripline within stripline block (including the clamp) does not have to be replaced every time a horn is replaced. It is designed to last the lifetime of NuMI (10 years). The concern is that the fingers of the transmission line will "weld" together or somehow the remote clamp will not be able to disengage the transmission line and horn from the remainder of the assembly. Thus the stripline block is bolted together such that the transmission line internal to the transmission line block can be removed and replaced.

Airflow through stripline stuffing block from top of module to horn cannot be obstructed (this airflow cools stripline). However, an air dam is needed at the H-block cover between the module and the stripline along the target hall wall (this is a lower radiation area, so a wider choice of materials is available). The air dam is intended to contain air-borne radiation.

The transmission line along the target hall wall will be covered with a sloping "roof" to keep people from leaning on it or putting items on it. This will also help minimize the accumulation of dust and dirt on it.

4.3.5.4 Transmission Line Internal to the Horn Power Supply

The internal stripline of the capacitor bank is constructed of 1/4" x 12" copper extruded bus. Provision is also made to allow the output current direction to be reversed by the exchange of "jumper" placement. The output stripline is that section leading from the center bay of the capacitor bank to the outside of the enclosure. It is constructed of 3/8" x 12" 6101-T6 aluminum electrical bus conductor alloy.

The assembly of eight conductors, four conductor pairs, is held together by bar type compression clamps and utilizing G-10 insulating spacers between layers. The clamps are spaced at 12-inch intervals. The assembly is supported from an aluminum I-beam running the length of the enclosure. The I-beam serves two purposes. It serves as a spreader bar when the enclosure is being lifted by a crane for transport, but more importantly it facilitates the removal of the output stripline should it become necessary for repair or replacement. In the cavern installation, the output (stripline) end of the capacitor bank is closely positioned with respect to the cavern wall, preventing removal of the output stripline on that end of the enclosure. The stripline suspension incorporates a jacking mechanism and is equipped with rollers that trolley on the I-beam, allowing the suspension and stripline to pass through the enclosure and out the opposite end.

Pre-drilled holes in the I-beam flanges at each end allow extensions to be coupled and secured to the beam, as needed, to extend trolley travel.

4.3.5.5 Compression Clamps and Stripline Contacts

At locations where it is necessary to couple/decouple the eight-layer stripline, a special compression clamp is utilized. The clamp incorporates twelve spring-loaded pistons in each bar to establish equal pressure across the width of the stripline conductors. The spring on each piston is comprised of a series stack of 2,700 lb. rated conical (Belleville) compression washers. The clamp assembly is capable of 30,000 lbs. total clamping force.

4.3.6. Power Supply Cables

Table 4.3-2 through **Table 4.3-4** give the number, type, and approximate length of the cables needed for the power supplies, with the exception of the RG220 cable that is used for the kicker power supply. Klixon cables are not shown in this table, but are installed in the same manner as elsewhere at FNAL. All cables in new construction will be fire retardant.

4.3.7. Performance Monitoring Plan

For the kicker and horn power supplies, the predicted line locked ripple will not noticeably affect the beam dynamics, and Autotune will correct slow drifts. Other power supplies will have regulation as described in Section 0. All power supplies will also be continually monitored by the ACNET alarm system (with tolerances set appropriately). These alarms plus logged data will point out required power supply repairs. All supplies will have current error detectors, which will inhibit beam if the supply is not tracking the ramp.

4.3.8. References

The following references need to be made into NuMI notes.

Zhijing's Notes

Horn PS Manual (too large?)

Safety Docs for MI8

T

Table 7: NuMI POWER SUPPLY REQUIREMENTS

Ramp Cycle Time: 1.9 seconds 04/17/02

CIRCUIT(ACNET if different then CKT Name)	MAGNET TYPE	# MAGs	MAG. IND. (henry)	MAG. RES. (ohms)	MAG. Max. Pwr. (kW)	CABLE TYPE kcmil	CABLE # 1 way	CABLE R/kFt ohms	CABLE L (ft)	CABLE RES. ohms	Passive Filter R ohms	Passive Filter L henry	Total Res. ohms	Total Ind. henry	PEAK CURR. (amps)	Min. Curr. (amps)	dI/dT (A/s)	PEAK VOLT. (volts)	RMS CURR. (amps)	Power per Mag. (kW)	PEAK PWR (kW)	Power Supply TYPE #, Man./Pwr	Power Supply Volt (volts)	Power Supply Curr. (amps)	Power Supply PS Loses (kW)	Total RMS PWR (kW)	Fdr Load kVA	Peak Fdr kVA
MI60 Power Supplies																												
Kicker (I:KPS6N))	kicker	3																										
LAMB (I:LAM601)	Lamb.	1	0.017	0.0130		500	2	0.026	132	0.0034	0.002	0.001	0.018	0.018	765.85	0	note 7	200	400	2	153	**1, Xrex/500kW**	**200**	**2500**	4.00	7	112	214
LAMB (I:LAM6023)	Lamb.	2	0.017	0.0130		500	3	0.026	154	0.0027	0.002	0.001	0.031	0.035	1806.25	0	note 8	200	794	8	361	**1, Xrex/500kW**	**200**	**2500**	7.94	27	222	506
CMAG (E:V100)	Cmagnet	1	0.002	0.0070		500	5	0.026	165	0.0017	0.002	0.001	0.011	0.003	3482.5	0	note 7	50	1560	17	174	**1, Xrex/500kW**	**50**	**5000**	3.90	30	109	244
E:Q101	3Q120	1	1.500	2.2500	24.1	1/0	1	0.125	98	0.0245	0.000	0.000	2.274	1.500	64.64	64.64	0	147	65	9	10	1, PEI/20kW	200	100	0.65	10	18	18
BND1(E:HV101)	EPB	6	0.030	0.0175	50.0	500	3	0.026	244	0.0042	0.002	0.001	0.111	0.181	1645.67	0	note 7	600	914	15	987	**3, Xrex/500kW**	**600**	**2500**	27.42	120	768	1382
E:HT102	MI Corr.	1	0.950	4.4000		10ga	1	1.2	197	0.4719	0.000	0.000	4.872	0.950	25	0	26	147	14	1	4	MI DipoleTrim	150	15	0.11	1	3	5
E:Q102	3Q120	1	1.500	2.2500	24.1	1/0	1	0.125	148	0.0371	0.000	0.000	2.287	1.500	64.64	64.64	0	148	65	9	10	1, PEI/20kW	200	100	0.65	10	18	18
E:Q103	3Q120	1	1.500	2.2500	24.1	1/0	1	0.125	206	0.0514	0.000	0.000	2.301	1.500	72.36	72.36	0	167	72	12	12	1, PEI/20kW	200	100	0.72	13	20	20
E:VT103	MI Corr.	1	0.950	4.4000		10ga	1	1.2	267	0.6397	0.000	0.000	5.040	0.950	25	0	26	151	14	1	4	MI DipoleTrim	150	15	0.11	1	3	5
E:Q104	3Q60	1	1.100	1.6000	17.0	1/0	1	0.125	225	0.0562	0.000	0.000	1.656	1.100	33.68	33.68	0	56	34	2	2	1, PEI/20kW	100	200	0.17	2	5	5
E:H104	200 Turn SY Trims	1	1.500	2.2500	24.1	1/0	1	0.125	250	0.0625	0.000	0.000	2.313	1.500	80	80		185	80	14	15	1, PEI/20kW	200	100	0.80	16	22	22
E:HT105	MI Corr.	1	0.950	4.4000		10ga	1	1.2	301	0.7227	0.000	0.000	5.123	0.950	25	0	26	153	14	1	4	MI DipoleTrim	150	15	0.11	1	3	5
E:Q105	3Q120	1	1.500	2.2500	24.1	1/0	1	0.125	253	0.0632	0.000	0.000	2.313	1.500	60.04	60.04	0	139	60	8	8	1, PEI/20kW	200	100	0.60	9	17	17
E:VT106	MI Corr.	1	0.950	4.4000		10ga	1	1.2	358	0.8584	0.000	0.000	5.258	0.950	25	0	26	156	14	1	4	MI DipoleTrim	150	15	0.11	1	3	5
E:Q106	3Q120	1	1.500	2.2500	24.1	1/0	1	0.125	310	0.0774	0.000	0.000	2.327	1.500	60.04	60.04	0	140	60	8	8	1, PEI/20kW	200	100	0.60	9	17	17
E:HT107	MI Corr.	1	0.950	4.4000		10ga	1	1.2	414	0.9941	0.000	0.000	5.394	0.950	25	0	26	160	14	1	4	MI DipoleTrim	150	15	0.11	1	3	5
E:VT108	MI Corr.	1	0.950	4.4000		10ga	1	1.2	471	1.1298	0.000	0.000	5.530	0.950	25	0	26	163	14	1	4	MI DipoleTrim	150	15	0.11	1	3	5
E:HT109	MI Corr.	1	0.950	4.4000		10ga	1	1.2	527	1.2655	0.000	0.000	5.666	0.950	25	0	26	167	14	1	4	MI DipoleTrim	150	15	0.11	1	3	5
E:VT110	MI Corr.	1	0.950	4.4000		10ga	1	1.2	583	1.3993	0.000	0.000	5.799	0.950	25	0	26	170	14	1	4	MI DipoleTrim	150	15	0.11	1	3	5
E:VT111	MI Corr.	1	0.950	4.4000		10ga	1	1.2	646	1.5503	0.000	0.000	5.950	0.950	25	0	26	174	14	1	4	MI DipoleTrim	150	15	0.11	1	3	5
E:HT112	MI Corr.	1	0.950	4.4000		10ga	1	1.2	662	1.5884	0.000	0.000	5.988	0.950	25	0	26	175	14	1	4	MI DipoleTrim	150	15	0.11	1	3	5
																							MI60N Power Totals:		49	**266**	**1359**	**2516**
MI62 Power Supplies																												
E:Q107	3Q120	1	1.500	2.2500	24.1	1/0	1	0.125	662	0.1655	0.000	0.000	2.416	1.500	60.04	60.04	0	145	60	8	9	1, PEI/20kW	200	100	0.60	9	17	17
E:Q108	3Q120	1	1.500	2.2500	24.1	1/0	1	0.125	637	0.1593	0.000	0.000	2.409	1.500	60.04	60.04	0	145	60	8	9	1, PEI/20kW	200	100	0.60	9	17	17
BND2 (E:V109)	B2	6	0.008	0.0072	162.0	500	8	0.026	624	0.0041	0.002	0.001	0.049	0.049	4446.98	0	note 7	400	2360	40	1779	**MR - type**	**470**	**5000**	6.66	280	1553	2926
E:Q109	3Q120	1	1.500	2.2500	24.1	1/0	1	0.125	581	0.1452	0.000	0.000	2.395	1.500	60.04	60.04	0	144	60	8	9	1, PEI/20kW	200	100	0.60	9	17	17
E:Q110	3Q60	1	1.100	1.6000	17.0	1/0	1	0.125	525	0.1313	0.000	0.000	1.731	1.100	24.69	24.69	0	43	25	1	1	1, PEI/20kW	100	200	0.12	1	3	3
E:Q111	3Q120	1	1.500	2.2500	24.1	1/0	1	0.125	520	0.1300	0.000	0.000	2.380	1.500	55.99	55.99	0	133	56	7	7	1, PEI/20kW	200	100	0.56	8	16	16
E:Q112	3Q120	1	1.500	2.2500	24.1	1/0	1	0.125	542	0.1355	0.000	0.000	2.385	1.500	59.03	59.03	0	141	59	8	8	1, PEI/20kW	200	100	0.59	9	17	17
																							MI62 Power Totals:		9	**317**	**1622**	**2995**
																						minus MR PS/Xformer						
Upstream Service Building and Horn Power Supplies																												
E:Q113	3Q120	1	1.500	2.2500	24.1	1/0	1	0.125	732	0.1830	0.000	0.000	2.433	1.500	59.03	59.03	0	144	59	8	8	1, PEI/20kW	200	100	0.59	9	17	17
E:VT113	MI Corr.	1	0.950	4.4000		10ga	1	1.2	701	1.6829	0.000	0.000	6.083	0.950	25	0	26	177	14	1	4	MI DipoleTrim	150	15	0.11	1	3	5
E:HT114	MI Corr.	1	0.950	4.4000		10ga	1	1.2	692	1.6612	0.000	0.000	6.061	0.950	25	0	26	177	14	1	4	MI DipoleTrim	150	15	0.11	1	3	5
E:Q114	3Q120	1	1.500	2.2500	24.1	1/0	1	0.125	710	0.1776	0.000	0.000	2.428	1.500	55.99	55.99		136	56	7	8	1, PEI/20kW	200	100	0.56	8	16	16
E:HT115	MI Corr.	1	0.950	4.4000		10ga	1	1.2	637	1.5287	0.000	0.000	5.929	0.950	25	0	26	173	14	1	4	MI DipoleTrim	150	15	0.11	1	3	5
E:Q115	3Q60	1	1.100	1.6000	17.0	1/0	1	0.125	655	0.1638	0.000	0.000	1.764	1.100	24.69	24.69	0	44	25	1	1	1, PEI/20kW	100	200	0.12	1	3	3
E:VT116	MI Corr.	1	0.950	4.4000		10ga	1	1.2	590	1.4168	0.000	0.000	5.817	0.950	25	0	26	170	14	1	4	MI DipoleTrim	150	15	0.11	1	3	5
E:Q116	3Q120	1	1.500	2.2500	24.1	1/0	1	0.125	608	0.1521	0.000	0.000	2.402	1.500	80.98	80.98		195	81	15	16	1, PEI/20kW	200	100	0.81	17	23	23
E:HT117	MI Corr.	1	0.950	4.4000		10ga	1	1.2	518	1.2443	0.000	0.000	5.644	0.950	25	0	26	166	14	1	4	MI DipoleTrim	150	15	0.11	1	3	5
E:H117	200 Turn SY Trims	1	1.500	2.2500	24.1	1/0	1	0.125	518	0.1296	0.000	0.000	2.380	1.500	80	80		190	80	14	15	1, PEI/20kW	200	100	0.80	16	22	22
E:Q117	3Q120	1	1.500	2.2500	24.1	1/0	1	0.125	537	0.1341	0.000	0.000	2.384	1.500	64.14	64.14		153	64	9	10	1, PEI/20kW	200	100	0.64	10	18	18
E:VT118	MI Corr.	1	0.950	4.4000		10ga	1	1.2	497	1.1928	0.000	0.000	5.593	0.950	25	0	26	165	14	1	4	MI DipoleTrim	150	15	0.11	1	3	5
E:Q118	3Q120	1	1.500	2.2500	24.1	1/0	1	0.125	515	0.1288	0.000	0.000	2.379	1.500	71.22	71.22	0	169	71	11	12	1, PEI/20kW	200	100	0.71	13	20	20
BND3 (E:V119)	B2	4	0.008	0.0072	162.0	500	7	0.026	483	0.0036	0.002	0.001	0.034	0.033	4142.08	0	note 7	400	1945	27	1657	**4, Xrex/500kW**	**400**	**5000**	4.67	134	1089	2320
E:HT119	MI Corr.	1	0.950	4.4000		10ga	1	1.2	441	1.0591	0.000	0.000	5.459	0.950	25	0	26	161	14	1	4	MI DipoleTrim	150	15	0.11	1	3	5
E:Q119	3Q60	1	1.100	1.6000	17.0	1/0	1	0.125	459	0.1149	0.000	0.000	1.715	1.100	48.09	48.09	0	82	48	4	4	1, PEI/20kW	200	100	0.48	4	13	13
E:Q120	3Q120	1	1.500	2.2500	24.1	1/0	1	0.125	399	0.0997	0.000	0.000	2.350	1.500	73.63	73.63	0	173	74	12	13	1, PEI/20kW	200	100	0.74	13	21	21
E:Q121	3Q120	1	1.500	2.2500	24.1	1/0	1	0.125	405	0.1013	0.000	0.000	2.351	1.500	73.44	73.44	0	173	73	12	13	1, PEI/20kW	200	100	0.73	13	21	21
E:HT121	MI Corr.	1	0.950	4.4000		10ga	1	1.2	347	0.8327	0.000	0.000	5.233	0.950	25	0	26	156	14	1	4	MI DipoleTrim	150	15	0.11	1	3	5
E:VT121	MI Corr.	1	0.950	4.4000		10ga	1	1.2	345	0.8291	0.000	0.000	5.229	0.950	25	0	26	156	14	1	4	MI DipoleTrim	150	15	0.11	1	3	5
HORN PS	Horn	2	3.655	0.9320		stripline	1				0.000	0.000	0.001	3.655	300	0	316	700	300	84	210	**2, PEI/240kW**	**1000**	**300**	15.00	210	420	420
																						Upstream Service Building Power Totals:			**27**	**462**	**1710**	**2960**
Upgrade with Most Addtional Magnets: Narrow Band Beam (very rough guess at NBR,NBN parameters)																												
NBB1	EPB	2	0.030	0.0175		500	2	0.026	400	0.0104			0.045	0.060	1000	0	1053	109	577	6	109	**1, Xrex/500kW**	200	2500	5.77	21	162	280
NBR	NBR	1	0.030	0.0175		500	2	0.026	400	0.0104	-	-	0.028	0.030	1000	0	1053	100	577	148	100	**1, Xrex/500kW**	200	2500	5.77	15	162	280
NBN	NBB	1	0.030	0.0175		500	2	0.026	400	0.0104	-	-	0.028	0.030	1000	0	1053	100	577	78	100	**1, Xrex/500kW**	200	2500	5.77	15	162	280
Notes:																						**Additional NBB Upstream Service Building Power Totals:**			17	**51**	**485**	**840**
1. Assumptions for transrex-type power supplies:					Regulation: +/- .05%																	**Upstream Service Building Power Totals (w/NBB):**			44	**513**	**2195**	**3800**

4.4 DECAY TUNNEL AND HADRON ABSORBER (WBS 1.1.4)

4.4.1 Introduction

Producing a neutrino beam requires a region where the secondary beam pions, produced by primary beam protons hitting the target in the Target Hall, can decay to muons and neutrinos. After some distance, when a sufficient quantity of the pions have decayed, the pions need to be stopped so they do not contaminate the neutrino beam. So any general neutrino beam design needs a decay region followed by a beam absorber.

In the NuMI facility, the Target Hall is followed by the 675m long Decay Tunnel which holds this decay region. The Decay Tunnel holds the Decay Pipe which the particle beam passes through. To avoid a reduction of pions due to interactions in air, the Decay Pipe is a vacuum vessel. The Decay Pipe begins at the downstream end of the Target Hall, runs the entire length of the Decay Tunnel, and terminates in the Absorber Enclosure.

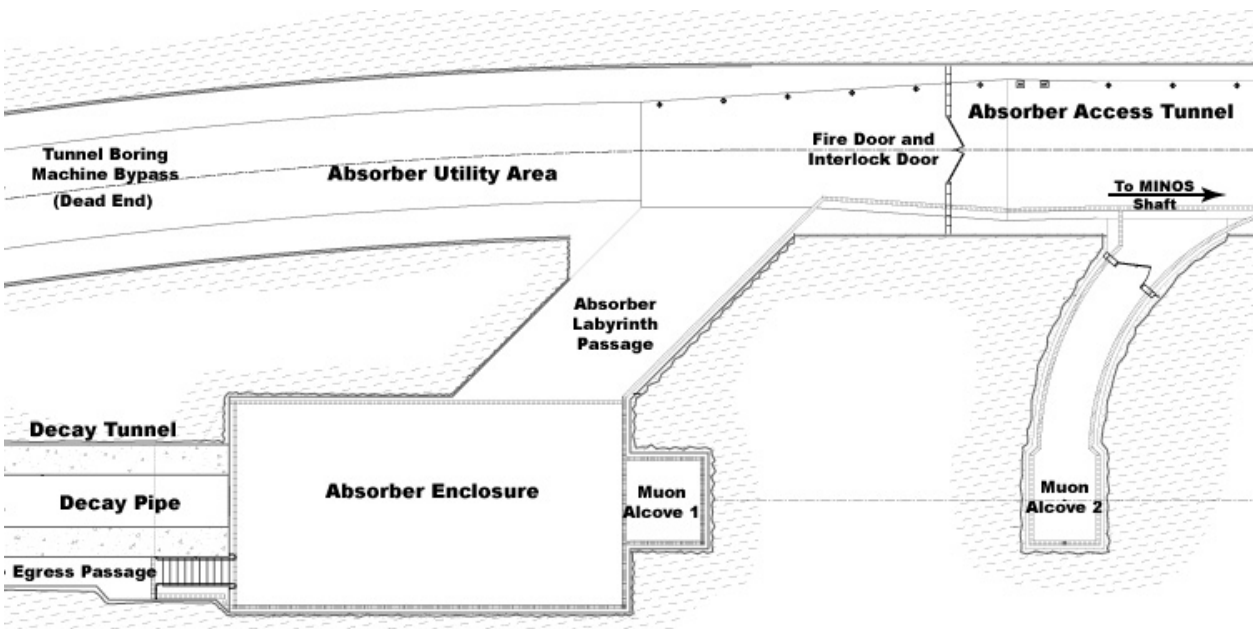

Fig. 4.4-01 : Layout of the Hadron Absorber Area. See text for description.

The Absorber Enclosure holds the Hadron Absorber, a beam dump made from a pile of aluminum, steel and concrete. All particles remaining in the beam at the downstream end of the Decay Pipe pass into the Absorber: primary protons which did not interact in the target, secondary pions which have not yet decayed, other secondary hadrons, and the muons and

neutrinos which result from pion decay. All the protons, pions and other hadrons interact in the material of the Absorber and their energy is deposited there as heat. The muons and neutrinos pass through the Absorber and continue on into rock. The muons range out in the rock and stop. To measure the decreasing numbers of muons, detectors are placed in muon alcoves – passages cut into the rock along the beamline. After some distance of rock, only the neutrinos remain, and these pass into the MINOS Hall at the very end of the tunnel excavation.

Figure 4.4-01 shows a layout of the Absorber area. The Absorber Enclosure a ~20-ft wide ~50-ft long ~40-ft high room; it is accessed from the MINOS Shaft elevator via the Absorber Access Tunnel. The tunneling machine which dug the Decay Tunnel was turned off the beam centerline upstream of the Absorber Enclosure, so as to allow the beam to pass through rock downstream of the Absorber Enclosure. This bypass tunnel was sealed with concrete when the Decay Tunnel shielding was poured, and is now a dead-end. The floor space in the bypass is used as utility area for the Decay and Absorber water pump and vacuum systems. A Labyrinth Passage connects the Access Tunnel to the Absorber Enclosure. The Labyrinth Passage is named for the concrete blocks placed there, which shield the Access Tunnel from slow neutrons which are emitted from the Absorber as a result of the beam deposited in it. A Controlled Access Interlock door is located at the fire door in the Absorber Access Tunnel, just downstream of the Absorber Enclosure.

4.4.2 System Description: Decay Tunnel and Decay Pipe

The decay tunnel is an approximately 22ft diameter excavation created by the tunnel-boring machine during the facility construction. The only beamline component within the tunnel is the Decay Pipe, a vacuum region where the produced pions decay to muons and neutrinos. The Decay Pipe is a 6-ft diameter steel pipe which runs the entire length of the tunnel, centered on the neutrino beam centerline; its basic parameters are given in Table 4.4-01. The pipe was made from sections 40-ft long, each with five stiffener-rings 3/8” wide and 5” tall in the radial dimension. Each pipe section was surveyed into place, held up by a supporting structure since it was positioned above the tunnel floor, and welded to its neighbors.

Inner Diameter	Wall Thickness	Length	Vacuum
1.98 meters	0.375 inch	677.1 meters	<1 torr

Table 4.4-01: Parameters describing the Decay Pipe

Once the pipe sections were in place, the Decay Tunnel was backfilled with concrete to shield groundwater from the particles which impact the walls of the pipe. Figure 4.4-02 shows a sample cross-section diagram of the Decay Tunnel. As shown, the tunnel was excavated and the concrete was formed so that a ~50-in wide egress passage remained along the east side of the original excavation; this passage provides emergency access between the upstream Target Hall areas and the downstream MINOS areas.

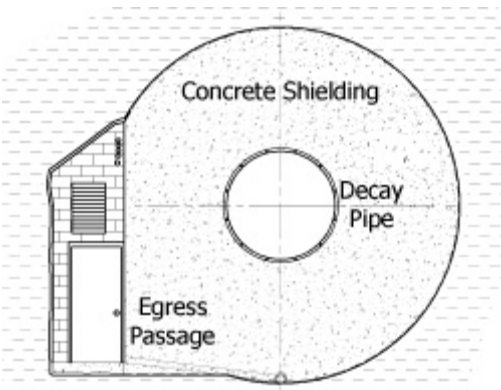

Fig 4.4-02 : A cross section of the Decay Tunnel, at midpoint. Portions of the Tunnel were enlarged from the initial 22-ft bore, to allow adequate space outside the shielding for the Egress passage.

The concrete shielding is not of a uniform radial thickness; it is thicker at the upstream end than at the downstream end, because more particles impact the sides of the Decay Pipe along the upstream end and more shielding was required there. See Table 4.4-02 for the shield thickness versus length down the tunnel. The effectiveness of the concrete shielding in protecting the groundwater is discussed in Chapter 5.

The particles which impact the sides of the pipe interact and create particle showers in the steel and the surrounding concrete. Heat is deposited as those particles are absorbed by these materials. An excessive amount of heat in the steel pipe might cause it to expand enough to crack the concrete shielding, and so copper cooling lines were installed along the length of the Decay Pipe, before the concrete was poured. Twelve lines were placed at 30° intervals of azimuth around the decay pipe. To prevent any chemistry between the steel pipe and copper lines, a thin insulator was placed between them. The cooling lines exit at each end of the Decay Pipe and are connected to a RAW circulating and heat exchanger system.

Length in meters along the Decay Pipe	50	150	350	425
Thickness of Shielding in inches	72	84	66	55

Table 4.4-02: Thickness of Decay Region Shielding versus location along the tunnel

The total energy deposited in the steel walls of the decay pipe and in the surrounding concrete was modeled using the MARS program, which simulates particle interactions in matter and is used to evaluate shielding designs. The MARS results are summarized in Table 4.4-03**.** Figure 4.4-03 shows the distribution of the energy deposition along the length of the decay pipe.

	Steel Decay Pipe	Concrete shielding		
		0-30 cm radius	30-60 cm radius	>60 cm radius
Low Energy Beam Configuration	kW	kW	kW	kW
	62.7	42.9	6.14	2.89

Table 4.4-03 Total energy deposition in kW in the decay pipe steel and the concrete surrounding the decay pipe, from MARS simulations of the NuMI beamline in low energy neutrino beam configuration.

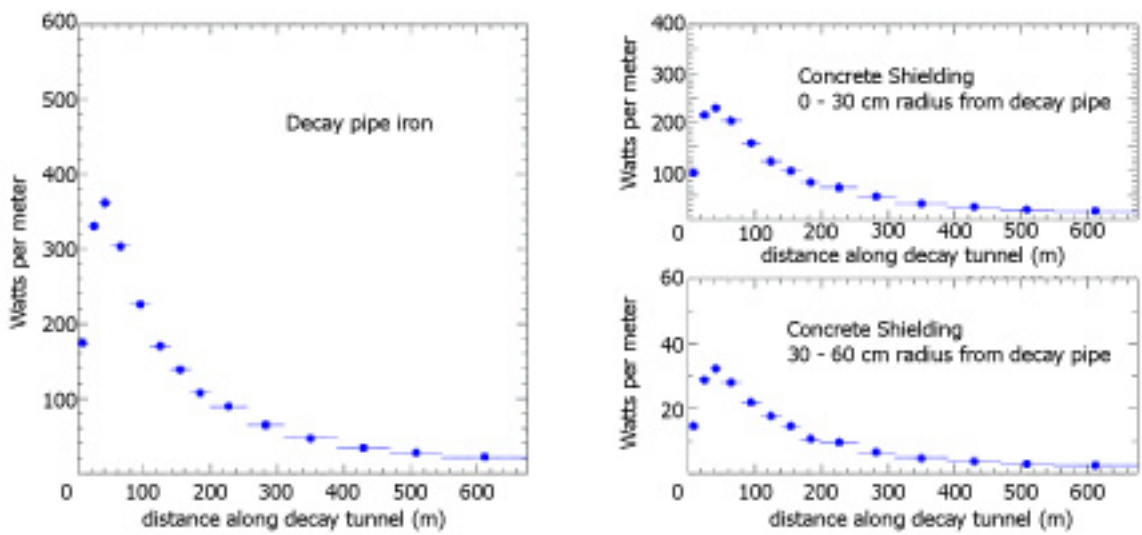

Figure 4.4-03: Energy deposition distribution for the low-energy neutrino beam configuration of target and horns

All of the decay pipe installation described above was part of the underground construction, and additional details may be found in the NuMI Facility TDR. Figure 4.4-04 shows photos of the decay pipe installation in progress. The only items remaining after the construction period were to attach end caps onto the Decay Pipe and then install the water and vacuum utilities; these tasks were performed as part of the NuMI Technical Components installation.

The decay pipe ends were sealed by end caps, concave in shape to minimize stress due to the vacuum inside the decay pipe. At the upstream end, one wishes to preserve as many of the secondary pions as possible in order to maximize the final flux of neutrinos. In general this

means making a thin vacuum window, although in this case thin was a relative term. At the downstream end all pions of interest have decayed and there are no concerns about preserving

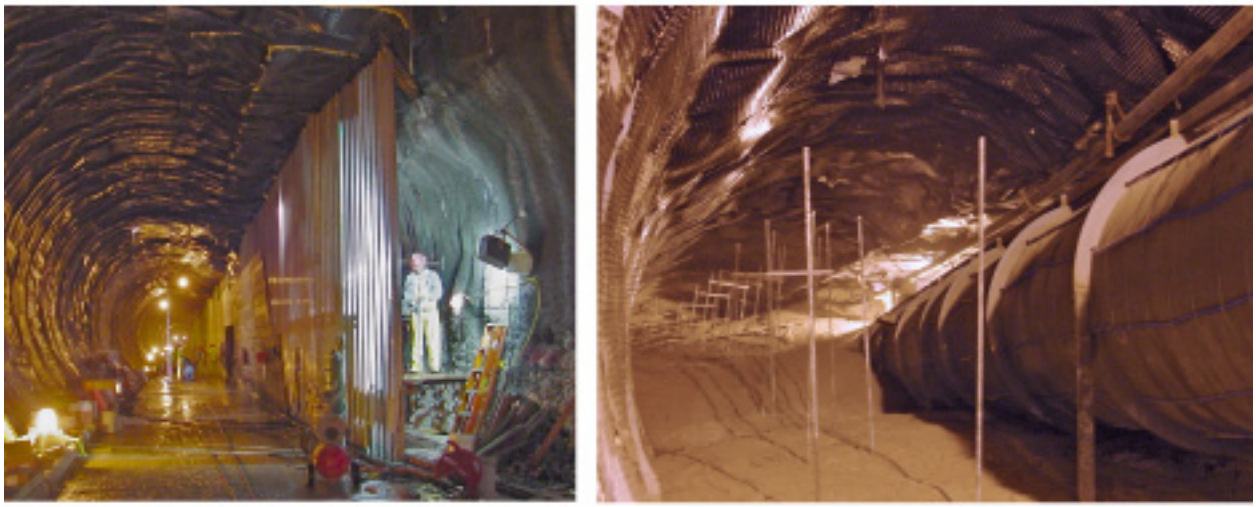

Figure 4.4-04: The left photo shows the Decay Tunnel before the Decay Pipe was installed. The wall is the form for the concrete shielding; the worker is standing in the egress passage. The right photo shows the installed Decay Pipe with concrete shielding being poured. Note the stiffening ribs around the pipe, and the copper cooling lines running along the length of the pipe.

particle flux; the Downstream End Cap can be made as thick as necessary to achieve straight-forward structural integrity.

Vacuum windows tens of mils in thickness and 6-ft diameter have been engineered and used. However, due to damage caused by a large particle flux, any such window will have a limited lifetime. This might not be an issue in some applications, but in the NuMI beamline, the Upstream End Cap is located at the downstream end of the Target Hall, under many feet of shielding blocks, and is quite inaccessible for repair or replacement. So the window thickness had to be sufficient to withstand the normal beam flux indefinitely and any possible accident conditions, yet be as thin as possible so as to minimize the window's effect on that same beam flux. These criteria were tempered by the fact that the window did not have to be the full 6-ft diameter. The particles exiting the Target Hall do not extend out to a 6-ft radius, but instead fill the space defined by the Target Hall cave, which is approximately 3-ft diameter. The resulting design is a thinner window embedded within a thicker end cap. Figure 4.4-05 shows the Upstream End Cap. The inner window material is specifically aluminum 6061-T6, selected as having the best performance among various types of aluminum or steel. The worst condition the material must withstand is the dynamic thermal stress due to an accident condition where the full

intensity primary proton beam misses the target and impacts the window with a small spot size. An ANSYS analysis of the Upstream End Cap under these conditions is reported in MSG-EAR-02317, *Thermal and Stress Analysis of Numi Decay Pipe Thin Head*, by Bob Wands, July 16, 2002.

The Downstream End Cap is a full 6-ft diameter semi-ellipsoidal concave sheet made of carbon steel 1/4-in thick attached to a short section of pipe, and is shown in Figure 4.4-06. The vacuum

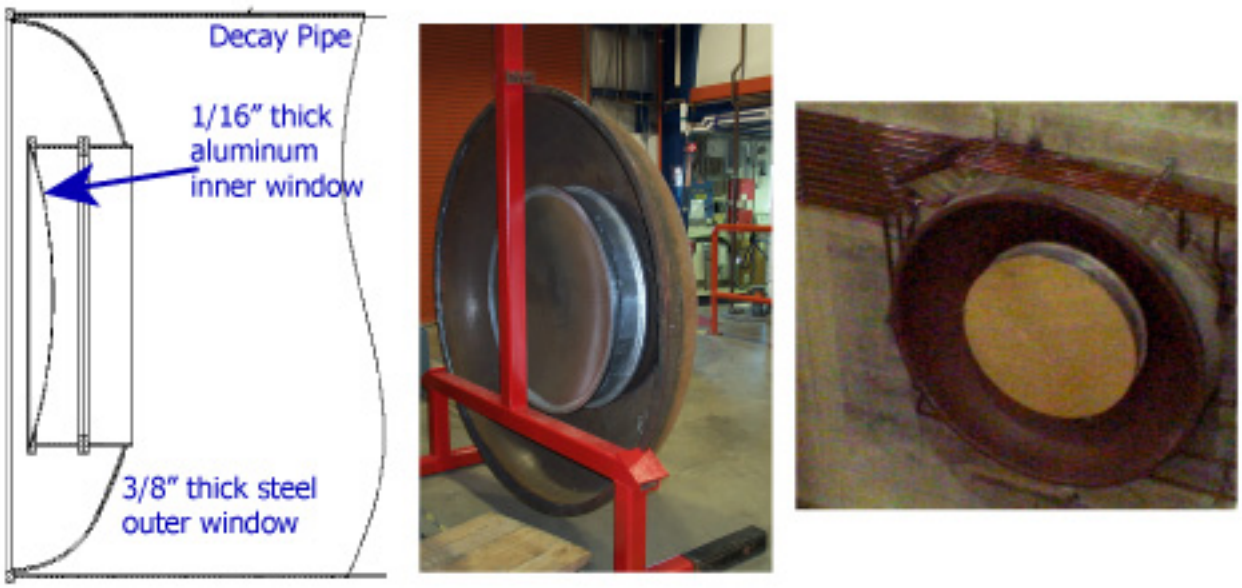

Figure 4.4-05 : Upstream End Cap. The left diagram shows a cross section sketch of the Upstream End Cap. The center photo shows the fabricated End Cap; the red frame is the lifting fixture for transport of the End Cap and was also used to hold the End Cap in position while being welded into place. The right photo shows the installed End Cap before it was surrounded by shielding. The central aluminum window is covered with plywood to protect it during installation of the Target Hall shielding. Note the copper cooling lines exiting the concrete around the perimeter of the Decay Pipe.

pump-out port is located on the upper part of the End Cap pipe, and at the base is a line to allow for drainage of water that may collect in the Decay Pipe before the End Caps were installed.

Both End Caps were constructed with an integrated carbon steel rim the same diameter as the Decay Pipe, which allowed them to be welded directly to the Pipe. The root weld is GTAW (a.k.a. TIG), the remaining passes are SMAW (a.k.a stick) using 7018 filler metal. The final fillet weld is 5/16" wide.

The Decay Pipe and End Caps have been designed to withstand the pressures of normal operation in the NuMI beam environment, indefinitely. The design meets the ASME pressure

vessel code for allowable stress (both primary and secondary), and the details are described in the Decay Pipe Engineering Notes. End Cap failure, while remote, is a hazard which must be examined, and a hazard analysis can be found in NuMI Note 0977.

Figure 4.4-06 : Downstream End Cap. The left photo shows the fabricated End Cap, viewed from its inner surface; the small pipe on the side is the drainage port. The right photo shows the installed End Cap, with all utilities attached: the 12 copper cooling lines distributed around the circumference, the vacuum pump-out line at upper right, and the drainage line at the bottom.

4.4.3 System Description: Hadron Absorber

The function of the Hadron Absorber is to stop most beam particles which remain at the end of the Decay Pipe and absorb their energy. The vast majority of these particles are hadrons, protons, pions and kaons, and essentially all of them are stopped by the Absorber. A relatively low rate of thermal neutrons are emitted from the Absorber as a by-product of the stopped hadrons. The muons in the beam are ranged out in rock downstream of the Absorber Enclosure. The neutrinos of course pass through all of this material and are the resulting product of the NuMI beam.

The Absorber must be able to easily handle the energy deposited by the beam, under all expected operating conditions and under all accident conditions which have any reasonable probability of

occurring. The basic design of any such beam dump is a central core of metal surrounded by additional steel shielding and by an outer layer of concrete. The metal serves to both create and contain the particle showers. The outer steel and concrete layers provide additional containment; the concrete also acts to absorb thermal neutrons, those with energies of 847 keV and below, as these are not stopped by iron.

4.4.3.1 Absorber Core

The detailed design for the Absorber core depends upon the size, energy and intensity of the entering hadron beam. A simulation of the NuMI beam impacting on a beam dump was used to define the basic design parameters of the Hadron Absorber; this work is reported in NuMI-B-652, *Advanced Conceptual Design of the NuMI Hadron Beam Absorber Core*, by A. Abramov, et. al. In summary, the Absorber consists of a core made from both aluminum and steel, surrounded by steel shielding blocks and an outer layer of concrete shielding blocks. The core is 51-in square transverse to the beam; this dimension was determined both by the beam size and by the availability of specific steel blocks for the surrounding shielding – a core made of a size similar to these blocks resulted in an easily stacked pile of material. The aluminum portion of the core is 8-ft deep, longitudinal to the beam, followed by a ~7.5-ft steel portion of the core. The aluminum portion is actively cooled by a circulating water system, described in more detail in Chapter 4.7. The temperature of the metal is monitored using thermocouples. An analysis of the water-cooled aluminum blocks subjected to the expected beam energy deposition is summarized in MSG-EAR-01-289, *Thermal Stress Analysis of Gun-drilled NuMI Absorber Core*, by Bob Wands.

Fig. 4.4-07: The first 3 Al core blocks, being assembled on the bench. Note the staggered arrangement of the pipes so that each block has two independant cooling circuits. The arrow points to the slot made for temperature monitoring thermocouples. This location, betweeen the 3rd and 4th blocks, is where the particle shower reaches it's maximum extent and the heat deposition is greatest.

The core is built up from smaller sections. The aluminum core is made from 8 blocks each 51” x 51” x 12”. Round channels were drilled within each block so that each of the 8 blocks has two independent water cooling circuits. The entrances and exits to these channels are set in a vertically staggered pattern along the sides, so that the water supply lines to each block do not interfere with each other in the final assembly. For ease of installation, the aluminum

blocks and their piping were assembled into two sections of 4 blocks each; this minimized the number of delivery trips of materials to the Absorber Enclosure, and minimized the amount of welding performed underground in the Enclosure, where working space was tight. Figure 4.4-07 shows the three upstream aluminum core blocks on the bench, being assembled into one of the sections. The pipes for each Al core block are routed through the core blocks from back to front; thus the number of pipes increases from upstream to downstream.

The steel part of the core is made from 10 blocks each 51” x 51” x 9.1”. The steel core blocks were likewise assembled on the bench into 4 sections, of 3, 3, 2 & 2 blocks. The cooling water pipes for the aluminum core blocks pass through the steel sections, and so the steel blocks are machined with holes for the pipes. During installation the pipes were carefully “threaded” through the steel core sections.

Each cooling pipe is a single continuous length through the core blocks, not from welded sections, so as to minimize the probability of leaks. Each pipe runs from where it is attached to its core block, through holes in the aluminum and steel core blocks downstream, ending several inches past the last steel core block which sits at the back face of the Absorber. At the rear of the Absorber, additional piping was installed to connect the core cooling pipes to a Radioactive Water (RAW) system. Each core block has two water circuits. The two circuits are each joined at two manifolds, so that the entire core can be cooled by one or both of these water circuits. The report MSG-EAR-01-289 calculates that one water circuit provides sufficient cooling. In the case of a water leak in one circuit in any given module, the entire circuit can be removed from the system, manually, at the manifold location outside of the Absorber. In the more unlikely case of a failure in the second circuit, then the piping to the particular leaking core block (on either circuit) can be physically disconnected from the manifolds, halting water flow in that particular block but no others; again, report MSG-EAR-01-289 shows there is sufficient heat transfer to the adjacent blocks under this condition that the temperature in the disconnected block would not become high enough for structural damage. The Absorber RAW system is described in more detail in Section 4.7.

4.4.3.2 Absorber Layout & Installation

The Hadron Absorber was constructed by a stacking of steel and concrete shielding blocks, and this Section describes the stacking in the order in which the parts were installed. Please refer to the diagrams in Figure 4.4-08 throughout the stacking description; a list at the end of this section gives the FNAL PPD Mechanical Dept. drawing numbers for the main parts and overall assembly. Also refer to the photos in Figures 4.4-09 through 4.4-17 for views of the Absorber

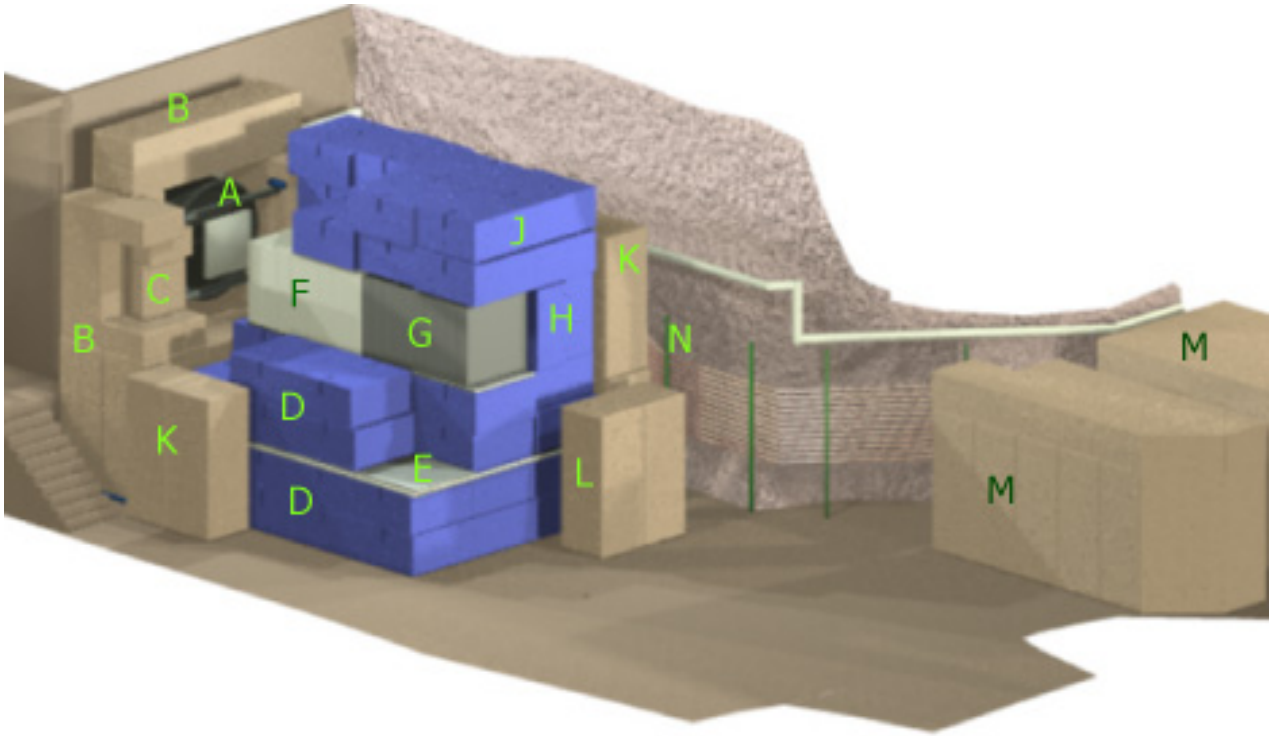

Fig. 4.4-08 : Cutaway isometric diagram of the Hadron Absorber, above, and a plan view, below. The letters label the same items in both diagrams. See text for description.

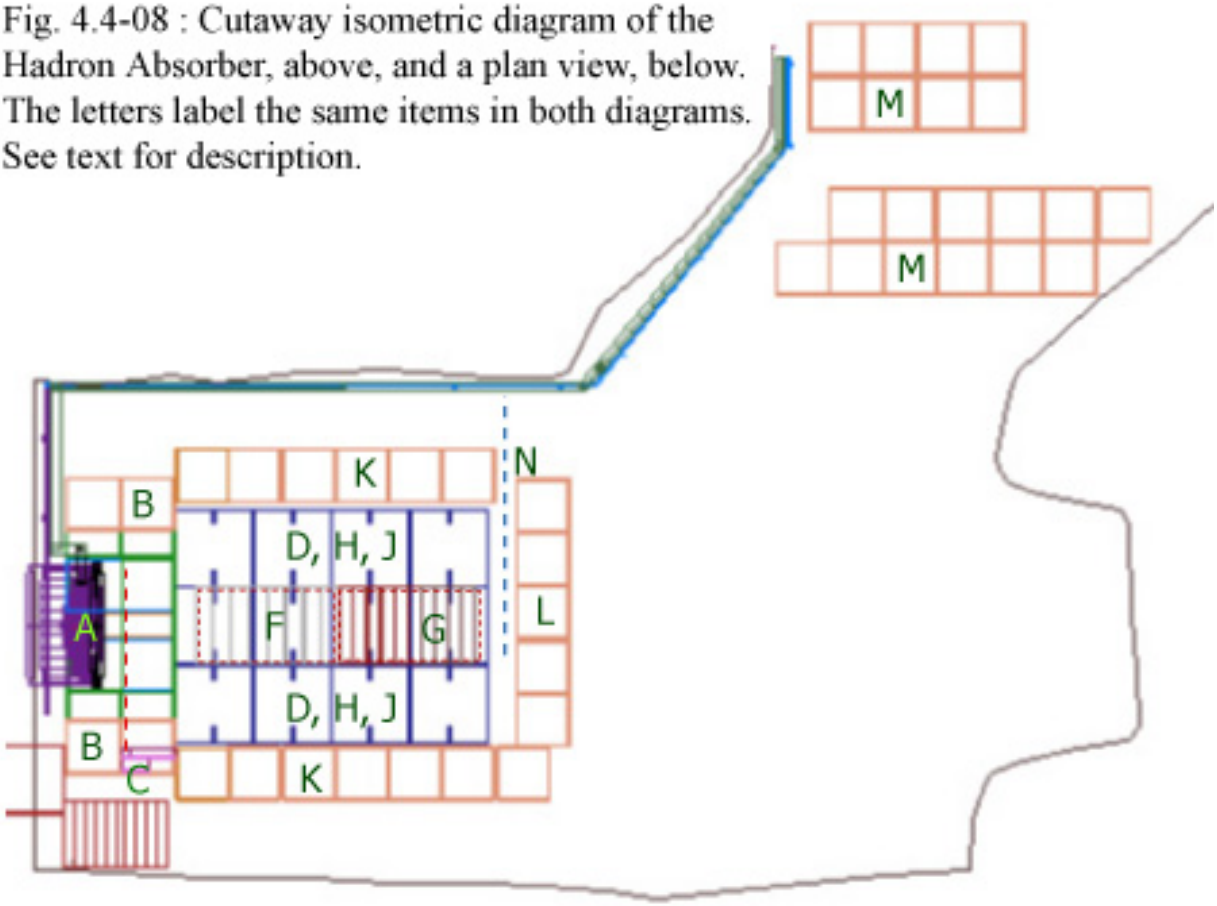

during installation. Installation started with stacked concrete shield blocks around the Decay Pipe and the Hadron Monitor. The

Monitor is located just a few inches downstream of the decay pipe Endcap, and both are labeled (A) in Figure 4.4-08. The concrete blocks, labeled (B) in Figure 4.4-08, can be considered an extension of the concrete shielding poured around the Pipe in the Decay Tunnel. The blocks sit flush against the base of the south wall of the Absorber enclosure, and extend 6-ft into the enclosure. The stacked blocks provide 3-ft of shielding around the top and sides of the decay pipe where the beam exits. The block base is built up about 7-ft high because of the elevation of the beam centerline and Decay Pipe in the Enclosure. On the upper east (beam-right) side, smaller blocks were stacked in a way to create an access slot, labeled (C) in the diagrams, for the installation of the Hadron Monitor. A sliding steel door covers the slot, and is shown in Figure 4.4-09. Also in that figure is a view of the Monitor support rails, showing it's location in relation to the decay pipe and shielding. Figure 4.4-10 shows the completed Decay Pipe concrete block shielding, before any further Absorber installation occurred.

Fig. 4.4-09 : Hadron Monitor access slot and mounting rails within the stacked concrete shielding around the Decay Pipe. The steel slot doors, covered with poly sheets, is equivalent in shielding to the concrete blocks it replaces.

As mentioned, specific steel blocks were obtained for use as the main stacking element for the Absorber shielding; these steel blocks were 52" x 52" x 26", and are the blue items labeled (D),(H) and (J) in Figure 4.4-09. The Absorber base was stacked up in four layers of 12 steel

blocks each, laid out 3 blocks wide transverse to the beam and 4 blocks deep longitudinal to the beam, labeled (D).

Figure 4.4-10 : Completed concrete block shielding around the downstream end of the Decay Pipe. The yellow beam is the temporary crane used during installation.

Between base layers 2 and 3 is a shallow steel pan which acts as a catch-basin for any cooling water leaking from the Absorber core, labeled (E). The pan drains to a tank, which has sufficient capacity for the entire volume of the Absorber primary RAW system. This tank can be seen at the back of the completed Absorber in Figure 4.4-16. Figure 4.4-11 shows two views of the base layers: the first two layers, and all four base layers. Each layer was shimmed to be level. Cracks between blocks were filled with grout. Note the edge of the water containment pan between layers 2 and 3. Note also that the middle row blocks in layers 3 and 4 sits lower than the outer rows. This is because the Absorber core carrier plate, a 1-in thick steel plate, sits on the middle row of blocks. The core carrier plate is machined level and provides a level base on which to set the core block sections. To compensate for the core carrier's extra inch of elevation, 1-in thick steel plates lie on the steel containment pan beneath the outer rows of layer 3 blocks, raising them relative to the middle row. In the end, the Absorber base, with the core carrier plate, sits at a level elevation.Installation of the Absorber Core came next. The upstream face of the core is inset from the upstream faces of the blue steel shield blocks which surround it, by 12-in. Combined with space downstream of the Hadron Monitor and inside the concrete blocks, this makes for a volume of approximately 130-ft^3 of air space which the beam travels through. Concerns about the release of excess activated air, discussed in Section 4.4.3.3, led to the filling of this volume by a box. The box is made from sheet aluminum, welded along all edges, and is filled with air at atmospheric pressure. The purpose of the box is simply to isolate the most intensely activated air within the box from any air in the nooks and crannies within the shield blocks which will eventually leak and mix with outside air. The box was set in position just before the first half-section of the aluminum core. Figure 4.4-12 shows the box, and then the first half-section of the core, with its long pipes supported behind it.

Figure 4.4-11 : Absorber base. At left is the first two layers, viewed from the side. At right layers 2,3,4 can be seen, viewed from the back. Note the upturned edge of the steel containment pan between layers 2 and 3. The outer blocks of layer 3 sit on 1-in steel plate, set within the pan, thus setting them higher than the middles blocks. The 1-in thick Core Carrier plate sits on top of the middle blocks of layer 4. All exposed cracks between blue blocks have been grouted.

Figure 4.4-12 : Absorber core installation, first stages. At left is a view of the air containment box which fills the space between the Hadron Monitor and the front face of the core. The front "stop" of the Core Carrier plate can be seen in front of the box. At right the first four modules of the aluminum core, pre-assembled as a unit with their piping, have been installed.

Fig. 4.4-13 : Absorber core installation. Top left - the 8 aluminum core blocks. Top right and lower left - the first 3 steel core blocks, welded beforehand into a single unit, being threaded onto the piping. Lower right - the completed core.

The second half-section of the aluminum core came next. The steel core sections were installed after the aluminum, and the steel sections were carefully threaded through the pipes from the aluminum core section. Figure 4.4-13 shows this installation process. A few inches of pipe extend beyond the last steel core block for attaching connections to the water system; this piping work was done later in the installation process after most of the heavy rigging was completed.

The side steel shield blocks were installed next, labeled (H) in the diagrams in Fig. 4.4-08. These are the same blocks as used for the base layers, but rotated so their 52-in length sits alongside the core. Two rows of steel blocks were placed on each side of the core. These blocks did not sit flush to the sides of the core but left an inch or so of space on each side. The side blocks were slightly higher than the core, so that when steel plates set on the side blocks bridged over the core about an inch of gap existed also above the core. These gaps were measured and steel plates fabricated to fill these small volumes, so as to exclude air which would otherwise add to the air

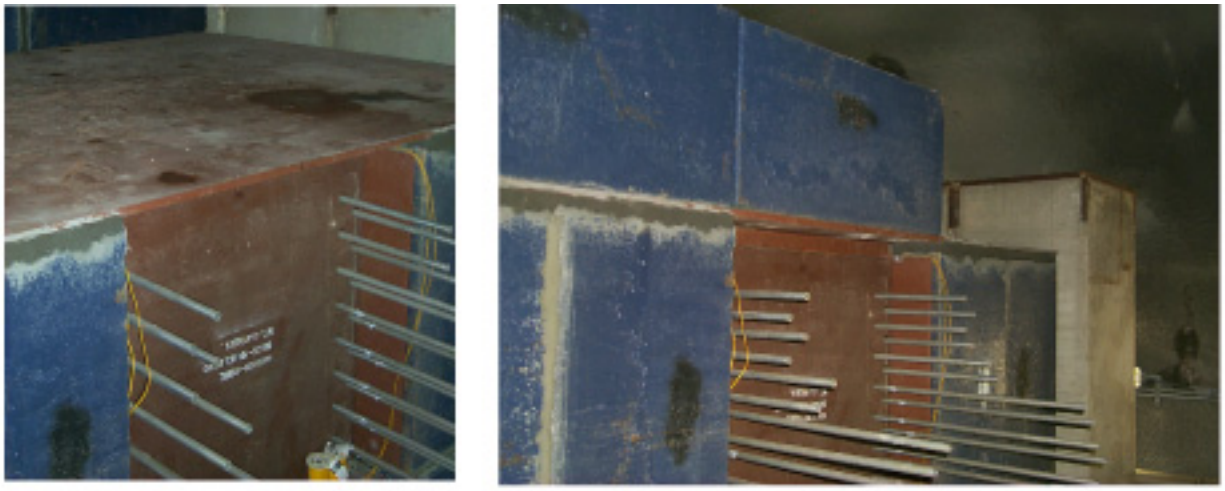

Figure 4.4-14 : Absorber side and top shielding. At left, the side blocks have been installed, their top surface leveled, and the steel bridging plates laid across them and the core. At right, nearly all of the first top layer has been installed. Note the additional steel plate which was installed around the core to fill in larger air gaps; the plate is painted brown making it visible against the blue blocks. The yellow wires are the thermocouple readout.

activation issues. The readout cables for the core thermocouples were carefully run through the steel filler plates out to the rear of the core.

Steel bridge plates spanning the entire width of the Absorber steel shield blocks were laid on the side blocks so that no weight from the top layers of shielding rest upon the core. Two more layers of steel blocks, laid in the same way as the base layers, were set on the bridge plates, and are labeled (J) in the diagrams. At this time, the side concrete blocks, labeled (K) were set in place, one row down each side, 3-ft x 3-ft x 7-ft tall, stacked two blocks high. A small air gap exists between the side concrete blocks and the steel shield blocks. A similar wall of concrete blocks were set across the back of the Absorber steel pile, labeled (L) in the diagrams, but only the bottom level at this point. Figure 4.4-14 shows the core with side shield blocks and steel bridge plate, and the first layer of top shield blocks.

At this point, the space remaining between the ceiling of the Enclosure and the top of the blue shield blocks did not allow for the installation of more blocks of that size, yet more shielding was required to satisfy groundwater activation levels. Nor was there space left for the usual 3-ft of outer concrete shielding on the top of the pile, which meant more thermal neutrons would escape along the top than on all other sides. It was determined that 18-in more steel would satisfy the shielding needs, and the absence of concrete would be tolerated – if too many thermal

neutrons escaped through the top and into the enclosure, then more concrete could be added to the Absorber Labyrinth to block them there.

In some areas on the top of the Absorber there was barely sufficient space for this 18-in of steel, and because of the lack of overhead space the gantry crane could no longer be used to position blocks. This meant using more basic rigging techniques and these techniques would be made easier if each block were relatively small. A total of 88 blue shield blocks had been used to this point. The final 18-in layer was made of 78 steel blocks of various sizes. This top layer of steel blocks was set on the side concrete blocks and on the main pile, and bridged across all gaps along the sides and along the boundary between the front concrete shielding and the main pile. A large gap exists at the back, between the main pile and the outer concrete, where the core cooling pipes are routed. A fixture was designed to support steel blocks across the top of this gap. The top steel layer is not shown in the diagrams. Fig. 4.4-15 shows the top steel layer during installation, from different viewpoints.

The core piping was routed along the back of the Absorber pile toward the west wall of the

Fig. 4.4-15 : Absorber roof shielding.
Top left - the variously sized blocks being set. In some spots only 2-in of clearance remained. Top right - view from the back, showing the steel blocks on top of the side concrete and bridging across the gap between the concrete and main steel pile. Note the fixture along the upper back. At right - view along the piping path. The purpose of the fixture can be seen clearly, to hold top steel blocks bridging across the gap between the main steel pile and back row of concrete.

enclosure; the path is labeled (N) in the diagrams. Before the final piping connections were made, a plywood box was constructed which filled the gap in the outer concrete shielding where the pipes were routed. Holes drilled in the box allowed the pipes to pass through. Once in place,

Figure 4.4-16 : Completed Hadron Absorber. The back wall of concrete blocks is in place, and the steel roof blocks bridge across the gap between them and the main pile of blue blocks. On the floor is the tank into which the secondary containment pan drains. At right the core pipes emerge and are connected to manifolds located along the wall. The white structure where the pipes emerge is the plywood box, filled with poly-beads. This box can be moved if access to the rear of the Absorber pile is necessary.

the box was filled with polyethelene beads, which are similar in shielding value to the concrete.

The completed Absorber is shown in Fig. 4.4-16. All of the outer concrete is in place. The piping emerges from the (painted) white bead-filled box. All the top steel is in place. The drain line from the metal containment pan, set in the base steel layers, is routed to a holding tank at the back of the Absorber. A heculite tarp is laid across the top, so that water from any drips in the enclosure roof runs off down the sides, and not down into cracks between the steel blocks. The worst (and only significant) ceiling drip in the enclosure is caught by a pan and drained into the gutters; however over time other drips may develop.

Once the Absorber was completed, the Absorber Labyrinth was installed in the passage between the Absorber enclosure and the Absorber utility area. The Labyrinth, labeled (M) in the diagrams, is simple, made from two rows of shield blocks, each row being 6-ft thick and running between floor and ceiling. Figure 4.4-17 shows the Labyrinth from each side. Also in that Figure is a view of the Absorber water and vacuum utility skids.

Figure 4.4-17 : Absorber Labyrinth. At left is a view of the entrance - the small corridor between the walls of concrete shield blocks - from the Absorber Access Tunnel, standing just by the fire doors. The equipment is the utility skids for the Absorber and Decay Pipe. At right is a view of the exit, from inside the Absorber Enclosure. In the foreground is the secondary containment tank at the back of the Absorber.

List of PPD Mechanical Dept drawing numbers for the main parts and overall assembly

427776 Overall Assembly, listing all sub-drawings
427334 Concrete block stacking, around DK pipe and along sides of Absorber
433146 Air containment box
431534 Hadron Monitor access slot shield door assembly
427127 Al core modules assembly – 427130:135+427620+427622 individual modules
427159 Core carrier plate assembly – 427160, 427162, 427164 individual plates
427154 Steel core blocks
406519, 433158, 431468, 431467 Core cooling pipes assembly
427337, 427376 Steel Blu block base assembly
427383 Containment pan assembly
427379 Steel Blu block side and top assembly

4.4.3.3 Control of Activated Air

The Absorber shielding was primarily designed to protect the groundwater in the surrounding rock from activation by particle showers, a requirement which the Absorber satisfies. The shielding is also sufficiently thick that residual activation rates on the outer surface of the surrounding concrete are reasonable for an enclosure locked off during beam and otherwise infrequently accessed. A third radiological concern is the release of activated air, and here some steps had to be taken.

Any stacked construction of slightly uneven blocks, such as used for the Absorber, will create variously sized gaps and cracks. The air within these gaps and cracks becomes activated by the

particle showers created in the Absorber material; the closer the gap or crack is to the beam centerline the more activated the air will become. If no effort is made to seal up the Absorber, the activated air will leak out of these gaps and cracks, and mix with un-activated air which is flowing through the Enclosure. The underground air flow pulls air from the Absorber Enclosure, up the decay egress passage, and out a ventilation stack halfway along the length of the decay tunnel. The time it takes for air to flow along this route is too short for all activated elements to decay, and some activated air will be released. There is an overall budget for released activated air, and so efforts were made to predict the contribution coming from the Absorber, which meant understanding all the volumes of air within the Absorber pile.

And there turned out to be significant volumes, not mere cracks, located in or near the beam center, where activation would be highest. The largest volume was the space between the Decay Pipe Endcap and the front face of the Absorber. The Hadron Monitor is located here, and because “backsplash” from beam hitting the front face of the core could affect the efficiency of the detector, by design there was some distance of open space between the two. The full beam intensity at the end of the decay pipe passes through this large volume of air. The next largest volume is the gaps between the core modules and the surrounding blue steel shield blocks. While only about an inch in thickness, the gaps exist on the top and two sides, and extend for the entire length of the core. Since these gaps surround the core, the air sees a large particle flux and becomes quite activated. The third main volume is around the upper portion of the south wall of the Enclosure, where the Decay Pipe exits. The shielding stacking plan assumed this wall was flat, but in fact it is not. The lower 5-ft of the wall extends 15-in further into the enclosure than the rest of the wall, above 5-ft. The shield blocks were placed where the wall met the floor, but that left a 15-in wide gap above the 5-ft level, all around the Decay Pipe. The actual particle flux passing through this volume is lower, because it is “behind” the poured Decay Pipe shielding and off the beam axis. However, this large gap is contiguous with the two other, more activated, air volumes mentioned above, inside the stacked shielding, giving a clear and easy path for the activated air inside the shielding to be pulled out and mix with the air in the Enclosure.

The amount and activation level of air from these volumes was calculated, and if the large gap around the Decay Pipe in the south wall was left as is, then all the activated air would mix freely with the air in the enclosure. From this, the predicted quantity of activated air released to the surface could be calculated, and that quantity was deemed to be too large a portion of the allowed fraction. But it was not necessary to make the Absorber air-tight – a small amount of activated air could be allowed to escape on a continuous basis. So, during Absorber installation, attention was paid to the particular large volumes mentioned, to minimize or eliminate them, and

to cracks between stacked blocks, with the goal of an overall “leakage” of a few percent of the total activated air through such cracks.

As blocks were set and leveled, cracks along the floor and between blocks were filled with grout. Typically only the cracks along the outer sides were filled. Certain layers were covered with grout to create a level surface, sealing all cracks on that layer’s surface: the layer on which the core sits, and the top layer of blue shield blocks, were treated in this way. Figure 4.4-11 shows this crack filling, and it can be seen in other photos as well.

The first large volume, between the Decay Pipe Endcap and the front face of the core, was mostly filled by the aluminum box shown in Figure 4.4-12. The box simply prevents the air inside of it from freely mixing with air outside of it, removing the volume within the box from the equation for total activated air. The box fills the space between the Hadron Monitor and the front face of the core, which accounts for 55% of the total volume in this area. The remainder, between the Decay Endcap and the Hadron Monitor, cannot be similarly filled, as a box in this

Fig. 4.4-18 : South wall filler shielding. The left photo shows the Absorber Enclosure south wall before shielding installation; the lower 5-ft of the wall extends 15-in further into the enclosure than the upper portion of the wall, making a shelf. The right photo shows the mortar and brick used to fill above the shelf, between the shielding blocks and the south wall.

location would interfere with the installation of the Monitor. As long as the remaining free volume of air can be held within the Absorber and have a low leak rate into the Enclosure, then it can be tolerated.

The second main activated volume is the one around the core. The strategy again was to mostly eliminate the volume of air from the equation by filling the space with something else. In this case thin steel plates were fabricated to fit as closely as possible between the core and the steel blocks. One of the plates can be seen in Figure 4.4-14, extending beyond the end of the core block. These plates reduced the volume of air in this space to 10% of the former amount.

The third area of attention was the 15-in gap around the Decay Pipe on the south wall. This gap provided a large escape route for all the activated air within the Absorber. Figure 4.4-18 shows two views of the south wall. The first view before any shielding was installed; the 15-in change in wall position can be seen at the level of the person's white hard hat. The second view is a close-up of the bricked-in gap after installation was completed. A protective foam wrap was placed around the piping before the mortar was applied. The brick wall is not air-tight, and was not required to be, as long as the leak rate was reduced to a few percent of what it would be if the wall was absent.

4.8 CONTROLS, INTERLOCKS AND CABLE INSTALLATION (WBS 1.1.8)

4.8.1 Controls

4.8.1.1 Introduction

Controls for NuMI are comprised of generally standard interface and networking components. These include a combination of VME, IRM, CAMAC and PLC hardware with necessary and appropriate modules to afford monitor and control of technical equipment through ACNET, the Accelerator Controls Network. Specific choices of interface are based on cost, availability, reliability and ease of interface. Connection of these interfaces to ACNET central services is accomplished by extension of existing single and multi mode fiber cable networks.

Installation of ACNET services for NuMI includes connectivity to accelerator time (TCLK) and beam synchronous (MIBS) clocks and to the NuMI Beam Permit System.

ACNET consoles enable the monitor and control of accelerator operations, including the NuMI beamline and associated technical components. While operations are generally concentrated in the Main Control Room with the use of these consoles, remote consoles may be connected to the extended network. In particular, remote consoles are to be made available at select locations to facilitate commissioning and operations as appropriate.

4.8.1.2 System Description: Controlled Equipment and Systems and Their Locations

Controls for NuMI are or will be installed at eight distinct geographical locations. Three of these locations are already outfitted with basic Controls infrastructure. Major items of equipment or systems to be controlled and monitored are listed for each of the locations in **Table 4.8-1**.

	MI-60 Service Building South	MI-60 Service Building North	MI-62 Service Building	MI-65 Service Building	Target Hall PS Support Room	MINOS Service Building	MINOS Near Detector Hall	Absorber Access Tunnel
Power Supplies	**60S**	**60N**	**62SB**	**65SB**	**THSR**	**MSB**	**MND**	**AAT**
Single Turn Extraction Kicker	X							
Lambertsons		X						
Dipole Magnets - Ramped		X	X	X				
Quadrupole Magnets - Ramped		X	X	X				
Trim Correction Elements		X		X				
Focusing Horns Including Stripline					X			
Loss and Profile Monitor High Voltage		X	X	X	X			
Near Detector Analysis Magnet							X	
Vacuum								
Primary Beam Transport - Including Isolation Valves, Gauges & Ion Pumps		X	X					
Decay Pipe (PLC)								X
Fluid Systems								
Flourinert Cooling for Extraction Kickers	X							
MI-62 LCW and Pond Water Systems (PLC)			X					
Target & Baffle RAW System (PLC)					X			
Horn 1 RAW System (PLC)					X			
Horn 2 RAW System (PLC)					X			
Target Pile Air Cooling System (PLC)					X			
MINOS LCW System (PLC)							X	
MINOS Sump Pumps						X	X	
Decay Pipe Cooling RAW System (PLC)					X			X
Intermediate Water Cooling for Absorber RAW System (PLC)								X
Absorber Cooling RAW System (PLC)								X
Instrumentation								
Primary Transport Beam Position Monitors		X		X				
Beam Profile Monitors		X		X				
Loss Monitors		X	X		X			
Total Loss Monitors			X					
Beam Intensity Toroids			X		X			

Baffle and Target Instrumentation (PLC)					X			
Target Budal Monitors					X			
Positioning Systems for Target and Horn 1					X			
Horn 1 and 2 Module and Stripline Instrumentation (PLC)					X			
Horn Bdot Magnetic Field Probes					X			
Absorber Instrumentation (PLC)								X
Hadron Monitor at Downstream End of Decay Pipe								X
Muon Monitors at Muon Alcoves #1, #2 and #3								X
Beam Permit System - Process Channel Interface (7 Total)	X	XX	X	X	XX			
ACNET Connectivity								
Ethernet	X	X	X	X	X	X	X	X
VME	X	X	X	X	X			X
Internet Rack Monitor - IRM					X			
Programmable Logic Controller - PLC		X	X	X	X		X	X
CAMAC	X	X	X	X	X	X	X	X

Table 4.8-1 Technical Equipment Interfaced to the Control System versus Location

4.8.1.3 System Description: Accelerator Clocks and NuMI Operations

The present accelerator complex uses a number of clock systems to control devices and to time beam transfers. Of particular interest to NuMI operations are the following:

TCLK The primary accelerator time clock is a 10 MHz clock known as TCLK. A TCLK event is realized by the transmission of 8 bits of data enveloped by a start and parity bit in the serial clock stream. TCLK events are designated by a two-character hexadecimal number preceded by a dollar sign and range from $00 through $FF. Six new or redefined TCLK events have been assigned to accommodate NuMI operations. These are $23, $A5, $19, $A9, $A6 and $A8. NuMI operations are planned to occur in a new Main Injector reset cycle signed by **TCLK $23**. This reset cycle is unique in that it can simultaneously support P-Bar production and NuMI operations. In the dual mode, one to five batches of Booster beam may be loaded into MI for NuMI. The total cycle time for the Main Injector running under the $23 reset is optimally established at 1.8 seconds.

MIBS The Main Injector has a separate beam synchronous clock system, MIBS, that is locked in frequency to the Main Injector rf system. This clock, that operates at

approximately 7.5 MHz (rf/7), is used to coordinate Main Injector transfers and beam related diagnostics. A most significant event on the MIBS clock is $AA, the revolution marker. For the MI, the $AA event occurs approximately every 10 microseconds. MIBS event $74 has been assigned to initiate the extraction of 120 GeV beam for NuMI. When issued, this extraction event is always synchronous with respect to the MIBS $AA revolution marker event.

Timing observations for the Main Injector $29 cycle for P-Bar Production are listed in **Table 4.8-2**. Expected timing for the Main Injector $23 cycle for P-Bar Production and NuMI Operations are listed in **Table 4.8-3**. TCLK and MIBS events of interest to NuMI operations are listed in **Table 4.8-4**.

Timing Observations of MI $29 Cycle for P-Bar Production Cycle

Event	Description / Comment	Time in Milliseconds	Note
$80	3 x 15 Hz Ticks Before $29 MI Reset or -201 ms	-201.0	
$29	Main Injector Reset	0.0	1
$22	Start of Ramp	89.0	
$25	Start of Flattop	778.9	
MIBS $79	Initiate P-Bar Production Beam Transfer	838.9	
	MI-52 Kicker Fire Time MIBS $79 + 24.918 MR Rev	839.2	
$26	End of Beam Operations	848.9	
	Total $29 Cycle Time	1,466.7	2
	Flattop to Actual P-Bar Production Beam Extraction	60.3	

Note 1 The $29 to $22 Interval Accommodates One $14 Booster Batch to Main Injector.

Note 2 The Current $29 Cycle is Judged to be Twenty-Two 15 Hz Ticks Long or 1.467 Seconds

Table 4.8-2 Timing Observations for MI $29 Cycle for P-Bar Production

Expected Timing for MI $23 Cycle for P-Bar Production and NuMI Operations

Event	Description / Comment	Time in Milliseconds	Note
$80	Signature Event for P-Bar Production Cycle	?	**3**
$A5	Signature Event for NuMI Beam Cycle	-0.001	**4**
$23	Main Injector Reset	0.0	**5 & 6**
$22	Start of Ramp	422.3	
$25	Start of Flattop	1,112.2	
MIBS $79	Initiate P-Bar Production Beam Transfer	1,172.2	
	MI-52 Kicker Fire Time MIBS $79 + 24.918 MI Rev	1,172.5	
MIBS $74	Initiate NuMI Beam Extraction	1,173.3	**7**
	I:KPS6N Kicker Fire Time MIBS $74 + 20.xxx MI Rev	1,173.5	**8**
$26	End of Beam Operations	1,182.2	
	Total $23 Cycle Time	1,800.0	**9**
	Flattop to Actual P-Bar Production Beam Extraction	60.3	
	Flattop to Actual NuMI Beam Extraction	61.3	

Note 3 $80 May be Placed Before or After the $23, but Must be Before the $14.

Note 4 The $A5 Event is Now Expected to be Imediately Before the $23 MI Reset. That Stated, $A5 May be Placed Before or After the $23, but Must be Before the $19s.

Note 5 The $23 to $22 Interval Will Accommodate Six Booster Batches to Main Injector. Normally a Single $14 Batch for P-Bar Production and 5 x $19 Batches for NuMI.

Note 6 The $29 to $22 Interval of 89 ms is Extended by Five 15 Hz Ticks for the $23 Ramp Scenario. Subsequent Times Generally Advance by 333.3 ms.

Note 7 Exact Placement of MIBS Extraction Event is Subject to Observed Peak of Longitudinal Bunch Length and Number of Integral MI Turns of Beam After MIBS $74.

Note 8 Time is About 1 ms After P-Bar Production Beam Extraction When Longitudinal Bunch Length is Peaked. 20 MI Revolutions is the Suggested Integral Value of Delay After MIBS $74. ".xxx" Fractional Turn Delay to be Field Determined.

Note 9 The Expected $23 Cycle is Judged to be Twenty-Seven 15 Hz Ticks Long or 1.8 Seconds[1]

Table 4.8-3 Expected Timing for MI $23 Cycle for P-Bar Production and NuMI Operations

[1] The cycle time was discussed at the 4/12/04 installation/L3 Managers' meeting. Bruce Baller reiterated that the baseline cycle time is 1.87 seconds—not 1.8 seconds. The meaning of this is that project funds should not be expended to reduce the cycle time from 1.87 seconds to 1.8 seconds.

NuMI TCLK and MIBS EVENTS

TCLK	DEFINITION	COMMENT
$A5	NuMI Reset for Extracted Beam	Expected to be Closely Synchronous With and Well in Advance of NuMI Extracted Beam. Primary Reset for NuMI Ramped Devices.
$23	Main Injector Cycle Reset for P-Bar Production and NuMI Operations	Usually Has Beam for Both P-Bar Production and NuMI Operations. But Could Have Beam for Only One Destination.
$14	Booster Reset for P-Bar Production Beam	Normally One High Intensity Batch.
$19	Booster Reset for NuMI Operations Beam	Normally One to Five Batches for NuMI with Programmable Intensity.
$52	Beam for Previous Booster Reset Will Be Accelerated.	A Generic Event.
$53	Beam for Previous Booster Reset Will Not Be Accelerated.	A Generic Event.
$1F	Booster Beam About to be Transferred to Main Injector	A Generic Event.
$22	Main Injector Ramp Begins	A Generic Event.
$25	Main Injector Flattop	A Generic Event.
$81	Reflected MIBS Event $79	Expected to be Synchronous Within a Few Microseconds.
$A9	Reflected MIBS Event $74	Expected to be Synchronous Within a Few Microseconds.
$27	Detected Fall of the Main Injector Beam Permit	Fires the Main Injector Abort Kicker
$2F	Fire the Main Injector Abort	Happens Every Cycle.
$26	End of Beam Operations in the Main Injector	All Beam Should be Gone.
$A6	NuMI Beam Permit Has Fallen to Non-Permit State	Serves to Inhibit Accelerating Beam Associated With Booster $19 Reset. Also Will Inhibit Generation of MIBS $74.
$A8	NuMI Beam Permit System Reset	Issued by Operator Command. Rcvd by C200 and C201 Modules. Clears Latched Inputs of C200.
$FA	Reflected MIBS $ED	A Generic Event.

MIBS	DEFINITION	COMMENT
$AA	Main Injector Revolution Marker	Once Every 588 RF Cycles. Approximate 10 Microsecond Period.
$79	Initiate Transfer of 120 GeV P-Bar Prod Beam to P-Bar Tgt	Reflected as TCLK $81.
$74	Initiate Transfer of 120 GeV NuMI Beam to NuMI Primary Beamline	Reflected as TCLK $A9.
$ED	Request for a MIBS Transfer Event Has Been Denied	Reflected as TCLK $FA. This is a Generic Event. If One Expects to See $74 or $79 and Does Not, This $ED Event Should Be Generated.

Table 4.8-4 NuMI Significant TCLK and MIBS Clock Events

4.8.1.4 System Description: NuMI Beam Permit System

The fundamental design of the NuMI Beam Permit System (NBPS) takes advantage of already designed hardware and methodologies for Beam Permit/Abort that were instituted in the early days of the Tevatron. While not necessarily redundant in architecture, the NBPS is simple and fail-safe in design.

The NBPS is realized by a dedicated fiber optic line linking all of the distinct geographic locations of NuMI controls. Its operation closely resembles that of a simple flip-flop being in either a beam permit or inhibit state. Inputs for the beam inhibit conditions are many, with each being latched. Bringing the NBPS communication line to the beam permit state is singularly accomplished by operator initiation of a specific TCLK event, but only after beam inhibit conditions have been cleared. The state of the line is examined at two significant locations. The NBPS state is examined at MI-60 as a necessary condition to launch the MIBS $74 extraction event and to allow the firing of the NuMI single turn extraction kicker. The NBPS state is also examined at the Main Control Room as an input to the Beam Switch Sum Box (BSSB) as one of the necessary conditions to allow acceleration of beam in the Linac that is destined for NuMI.

The NBPS distinguishes itself from other installed permit systems in the number and type of inputs. Specifically it is intended to monitor as many technical components and sub-systems as practical that portend successful operation of the NuMI beamline and meaningful operations. The NBPS is especially unique in that it examines data for proper state and operation both closely before and immediately subsequent to NuMI beam extraction. Central to this unique capability is the development of the Process Channel Interface (PCI) and its companion ACNET interface, the CAMAC C204 module. The C204/PCI facility is capable of examining analog and digital inputs with respect to down loaded limit values. The decision process is localized, prompt and not centrally reliant on ACNET services for execution. ACNET services are required for set-up.

The following is a condensed list of significant inputs to the NuMI Beam Permit System:

- NuMI Radiation Safety System
- Main Injector Performance Parameters
- Single Turn Extraction Kicker Power Supply
- Dipole and Quadrupole Magnet Power Supplies

- Beam Loss Monitors
- Total Beam Loss Monitors
- Horn Power Supply
- Low Conductivity and Radioactive Water Systems
- Extraction Beamline Vacuum System Isolation Valves
- Temperature Monitors of Various Technical Components

4.8.2 Interlocks

4.8.2.1 Introduction

The Radiation Safety System (RSS) for NuMI encompasses the underground enclosure with the exception of the following areas. These areas are to be accessible during NuMI beam operations.

- MI-65 Access Shaft Including Stairwell and Elevator
- MI-65 Below Ground Elevator and Shaft Landing Area
- Target Hall Power Supply and RAW Support Rooms
- MINOS Access Shaft Including Elevators
- MINOS Below Ground Elevator Landing Area
- MINOS Below Ground Shaft Landing Area
- Absorber Access Tunnel up to the Absorber Area
- MINOS Experimental Hall Access Tunnel
- MINOS Experimental Hall.

Areas of exclusion during NuMI beam operations are divided into eight separated areas with most being under the domain of the NuMI RSS. All areas are contiguous with the exception of three Muon Alcoves. **Table 4.8-5** indicates the NuMI interlocked areas and barriers.

Area #	Area Description	RSS	Associated Barrier
Area 1	Upstream Carrier Tunnel	Main Inj	G1 D2
Area 2	Downstream Carrier Tunnel, Pre-Target Enclosure and Target Hall, Including Entrance Labyrinth	NuMI	D2 G3 D4
Area 3	Decay Pipe Passageway (Mini-Loop)	NuMI	D4 G5
Area 4	Absorber Hall Including Upstream End of Absorber Access Tunnel, Entrance Labyrinth and Muon Alcove #1	NuMI	G5 D6
Area 5	Muon Alcove #2	NuMI	D7
Area 6	Muon Alcove #3	NuMI	D8
Area 7	Muon Alcove #4	NuMI	D9

Gate or Door#	Barrier Location	RSS	Area
Gate 1	Upstream End of Carrier Tunnel	MI	Area 1
Door 2	Fire Door and CMU Wall at Mid-Point of Carrier Tunnel	MI + NuMI	Areas 1 & 2
Gate 3	Beginning of Entrance Labyrinth to Pre-Target and Target Hall at Bottom of MI-65 Shaft Stairway	NuMI	Area 2
Door 4	Fire Door at Upstream End of Decay Pipe Passageway	NuMI	Areas 2 & 3
Gate 5	Gate at Downstream End of Decay Pipe Passageway	NuMI	Areas 3 & 4
Door 6	Fire Door Across Absorber Access Tunnel Between Absorber Hall and Muon Alcove #2	NuMI	Area 4
Door 7	Entrance to Muon Alcove #2	NuMI	Area 5
Door 8	Entrance to Muon Alcove #3	NuMI	Area 6
Door 9	Entrance to Muon Alcove #4 (This Door May Be Simply Locked Closed by RSO Lock)	NuMI	Area 7

Table 4.8-5 NuMI Interlocked Areas and Barriers

The NuMI RSS must be cleared for beam to be transmitted down the NuMI beamline. The state of the RSS is also an input to the NuMI Beam Permit System. While not integral to the NuMI RSS, radiation "stack" monitors sample and record levels of activated air from the Pre-Target, Target Hall and Absorber areas.

4.8.2.2 System Description: Critical Devices

The critical devices for the NuMI area have been established as the **Lambertson** and **HV101** magnet strings in the Main Injector enclosure Q608 to Q611 area. Power supplies for these devices are located at the North end of the MI-60 Service Building.

Lambertsons - There are two power supplies at the North end of the MI-60 equipment gallery for the three Lambertson magnets located in the MI enclosure by Main Injector quadrupole Q608. The first Lambertson supply, I:LAM60, powers the first Lambertson magnet immediately upstream of Q608. The second supply, I:LAM61, powers the two Lambertsons positioned immediately downstream of Q608. Both of these two supplies are considered as the first of two critical devices for NuMI. A single AC contactor for these supplies is located nearby on the East wall of the equipment gallery and is controlled by the first Critical Device Controller of the NuMI RSS.

HV101 - The second critical device is the HV101 string of six EPB magnets located between Q609 and Q612. The three power supplies for HV101 are located in the North power supply room of MI-60. An AC contactor for these supplies is located nearby on the South wall of the power supply room and is controlled by the second Critical Device Controller of the NuMI RSS.

4.8.2.3 System Description: Search and Secure Areas

The NuMI beamline spans two radiation safety systems, the first being the **existing Main Injector RSS** and then the new **NuMI RSS**. The boundary between the two systems is the (Hobbit) door located at the mid-point of the Carrier Tunnel. The upstream end of the Carrier Tunnel (Upper Hobbit) is to be guarded by a separately accessible mini-loop so as to avoid necessity of routine search and secure of this area. The downstream end of the Carrier Tunnel (Lower Hobbit) is associated with the NuMI RSS. In that the Carrier Tunnel is to be considered an alternate emergency exit for personnel, installed gates or doors must be capable of being opened without necessity of regular access keys.

From the MI-65 Service Building, the main area of the NuMI RSS includes the downstream Carrier Tunnel, Pre-Target enclosure, Target Hall and the labyrinth access to these areas. These are the areas subject to a normal search and secure procedure. From the Target Hall, there is also access to the Decay Pipe passageway. This passageway is approximately 2,200 feet in length on the East side of the concrete embedded Decay Pipe. There is a fire door at its mid-point that

serves as a boundary between the MI-65 and MINOS fire protection systems. (The mid-point door also serves to isolate the MI-65 and MINOS air circulation systems.) The downstream end of this passageway terminates at the Absorber Hall. The Decay Pipe passageway is guarded as a separately accessible area so as to avoid necessity of routine search and secure of this area. As is the case for the Carrier Tunnel, the Decay Pipe passageway is considered an alternate emergency exit for personnel. The associated doors and gates are capable of being opened without necessity of regular access keys.

One or more radiation monitoring scarecrows will be placed in the Carrier Tunnel and or Pre-Target regions and connected to the NuMI RSS. Scarecrow placement here will preclude repetitive higher loss operation of the NuMI beamline in these areas.

The MI-65 shaft, its stairwell, the elevator landing area, the shaft landing area and Target Hall support rooms may be occupied during NuMI operations. Though not part of the NuMI RSS, the RAW support room is expected to have some level of access control due to expected activation at the de-ionization bottles associated with the RAW systems.

From the MINOS Service Building, the main areas of the NuMI RSS include the Muon Alcoves, the very upstream end of the Absorber Access Tunnel and the Absorber Hall itself. The Absorber Hall enclosure area accommodates entry to the Decay Pipe passageway. The MINOS shaft, its elevator landing area, the shaft landing area, most of the Absorber Access Tunnel and all downstream areas, including the MINOS Near Detector Experimental Hall and its access tunnel, may be occupied during NuMI operations.

There are four entry points to the NuMI radiation area from the Absorber Access Tunnel. The first three are at entrances to the Muon Alcoves (No. 4, No. 3 and No. 2), each being a dead end for access to muon detectors positioned in the beam flux path. The two most upstream of the three alcoves (No. 2 and No. 3) house arrays of muon detectors. Beyond the alcoves and moving upstream toward the Absorber, there is a fire door that is the fourth entry point. Immediately South of this interlocked door is the access labyrinth to the Absorber Hall. Passing through the Absorber Hall area (an area that includes Muon Alcove No. 1), there is an access gate to the downstream end of the Decay Pipe passageway. Access to the Decay Pipe passageway is to be supported by a separate mini-loop to preclude necessity of routine search and secure. The most upstream end of the Absorber Access Tunnel houses Decay Pipe vacuum equipment, RAW skids for the Absorber and Decay Pipe Cooling water systems and electrical equipment.

The Absorber Access Tunnel, Absorber Hall and the Decay Pipe passageway are considered as an alternate emergency exit for personnel in the downstream MINOS areas. The associated doors and gates are capable of being opened without necessity of regular access keys.

It is expected that no more than two personnel will be required to satisfactorily search and secure areas in the domain of the NuMI Radiation Safety System.

4.8.2.4 System Description: Electrical Safety System for NuMI

Electrical hazards from exposed conductors and connections exist in the NuMI beamline from point of extraction to the magnetic focusing horns. These hazards are typically associated with the beamline magnetic elements such as dipole and quadrupole magnets. Such hazards are also associated with the extraction kicker, Lambertsons, and horns. **The Electrical Safety System (ESS)** extensions of both the Main Injector and NuMI RSS provide permitting inputs to associated power supplies to partially mitigate the hazard of exposed conductors that are not otherwise guarded. The MI ESS connects to supplies in MI-60 and MI-62, while the NuMI ESS connects to supplies at the MI-65 area, both above and below ground. Trim element conductors and connections are guarded and connection of their associated power supplies to either ESS is not necessary.

Accommodating access into the Main Injector and NuMI stub is further provided by connection of selected supplies to the “Beamline” Feeder 96/97. This feeder is de-energized during MI access. Technical power supplies at the MI-65 location are powered from conventional power feeders through a single 2000 kVA pulsed power transformer. Opening of a single point disconnect of 13.8 kV power to this transformer facilitates access to the downstream end of the Carrier Tunnel, Pre-Target enclosure and Target Hall. For purposes of Electrical Safety, this disconnect need not be opened for access to the Muon Alcoves, Absorber Hall or Decay Pipe passageway.

4.8.3 Cables

Cables associated with the NuMI Project are generally quite conventional in nature. The uniqueness of the NuMI underground enclosure, however, requires utilization of fire retardant cable insulation or jacketing unless the cables are installed in conduit. Certain cables in the high radiation environment of the target chase and absorber have suitably radiation tolerant insulation.

Cabling between MI-65 and MINOS areas is accomplished via buried communication duct pathways. All cables are labeled in accord with Accelerator Division standards.

4.8.3.1 System Description: General Cable Plant

The general cable plant of the NuMI Project has two fundamental aspects. The first aspect involves connectivity of both MI-65 and MINOS Service Buildings to established Laboratory infrastructure. An additional attribute here is the connection of certain services between these two service buildings. The second aspect of the cable plant involves connectivity between MI-60, MI-62 and MI-65 and MINOS Service Buildings and technical and experimental equipment in the accelerator and beamline enclosures.

The established Laboratory infrastructure required at the MI-65 and MINOS Service Buildings includes the following. These elements of infrastructure are already available at the MI-60 and MI-62 Service Buildings.

- Accelerator Radiation Safety System
- Accelerator Controls Network (ACNET)
- Wide Area Network Connectivity including access to Fermilab Central Analysis and Data Storage Facilities
- CATV
- Fire & Utility Monitoring System (FIRUS)
- Telephone Communications (POTS)
- MI-62, MI-65 and MINOS Fire Detection System Connectivity

The second aspect of the cable plant includes the following.

- Extension of above infrastructure (excluding Fire Detection System) to the new underground areas as appropriate
- Connections between various Power Supplies and enclosure Beamline Elements (Kickers, Lambertsons, Dipole and Quadrupole Magnets, Trim Elements)
- Connections between MI-62 based Vacuum System Electronics and Ion Pump Power Supplies and Beamline Vacuum Equipment (Ion pumps, Gauges, Isolation Valves)
- Connections between service building based electronics and beamline instrumentation (Beam Position Detectors, Beam Toroids, Profile Monitors, Regular and Total Loss Monitors)

- Localized connections in and between technical, scientific components and infrastructure hardware

4.8.3.2 System Description: MI-65 and MINOS Access Shaft Cables

At the MI-65 access shaft, cables are generally installed in cable tray. At the MINOS access shaft, all cables are installed in conduit. The depth of the MINOS shaft, approximately 350 feet, demands that cables have several points of support so as not to exceed cable tensile strength. Advantage is being taken of the "Outfitting" civil construction work activities. These involve similar installations in the shafts for the AC power distribution system, fire detection and utility infrastructure. Adding the installation of technical and infrastructure cabling to the Outfitting scope of work is simplifying installation. **Table 4.8-6** and **Table 4.8-7** summarize the various cables installed under the Service Building and Outfitting subcontract for the MI-65 and MINOS Access Shafts respectively.

MI-65 Service Building Shaft Wire and Cable - Installed Under SB&O Subcontract

Quantity	Avg Length	Type of Cable	Start	Finish	Route	Utilization	Provided & Used By
14	491	Insulated Copper Building Wire 500 MCM THHN Black	Electrical Room	Two Locations in Pre-Target	Power Tray	E:V118 String of Four B2 Dipoles	Subcontractor WBS 1.1.3
20	583	Insulated Copper Building Wire 1/0 THHN Black	Electrical Room	Varied Locations in Carrier Tunnel & Pre-Target	Power Tray	Q113-Q121 Quads and H117 Dipole	Subcontractor WBS 1.1.3
9	585	Shielded Twisted Pair 10 AWG	Electronics Room	Varied Locations in Carrier Tunnel & Pre-Target	Power Tray	Trim Elements	Fermilab WBS 1.1.3
24	536	3/8" Low Loss Heliax Coax Andrew LDF2RN-50	Electronics Room	Varied Locations in Carrier Tunnel & Pre-Target	Signal Tray	Beam Position Monitors & Calibration Signals	Fermilab WBS 1.1.1
12	555	Amphenol Spectra Strip Round 'n' Flat #843-159-2801-050	Electronics Room	Varied Locations in Carrier Tunnel & Pre-Target	Signal Tray	Profile Monitor Signal	Fermilab WBS 1.1.1
2	500	Multiconductor, 19 Conductor, 18 AWG, Alpha 1898/19C	Electronics Room	Pre-Target	Power Tray	Profile Monitor Motors Trunk	Fermilab WBS 1.1.1
4	500	Multiconductor, 9 Shielded Twisted Pairs, 18 AWG, Alpha 6025C	Electronics Room	Pre-Target	Signal Tray	Profile Monitor LVDTs Trunk	Fermilab WBS 1.1.1
1	500	Multiconductor, 15 Shielded Twisted Pairs, 22 AWG, Alpha 6018C	Electronics Room	Pre-Target	Signal Tray	Profile Monitor Limit Switches Trunk	Fermilab WBS 1.1.1

1	500	Multiconductor, 15 Shielded Twisted Pairs, 22 AWG, Alpha 6018C	Electronics Room	Pre-Target	Signal Tray	Magnet Klixons Trunk	Fermilab WBS 1.1.3
1	300	Fiber Optic Trunk Cable 24 Fiber Singlemode	Electronics Room	Target Hall PS Support Room	Signal Tray	Networking	Fermilab WBS 1.1.8
1	300	Fiber Optic Trunk Cable 36 Fiber Multimode	Electronics Room	Target Hall PS Support Room	Signal Tray	Controls	Fermilab WBS 1.1.8
2	300	Multiconductor, 20 Conductor, 18 AWG, Custom, Blue Jkt	Electronics Room	Target Hall PS Support Room	Signal Tray	Radiation Safety System	Fermilab WBS 1.1.8
2	300	Multiconductor, 4 Shielded Twisted Pairs, 18 AWG, Custom, Blue Jkt	Electronics Room	Target Hall PS Support Room	Signal Tray	RSS Data Links & Audio Warning	Fermilab WBS 1.1.8
1	300	Multiconductor, 15 Shielded Twisted Pairs, 22 AWG, Alpha 6018C	Electrical Room	Target Hall PS Support Room	Signal Tray	FIRUS Utility Monitors & Spare Utility	Fermilab WBS 1.1.8
2	300	RG213/U 50 Ohm Coax Red Jkt, Stk #1170-044500	Electronics Room	Target Hall PS Support Room	Signal Tray	EAV-2 and EAV-3 Stack Rad Monitors	Fermilab WBS 1.1.8
1	300	Multicoax, 16 x RG58C/U, 50 Ohm, Custom, Orange Jacket	Electronics Room	Target Hall PS Support Room	Signal Tray	Profile Monitor Clearing HV & Spare Utility	Fermilab WBS 1.1.1
2	300	CAC-6 75 Ohm Coax	Electronics Room	Target Hall PS Support Room	Signal Tray	CATV Monitors	Fermilab WBS 1.1.8
4	300	RG59/U 75 Ohm Coax	Electronics Room	Target Hall PS Support Room	Signal Tray	CATV Cameras	Fermilab WBS 1.1.8
1	300	Multiconductor, 25 Twisted Pairs, 24 AWG, Teflon Jacket	Electrical Room Inside Terminal	Target Hall PS Support Room	Signal Tray	Telecom POTS	Fermilab WBS 1.1.8

Table 4.8-6 MI-65 Access Shaft Cables Installed Under SB&O Subcontract

MINOS Service Building Shaft Wire and Cable - Installed Under SB&O Subcontract

Quantity	Length Each	Type of Cable	Start	Finish	Route	Utilization	Provided & Used By
1	725	Fiber Optic Trunk Cable 24 Fiber Singlemode	Mechanical - Electrical Area	MINOS Hall	Signal Conduit	Network Fiber	Fermilab WBS 1.1.8
1	725	Fiber Optic Trunk Cable 36 Fiber Multimode	Mechanical - Electrical Area	MINOS Hall	Signal Conduit	Controls Fiber	Fermilab WBS 1.1.8
1	725	Multiconductor, 15 Shielded Twisted Pairs, 22 AWG, Alpha 6018C	Mechanical - Electrical Area	MINOS Hall	Signal Conduit	FIRUS Utility Monitors & Spare Utility	Fermilab WBS 1.1.8
4	725	CAC-6 75 Ohm Coax	Mechanical - Electrical Area	MINOS Hall	Signal Conduit	CATV Monitors	Fermilab WBS 1.1.8
6	725	RG59/U 75 Ohm Coax	Mechanical - Electrical Area	MINOS Hall	Signal Conduit	CATV Cameras	Fermilab WBS 1.1.8
3	725	RG213/U 50 Ohm Coax Red Jkt, Stk #1170-044500	Mechanical - Electrical Area	MINOS Hall	Signal Conduit	Spare Utility	Fermilab WBS 1.1.8
1	725	Multicoax, 16 x RG58C/U, 50 Ohm, Custom, Orange Jacket	Mechanical - Electrical Area	MINOS Hall	Signal Conduit	Spare Utility	Fermilab WBS 1.1.8
1	725	Multiconductor, 25 Twisted Pairs, 24 AWG, Teflon Jacket	Mechanical - Electrical Area	MINOS Hall	Signal Conduit	Telecom POTS	Fermilab WBS 1.1.8
2	1100	Multiconductor, 20 Conductor 18 AWG, Custom, Blue Jkt	Mechanical - Electrical Area	Upstream End of Absorber Access Tunnel	Signal Conduit and Tray	Radiation Safety System	Fermilab WBS 1.1.8
2	1100	Multiconductor, 4 Shielded Twisted Pairs, 18 AWG, Custom, Blue Jkt	Mechanical - Electrical Area	Upstream End of Absorber Access Tunnel	Signal Conduit and Tray	Radiation Safety System Data Links	Fermilab WBS 1.1.8

Table 4.8-7 MINOS Access Shaft Cables Installed Under SB&O Subcontract

4.8.3.3 System Description: Communication Ducts

The MI-65 Service Building connects directly to the Main Injector communication duct system that generally follows Indian and Kautz Road pathways at communications manhole CMH-CUB-1. This system also affords connection to the Accelerator Cross Gallery and the new MI-12 MiniBooNE Target Building. While the MI system has connections to MI-8 and MI-62, more direct communication duct paths have been installed that connect MI-65 to both MI-62 and MI-

8. Infrastructure requirements at the MI-65 Service Building are primarily supported by installation of cables between MI-62 and MI-65. **Table 4.8-8** lists the cables to be found in the MI-62 to MI-65 communications ducts.

Comm Duct Cables from MI-62 to MI-65 Service Building 900 Feet

Qty	Type of Cable	Utility
1	Fiber Optic Trunk 24 Singlemode Fibers	Accelerator Computer Network
3	Fiber Optic Trunks 12 Multimode Fibers Each	Accelerator Controls including: Main Injector CAMAC Link Tevatron Clock (TCLK) Main Inj Beam Sync (MIBS) Machine Data (MDAT) NuMI Beam Permit DDC Utility Monitor System
2	20 Conductor 18 AWG Cables	Safety Interlock
2	Four Twisted Pair Cables, 18 AWG	Safety Data Links and Audio Warning
1	Three Twisted Pair, 18 AWG	ES&H Radiation Mux Trunk
3	1/2" 75 Ohm Hardline Coax Cables	FIRUS
3	1/2" 75 Ohm Hardline Coax Cables	CATV
1	Four Twisted Pairs 16 AWG	NuMI Fire Protection Connectivity between MI-62 and MI-65 Bldgs
1	Telephone Trunk Cable 50 Pair 24 AWG	Telephone Communications (POTS)

Table 4.8-8 Communication Duct Cables Between MI-62 and MI-65

A single communications duct has been installed between MBD and MI-12. Multiple ducts have been installed between MI-12 and the Main Injector system proximate to MI-10. These ducts have installed cables for infrastructure, MiniBooNE specific applications, and NuMI specific applications. **Table 4.8-9** lists the NuMI related cables to be found in the communication duct system connecting MI-65 to MiniBooNE Detector Building (MBD).

MI-65 to MiniBooNE Detector Building 4,000 Feet

Qty	Type of Cable	Utility
2	20 Conductor 18 AWG Cables	Safety Interlock
2	Four Twisted Pair Cables 18 AWG	Safety Data Links and Audio Warning
1	Four Twisted Pairs 16 AWG	NuMI Fire Protection Connectivity between MI-65 and MINOS Bldgs

Table 4.8-9 Communication Duct Cables Between MI-65 and MBD

The MINOS Service Building is directly served by a communication duct system installed under the NuMI Site Preparation and Service Building and Outfitting civil subcontracts. This system has connection to the MiniBooNE Detector Building and the MiniBooNE communication duct system that connects MI-10, MI-12 and MBD. This system also has connection to the Lederman Science Education Center and the accelerator footprint area. The path to Science Center facilitates connection to telephone, FIRUS, CATV and computing network infrastructures. This basic infrastructure has already been installed at the MBD. Supporting MINOS infrastructure has been accomplished by extension of the MBD infrastructure. **Table 4.8-10** lists the cables to be found in the communications ducts between MBD and the MINOS Service Building.

MiniBooNE Detector Building to MINOS Service Building 1,600 Feet

Qty	Type of Cable	Utility
1	Fiber Optic Trunk 24 Singlemode Fibers	Accelerator Computer Network Including Wide Area Network Connectivity and Access to Fermilab Central Analysis and Data Storage Facilities
3	Fiber Optic Trunks 12 Multimode Fibers Each	Accelerator Controls including: Main Injector CAMAC Link Tevatron Clock (TCLK) Main Inj Beam Sync (MIBS) Machine Data (MDAT) NuMI Beam Permit DDC Utility Monitor System
2	20 Conductor 18 AWG Cables	Safety Interlock
2	Four Twisted Pair Cables, 18 AWG	Safety Data Links and Audio Warning
3	1/2" 75 Ohm Hardline Coax Cables	FIRUS (Sourced from Science Education Building and Accelerator Cross Gallery)
3	1/2" 75 Ohm Hardline Coax Cables	CATV (Sourced from Science Education Building and Accelerator Cross Gallery)
1	Telephone Trunk Cable 50 Pair 24 AWG	Telephone Communications (POTS) (Sourced from Science Education Building Area and Accelerator Cross Gallery)
1	Four Twisted Pairs 16 AWG	NuMI Fire Protection Connectivity between MI-65 and MINOS Bldgs

Table 4.8-10 Communication Duct Cables Between MBD and MINOS Service Building